

Advances in inhalation safety assessment

Edited by

Victoria Hutter, Ewelina Hoffman, Thomas Hofmann
and Mary Catherine McElroy

Published in

Frontiers in Toxicology



FRONTIERS EBOOK COPYRIGHT STATEMENT

The copyright in the text of individual articles in this ebook is the property of their respective authors or their respective institutions or funders. The copyright in graphics and images within each article may be subject to copyright of other parties. In both cases this is subject to a license granted to Frontiers.

The compilation of articles constituting this ebook is the property of Frontiers.

Each article within this ebook, and the ebook itself, are published under the most recent version of the Creative Commons CC-BY licence. The version current at the date of publication of this ebook is CC-BY 4.0. If the CC-BY licence is updated, the licence granted by Frontiers is automatically updated to the new version.

When exercising any right under the CC-BY licence, Frontiers must be attributed as the original publisher of the article or ebook, as applicable.

Authors have the responsibility of ensuring that any graphics or other materials which are the property of others may be included in the CC-BY licence, but this should be checked before relying on the CC-BY licence to reproduce those materials. Any copyright notices relating to those materials must be complied with.

Copyright and source acknowledgement notices may not be removed and must be displayed in any copy, derivative work or partial copy which includes the elements in question.

All copyright, and all rights therein, are protected by national and international copyright laws. The above represents a summary only. For further information please read Frontiers' Conditions for Website Use and Copyright Statement, and the applicable CC-BY licence.

ISSN 1664-8714
ISBN 978-2-8325-6706-7
DOI 10.3389/978-2-8325-6706-7

Generative AI statement

Any alternative text (Alt text) provided alongside figures in the articles in this ebook has been generated by Frontiers with the support of artificial intelligence and reasonable efforts have been made to ensure accuracy, including review by the authors wherever possible. If you identify any issues, please contact us.

About Frontiers

Frontiers is more than just an open access publisher of scholarly articles: it is a pioneering approach to the world of academia, radically improving the way scholarly research is managed. The grand vision of Frontiers is a world where all people have an equal opportunity to seek, share and generate knowledge. Frontiers provides immediate and permanent online open access to all its publications, but this alone is not enough to realize our grand goals.

Frontiers journal series

The Frontiers journal series is a multi-tier and interdisciplinary set of open-access, online journals, promising a paradigm shift from the current review, selection and dissemination processes in academic publishing. All Frontiers journals are driven by researchers for researchers; therefore, they constitute a service to the scholarly community. At the same time, the *Frontiers journal series* operates on a revolutionary invention, the tiered publishing system, initially addressing specific communities of scholars, and gradually climbing up to broader public understanding, thus serving the interests of the lay society, too.

Dedication to quality

Each Frontiers article is a landmark of the highest quality, thanks to genuinely collaborative interactions between authors and review editors, who include some of the world's best academicians. Research must be certified by peers before entering a stream of knowledge that may eventually reach the public - and shape society; therefore, Frontiers only applies the most rigorous and unbiased reviews. Frontiers revolutionizes research publishing by freely delivering the most outstanding research, evaluated with no bias from both the academic and social point of view. By applying the most advanced information technologies, Frontiers is catapulting scholarly publishing into a new generation.

What are Frontiers Research Topics?

Frontiers Research Topics are very popular trademarks of the *Frontiers journals series*: they are collections of at least ten articles, all centered on a particular subject. With their unique mix of varied contributions from Original Research to Review Articles, Frontiers Research Topics unify the most influential researchers, the latest key findings and historical advances in a hot research area.

Find out more on how to host your own Frontiers Research Topic or contribute to one as an author by contacting the Frontiers editorial office: frontiersin.org/about/contact

Advances in inhalation safety assessment

Topic editors

Victoria Hutter — University of Hertfordshire, United Kingdom

Ewelina Hoffman — ImmuONE, United Kingdom

Thomas Hofmann — Thomas Hofmann Toxicological Consulting (THC), Germany

Mary Catherine McElroy — Charles River Laboratories, United Kingdom

Citation

Hutter, V., Hoffman, E., Hofmann, T., McElroy, M. C., eds. (2025). *Advances in inhalation safety assessment*. Lausanne: Frontiers Media SA.

doi: 10.3389/978-2-8325-6706-7

Table of contents

- 05 **Twenty-eight day repeated exposure of human 3D bronchial epithelial model to heated tobacco aerosols indicates decreased toxicological responses compared to cigarette smoke**
Fiona Chapman, Sarah Jean Pour, Roman Wieczorek, Edgar Trelles Sticklen, Jessica Budde, Karin Röwer, Sandra Otte, Elizabeth Mason, Lukasz Czekala, Thomas Nahde, Grant O'Connell, Liam Simms and Matthew Stevenson
- 20 **Inhalation of electronic cigarettes slightly affects lung function and inflammation in mice**
Yuxing Dai, Kun Duan, Guangye Huang, Xuemin Yang, Xingtiao Jiang, Jianwen Chen and Peiqing Liu
- 29 **Refinement of the acute inhalation limit test for inert, nano-sized dusts by an *in silico* dosimetry-based evaluation: case study for the dissolution of a regulatory dilemma**
Heidi Stratmann, Lan Ma-Hock, Simone Tangermann and Richard A. Corley
- 41 **Liquid application dosing alters the physiology of air-liquid interface (ALI) primary human bronchial epithelial cell/lung fibroblast co-cultures and *in vitro* testing relevant endpoints**
Nicholas M. Mallek, Elizabeth M. Martin, Lisa A. Dailey and Shaun D. McCullough
- 60 **Use of quantitative *in vitro* to *in vivo* extrapolation (QIVIVE) for the assessment of non-combustible next-generation product aerosols**
Marjory Moreau, Liam Simms, Melvin E. Andersen, Edgar Trelles Sticklen, Roman Wieczorek, Sarah Jean Pour, Fiona Chapman, Karin Roewer, Sandra Otte, Jeffrey Fisher and Matthew Stevenson
- 76 **Applying new approach methodologies to assess next-generation tobacco and nicotine products**
David Thorne, Damian McHugh, Liam Simms, K. Monica Lee, Hitoshi Fujimoto, Sara Moses and Marianna Gaca
- 91 **Corrigendum: Applying new approach methodologies to assess next-generation tobacco and nicotine products**
David Thorne, Damian McHugh, Liam Simms, K. Monica Lee, Hitoshi Fujimoto, Sara Moses and Marianna Gaca
- 93 **New approach methodologies (NAMs) for the *in vitro* assessment of cleaning products for respiratory irritation: workshop report**
Lynne T. Haber, Mark A. Bradley, Amanda N. Buerger, Holger Behrsing, Sabina Burla, Phillip W. Clapp, Scott Dotson, Casey Fisher, Keith R. Genco, Francis H. Kruszewski, Shaun D. McCullough, Kathryn E. Page, Vivek Patel, Nathan Pechacek, Clive Roper, Monita Sharma and Annie M. Jarabek

- 122 **Evaluation of a non-animal toolbox informed by adverse outcome pathways for human inhalation safety**
Renato Ivan de Ávila, Iris Müller, Hugh Barlow, Alistair Mark Middleton, Mathura Theiventhran, Danilo Basili, Anthony M. Bowden, Ouarda Saib, Patrik Engi, Tymoteusz Pietrenko, Joanne Wallace, Bernadett Boda, Samuel Constant, Holger Peter Behrsing, Vivek Patel and Maria Teresa Baltazar
- 152 **Immunotoxicity assessment of multiwalled carbon nanotubes following whole-body inhalation exposure for 30 and 90 days in B6C3F1/N mice and 30 days in HSD:Harlan Sprague Dawley SD® rats**
Victor J. Johnson, Nigel J. Walker, Michael I. Luster, Gary R. Burleson, Michelle Cora, Gregory L. Baker, Barney Sparrow and Dori R. Germolec



OPEN ACCESS

EDITED BY

Gabino Garrido,
Catholic University of the North, Chile

REVIEWED BY

Aditya Reddy Kolli,
Philip Morris International, Switzerland
Maciej Stepnik,
QSAR Lab Ltd., Poland

*CORRESPONDENCE

Fiona Chapman,
✉ fiona.chapman@uk.imptob.com

SPECIALTY SECTION

This article was submitted to
In Vitro Toxicology,
a section of the journal
Frontiers in Toxicology

RECEIVED 21 October 2022

ACCEPTED 09 January 2023

PUBLISHED 16 February 2023

CITATION

Chapman F, Pour SJ, Wieczorek R,
Trelles Sticklen E, Budde J, Röwer K, Otte S,
Mason E, Czekala L, Nahde T, O'Connell G,
Simms L and Stevenson M (2023), Twenty-
eight day repeated exposure of human 3D
bronchial epithelial model to heated
tobacco aerosols indicates decreased
toxicological responses compared to
cigarette smoke.
Front. Toxicology 5:1076752.
doi: 10.3389/ftox.2023.1076752

COPYRIGHT

© 2023 Chapman, Pour, Wieczorek,
Trelles Sticklen, Budde, Röwer, Otte,
Mason, Czekala, Nahde, O'Connell, Simms
and Stevenson. This is an open-access
article distributed under the terms of the
[Creative Commons Attribution License
\(CC BY\)](https://creativecommons.org/licenses/by/4.0/). The use, distribution or
reproduction in other forums is permitted,
provided the original author(s) and the
copyright owner(s) are credited and that
the original publication in this journal is
cited, in accordance with accepted
academic practice. No use, distribution or
reproduction is permitted which does not
comply with these terms.

Twenty-eight day repeated exposure of human 3D bronchial epithelial model to heated tobacco aerosols indicates decreased toxicological responses compared to cigarette smoke

Fiona Chapman^{1*}, Sarah Jean Pour², Roman Wieczorek²,
Edgar Trelles Sticklen², Jessica Budde², Karin Röwer², Sandra Otte²,
Elizabeth Mason¹, Lukasz Czekala¹, Thomas Nahde²,
Grant O'Connell¹, Liam Simms¹ and Matthew Stevenson¹

¹Imperial Brands PLC, Bristol, United Kingdom, ²Reemtsma Cigarettenfabriken GmbH, Hamburg, Germany

Tobacco harm reduction (THR) involves providing adult smokers with potentially reduced harm modes of nicotine delivery as alternatives to smoking combustible cigarettes. Heated tobacco products (HTPs) form a category with THR potential due to their ability to deliver nicotine and flavours through heating, not burning, tobacco. By eliminating burning, heated tobacco does not produce smoke but an aerosol which contains fewer and lower levels of harmful chemicals compared to cigarette smoke. In this study we assessed the *in vitro* toxicological profiles of two prototype HTPs' aerosols compared to the 1R6F reference cigarette using the 3D human (bronchial) MucilAir™ model. To increase consumer relevance, whole aerosol/smoke exposures were delivered repeatedly across a 28 day period (16, 32, or 48 puffs per exposure). Cytotoxicity (LDH secretion), histology (Alcian Blue/H&E; Muc5AC; FoxJ1 staining), cilia active area and beat frequency and inflammatory marker (IL-6; IL-8; MMP-1; MMP-3; MMP-9; TNFα) levels were assessed. Diluted 1R6F smoke consistently induced greater and earlier effects compared to the prototype HTP aerosols across the endpoints, and in a puff dependent manner. Although some significant changes across the endpoints were induced by exposure to the HTPs, these were substantially less pronounced and less frequently observed, with apparent adaptive responses occurring over the experimental period. Furthermore, these differences between the two product categories were observed at a greater dilution (and generally lower nicotine delivery range) for 1R6F (1R6F smoke diluted 1/14, HTP aerosols diluted 1/2, with air). Overall, the findings demonstrate the THR potential of the prototype HTPs through demonstrated substantial reductions in toxicological outcomes in *in vitro* 3D human lung models.

Abbreviations: ALI, air-liquid interface; COPD, chronic obstructive pulmonary disease; HPHCs, Harmful and potentially harmful constituents; HTP, heated tobacco product; ISO, international organization for standardization; NGP, next-generation product; p-HTP, prototype heated tobacco product; SAEIVS, smoke aerosol exposure *in vitro* system; THR, tobacco harm reduction.

KEYWORDS

in vitro, MucilAir™, heated tobacco, cigarette, tobacco harm reduction, repeat exposure

Introduction

Combustible cigarette smoking is cause of serious diseases, including heart disease, lung cancer and emphysema (United States Surgeon General, 2010; International Agency for Research on Cancer, 2012; US Department of Health and Human Services, 2014). This is largely attributed to the repeated exposure of cells to a vast number of toxicants within the smoke generated upon the combustion of tobacco, which in turn can cause the initiation of cellular and molecular processes leading to disease (US Department of Health and Human Services, 2014). Tobacco harm reduction (THR) is the concept of providing adult smokers who would otherwise continue to smoke with potentially less harmful forms of nicotine delivery (Stratton et al., 2001; O'Leary and Polosa, 2020). This is achieved through offering adult smokers nicotine delivery innovations, or next-generation products (NGPs), which deliver satisfactory levels of nicotine but with substantially reduced levels of, and fewer, toxicants compared to combustible cigarette smoke (O'Leary and Polosa, 2020). Further to this, nicotine delivery products are proposed to sit on a product risk scale relative to one another, with medically licenced nicotine replacement therapies, such as gum and patches, at the lower risk end, combustible cigarette smoking at the highest risk by a large margin, and NGPs in between (McNeill and Munafò, 2013; Abrams et al., 2018; Zeller, 2019; Murkett et al., 2020). NGPs which deliver nicotine *via* the inhalation route and do not involve tobacco combustion include e-cigarettes and heated tobacco products (HTPs). By eliminating burning, these products do not produce smoke but an inhalable aerosol which contains fewer and lower levels of potentially harmful chemicals (Forster et al., 2018; Bentley et al., 2020; Rudd et al., 2020; Chapman et al., 2023).

Increasing evidence in the scientific literature suggests that the reduction in levels and number of toxicants within the aerosols of NGPs, including e-cigarettes and heated tobacco, correlates with reductions in *in vitro* toxicological responses compared to combustible cigarette smoke (Schaller et al., 2016; Jaunky et al., 2018; Hattori et al., 2020; Rudd et al., 2020; Simms et al., 2020; Simms et al., 2021; Chapman et al., 2023). Furthermore, the substantially reduced toxicological responses of NGPs compared to combustible cigarette has been demonstrated in a number of *in vitro* studies, in both 2D and 3D cell models (Iskandar et al., 2018; Czekala et al., 2019; Czekala et al., 2020; Haswell et al., 2021; Simms et al., 2021; Simms et al., 2022). Three dimensional (human) lung cell models are a useful tool in the assessment of the effects of inhalable test articles such as combustible cigarette smoke or NGP aerosols (Bedford et al., 2022). These models offer a human-relevant cellular system, grown and/or stimulated under air-liquid interface (ALI) conditions, and can include a variety of relevant cell types (e.g., basal, goblet and ciliated cells); this is more closely representative of an *in vivo* scenario than using single cell-type 2D cultures, for example (Huang et al., 2013; Cervená et al., 2019). This, coupled with the application of whole aerosol/smoke exposures at the ALI can model exposure of cells to as representative a chemical mixture to that which the consumer would be exposed to as possible (Chapman et al., 2023). *In vitro* 3D models exposed to whole NGP aerosol or combustible cigarette smoke have been used to assess a number of endpoints associated with the development and progression of respiratory

diseases, including functional and morphological changes like cilia activity and ratios of cell types (e.g., goblet cells, ciliated cells), inflammatory readouts and genomic level changes (Czekala et al., 2019; Rayner et al., 2019; Ghosh et al., 2020; Haswell et al., 2021; Bedford et al., 2022).

Most of the previous *in vitro* studies utilising human 3D lung tissue models in the assessment of the effects of NGPs compared to combustible cigarettes have applied acute (single) exposures (Iskandar et al., 2018; Czekala et al., 2019; Giralt et al., 2021). However, it is recognised that development of disease phenotypes occurs following a period of time, and additionally is likely the effect of more than a single exposure or cellular/molecular event (Yoshida and Tuder, 2007; Haswell et al., 2021; Luettich et al., 2021). Furthermore, upregulation of responses to exogenous agents may have protective effects in the event of any subsequent exposures, or may result in increased susceptibility and instability of cellular processes (Chapman et al., 2015). Czekala et al. (2021) recently compared the effects of repeat exposures of diluted fresh whole 3R4F reference cigarette smoke to whole fresh undiluted e-cigarette aerosol and found that whilst 3R4F induced strong declines in cellular functionality and integrity over a 28 days repeated exposure period compared to Sham, the e-cigarette did not. At lower exposures repeated over a 6 week period, diluted (1:80, then later 1:100) 1R6F reference cigarette smoke induced increases in the population of mucin-producing cells, or goblet cell hyperplasia, a pathology associated with development of COPD (Haswell et al., 2021). Crucially, application of repeat exposures, over a long-term period, is more representative of a consumer relevant scenario, i.e., repeated, regular product use. The 3D MucilAir model is considered a useful tool in such repeat exposure studies as it can be maintained in the incubator in its fully differentiated state for up to 1 year (Cervená et al., 2019; Epithelix Sàrl, 2022). However, studies on repeat exposure to NGPs compared to combustible cigarettes *in vitro* are limited, particularly with regards to HTPs.

Mucociliary clearance, which involves both cilia activity and the airway surface liquid (including mucus and the periciliary layer) play a key role in maintenance of airway functionality, and dysfunction is linked to the development of pathologies such as COPD (Luettich et al., 2021). This adverse event pathway, which may occur upon exposure to combustible cigarette smoke, has recently been mapped out by Luettich et al. (2021). As part of this pathway, FoxJ1 has a role in ciliogenesis, and its decreased expression, which has been linked with combustible cigarette smoke exposure, is associated with loss/absence of cilia (Luettich et al., 2021). Goblet cell hyperplasia is another process associated with respiratory disease pathologies, and has recently been modelled *in vitro* during sub-cytotoxic repeated exposures to diluted combustible cigarette smoke (but was not induced by HTP aerosol exposure) (Haswell et al., 2021); Muc5AC is often used as a marker for mucin gene expression (Behrsing et al., 2016; Bedford et al., 2022). Additionally, changes in inflammatory markers are used as a proxy of inflammatory responses *in vitro*, and a number of mediators, including the cytokines, TNF α and interleukins (ILs), and matrix metalloproteinases (MMPs), are associated with exposure to inhaled toxicants, including combustible cigarette smoke (Behrsing et al., 2016; Czekala et al., 2021; Bedford et al., 2022; Langel et al., 2022). It is for the above reasons that these cellular processes (cilia activity

(beat frequency and active area), FoxJ1 expression, changes in goblet cells, inflammatory readouts) are often used as *in vitro* indicators of potential responses to inhaled test articles (Behrsing et al., 2016; Iskandar et al., 2017; Czekala et al., 2021; Bedford et al., 2022). Therefore in the current study, we looked to assess these endpoints.

The current study aimed to assess the effects of two prototype HTPs (p-HTPs) on the MucilAir 3D reconstituted human bronchial epithelial cell model compared to the 1R6F reference combustible cigarette. To increase the human-use relevance of the study, cells were exposed to (air) diluted whole smoke/aerosol, and under repeated exposure conditions over 28 days. Effects on cells were assessed throughout the 28-day exposure period using secreted LDH levels as a marker of cytotoxicity, histological evaluation of tissue architecture, goblet cell (Muc5AC) and ciliated cell (FoxJ1) markers, and cilia beat frequency and active area as a measure of cell functionality. To assess the inflammatory responses of the tissues, levels of six markers associated with combustible cigarette smoke exposure were additionally assessed, IL-6, IL-8, MMP-1, MMP-3, MMP-9 and TNF α . This is the first study on the effects of these p-HTPs on the MucilAir (bronchial cell) model, and using a prolonged (28 days), repeat exposure regime.

Materials and methods

Test articles

Three test articles were assessed in this study, two prototype heated tobacco products (p-HTPs) (obtained directly from production by Imperial Brands PLC) and the 1R6F Reference Cigarette (Kentucky Tobacco Research and Development Centre, University of Kentucky). The p-HTPs consist of a rechargeable device into which a consumable stick with a reconstituted tobacco portion is inserted (illustrated in Supplementary Figures S1, S2). Upon device activation by the user, the tobacco portion is heated directly with a ceramic heating pin, which generates an aerosol, delivered to the user as they draw air through the filter. The device has two heating temperatures, 315°C and 345°C; the higher temperature of the two was used in this study. Two stick variants were tested, Regular and Intense. The p-HTP sticks were stored at room temperature, protected from light, in sealed portions per test within airtight containers, until use; the 1R6F reference cigarettes were stored frozen, sealed in the original packaging until conditioning according to International Organization for Standardization (ISO, 2018) Guideline 3402 (1999) (at least 48 h at 22 \pm 1°C and 60 \pm 3% relative humidity) prior to use.

Cell culture

Fully differentiated reconstituted 3D human bronchial epithelial models (MucilAir™) were purchased from Epithelix Sàrl (Switzerland). The donor was a 41 year-old male Caucasian non-smoker with no pathology (Batch No.: MD072001). Upon receipt, tissues were incubated at 37°C, 5% CO₂ for 7 days, to acclimatise, according to manufacturer's instructions. Cells were maintained with 700 μ L basal medium (standard manufacturer's culture medium, Epithelix Sàrl, Switzerland), supplemented with 1% Amphotericin B (Sigma-Aldrich, Germany) (final medium concentration, 2.5 μ g/mL). Basal cell culture medium was changed every 3 days, collected in

200 μ L aliquots and stored frozen at –80°C until analysis. Once a week mucus was removed from the surface of the tissues: 4 hours following exposure, 200 μ L PBS (Mg²⁺/Ca²⁺) was added apically to the tissues and allowed to incubate (37°C, 5% CO₂) for 30 min, then gently washed from the tissue together with the mucus by manual pipetting. PBS/mucus samples were stored frozen at –80°C for cytotoxicity evaluation (see section, 'Cytotoxicity Evaluation').

Exposures

Whole aerosol/smoke aerosols were applied to the apical surfaces of the 3D models (at the ALI) using the custom-built Smoke Aerosol Exposure *In Vitro* System (SAEIVS) (Rudd et al., 2020; Wiecek et al., 2020). Exposures were carried out over an experimental period of 28 days (treatment and sampling regimes are detailed in Figure 1). The SAEIVS consists of five smoking chambers into which the test products were placed for respective runs. The 1R6F reference cigarette was smoked according to the ISO 20778 smoking regime (2018) (formerly known as the Health Canada Intense regime) (55 mL puff volume, 2 s puff duration, 30 s puff interval, bell shaped puff profile, ventilation blocking). The p-HTP aerosols were generated using a modified ISO 20778 regime (55 mL puff volume, 2 s puff duration, 30 s puff interval, bell shaped puff profile), with no ventilation blocking. This regime was used for the p-HTPs as there is currently no published ISO regime for HTPs; ventilation blocking was not applied as this is more representative of how the product would be used, i.e., ventilation holes would not be blocked by the user's fingers or lips as has been suggested with combustible cigarettes (Gee et al., 2018). After each puff, the smoke or aerosol from the five smoking chambers was combined in a mixing pump and diluted with fresh filtered humidified air according to the following ratios (smoke/aerosol in air): 1R6F, 1 in 14 (92.7% dilution; 7.3% smoke concentration); p-HTP Regular, 1 in 2 (50% dilution; 50% aerosol concentration); p-HTP Intense, 1 in 2. Dilutions were applied to prevent excessive toxicity to the cell models (i.e., to achieve sub-cytotoxic exposures) where possible. The diluted aerosol/smoke then moved into exposure chambers where the cell culture plates were placed. Within these chambers (two in parallel) aerosol/smoke is delivered to individual wells *via* a dilution manifold, and a sliding lid allows columns of wells to be sequentially covered to achieve puff-wise exposures across the plate. In this study, 16, 32 or 48 (diluted as described above) puffs were delivered to the cells at each exposure (i.e., equivalent to 1.14, 2.29 and 3.43 puffs for 1R6F; 8, 16 and 24 puffs for p-HTPs Regular and Intense). Following each puff, aerosol/smoke is drawn out of the exposure chamber *via* an exhaust. The SAEIVS achieves delivery of aerosol/smoke generated to cells in <10 s, ensuring that ageing effects are prevented and that maximal aerosol/smoke chemical constituents are delivered to the cells. The numbers of puffs applied were selected to allow for puff count and exposure time comparability between the cigarette smoke and heated tobacco aerosols. This was derived from preliminary dose range finding experiments with the 1R6F reference cigarette smoke (the most toxic test article) (data not shown), where smoke dilutions and puff counts were selected based on non-, sub- and weakly cytotoxic responses in 3D tissues derived from the same donor as used in the main study presented. The pre-study also included selecting the levels of dilution of the fresh 1R6F smoke/p-HTP aerosols with air.

Day	1	2	3	4	5	6	7	8	9	10	11	12	13	14	15	16	17	18	19	20	21	22	23	24	25	26	27	28
Exposure																												
Medium sampling (nicotine)																												
Medium sampling (LDH)																												
Mucus collection (LDH)																												
Fixation for histology																												
CBF/ AA measurement																												
Medium sampling (cytokines)																												

FIGURE 1

Exposure and sampling/measurement regimes for the 3D models over the experimental period. Samples of medium were taken (following exposures; prior to harvesting on day 28) and mucus (4 h prior to exposures) over the experimental period for LDH release measurement; medium was also sampled for cytokine analysis directly before exposure; on days denoted with *, samples were taken both directly before exposure and 4 h following exposure. Cilia beat frequency (CBF)/active area (AA) measurements were taken on days where exposure did not occur (these measurements were additionally taken on days -5 and 0 to assess tissue functionality prior to the experimental period). Treatments of additionally allocated tissues with 5 ng/mL positive control, IL-13, were also included in the study (days 13, 15, 17, 20, 22 and 24); cells were treated with CBF positive control, procaterol on day 21 (positive controls not included in this figure to increase readability). On day 28, a subset of tissues were fixed for histological analyses.

Nicotine dosimetry

Nicotine dosimetry of the cell culture medium was carried out at the timepoints detailed in Figure 1. Nicotine quantification in medium samples was carried out using LC-MS/MS (AB Sciex API 6500 QTRAP (SCIEX, USA)). For analysis, medium samples were diluted 1:1,000 and 1:2000 with MilliQ water and 1:1 in the autosampler with the internal standard solution in methanol. A Gemini NX-C18 column (110Å, 100 × 2.0 mm, 3 µm) (Phenomenex, USA) was used for the liquid chromatography (oven temperature 55°C ± 1°C), sample injection volume was 5 µL and the autosampler temperature was 5°C. The eluent gradient was applied according to the following: 0min: 2% B (methanol)/98% A (0.05% acetic acid) (flow rate: 400 mL/min); 1.2 min: 65% B/35% A (400 mL/min); 1.5 min: 95% B/5% A (400 mL/min); 2.5 min: 98% B/2% A (400 mL/min); 3.0 min: 98% B/2% A (400 mL/min). The following conditions were used for the mass spectrometry: Ion spray voltage: 450 V, Ion source temperature: 500°C, MRM: 163/132 quantification; 163/106 qualifier. Three replicates were analysed per treatment.

Cytotoxicity evaluation

Cytotoxicity was assessed based on measurement of levels of LDH release into the cell culture medium and mucus. Medium samples were taken, at the timepoints detailed in Figure 1, prior to exposure, whereas mucus was collected by washing with PBS once a week (see section 'Cell culture'). For analysis, samples were thawed and analysed using the Promega CytoTox 96® Non-Radioactive Cytotoxicity Assay kit, according to manufacturer instructions. A standard row was used to calculate the total amount of LDH in pg.

Histology

Tissues from each treatment group, harvested at day 28, were prepared for histological analysis. Tissues were fixed with 3 × 20 min

incubations in 4% formaldehyde in PBS (Mg²⁺/Ca²⁺), following this, they were stored in 50 mL tubes filled with PBS at 4°C until processed. Histological analysis was carried out by Epithelix Sàrl. The tissues and culture insert membranes were removed and this disc was cut in half (to be embedded in the same paraffin block). The samples were processed according to the Peloris Automaton (Leica Biosystems, Germany) 1 h protocol, then embedded in paraffin. For each sample, two sections, approximately 3 µm thick, were cut and placed on the same glass slide. Cells were stained with Haematoxylin Eosin (HE)/Alcian Blue (AB) according to Epithelix's internal protocol. Additional immunohistochemistry staining was carried out on complementary sections using the Ventana Benchmark XT and Ultraview DAB detection kit (760-500) (both Ventana-Roche). Antibodies: staining was carried out for Mucin-5AC protein (Muc5AC) (ThermoFisher Scientific, MA5-12178 (mouse monoclonal)) and forkhead box transcription factor (Fox-J1) (Novus Biological, NBP1-87928 (rabbit polyclonal)). Slides were imaged and digitalised using a Nanozoomer (Hamamatsu) under brightfield conditions, with a ×20 objective (without Z stack mode). Histological quantification was carried out using NDPiExport, developed by Epithelix. For Alcian blue/H&E staining, results were expressed as % positive cells/total area; for Muc5AC, % positive area/total area; and for Fox-J1, % positive nuclei/number of nuclei.

Cell imaging (CBF, CAA)

Cilia beat frequency (CBF) and cilia active area (CAA) were recorded throughout the experiment, at the timepoints detailed in Figure 1, as an assessment of tissue functionality. The timepoints were selected to fall 24 h pre-/post-exposure to so as not to add any additional stress to the tissues too close to the exposures, and to take the measurements when the tissues are stabilised in the time between exposures. Prior to measurement, tissues were placed into an ibidi Heating System for multiwell plates (ibidi GmbH, Germany) for 20 min at 37°C to acclimatise. Video images of the apical surface of the tissues were captured using the ×4 objective of an Olympus 1×53P1F

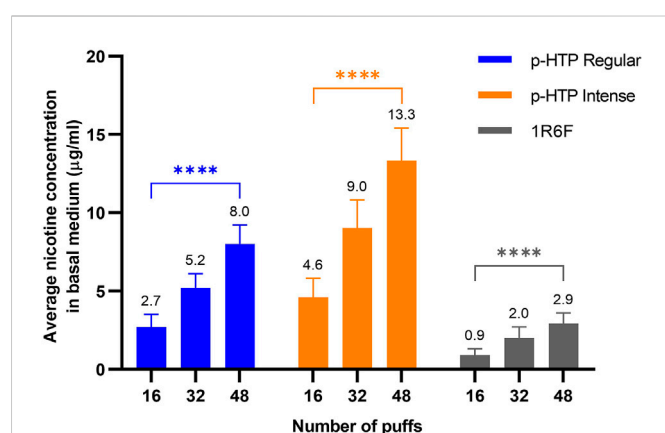


FIGURE 2

Average (values detailed above each bar) nicotine concentration in basal cell culture medium samples collected directly following exposure of the 3D tissues to 16, 32 or 48 puffs of p-HTP aerosols (diluted 1 in 2) or 1R6F reference cigarette smoke (diluted 1 in 14). Data is an average of measurements in samples taken at the timepoints detailed in Figure 1. Error bars represent standard deviation; $n = 3$ per day \times 12 days. Differences between the puff levels of each product were analysed using a two-way ANOVA; **** $p < 0.0001$ (two-way ANOVA with Tukey's post-hoc test).

inverted microscope (Olympus, Japan) and analysed using Sisson-Ammons Video Analysis software. The captured image was divided into two blocks (top and bottom), each block was analysed separately using the same routine analysis. Videos were recorded at 200 frames/s (total 1,024 frames/video). Pixel intensities were extracted by the analysis software for a region of interest over time, then data underwent a fast Fourier transformation; noise reduction was applied using a Gaussian distribution. Outputs were displayed as intensity graphs for each of the two endpoints (CBF and CAA).

Procaterol hydrochloride (10 μ M final concentration) (Sigma-Aldrich, Germany) was used as a positive control for CBF (increased activity), added to the basolateral medium of dedicated tissues for this analysis. Following addition of procaterol hydrochloride, tissues were allowed 15 min to equilibrate with the compound prior to imaging; the basal medium was removed and exchanged for fresh culture medium after 1 h.

Representative images are included in Supplementary Figure S3.

Analysis of inflammatory markers

Levels of pro-inflammatory markers tumour necrosis factor alpha (TNF α) and interleukin (IL)-6, the chemokine IL-8 and the matrix metalloproteinases (MMP)-1, MMP-3 and MMP-9 secreted into the basal cell culture medium were assessed at the timepoints detailed in Figure 1. Medium was sampled either directly prior to next exposure (days 3, 6, 10, 17, 24, 28) or 4 h following exposures (days 3, 10, 17, 24). The markers were measured using an MSD® Multi-Spot Assay System MESO Scale QuickPlex™ (MSD Maryland, USA). IL-8 was determined *via* the Chemokine Panel one Kit and a 1:4 dilution of the sampled medium. The other cytokines were measured together on Custom U-Plex plates with undiluted medium samples according to the manufacturer's protocol.

Statistical analyses

For the nicotine dosimetry (two-way analysis of variance (ANOVA) with Tukey's post-hoc test; comparison between numbers of puffs for the respective study products), LDH (two-way ANOVA with Dunnett's post-hoc test; comparison of the study product responses to Sham for respective timepoints), CBF, CAA (both ordinary one-way ANOVA with Bonferroni's post-hoc test; comparison of the study product responses to Sham (fold-change) for respective timepoints) and inflammatory marker (two-way ANOVA with Dunnett's post-hoc test; comparison of the study product responses to Sham (fold-change) for respective timepoints) data, statistical analyses were carried out using GraphPad Prism version 8.

Results

Exposure measurement (delivered nicotine)

Samples of basal cell culture medium were collected directly following exposure of the models to 16, 32 or 48 puffs of the p-HTP aerosols/1R6F smoke. Nicotine levels within these samples were then quantified to provide an indication of relative exposures to the cultures according to the different exposure levels/products (Figure 2). Measured nicotine levels were approximately proportional to number of puffs delivered for each product, i.e., 16:32:48 puffs = 1:2:3 times the amount of nicotine measured. The p-HTP Intense product variant delivered around 1.7 times more nicotine per puff (diluted 1 in 2) compared to p-HTP Regular, despite the same dilution factor. The lower levels of nicotine observed for 1R6F were due to increased dilution per puff (i.e., 1 in 14) prior to exposures in the cell culture chambers. However, 48 puffs of 1R6F smoke diluted 1 in 14 delivered comparable nicotine levels to 16 puffs of 1 in 2 diluted p-HTP Regular aerosol, indicating that exposures for this study fell within a comparable nicotine delivery range.

Cytotoxicity

Over the 28-day experimental period, levels of LDH secreted from cells (into basal medium and mucus) were generally consistent between all test articles and Sham at the 16 and 32 puff levels. Although there were a few significant differences to Sham at some timepoints (p-HTP Intense 16 puffs, day 17; 1R6F 16 puffs, day 24 and 32 puffs, days 17 and 22), these were not sustained trends. This was also the case for both p-HTPs with the 48 puff exposures. However, in contrast, increased release of LDH was observed following exposures to 48 puffs of 1R6F smoke compared to Sham, which reached significance at day 10 and generally increased from this point onwards. It was also noted that greater variability was observed for the p-HTP Regular tissues exposed to 32 puffs particularly.

Histology

Following the 28-day experimental period, a subset of tissues were harvested and fixed for histological analysis (Figure 3). Alcian Blue/H&E staining was carried out to assess tissue architecture, Muc5AC staining was used to indicate the presence of goblet cells and FoxJ1 was used to stain for ciliated cells (Figure 3; Table 1). In the Sham treated tissues,

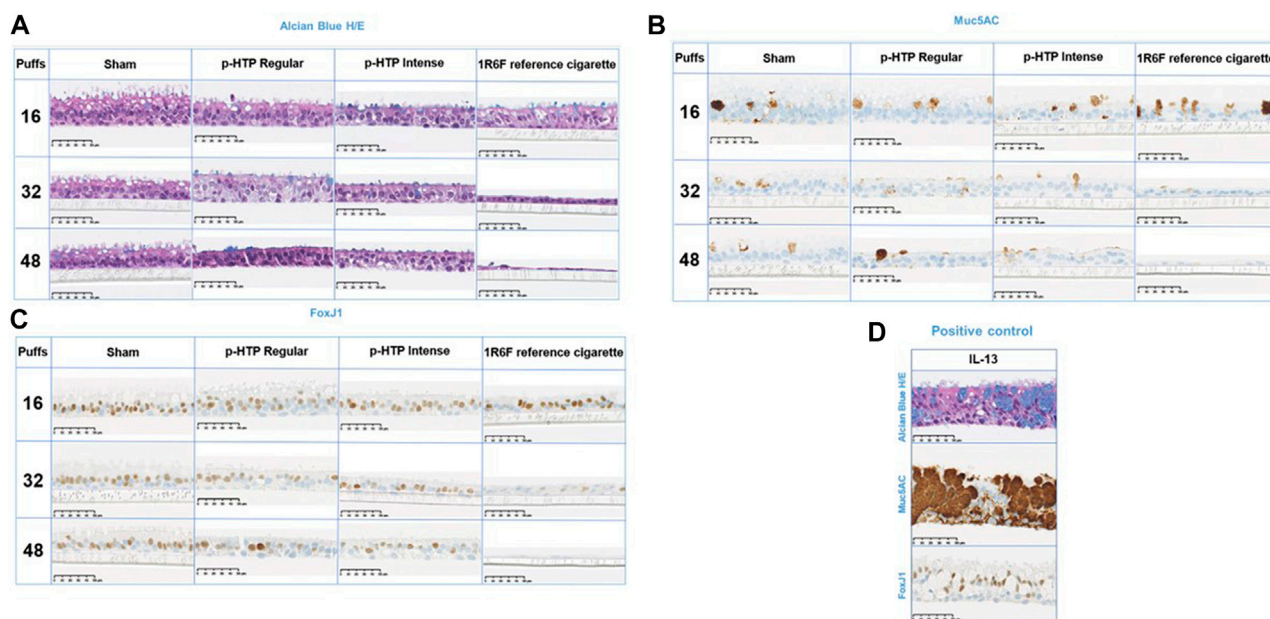


FIGURE 3

Representative histological images of the tissues exposed to 16, 32 and 48 puffs of air (sham), p-HTP Regular aerosol, p-HTP Intense aerosol or 1R6F reference cigarette smoke, harvested at the end of the 28 days repeated exposure experimental period. Fixed tissue slices were stained with Alcian Blue and H/E (A), Muc5AC (B) and FoxJ1 (C). A subset of tissues were treated with IL-13 as a positive control (D). Sham: $n = 1$ per condition; test products: $n = 2$ per condition; IL13: $n = 3$.

TABLE 1 Average staining in treated tissues (16, 32 or 48 puffs of air (Sham), p-HTP Regular, p-HTP Intense, 1R6F), fixed and stained at the end of the 28 days repeated exposure period. Positive control treatment, IL-13, is also included. ND: no staining detected.

		16 puffs	32 puffs	48 puffs
Alcian Blue/H&E (% positive cells/total area)	Sham	0.16	0.10	0.10
	p-HTP Regular	1.66	0.20	0.03
	p-HTP Intense	0.38	0.10	0.08
	1R6F	0.25	0.22	0.06
	IL-13	19.99		
Muc5AC (% positive area/total area)	Sham	4.50	2.97	2.57
	p-HTP Regular	5.97	2.07	2.68
	p-HTP Intense	3.23	1.75	2.68
	1R6F	5.48	1.23	0.54
	IL-13	77.26		
FoxJ1 (% positive nuclei/number of nuclei)	Sham	47.02	45.93	44.54
	p-HTP Regular	45.54	42.17	32.09
	p-HTP Intense	42.33	34.10	24.73
	1R6F	40.64	17.16	ND
	IL-13	43.23		

slight declines in all endpoints were observed with increasing numbers of puffs, which may be the result of repeated exposures to puffs, i.e., mechanical stress, over the prolonged 28-day exposure period. For the Alcian Blue/H&E staining, compared to Sham treated tissues, there appeared to be a small decline in tissue height with

increasing puffs of the p-HTP aerosols, however, this was not pronounced. For 1R6F, there were clear declines in tissue height and number of cells present, along with changes in morphology with increasing puffs. When stained for Muc5AC, the presence of goblet cells appeared to decrease for all treatments with increasing puffs

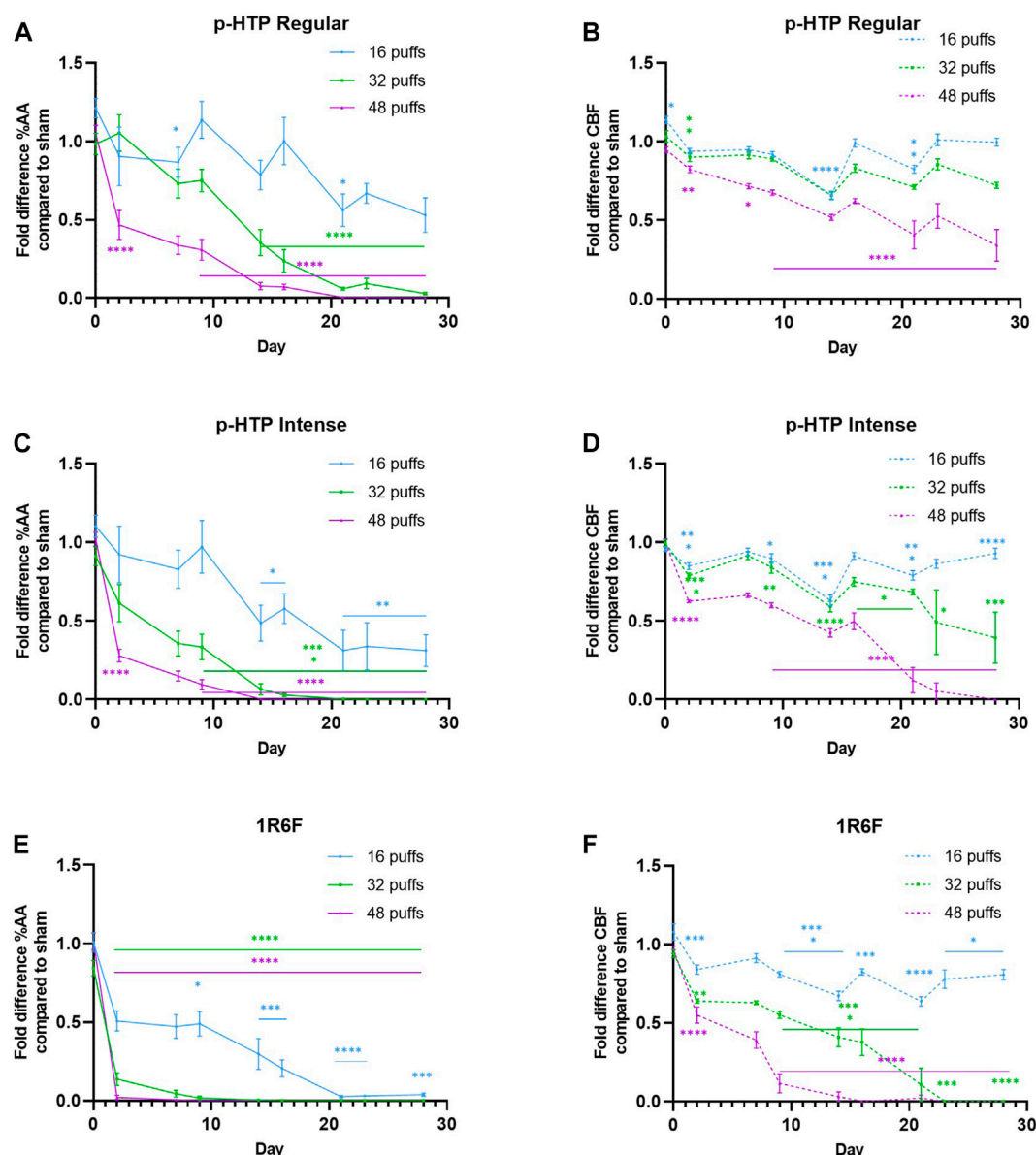


FIGURE 4

(A, C, E) Fold changes in % cilia active area (AA) compared to sham (air) treatment of 3D bronchial tissue models exposed to 16, 32 or 48 puffs of aerosol or smoke (B, D, F) Fold changes in cilia beat frequency (CBF) compared to sham (air) treatment of 3D bronchial tissue models exposed to 16, 32 or 48 puffs of aerosol or smoke. Error bars represent standard deviation; Sham: up to day 17, $n = 5$, day 15 onwards, $n = 3$; test products: up to day 17, $n = 8$, day 15 onwards, $n = 5$ (some tissues were lysed for analyses on day 17). * $p \leq 0.05$; ** $p \leq 0.01$; *** $p \leq 0.001$; **** $p \leq 0.0001$ (ordinary one-way ANOVA with Bonferroni's *post-hoc* test).

(including for Sham). However, this effect was especially pronounced for the 1R6F treated tissues with increasing puffs (around 10-fold decrease between 16 and 48 puffs). Puff-wise declines in ciliated cells were observed for the p-HTPs, with slightly stronger effects for p-HTP Intense. However, with increasing puffs of 1R6F smoke, declines in ciliated cells were stronger, with none detected at 48 puffs.

Tissue functionality: Cilia active area and cilia beat frequency

Over the 28 day period, increasing declines in both CAA and CBF compared to Sham (Sham values are detailed in Supplementary Figure

S4) over time were observed for all three test articles (Figure 4). The sizes of these declines correlated with the number of puffs to which the tissues were exposed. Additionally, for all test articles, declines in CAA were observed earlier than the declines in CBF. Upon comparison of tissue responses to the two p-HTP aerosols, p-HTP Intense exhibited greater potency than p-HTP Regular, with slightly greater, but not earlier declines in CBF and CAA observed. However, for 1R6F smoke, diluted to a much greater level, declines in CAA and CBF compared to Sham were observed at earlier timepoints and to a much greater degree relative to both the p-HTPs. Some evidence of tissue variability was observed, indicated by differences between Sham and aerosol/smoke-exposed tissues (significant for some p-HTP Regular tissues) at the 0 days timepoint (before any exposures had occurred).

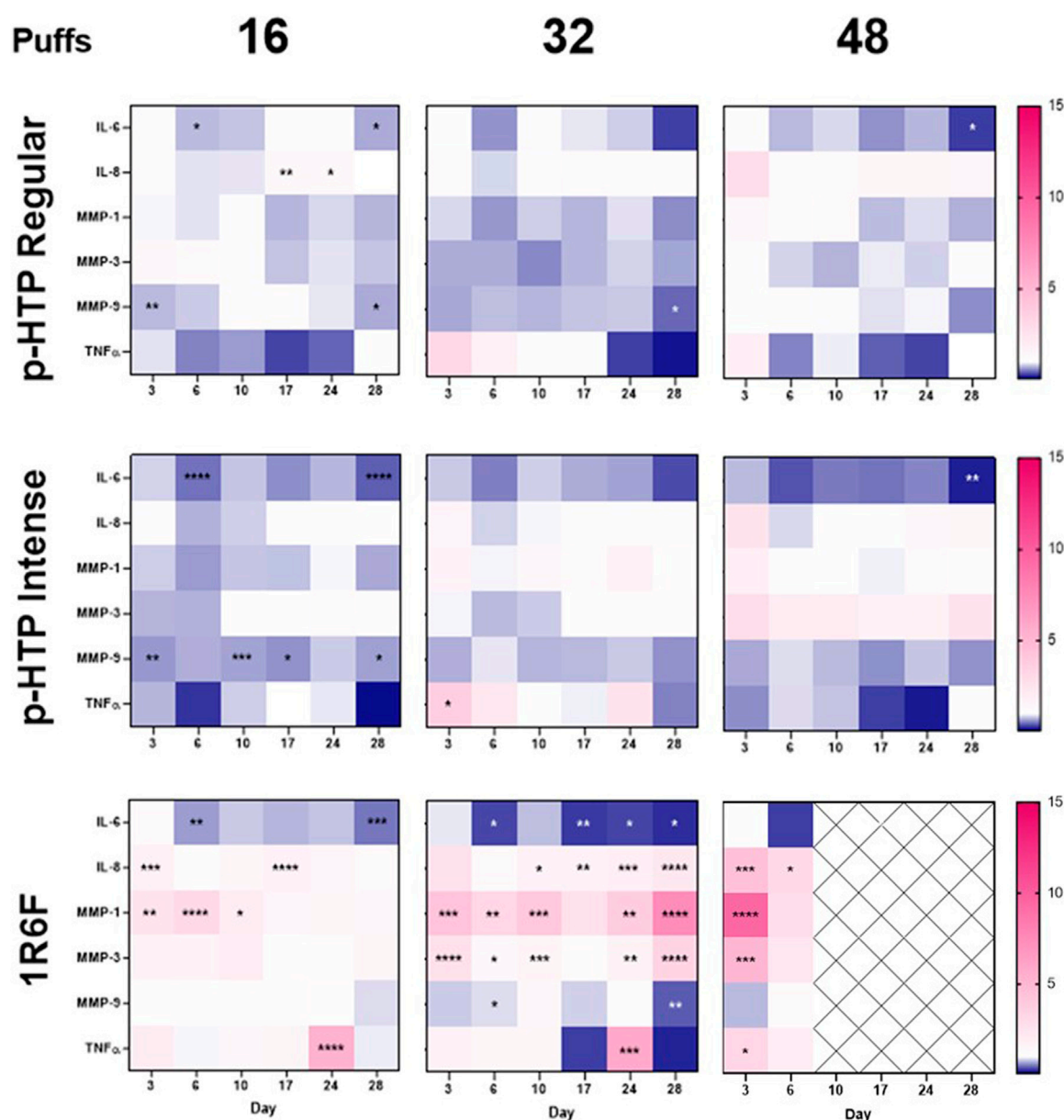


FIGURE 5

Heatmap representation of inflammatory markers in the cell culture medium of models exposed to 16, 32 or 48 puffs of p-HTP Regular or Intense aerosol or 1R6F smoke. Cells were exposed according to the regime detailed in Figure 1 and levels in basal medium samples taken pre-exposure on days 3, 6, 10, 17, 24 and 28 are shown. Data is plotted as fold-change relative to Sham (1-fold); the highest value on the heatmap is set to the highest observed fold-change across the six markers measured (15-fold) and the lowest value is set to the equivalent inverse. Pink indicates an increase in secretion of markers in the medium compared to Sham levels, and blue indicates a decrease; crossed out cells indicate timepoints where significant cytotoxicity was first observed for 1R6F. Statistically significant changes from Sham levels are denoted by asterisks (*): $p \leq 0.05$; $**p \leq 0.005$; $***p \leq 0.001$; $****p \leq 0.0001$ (two-way ANOVA with Dunnett's post-hoc test). Data plots can also be found in the supplementary information (Supplementary Figures S5–S10), along with measurements from samples taken 4 h post-exposure. $n = 3$.

Inflammatory readouts

Measurement of the levels of six inflammatory markers secreted into the basal cell culture medium was carried out; samples were taken either directly before exposure (Figure 5; Supplementary Figures S3–S8) or 4 h post-exposure (Supplementary Figures S6–S9). For IL-6 and TNFα, no signal was detected in the samples post-exposure, and therefore data is not shown. Although there were few significant changes in TNFα levels across the timepoints

measured (p-HTP Intense on day 3, 32 puffs; 1R6F on days 3 (48 puffs) and 24 (16 and 32 puffs)), there were some initially elevated levels on day 3. This response was similar for 1R6F, however, on day 24 there was a large peak in response for 16 and 32 puffs. The IL-6 response measured following one exposure (measured on day 3) to the test articles did not significantly differ to Sham. However, a second exposure led to declines in levels, which was significant for both p-HTPs for 16 puffs only and for 1R6F at 16 and 32 puffs only (Figure 5; Supplementary Figure S3). For the

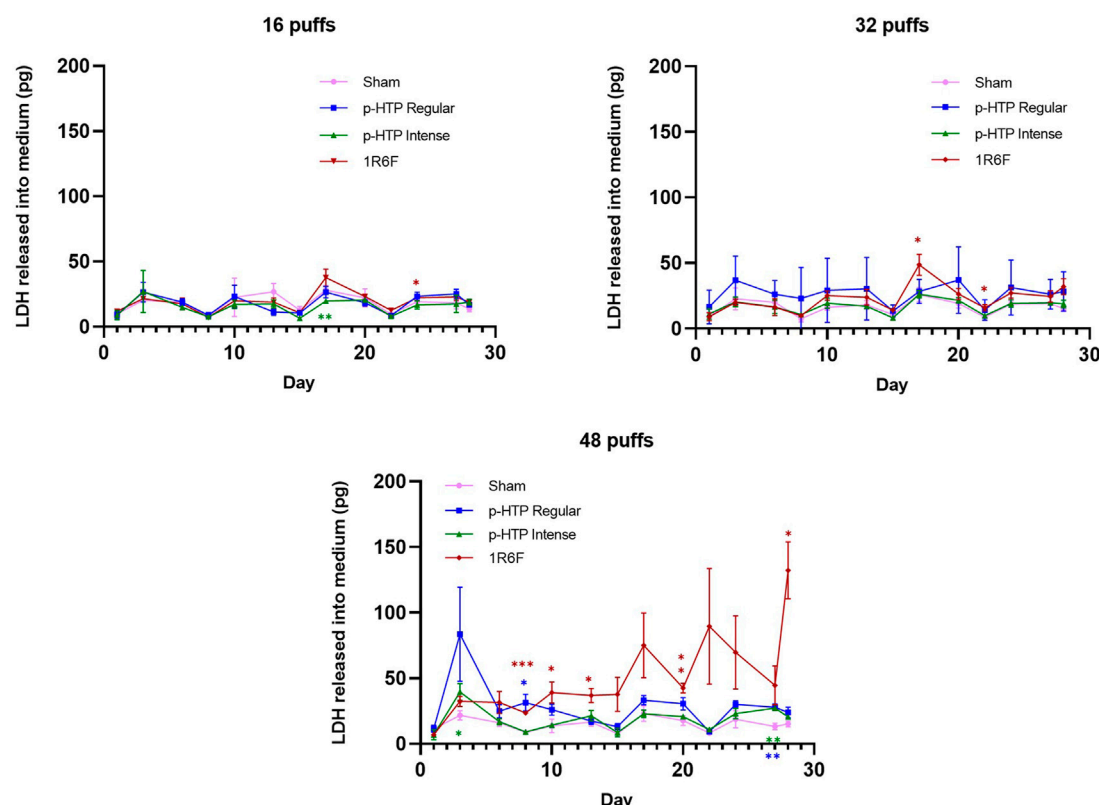


FIGURE 6

LDH released into cell culture medium and mucus from tissues exposed to 16, 32 and 48 puffs of sham (air), p-HTP Regular, p-HTP Intense and 1R6F Reference Cigarette. For each puff level, responses for p-HTP Regular, p-HTP Intense and 1R6F were statistically compared to sham measurements for each day measured (1, 3, 6, 8, 10, 13, 15, 17, 20, 22, 24, 27, 28); * $p \leq 0.05$, ** $p \leq 0.005$, *** $p \leq 0.001$ (two-way ANOVA with Dunnett's post-hoc test). Error bars represent standard deviation; $n = 3$.

p-HTPs, levels of IL-6 did not significantly differ to Sham again until the measurement on day 28, and this was for 16 and 48 puffs only. In slight contrast, significant decreases were observed for 1R6F from day 17 onwards, however, for 48 puffs, on day 28, there was a sharp increase in levels secreted into the medium. The strongest IL-8 responses were induced by exposure to 1R6F smoke in both the pre- and post-exposure samples, with both immediate and sustained elevations in levels secreted. At the second post-exposure timepoint (day 10), there were significant elevations in the levels of IL-8 at all three puff levels for the p-HTPs, however, there were no significant changes relative to Sham in the pre-exposure samples. These responses were reflected in the levels of MMP-1 secreted, in both the pre- and post-exposure samples. For both IL-8 and MMP-1, effects were clearly puff dependent, particularly for 1R6F, which elicited substantially greater responses than the p-HTPs. MMP-3 and MMP-9 responses were generally less pronounced, with little trend in significant deviations from Sham for MMP-9. However, MMP-3 secretion was significantly increased for 1R6F exposures at 32 and 48 puffs in the pre-exposure samples. Post-exposure at the earlier timepoints and higher puffs, there were some significant increases in MMP-3 secretion, however, in contrast, p-HTP Regular induced increasing secretions post-exposure with time at the 32 puffs level only, which was coupled with high variability between replicates. However, as 48 puffs of 1R6F induced significant cytotoxicity from day 10 until the end of the

experimental period (Figure 6), this data was omitted from further interpretation with regards to inflammatory responses, as these responses would likely be associated with cell death rather than progression to disease-representative pathologies (Iskandar et al., 2018).

Discussion

This study was the first to assess the effects of the two p-HTP variants' whole aerosols on the 3D MucilAir model. Furthermore, this study was carried out over an extended (28 days) period, using repeat exposures, and therefore more representative of a realistic adult smoker exposure scenario.

Exposure to p-HTP aerosols resulted in substantially reduced toxicological outcomes compared to 1R6F smoke

The 3D tissues were exposed to 16, 32 or 48 puffs of diluted p-HTP aerosol (1 in 2) or 1R6F smoke (1 in 14) and across the endpoints assessed, both p-HTP variants were substantially less toxic than 1R6F. Upon assessment of LDH secretion into both the basal cell culture medium and mucus across the experimental period, at 16 and 32 puffs,

the LDH levels released by tissues exposed to the p-HTPs did not significantly differ when compared to Sham across the timepoints measured. There was increased variability in tissue responses to p-HTP Regular exposures (particularly for 32 puffs), which was also observed across the experimental endpoints assessed within this study, and therefore may be due to comparatively increased sensitivity of certain tissues. Tissues repeatedly exposed to 48 puffs of 1R6F smoke demonstrated the greatest increase in LDH secretion, which generally increased with time, and furthermore, the dilution level of smoke was one in 14, much greater than for the p-HTP aerosols (1 in 2). With the exception of the high cytotoxicity induced by 1R6F at 48 puffs from day 10 onwards, exposures delivered were generally sub-cytotoxic and therefore responses observed in the subsequent endpoints assessed were deemed to be related to processes potentially leading to disease pathologies rather than cell death.

Upon histological analysis of the tissues, slight declines in staining were observed with increasing puffs for the Sham treatment, which mirrors the secretion of LDH by the Sham tissues over the experimental period (Figure 6). However, as tissues were fixed for histological analysis at the end of the experimental period, they may have undergone some effects from mechanical stress of puffing with air over a long-term period. Declines in function in both incubator and air control MucilAir tissues following an extended experimental period were also observed by Haswell et al. (2021) and following a single non-cytotoxic exposure (Phillips et al., 2021). It must be acknowledged that these models cannot fully replicate a human *in vivo* scenario, where interplay of other cell types, in addition to being part of a whole tissue, as well as mechanical stimulation *in situ*, may have an effect on cellular and tissue maintenance.

However, upon comparison of Sham tissues to both the p-HTP aerosols and 1R6F smoke, there were clear differences between the responses observed. 1R6F induced increasing declines in normal tissue morphology (Alcian Blue/H&E staining) and the greatest loss of goblet (Muc5AC staining) and ciliated (Fox-J1 staining) cells with increasing numbers of puffs. Changes followed a similar trend for the p-HTPs, but these were more subtle and more closely resembled Sham responses. Some measures were relatively elevated for certain staining endpoints for p-HTP Regular (16 puffs, Alcian Blue/H&E and Muc5AC), which may be attributed to tissue variability, as observed across the other study assays for this product variant. However, p-HTP Intense generally demonstrated the higher potency of the two variants in the histological analyses (discussed further in 'Nicotine dosimetry and translation to exposure to other chemicals' section). In the study conducted by Haswell et al. (2021), sub-cytotoxic, and much higher dilutions, of 1R6F smoke (but not HTP aerosol) induced goblet cell hyperplasia within a 6 weeks experimental period. Although the current study did not cover as long a time period, and applied higher exposures of smoke, we only observed some decline in goblet cells. This indicates that both exposure dose and duration are potentially important factors in the experimental design.

Changes in CAA and CBF are recognised indicators of airway epithelial dysfunction (Gindele et al., 2020; Luettich et al., 2021); Luettich et al. (2021) recently described their role in the AOP to decreased lung functionality upon exposure to inhaled toxicants. In this study, CBF and CAA were recorded at timepoints across the 28 day period to understand changes in functionality in response to the repeat exposure regimens. Across the experimental timepoints

(particularly at the lower puffs levels for the p-HTPs) variation in the levels of change compared to Sham were observed. This could be due to some capacity of cells/tissues to recover between exposures. However, pronounced declines in CAA were followed by those in CBF and the effects on the presence and functionality of cilia correspond to the histological outcomes. Overall, it was clear that the effects of 1R6F smoke (diluted to a higher level) were substantially greater, and generally occurred earlier, than those of the p-HTPs. Generally greater effects of combustible cigarette smoke, compared to other test articles, in repeated exposure studies with such models have also been previously observed (Czekala et al., 2021; Haswell et al., 2021).

Inflammation is another key process in airway damage and dysfunction and the associations of inflammatory mediators with exposure to combustible cigarette smoke have been extensively mapped (Aghapour et al., 2018). Many *in vitro* studies into NGP aerosol/cigarette smoke exposures have included inflammatory cytokine panels as an indicator of cellular/tissue responses to exposure (Iskandar et al., 2019; Czekala et al., 2021; Phillips et al., 2021). Here, we selected six markers associated with combustible cigarette smoking to assess how responses compared between the p-HTP aerosols and 1R6F smoke. As observed with CAA/CBF, across the experimental period, there was some variation in levels of responses compared to Sham dependent on the timepoint, which again, could be due to some adaptive responses of the tissues. Across all of the selected markers, 1R6F induced the strongest and most sustained responses, which were substantially greater than those to the p-HTPs. Due to the significant and increasing cytotoxicity from day 10 onwards for 48 puffs of diluted 1R6F smoke, the readouts were regarded to be due to pathways related to cellular death rather than to a disease pathological state, as described by Iskandar et al. (2018).

The six inflammatory markers assessed within this study have all demonstrated associations with exposure to cigarette smoke, and particularly associated with disease pathologies including the chronic inflammatory condition, COPD (Zhang et al., 2011; Tanaka et al., 2014; Ostridge et al., 2016; Kraen et al., 2019; Huang et al., 2021). Four hours following the exposures, across the experimental days, IL-6 and TNF α were not consistently detectable in the medium for any of the treatments (including Sham), which may be due to the sensitivity of the method coupled with low, if any, secretion by that sampling timepoint. Therefore, data is not shown. IL-6 secretion was generally suppressed compared to Sham following exposures to all three test articles, however, this effect was generally not significant for the p-HTPs (with the exception of 16 puffs on day 6 and 16 and 48 puffs on day 28). Pathways involving c-jun and NF κ B have an association with IL-6 suppression (Tanaka et al., 2014), and in the previous study by Chapman et al. (2023), both the p-HTP Regular product and 1R6F induced significant (dose dependent) increases in c-jun and NF κ B activity, albeit to different degrees (and in a single human bronchial cell type model and measured at two timepoints only). Iskandar et al. (2018) also observed decreases in IL-6 upon single exposure of tissues to 1R6F, however, not following exposure to HTP aerosol. The increase in IL-6 secretion at day 28 for cells exposed to 1R6F may be the artefact of high cell death by this timepoint for this exposure.

Following an initial non-significant increase in IL-8, particularly at 48 puffs, for the p-HTPs, limited changes in the pre-exposure collected medium suggested that there was limited to no sustained response over the experimental period. However, for 1R6F, IL-8 levels remained

significantly elevated across the experimental period for 48 puffs, with a sharp increase in secretion between days 10 and 24, followed by a decline, correlating with the observed cytotoxicity for this treatment. Tissues exposed to 32 puffs of 1R6F exhibited consistently significantly elevated levels of IL-8 secretion present in the pre-exposure medium samples, however to a lesser degree than observed with the cytotoxic 48 puffs. This trend was also observed, but again to a slightly lesser extent, for 16 puffs of 1R6F. For the p-HTPs, secretions measured 4 h post-exposure indicated some initial responses to exposure up to day 10, however, for the two timepoints measured following this (days 17 and 24), there were no significant changes, potentially indicating an adaptive response of the tissues. In contrast, exposures to all puff levels of 1R6F smoke induced secretion of IL-8 following exposure. Interestingly, although IL-8 (and TNF α) has been implicated in the post-transcriptional regulation of MUC5AC gene expression (Bautista et al., 2009), we observed puff-dependent declines in MUC5AC staining across all treatments.

Upon assessment of MMP-9, despite some significant changes compared to Sham, there was no clear trend in responses, which were weak compared to those seen for the other two MMPs, particularly in response to 1R6F exposure. For the p-HTPs, there were few and small significant changes compared to Sham for MMP-3, with the exception of at day 24 for 16 puffs, 4 h post-exposure for p-HTP Regular. However, this was coupled with high variability, as seen in the other endpoints for this set of tissues, and therefore it is unclear how reliable this particular response is. Despite some apparent adaption of tissues to exposure to 1R6F at day 17, and increase in MMP-3 was observed at the later timepoints, again correlating with the cytotoxicity/cell loss observed towards the end of the experimental period. On day 10, in the medium sampling following exposure to the p-HTPs, the tissues demonstrated significant increases in MMP-1 secretion at all three puff levels; however, as observed with the other inflammatory markers, this was followed by subsequent apparent adaption of the tissues to this treatment. In contrast, 1R6F elicited significant increases in secretion of MMP-1 from the first measurement of the experimental period, and these responses to 1R6F were particularly sustained and apparent throughout the experimental period. MMPs have a number of roles within the inflammatory response, for example in regulation of cytokines and chemokines and in tissue remodelling (Czekala et al., 2021), however, their activity and exact roles in the human lung is complex (Churg et al., 2012). A lower MMP-9 response in such tissues compared to MMP-1 and MMP-3 to combustible cigarette exposure was also observed by Czekala et al. (2021).

Although broadly non-significant, TNF α levels were variable compared to Sham, and were particularly elevated at the first measured timepoint (day 3), potentially due to an initial stress response. However, lower levels of TNF α are involved in various cellular/tissue processes under homeostatic conditions (Mukhopadhyay et al., 2006), and therefore the lowered TNF α levels observed here may correlate with the adaptive responses observed in tissues, particularly those exposed to the p-HTPs. At day 24, there was a peak in TNF α secretion for 16 and 32 puffs of 1R6F, which may signal a heightened stress response in the tissues following cumulative exposures. However as TNF α is known to be involved in many cellular processes, including driving inflammatory responses and also apoptosis (Mukhopadhyay et al., 2006; Malaviya et al., 2017), the readouts here require further investigation, as is true for all the markers assessed. Furthermore, inflammatory responses are complex and involve the interaction of many molecules and pathways,

therefore further resolution on the effects of the test articles on these would be the focus of future studies, for example through transcriptomics analyses.

Overall, the *in vitro* assessment findings support the observations in other studies with 3D models exposed to combustible cigarette smoke and HTP aerosols, that effects are substantially greater upon exposure to cigarette at lower concentrations (Iskandar et al., 2017; Iskandar et al., 2018; Haswell et al., 2021). However, further studies are required on the effects of HTPs following repeated exposures to substantiate the observations from this study.

Whole aerosol/smoke repeated exposures to 3D human cell models increase human relevance of the outcomes

This study utilised the MucilAir 3D reconstituted human bronchial epithelial cell model, an established and robust model which has been utilised in a number of inhalation toxicological assessments (Huang et al., 2013; Frieke Kuper et al., 2015; Bedford et al., 2022). The use of human-derived cells increases the relevance of the outputs to consumers and can more closely represent human-specific molecular pathways and responses (Krewski et al., 2010; Adeleye et al., 2015). Furthermore, the repeated exposure element of the study more accurately models likely human exposure patterns than a single, acute, *in vitro* exposure (Mallock et al., 2019; Jones et al., 2020; Laverty et al., 2021). Interestingly, lower or absent responses in 3D respiratory tissue models exposed to heated tobacco aerosol, compared to cigarette smoke, in the short term (e.g., up to 72 h), following an acute exposure (Iskandar et al., 2018; Mori et al., 2021) was a relative response observed to be maintained over the 28 days of the current study. The findings of the current study therefore indicate reduced harm potential of the p-HTPs over the longer period tested. However, the 28 days exposures applied within this study still provide valuable insight into outcomes upon repeated exposures over a prolonged period for both the p-HTPs and cigarette.

In combination with this, whole aerosol/smoke exposures were achieved using the SAEIVS, which enables a number of human-relevant conditions to be met during exposure. Firstly, the whole aerosol/smoke exposures allow the delivery of all chemical fractions generated upon heating/combustion (respectively) of the products, including particulate and gas/vapour phases; delivery of a combination of these fractions is often challenging in *in vitro* systems, for example, in submerged cell cultures, as evaluated previously (Smart and Phillips, 2021). In addition to the delivery of all chemical fractions, the SAEIVS ensures exposures of cells to aerosol/smoke within 10 s of generation, preventing ageing effects. These, in combination, ensure that cells are exposed to as consumer-relevant chemical mixture as possible. Further to this, humidity within the SAEIVS is maintained at 70%–80%, to prevent tissue drying effects throughout the exposures. A vacuum pump also acts to remove aerosol/smoke from the exposure chambers following each puff, mimicking exhalation of some chemicals.

Nicotine dosimetry and translation to exposure to other chemicals

Nicotine is often used as a marker of aerosol/smoke exposure *in vitro* as it is considered to be a reliable dosimetry measure

(Adamson et al., 2016; Behrsing et al., 2018). In this study, nicotine dosimetry using the levels trapped within the basal medium was carried out to gain an understanding of relative exposures to the tissues. During exposure, gaps present at the sides of the culture inserts for gaseous exchange in the basal medium of the system enable delivery to and trapping of the aerosol/smoke constituents in this compartment. Although this does not model deposition on the tissue surface, it does provide an indication of relative exposures and has previously been used as a dosimetry method in similar 3D culture exposure set-ups (Haswell et al., 2017).

Although exposures were matched on a puff basis, matching delivered nicotine levels across all exposure levels was not possible in combination with this due to the high cytotoxicity potential of 1R6F smoke at lower dilutions. However, average nicotine levels delivered by 16 puffs of the p-HTP Regular product did match those delivered by 48 puffs of 1R6F, allowing some comparison of effects upon a nicotine basis. Overall, it is clear that 1R6F smoke induced substantially greater toxicological effects compared to the p-HTPs, across a comparable nicotine delivery range. Although adult smokers smoke for nicotine amongst other reasons, tobacco combustion generates more than 7,000 chemicals (US Department of Health and Human Services, 2014), to which the consumer is exposed. A number of studies have demonstrated, however, that aerosols generated from HTPs are less complex and contain fewer and substantially lower levels of toxicants compared to combustible cigarette smoke, attributed to the heating, as opposed to burning of tobacco (Jaccard et al., 2017; Forster et al., 2018; Malt et al., 2022). A recent study by Chapman et al. (2023) characterised the aerosols generated by two p-HTPs, one of which was used in this study (p-HTP Regular) and reported substantial reductions in the levels and numbers of toxicants present in the aerosol compared to 1R6F smoke. On a per puff basis, nicotine delivery was around half that for the p-HTPs compared to 1R6F, however, on a nicotine equivalent basis, substantial reductions in *in vitro* toxicological outcomes were observed upon exposure of cells to the p-HTP aerosols. To maximise adult smoker satisfaction, the p-HTP Intense variant used in this study was designed to deliver increased aerosol, and therefore nicotine per puff, and indeed greater levels of nicotine were measured in the basal medium following exposures. In the case that correspondingly increased toxicant levels were delivered to the tissues, in line with the HT product category, these levels are still expected to be substantially reduced compared to (1R6F) combustible cigarette smoke. Indeed, toxicological responses observed were similar between the two p-HTP variants used in this study, supporting the growing evidence for the THR potential of this category (Committee On Toxicity, 2017; Mallock et al., 2018; McNeill et al., 2018; RIVM, 2018; SHC, 2020). *In vitro* analyses with more mechanistic resolution, for example, transcriptomics approaches, may provide more resolution between toxicological responses to individual variants within the same product category, and will be the subject of future studies.

Although aerosol/smoke deposition on the tissue surfaces was not measured, it would be informative to gain an understanding of aerosol/smoke deposition and therefore apical exposures to the tissues. Additionally, this information, in combination aerosol particle size data, could be inserted into lung deposition models to predict human relevant exposure scenarios. This will also be addressed in future studies. Furthermore, the basal nicotine concentrations measured within this study were markedly higher than physiological blood plasma nicotine levels in smokers or heated tobacco product users (10–50 ng/mL, Benowitz et al., 2009;

Phillips-Waller et al., 2021). Whilst not at physiological levels, the quantification of nicotine was useful in providing an indication of relative exposures to the cultures according to the different exposure levels/products.

The role of NGPs in THR

This study has demonstrated that the human 3D bronchial epithelial cell models exhibit substantially reduced toxicological responses following exposure to the p-HTP aerosols compared to 1R6F reference cigarette smoke. This is consistent with the current scientific evidence base underpinning the HTP category and reflects the previously described substantial reductions in the levels and numbers of toxicants present in the aerosols of p-HTPs compared to 1R6F smoke correlating with reduced toxicological outcomes observed across a range of *in vitro* models (Chapman et al., 2023). As may be expected, although the p-HTPs do not exhibit the same level of reduction in toxicological responses as typically observed with ENDS (Czekala et al., 2021), the data in this manuscript does support the proposed placement of nicotine delivery products across a relative risk scale (Abrams et al., 2018; Murkett et al., 2020). However, HTPs, as demonstrated in this study, still offer substantially reduced harm nicotine delivery compared to combustible cigarette smoking (Committee On Toxicity, 2017). Further to this, for NGPs to reach their full THR potential, they must offer adult smokers an acceptable form of nicotine delivery, which includes sensory satisfaction, which HTPs may provide to adult smokers as a closer experience to cigarette smoking (Roulet et al., 2019; Haziza et al., 2020).

Limitations of the study and future directions

This study provides valuable information on the effects of repeated exposures, over a prolonged period of 28 days, to p-HTP aerosols in the MucilAir bronchial cell model compared to combustible cigarette smoke. The study does have a number of limitations which must be acknowledged, and the data viewed within this context. Some variability between tissues was observed, particularly for the subset of models used for the p-HTP Regular exposures, which may remove some resolution of the subtle differences in effects of the two product variants. Whilst technical replication was carried out to mediate such biological variability, and tissues underwent quality control measures prior to the start of experimentation (transepithelial electrical resistance (TEER) measurement/visual (microscopic) inspection), the study was conducted using models derived from one donor, and therefore does not account for donor variability. This is an important consideration as, for example, in the study by Czekala et al. (2021), tissues were exposed to greater numbers of reference cigarette puffs, which although diluted slightly more than in the current study (1:17 vs 1:14 respectively), tissues appeared more sensitive to combustible cigarette smoke in the present study, and puffs were limited to 48 to prevent excessive cytotoxicity. However, it is difficult to fully model consumer variability *in vitro*, and the recent findings of Bowers et al. (2021) indicate that 13–299 donors would be required to provide information on various inflammatory readouts. Additionally, the current study was carried out on models derived from human bronchial cells, however, this does not model other regions of the respiratory tract, for example the alveoli, and does

indicate the interaction with other cell types present *in vivo*, including fibroblasts, endothelium and immune cells. Assessment of the effects of the test products in models including alveolar tissues and those in the presence of immune cells will be the focus of future work.

To further expand upon the mechanistic insights into the effects of the test products, it would also be beneficial to expand upon the endpoints assessed in the current study to include analyses at the transcriptomic level, to identify further pathways involved in the responses, and gain information on important processes to screen for in future *in vitro* assessments. For example, the 3D models demonstrate metabolic capability (Huang et al., 2013; Cervenka et al., 2019) and whilst no measurements of this activity were taken in the current study, it would be interesting to gain some insight into metabolic activity and upregulation upon exposure to the respective test articles. From this capacity of the tissues, however, it could be assumed that exposure outcomes within the current study may have involved the effects of the metabolism pro-toxicants, and warrants further investigation.

The experimental design would also benefit, in future studies of this type, from switching/dual exposure arms. These are two important use scenarios to model *in vitro*, and would further increase the consumer relevance of such studies: NGPs offer adult smokers an alternative, reduced harm form of nicotine delivery to adult smokers, therefore switching from cigarette use to NGP use could be modelled by a period of exposure to combustible cigarette smoke followed by a period of exposure to NGP. Switching is often accompanied by a period of dual use of combustible cigarettes and NGPs (Farsalinos et al., 2015; Adriaens et al., 2017; Sutanto et al., 2020), therefore, an *in vitro* model of this may also be informative. However, how *in vitro* responses translate to *in vivo* effects still remains to be elucidated.

Finally, in future studies it would be beneficial to extend endpoints to add to the weight of evidence with regards to the outcomes. For example, transepithelial electrical resistance (TEER) measurement can provide an additional measure for barrier integrity and will be incorporated as an endpoint in future studies of this kind.

Conclusion

This study has demonstrated that the effects of repeated exposures of 3D human reconstituted bronchial cell models *in vitro*, over an extended 28 day period, to p-HTP variant aerosols are substantially reduced compared to the effects of 1R6F combustible reference cigarette smoke. This is in line with the findings of previous *in vitro* studies on both the p-HTPs and HTP category, and supports a growing weight of evidence for the tobacco harm reduction potential of such products,

through offering a potentially less harmful form of nicotine delivery to adult smokers. The combination of the human MucilAir models, whole aerosol/smoke exposures and an extended, repeated exposure regime additionally increases the human, and therefore consumer, relevance of the outcomes observed.

Data availability statement

The original contributions presented in the study are included in the article/supplementary material, further inquiries can be directed to the corresponding author.

Author contributions

FC, SP, RW, ES, LS, and MS contributed to the conception and the design of the study. SP, RW, ES, JB, KR, and SO carried out the laboratory testing. FC, SP, RW, ES, and JB carried out the statistical analyses. FC wrote the first draft of the manuscript. All authors contributed to manuscript draft review and revision and approved the final version.

Conflict of interest

Authors FC, EM, LC, GO'C, LS and MS were employed by the company Imperial Brands PLC. Authors SP, RW, ES, JB, KR, SO and TN were employed by the company Reemtsma Cigarettenfabriken GmbH, a subsidiary of Imperial Brands PLC.

Publisher's note

All claims expressed in this article are solely those of the authors and do not necessarily represent those of their affiliated organizations, or those of the publisher, the editors and the reviewers. Any product that may be evaluated in this article, or claim that may be made by its manufacturer, is not guaranteed or endorsed by the publisher.

Supplementary material

The Supplementary Material for this article can be found online at: <https://www.frontiersin.org/articles/10.3389/ftox.2023.1076752/full#supplementary-material>

References

- Abrams, D. B., Glasser, A. M., Pearson, J. L., Villanti, A. C., Collins, L. K., and Niaura, R. S. (2018). Harm minimization and tobacco control: Reframing societal views of nicotine use to rapidly save lives. *Annu. Rev. Public Health* 39, 193–213. doi:10.1146/annurev-publhealth-040617-013849
- Adamson, J., Azzopardi, D., Errington, G., Dickens, C., McAughey, J., and Gaca, M. D. (2016). Assessment of an *in vitro* whole cigarette smoke exposure system: The Borgwaldt RM20S 8-syringe smoking machine. *Chem. Central J.* 10, 50. doi:10.1186/1752-153X-5-50
- Adeleye, Y., Andersen, M., Clewell, R., Davies, M., Dent, M., Edwards, S., et al. (2015). Implementing Toxicity Testing in the 21st Century (TT21C): Making safety decisions using toxicity pathways, and progress in a prototype risk assessment. *Toxicology* 332, 102–111. doi:10.1016/j.tox.2014.02.007
- Adriaens, K., Van Gucht, D., and Baeyens, F. (2017). Differences between dual users and switchers center around vaping behavior and its experiences rather than beliefs and attitudes. *Int. J. Environ. Res. public health* 15 (1), 12. doi:10.3390/ijerph15010012
- Aghapour, M., Raei, P., Moghaddam, S. J., Hiemstra, P. S., and Heijink, I. H. (2018). Airway epithelial barrier dysfunction in chronic obstructive pulmonary disease: Role of cigarette smoke exposure. *Am. J. Respir. Cell Mol. Biol.* 58 (2), 157–169. doi:10.1165/rcmb.2017-0200TR
- Bautista, M. V., Chen, Y., Ivanova, V. S., Rahimi, M. K., Watson, A. M., and Rose, M. C. (2009). IL-8 regulates mucin gene expression at the posttranscriptional level in lung epithelial cells. *J. Immunol.* 183 (3), 2159–2166. doi:10.4049/jimmunol.0803022

- Bedford, R., Perkins, E., Clements, J., and Hollings, M. (2022). Recent advancements and application of *in vitro* models for predicting inhalation toxicity in humans. *Toxicol. Vitro* 79, 105299. doi:10.1016/j.tiv.2021.105299
- Behrsing, H., Raabe, H., Manuppello, J., Bombick, B., Curren, R., Sullivan, K., et al. (2016). Assessment of *in vitro* COPD models for tobacco regulatory science: Workshop proceedings, conclusions and paths forward for *in vitro* model use. *Altern. Lab. Anim.* 44 (2), 129–166. doi:10.1177/026119291604400206
- Behrsing, H., Aragon, M., Adamson, J., Sheehan, D., Gaca, M., Curren, R., et al. (2018). Characterization of a vitroculture VCI using nicotine dosimetry: An essential component toward standardized *in vitro* aerosol exposure of tobacco and next generation nicotine delivery products. *Appl. Vitro Toxicol.* 4 (2), 159–166. doi:10.1089/aivt.2018.0001
- Bekki, K., Inaba, Y., Uchiyama, S., and Kunugita, N. (2017). Comparison of chemicals in mainstream smoke in heat-not-burn tobacco and combustion cigarettes. *J. Uoeh.* 39 (3), 201–207. doi:10.7888/juoe.39.201
- Benowitz, N., Hukkanen, J., and Jacob, P. (2009). Nicotine chemistry, metabolism, kinetics and biomarkers. *Handb. Exp. Pharmacol.* (192), 29–60. doi:10.1007/978-3-540-69248-5_2
- Bentley, M. C., Almstetter, M., Arndt, D., Knorr, A., Martin, E., Pospisil, P., et al. (2020). Comprehensive chemical characterization of the aerosol generated by a heated tobacco product by untargeted screening. *Anal. Bioanal. Chem.* 412 (11), 2675–2685. doi:10.1007/s00216-020-02502-1
- Bowers, E. C., Martin, E. M., Jarabek, A. M., Morgan, D. S., Smith, H. J., Dailey, L. A., et al. (2021). Ozone responsive gene expression as a model for describing repeat exposure response trajectories and interindividual toxicodynamic variability *in vitro*. *Toxicol. Sci.* 185 (1), 38–49. doi:10.1093/toxsci/kfab128
- Cervena, T., Vrbova, K., Rossnerova, A., Topinka, J., and Rossner, P. (2019). Short-term and long-term exposure of the MucilAir™ model to polycyclic aromatic hydrocarbons. *Altern. Lab. Animals* 47 (1), 9–18. doi:10.1177/0261192919841484
- Chapman, K. E., Doak, S. H., and Jenkins, G. J. S. (2015). Acute dosing and p53-deficiency promote cellular sensitivity to DNA methylating agents. *Toxicol. Sci.* 144 (2), 357–365. doi:10.1093/toxsci/kfv004
- Chapman, F., Sticken, E. T., Wiczorek, R., Pour, S. J., Dethloff, O., Budde, J., et al. (2023). Multiple endpoint *in vitro* toxicity assessment of a prototype heated tobacco product indicates substantially reduced effects compared to those of combustible cigarette. *Toxicol. Vitro* 86, 105510. doi:10.1016/j.tiv.2022.105510
- Churg, A., Zhou, S., and Wright, J. L. (2012). Series "matrix metalloproteinases in lung health and disease": Matrix metalloproteinases in COPD. *Eur. Respir. J.* 39 (1), 197–209. doi:10.1183/09031936.00121611
- Committee On Toxicity (2017). *Statement on the toxicological evaluation of novel heat not-burn tobacco products*. Available at: https://cot.food.gov.uk/sites/default/files/heat_not_burn_tobacco_statement.pdf (Last assessed 03 03, 2022).
- Crosswhite, M. R., Bailey, P. C., Jeong, L. N., Lioubimirov, A., Yang, C., Ozvald, A., et al. (2021). Non-targeted chemical characterization of JUUL Virginia tobacco flavored aerosols using liquid and gas chromatography. *Separations* 8 (9), 130. doi:10.3390/separations8090130
- Czekala, L., Simms, L., Stevenson, M., Tschierske, N., Maione, A. G., and Walele, T. (2019). Toxicological comparison of cigarette smoke and e-cigarette aerosol using a 3D *in vitro* human respiratory model. *Regul. Toxicol. Pharmacol.* 103, 314–324. doi:10.1016/j.yrtph.2019.01.036
- Czekala, L., Wiczorek, R., Simms, L., Yu, F., Budde, J., Trelles Sticken, E., et al. (2021). Multi-endpoint analysis of human 3D airway epithelium following repeated exposure to whole electronic vapor product aerosol or cigarette smoke. *Curr. Res. Toxicol.* 2, 99–115. doi:10.1016/j.crt.2021.02.004
- Epithelix Sàrl (2022). *MUCILAIR™: IN vitro 3D human upper airway epithelium*. Available at: <https://www.epithelix.com/products/mucilair> (Last accessed March 3rd, 2022).
- Farsalinos, K. E., Romagna, G., and Voudris, V. (2015). Factors associated with dual use of tobacco and electronic cigarettes: A case control study. *Int. J. Drug Policy* 26 (6), 595–600. doi:10.1016/j.drugpo.2015.01.006
- Forster, M., Fiebelkorn, S., Yurteri, C., Mariner, D., Liu, C., Wright, C., et al. (2018). Assessment of novel tobacco heating product THP1.0. Part 3: Comprehensive chemical characterisation of harmful and potentially harmful aerosol emissions. *Regul. Toxicol. Pharmacol.* 93, 14–33. doi:10.1016/j.yrtph.2017.10.006
- Frieke Kuper, C., Grollers-Mulderij, M., Maarschalkerweerd, T., Meulendijks, N. M. M., Reus, A., van Acker, F., et al. (2015). Toxicity assessment of aggregated/agglomerated cerium oxide nanoparticles in an *in vitro* 3D airway model: the influence of mucociliary clearance. *Toxicol. Vitro* 29 (2), 389–397. doi:10.1016/j.tiv.2014.10.017
- Gee, J., Prasad, K., Slayford, S., Gray, A., Nother, K., Cunningham, A., et al. (2018). Assessment of tobacco heating product THP1.0. Part 8: Study to determine puffing topography, mouth level exposure and consumption among Japanese users. *Regul. Toxicol. Pharmacol.* 93, 84–91. doi:10.1016/j.yrtph.2017.08.005
- Ghosh, B., Reyes-Caballero, H., Akgun-Olmez, S. G., Nishida, K., Chandrala, L., Smirnova, L., et al. (2020). Effect of sub-chronic exposure to cigarette smoke, electronic cigarette and waterpipe on human lung epithelial barrier function. *BMC Pulm. Med.* 20 (1), 216. doi:10.1186/s12890-020-01255-y
- Gindele, J. A., Kiechle, T., Benediktus, K., Birk, G., Brendel, M., Heinemann, F., et al. (2020). Intermittent exposure to whole cigarette smoke alters the differentiation of primary small airway epithelial cells in the air-liquid interface culture. *Sci. Rep.* 10 (1), 6257. doi:10.1038/s41598-020-63345-5
- Giralt, A., Iskandar, A. R., Martin, F., Moschini, E., Serchi, T., Kondylis, A., et al. (2021). Comparison of the biological impact of aerosol of e-vapor device with MESH® technology and cigarette smoke on human bronchial and alveolar cultures. *Toxicol. Lett.* 337, 98–110. doi:10.1016/j.toxlet.2020.11.006
- Haswell, L. E., Baxter, A., Banerjee, A., Verrastro, I., Mushongano, J., Adamson, J., et al. (2017). Reduced biological effect of e-cigarette aerosol compared to cigarette smoke evaluated *in vitro* using normalized nicotine dose and RNA-seq-based toxicogenomics. *Sci. Rep.* 7 (1), 888. doi:10.1038/s41598-017-00852-y
- Haswell, L. E., Smart, D., Jaunky, T., Baxter, A., Santopietro, S., Meredith, S., et al. (2021). The development of an *in vitro* 3D model of goblet cell hyperplasia using MUC5AC expression and repeated whole aerosol exposures. *Toxicol. Lett.* 347, 45–57. doi:10.1016/j.toxlet.2021.04.012
- Hattori, N., Nakagawa, T., Yoneda, M., Nakagawa, K., Hayashida, H., and Ito, T. (2020). Cigarette smoke, but not novel tobacco vapor products, causes epigenetic disruption and cell apoptosis. *Biochem. Biophys. Res. Commun.* 24, 100865. doi:10.1016/j.bbrc.2020.100865
- Haziza, C., de La Bourdonnaye, G., Donelli, A., Poux, V., Skiada, D., Weitkunat, R., et al. (2020). Reduction in exposure to selected harmful and potentially harmful constituents approaching those observed upon smoking abstinence in smokers switching to the menthol tobacco heating system 2.2 for 3 Months (Part 1). *Nicotine Tob. Res.* 22 (4), 539–548. doi:10.1093/ntr/ntz013
- Huang, S., Wiszniewski, L., Constant, S., and Roggen, E. (2013). Potential of *in vitro* reconstituted 3D human airway epithelia (MucilAir™) to assess respiratory sensitizers. *Toxicol. Vitro* 27 (3), 1151–1156. doi:10.1016/j.tiv.2012.10.010
- International Agency for Research on Cancer (2012). *Personal habits and indoor combustions. A review of human carcinogens: IARC monographs on the evaluation of carcinogenic risks to humans*, Vol. 100E. Available at: <https://monographs.iarc.fr/wp-content/uploads/2018/06/mono100E.pdf> (Last accessed 02 13, 2021).
- Iskandar, A. R., Mathis, C., Martin, F., Leroy, P., Sewer, A., Majeed, S., et al. (2017). 3-D nasal cultures: Systems toxicological assessment of a candidate modified-risk tobacco product. *Altox* 34 (1), 23–48. doi:10.14573/altox.1605041
- Iskandar, A., Martin, F., Leroy, P., Schlage, W., Mathis, C., Titz, B., et al. (2018). Comparative biological impacts of an aerosol from carbon-heated tobacco and smoke from cigarettes on human respiratory epithelial cultures: A systems toxicology assessment. *Food Chem. Toxicol.* 115, 109–126. doi:10.1016/j.fct.2018.02.063
- ISO (2018). ISO 20778:2018 - cigarettes - Routine analytical cigarette smoking machine - definitions and standard conditions with an intense smoking regime. ICS 65, 65–160. Available at: <https://www.iso.org/standard/69065.html>.
- Jaccard, G., Tabin Djoko, D., Moennikes, O., Jeannet, C., Kondylis, A., and Belushkin M. (2017). Comparative assessment of HPHC yields in the Tobacco Heating System THS2.2 and commercial cigarettes. *Regul. Toxicol. Pharmacol.* 90, 1–8. doi:10.1016/j.yrtph.2017.08.006
- Jaunky, T., Adamson, J., Santopietro, S., Terry, A., Thorne, D., Breheny, D., et al. (2018). Assessment of tobacco heating product THP1.0. Part 5: *In vitro* dosimetric and cytotoxic assessment. *Regul. Toxicol. Pharmacol.* 93, 52–61. doi:10.1016/j.yrtph.2017.09.016
- Jones, J., Slayford, S., Gray, A., Brick, K., Prasad, K., and Proctor, C. (2020). A cross-category puffing topography, mouth level exposure and consumption study among Italian users of tobacco and nicotine products. *Sci. Rep.* 10 (1), 12. doi:10.1038/s41598-019-55410-5
- Kraen, M., Frantz, S., Nihlen, U., EnGstrom, G., Lofdahl, C. G., Wollmer, P., et al. (2019). Matrix Metalloproteinases in COPD and atherosclerosis with emphasis on the effects of smoking. *PLoS One* 14 (2), e0211987. doi:10.1371/journal.pone.0211987
- Krewski, D., Acosta, D., Andersen, M., Anderson, H., Bailar, J. C., Boekelheide, K., et al. (2010). Toxicity testing in the 21st century: a vision and a strategy. *J. Toxicol. Environ. Health Part B, Crit. Rev.* 13 (2–4), 51–138. doi:10.1080/10937404.2010.483176
- Langel, S. N., Kelly, F. L., Brass, D. M., Nagler, A. E., Carmack, D., Tu, J. J., et al. (2022). E-cigarette and food flavoring diacetyl alters airway cell morphology, inflammatory and antiviral response, and susceptibility to SARS-CoV-2. *Cell Death Discov.* 8 (1), 64. doi:10.1038/s41420-022-00855-3
- Laverty, A. A., Vardavas, C. I., and Filippidis, F. T. (2021). Prevalence and reasons for use of heated tobacco products (HTP) in Europe: an analysis of eurobarometer data in 28 countries. *Lancet Regional Health - Eur.* 8, 100159. doi:10.1016/j.lanpe.2021.100159
- Luettich, K., Sharma, M., Yepiskoposyan, H., Breheny, D., and Lowe, F. J. (2021). An adverse outcome pathway for decreased lung function focusing on mechanisms of impaired mucociliary clearance following inhalation exposure. *Front. Toxicol.* 3, 750254. doi:10.3389/ftox.2021.750254
- Malaviya, R., Laskin, J. D., and Laskin, D. L. (2017). Anti-TNFα therapy in inflammatory lung diseases. *Pharmacol. Ther.* 180, 90–98. doi:10.1016/j.pharmthera.2017.06.008
- Mallock, N., Boss, L., Burk, R., Danziger, M., Welsch, T., Hahn, H., et al. (2018). Levels of selected analytes in the emissions of "heat not burn" tobacco products that are relevant to assess human health risks. *Arch. Toxicol.* 92, 2145–2149. doi:10.1007/s00204-018-2215-y
- Mallock, N., Pieper, E., Hutzler, C., Henkler-Stephani, F., and Luch, A. (2019). Heated tobacco products: A review of current knowledge and initial assessments. *Front. Public Health* 7, 287. doi:10.3389/fpubh.2019.00287

- Malt, L., Thompson, K., Mason, E., Walele, T., Nahde, T., O'Connell, G., et al. (2022). The product science of electrically heated tobacco products: a narrative review of the scientific literature [version 1; peer review: awaiting peer review]. *F1000Research* 11, 121. doi:10.12688/f1000research.74718.1
- Margham, J., McAdam, K., Cunningham, A., Porter, A., Fiebelkorn, S., Mariner, D., et al. (2021). The chemical complexity of e-cigarette aerosols compared with the smoke from a tobacco burning cigarette. *Front. Chem.* 9, 743060. doi:10.3389/fchem.2021.743060
- McNeill, A., and Munafo, M. R. (2013). Reducing harm from tobacco use. *J. Psychopharmacol.* 27, 13–18. doi:10.1177/0269881112458731
- McNeill, A., Brose, L., Calder, R., Bauld, L., and Robson, D. (2018). *Evidence review of e-cigarettes and heated tobacco products 2018*. A report commissioned by Public Health England. London: Public Health England.
- Mori, S., Ishimori, K., Tanabe, I., and Ishikawa, S. (2021). Evaluation of the biological effects of novel tobacco product vapor using two- or three-dimensional culture systems of human bronchial epithelia. *Appl. Vitro Toxicol.* 7 (1), 24–33. doi:10.1089/aivt.2020.0022
- Mukhopadhyay, S., Hoidal, J. R., and Mukherjee, T. K. (2006). Role of TNFalpha in pulmonary pathophysiology. *Respir. Res.* 7 (1), 125. doi:10.1186/1465-9921-7-125
- Murkett, R., Rugh, M., and Ding, B. (2020). Nicotine products relative risk assessment: a systematic review and meta-analysis. *F1000Research* 9, 1225. [version 1; peer review: 1 approved]. doi:10.12688/f1000research.26762.1
- O'Farrell, H. E., Brown, R., Brown, Z., Milijevic, B., Ristovski, Z. D., Bowman, R. V., et al. (2021). E-cigarettes induce toxicity comparable to tobacco cigarettes in airway epithelium from patients with COPD. *Toxicol. Vitro* 75, 105204. doi:10.1016/j.tiv.2021.105204
- O'Leary, R., and Polosa, R. (2020). Tobacco harm reduction in the 21st century. *Drugs Alcohol Today* 20 (3), 219–234. doi:10.1108/DAT-02-2020-0007
- Ostridge, K., Williams, N., Kim, V., Bennett, M., Harden, S., Welch, L., et al. (2016). Relationship between pulmonary matrix metalloproteinases and quantitative CT markers of small airways disease and emphysema in COPD. *Thorax* 71 (2), 126–132. doi:10.1136/thoraxjnl-2015-207428
- Phillips, G., Czekala, L., Behrsing, H. P., Amin, K., Budde, J., Stevenson, M., et al. (2021). Acute electronic vapour product whole aerosol exposure of 3D human bronchial tissue results in minimal cellular and transcriptomic responses when compared to cigarette smoke. *Toxicol. Res. Appl.* 5, 239784732098849. doi:10.1177/2397847320988496
- Phillips-Waller, A., Przulj, D., Pesola, F., Smith, K. M., and Hajek, P. (2021). Nicotine delivery and user ratings of IQOS heated tobacco system compared with cigarettes, juul, and refillable E-cigarettes. *Nicotine Tob. Res.* 23 (11), 1889–1894. doi:10.1093/ntr/ntab094
- Rayner, R. E., Makena, P., Prasad, G. L., and Cormet-Boyaka, E. (2019). Optimization of normal human bronchial epithelial (NHBE) cell 3D cultures for *in vitro* lung model studies. *Sci. Rep.* 9 (1), 500. doi:10.1038/s41598-018-36735-z
- RIVM (2018). *Addictive nicotine and harmful substances also present in heated tobacco*. Bilthoven: National Institute for Public Health and the Environment RIVM. Available at: <https://www.rivm.nl/en/news/addictivenicotine-and-harmful-substances-also-present-in-heated-tobacco>.
- Roulet, S., Chrea, C., Kanitscheider, C., Kallischnigg, G., Magnani, P., and Weitkunat, R. (2019). Potential predictors of adoption of the Tobacco Heating System by U.S. adult smokers: An actual use study. *F1000Research* 8, 214. doi:10.12688/f1000research.17606.1
- Rudd, K., Stevenson, M., Wieczorek, R., Pani, J., Trelles Sticken, E., Dethloff, O., et al. (2020). Chemical composition and *in vitro* toxicity profile of a pod-based E-cigarette aerosol compared to cigarette smoke. *Appl. Vitro Toxicol.* 6 (1), 11–41. doi:10.1089/aivt.2019.0015
- SHC (2020). *Superior Health council. New tobacco products: Heated tobacco products*. Report 9538. Brussels: SHC. Available at: https://www.health.belgium.be/sites/default/files/uploads/fields/fpshealth_theme_file/201026_shc-9538_new_tobacco_products_vweb.pdf.
- Simms, L., Rudd, K., Palmer, J., Czekala, L., Yu, F., Chapman, F., et al. (2020). The use of human induced pluripotent stem cells to screen for developmental toxicity potential indicates reduced potential for non-combusted products, when compared to cigarettes. *Curr. Res. Toxicol.* 1, 161–173. doi:10.1016/j.crttox.2020.11.001
- Simms, L., Mason, E., Berg, E. L., Yu, F., Rudd, K., Czekala, L., et al. (2021). Use of a rapid human primary cell-based disease screening model, to compare next generation products to combustible cigarettes. *Curr. Res. Toxicol.* 2, 309–321. doi:10.1016/j.crttox.2021.08.003
- Simms, L., Yu, F., Palmer, J., Rudd, K., Sticken, E. T., Wieczorek, R., et al. (2022). Use of human induced pluripotent stem cell-derived cardiomyocytes to predict the cardiotoxicity potential of next generation nicotine products. *Front. Toxicol.* 4, 747508. doi:10.3389/ftox.2022.747508
- Smart, D. J., and Phillips, G. (2021). Collecting e-cigarette aerosols for *in vitro* applications: A survey of the biomedical literature and opportunities to increase the value of submerged cell culture-based assessments. *J. Appl. Toxicol.* 41 (1), 161–174. doi:10.1002/jat.4064
- Stratton, K., Shetty, P., Wallace, R., and Bondurant, S. Institute of Medicine Committee to Assess the Science Base for Tobacco Harm (2001). *Clearing the smoke: Assessing the science base for tobacco harm reduction*. Washington (DC): National Academies Press US. Copyright 2001 by the National Academy of Sciences. All rights reserved.
- Sutanto, E., Miller, C., Smith, D. M., Borland, R., Hyland, A., Cummings, K. M., et al. (2020). Concurrent daily and non-daily use of heated tobacco products with combustible cigarettes: Findings from the 2018 ITC Japan survey. *Int. J. Environ. Res. public health* 17 (6), 2098. doi:10.3390/ijerph17062098
- United States Surgeon General (2010). *Surgeon General's Report – how tobacco smoke causes disease: The biology and behavioural analysis for smoking-attributable disease*. Available at: https://www.cdc.gov/tobacco/data_statistics/sgr/2010/index.htm (Last accessed 02 13, 2021).
- US Department of Health and Human Services (USDHHS) (2014). *The health consequences of smoking—50 Years of progress: A report of the surgeon general*. Atlanta, GA: US Department of Health and Human Services, Centers for Disease Control and Prevention, National Center for Chronic Disease Prevention and Health Promotion, Office on Smoking and Health.
- Yoshida, T., and Tuder, R. M. (2007). Pathobiology of cigarette smoke-induced chronic obstructive pulmonary disease. *Physiol. Rev.* 87 (3), 1047–1082. doi:10.1152/physrev.00048.2006
- Zeller, M. (2019). The future of nicotine regulation: Key questions and challenges. *Nicotine Tob. Res.* 21 (3), 331–332. doi:10.1093/ntr/nty200
- Zhang, X., Zheng, H., Zhang, H., Ma, W., Wang, F., Liu, C., et al. (2011). Increased interleukin (IL)-8 and decreased IL-17 production in chronic obstructive pulmonary disease (COPD) provoked by cigarette smoke. *Cytokine* 56 (3), 717–725. doi:10.1016/j.cyt.2011.09.010



OPEN ACCESS

EDITED BY

Mary Catherine McElroy,
Charles River Laboratories,
United Kingdom

REVIEWED BY

Jonathan Shannahan,
Purdue University, United States
Jason Michael Fritz,
US Federal Employee Scientist,
United States

*CORRESPONDENCE

Jianwen Chen,
✉ chenjwen@mail.sysu.edu.cn
Peiqing Liu,
✉ liupq@mail.sysu.edu.cn

RECEIVED 31 May 2023

ACCEPTED 14 July 2023

PUBLISHED 04 September 2023

CITATION

Dai Y, Duan K, Huang G, Yang X, Jiang X,
Chen J and Liu P (2023), Inhalation of
electronic cigarettes slightly affects lung
function and inflammation in mice.
Front. Toxicol. 5:1232040.
doi: 10.3389/ftox.2023.1232040

COPYRIGHT

© 2023 Dai, Duan, Huang, Yang, Jiang,
Chen and Liu. This is an open-access
article distributed under the terms of the
[Creative Commons Attribution License
\(CC BY\)](https://creativecommons.org/licenses/by/4.0/). The use, distribution or
reproduction in other forums is
permitted, provided the original author(s)
and the copyright owner(s) are credited
and that the original publication in this
journal is cited, in accordance with
accepted academic practice. No use,
distribution or reproduction is permitted
which does not comply with these terms.

Inhalation of electronic cigarettes slightly affects lung function and inflammation in mice

Yuxing Dai¹, Kun Duan², Guangye Huang¹, Xuemin Yang²,
Xingtao Jiang², Jianwen Chen^{1,3*} and Peiqing Liu^{1,3*}

¹Department of Pharmacology and Toxicology, School of Pharmaceutical Sciences, Sun Yat-Sen University, Guangzhou, Guangdong, China, ²RELX Science Center, Shenzhen RELX Tech Co., Ltd., Shenzhen, China, ³National and Local Joint Engineering Laboratory of Druggability and New Drugs Evaluation, Guangdong Engineering Laboratory of Druggability and New Drug Evaluation, School of Pharmaceutical Sciences, Sun Yat-sen University, Guangzhou, China

Electronic cigarettes have become increasingly popular, but the results of previous studies on electronic cigarette exposure in animals have been equivocal. This study aimed to evaluate the effects of electronic cigarette smoke (ECS) and cigarette smoke (CS) on lung function and pulmonary inflammation in mice to investigate whether electronic cigarettes are safer when compared to cigarettes. 32 specific pathogen-free BALB/c male mice were randomly grouped and exposed to fresh air (control), mint-flavored ECS (ECS1, 6 mg/kg), cheese-flavored ECS (ECS2, 6 mg/kg), and CS (6 mg/kg). After 3 weeks exposure to ECS or CS, we measured lung function (PIF and Penh) and blood oxygen saturation. The levels of TNF- α and IL-6 in the bronchoalveolar lavage fluid (BALF) and serum were measured using ELISA. HE staining was performed to observe the pathological changes in the lung tissues. The levels of IL-6 in BALF and serum, and TNF- α in BALF, were elevated similarly in the ECS and CS groups compared to the control group. Significant elevation was observed in serum TNF- α levels in the CS group. The total count of cells in BALF were increased after ECS1 exposure and CS exposure. PIF and oxygen saturation decreased, and Penh increased markedly in the CS group but not in the ECS groups. Compared with the ECS groups, mice in the CS group had widened lung tissue septa and increased inflammatory cell infiltration. However, we did not detect significant differences between mint-flavored and cheese-flavored e-cigarettes in our study. Overall, our findings suggested that both ECS and CS impair lung function and histopathology while promoting inflammation. In contrast, ECS has a less negative impact than CS.

KEYWORDS

electronic cigarette, lung function, cigarette, inflammation, toxicology

Introduction

Smoking is a major cause of morbidity and mortality, responsible for nearly 200 million deaths per year (Beaglehole et al., 2019). Tobacco smoking is the leading risk factor for serious lung diseases, including lung cancer and chronic obstructive pulmonary disease (Traboulsi et al., 2020). While traditional cigarette smoking has declined in recent years, the use of electronic cigarettes or e-cigarettes has increased dramatically (Bilano et al., 2015). E-cigarettes, also known as a type of electronic nicotine delivery system (ENDS), comprise a rechargeable battery, an atomizer, and liquid containing nicotine, solvent, and flavors, but do

not contain natural tobacco. Electronic cigarette aerosols, produced by the heating and atomization of nicotine liquid via an atomizer, directly enter the lungs through the respiratory tract. The toxic and carcinogenic substances contained in cigarette smoke, including carbonyl compounds, volatile organic compounds, nitrosamines, and heavy metals, can still be detected in electronic cigarette aerosols, but their levels are much lower than those in cigarette smoke under the same average puffing conditions (Goniewicz et al., 2014).

E-cigarettes are marketed as a safer alternative to cigarettes, yet their health effects remain largely controversial (Rom et al., 2015). Reliable and direct support data on the safety of using electronic cigarettes for human health remains scanty (Wagner et al., 2017), and the effects of electronic cigarettes on human health have not been adequately clarified (Dinakar and O'Connor, 2016; Pisinger and Dossing, 2014). Due to a lack of preclinical scientific data in the field, it is critical to evaluate the *in vivo* safety of electronic cigarettes.

Previous research on e-cigarettes has focused on acute exposure, with studies showing that e-cigarette aerosol can induce inflammation, impair lung function and increase oxidative stress. Acute exposure to electronic cigarette vapor increases blood pressure (Fogt et al., 2016) and airway resistance (Vardavas et al., 2012). E-cigarette aerosols increase levels of monocyte chemoattractant protein-1 (MCP-1) and IL-6 in BALF after acute exposure to e-cigarettes (Lerner et al., 2015). Another study found that mice exposed to e-cigarettes for 6 h per day had higher IL-6 and TNF- α transcripts levels after 3 days. However, some studies have shown that e-cigarette exposure did not induce oxidative stress and cell death, and only a limited focus of inflammatory cell infiltration was observed on lung histology (Husari et al., 2016). It has been reported that the inflammation was not increased in mice exposed to e-cigarettes, but the lung function was decreased (Larcombe et al., 2017a).

More and more studies have examined the pulmonary effects of e-cigarettes short-term and long-term exposure. A *in vivo* study reported that 4 weeks exposure to e-cig vapor can induce inflammatory responses and adversely affect respiratory system mechanics (Glynos et al., 2018). Another study has shown that mice exposed to e-cigarette aerosol for 8 weeks did not have increased inflammation but did display decrements in parenchymal lung function while less worsening than combusted cigarette smoke (Larcombe et al., 2017b). It has also reported that exposure to inhaled nicotine-containing e-cigarette fluids for 4 months triggered adverse effects including cytokine expression, airway hyper-reactivity and lung tissue destruction (Garcia-Arcos et al., 2016).

E-cigarettes flavors have been found to increase e-cigarettes use frequency among adolescent (Morean et al., 2018). However, it is widely validated that the flavorings used in e-cigarettes may exacerbate the adverse pulmonary effects induced by e-cigarettes. Thermal decomposition of flavoring compounds dominates formation of aldehydes during vaping, which toxic to human health (Khlystov and Samburova, 2016). Glynos et al. also have examined that the added flavor in e-cigs exacerbated the detrimental effects of e-cig vapor, inducing more severe health concerns.

Understanding the pulmonary impacts of e-cigarette use is critical to informing product regulations and user safety. This

study aimed to determine the effects of short-term exposure to e-cigarette aerosol *versus* cigarette smoke on inflammation and lung function in mice. Before the products exposure, we collected the e-cigarettes aerosol and cigarette smoke for UPLC measurement to determine the equivalent nicotine concentration as exposure dose. The nicotine concentration, which served as the exposure dosage, was determined by UPLC analysis of the collected aerosol and smoke samples. BALB/c mice, aged 8 weeks, were selected to be exposed to either conventional cigarette smoke or e-cigarette aerosols with mint or cheese flavorings for 3 weeks. The pulmonary physiology, the levels of inflammatory cytokines in BALF and serum, and histopathological changes in the lung tissues were assessed. Our hypothesis postulates that e-cigarette inhalation results in heightened pulmonary inflammation, compromised lung function, and these adverse effects exhibit variations with diverse flavors.

Materials and methods

Animals

BALB/c mice were susceptible to cigarette smoke induced lung pathology and systemic inflammatory and fibrotic responses (H. Chen et al., 2021), so we purchased specific pathogen-free male BALB/c mice aged 8 weeks from Guangdong Medical Laboratory Animal Centre (China). They were kept in a 12-h light/dark cycle with a room temperature of 22°C and had *ad libitum* access to food and water. All animal procedures were approved by the Institutional Animal Care and Use Committee (IACUC), Sun Yat-Sen University (Approval No. SYSU-IACUC-2020-000259).

Smoke collection and UPLC method for measuring nicotine

ESC or CS was generated by a smoking machine and following collected with a Cambridge filter in a whole-body chamber delivering the relevant smoke. The size of the chamber was 3.8 L, where the flow rate of the air pump was 2.0 L/min. Smoke delivery methods simulated the way humans inhale smoke. 55 mL of smoke was released in 3 s, paused for 27 s, and released again. Smoke was released at a rate of 2 times per minute. The total amount of smoke released was 110 mL/min and after 30 min the Cambridge filter was extracted with 10 mL of DMSO. The average nicotine content of ECS and CS was determined within 30 min using ultra-performance liquid chromatography (UPLC). An external standard approach was used for quantitative analysis. The mobile phase was made up of 10 mM ammonium acetate (A) and 0.3 mL/min acetonitrile (B). The analytical column was an ACQUITY UPLC HSS T3 2.1 \times 100 mm \times 1.8 μ m. The injection volume and temperature of the column were 0.5 μ L and 40°C, respectively. The following was the best gradient elution: from 0.0 to 6.0 min, A-B of 80:20; from 6.01 to 9.0 min, A-B of 10:90; from 9.01 to 12.0 min, A-B of 80:20. At a wavelength of 260 nm, UV chromatograms were detected.

Design and dosage of exposure to ECS and CS design

The electronic cigarettes consumed by an adult contain approximately 40 mg of nicotine per day (Prochaska et al., 2022). For 60 kg, an average human body weight, the nicotine dosage for human is approximately 0.67 mg/kg (nicotine-by-weight). The Meeh-Rubner formula is a calculation formula of total body surface area most commonly used for small animals ($TBSA = kW^{2/3}$, mean k value is 9.83) (Gouma et al., 2012). According to the Meeh-Rubner formula, the equivalent dosage for mice was approximately 6 mg/kg, thus the nicotine inhaled by mice weighing 0.02 kg is 12 mg. The results of the pre-experiment showed that the average concentration of nicotine was 0.1 mg/L. So, it can be calculated the equivalent nicotine volume inhaled by mice is approximately 1.2 L. The ventilation volume per minute of mice was 0.0217 L/min (Alexander et al., 2008). Thus, the mice exposed to the aerosol for 60 min could reach the nicotine dose of 6 mg/kg, which is equivalent to human nicotine consumption per day.

The procedure for ECS and CS exposure

Thirty-two specific pathogen-free BALB/c mice were randomly divided into four groups. The control group was exposed to fresh air. The ECS1 group was exposed to mint-flavored electronic cigarette smoke (RELX Tech. Co., Ltd.). The ECS2 group was exposed to cheese-flavored electronic cigarette smoke (RELX Tech. Co., Ltd.). The CS group was exposed to cigarette smoke. Except for the control group, the other groups were exposed to smoke twice a day for 30 min each. The exposure lasted 3 weeks, 5 days a week. During smoke exposure, every four mice were exposed to one batch of smoke. Smoke is delivered in the same manner as the above collection method.

Lung function tests

The lung function of mice after smoke exposure was assessed using a whole-body plethysmograph (EMKA Technologies, Paris, France) (Moriya et al., 2016). The mice were placed into chambers of the whole-body plethysmograph and recorded for 5 min to detect peak inspiratory flow (PIF) and decrease in enhanced pause (Penh) of the lungs.

Blood oxygen saturation

Blood oxygen saturation in mice was monitored with a Mouse Ox Plus pulse oximeter (Chang et al., 2013) for mice, rats, and other small animals (Starr Life Sciences Corp., Oakmont, United States). The blood oxygen sensor was collared around the necks of mice, and the instrument was electrified to detect and record the blood oxygen saturation for 3 min after stabilization.

BALF and serum acquire

Mice were anesthetized with 3% pentobarbital sodium (Van Hoesche et al., 2017). Further, the blood of the mice was acquired

from the fundus venous plexus. The blood was centrifuged at 3,000 rpm for 10 min at 4°C to obtain serum. The mice were sacrificed, and their chests were opened fully to expose the lungs. 0.5 mL of 4°C normal saline was injected into the trachea and withdrawn slowly three times during 30 s. This procedure was repeated. The BALF obtained twice was mixed, and the total number of leukocytes in the BALF was counted using a hemocytometer under a microscope. After counting, the BALF was centrifuged and the cell-free supernatant was stored at −80°C until subsequent measurement of TNF-α and IL-6. The levels of IL-6 and TNF-α in the supernatant of BALF and serum were detected using ELISA kits.

ELISA

Using mouse ELISA kits for IL-6 (9680008061219) and TNF-α (9680010061219) from ABclonal Biotechnology Co., Ltd. (Wuhan, China), the inflammatory cytokines IL-6 and TNF-α were quantified using enzyme-linked immunosorbent assay. The technical protocols are available on manufacturer's website (<https://abclonal.com.cn/mouse-elisa-kits/>) To begin, place 100 ul of standard or test samples in each well and incubate for 2 h at 37°C before washing. Incubate for 1 h at 37°C with 100 ul Working Biotin Conjugate Antibody, then wash three times. Add 100 ul Working Streptavidin-HRR and incubate for 0.5 h at 37°C. Then wash 3 times. Incubate for 15–20 min at 37°C in the dark with 100 ul Substrate Solution. Add 50 ul Stop Solution to the mix. Detect the optical density within 5 min under 450 nm. Each test sample was loaded in triplicate, with the results being averaged to minimize random errors and ensure reliability.

HE staining

The lung tissue, which not used to acquire for BALF, was fixed in formalin, embedded in paraffin, and sliced for hematoxylin-eosin staining with an HE staining kit (Boster Biological Technology Co., Ltd., Wuhan, China). Pathological changes in the lung tissues were observed under a microscope (Life Technologies Co., Ltd., New York, America), and each lung tissue sample was qualitatively analyzed.

Statistical analysis

Means ± standard deviation was calculated and statistical analysis was performed using GraphPad Prism version 8.0 for Windows. Statistical differences of measurement data were ascertained by one-way analysis of variance, with Tukey's multiple comparisons test. Count data were analyzed by Kruskal–Wallis test with Dunn's multiple comparisons test. Statistical significance was set at p -value <0.05.

Results

Effects of ECS and CS on lung function

As the lung is exposed to smoke and is the main target organ for cigarettes, we assessed the lung function in the mice

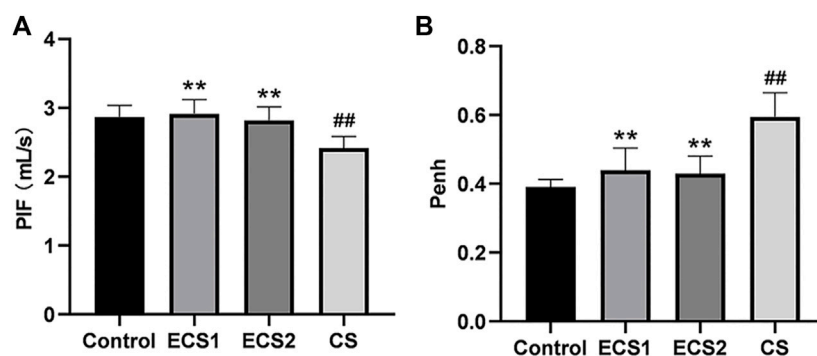


FIGURE 1

Effects of ECS and CS on PIF and Penh. PIF and Penh, as common indicators of lung function, were detected by a whole-body plethysmograph. Levels of PIF (A) and Penh (B) are presented ($n = 8$). Data are represented as mean \pm SD. ** $p < 0.01$, significantly different to the CS group; ## $p < 0.01$, significantly different to the control group.

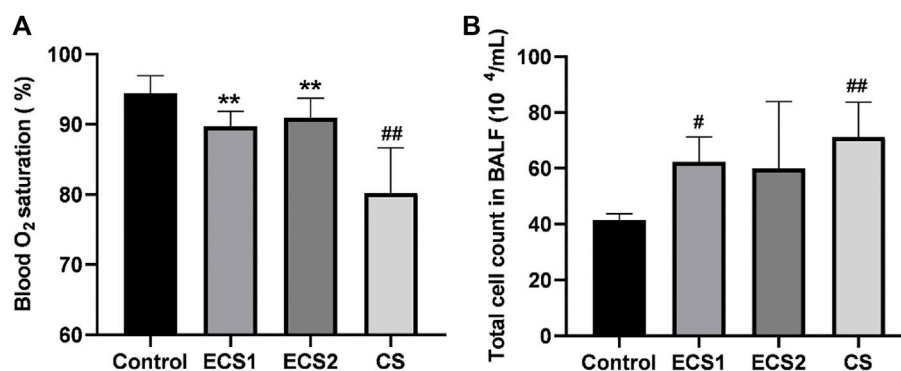


FIGURE 2

Effects of ECS and CS on blood oxygen saturation and the total cell count in BALF. Blood oxygen saturation was monitored with a Mouse Ox Plus pulse oximeter. The total cell count in BALF was counted under the microscope. Levels of blood oxygen saturation (A) and total count of cells in the BALF (B) are presented ($n = 3-4$). Data are represented as mean \pm SD. ** $p < 0.01$, significantly different to the CS group; # $p < 0.05$, significantly different to the control group; ## $p < 0.01$, significantly different to the control group.

immediately after the completion of smoke exposure. The results of lung function testing showed PIF decreased and Penh increased significantly in the CS group compared to the control group ($p < 0.01$). Notably, in comparison to ECS group, PIF also fell drastically ($p < 0.01$), while Penh elevated significantly in CS-exposed mice ($p < 0.01$) (Figure 1).

Effects of ECS and CS on blood oxygen saturation

To further define lung function, the oxygen saturation of mice was examined. The study indicated that ECS exposure had no significant effect on blood oxygen saturation compared to air exposure, and the blood oxygen saturation in the CS group was markedly lower than that in the control group ($p < 0.01$). The blood oxygen saturation in each ECS group was significantly higher than that in the CS group ($p < 0.01$) (Figure 2).

Effect of ECS and CS on the total count of cells in the BALF

Furthermore, we also measured the number of cells in the BALF. The results indicated that the total cell count in the BALF in the CS group was significantly higher than that in the control group ($p < 0.01$). The total count of cells in the ECS1 group was significantly higher compared to the control group ($p < 0.05$). Moreover, the total cell count in BALF in each ECS group decreased to a different degree than that in the CS group, but there was no significant difference ($p > 0.05$) (Figure 2).

Effect of ECS and CS on the contents of TNF- α and IL-6 in BALF and serum

We examined the levels of inflammatory factors in serum and BALF to explore whether ECS caused an inflammatory response.

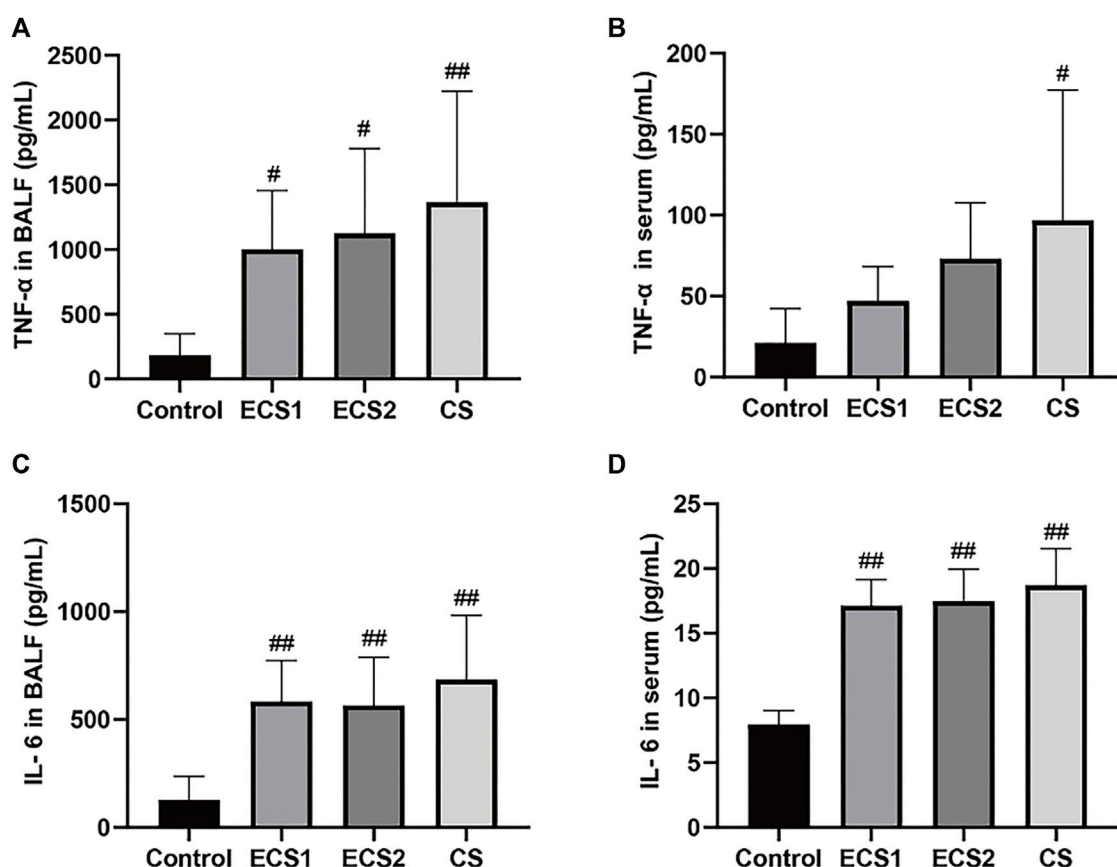


FIGURE 3

Effects of ECS and CS on TNF- α and IL-6 levels in BALF and serum. Levels of TNF- α in BALF (A), TNF- α in serum (B), IL-6 in BALF (C), and IL-6 in serum (D) are presented ($n = 3-4$). Data are represented as mean \pm SD. # $p < 0.05$, significantly different to the control group; ## $p < 0.01$, significantly different to the control group.

When compared to the control group, the ECS groups had considerably greater levels of TNF- α in BALF ($p < 0.05$) and IL-6 in both BALF and serum ($p < 0.01$). TNF- α levels in BALF ($p < 0.01$) and serum ($p < 0.05$) were significantly higher in the CS group compared with the control group, as were IL-6 levels ($p < 0.01$). TNF- α and IL-6 values in BALF and serum were marginally lower in the ECS groups than in the CS group, but there was no significant difference (Figure 3).

Effect of ECS and CS on HE staining in lung tissue

To observe the effect of ECS on the lung tissue structure, HE staining of lung tissue was performed. The analysis suggested that the lung tissue septum in animals exposed to cigarettes was significantly broadened, inflammatory cell infiltration was obvious, and increased local pulmonary hemorrhage and pulmonary interstitial congestion were found in comparison to animals exposed to air. Furthermore, the lung tissue septum was less widened, inflammatory cell infiltration was decreased, and pulmonary hemorrhage was less common in each ECS group than in the CS group (Figure 4).

Discussion

The present study aimed to analyze the effects of short-term exposure to ECS and CS on lung function and inflammation in mice. Our findings suggested that ECS had a negative impact on pulmonary inflammation, whereas CS exerted more pronounced detrimental effect on lung function injury and inflammation. These results contribute to the ongoing controversy surrounding the potential benefits and harms of electronic cigarettes.

Electronic cigarettes have become increasingly popular recently, especially among teenagers. Consumption of electronic cigarettes may not be effective in promoting tobacco cessation (Kalkhoran and Glantz, 2016), but the reduction in tobacco smoking is indeed closely related to the use of electronic cigarettes in adolescent smokers with severe nicotine addiction (Selya et al., 2018). It is unclear whether they are beneficial or harmful for smokers and adolescents (Lam et al., 2014). The increasing prevalence of electronic cigarettes has raised serious concerns about their impact on public health (Pearson et al., 2012).

Lung function is an important indicator of lung health. As an overall indicator, the lung function in animals can directly represent the effect of ECS exposure. While many respiratory parameters were detected using EMKA system, most indicators lacked statistical differences to be included in our study. Penh is an important

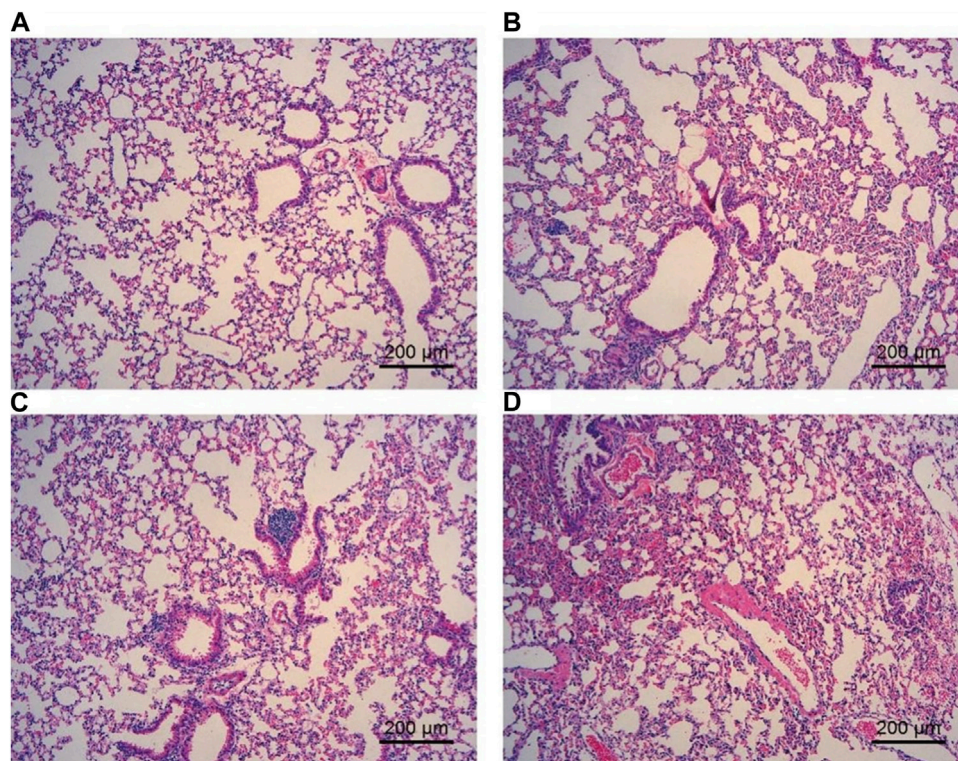


FIGURE 4

Effect of ECS and CS on HE staining of the lung tissue. The lung tissue was fixed, embedded in paraffin, and sliced for hematoxylin-eosin staining with an HE staining kit ($n = 3-4$). (A) represents the control group; (B) represents the ECS1 group; (C) represents the ECS2 group; (D) represents the CS group. Scale bar: 200 μm .

parameter that represents the gas exchange capacity and the severity of airway resistance (Ghorani et al., 2017). Penh reflects changes in lung function and airway resistance in conscious animals by using a whole-body thoracoscopic system (Halloy et al., 2004). Measurement of PIF is useful for interpreting inspiratory resistance to assess lung function in mice (Bentur et al., 2004). Decreased gas exchange capacity and increased airway resistance are typical clinical manifestations of decreased lung function (Jobse et al., 2013), and they are important diagnostic indicators of decreased lung function. Smoking is known to cause lung dysfunction (Zalokar, 1979). Regarding whether e-cigarettes impair lung function, several informative studies have addressed the effects of electronic cigarettes on lung health *in vivo* (Sussan et al., 2015; Husari et al., 2016), but they lack investigation into lung function mechanics. To address this problem, we evaluated the effect of ECS exposure on lung function. In this study, Penh and PIF values in mice were detected consciously. The results showed that CS exposure caused significant changes in PIF and Penh, but not in ECS exposure. These results suggest that exposure to CS is harmful and that it significantly affects lung function in mice. In contrast, exposure to ECS had slightly but no significant adverse effects on lung function in mice, but the damage to the lung function was significantly less than that of CS. Notably, more common lung function parameters should be evaluated again to expand the scope of endpoints including respiratory rate (RR), tidal volume (TV), peak expiratory flow (PEF), total lung volume (TLV), and forced expiratory volume (FEV).

Blood oxygen saturation is an important characteristic of the functioning of the respiratory and circulatory systems. The lungs are organs for oxygen exchange in mice. When lung function is impaired, the blood oxygen saturation may also change. The saturation changes with the severity of lung dysfunction in mice (Gross et al., 2020). In this study, we measured the blood oxygen saturation in conscious mice. The results showed that both CS and ECS caused a reduction in blood oxygen saturation, while ECS exposure exhibiting a significantly distinct effect on blood oxygen saturation compared to CS exposure. Taken together, lung dysfunction caused by exposure to CS but not ECS affects blood oxygen saturation in mice.

Lung injury in mice leads to an inflammatory response. Studies have shown that smoking reduces levels of the antioxidant glutathione (GSH) in the lung, which further activates redox-sensitive transcription factors including nuclear factor- κB (NF- κB) and activator protein-1 (AP-1), initiating a pulmonary inflammatory response (Rahman, 2003). During the inflammatory response, some cytokines influence the activation of inflammatory cells and they are recruited into the airways, which further leads to lung dysfunction (Szafran et al., 2020). It has been reported that passive smoking leads to slow weight gain, lung pathology in mice, and markedly elevated levels of serum IL-6 and TNF- α (Onishi et al., 2018; Romo et al., 2019). TNF- α has been identified as a key cytokine in the immunological response to CS exposure, regulating inflammation and promoting neutrophil recruitment via activating endothelial cells (Churg et al., 2003).

In this research, we measured the total cell count in BALF, TNF- α , and IL-6 in the BALF and serum to study the effect of ECS exposure on lung inflammation. The results suggested that ECS exposure resulted in an increase in total cell count as well as increased inflammatory levels, but the effects were minor when compared to CS exposure. Therefore, exposure to both ECS and CS can cause inflammation in the body and lungs of mice, but the inflammation caused by CS is more serious. However, a more comprehensive evaluation of systemic inflammation including more inflammatory markers would provide a more detailed understanding. In addition to smoking, inhalation of other foreign substances can also cause lung injury and inflammation (Wang et al., 2019). Moreover, the severity of lung injury and inflammation is closely related to the amount of inhaled substances (Deb et al., 2012).

HE staining is an important method to determine pathological changes in tissue structure, and it is one of the most widely used methods for pathological biopsy (Zheng et al., 2019). The lung tissue of mice was sectioned and stained with an HE staining kit in this experiment. The results showed that exposure to both ECS and CS caused pathological changes in the lung tissue of mice, but the lung tissue lesions caused by exposure to CS were more serious than those caused by ECS. Therefore, these results suggest that both ECS and CS can cause changes in the lung tissue of mice, although CS is more toxic than ECS.

However, we recognize that our evaluation of total BALF cellularity and images of HE-stained histological lung sections provides a summary-level survey, which may limit our ability to make specific connections between BALF cytokine levels and the mechanisms of inflammation on pulmonary function. A more comprehensive analysis of BALF cellular constituents and immunohistochemical evaluation of lung sections would provide a clearer understanding of the potential mechanistic linkages to changes in pulmonary function.

One limitation of our study is that it did not address the potential impact of different flavors on lung function and inflammation. Previous research has suggested that certain flavors may have differential effects on lung health. Bahl et al. (2012) first suggested that cytotoxicity of e-cigarette liquids (e-liquids) was related to flavors. However, Misra et al. (2014) indicated that e-liquids or collected aerosol produced any meaningful toxic effects *in vitro*. This controversy may be driven from cell lines. As in our mice model, we did not find any significant differences between different flavors in terms of lung function and inflammation. Further research is needed to explore the role of flavorings in electronic cigarette toxicity using more widely marketed flavorings.

Another important aspect to consider is the aerosol components of electronic and traditional cigarette smoke, which may contribute to the differential lung effects observed in our study. While both ECS and CS contain nicotine, the chemical composition of their aerosols differs significantly (Li et al., 2020). The aerosol from the e-cigarette is compositionally less complex than conventional cigarette smoke, containing significantly lower levels of toxicants (Margham et al., 2016). This difference in composition may partially explain the observed differences in lung function and inflammation between ECS and CS exposure in our study.

In this study, we used a whole-body exposure chamber as opposed to nose-only exposure system, which may introduce some uncertainty due to the grooming and cleaning behaviors of

rodents between exposures. This behavior could result in incidental ingestion of cigarette smoke and related substances, in addition to inhalation exposures. Studies have reported that whole-body exposure systems may lead to a combination of oral and inhalation exposures in rodents (L.-C. Chen and Lippmann, 2015), which could potentially confound the interpretation of our findings. Despite this limitation, however, whole-body exposure systems have been widely used in inhalation toxicology studies since it could mimic real-world exposure behavior, where humans are also exposed to both inhalation and incidental ingestion of environmental pollutants (Serré et al., 2021). Compared to whole-body exposure, the use of a nose-only exposure system could help to minimize confounding factors related to incidental ingestion, allowing for a more precise assessment of inhalation-specific effects on pulmonary function (Kogel et al., 2021).

Our study evaluated the toxicity of ECS and CS using equivalent dosing, which may not accurately represent real-world smoking patterns because smokers tailor their smoking to different products and toxicologic effects change with different smoking profiles (Marian et al., 2009). It is essential to consider that electronic cigarette users and traditional smokers may exhibit differences in smoking patterns, such as puff frequency, duration, and intensity. Moreover, the nicotine content and other toxic matters also vary in electronic cigarettes with different brands, model numbers, and flavors, inducing variability in potential human exposures (Stratton et al., 2018). These variations in smoking behavior could potentially alter the toxicity of the aerosols and their impact on lung function and inflammation. Future studies should investigate the effects of different smoking patterns on lung health to better understand the potential risks associated with electronic cigarette use in comparison to traditional smoking.

In terms of the global public health impact, our findings suggest that electronic cigarettes may be less harmful to lung health than conventional cigarettes, at least in the context of short-term exposure. This information could be useful in guiding public health policies and strategies aimed at reducing the harm associated with tobacco smoking. However, it is crucial to emphasize that our study was conducted in mice, and the results may not directly translate to humans. Additional research is needed to confirm the effects of electronic cigarette use on lung function and inflammation in human populations, as well as to identify any potential long-term consequences.

Overall, our study provides new insights into the effects of short-term exposure to ECS and CS on lung function and inflammation in mice. While both ECS and CS exposure can induce lung dysfunction and inflammation, the severity of these effects is considerably higher following CS exposure. Our findings contribute to the ongoing debate surrounding the potential benefits and harms of electronic cigarettes, highlighting the need for further research to better understand their long-term consequences and inform public health policies.

Conclusion

The study compared the effects of short-term exposure to ECS with mint and cheese flavors and CS in mice. Our findings revealed

that exposure to both electronic cigarettes and conventional cigarettes negatively impacts lung physiology. However, the lung function and blood oxygen saturation in the group of electronic cigarettes improved compared to those in the conventional cigarette group. There is no significant difference between mint-flavored and cheese-flavored electronic cigarettes in our model. Notably, our findings seem supported that the harmful effects of electronic cigarettes were less than those of conventional cigarettes in mice.

Data availability statement

The original contributions presented in the study are included in the article/Supplementary Material, further inquiries can be directed to the corresponding authors.

Ethics statement

The animal study was reviewed and approved by the Institutional Animal Care and Use Committee (IACUC), Sun Yat-Sen University.

Author contributions

Methodology: JC and PL; Formal analysis and investigation: YD; Writing-original draft preparation: YD and KD; Writing-review and editing: JC, GH, XY, and XJ. All authors contributed to the article and approved the submitted version.

References

- Alexander, D. J., Collins, C. J., Coombs, D. W., Gilkison, I. S., Hardy, C. J., Healey, G., et al. (2008) Association of Inhalation Toxicologists (AIT) working party recommendation for standard delivered dose calculation and expression in non-clinical aerosol inhalation toxicology studies with pharmaceuticals. *Inhal. Toxicol.* 20, 1179–1189. doi:10.1080/08958370802207318
- Bahl, V., Lin, S., Xu, N., Davis, B., Wang, Y., and Talbot, P. (2012). Comparison of electronic cigarette refill fluid cytotoxicity using embryonic and adult models. *Reprod. Toxicol.* 34 (4), 529–537. doi:10.1016/j.reprotox.2012.08.001
- Beaglehole, R., Bates, C., Youdan, B., and Bonita, R. (2019). Nicotine without smoke: fighting the tobacco epidemic with harm reduction. *Lancet* 394 (10200), 718–720. doi:10.1016/S0140-6736(19)31884-7
- Bentur, L., Mansour, Y., Hamzani, Y., Beck, R., Elias, N., and Amirav, I. (2004). Measurement of inspiratory flow in children with acute asthma. *Pediatr. Pulm.* 38, 304–307. doi:10.1002/ppul.20109
- Bilano, V., Gilmour, S., Moffiet, T., d'Espaignet, E. T., Stevens, G. A., Commar, A., et al. (2015). Global trends and projections for tobacco use, 1990–2025: an analysis of smoking indicators from the WHO comprehensive information systems for tobacco control. *Lancet* 385 (9972), 966–976. doi:10.1016/S0140-6736(15)60264-1
- Chang, Z., Ballou, E., Jiao, W., McKenna, K. E., Morrison, S. F., and McCrimmon, D. R. (2013). Systemic leptin produces a long-lasting increase in respiratory motor output in rats. *Front. Physiol.* 4, 16. doi:10.3389/fphys.2013.00016
- Chen, H., Li, G., Chan, Y. L., Zhang, H. E., Gorrell, M. D., Pollock, C. A., et al. (2021). Differential effects of 'vaping' on lipid and glucose profiles and liver metabolic markers in obese versus non-obese mice. *Front. Physiology* 12, 755124. doi:10.3389/fphys.2021.755124
- Chen, L.-C., and Lippmann, M. (2015). Inhalation toxicology methods: the generation and characterization of exposure atmospheres and inhalational exposures. *Curr. Protoc. Toxicol./Editor. Board* 63, 1–24. doi:10.1002/0471140856.tx2404s63
- Churg, A., Wang, R. D., Tai, H., Wang, X., Xie, C., Dai, J., et al. (2003). Macrophage metalloelastase mediates acute cigarette smoke-induced inflammation via tumor necrosis factor- α release. *Am. J. Respir. Crit. Care Med.* 167, 1083–1089. doi:10.1164/rccm.200212-1396OC
- Deb, U., Lomash, V., Raghuvanshi, S., Pant, S. C., and Vijayaraghavan, R. (2012). Effects of 28 days silicon dioxide aerosol exposure on respiratory parameters, blood biochemical variables and lung histopathology in rats. *Environ. Toxicol. Phar* 34, 977–984. doi:10.1016/j.etap.2012.07.009
- Dinakar, C., and O'Connor, G. T. (2016). The health effects of electronic cigarettes. *New Engl. J. Med.* 375, 1372–1381. doi:10.1056/NEJMr1502466
- Fogt, D. L., Levi, M. A., Rickards, C. A., Stelly, S. P., and Cooke, W. H. (2016). Effects of acute vaporized nicotine in non-tobacco users at rest and during exercise. *Int. J. Exerc. Sci.* 9, 607–615.
- Garcia-Arcos, I., Geraghty, P., Baumlin, N., Campos, M., Dabo, A. J., Jundi, B., et al. (2016). Chronic electronic cigarette exposure in mice induces features of COPD in a nicotine-dependent manner. *Thorax* 71 (12), 1119–1129. doi:10.1136/thoraxjnl-2015-208039
- Ghorani, V., Boskabady, M. H., Khazdair, M. R., and Kianmehr, M. (2017). Experimental animal models for COPD: A methodological review. *Tob. Induc. Dis.* 15, 25. doi:10.1186/s12971-017-0130-2
- Glynos, C., Bibli, S. I., Katsaounou, P., Pavlidou, A., Magkou, C., Karavana, V., et al. (2018). Comparison of the effects of e-cigarette vapor with cigarette smoke on lung function and inflammation in mice. *Am. J. Physiol. Lung Cell Mol. Physiol.* 315, L662–L672. doi:10.1152/ajplung.00389.2017
- Goniewicz, M. L., Knysak, J., Gawron, M., Kosmider, L., Sobczak, A., Kurek, J., et al. (2014). Levels of selected carcinogens and toxicants in vapour from electronic cigarettes. *Tob. Control* 23, 133–139. doi:10.1136/tobaccocontrol-2012-050859
- Gouma, E., Simos, Y., Verginadis, I., Lykoudis, E., Evangelou, A., and Karkabounas, S. (2012). A simple procedure for estimation of total body surface area and determination of a new value of Meeh's constant in rats. *Lab. Anim.* 46 (1), 40–45. doi:10.1258/la.2011.011021
- Gross, C. M., Kovacs-Kasa, A., Meadows, M. L., Cherian-Shaw, M., Fulton, D. J., and Verin, A. D. (2020). Adenosine and ATPyS protect against bacterial pneumonia-induced acute lung injury. *Sci. Rep.* 10, 18078. doi:10.1038/s41598-020-75224-0

Funding

This research was funded by the National Major Special Projects for the Creation and Manufacture of New Drugs (grant number 2018ZX09301031-001).

Acknowledgments

We thank the New Drug Research and Development Center, School of Pharmaceutical Science, Sun Yat-sen University, and the Medical Laboratory Animal Center of Sun Yat-sen University for their help in the project.

Conflict of interest

Authors KD, XY, and XJ Shenzhen RELX Tech Co., Ltd.

The remaining authors declare that the research was conducted in the absence of any commercial or financial relationships that could be construed as a potential conflict of interest.

Publisher's note

All claims expressed in this article are solely those of the authors and do not necessarily represent those of their affiliated organizations, or those of the publisher, the editors and the reviewers. Any product that may be evaluated in this article, or claim that may be made by its manufacturer, is not guaranteed or endorsed by the publisher.

- Halloy, D. J., Kirschvink, N. A., Vincke, G. L., Hamoir, J. N., Delvaux, F. H., and Gustin, P. G. (2004). Whole body barometric plethysmography: A screening method to investigate airway reactivity and acute lung injuries in freely moving pigs. *Vet. J.* 168, 276–284. doi:10.1016/j.tvjl.2003.10.015
- Husari, A., Shihadeh, A., Tali, S., Hashem, Y., El Sabban, M., and Zaatari, G. (2016). Acute exposure to electronic and combustible cigarette aerosols: effects in an animal model and in human alveolar cells. *Nicotine Tob. Res.* 18, 613–619. doi:10.1093/ntr/ntv169
- Jobse, B. N., Rhem, R. G., Wang, I. Q., Counter, W. B., Stämpfli, M. R., and Labiris, N. R. (2013). Detection of lung dysfunction using ventilation and perfusion SPECT in a mouse model of chronic cigarette smoke exposure. *J. Nucl. Med.* 54, 616–623. doi:10.2967/jnumed.112.111419
- Kalkhoran, S., and Glantz, S. A. (2016). E-Cigarettes and smoking cessation in real-world and clinical settings: A systematic review and meta-analysis. *Lancet Resp. Med.* 4, 116–128. doi:10.1016/S2213-2600(15)00521-4
- Khlstov, A., and Samburova, V. (2016). Flavoring compounds dominate toxic aldehyde production during E-cigarette vaping. *Environ. Sci. Technol.* 50 (23), 13080–13085. doi:10.1021/acs.est.6b05145
- Kogel, U., Wong, E. T., Szostak, J., Tan, W. T., Lucci, F., Leroy, P., et al. (2021). Impact of whole-body versus nose-only inhalation exposure systems on systemic, respiratory, and cardiovascular endpoints in a 2-month cigarette smoke exposure study in the ApoE^{-/-} mouse model. *J. Appl. Toxicol.* 41 (10), 1598–1619. doi:10.1002/jat.4149
- Lam, D. C. L., Nana, A., Eastwood, P. R., and Apss, (2014). Electronic cigarettes: 'Vaping' has unproven benefits and potential harm. *Respirology* 19, 945–947. doi:10.1111/resp.12374
- Larcombe, A. N., Janka, M. A., Mullins, B. J., Berry, L. J., Bredin, A., and Franklin, P. J. (2017b). The effects of electronic cigarette aerosol exposure on inflammation and lung function in mice. *Am. J. Physiol. Lung Cell Mol. Physiol.* 313, L67–L79. doi:10.1152/ajplung.00203.2016
- Larcombe, A. N., Janka, M. A., Mullins, B. J., Berry, L. J., Bredin, A., and Franklin, P. J. (2017a). The effects of electronic cigarette aerosol exposure on inflammation and lung function in mice. *Am. J. Physiology-Lung Cell. Mol. Physiology* 313 (1), L67–L79. doi:10.1152/ajplung.00203.2016
- Lerner, C. A., Sundar, I. K., Yao, H., Gerloff, J., Ossip, D. J., McIntosh, S., et al. (2015). Vapors produced by electronic cigarettes and e-juices with flavorings induce toxicity, oxidative stress, and inflammatory response in lung epithelial cells and in mouse lung. *PLoS One* 10, e0116732. doi:10.1371/journal.pone.0116732
- Li, L., Lin, Y., Xia, T., and Zhu, Y. (2020). Effects of electronic cigarettes on indoor air quality and health. *Annu. Rev. Public Health* 41 (1), 363–380. doi:10.1146/annurev-publhealth-040119-094043
- Margham, J., McAdam, K., Forster, M., Liu, C., Wright, C., Mariner, D., et al. (2016). Chemical composition of aerosol from an E-cigarette: A quantitative comparison with cigarette smoke. *Chem. Res. Toxicol.* 29 (10), 1662–1678. doi:10.1021/acs.chemrestox.6b00188
- Marian, C., O'Connor, R. J., Djordjevic, M. V., Rees, V. W., Hatsukami, D. K., and Shields, P. G. (2009). Reconciling human smoking behavior and machine smoking patterns: implications for understanding smoking behavior and the impact on laboratory studies. *Cancer Epidemiol. Biomarkers Prev. A Publ. Am. Assoc. Cancer Res.* 18 (12), 3305–3320. doi:10.1158/1055-9965.EPI-09-1014
- Misra, M., Leverette, R. D., Cooper, B. T., Bennett, M. B., and Brown, S. E. (2014). Comparative *in vitro* toxicity profile of electronic and tobacco cigarettes, smokeless tobacco and nicotine replacement therapy products: E-Liquids, extracts and collected aerosols. *Int. J. Environ. Res. Public Health* 11 (11), 11325–11347. doi:10.3390/ijerph111111325
- Morean, M. E., Butler, E. R., Bold, K. W., Kong, G., Camenga, D. R., Cavallo, D. A., et al. (2018). Preferring more e-cigarette flavors is associated with e-cigarette use frequency among adolescents but not adults. *PLOS ONE* 13 (1), e0189015. doi:10.1371/journal.pone.0189015
- Moriya, R. (2016). Optogenetic silencing of selected serotonin neurons in the control of CO₂-induced arousal. *Eur. Respir. J.* 48, 2299.
- Onishi, M., Kobayashi, T., D'Alessandro-Gabazza, C. N., Fujimoto, H., Chelakkot-Govindalayathil, A. L., Takahashi, Y., et al. (2018). Mice overexpressing latent matrix metalloproteinase-2 develop lung emphysema after short-term exposure to cigarette smoke extract. *Biochem. Biophys. Res. Commun.* 497, 332–338. doi:10.1016/j.bbrc.2018.02.081
- Pearson, J. L., Richardson, A., Niaura, R. S., Vallone, D. M., and Abrams, D. B. (2012). E-cigarette awareness, use, and harm perceptions in US adults. *Am. J. Public Health* 102, 1758–1766. doi:10.2105/AJPH.2011.300526
- Pisinger, C., and Dossing, M. (2014). A systematic review of health effects of electronic cigarettes. *Prev. Med.* 69, 248–260. doi:10.1016/j.ypmed.2014.10.009
- Prochaska, J. J., Vogel, E. A., and Benowitz, N. (2022). Nicotine delivery and cigarette equivalents from vaping a JUULpod. *Tob. Control* 31 (1), e88–e93. doi:10.1136/tobaccocontrol-2020-056367
- Rahman, I. (2003). Oxidative stress, chromatin remodeling and gene transcription in inflammation and chronic lung diseases. *J. Biochem. Mol. Biol.* 36, 95–109. doi:10.5483/bmbrep.2003.36.1.095
- Rom, O., Pecorelli, A., Valacchi, G., and Reznick, A. Z. (2015). Are E-cigarettes a safe and good alternative to cigarette smoking? *Ann. N. Y. Acad. Sci.* 1340, 65–74. doi:10.1111/nyas.12609
- Romo, D., Velmurugan, K., Upham, B. L., Dwyer-Nield, L. D., and Bauer, A. K. (2019). Dysregulation of gap junction function and cytokine production in response to non-genotoxic polycyclic aromatic hydrocarbons in an *in vitro* lung cell model. *Cancers (Basel)* 11, 572. doi:10.3390/cancers11040572
- Selya, A. S., Dierker, L., Rose, J. S., Hedeker, D., and Mermelstein, R. J. (2018). The role of nicotine dependence in E-cigarettes' potential for smoking reduction. *Nicotine Tob. Res.* 20, 1272–1277. doi:10.1093/ntr/ntx160
- Serré, J., Tanjeko, A. T., Mathysen, C., Vanherwegen, A.-S., Heigl, T., Janssen, R., et al. (2021). Enhanced lung inflammatory response in whole-body compared to nose-only cigarette smoke-exposed mice. *Respir. Res.* 22 (1), 86. doi:10.1186/s12931-021-01680-5
- Stratton, K., Kwan, L. Y., and Eaton, D. L. (2018). *Public health consequences of E-cigarettes*. Washington, D.C., United States: National Academies Press.
- Sussan, T. E., Gajghate, S., Thimmulappa, R. K., Ma, J., Kim, J. H., Sudini, K., et al. (2015). Exposure to electronic cigarettes impairs pulmonary anti-bacterial and anti-viral defenses in a mouse model. *PLoS One* 10, e0116861. doi:10.1371/journal.pone.0116861
- Szafran, B. N., Pinkston, R., Perveen, Z., Ross, M. K., Morgan, T., Paulsen, D. B., et al. (2020). Electronic-cigarette vehicles and flavoring affect lung function and immune responses in a murine model. *Int. J. Mol. Sci.* 21, 6022. doi:10.3390/ijms21176022
- Taboulsi, H., Cherian, M., Abou Rjeili, M., Preteroti, M., Bourbeau, J., Smith, B. M., et al. (2020). Inhalation toxicology of vaping products and implications for pulmonary health. *Int. J. Mol. Sci.* 21, 3495. doi:10.3390/ijms21103495
- Van Hoecke, L., Job, E. R., Saelens, X., and Roose, K. (2017). Bronchoalveolar lavage of murine lungs to analyze inflammatory cell infiltration. *J. Vis. Exp.* 55398. doi:10.3791/55398
- Vardavas, C. I., Anagnostopoulos, N., Kougias, M., Evangelopoulou, V., Connolly, G. N., and Behrakis, P. K. (2012). Short-term pulmonary effects of using an electronic cigarette impact on respiratory flow resistance, impedance, and exhaled nitric oxide. *Chest* 141, 1400–1406. doi:10.1378/chest.11-2443
- Wagner, N. J., Camerota, M., and Propper, C. (2017). Prevalence and perceptions of electronic cigarette use during pregnancy. *Matern. Child. Hlth J.* 21, 1655–1661. doi:10.1007/s10995-016-2257-9
- Wang, D. (2019). Construction of animal models of inhalation lung injury: A review. *Chin. J. Comp. Med.* 29, 126–130.
- Zalokar, J. B. (1979). Pulmonary dysfunction, smoking, and coronary heart-disease. *Lancet* 1, 1348–1349. doi:10.1016/s0140-6736(79)91979-2
- Zheng, J. H., Jin, Y. L., and Zou, Z. Y. (2019). Effect contrast of conventional HE staining and HE staining of environmental protection reagent. *China Med. Equip.* 16, 99–102.



OPEN ACCESS

EDITED BY

Ewelina Hoffman,
ImmuONE, United Kingdom

REVIEWED BY

Anna Babin Morgan,
Kingston University, United Kingdom
Otto Creutzenberg,
Fraunhofer Institute for Toxicology and
Experimental Medicine (FHG), Germany

*CORRESPONDENCE

Heidi Stratmann,
✉ heidi.stratmann@sunchemical.com

RECEIVED 14 July 2023

ACCEPTED 03 November 2023

PUBLISHED 05 December 2023

CITATION

Stratmann H, Ma-Hock L, Tangermann S
and Corley RA (2023), Refinement of the
acute inhalation limit test for inert, nano-
sized dusts by an *in silico* dosimetry-
based evaluation: case study for the
dissolution of a regulatory dilemma.
Front. Toxicol. 5:1258861.
doi: 10.3389/ftox.2023.1258861

COPYRIGHT

© 2023 Stratmann, Ma-Hock,
Tangermann and Corley. This is an open-
access article distributed under the terms
of the [Creative Commons Attribution
License \(CC BY\)](https://creativecommons.org/licenses/by/4.0/). The use, distribution or
reproduction in other forums is
permitted, provided the original author(s)
and the copyright owner(s) are credited
and that the original publication in this
journal is cited, in accordance with
accepted academic practice. No use,
distribution or reproduction is permitted
which does not comply with these terms.

Refinement of the acute inhalation limit test for inert, nano-sized dusts by an *in silico* dosimetry-based evaluation: case study for the dissolution of a regulatory dilemma

Heidi Stratmann^{1*}, Lan Ma-Hock ^{2†}, Simone Tangermann² and Richard A. Corley ^{3†}

¹Colors and Effects Switzerland AG Efringerstrasse, Basel, Switzerland, ²Experimental Toxicology and Ecology, BASF SE, Ludwigshafen, Germany, ³Greek Creek Toxicokinetics Consulting, LLC, Boise, ID, United States

This case study aims to describe the dilemma faced when exposing rats to very high concentrations of fine, pulverulent materials for acute inhalation studies and to address the regulatory question of whether the effects seen here are relevant to humans and the subject of classification according to the Globally Harmonized System of Classification and Labeling of Chemicals (GHS). Many powders match the definition of nanomaterials in the EU; therefore, information on acute inhalation testing of powders up to the GHS cutoff of 5 mg/L is required. However, testing rats at such a high aerosol concentration can cause physical obstruction of the airways and even mortality by suffocation. Therefore, to evaluate whether the physical effects on airway obstruction in rats exposed to 5 mg/L for 4 hours and alternative exposures to 1 and 2 mg/L are relevant for humans, an *in silico* evaluation of aerosol deposition was conducted using the multiple-path particle dosimetry (MPPD) model. For this evaluation, actual exposure conditions for an organic, nano-sized pigment which produced 100% lethality in rats at 5 mg/L, but not at 1 mg/L, were used to assess the potential for airway obstruction in rats and accordingly in humans. As an indicator of the potential for airway obstruction, the ratio of the diameter of the deposited, aggregated aerosol to airway diameter was calculated for each exposure condition. For rats exposed to 5 mg/L for 4 h, approximately 75% of tracheobronchial and 22% of pulmonary/alveolar airways were considered vulnerable to significant or complete obstruction (ratios >0.5). In humans, an equivalent exposure resulted in just over 96% of human tracheobronchial airways that received deposited mass to airway diameter ratios between 0.3 and 0.4 (nasal) or 0.4 and 0.5 (oral), with no airways with ratios >0.5. For the pulmonary/alveolar region, ~88% of the airways following nasal or oral breathing were predicted to have deposited aerosol diameter to airway diameter ratios <0.1, with no airways with ratios >0.5. Thus, the *in silico* results obtained for rats are in line with the

pathological findings of the animal test. The predicted results in humans, however, affirm the hypothesis of a rat-specific high dose effect which does not justify a classification according to GHS.

KEYWORDS

MPPD, aerosol deposition, acute inhalation testing, REACH, GHS, nanomaterial, modeling, dust

1 Introduction

When REACH came into force in 2007, producers and importers of chemicals in Europe began to register their substances according to this new regulation. One of the key points of REACH is “no data, no market.” Thus, affected companies collected and evaluated existing experimental data required for the registration deadlines, with the relevant deadline depending on the tonnage. The REACH regulation was amended in 2020 by the notification obligation for nanomaterials. With this amendment, acute inhalation testing was no longer an option depending on the most likely route of exposure but a mandatory information requirement even for low-volume substances.

For poorly soluble particles that are either known or expected to be virtually non-toxic, the current OECD guidelines for acute inhalation toxicity assessments incorporate a limit test concentration for aerosols (OECD, 2009). Depending upon the regulatory requirements, the limit test concentration for aerosols can be as high as 5 mg/L (or the maximum attainable concentration) if the United Nations (UN) Globally Harmonized System of Classification and Labeling of Chemicals (GHS) is applied. The OECD guidance document for inhalation toxicity testing (OECD, 2018) points out that the GHS limit concentration of 5 mg/L is technically challenging for most aerosols and exceeds real-world human exposure. A maximum aerosol concentration of 2 mg/L is therefore recommended. However, according to the GHS, an exposure concentration below 5 mg/L is a criterion for placement in hazard category 4 and labeling as “harmful after inhalation,” even if no mortality was observed. Thus, the regulatory thresholds for classification and labeling are at this point in contradiction with the recommendations of the OECD guidelines. Eventually, the registrant of a nanomaterial is forced to weigh the OECD recommendations and animal welfare against a possible erroneous classification for product labeling.

The aim of this case study is to examine whether *in vivo* effects of obstructed airway-induced lethality observed in a recently conducted, regulatory-required acute inhalation toxicity study in rats with an organic, nano-sized pigment (Wittmer et al., 2021) are relevant for toxicity classification and labeling. Similar findings of airway obstruction in rats following acute inhalation exposures have also been observed in the past for other organic, nano-sized pigments (Hofmann et al., 2018). This latest toxicity study by Wittmer et al. thus prompted the need for additional evaluations beyond those by Hoffmann et al. regarding the importance of physicochemical properties in causing airway obstruction to include an *in silico* analysis of aerosol dosimetry. We therefore used the well-established multiple-path particle dosimetry (MPPD)

model to provide a respiratory dosimetry assessment of the potential for airway obstruction following *in vivo* exposures of rats and humans to aerosols under the relevant aerosol exposure conditions used in Wittmer et al. (2021).

It is widely recognized that external exposure concentrations of airborne particulates are not directly equivalent to the amount that is inhaled, deposited, and retained in airways of laboratory animals *versus* humans due to major differences in airway anatomy and physiology (c.f. Menache et al., 1995; Werner and Asgharian, 2003; Tawhai et al., 2004; Brown et al., 2005; Phalen and Mendez, 2009; Miller et al., 2016; Bevan et al., 2018; Corley et al., 2021). Without factoring in these differences across species, the results from inhalation toxicity studies may not be directly translatable to human health risk. As a result, computational approaches such as MPPD that combine species-specific data and the physics of aerosol transport and deposition are increasingly utilized by regulatory agencies to carry out their assessments (c.f. EPA, 2021).

The purpose of our computational approach using MPPD is to provide a generic aerosol respiratory dosimetry assessment tool for calculating the potential for airway obstruction in rats using the physical attributes of aerosol exposure (e.g., concentration, size, density, and duration) from the acute toxicity case study. Emphasis was placed on estimations of particle load in individual airways following multiple acute exposures to assess the potential for physical obstruction of bronchial and terminal pulmonary airways in rats due to high rates of local aerosol deposition, and the resulting challenges for study interpretation and product classification and labeling. For comparison, human simulations for 5 mg/L exposure were also conducted to highlight cross-species differences in regional and airway-specific deposition where lethality was observed in rats. In this way, we hope to encourage future action to resolve the discrepancies between regulatory classification and guidelines for acute inhalation toxicity testing requirements and thereby reduce unnecessary testing in laboratory animals, especially when airway obstruction-induced lethality can be anticipated.

2 Materials and methods

2.1 Test material

An organic pigment, CAS 27614-71-7, was used as the test item in the acute inhalation toxicity study in rats. The sample is handled as blue powder (median D50 14.9 nm) having a purity of >99%. Although the test material mainly consisted of nano-sized particles, the need to comply with the high atmospheric concentration stipulated by the OECD test guideline 403 limit test led to

TABLE 1 Species, physiology, and aerosol properties used in each MPPD simulation.

Species	Position	Physiology				Aerosol properties				
		Breathing modality	Activity	Tidal Vol. (ml/breath)	Frequency (BPM)	Conc. (mg/m ³)	MMAD (μm)	GSD	Density (g/cm ³)	Inhalability adjustment (yes/no)
SD rat, asymmetric, 300 g BW	Upright	Nose only	Resting	2.12614 (scaled by BW)	166	5212 ^a	2.74 ^a	2.8 ^a	1.0	Yes
SD rat, asymmetric, 300 g BW	Upright	Nose only	Resting	2.12614 (scaled by BW)	166	2000 ^b	2.01	3.0	1.0	Yes
SD rat, asymmetric, 300 g BW	Upright	Nose only	Resting	2.12614 (scaled by BW)	166	1084 ^a	2.01 ^a	3.0 ^a	1.0	Yes
Human, Yeh and Schum, symmetric	Upright	Nasal	Resting	625 (default)	12 (default)	5212	2.74	2.8	1.0	No
Human, Yeh and Schum, symmetric	Upright	Oral	Resting	625 (default)	12 (default)	5212	2.74	2.8	1.0	No

^aExposure conditions from Wittmer et al. (2021).

^bOECD, recommended alternate limit test exposure concentration (OECD, 2009).

substantial and inevitable agglomeration of particles. As a result, the test atmosphere contained micro-sized agglomerates/particles instead (Wittmer et al., 2021).

2.2 Acute inhalation study

According to OECD guideline 403, male and female Wistar rats were exposed by inhalation to dust atmosphere of the test substance in two sequential experiments at gravimetrically determined concentrations of 5.212 mg/L and 1.084 mg/L. No mortality was observed at 1.084 mg/L, but all animals exposed to 5.212 mg/L died either during exposure or on study days 1–2 post-exposure. Therefore, gross pathological examinations were performed on all animals, and histological examinations of the respiratory tract were performed in three representative dead male and female rats (Wittmer et al., 2021). A summary of the study design, exposure generation and characterization, and results are provided in the [Supplementary Material](#).

2.3 Choice of the *in silico* model

The MPPD model developed for calculating the deposition and clearance of inhaled insoluble particles was utilized for this dosimetry-based analysis of the limit test exposure conditions for poorly soluble, low-toxicity materials to meet the regulatory requirements of GHS (OECD, 2009). The MPPD model was chosen as it is a mechanistic model that combines many of the complexities of species-specific anatomy, physiology, and aerosol physics in an easy-to-use platform for personal computers.

Two versions of the model were available and utilized for this project: (a) the public version (v3.041), which can be obtained freely from Applied Research Associates (ARA; <https://www.ara.com/>

[mppd/](#)), and (b) a modification of the public version obtained from ARA (v 3.24C57) that fixed an issue with the asymmetric Sprague–Dawley rat airway geometry used in the model for the head region.

2.4 MPPD input conditions for aerosol dosimetry in rats

While the acute inhalation test case study was carried out on Wistar rats, the MPPD model is currently configured only for Sprague–Dawley and Long Evans rat strains. Due to their age- and body weight-dependent anatomic similarities, the MPPD model for Sprague–Dawley rats was used to determine regional and airway-specific aerosol deposition representative of a guideline limit test acute inhalation toxicity study (OECD, 2009). Specifically, a 4-hr nose-only inhalation exposure to aerosol particles with mass median aerosol diameters (MMADs), geometric standard deviations (GSDs), and aerosol concentrations from the Wittmer et al. acute toxicity study were simulated along with an additional aerosol concentration (2 mg/L) that is recommended for an alternative limit test. For rats simulations, breathing physiology used MPPD's default, resting physiology for a male Sprague–Dawley rat adjusted for a body weight of 300 g was used (Table 1). Simulations were not performed for female Sprague–Dawley rats as results would be similar as MPPD provides for adjustments in anatomy and physiology for the lower body weights (Miller et al., 2014). Since the inhalability of aerosol particles in rats decreases for particles >1 μm MMAD (Ménache et al., 1995), inhalability correction was used in all rat simulations.

The asymmetric (multiple-path) Sprague–Dawley rat model in MPPD was used to provide a detailed (airway-specific) analysis of the heterogeneity of aerosol deposition across the lungs. This feature (asymmetry) is particularly important for rats due to their

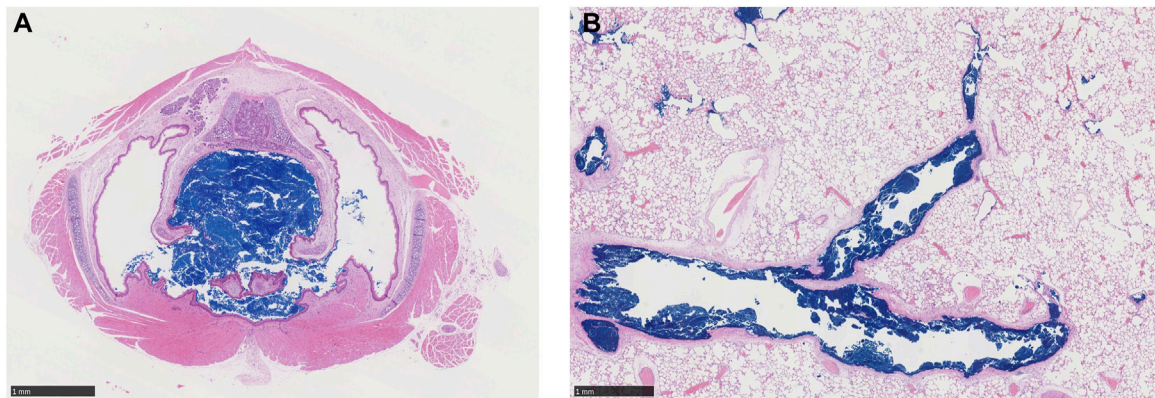


FIGURE 1

Representative histology sections (H&E stain, x20 magnification, black bar scale of 1 mm in each panel) through (A) larynx level 1 and (B) lungs of a male rat showing accumulation of deposited copper phthalocyanine pigment (dark blue) in respiratory airways and complete obstruction of the larynx during an acute, 4-h exposure to 5.212 mg/L aerosol (Wittmer et al., 2021).

monopodial branching patterns, where a significant number of respiratory bronchioles and alveolar regions branch off from early generations of conducting airways, unlike the symmetric model included in MPPD where terminal alveolar regions are represented only in the final eight generations of each tracheobronchial conducting airway.

2.5 MPPD input conditions for aerosol dosimetry in humans

Human simulations were conducted under the same aerosol exposure conditions used for rats simulation (high concentration) as this was the only concentration associated with mortality in the study of acute inhalation exposures in rats. Since humans are not obligate nose-breathers like rats and potential human exposures to many aerosols may occur under both residential and occupational exposure conditions, both nasal and oral breathing were simulated under resting conditions (ICRP, 1994) (Table 1). The Yeh and Schum symmetric (typical path) model was used for all simulations as this is the recommended default human geometry by the U.S. EPA (EPA, 2021). The inhalability of aerosols in humans decreases for particles $>10\ \mu\text{m}$ MMAD (Menache et al., 1995), so inhalability correction was not necessary for these simulations.

2.6 Calculating the potential for airway obstruction

In addition to a variety of potential aerosol dose metrics, such as the fraction, mass, particle number, particle surface area, or volume of inhalable particle deposition by region or airway or airway surface area, MPPD also provides airway-segment and/or generation-specific calculations of deposited aerosol volume and mass depending on the choice of the model, exposure conditions, and aerosol properties. As an indicator of the potential for airway obstruction, ratios of the diameter of the deposited, aggregated aerosol, calculated from the volume or mass of the aerosol

deposited in each airway, to the diameter of the corresponding airway were calculated for each exposure condition.

3 Results

3.1 Results of the acute inhalation study

Cascade impactor measurements resulted in mass median aerodynamic diameters (MMADs) between 1.93 and 2.98 μm , with high fractions of particles $< \text{MMAD } 3\ \mu\text{m}$. The particles were larger at high concentration than at low concentration, which was unavoidable due to agglomeration. When exposed to 5.212 mg/L, all animals died either during exposure or during the first 2 days after the exposure, while no animals died when exposed to 1.084 mg/m³ (Wittmer et al., 2021). Clinical signs of toxicity comprised accelerated, abdominal respiration and respiration sounds of different severity patterns and durations, indicating impairment of respiration. There were no substance-related gross pathological findings in the surviving animals at the end of the post-exposure observation period (day 14). In animals that died, many black foci were seen in the lung lobes with a sunken surface. Blue discoloration of the content of the stomach was seen in four males and three females, and blue depositions in the trachea were present in four males and two females (Supplementary Table S1.2). There were no gross pathological changes in the remote organs of these prematurely dead animals. Since this was a guideline toxicity study, histological examinations were carried out only on rats that died during exposure or during the 2-week post-exposure observation period. These examinations revealed that large amounts of blue pigment were deposited in the larynx, bronchi, bronchioles, and terminal bronchioles, causing obstruction of the airway and subsequently leading to death (Figure 1 and Supplementary Table S1.3). In the nasal cavity, small to moderate amounts of the blue pigment were observed. Based on the lethality rate, clinical signs of toxicity, body weight development, and gross necropsy, there were no differences in response between male and female animals.

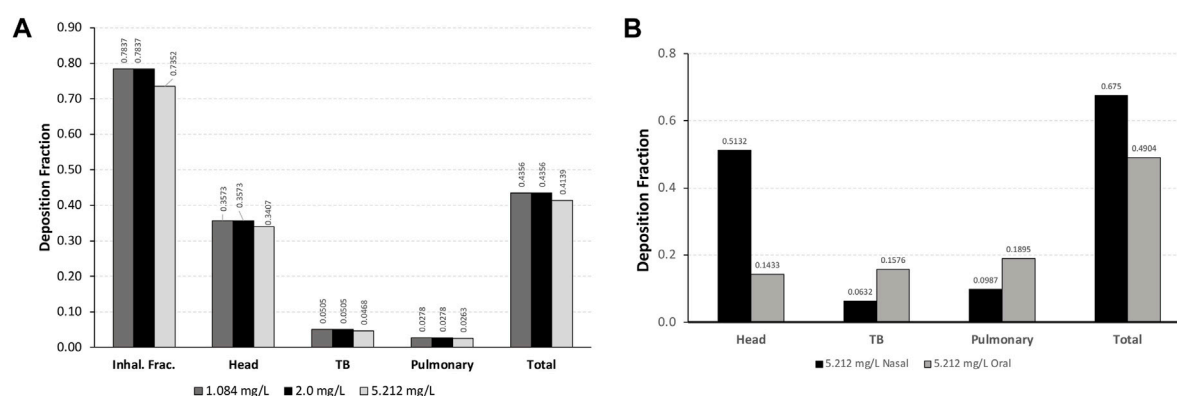


FIGURE 2

Comparisons of the inhalable fraction (rat only) and deposition fractions of aerosol particles in each region of (A) a asymmetric Sprague–Dawley rat following a 4-h exposure to aerosol concentrations of 1.084, 2.0, and 5.212 mg/L and (B) Yeh and Schum symmetric human models following nasal and oral breathing at 5.212 mg/L under resting ventilation conditions. For human simulations, the inhalable fraction of particle sizes at 5.212 mg/L was 1.0 (see Table 1 for simulation details).

3.2 *In silico* aerosol deposition in rats

For each exposure, 41–44% of the total inhalable particles deposited in the head (~34–35%; nose through larynx/throat), conducting airways in the chest (~5%; tracheobronchial, TB), and pulmonary/alveolar (~3%) regions in the Asymmetric rat models (Figure 2A). In the chest region in the asymmetric Sprague–Dawley rat model, tracheobronchial airways cover the first 28 generations (generation 1 representing the trachea), with the pulmonary airways branching off of the tracheobronchial airways from generations 8 to 28 and an additional eight generations terminating each complete tracheobronchial airway for a total of 36 generations (Figure 2A). Airway generation-specific deposition over the entire lung is shown in Figure 3A. However, the distribution of particles deposited at each generation varied up to an order of magnitude between the lobes (Figure 3B), reflecting the realistic monopodial airway branching and geometry measured from lung casts used in the MPPD asymmetric Sprague–Dawley rat model (Schroeter et al., 2012; Miller et al., 2014).

3.3 Potential for obstructive disruption of airway function in rats

While MPPD is not designed to specifically address the question of whether deposited aerosols can be of sufficient magnitude to alter local airflows and thus *pulmonary* function (i.e., gas exchange), the significant amounts of aerosol that deposit in individual tracheobronchial and pulmonary regions of the asymmetric Sprague–Dawley rat simulations suggest that the potential for disruption in airflows and lung function is possible or even likely. To assess this possibility, the total mass and volume of aerosol particles deposited in each tracheobronchial and pulmonary airway over the 4-h exposure were assumed to coalesce into a single spherical volume whose dimensions (diameter) were then compared with each corresponding airway diameter. While MPPD has no equations describing the influence of particles on airflows, significant deposition and accumulation

certainly occurs in discrete regions within each airway over a 4-h exposure. This comparative calculation from MPPD currently ignores this potential effect on local airflow that would enhance deposition in proximal airways rather than allowing aerosols to penetrate distally without obstruction.

Given this scenario, the ratios of the theoretical diameter of the total deposited mass in each airway to its corresponding airway diameter in the asymmetric Sprague–Dawley rat simulations were determined at the end of the 4-h exposure. In this model, the ratios of deposited aerosol volume diameters to the corresponding diameter of each airway in the tracheobronchial and pulmonary regions show a significant number of airways with ratios >0.5 and, in many cases, ratios significantly >1.0 (fully blocked) after exposure to 5.212 mg/L (Figure 4).

The total number of airways and the percentage of airways were sorted into quartile intervals of the ratio of deposited volume to airway diameter ranging from 0 to 0.25, 0.25 to 0.5, 0.5 to 0.75, 0.75 to 1.0, and >1.0 to gauge the relative potential for biologically significant airway obstruction following exposures to 1.084 and 5.212 mg/L of aerosols and the alternative limit test concentration of 2 mg/L (Figure 5). At the highest exposure, 5.212 mg/L, with 100% mortality in the acute inhalation study, most airways in the tracheobronchial region (4,699 airways or 59.1%) had diameter ratios between 0.5 and 0.75, 8.6% (685 airways) had ratios between 0.75 and 1.0, and 7.7% of airways (613 airways) had ratios >1.0. In the pulmonary region, the number and percentages of airways having ratios >0.5 were smaller than that predicted for the tracheobronchial region, at just over 22% (7,034 airways). However, there were numerous airways with deposited aerosol volume to airway diameter ratios significantly greater than 1.0, some with ratios up to 28. These high ratios are consistent with the number of airways that branch off from the upper bronchiolar airways (Miller et al., 2014), indicating greater exposure potential for aerosols in these locations (Figure 4).

At the lowest concentration used in the acute inhalation toxicity study (1.084 mg/L) with no mortality and at 2 mg/L, which has been suggested by OECD as an alternative limit test concentration, there was a shift toward greater numbers and percentages of airways with

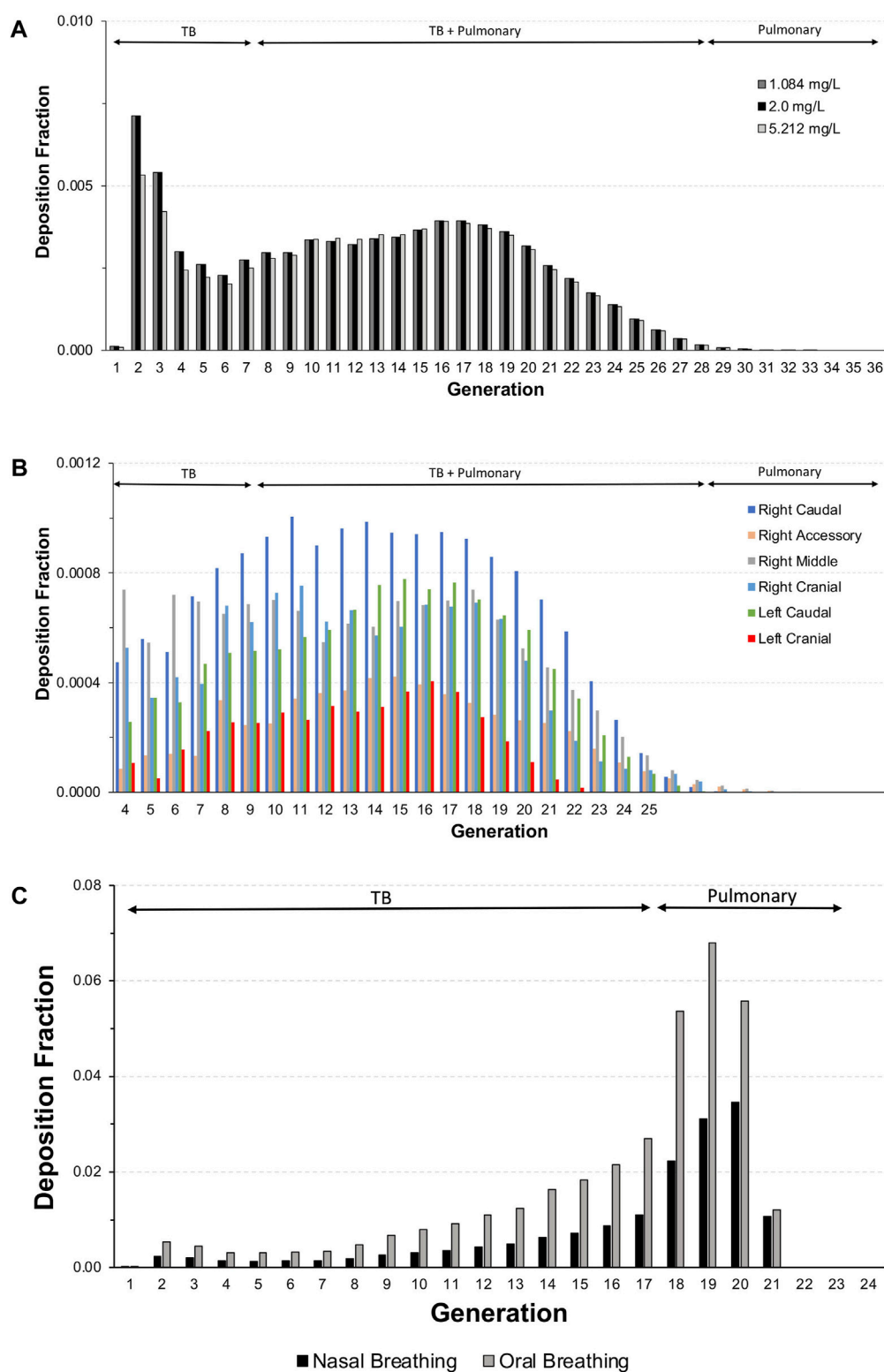


FIGURE 3

Deposition fractions in each generation of the lung (sum of all tracheobronchial and pulmonary airways in each generation) in (A) the entire lung and (B) individual lobes of the asymmetric Sprague–Dawley rat model following a 4-h exposure to aerosol concentrations of 1.084, 2.0, and 5.212 mg/L and (C) the Yeh and Schum human model following nasal and oral breathing (5.212 mg/L only) under resting ventilation conditions (see Table 1 for simulation details).

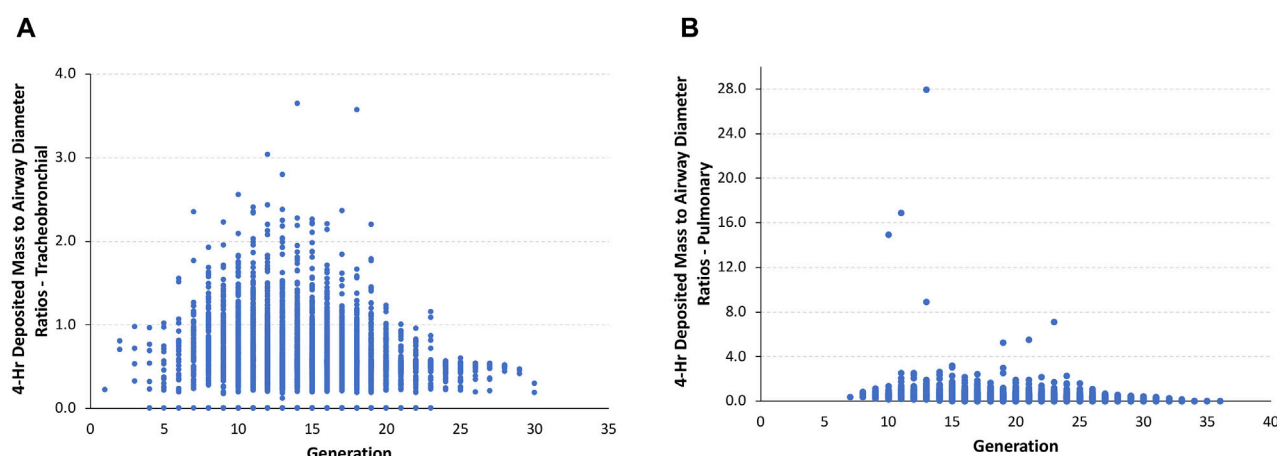


FIGURE 4

Ratios of the theoretical diameters of retained particle mass (volume) to their corresponding airway diameters in (A) tracheobronchial and (B) pulmonary airways within each generation of the asymmetric Sprague–Dawley rat models following a 4-h exposure to a limit test concentration of 5.212 mg/L aerosol.

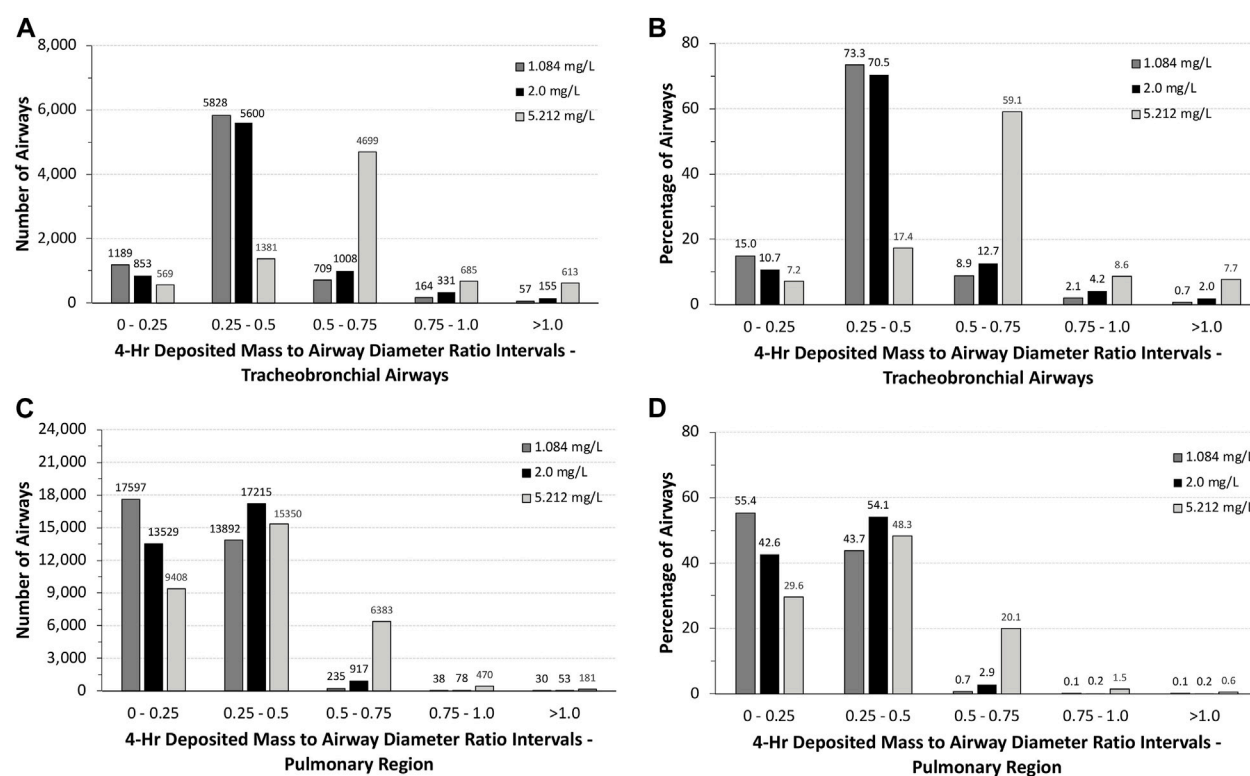
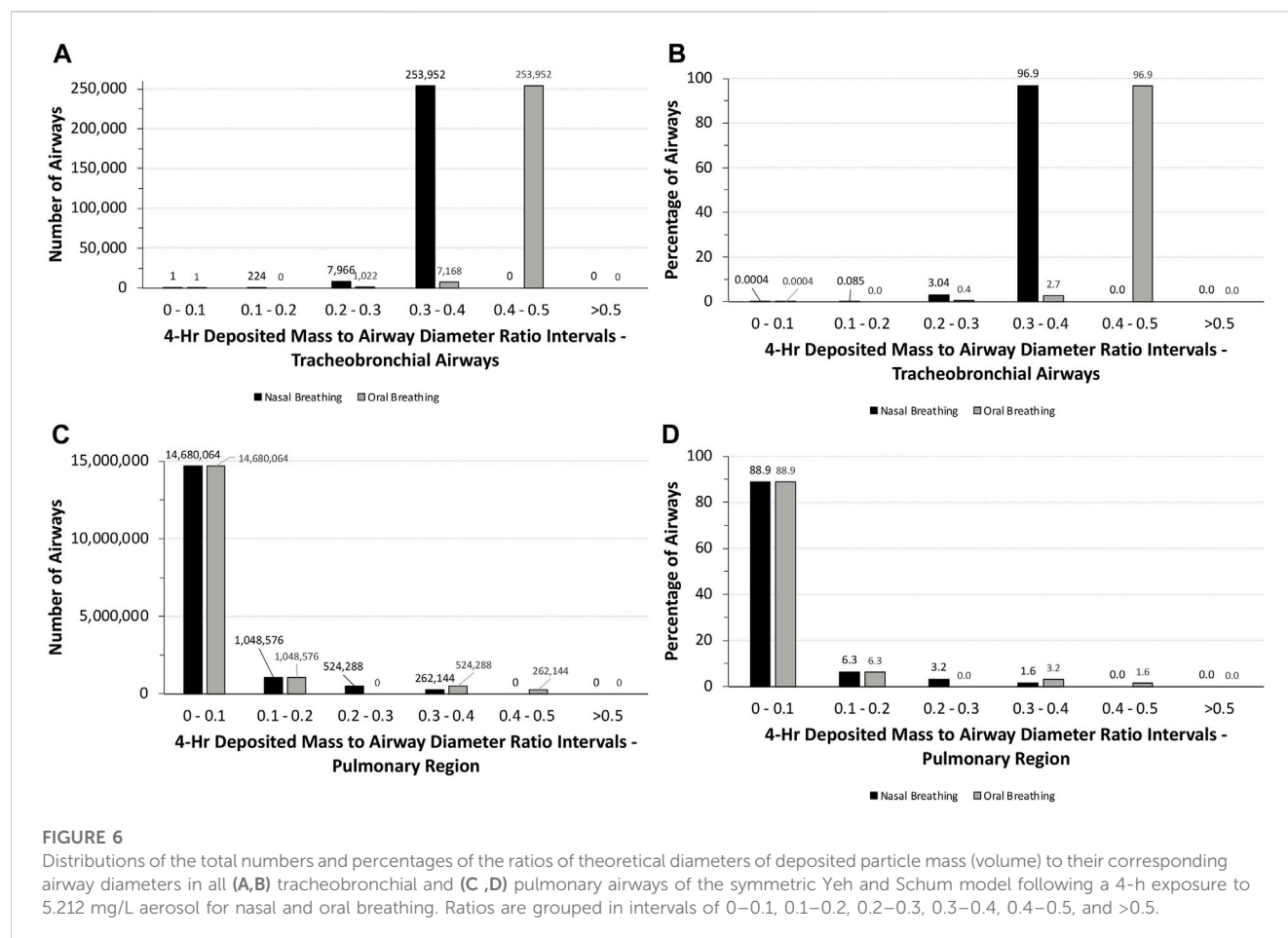


FIGURE 5

Distributions of the total numbers and percentages of the ratios of theoretical diameters of deposited particle mass (volume) to their corresponding airway diameters in all (A,B) tracheobronchial and (C,D) pulmonary airways of the asymmetric Sprague–Dawley rat model following a 4-h exposure to 1.084, 2.0, and 5.212 mg/L aerosol concentrations. Ratios are grouped in intervals of 0–0.25, 0.25–0.5, 0.5–0.75, 0.75–1.0, and >1.0.

ratios of deposited aerosol volume to airway diameters <0.5 in both tracheobronchial and pulmonary airways (Figure 5). While the number and percentages of airways with ratios >1 also significantly decreased at the two lower exposure concentrations

vs. 5.212 mg/L, there were still a significant percentage of airways with ratios >0.5 in both tracheobronchial and pulmonary airways combined (~3 to 6%), 87–208 airways (mostly tracheobronchial) with ratios >1.0, and some airways with ratios nearly 18-fold greater



than 1.0, indicating that some airways may yet be compromised by physical obstruction at lower exposure concentrations even if mortality did not occur at the lowest concentration (1.084 mg/L) in the acute inhalation study (the alternative limit test concentration of 2 mg/L was not tested in the acute inhalation study).

3.4 Aerosol dosimetry in humans

Following nasal breathing, 51.3% of the inhaled fraction of aerosols deposited in the head, while 6.3% deposited in the tracheobronchial and 9.9% in the pulmonary regions (68% total; Figure 2B). This is in contrast with oral breathing, where under resting conditions only 14.3% of the inhaled fraction of aerosols deposited in the head, with deposition increasing to 15.8% in the tracheobronchial and 19% in the pulmonary regions (49% total).

For the chest region, the symmetric Yeh and Schum human model consists of 17 generations of tracheobronchial airways (the trachea is generation 1), with seven generations of pulmonary airways appended to each terminal bronchiole airway for a total of 24 generations. In contrast to rats model, generation-specific deposition fractions for each breathing modality, especially oral breathing, indicate a significant shift in fractional deposition from the upper conducting airways toward the deeper pulmonary airways in generations 18–21 (Figure 3C). However, no deposition was

predicted for terminal alveolar generations 22–24, which contain nearly 88% of the airways in the symmetric Yeh and Schum human model. Given the large airway surface in the pulmonary region, the cumulative mass deposited in 4 h per airway surface area remained significantly lower in the pulmonary region compared to the first few generations of the tracheobronchial airways.

3.5 Potential for obstructive disruption of airway function in humans

Although humans would not be expected to tolerate unrealistic exposures to 5.212 mg/L aerosol concentration for 4 h, a similar analysis of the potential for airway obstruction was used for human simulations following nasal and oral breathing (Table 1). Under these exposure conditions, no airway had theoretical deposited mass to airway diameter ratios >0.5, with nearly 88% of all airways (~14.7 million) having ratios <0.1 (Figure 6). While the latter number was primarily associated with the pulmonary airways, nearly 790,000 airways (~4.8%) in the pulmonary region had deposited mass to airway diameter ratios between 0.2 and 0.5 depending on the breathing modality. In the tracheobronchial region, however, nearly 97% (~254,000) of airways, primarily in generations 13–18, had deposited mass to airway diameter ratios between 0.3 and 0.4 (nasal) or 0.4 and 0.5 (oral), showing the shift in penetration to deeper airways following oral breathing. Thus, there

may be some degree of potential vulnerability for airway obstruction in a significant portion of humans lung, albeit to a significantly lesser degree than that predicted for rats assuming such a theoretical exposure was even possible.

4 Discussion

The MPPD model was used to evaluate differences between rats and humans in predicted regional airway deposition and retention of an organic pigment under exposure conditions obtained from an OECD guideline acute inhalation toxicity study. Although the test material is classified as a nanomaterial, current capabilities for generating atmospheres of low mg/L concentrations, including a limit test concentration of 5 mg/L, invariably resulted in agglomeration of the nano-sized particles, resulting in aerosols ranging in size from 2.01 to 2.74 microns MMAD in the acute inhalation case study in rats (Wittmer et al., 2021; Supplementary Table S1.1). This agglomeration behavior was also observed for other organic pigments in several dustiness measurements (EN 17199-4:2019-03), with peak aerodynamic diameters ranging from 1 to 5 μm with aerodynamic diameters increasing as aerosol concentrations increased. While Wessely et al. (2022) suggested that cascade impactors are not appropriate for characterizing particle sizes of low-density powders, due to the shearing of the fragile structure of the agglomerates during impactor measurements, the material used in the case study was not a low-density material, and no significant changes in particle sizes occurred in cascade impactor measurements taken over 2 h apart.

Under these exposure conditions, only 74%–78% of the 2.01- to 2.74- μm MMAD-sized atmospheric aerosols are predicted by MPPD to be inhalable by rats, while 100% is inhalable by humans. For nasal breathing under resting ventilation conditions, approximately 34% of respirable 2.74- μm MMAD aerosols deposited in the head of rats compared to 51% in humans (14% for oral breathing).

Since MPPD uses an empirical model for the head region (nose/mouth through the larynx), deposition within this region is not determined. However, previous simulations of comparable aerosols are available to estimate local deposition within the head regions of rats and humans by applying computational fluid particle dynamic (CFPD) modeling (Corley et al., 2021). Using CFPD modeling as a guide (see Supplementary Material), inhalable aerosols from the MPPD simulations for rats are predicted to deposit in the most anterior portions of the nose (nasal vestibule and wet squamous epithelium), followed by the most anterior portions of the respiratory and transitional epithelium of the nasal turbinates and maxilloturbinates, and larynx, the latter of which is consistent with the histopathological findings in a representative rat exposed to 5.212 mg/L in the acute inhalation study (Figure 1A). For humans, the CFPD analysis indicates that the nasal respiratory epithelium and the larynx also receive the highest deposited fractions following nasal breathing, whereas the mouth and larynx receive the highest deposition fractions following oral breathing. While each of these regions has high rates of aerosol clearance (ICRP, 2015), depending on the aerosol mode of action, the nasal respiratory epithelium (nasal breathing) and larynx (both nasal and oral breathing) could represent tissues of potential

concern based on the local deposited dose in the head region of the MPPD model following exposures to high concentrations (5.212 mg/L) of aerosols of size 2.74 μm MMAD, unless cell-specific sensitivity factors across this region are known and suggest otherwise.

For the tracheobronchial region, MPPD provides both regional and generation- or airway-specific model analyses with comparable overall fractional depositions predicted for rats (~5%) vs. humans (~6%) for nasal breathing (~16% for oral breathing). Overall, there is a generally higher fractional pulmonary deposition of 2.74 μm MMAD aerosols in humans (~10–19%) than in rats (~3%). There is also a shift toward significantly less deposition in the head and higher pulmonary deposition and deeper penetration into the pulmonary airways following oral breathing in humans.

Given the observation of significant airway obstruction in rats that died during or within 2 days following the 4-h exposure to the limit test concentration of 5 mg/L (5.212 mg/L actual) that were evaluated histologically (Figure 1; Wittmer et al., 2021), the calculations of potential airway obstruction from MPPD simulations in rats were consistent with the primary cause of death in that study. Not surprisingly, many tracheobronchial and pulmonary airways in rats were predicted to be vulnerable to obstruction and at risk for impairment of normal airflow and delivery to the gas-exchange region (Figures 4, 5). This prediction also supports findings of other similar chemicals in its class (Hofmann et al., 2018). Even after lowering the concentration from 5.212 mg/L, which caused all animals to die in the case study, to 2 mg/L, an alternative limit test concentration in the OECD guideline (not tested in the case study), or 1.084 mg/L (which did not cause lethality in the case study), a significant number of tracheobronchial and pulmonary airways might still be vulnerable to at least partial obstruction, albeit at a much lower percentage. These *in silico* results for the low-dose group are in accordance with the changed respiration pattern observed *in vivo* that persisted up to day 6 post-exposure and strongly indicated the presence of the previously described partial obstruction and altered airflow of the tracheobronchial and pulmonary airways. Given that these are the only effects observed in the case study (asphyxiation and altered respiration), these are not toxicity effects *per se* and raise questions about the classification of the potential human health risk of inhalation toxicity when labeling requirements are incongruent with the realities of guideline testing.

Clearly, humans would not be expected to tolerate exposures to the high aerosol concentrations of the pigment used in rats acute inhalation toxicity study even for a short period of time, much less for 4 h. However, with MPPD, *in silico* theoretical comparison of the potential for airway obstruction in rats is possible. In this case, differences across species in airway anatomy and physiology are major factors. Given the overall larger airway sizes and lower ventilation rate per kilogram body weight, it is not surprising that nearly 88% of all tracheobronchial and pulmonary airways (~14.7 million) in humans following nasal breathing have deposited aerosol mass to airway diameter (obstruction) ratios <0.1 and ~95% with ratios no more than 0.2. No airways were predicted to have ratios greater than 0.5 (Figure 6). By comparison, more than 75% of tracheobronchial and over 22% of pulmonary airways were predicted to have theoretical ratios >0.5 for deposited aerosol mass to airway diameters in rats, with nearly 8% of

tracheobronchial and 0.6% of pulmonary airways with ratios >1.0 (Figure 5). While there is less chance for airway obstruction in humans, even under this extraordinary exposure condition, there still remains a concern given that nearly 97% (~254,000) of tracheobronchial airways, primarily in generations 13–18, received deposited mass to airway diameter ratios between 0.3 and 0.4 (nasal breathing) or 0.4 and 0.5 (oral breathing), indicating a significant portion of the lung could still be vulnerable to physical obstruction if such a theoretical aerosol exposure was even possible in the real world.

There are acknowledged limitations to this study. Since MPPD cannot address the impact of particles on airflow (only the effect of airflow on particle transport), we assumed that particles deposited in each airway likely deposited in local hot spots (this typically occurs around bifurcations or when convective flow changes and impaction forces dominate (c.f. Anjivel and Asgharian, 1995; Corley et al., 2021)) and then coalesced together as each breath contributed additional particles to the same areas. The potential for further agglomeration over repeated breaths was considered likely given the propensity for the nanomaterial to agglomerate into micron-sized aerosols during aerosol generation. Assuming the aerosol mass was spherical, the resulting aerosol diameters could be compared with the diameter of each corresponding airway as a predictor of airway obstruction potential. One aspect to this assumption is that even with a calculated full airway obstruction, without a two-way coupled airflow–particle interaction, MPPD will predict that particles still penetrate deeper into the lung periphery as if no upstream obstruction exists. This in effect reduces the impact of the calculations as we ignore the fact that airways and respiratory regions beyond an obstruction are no longer ventilated, and more particles build up near each obstruction with each subsequent breath. This is one justification for the importance of histopathology observations and *in silico* predictions of obstruction in the tracheobronchial region of conducting airways that ventilate the pulmonary/alveolar regions.

The other potential limitation is that the current analysis focuses on total deposition over 4 h of exposure and ignores the potential for particle clearance. When particle clearance was factored into simulations, no pulmonary clearance of particles (primarily macrophages) was predicted to occur within the 4-h exposure in either rats or humans. In the tracheobronchial region, mucociliary clearance, which is normally faster in rats and humans, could result in ~22% of deposited mass retained at the end of the exposure in rats, while ~81% would be retained in humans based on comparative simulations at the limit test exposure concentration. However, this means that mucociliary clearance would be unaffected by such an exposure. Furthermore, it is theoretically possible, if not probable at such high exposures, that as the mucociliary escalator transports deposited aerosol mass from distal generations toward the proximal upper conducting airways, more particles can agglomerate and impede mucociliary transport as airways come together. For repeated exposure or longer-term studies, incorporating aerosol clearance would be important, but for an acute 4-h exposure, as in the current analysis, deposited dose is a reasonable dose metric.

In addition to direct evidence from histopathology, there is also supporting, indirect information that the coalescing of

deposited material likely occurs for the specific organic nano-sized pigment evaluated in the acute inhalation study by Wittmer et al. (2021). The first is that all efforts to generate test atmospheres from the nanomaterial pigment up to concentrations of 1–5 mg/L still resulted in aerosol sizes in the micrometer range. In addition, *in vitro* studies measuring the hydrophobicity of a series of nano-sized organic pigments showed that hydrophilic materials spread out on the surface of an adhesive, transparent tape, whereas hydrophobic materials “clumped up” into droplet shapes using a drop shape analyzer, one of several measured properties that were associated with acute inhalation lethality through asphyxiation (Hofmann et al., 2018). Even with these acknowledged limitations, taken together, this *in silico* approach serves as a simplified, yet useful, comparison for materials with properties similar to the organic, nano-sized pigment evaluated in the acute inhalation study.

In keeping with the decades-old 3R principles for humane use of animals in research (replace, reduce, and refine; Russell and Burch, 1959), OECD test guidelines for acute inhalation studies were originally designed to minimize the number of animals to meet the scientific objectives of the study. Furthermore, limit concentrations were established to provide an upper bound on exposures for materials that are relatively non-toxic. If animals survive and recover from 4-h exposures to the limit concentration, no further testing is required, and animal use is minimized. While OECD recognizes that a limit test of 5 mg/L is challenging for many aerosols and can exceed real-world exposures, a lower limit of 2 mg/L may be justified, which prompted the use of this exposure concentration in the case study. This (2 mg/L) is also the limit test concentration used in the U.S. EPA acute inhalation guidelines (EPA, 1996). However, testing of insoluble, nano-sized dust particles for acute toxicity according to the current OECD guidelines continues to present several ethical, regulatory, and technical problems even for a 2 mg/L alternative limit exposure based on this *in silico* analysis.

Although an update of the GHS labeling criteria for acute inhalation toxicity and harmonization with OECD guidance documents 403 and 39 for nanomaterials is time-consuming and changes in an international regulation even more so, the results from this study and those of other materials in this class suggest that a thorough update is overdue. The technical performance and the obstacles in the *in vivo* experiment when testing insoluble dust particles are also subjects for further investigations, and the results should be incorporated in updated guidelines reflecting nanomaterial properties. Moreover, the re-worked guidance documents and the classification and labeling regulation must be harmonized with testing guidelines to enable a regulatory assessment for this category of testing materials. For the time being, MPPD simulations of airway deposition at high exposure concentrations between rats and humans, in addition to estimating the extent to which airways may be vulnerable to obstruction, form a reasonable basis for an interim assessment on potential health hazards for certain classes of nanomaterials and their relevance, or lack thereof, for humans.

Data availability statement

The original contributions presented in the study are included in the article/[Supplementary Material](#); further inquiries can be directed to the corresponding author.

Ethics statement

The animal study was approved by the Ethical Committee, Landesärztekammer Rheinland Pfalz, Chair Univ.-Prof. Dr. med. Dipl. Ing. Stephan Letzel. The study was conducted in accordance with the local legislation and institutional requirements.

Author contributions

HS: writing–original draft, writing–review and editing, and project administration. LM-H: methodology, writing–original draft, and writing–review and editing. ST: Writing–original draft, Investigation. RC: writing–original draft and writing–review and editing.

Funding

The author(s) declare that financial support was received for the research, authorship, and/or publication of this article. All MPPD simulations and subsequent analyses of MPPD and previously published CFD results were supported by Colors & Effects Switzerland AG, which had no restrictions in the study design, collection, analysis, interpretation of data, the writing of this article, or the decision to submit for publication.

Acknowledgments

The authors are grateful to Owen Price, ARA, for the updated version of the publicly available MPPD model that

corrected the head model of the asymmetric Sprague–Dawley rat (MPPD v3. 24C57). The authors would also like to thank (BASF SE) for the preparation of the histopathological images.

Conflict of interest

HS was employed by Colors & Effects Switzerland AG; HS and LM-H are current employees of Colors & Effects Switzerland AG and BASF SE, respectively. RC is the sole proprietor of Greek Creek Toxicokinetics Consulting, LLC and served as a consultant to Colors & Effects Switzerland AG under a service agreement.

Publisher's note

All claims expressed in this article are solely those of the authors and do not necessarily represent those of their affiliated organizations, or those of the publisher, the editors, and the reviewers. Any product that may be evaluated in this article, or claim that may be made by its manufacturer, is not guaranteed or endorsed by the publisher.

Author disclaimer

The opinions expressed in this publication are those of the authors. They do not purport to reflect the opinions or views of Colors & Effects Switzerland AG, or any of its affiliated companies.

Supplementary material

The Supplementary Material for this article can be found online at: <https://www.frontiersin.org/articles/10.3389/ftox.2023.1258861/full#supplementary-material>

References

- Anjilvel, S., and Asgharian, B. (1995). A multiple-path model of particle deposition in the rat lung. *Fundam. Appl. Toxicol.* 28 (1), 41–50. doi:10.1006/faat.1995.1144
- Bevan, R. J., Kreiling, R., Levy, L. S., and Warheit, D. B. (2018). Toxicity testing of poorly soluble particles, lung overload and lung cancer. *Reg. Toxicol. Pharmacol.* 100, 80–91. doi:10.1016/j.yrtph.2018.10.006
- Brown, J. S., Wilson, W. E., and Grand, L. D. (2005). Dosimetric comparisons of particle deposition and retention in rats and humans. *Inhal. Toxicol.* 17, 355–385. doi:10.1080/08958370590929475
- Christie, R. (2014). *Colour chemistry*. Royal society of chemistry.
- Corley, R. A., Kuprat, A. P., Suffield, S., Kabilan, S., Hinderliter, P., Yugulis, K., et al. (2021). New approach methodology for assessing inhalation risks of a contact respiratory cytotoxicant: computational fluid dynamics-based aerosol dosimetry modeling for cross-species and *in vitro* comparisons. *Toxicol. Sci.* 182 (2), 243–259. doi:10.1093/toxsci/kfab062
- Corley, R. A., Kuprat, A. P., Suffield, S. R., Kabilan, S., Hinderliter, P. M., Yugulis, K., et al. (2021). New approach methodology for assessing inhalation risks of a contact respiratory cytotoxicant: computational fluid dynamics-based aerosol dosimetry modeling for cross-species and *in vitro* comparisons. *Toxicol. Sci.* 182 (2), 243–259. doi:10.1093/toxsci/kfab062
- EPA (1996). *Health effects test guidelines OPPTS 870.1300 acute inhalation toxicity*.
- EPA (2021). *Multiple-path particle dosimetry (MPPD) model: U.S. EPA technical support documentation and user's guide*. China: MPPD EPA. 2021_v1.01).
- European Commission (2011). Commission recommendation of 18 October 2011 on the definition of nanomaterial. *Off. J. Eur. Union* 275, 38.
- Hofmann, T., Ma-Hock, L., Teubner, W., Athas, J. C., Neubauer, N., Wohleben, W., et al. (2018). Reduction of acute inhalation toxicity testing in rats: the contact angle of organic pigments predicts their suffocation potential. *Appl. Vitro Toxicol.* 4 (2), 220–228. doi:10.1089/aivt.2018.0006
- Hofmann, W., and Asgharian, B. (2003). The effect of lung structure on mucociliary clearance and particle retention in human and rat lungs. *Tox. Sci.* 73, 448–456. doi:10.1093/toxsci/kfg075
- Hunger, K., and Schmidt, M. U. (2018). *Industrial organic pigments: production, crystal structures, properties, applications, fourth*. USA, Completely Revised Edition.
- ICRP (1994). “Human respiratory tract model for radiological protection,” in *ICRP (international commission on radiological protection) publication 66* (Pergamon).
- ICRP (2015). “Occupational intakes of radionuclides: Part 1,” in *Annals of the ICRP (international commission on radiological protection)*. IEEE, China,
- ICRP (International Commission on Radiological Protection) (2015). Occupational intakes of radionuclides: Part 1. ICRP publication 130. *Sage* 44 (2).

- Ménache, M. G., Miller, F. J., and Raabe, O. G. (1995). Particle inhalability curves for humans and small laboratory animals. *Ann. Occup. hygiene* 39 (3), 317–328. doi:10.1016/0003-4878(95)00002-v
- Miller, F. J., Asgharian, B., Schroeter, J. D., and Price, O. (2016). Improvements and additions to the multiple path particle dosimetry model. *J. Aerosol Sci.* 99, 14–26. doi:10.1016/j.jaerosci.2016.01.018
- Miller, F. J., Asgharian, B., Schroeter, J. D., Price, O., Corley, R. A., Einstein, D. R., et al. (2014). Respiratory tract lung geometry and dosimetry model for male Sprague-Dawley rats. *Inhal. Toxicol.* 26 (9), 524–544. doi:10.3109/08958378.2014.925991
- OECD (2009). *OECD guideline for the testing of chemicals 403, Acute inhalation toxicity*.
- OECD (2018). *Guidance document on inhalation toxicity studies, Series on testing and assessment*. USA, OECD., 39.
- Phalen, R. F., and Mendez, L. B. (2009). Dosimetry considerations for animal aerosol inhalation studies. *Biomarker* 14 (S1), 63–66. doi:10.1080/13547500902965468
- Russell, W. M. S., and Burch, R. L. (1959). *The principles of humane experimental technique*. London: Methuen & Co, Ltd.
- Schroeter, J. D., Kimbell, J. S., Asgharian, B., Tewksbury, E. W., and Singal, M. (2012). Computational fluid dynamics simulations of submicrometer and micrometer particle deposition in the nasal passages of a sprague-Dawley rat. *J. aerosol Sci.* 43, 31–44. doi:10.1016/j.jaerosci.2011.08.008
- Wessely, B., Stintz, M., Nolde, J., and Creutzenberg, O. (2022). Experimental study on the transport and alteration behavior of aerosols from low density powders for acute inhalation Toxicology studies. *Front. Public Health* 10, 907202. doi:10.3389/fpubh.2022.907202
- Wittmer, E., Tangermann, S., and Landsiedel, R. (2021). *Low chlorinated copper, [29H,31H-phthalocyaninato(2-)-N29,N30,N31,N32]-, wherein the number of chlorines is more than or equal to 0 and less than or equal to 7. Acute inhalation toxicity study in Wistar rats. 4-Hour dust exposure (nose only). Final Report Experimental toxicology and Ecology, BASF SE*.
- Zweifel, H., Maier, R. D., Schiller, M., and Amos, S. E. (2001). *Plastics additives handbook*.



OPEN ACCESS

EDITED BY

Victoria Hutter,
University of Hertfordshire,
United Kingdom

REVIEWED BY

Ishita Choudhary,
North Carolina State University,
United States
Ewelina Hoffman,
ImmuONE, United Kingdom

*CORRESPONDENCE

Shaun D. McCullough,
✉ smccullough@rti.org

RECEIVED 20 July 2023

ACCEPTED 14 December 2023

PUBLISHED 23 January 2024

CITATION

Mallek NM, Martin EM, Dailey LA and
McCullough SD (2024), Liquid application
dosing alters the physiology of air-liquid
interface (ALI) primary human bronchial
epithelial cell/lung fibroblast co-cultures
and *in vitro* testing relevant endpoints.
Front. Toxicol. 5:1264331.
doi: 10.3389/ftox.2023.1264331

COPYRIGHT

© 2024 Mallek, Martin, Dailey and
McCullough. This is an open-access
article distributed under the terms of the
[Creative Commons Attribution License
\(CC BY\)](https://creativecommons.org/licenses/by/4.0/). The use, distribution or
reproduction in other forums is
permitted, provided the original author(s)
and the copyright owner(s) are credited
and that the original publication in this
journal is cited, in accordance with
accepted academic practice. No use,
distribution or reproduction is permitted
which does not comply with these terms.

Liquid application dosing alters the physiology of air-liquid interface (ALI) primary human bronchial epithelial cell/lung fibroblast co-cultures and *in vitro* testing relevant endpoints

Nicholas M. Mallek¹, Elizabeth M. Martin², Lisa A. Dailey³ and
Shaun D. McCullough ^{3,4*}

¹Curriculum in Toxicology and Environmental Medicine, University of North Carolina, Chapel Hill, NC, United States, ²Epigenetics and Stem Cell Biology Laboratory, National Institute of Environmental Health Sciences, National Institutes of Health, Department of Health and Human Services, Durham, NC, United States, ³Public Health and Integrated Toxicology Division, Center for Public Health and Environmental Assessment, United States Environmental Protection Agency, Chapel Hill, NC, United States, ⁴Exposure and Protection, RTI International, Durham, NC, United States

Differentiated primary human bronchial epithelial cell (dpHBEC) cultures grown under air-liquid interface (ALI) conditions exhibit key features of the human respiratory tract and are thus critical for respiratory research as well as efficacy and toxicity testing of inhaled substances (e.g., consumer products, industrial chemicals, and pharmaceuticals). Many inhalable substances (e.g., particles, aerosols, hydrophobic substances, reactive substances) have physiochemical properties that challenge their evaluation under ALI conditions *in vitro*. Evaluation of the effects of these methodologically challenging chemicals (MCCs) *in vitro* is typically conducted by “liquid application,” involving the direct application of a solution containing the test substance to the apical, air-exposed surface of dpHBEC-ALI cultures. We report that the application of liquid to the apical surface of a dpHBEC-ALI co-culture model results in significant reprogramming of the dpHBEC transcriptome and biological pathway activity, alternative regulation of cellular signaling pathways, increased secretion of pro-inflammatory cytokines and growth factors, and decreased epithelial barrier integrity. Given the prevalence of liquid application in the delivery of test substances to ALI systems, understanding its effects provides critical infrastructure for the use of *in vitro* systems in respiratory research as well as in the safety and efficacy testing of inhalable substances.

KEYWORDS

inhalation, IVIVE, new approach methodologies (NAMs), air-liquid interface (ALI), epithelial, risk assessment, bronchial, respiratory tract

Introduction

Exposure to a broad range of inhalable substances including inhaled pharmaceuticals, consumer products, industrial chemicals, and ambient air pollutants influences human health worldwide. Inhalation is one of the three primary routes of chemical and pharmaceutical exposure and many inhaled substances elicit their effects, beneficial or adverse, in the respiratory tract, which serves as the portal of entry. The vast number of data-poor new and existing inhalable substances, including ambient or occupational exposure-related chemicals/substances, pharmaceuticals, and consumer and commercial products, as well as mixtures of different substances, and repeated exposure scenarios precludes the feasibility of using traditional *in vivo* animal studies to evaluate the potential adverse effects of these exposures and scenarios (National Research Council, 2007). The 2007 National Research Council report, *Toxicity Testing in the 21st Century: A Vision and a Strategy*, outlined a strategy to address these limitations through the use of *in vitro* and computational new approach methodologies (NAMs) to advance the throughput and human relevance of toxicity testing. These recommendations have been used by regulatory agencies, including the US Environmental Protection Agency, to develop strategic plans to increase the use of NAMs to generate data for decision making (United States Environmental Protection Agency, 2020; US Environmental Protection Agency, 2021).

The respiratory tract epithelium functions as a physical barrier between inhaled materials and underlying tissues. In the nasal and tracheobronchial airways, the secretion of mucus and presence of beating cilia also function as a mucociliary escalator to facilitate clearance of inhaled materials and pathogens. Further, respiratory epithelial cells participate in the induction and regulation of the immune response to injury and inhaled insults through the secretion of pro-inflammatory cytokines (Reviewed in Polito and Proud, 1998; Hiemstra, McCray, and Bals, 2015; Hewitt and Lloyd, 2021). Primary human airway epithelial cell cultures that have been differentiated and subsequently maintained under ALI conditions exhibit key features of their respective regions of the human respiratory tract *in vivo* including the formation of a selectively permeable and electrically resistant barrier, the presence of beating cilia, release of pro-inflammatory cytokines, and secretion of mucus (Fulcher et al., 2005; Ross et al., 2007; Pezzulo et al., 2011; Randell et al., 2011; Rayner et al., 2019). ALI-differentiated primary human bronchial epithelial cell (dpHBEC-ALI) and primary human nasal epithelial cell (dpHNEC-ALI) systems have been widely used to model their respective regions of the respiratory tract to advance our understanding of respiratory tract development and disease. They are also a critical resource in support of efforts to increase the *in vivo* human relevance of inhaled test substance evaluation (Clippinger et al., 2018a; Clippinger et al., 2018b; Faber and McCullough, 2018; Hiemstra et al., 2018).

Evaluating the effects of inhaled gases and vapors on differentiated primary airway epithelial cell culture models while maintaining ALI conditions can generally be accomplished using existing *in vitro* exposure apparatus/technology. In contrast, many other types of test substances (e.g., particles, aerosols, hydrophobic substances, reactive substances, biomolecules, *et cetera*) have physical and/or chemical properties that pose challenges to their evaluation under ALI conditions (examples reviewed in Lacroix

et al., 2018). The evaluation of these inhaled methodologically challenging chemicals (MCCs) using *in vitro* systems has often relied on the application of test substances in aqueous solutions/suspensions to the apical surface of ALI models of the respiratory tract (described here as “liquid application”, but also commonly referred to as “direct application” or “liquid dosing”). Liquid application dosing is also often used to deliver exogenous stimuli (e.g., lipopolysaccharide (LPS), tumor necrosis factor alpha (TNF- α), or small molecules to ALI cultures for respiratory biology research and pharmaceutical development, respectively).

When using liquid application dosing, the effect of the test substance treatment is typically assessed by comparison to the respective aqueous solvent (e.g., water, saline, buffered saline, cell culture medium, *et cetera*) as a vehicle control. The application of exogenous liquid alone (*i.e.*, in the absence of a test substance) disrupts ALI conditions, a key physiologically relevant feature of these culture models; however, the effects of applying liquid to differentiated ALI cultures are typically not considered in the analysis and interpretation of study data. Maintaining ALI conditions is key for the successful differentiation of pHBECS into dpHBECs as ALI increases the available oxygen at the epithelial cell layer, which is critical for successful cell differentiation; and the loss of ALI conditions by exogenous liquid application reduces oxygen availability and may alter dpHBEC characteristics (Kouthouridis et al., 2021). Further, while liquid application dosing is commonly used for the delivery of test substances and biological stimuli in ALI systems in inhalation toxicology research and testing, the effects of applying liquid to ALI cultures have not been well characterized. Thus, the potential for liquid application dosing to affect the physiological relevance of the differentiated ALI *in vitro* system, as well as confound test substance exposure effects and the extrapolation of study data to human health outcomes are poorly understood. Addressing this knowledge gap by determining whether disrupting the *in vivo*-relevant ALI conditions alters dpHBEC culture physiology is critical to providing context for the use of liquid application dosing of *in vitro* ALI systems for respiratory biology, inhalation toxicology, pharmaceutical development, and disease research. Here, we report the results of a study describing the effects of the application of liquid, in the absence of a test substance, to a dpHBEC-ALI co-culture model on endpoints that are relevant to *in vivo* bronchial epithelial tissue physiology. These endpoints included global transcriptional regulation, biological pathway activity, ciliary beat frequency, regulation of stress-responsive cellular signaling pathways, release of pro-inflammatory cytokines and growth factors, and epithelial barrier function.

Methods

Differentiated dpHBEC/HLF co-culture ALI model

Fibroblasts exist immediately beneath the bronchial epithelial barrier and contribute to respiratory tract homeostasis and disease (Kendall and Feghali-Bostwick, 2014; White, 2015). We have also recently observed that lung fibroblasts are both a target and mediator of the effects of inhaled toxicant exposure *in vitro*

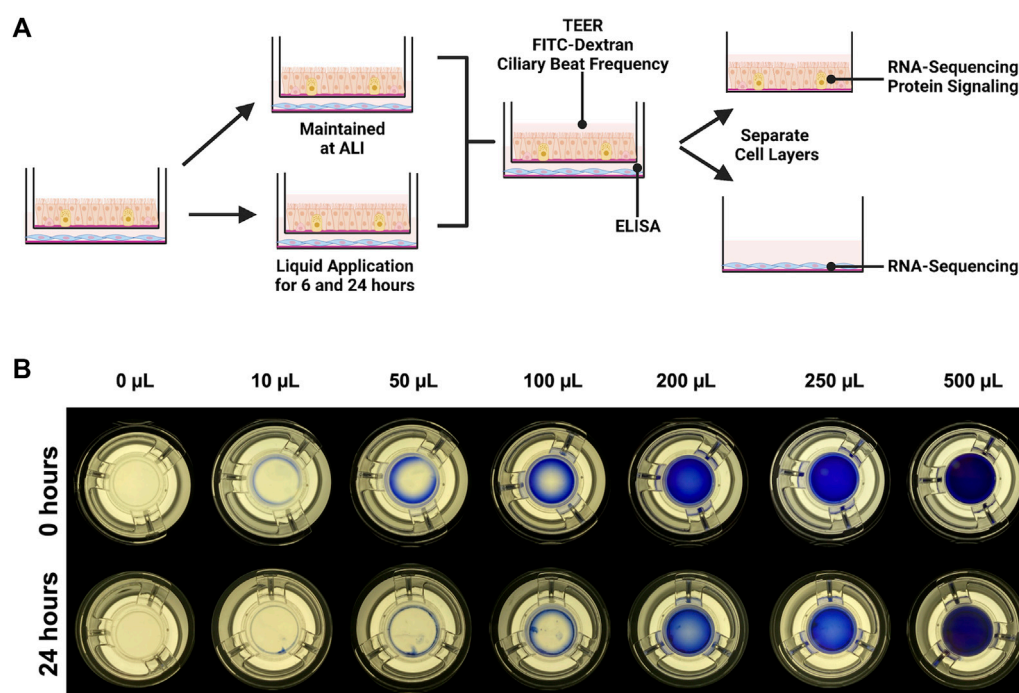


FIGURE 1

Experimental design. (A) IMR90 fibroblasts were seeded onto collagen-coated tissue culture wells 24 h before being combined with dpHBEC under ALI conditions. 24 h after the cells were combined, 250 µL of liquid (ALI medium) was applied to the apical surface of the dpHBECs for either 6 or 24 h. A matched set of cultures was maintained under ALI conditions to serve as the control. The indicated endpoints were evaluated to determine the effect of the application of liquid on dpHBEC cultures. (B) Titration of apical volumes of crystal violet solution in 12 mm Transwell® inserts used to visualize the relative coverage of the insert surface area at different applied liquid volumes. The 250 µL volume was determined to provide the best balance between the smallest volume and uniformity of liquid coverage. (A) created with BioRender.com.

(Faber et al., 2000). Thus, we utilized a modified version of the co-culture model used by Faber *et al.* (2000) that combined dpHBEC on cell cultures inserts at ALI with confluent monolayers of IMR90 lung fibroblasts. The use of this system allowed for an improved relevance to the *in vivo* tissue compared to the use of dpHBEC cultures alone while also allowing for the evaluation of cell type-specific effects of liquid application.

pHBEC were obtained via bronchial brushing from healthy donors of 18–40 years of age that were not currently smoking and had no more than a one pack-year of lifetime smoking history. Donors gave their consent after being informed of risks and procedures. The consent and collection protocol were approved by the UNC School of Medicine Committee on the Protection of the Rights of Human Subjects and by the US EPA. Collection of pHBEC from volunteers was performed in accordance with relevant guidelines and regulations. pHBEC were isolated from brush biopsy (“passage 0”) and expanded to passage 3 prior to being plated on 12 mm Transwell® inserts (Corning #3460; 0.4 µm pore polyester membranes), becoming confluent, and differentiating for 24 days under ALI conditions. Detailed descriptions of the techniques, reagents, and materials used for the culture/expansion of pHBEC and differentiation of pHBEC at ALI used in this study are available as open access methods document by Dailey and McCullough (Dailey and McCullough, 2021). Day 24 ALI cultures were visually evaluated for the presence of beating cilia and the production of mucus as indicators of differentiation status to qualify their use in experiments. Donor demographics are listed in Supplementary Table S1. All cultures were at ALI day 24 at the

beginning of experiments. The human lung fibroblast cell line IMR90 (Nichols et al., 1977) was obtained from the American Type Culture Collection (ATCC, No. CCL-186, Batch #64155514), and cultured as described in detail in the open-access methods document by Mallek and McCullough (Mallek and McCullough, 2021a). Short tandem repeat (STR) service provided by ATCC (cat #135-XV) was used to authenticate IMR90 cells (Supplementary Figure S1). As described in Figure 1A, IMR90 fibroblasts were seeded onto a collagen-coated 12-well plate (Corning, #3512) at a density of 1×10^5 cells/mL in 800 µL of Pneumacult ALI medium (StemCell Technologies, #05001). The following day, day 23 dpHBEC-ALI inserts were added into the fibroblast-seeded wells (dpHBEC-IMR90 ALI model). The dpHBEC-IMR90 ALI model was used for experiments on the following day. The dpHBEC-IMR90 ALI model was maintained at ALI or subjected to the addition of ALI medium to the apical surface of the culture (“liquid application”). The methods for the selection of the volume of medium applied are described in the following section. The cells were kept submerged in ALI medium for either 6 or 24 h to represent “early” and “late” effects, respectively. The 24-h treatment is consistent with the liquid application treatment duration utilized in the recent OECD case study on the use of an ALI-differentiated *in vitro* NAM for an IATA to refine inhalation risk assessment for point of contact toxicity (Vinall, 2017; Hiemstra et al., 2018; Paulo, 2020; Welch et al., 2021). The effect of liquid application on global gene expression, stress-responsive signaling protein phosphorylation, growth factor secretion, pro-inflammatory cytokine secretion, trans-epithelial electrical resistance (TEER), and permeability

to a 20 kDa fluorescent dextran was then determined immediately after 6 and 24 h of liquid application (Figure 1A). A set of $n = 3$ donors were used for RNA-Sequencing, differential gene expression analysis, TEER, and FITC-dextran permeability. Follow-up experiments including immunoblotting and ELISAs were performed with an additional $n = 3$ donor set, unique from the donors used in initial experiments.

Determination of liquid application volume

We were not able to find any published studies evaluating the completeness of culture coverage resulting from different applied liquid volumes. The development of discontinuous coverage of the culture surface by the applied liquid would be expected to result in inconsistencies in test substance concentration and flux, ion and/or nutrient concentrations, and exposed oxygen concentrations across the culture. Thus, we sought to determine the smallest applied liquid volume that resulted in complete, and most uniform, coverage of the cell layer during a 24-h treatment period. To accomplish this, we titrated a range of apical volumes (10 μ L–500 μ L) of a 1:10 Trypan Blue (Sigma, #T8154-20 ML) solution in Dulbecco's Phosphate Buffered Saline (Gibco #14190-144) to the apical surface of dpHBEC-ALI cell layers grown on 12 mm Transwell® inserts (Figure 1B). After the 24-h treatment duration, inserts were placed on a white light transilluminator (FUJIFILM #IPE4046) and photographed with an iPhone SE (Apple, Model #MX9M2LL/A). The lowest volume that maintained complete coverage of the cell layer during the 24-h treatment duration with the best uniformity was selected for use in the study.

RNA isolation

Total RNA was isolated using the PureLink RNA Mini kit (ThermoFisher #12183025) according to the detailed open access method by McNabb and McCullough (McNabb and McCullough, 2020). Briefly, dpHBEC samples were harvested by the addition of 250 μ L RNA lysis buffer containing 1% β -mercaptoethanol, triturated, and transferred to Eppendorf tubes on ice prior to storage at -80°C until extraction. Total RNA was eluted in nuclease-free water (ThermoFisher, #AM9937) following extraction and column purification. Total RNA was quantified using a NanoDrop OneC UV-Vis Spectrophotometer. Purified RNA was stored at -80°C until submission for RNA-sequencing or preparation of cDNA for quantitative real-time polymerase chain reaction (qRT-PCR).

Sequencing, DESeq2, and qRT-PCR validation

Library preparation and sequencing were performed by the University of North Carolina at Chapel Hill High Throughput Genomic Sequencing Facility. Briefly, 100–500 ng of RNA were used to make libraries using a KAPA Stranded mRNA-Seq Kit, with KAPA mRNA Capture Beads (Roche Sequencing and Life Science #07962207001). Libraries underwent quality control via

dsDNA High Sensitivity Qubit following cDNA synthesis and adaptor ligation (Q32851). Libraries were normalized to 5 nM and pooled in equal amounts and then processed on a miSeq nano flowcell (MS-103–1001). Samples were run on an Illumina Novaseq 6,000 (Illumina, San Diego, CA), and calibrated against 1% PhiX as a positive control during sequencing. Base call files were transformed into FASTQ files using bcl2fastq software (version 2.20.0). Mapping of sequence reads to the human genome (GRCh38) was performed by STAR (version 2.5) with the following parameters: - outSAMAttrIHstart 0 --outFilterType BySJout--alignSJoverhangMin 8 -- outMultimapperOrder Random (other parameters at default settings). Mapped read counts per gene were collected by Subread feature Counts (version 1.5.0-0-p1). Genes with a minimum average of normalized mapped read counts >50 in at least one category were selected for differential gene expression analysis. Differentially expressed genes (DEGs) were identified by DESeq2 (v 3.13) using filters of $\text{FDR} < 0.01$. Read counts and the processed data matrix are available to the public on the NCBI Gene Expression Omnibus (series number: GSE198884). DEG datasets were also generated for the underlying IMR90 fibroblasts after the application of liquid to the apical dpHBECs for either 6 or 24 h (Supplementary Figure S2). Fold change expression values derived from RNA-sequencing-derived DESeq2 were validated against standard real-time qRT-PCR methods (Supplementary Figure S4). Briefly, cDNA was synthesized using the iScript Reverse Transcription Kit (Bio-Rad, #1708891) according to the manufacturer's protocol. Fold change values were assessed via primers, hydrolysis probes (Supplementary Table S2), and iTaq universal Probes Supermix (Bio-Rad, #1725131) on a CFX96 Touch (Bio-Rad). Target gene C_q values were normalized to β -actin and expressed as fold changes between liquid application and ALI conditions using the Pfaffl method (Pfaffl, 2001).

Ingenuity Pathway Analysis

The number of statistically significant alternatively regulated genes identified in dpHBECs following 24-h liquid application treatment (10,239 genes) exceeded the maximum number of genes (8,000) that can be analyzed by the IPA software. Thus, we generated a sub-set of each DEG list that included only statistically significant genes that were alternatively regulated with an absolute value \log_2 fold change >2.0 . These “pathway analysis” gene sets were uploaded to Ingenuity Pathway Analysis software (Version 65367011). Gene lists were exported for each of the top 10 canonical pathways as determined by $-\log(p\text{-value})$. The 10 genes with the greatest absolute fold change value were exported as tables for the top 10 most significant canonical pathways. IPA was also used to determine canonical pathways and top genes for underlying IMR90s after liquid application to apical dpHBECs (Supplementary Figure S3, 4).

Protein collection and immunoblotting

Total protein was isolated via a RIPA extraction. Briefly, dpHBEC samples were harvested by the addition of 250 μ L of

RIPA lysis buffer (50 mM Tris-base, pH 8.0, 150 mM NaCl, 400 μ M EDTA, 10% glycerol, 1% Triton-X, 0.1% SDS, 0.1% sodium deoxycholate, with 1X protease inhibitor (Sigma, #11697498001) and phosphatase inhibitor (Sigma, #04906837001) cocktails) to each insert, scraping with a wide-bore P200 pipette tip (United States Scientific, #10118410), and transfer to an Eppendorf tube prior to incubation on ice for 20 min. Samples were centrifuged at $13,000 \times g$ for 15 min to pellet cell debris and supernatants were transferred to new Eppendorf tubes on ice. Three aliquots (10 μ L) were removed from each sample for determination of protein concentration by BCA assay. 5X Laemmli buffer (120 mM Tris, pH 6.8, 400 mM dithiothreitol, 20% glycerol, 4% SDS, 0.025% bromophenol blue) was then added to the remaining sample volume before the samples were incubated at 95°C for 5 min. Samples were stored at -80°C until used for immunoblotting. The antibodies and dilutions used for immunoblotting are provided in [Supplementary Table S3](#). All samples were electrotransferred on 0.45 μ M nitrocellulose membranes (Bio-Rad, #1620115) in transfer buffer (48 mM Tris-base, 39 mM glycine, 20% methanol). Chemiluminescence was generated via a horseradish peroxidase-conjugated secondary antibody (Jackson ImmunoResearch, #711-036-152) and Clarity Western ECL Blotting Substrate (Bio-Rad #1705060). Images were taken on a ChemiDoc MP Imaging System (Bio-Rad), and densitometry was generated using Bio-Rad Image Lab Software (Version 6.1.0, Build 7).

Evaluation of growth factor and pro-inflammatory cytokine secretion

Conditioned medium was collected from the basolateral compartment of dpHBEC-ALI cultures immediately before liquid application, and 6 or 24 h after liquid application. Conditioned media were centrifuged and syringe filtered through 0.22 μ m pore PVDF membranes (Millipore Sigma, #SLGV033RS) to remove cellular debris before storage at -80°C until use. Conditioned media were probed for cytokine secretion by the V-PLEX Human Proinflammatory Panel II (4-Plex) (Mesoscale Discovery, K15053D-1) and growth factor secretion by the U-PLEX Development Pack (Mesoscale Discovery, K15228N-1) according to the manufacturer's protocols. Briefly, conditioned media samples were diluted two-fold, and assayed in triplicate with either four 10-fold serial dilutions (for cytokines) or four two-fold serial dilutions (for growth factors) to determine the limits of detection in our dpHBEC-ALI cultures. The MSD plate was washed thrice with 150 μ L of wash buffer per well prior to the addition of 50 μ L of diluted sample to individual wells and incubation with shaking (300 RPM) for 2 hours at room temperature. Samples were then aspirated and the plate was washed thrice with 150 μ L of wash buffer prior to the addition of 25 μ L of detection antibody solution to each well and incubation with shaking (300 RPM) for 2 hours at room temperature. The antibody solution was then aspirated and the plate was washed thrice with 150 μ L wash buffer before the addition of 150 μ L of 2X Read Buffer T to each well. The sample plate was read on the Meso Quickplex SQ 120, and analyte concentrations were determined using the MSD Discovery Workbench software (Version 4.0.12).

Trans-epithelial electrical resistance

Trans-epithelial electrical resistance (TEER) was measured using the EVOM2 (World Precision Instruments) with EndOhm cup for 12 mm inserts (World Precision Instruments) at the indicated time points as described in a detailed open-access methods document by Mallek and McCullough ([Mallek and McCullough, 2021b](#)). Briefly, resistance measurements were obtained for both experimental samples and insert only (without cells). TEER values from insert only samples were subtracted from experimental sample resistance values and the resulting values were then multiplied by the insert surface area to calculate values in $\Omega \times \text{cm}^2$ ([Srinivasan et al., 2015](#)). Three cultures were used for each condition per experiment and each culture was assayed in technical triplicate. The mean (\pm SD) of three independent experiments is shown. TEER was treated as a destructive assay and no additional assays were conducted on cultures that were analyzed by TEER.

Fluorescein isothiocyanate-labeled dextran assay

The translocation of a 20 kDa fluorescein isothiocyanate (FITC)-labeled dextran (Sigma, FD20) was measured as described in a detailed open-access methods document by Faber and McCullough ([Faber and McCullough, 2020](#)). Briefly, experimental sample inserts and insert only (without cells) were transferred to a new multi-well plate containing 800 μ L of phenol-red free MEM (ThermoFisher, #51200038) in each well. The apical medium was carefully aspirated from cultures after liquid application for 6 or 24 h and 250 μ L of a 1 mg/mL suspension of FITC-dextran in Pneumacult ALI medium (StemCell Technologies, #05001) was added to the apical compartment of each insert. Samples were incubated in the dark for 20 min at 37°C, and the basolateral media containing translocated FITC-dextran suspension was collected and transferred to a 96-well clear bottom microplate (Corning, #3904) prior to determination of the fluorescence of each sample at 490/520 nm Ex/Em on a ClarioStar Plus plate reader. Three cultures were used for each condition per experiment and each culture was assayed in technical triplicate. The mean (\pm SD) of three independent experiments is shown. The FITC-dextran assay was considered to be destructive and no additional assays/endpoints were conducted/evaluated on cultures after this assay.

Statistical analysis

Statistical analyses for protein densitometry, cytokine and growth factor secretion, TEER, FITC-dextran, ciliary beat frequency and total ciliated area, and viability were conducted using GraphPad Prism 9.0.1 (GraphPad Software). The statistical significance of differences between each duration of liquid application and untreated controls were evaluated using a parametric unpaired *t*-test. A *p*-value of ≤ 0.05 was considered statistically significant for all analyses.

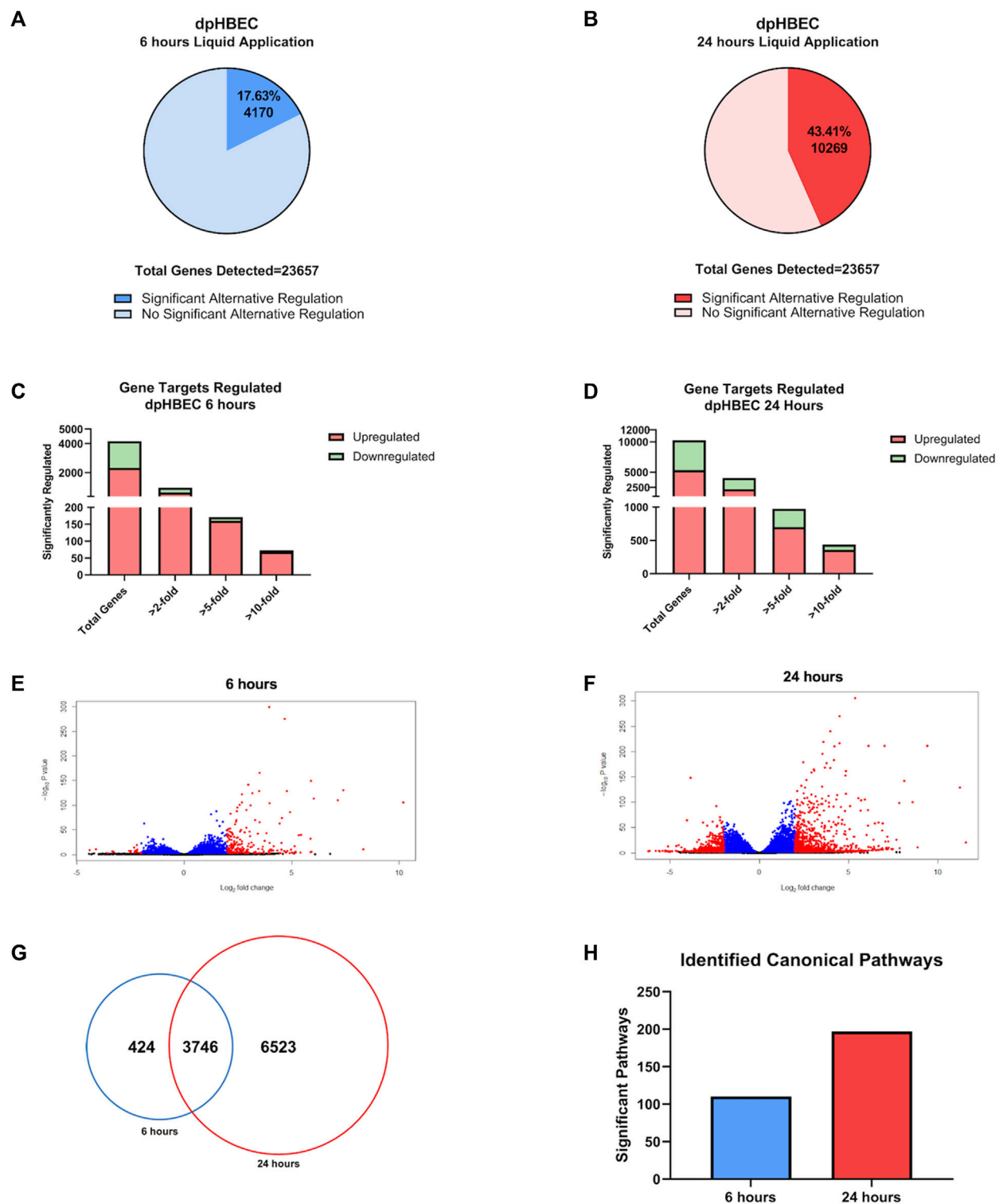
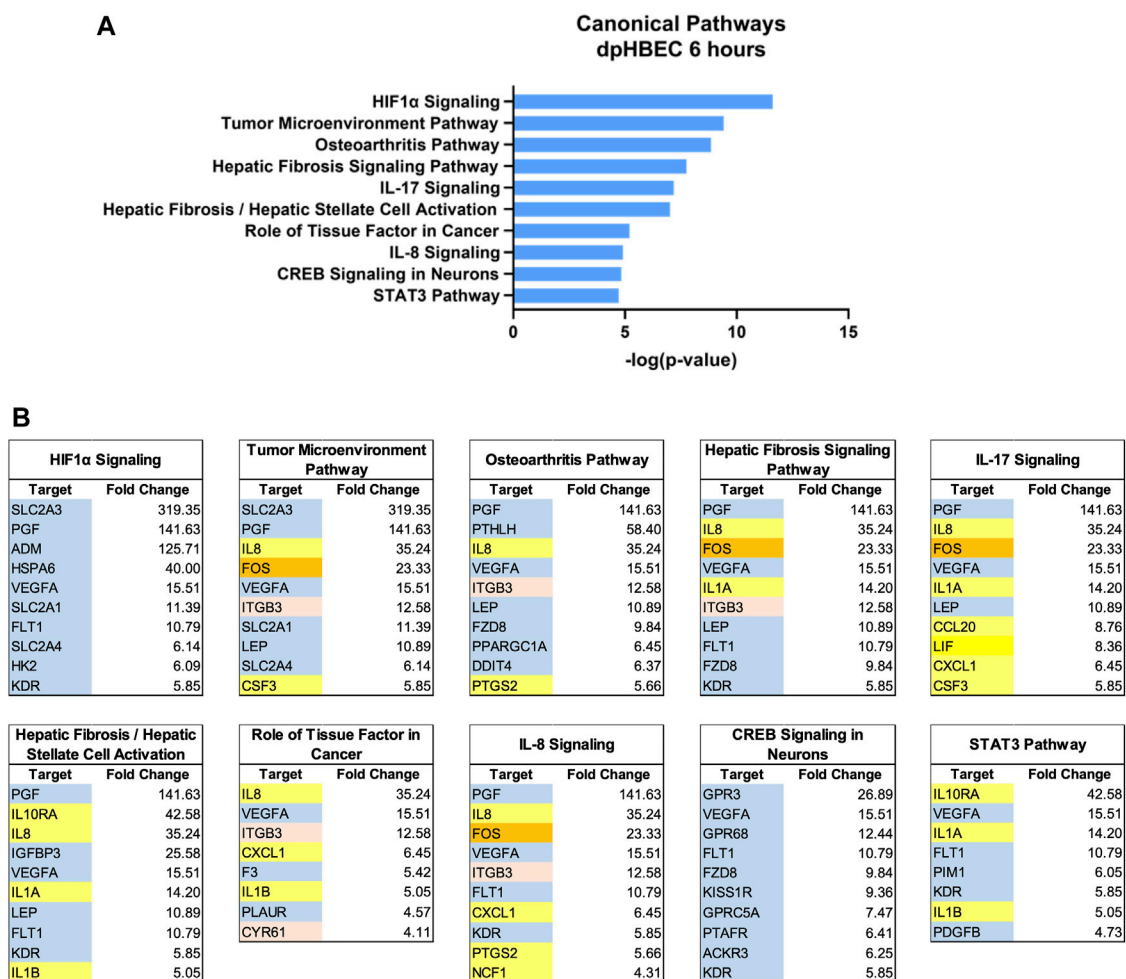


FIGURE 2

Global transcriptome changes following liquid application exposure for 6 or 24 h (A, B) The total amount of significantly alternatively regulated genes (adjusted p -value < 0.05) after 6 h (A) or 24 h (B) of liquid application, respectively. (C, D) The total number of significant alternatively regulated genes from (A, B) separated into fold change expression thresholds after 6 h (C) or 24 h (D) of liquid application, respectively. (E, F) Volcano plots of the gene datasets described in (A, B). Blue points have an adjusted p -value of <0.01, and red points have an adjusted p -value of <0.05 and a \log_2 (foldchange) > 1. (G) Venn Diagram comparison displaying the number of significant (adjusted p -value < 0.05) unique and shared genes between the 6- and 24-h liquid application dataset described in (A, B). (H) Total number of significant canonical pathways regulated after liquid application for 6 or 24 h according to Ingenuity pathway analysis of the dataset from (A, B). Data shown represent $n = 3$ donors.

**FIGURE 3**

Ingenuity pathway analysis of alternatively regulated genes after 6 h of liquid application on dpHBEC-ALI cultures. **(A)** The top 10 most significant canonical pathways by the $-\log(p\text{-value})$ identified after 6 h of liquid application. **(B)** The top 10 genes, by absolute value, in each canonical pathway identified in **(A)**, and their respective fold change expression over ALI cultures. Only genes exhibiting a $\pm \log_2$ fold change ≥ 2.0 were used in this analysis. In **(B)**, blue shading indicates cell signaling-related genes, orange shading indicates transcription factors, red shading indicates adhesion-related genes, and yellow shading indicates inflammation-related genes.

Results

Applied volume affects the completeness of culture exposure

There are a broad range of applied liquid volumes used for the delivery of experimental treatments to ALI cultures reported in the literature; however, we were not able to identify any published studies that evaluated the completeness of culture coverage at the beginning or end of experiments utilizing liquid application dosing. Thus, we sought to empirically determine the smallest volume that maintained the most complete coverage of the culture over the 24-h treatment. The application of 200 μL (177 $\mu\text{L}/\text{cm}^2$) provided complete coverage immediately after liquid application; however, coverage became markedly uneven during the 24-h treatment duration (Figure 1B). In contrast, the application of 250 μL (221 $\mu\text{L}/\text{cm}^2$, equivalent to the addition of 73.5 μL to a 6.5 mm cell culture insert) was the smallest volume tested that maintained complete coverage across the insert,

while also exhibiting better uniformity than the 200 μL volume, by 24 h. Thus, we utilized an applied liquid volume of 250 μL per 12 mm cell culture insert for subsequent experiments. The application of lower volumes (*i.e.*, $\leq 100 \mu\text{L}$; $\leq 88 \mu\text{L}/\text{cm}^2$, equivalent to $\leq 30 \mu\text{L}$ applied to a 6.5 mm cell culture insert) failed to completely cover the culture surface at the time of application. The completeness of culture coverage at these volumes was diminished over the 24-h incubation period. Importantly, there is no way to achieve completely uniform depth across the surface area of the insert due to the formation of a meniscus.

Liquid application alternatively regulates global gene expression in dpHBEC cultures

Following ALI differentiation, the transcriptional profiles of dpHBEC cultures recapitulate those of their corresponding *in vivo* tissue (Fulcher et al., 2005; Pezzulo et al., 2011; Randell et al., 2011). We began our assessment of the impact of liquid application on dpHBEC-

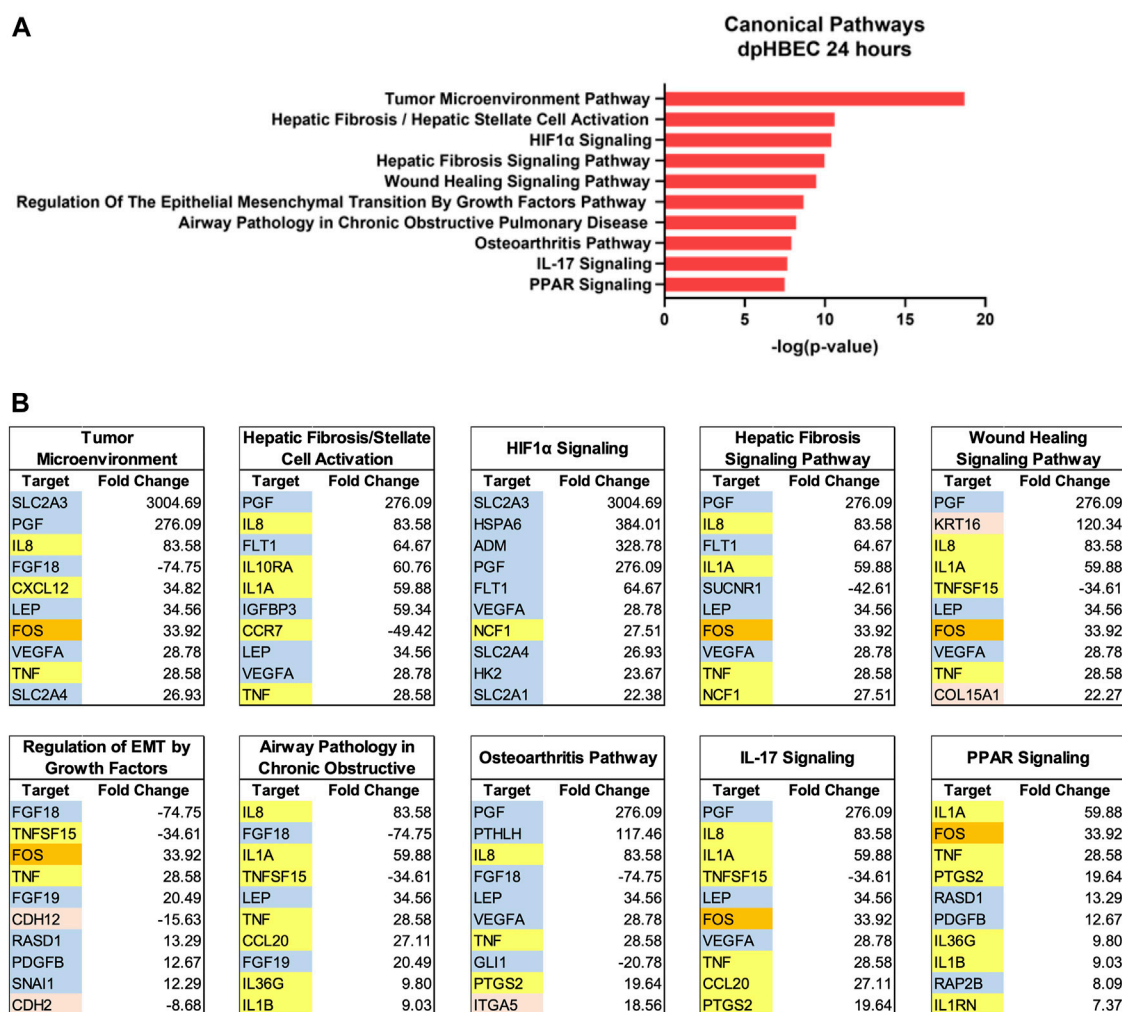


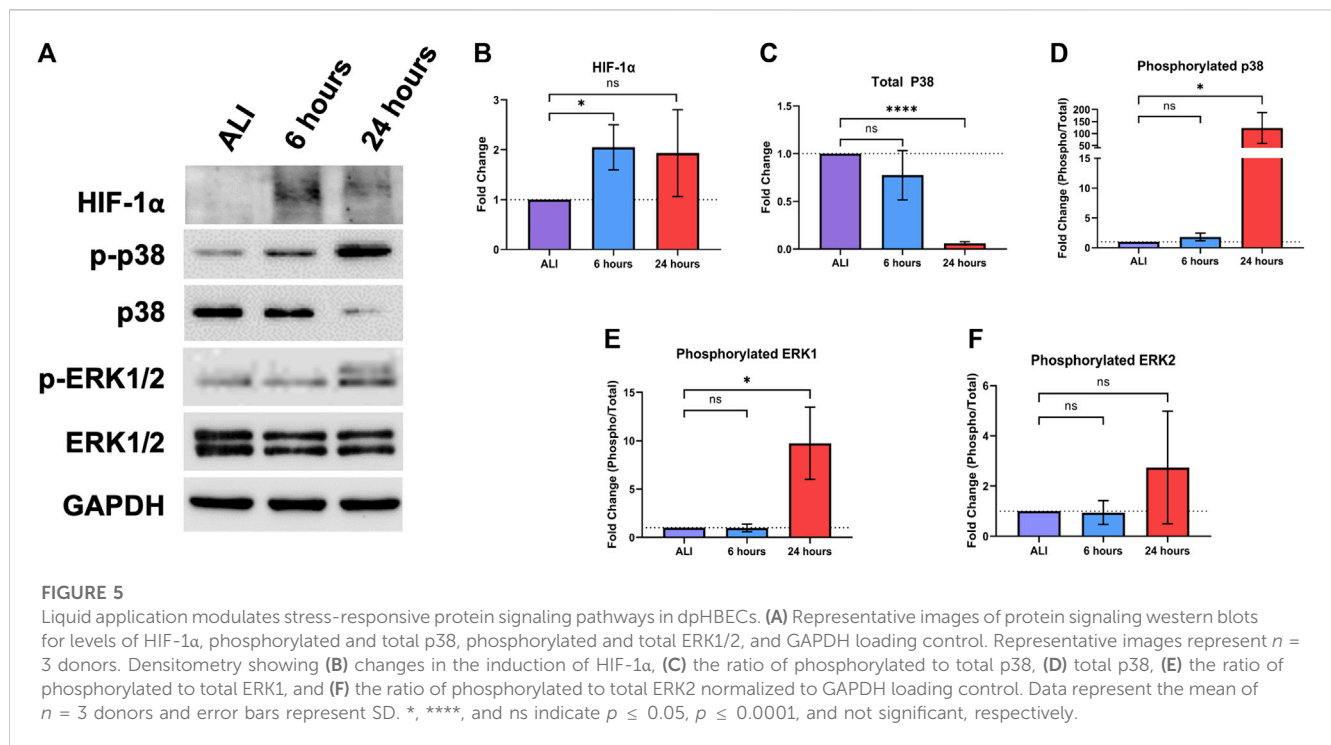
FIGURE 4

Ingenuity pathway analysis after 24 h of liquid application on dpHBEC-ALI cultures. (A) The top 10 most significant canonical pathways by the $-\log(p\text{-value})$ identified after 24 h of liquid application. (B) The top 10 genes, by absolute value, in each canonical pathway identified in (A), and their respective fold change expression over ALI cultures. Only genes exhibiting a $\pm \log_2$ fold change ≥ 2.0 were used in this analysis. In (B), blue shading indicates cell signaling-related genes, orange shading indicates transcription factors, red shading indicates adhesion-related genes, and yellow shading indicates inflammation-related genes.

ALI cultures with the evaluation of its effect on global transcriptional programming using RNA-sequencing. Of the tested transcripts ($n = 33,121$ in the RNA-seq Data set), 23,657 (71%) were detected in dpHBECs. The application of liquid to dpHBEC-ALI cultures for 6 and 24 h resulted in the significant (adjusted $p \leq 0.05$) alternative expression of 4,170 and 10,269 genes, respectively (Figures 2A, B). Of the 4,170 genes that were alternatively expressed at 6 h of liquid application, 626 and 326 were up- and downregulated greater than 2-fold, 160 and 11 were up- and downregulated greater than 5-fold, and 68 and 5 were up- and downregulated greater than 10-fold, respectively (Figure 2C). Of the 10,269 genes that were alternatively expressed at 24 h of liquid application, 2,159 and 1,865 were up- and downregulated greater than 2-fold, 700 and 274 were up- and downregulated greater than 5-fold, and 358 and 79 were up- and downregulated greater than 10-fold, respectively (Figure 2D). The 6- and 24-h time points had 424 and 6,523 unique alternatively expressed genes, respectively, and 3,746 alternatively expressed genes in common (Figure 2G). The

alternative expression of selected targets identified in the RNA-seq analysis (IL-8, IL-1α, and COX-2) were validated by qRT-PCR (Supplementary Figure S2).

Ingenuity Pathway Analysis of significantly alternatively expressed genes indicated that liquid application resulted in the significant alternative regulation of 110 and 197 canonical pathways in pHBEC-ALI cultures at 6 and 24 h, respectively (Figure 2H). The 10 most significant pathways (by $-\log(p\text{-value})$) identified at 6 and 24 h are listed in Figures 3A; Figure 4A and the 10 genes with the largest magnitude of fold change expression, by absolute value, for each of the top alternatively regulated pathways are listed in Figures 3B; Figure 4B, respectively. Several alternatively expressed genes were common to the 10 most significantly alternatively regulated pathways following 6 h of liquid application, including: the growth factors placental growth factor (PGF, 141.6-fold) and vascular endothelial growth factor A (VEGFA, 15.5-fold) and pro-inflammatory mediators such as interleukin (IL)-8 (IL-8, 35.2-



fold), IL-1α (IL-1α, 14.2-fold), IL-1β (IL-1β, 5.1-fold), and cyclooxygenase-2 (COX-2 5.7-fold). Many alternatively expressed genes were also common to the alternatively regulated pathways after 24 h of liquid application including: the growth factors PGF (276.1-fold) and VEGFA (28.9-fold), and the pro-inflammatory mediators IL-8 (83.6-fold), IL-1α (59.9-fold), IL-1β (9.0-fold), and PTGS2 (19.6-fold). Additional highly expressed genes at 24 h included platelet derived growth factor subunit B (PDGF-B, 12.7-fold), and tumor necrosis factor (TNF, 28.6-fold).

Liquid application increases HIF-1a protein levels and the phosphorylation of ERK and p38 cellular signaling pathways in dpHBEC cultures

HIF-1 is a heterodimeric transcription factor that regulates the expression of genes involved in the cellular response to hypoxia, as well as tissue vascularization and the maintenance of tissue homeostasis (Ziello et al., 2007; Shimoda and Semenza, 2011). HIF-1 activation is regulated by the stabilization of the HIF-1α subunit, which occurs in response to hypoxic conditions (Shimoda and Semenza, 2011). The application of liquid to an ALI culture reduces exposure of the apical culture surface to oxygen. Thus, we evaluated whether liquid application resulted in the stabilization of HIF-1α, the regulatory subunit of HIF-1, which was significantly increased (2.05-fold (± 0.45)) at 6, but not 24, hours of liquid application (Figure 5B).

The ERK and p38 mitogen activated protein kinase (MAPK) signaling pathways regulate the response of the respiratory epithelium to oxidative, inflammatory, and pathogenic stimuli (Roux and Blenis, 2004; Lu and Xu, 2006; Guo et al., 2020; Canovas and Nebreda, 2021). Hyperactivation of these pathways also leads to respiratory disease including asthma, COPD, lung injury, and lung cancer (Arcaroli

et al., 2001; Vitos-Faleato et al., 2020). Given their role in mediating homeostasis in the respiratory tract, we sought to determine whether these signaling pathways would be alternatively regulated in response to liquid application (Figure 5A). We observed a significant 122.9-fold (± 64.56) increase in p38 MAPK phosphorylation that was accompanied by a 16.5-fold (± 3.75) decrease in total p38 protein levels at 24 h of liquid application exposure (Figures 5C, D). Phosphorylation levels of ERK1 were significantly increased after 24 h of liquid application exposure, whereas ERK2 phosphorylation levels were unchanged (Figures 5E, F).

Liquid application increases pro-inflammatory cytokine and growth factor secretion in dpHBEC cultures

Bronchial epithelial cells play a key role in orchestrating inflammation within the respiratory tract in response to inhaled toxicants and other cellular stressors through the secretion of pro-inflammatory cytokines (Hewitt and Lloyd, 2021). After observing the upregulation of pro-inflammatory cytokine transcripts at both 6 and 24 h of liquid application, we sought to determine whether these changes also resulted in the increased release of the corresponding pro-inflammatory cytokine proteins. We observed significant increases in the secretion of IL-8, IL-1β, and TNFα into the basolateral medium at both 6 and 24 h of liquid application exposure (Figures 6A, B, D). While IL-6 secretion exhibited an upward trend after 24 h of liquid application exposure, the change was not statistically significant (Figure 6C). Cytokine concentration and fold change values are reported in Table 1.

The regulation of growth factor signaling plays an important role in normal airway homeostasis. Aberrant growth factor signaling occurs in response to chemical exposures and plays a role in airway

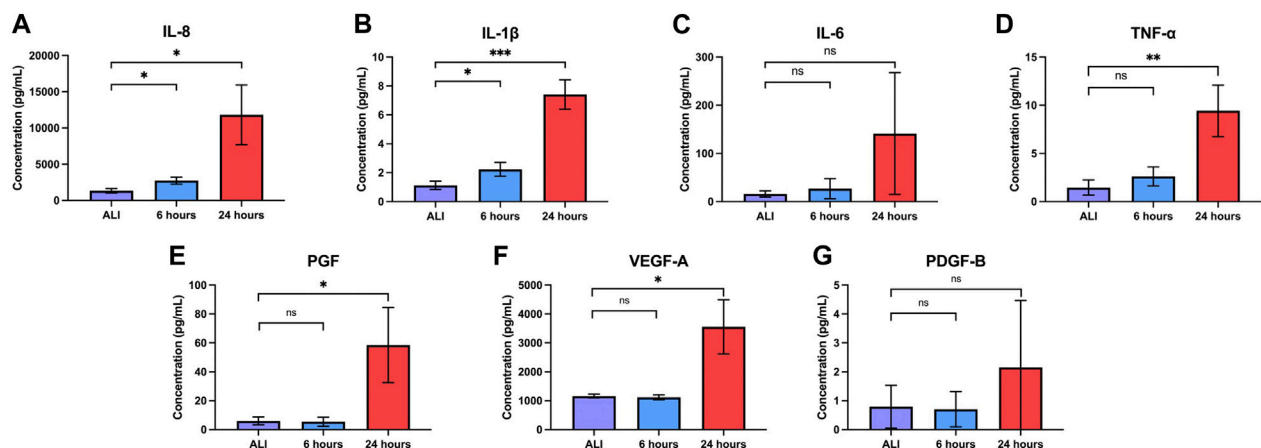


FIGURE 6

Liquid application increases the release of pro-inflammatory cytokines and growth factors. Effects of 6- and 24-h liquid application on the amount of (A) IL-8, (B) IL-1β, (C) IL-6, (D) TNF-α, (E) PGF, (F) VEGF-A, and (G) PDGF-B detected in the basolateral medium. Data represent the mean of $n = 3$ donors and error bars indicate SD. *, **, ***, and ns indicate $p \leq 0.05$, $p \leq 0.01$, $p \leq 0.001$, and not significant, respectively.

TABLE 1 Summary of pro-inflammatory cytokine and growth factor ELISA data.

Analyte	ALI concentration (pg/mL)	Concentration at 6 h LAE (pg/mL)	Fold change at 6 h (LAE/ALI)	<i>p</i> -value	Concentration at 24 h LAE (pg/mL)	Fold change at 24 h (LAE/ALI)	<i>p</i> -value
IL-8	1,338 (±319.9)	2,739 (±482.0)	2.0	0.014	11,820 (±4,116)	8.8	0.012
IL-1β	1.127 (±0.3)	2.233 (±0.5)	2.0	0.027	7.41 (±1.0)	6.6	0.001
IL-6	15.9 (±6.4)	26.88 (±20.9)	1.7	0.434	141.4 (±126.3)	8.9	0.161
TNF-α	1.46 (±0.8)	2.617 (±1.0)	1.8	0.189	9.427 (±2.7)	6.5	0.008
PDGF-B	0.7923 (±0.7)	0.7048 (±0.6)	0.9	0.883	2.157 (±2.3)	2.7	0.385
PGF	6.007 (±2.7)	5.417 (±3.1)	0.9	0.817	58.56 (±26.0)	9.7	0.025
VEGFA	1161 (±64.7)	1119 (±85.9)	1.0	0.532	3,557 (±937.0)	3.1	0.012

Values presented are the mean (± SD) of $n = 3$ donors. LAE refers to liquid application exposure.

disease (Desai and Cardoso, 2001; Woo et al., 2004; Voelkel et al., 2006; Wu et al., 2016). Liquid application resulted in the upregulation of several growth factor transcripts at 6 and 24 h so we sought to determine whether changes translated to increased growth factor secretion. We observed significant increases in the secretion of both PGF and VEGF-A, but not PDGF-B, into the basolateral medium after 24 h of liquid exposure (Figures 6E–G). Growth factor concentrations and fold change values are reported in Table 1.

Liquid application decreases dPHBEC culture epithelial barrier function but not ciliary function

In vivo, the normal bronchial epithelium functions in host defense as a physical barrier and a mucociliary escalator. In its role as a barrier, the normal bronchial epithelium forms an electrically resistant tissue layer that is selectively permeable to

small molecules that separates inhaled substances from underlying host tissue (Rezaee and Georas, 2014). While often affected by exposure to inhaled insults, loss of bronchial epithelial barrier integrity is also a hallmark of both acute and chronic respiratory disease (Peterson et al., 1993; Gerloff et al., 2017; Smyth et al., 2020; Carlier et al., 2021). Further, loss of epithelial barrier integrity also results in the loss of apical-basolateral polarization and is a key aspect of epithelial-to-mesenchymal transition (EMT), an early step in epithelial carcinogenesis (Saitoh, 2018). We evaluated the effect of liquid application on epithelial barrier integrity by determining the electrical resistance of the epithelial layer by trans-epithelial electrical resistance (TEER). Cultures maintained at ALI exhibited a mean TEER of $373.7 (\pm 83.9) \Omega \times \text{cm}^2$, which was significantly reduced to $212.7 (\pm 33.3) \Omega \times \text{cm}^2$ after 24 h of liquid application (Figure 7A); however, TEER was not significantly affected after 6 h of liquid application ($349.7 \pm 109.2 \Omega \times \text{cm}^2$). We then evaluated whether the decreased electrical resistance coincided with an increase in the small molecule permeability of the epithelial barrier. In concordance with the

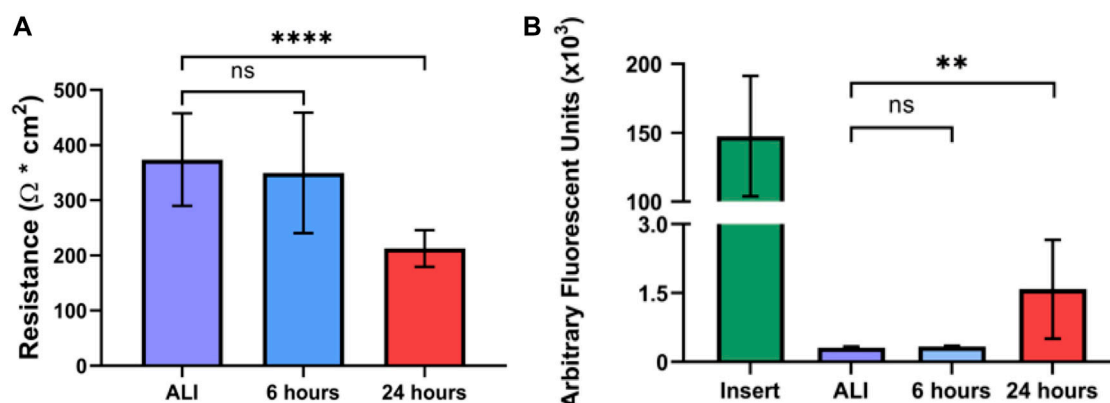


FIGURE 7

Liquid application reduces epithelial barrier integrity of dpHBEC cultures. (A) Effects of 6- and 24-h liquid application on TEER of dpHBEC layer. (B) Effects of 6- and 24-h liquid application on permeability of the dpHBEC layer to the translocation of 20 kDa FITC-dextran. Data represent the mean of $n = 3$ donors and error bars represent SD. ****, **, and ns indicate $p \leq 0.0001$, $p \leq 0.01$, and not significant, respectively. Data shown represent $n = 3$ donors.

observation of decreased TEER, liquid application significantly increased the permeability of the epithelial layer to 20 kDa FITC-conjugated dextran, which is a similar molecular weight to small biomolecules (e.g., IL-6), after 24 h (1581 ± 1076 arbitrary fluorescent units (AFU)), but not at 6 h (329.9 ± 19.6 AFU), when compared to cultures maintained at ALI (310.0 ± 21.9 AFU) (Figure 7B).

The normal *in vivo* bronchial epithelium contains actively beating cilia, a biological feature that is recapitulated *in vitro* by dpHBEC cultures. Despite observing the effects on barrier integrity described above, we did not observe any significant effect of liquid application on CBF or the percentage of active ciliated surface area of dpHBEC cultures (Supplementary Figure S3).

Discussion

The direct application of experimental treatments in aqueous solvents to differentiated primary human airway epithelial cell cultures is, and has been, a common practice for the dosing of *in vitro* ALI systems with biological stimuli, experimental interventions, and other test substances. Liquid application dosing is considered to be practical due to its expediency, low cost, and minimal technical requirements. The application of liquid to the apical surface of differentiated primary human airway epithelial cell cultures disrupts ALI conditions that are a critical component of their ability to represent the luminal surface of the respiratory tract *in vivo*; however, the effects of different liquid application conditions (e.g., liquid volume, type of solvent, and treatment duration) are poorly understood. The success of initiatives to leverage *in vitro* test systems in respiratory biology, pharmaceutical development, disease research, and inhaled chemical testing depends on building confidence in their ability to represent *in vivo* human-relevant physiology. Additionally, characterizing the effects of liquid application as a dosing modality for ALI-dpHBEC cultures is critical to create context for the interpretation and integration of data collected with this method into applicable decision-making processes.

Considerations for liquid application conditions

The conditions in which liquid application dosing is used, including the aqueous solvent used, volume of liquid applied, and duration of treatment, vary widely. We selected ALI medium as the applied liquid instead of PBS, 0.9% saline, or water to avoid generating an ionic gradient across the epithelial barrier and reducing nutrient availability. Additionally, while 0.9% saline is commonly used as a vehicle, it does not contain a pH buffer and has a broad pH range (manufacturer specification range of 4.5–7.0), which is often below pH 6.0 based on our evaluation of certificates of analysis from the commonly used manufacturers Baxter (#2F7123/#2F7124, lots #G154987, G139168, G160308, and G140409; mean pH 5.63 at room temperature according to certificates of analysis) and Cytiva (#Z1376, lots #WH30698322, WH30698323, WH30698324, and WH30698325; mean pH 5.79 at room temperature according to certificates of analysis). We used 250 μL of ALI medium in 12 mm Corning Transwell® inserts (221 $\mu\text{L}/\text{cm}^2$; equal to 73 μL in a 6.5 mm Transwell® insert) for this study because it was the smallest volume that we were able to use while maintaining complete coverage of the apical surface of the dpHBEC culture for the 24-h treatment duration. While smaller volumes are often used in studies involving liquid application dosing, the reduction in apical volume that occurs over the course of the treatment duration results in variable and ultimately discontinuous coverage of the treated culture. The ability of volumes often used to dose ALI cultures, such as 10–50 μL on a 6.5 mm cell culture insert (equivalent to 34–170 μL in the 12 mm inserts used in this study), to achieve and maintain complete coverage of the treated culture over the course has not been characterized. Based on observations reported here (Figure 1B), the use of applied liquid volumes below that used in this study would result in a gradient of liquid coverage that would be expected to lead to inconsistent test substance concentration and flux, ion and/or nutrient concentrations, and exposed oxygen concentrations across the exposed culture. Unfortunately, the potential impact of applied liquid volume on any, or all, of these

aspects of experimental exposures remains uncharacterized. Thus, the data collected from these smaller volumes may reflect the impact of either, or both, of these scenarios instead of just the effects of the test substance.

The application of liquid causes dpHBEC co-cultures to deviate from a normal phenotype

The use of differentiated primary airway epithelial cell systems as an *in vitro* model with enhanced physiological relevance compared to either their undifferentiated counterparts or analogous cell lines is predicated on the assumption that the cultures are comparable to their donor tissue of origin. That is, cultures generated from “normal healthy” donors are representative of the respective region of the respiratory tract *in vivo* in the “normal healthy” population. Here we report that the application of liquid to dpHBEC caused significant transcriptional reprogramming of 4,169 and 10,268 genes, which represented 17.6% and 43.4% of expressed genes, at 6 and 24 h of liquid application, respectively (Figure 2). Pathway analysis of changes in transcriptional profiles, as well as phenotypic and functional endpoints, indicated that the application of liquid to dpHBEC cultures caused effects that were consistent with cancer/epithelial-to-mesenchymal transition (EMT), fibrosis, hypoxia, wound healing, and pro-inflammation (Figures 3, 4). Thus, dpHBEC cultures were no longer consistent with their “normal healthy” counterparts (*i.e.*, incubator controls maintained at ALI) following the application of liquid to their apical surface. In addition to this deviation, liquid application also caused effects similar to those elicited by a broad range of inhaled toxicants within the respiratory tract.

While this study focused on the effects of liquid application on the dpHBEC cell layer, we also observed significant transcriptional reprogramming in IMR90 fibroblasts residing beneath liquid-treated dpHBECs (Supplementary Figures S2–4). While there were only modest transcriptional changes in the fibroblasts by 6 h, more substantial changes occurred by 24 h. At this later time point, the majority of alternatively regulated pathways indicated the development of a pro-carcinogenesis phenotype that complemented observations in the adjacent dpHBECs. Future studies examining the auto- and paracrine signaling events involved in the interactions of these 2 cell types, as well as the intracellular signaling in fibroblasts, will be a valuable advancement to the field.

Cell signaling

The response of the bronchial epithelium to inhaled toxicants and biological stimuli is mediated through the modulation of cellular signaling pathways, which regulate gene expression, cell survival and growth, and functional properties of the cell layer. Here, we observed that the application of liquid induces a significant increase in HIF-1 α protein stabilization at 6 h that is followed by increased p38 and ERK1 phosphorylation at 24 h (Figure 5). Activity of the HIF-1 signaling pathway is minimal under normoxic conditions in the healthy airway epithelium (Shimoda and Semenza, 2011). Under reduced oxygen concentrations, hypoxia-responsive gene expression is upregulated by the activation of the HIF-1 transcription factor

following stabilization and nuclear translocation of its regulatory HIF-1 α subunit (Dengler et al., 2014). Expression of HIF-1-responsive genes, including VEGF-A, ADM, and GLUT3, play key roles in angiogenesis, metabolism, and cell survival (Masoud and Li, 2015). While the induction of HIF-1 signaling is often considered in the context of tumorigenesis/carcinogenesis, aberrant HIF-1 α signaling also occurs in asthma, COPD, lung inflammation, acute lung injury, and ischemic lung injury (Ziello et al., 2007; Shimoda and Semenza, 2011; Ahmad et al., 2012; Masoud and Li, 2015; Tam et al., 2020). HIF-1 activation also results from exposure to inhaled substances including cigarette smoke, particulate matter, and many natural product-derived small molecules (Nagle and Zhou, 2006; Brant and Fabisiak, 2013; Daijo et al., 2016). HIF-1 α activation also contributes to EMT and enhanced pro-survival signaling (Chen and Sang, 2016).

Differences in oxygen content affect the physiology of cell culture systems, with a notable role for the activation of HIF-1-dependent signaling (Shimoda and Semenza, 2011; Masoud and Li, 2015). The availability of oxygen depends upon factors such as medium volume, culture configuration, cell type, and seeding density (Stuart et al., 2018). While medium volume affects diffusion of ambient oxygen to the cells, cell type and seeding density both influence consumption of available dissolved oxygen (Stuart et al., 2018). dpHBEC cultures grown under ALI cultures experience an oxygen concentration that is similar to the lumen of the respiratory tract *in vivo*, which is critical to their differentiation under ALI conditions (Kouthouridis et al., 2021). The increase in oxygen exposure that follows the transition of pHBEC cultures to ALI conditions is also accompanied by decreased HIF-1 α protein levels (Klasvogt et al., 2017; Kouthouridis et al., 2021). The importance of oxygen concentration on pHBEC differentiation has been further indicated by the demonstration that pHBECs grown in a submerged system with greater oxygen availability results in a phenotype identical to dpHBECs grown at ALI (Kouthouridis et al., 2021). In contrast, here we have demonstrated that the reduction of available oxygen by the application of liquid to dpHBEC-ALI cultures appears to initiate their dedifferentiation, which coincides with the stabilization of HIF-1 α . Future studies are required to characterize the relationship between oxygen availability, HIF-1 activation, dpHBEC culture physiology and exposure outcomes in the context of liquid application exposures.

ERK and p38 have diverse biological functions that include responding to cellular stress as well as promoting cell growth and survival (Roux and Blenis, 2004; Zarubin and Han, 2005; Lu and Xu, 2006; Martínez-Limón et al., 2020). The alternative regulation of cellular signaling proteins such as ERK1 and p38, alone or in concert, has been observed in response to exposures to a broad range of inhaled toxicants including ozone, diesel exhaust particulates, acrolein, asbestos, cigarette smoke, and diacetyl (2,3-butanedione) (Hashimoto et al., 2000; Cummins et al., 2003; Moretto et al., 2012; McCullough et al., 2014; Xu et al., 2015; Kelly et al., 2019). Further, the alternative regulation of these signaling proteins also occurs in a variety of respiratory diseases including COPD, asthma, fibrosis, EMT, and cancer (Yoshida et al., 2002; Renda et al., 2008; Alam and Gorska, 2010; Gui et al., 2012; Madala et al., 2012). Similar to HIF-1, the activation of these signaling proteins by liquid application alone has the potential to

confound exposure outcomes and interpretation. For example, the activation of ERK and p38 by the application of liquid alone may have an additive or synergistic effect on the activation of these proteins, or other signaling pathways, that occurs as a result of exposure to a test substance. Thus, exposure to the test substance by liquid application could enhance toxicity-related exposure outcomes that are dependent on ERK and/or p38 activation such as the induction of pro-inflammatory gene expression in pHBEC cultures (McCullough et al., 2014; Bowers et al., 2018). Alternatively, the role of HIF-1 α , ERK, and/or p38 activation in pro-survival and growth signaling may mean that the activation of these pathways by the application of liquid alone could diminish the cytotoxic effects of a test substance applied by liquid dosing. The pleiotropic effects of HIF-1 α , ERK, and p38 provide many possible avenues by which the effect of liquid application could impact the outcome and/or interpretation of chemical testing studies that utilize liquid dosing of dpHBEC-ALI cultures.

Induction of pro-inflammatory mediators

The airway epithelium plays a central role in the release of pro-inflammatory cytokines that play concerted roles in the response to inflammatory stimuli, airway insult/injury, and tissue homeostasis. While beneficial in the resolution of damage, their dysregulation results in airway remodeling, a chronic inflammatory state, impaired lung function, and disease (Reynolds et al., 2018). Given the role of inflammation and response to tissue injury in the etiology of toxicant-induced effects, several pro-inflammatory cytokines, such as IL-8 and TNF- α , are common endpoints in the evaluation of chemical toxicity. In the study reported here, the application of liquid alone induced significant increases in the release of IL-8 and IL-1 β at 6 h and IL-8, IL-1 β , and TNF- α at 24 h (Figure 6). The increased release of these pro-inflammatory cytokines has been implicated in a variety of respiratory diseases including COPD, acute lung injury, epithelial-to-mesenchymal transition, and squamous cell metaplasia (Chung, 2001; Goodman et al., 2003; Herfs et al., 2012; Pain et al., 2014). Further, the dysregulation of pro-inflammatory cytokine secretion also results from exposure to a diverse range of inhaled substances including diesel exhaust particulates, ambient particulate matter, acrolein, cigarette smoke, e-cigarette flavorings, and zinc oxide nanoparticles (Stoehr et al., 2015; Zhou et al., 2015; Gerloff et al., 2017; Murray et al., 2017; Grytting et al., 2022). Therefore, the observation that liquid application alone significantly enhances pro-inflammatory cytokine secretion indicates that the effects of this dosing method alone can induce a disease-like phenotype and could limit the identification of test substances that induce a pro-inflammatory response in the bronchial epithelium. Further, the induction of pro-inflammatory mediators by liquid application alone could account for the significantly lower levels of IL-8 induction in dpHBEC exposed to reactive aldehydes by liquid application dosing compared to matched ALI dosing reported by Dwivedi et al. (Dwivedi et al., 2018). The increased secretion of pro-inflammatory mediators by the bronchial epithelium also has the potential to prime the culture to respond more strongly to test substance exposure compared to the epithelium at ALI or the *in vivo* airway. For example, HTB-54 lung epithelial cells primed with TNF-

α , were found to secrete more IL-8 following particulate matter exposure compared to non-primed cells (Ning et al., 2004). Additionally, the detection of elevated IL-8, TNF- α , or IL-1 β is considered a biomarker for a wide variety of inflammatory conditions *in vivo* (Shahzad et al., 2010; Andreasson et al., 2017; Aghapour et al., 2018; Tutkun et al., 2019). Thus, the use of liquid application dosing may invalidate the use of pro-inflammatory cytokine release as an *in vitro* biomarker that is directly linked to *in vivo* mediators of toxicity.

Airway epithelial barrier integrity

The healthy bronchial epithelium functions as the barrier that protects the underlying lung tissue from inhaled pathogens, chemicals, and other materials. We observed that the application of liquid to dpHBEC significantly decreased barrier integrity and increased permeability as measured by a reduction in TEER and an increase in 20 kDa FITC-Dextran permeability at 24 h, respectively (Figure 7). Loss of epithelial barrier integrity is a hallmark of airway injury and occurs in airway diseases including COPD, acute respiratory distress syndrome, asthma, fibrosis, and EMT/cancer, thus supporting the conclusion that the application of liquid to dpHBEC causes a phenotype that is consistent with a range of respiratory diseases (Georas and Rezaee, 2014; Lamouille et al., 2014; Brune et al., 2015; Aghapour et al., 2018; Carlier et al., 2021). In contrast, hypoxia is protective against oxidant-induced loss of barrier integrity (Olson et al., 2011); however, our observations indicate that the stabilization of HIF-1 α protein alone (Figure 5) is not sufficient to prevent the loss of barrier integrity following liquid application. Epithelial barrier integrity is also adversely affected following exposure to a diverse range of inhaled substances including diesel exhaust particulates, ambient particulate matter, acrolein, asbestos, ozone, wood smoke particulates, and e-cigarette flavorings (Peterson et al., 1993; Yu et al., 1994; Olson et al., 2011; Gerloff et al., 2017; Xiong et al., 2018; Zeglinski et al., 2019; Smyth et al., 2020; Xian et al., 2020; Bowers et al., 2022). Thus, the observation that liquid application alone significantly reduces barrier integrity indicates the potential for this manner of dosing to limit the sensitivity of this approach to identify test substances that disrupt barrier function.

The polarized nature of the respiratory epithelial barrier results in the segregation of receptors and other factors between their apical and basolateral surfaces, which is important in maintaining tissue homeostasis. Liquid-induced disruption of barrier integrity could result in aberrant distribution of both cell surface receptors and/or the test substance relative to exposures conducted under ALI conditions or by inhalation *in vivo*. For example, members of the human epidermal growth factor receptor (HER) family are differentially localized to the apical and basolateral compartments of the airway epithelium, which plays a critical role in their function *in vivo* (Brune et al., 2015). Under homeostatic conditions, the epidermal growth factor receptor (EGFR; dimer of HER1) and the heterodimeric HER2/3 receptor are localized to the basolateral surface of the airway epithelium where they are separated from their ligands, epidermal growth factor (EGF) and heregulin, respectively, which are expressed in the apical compartment (Takeyama et al., 2001; Vermeer et al., 2003). When this

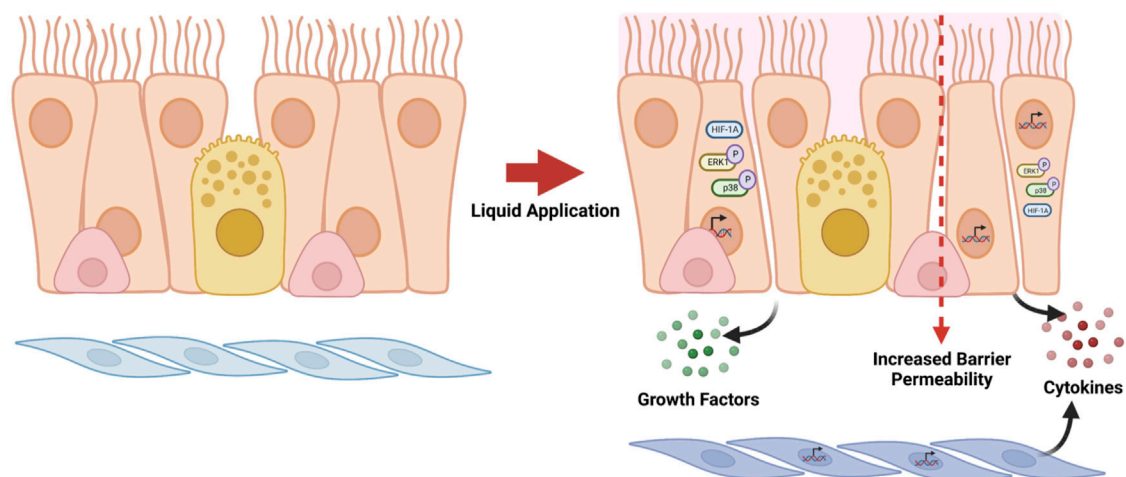


FIGURE 8

Summary of effects caused by liquid application to dpHBEC-ALI cultures. The application of 250 μ L ALI medium induces the alternative regulation of transcripts, the activation of stress-responsive protein signaling pathways, the secretion of pro-inflammatory cytokines and growth factors, and the breakdown of epithelial barrier integrity. Figure made with [BioRender.com](https://www.biorender.com).

compartmentalization is disrupted by damage to the epithelium, EGF and heregulin are able to access their respective receptors to promote repair of the epithelium through cell proliferation, differentiation, and protection (van der Geer et al., 1994; Walker, 1998; Yarden and Sliwkowski, 2001; Brune et al., 2015). Further, members of the toll-like receptor (TLR) family are also selectively localized to the apical or basolateral surfaces of airway epithelial cells where they play distinct roles in the recognition of exogenous pathogen-associated molecular patterns (PAMPs) and endogenous damage-associated molecular patterns (DAMPs) (Ioannidis et al., 2013; Arora et al., 2019). Activation of the HER and TLR families are involved in various diseases of the respiratory tract and are activated in response to a wide range of inhaled chemicals/materials as well as DAMPs resulting from the effects of reactive oxygen species that are common mediators of inhaled toxicants (Lucas and Maes, 2013; Luettich et al., 2017; Arora et al., 2019). Thus, loss of barrier integrity resulting from liquid application could result in the artificial exposure of test substances to receptors that they would not interact with under ALI conditions. Liquid application-induced decompartmentalization could also induce a pro-repair response that could limit the effects of test substances on cell survival. Further, activation of EGFR due to loss of epithelial barrier function also promotes mucus production (Burgel and Nadel, 2004), which could be interpreted as an adverse effect of exposure and/or alter the interaction of the test substance with the epithelial cell surface. Importantly, these effects may not be easily accounted for by the normalization of the effects of test substance exposures to vehicle controls.

Potential impact of a hypertonic environment

The reduction of apical volume occurring during the treatment duration observed in Figure 1B may result from evaporation, para-

or transcellular transport, or both. If occurring by evaporation, this change in apical volume will result in a hypertonic environment. We were unable to find any reports describing the effect of apical solvent evaporation in air-liquid interface *in vitro* respiratory tract cultures; however, the effects of exposure to hypertonic saline *in vitro* and *in vivo* have been previously reported. Nebulized hypertonic saline (HS) increases mucus clearance *in vivo* by increasing airway hydration and reduced viscosity through the disruption of ionic bonds and induced conformational changes in mucus proteins (Ziment, 1978; Robinson et al., 1997; Graeber et al., 2013). Treatment-induced increases in airway hydration were supported by the observation that aerosolized HS increased airway surface liquid (ASL) height in dpHBEC-ALI cultures *in vitro* (Goralski et al., 2018). Unfortunately, we did not evaluate mucus viscosity or ASL height in this study; however, understanding the impacts of liquid application and solvent evaporation on these parameters would be valuable given the potential for mucus to trap and sequester inhaled toxicants. Changes in ASL volume may also impact test substance concentrations, especially when experimental treatments are delivered in low applied liquid volumes. While hypertonic saline did not affect inflammation in a mouse model of chronic obstructive lung disease (Graeber et al., 2013), it did attenuate inflammation following trauma and hemorrhagic shock in rats (Wohlauer et al., 2012) and pro-inflammatory gene expression following treatment of primary human small airway epithelial cells with TNF- α , IL-1 β , and interferon (IFN)- γ *in vitro* (Mitra et al., 2017). While we expected some level of evaporation to occur during these treatments, we observed that the effects of liquid application increased the expression and secretion of pro-inflammatory cytokines (Figures 3, 4, 6). Thus, our observations indicate that either the evaporation in our approach did not create a sufficiently hypertonic condition, or the anti-inflammatory potential of hypertonic conditions is not sufficient to prevent the induction of pro-inflammatory mediators the results from liquid application. Additional studies are required to determine whether the mitigation of pro-inflammatory stimuli by hypertonic conditions described by

Mitra et al. (2017) alters the ability of low-volume liquid application dosing approaches to represent the induction of pro-inflammatory mediators by test substances.

Study limitations

The study reported here provides novel insight into the effects of liquid application on dpHBEC but has limitations that should be considered. First, we have previously shown that some endpoints vary based on inter-individual variability (Bowers et al., 2018; 2022). While the range of inter-individual variability for the endpoints evaluated here has not been evaluated, this study utilized an *n* of three dpHBEC donors for each endpoint evaluated. It remains unclear whether this sample size is sufficient to fully reflect the range of variability in the effects of liquid application on dpHBEC in the “normal healthy” donor population. Further, future studies using donor-matched primary HLF will be required to address the potential for inter-individual variability on the effects of liquid application on HLF beneath the epithelial barrier. Second, the liquid application dosing method has been used with a broad range of applied liquid volumes and in different permeable cell culture insert configurations (e.g., manufacturers, insert diameters, pore sizes, pore densities, membrane materials, *et cetera*). The observations reported here only evaluated one set of conditions. Third, different aqueous solvents including water, 0.9% saline, buffered (phosphate or other) saline, or cell culture medium have been used in reported studies that utilized liquid application dosing.

The impact of the type, volume, and duration of liquid application on the effects observed in dpHBEC cultures should be evaluated in future studies to provide a more comprehensive understanding of these variables on *in vivo* physiology-relevant endpoints, exposure outcomes, and test substance delivery/dosimetry. While this study sought to describe the effects of liquid application on the dpHBEC-ALI system, future studies could also provide a thorough characterization of the molecular mechanisms underlying the effects reported here. More specifically, additional work could more comprehensively evaluate the hypotheses generated with the RNA-sequencing data regarding the alternative regulation of biological pathways by liquid application. Additional studies could also determine the relative contributions of the MAPK pathways and HIF1 α signaling in the response of dpHBEC-ALI cultures to liquid application. Further studies are also required to determine whether differentiated primary human airway epithelial cell ALI models of other regions of the respiratory tract are similarly affected by the application of liquid alone.

Conclusion

In vitro studies that utilize differentiated primary human airway cell systems to evaluate inhalable test substances frequently rely on direct application dosing; however, publications describing these studies rarely report the use of an ALI control (*i.e.*, not subjected to liquid application) to account for the effects of the application of liquid alone in the data analysis and interpretation. The findings described here demonstrate that the application of liquid alone can

cause large-scale reprogramming of gene expression in differentiated ALI cultures and significant changes to aspects of the cell culture physiology that are of great importance with respect to the ability of the dpHBEC-ALI system to represent key aspects of *in vivo* respiratory tract physiology. Importantly, the effects liquid application on culture physiology occurred in the absence of changes in the cultures that would be detectable by basic visual microscopic examination. Thus, they would likely go unnoticed without more thorough evaluation. Further, the changes that result from liquid application involve the alternative regulation of cellular pathways that are often involved in mediating the response to exogenous stimuli and diseases of the respiratory tract. The endpoints that we observed to be alternatively regulated by liquid application are also commonly used to identify and quantify the toxicity or efficacy of test substances (*i.e.*, epithelial barrier function, cellular signaling pathway activation, pro-inflammatory cytokine release, and growth factor production) (Figure 8).

The findings reported here support the conclusion that the impact of the application of liquid alone has the potential to confound the accuracy, sensitivity, and translation of data resulting from the use of liquid dosing of dpHBEC-ALI systems for respiratory biology research and the evaluation of inhaled substances. Further, given the observations reported here, the comparison of test substance exposures to their respective vehicle treatment may not be sufficient to normalize data for comparison or extrapolation to *in vivo* human exposure outcomes. Additional studies are required to characterize the impact of liquid application on ALI cultures and exposure outcomes and provide a better understanding of the impact of liquid application on exposure outcomes and comparability of liquid application and ALI dosing outcomes in differentiated primary human airway epithelial tissue models.

The use of differentiated ALI cultures to inform inhaled chemical hazard identification and human health risk assessment is in its relative infancy, but the demand of the use of the approach is increasing. This is evidenced by the use of this dosing method in a recent case study for the use of an ALI-differentiated *in vitro* system as a part of an integrated approach to testing and assessment (IATA) to refine an inhalation risk assessment by the Organisation for Economic Co-operation and Development (OECD) (National Research Council, 2007; United States Environmental Protection Agency, 2020), an organization that develops international guidelines for studies used to evaluate pharmaceuticals, as well as commercial and industrial chemicals. Identification of considerations and limitations to the use of direct application dosing of ALI cultures at this early stage is critical for defining the context for their use in the assessment of inhalable substances. It also provides guidance on important aspects of study design and reporting, as well as considerations for the interpretation of data derived from liquid application dosing of dpHBEC-ALI systems, and potentially differentiated primary cell-based ALI models of other regions of the human respiratory tract. Additional studies are needed to determine whether the effect of liquid application alone impacts the outcomes of *in vitro* inhaled chemical testing, whether the effects observed here are specific to the conditions used in this study, and if these effects apply to differentiated ALI models of other regions of the human respiratory tract. Future studies are also needed to determine whether aspects of this dosing method

(e.g., type of aqueous buffer used, liquid volume, exposure duration, *et cetera*) can be optimized to minimize the effects on culture physiology. Ultimately, improving our understanding of how key aspects of differentiated ALI models of the human respiratory tract impact their physiology, response to test substance exposures, and data analysis and interpretation is central to building confidence in their ability to reflect *in vivo* human outcomes and advancing the translation of data from these *in vitro* systems into decision making.

Data availability statement

The datasets presented in this study can be found in online repositories. The names of the repository/repositories and accession number(s) can be found below: <https://www.ncbi.nlm.nih.gov/geo/>, GSE198884. <https://catalog.data.gov/dataset/epa-sciencehub>, by searching the manuscript title or DOI: 10.23719/1526421.

Ethics statement

These studies involved the use of de-identified primary human cells obtained from a biobank. The protocol for the collection of these cells from human volunteers was approved by the University of North Carolina at Chapel Hill Institutional Review Board and the US Environmental Protection Agency Office of Human Research Protection. Volunteers provided their written informed consent prior to sample collection for biobank storage.

Author contributions

NM: Formal Analysis, Methodology, Visualization, Writing—original draft, Writing—review and editing. EM: Data curation, Formal Analysis, Visualization, Writing—review and editing. LD: Investigation, Methodology, Writing—review and editing. SM: Conceptualization, Funding acquisition, Project administration, Resources, Supervision, Visualization, Writing—original draft, Writing—review and editing.

Funding

The author(s) declare financial support was received for the research, authorship, and/or publication of this article. NM was supported by a NIEHS T32 training grant (#2T32ES007126) and a

cooperative agreement between the US Environmental Protection Agency and the UNC Center for Environmental Medicine, Asthma, and Lung Biology (#CR82952201). EM was supported through the Intramural Research Program of the National Institute of Environmental Health Sciences, NIH (ES103372-01). SM and LD were supported by intramural research funding through the US Environmental Protection Agency. SM was also supported by RTI International.

Acknowledgments

We would also like to thank Drs. Phillip Clapp, Ana Rappold, David Diaz-Sanchez, Adam Speen, Jessica Murray, Annie Jarabek, and Ron Hines for critical reading of the manuscript prior to submission. Figures 1, 8 were made using BioRender.com. The research described in this manuscript has been reviewed and approved for publication by the United States Environmental Protection Agency's Office of Research and Development. Approval does not signify that contents necessarily reflect the views and policies of the agency, nor does the mention of trade names or commercial products constitute endorsement or recommendation for use.

Conflict of interest

The authors declare that the research was conducted in the absence of any commercial or financial relationships that could be construed as a potential conflict of interest.

Publisher's note

All claims expressed in this article are solely those of the authors and do not necessarily represent those of their affiliated organizations, or those of the publisher, the editors and the reviewers. Any product that may be evaluated in this article, or claim that may be made by its manufacturer, is not guaranteed or endorsed by the publisher.

Supplementary material

The Supplementary Material for this article can be found online at: <https://www.frontiersin.org/articles/10.3389/ftox.2023.1264331/full#supplementary-material>

References

- Aghapour, M., Raee, P., Moghaddam, S. J., Hiemstra, P. S., and Heijink, I. H. (2018). Airway epithelial barrier dysfunction in chronic obstructive pulmonary disease: role of cigarette smoke exposure. *Am. J. Respir. Cell Mol. Biol.* 58 (2), 157–169. doi:10.1165/rcmb.2017-0200TR
- Ahmad, T., Kumar, M., Mabalirajan, U., Pattnaik, B., Aggarwal, S., Singh, R., et al. (2012). Hypoxia response in asthma: differential modulation on inflammation and epithelial injury. *Am. J. Respir. Cell Mol. Biol.* 47 (1), 1–10. doi:10.1165/rcmb.2011-0203OC
- Alam, R., and Gorska, M. M. (2010). Mitogen-activated protein kinase signalling and ERK1/2 bistability in asthma. *Clin. Exp. Allergy* 41, 149–159. doi:10.1111/j.1365-2222.2010.03658.x
- Andreasson, A. S. I., Borthwick, L. A., Gillespie, C., Jiwa, K., Scott, J., Henderson, P., et al. (2017). The role of interleukin-1 β as a predictive biomarker and potential therapeutic target during clinical *ex vivo* lung perfusion. *J. Heart Lung Transplant.* 36 (9), 985–995. doi:10.1016/j.healun.2017.05.012
- Arcaroli, J., Yum, H. K., Kupfner, J., Park, J. S., Yang, K. Y., and Abraham, E. (2001). Role of p38 MAP kinase in the development of acute lung injury. *Clin. Immunol.* 101 (2), 211–219. doi:10.1006/clim.2001.5108
- Arora, S., Ahmad, S., Irshad, R., Goyal, Y., Rafat, S., Siddiqui, N., et al. (2019). TLRs in pulmonary diseases. *Life Sci.* 233, 116671. doi:10.1016/j.lfs.2019.116671

- Bowers, E. C., Martin, E. M., Jarabek, A. M., Morgan, D. S., Smith, H. J., Dailey, L. A., et al. (2022). Ozone responsive gene expression as a model for describing repeat exposure response trajectories and interindividual toxicodynamic variability *in vitro*. *Toxicol. Sci.* 185 (1), 38–49. doi:10.1093/toxsci/kfab128
- Bowers, E. C., McCullough, S. D., Morgan, D. S., Dailey, L. A., and Diaz-Sanchez, D. (2018). ERK1/2 and p38 regulate inter-individual variability in ozone-mediated IL-8 gene expression in primary human bronchial epithelial cells. *Sci. Rep.* 8 (1), 9398–9409. doi:10.1038/s41598-018-27662-0
- Brant, K. A., and Fabisiak, J. P. (2013). Role of hypoxia-inducible factor 1, α subunit and cAMP-response element binding protein 1 in synergistic release of interleukin 8 by prostaglandin E2 and nickel in lung fibroblasts. *Am. J. Respir. Cell Mol. Biol.* 49 (1), 105–113. doi:10.1165/rcmb.2012-0297OC
- Brune, K., Frank, J., Schwingshackl, A., Finigan, J., and Sidhaye, V. K. (2015). Pulmonary epithelial barrier function: some new players and mechanisms. *Am. J. Physiology - Lung Cell. Mol. Physiology* 308 (8), L731–L745. doi:10.1152/ajplung.00309.2014
- Burgel, P.-R., and Nadel, J. A. (2004). Roles of epidermal growth factor receptor activation in epithelial cell repair and mucin production in airway epithelium. *Thorax* 59 (11), 992–996. doi:10.1136/thx.2003.018879
- Canovas, B., and Nebreda, A. R. (2021). Diversity and versatility of p38 kinase signalling in health and disease. *Nat. Rev. Mol. Cell Biol.* 22 (5), 346–366. doi:10.1038/s41580-020-00322-w
- Carlier, F. M., de Fays, C., and Pilette, C. (2021). Epithelial barrier dysfunction in chronic respiratory diseases. *Front. Physiology* 12, 691227–27. doi:10.3389/fphys.2021.691227
- Chen, S., and Sang, N. (2016). Hypoxia-Inducible Factor-1: a critical player in the survival strategy of stressed cells. *J. Cell. Biochem.* 117 (2), 267–278. doi:10.1002/jcb.25283
- Chung, K. F. (2001). Cytokines in chronic obstructive pulmonary disease. *Eur. Respir. J.* 18 (34), 50–59. *Supplement*. doi:10.1183/09031936.01.00229701
- Clippinger, A. J., Allen, D., Behrsing, H., Bérubé, K. A., Bolger, M. B., Casey, W., et al. (2018b). Pathway-based predictive approaches for non-animal assessment of acute inhalation toxicity. *Toxicol. Vitro* 52, 131–145. doi:10.1016/j.tiv.2018.06.009
- Clippinger, A. J., Allen, D., Jarabek, A. M., Corvaro, M., Gaça, M., Gehen, S., et al. (2018a). Alternative approaches for acute inhalation toxicity testing to address global regulatory and non-regulatory data requirements: an international workshop report. *Toxicol. Vitro* 48, 53–70. doi:10.1016/j.tiv.2017.12.011
- Cummins, A. B., Palmer, C., Mossman, B. T., and Taatjes, D. J. (2003). Persistent localization of activated extracellular signal-regulated kinases (ERK1/2) is epithelial cell-specific in an inhalation model of asbestosis. *Am. J. Pathology* 162 (3), 713–720. doi:10.1016/S0002-9440(10)63867-9
- Daijo, H., Hoshino, Y., Kai, S., Suzuki, K., Nishi, K., Matsuo, Y., et al. (2016). Cigarette smoke reversibly activates hypoxia-inducible factor 1 in a reactive oxygen species-dependent manner. *Sci. Rep.* 6, 1–12. doi:10.1038/srep34424
- Dailey, L. A., and McCullough, S. D. (2021). Culture and differentiation of primary human tracheobronchial epithelial cells using STEMCELL Technologies Pneumacult media. *Protoc. Exch., PROTOCOL* (Version 1). doi:10.21203/rs.3.pex-1674/v1
- Dengler, V. L., Galbraith, M. D., and Espinosa, J. M. (2014). Transcriptional regulation by hypoxia inducible factors. *Crit. Rev. Biochem. Mol. Biol.* 49 (1), 1–15. doi:10.3109/10409238.2013.838205
- Desai, T. J., and Cardoso, W. V. (2001). Growth factors in lung development and disease: friends and foe? *Respir. Res.* 3, 1–4. doi:10.1186/rr169
- Dwivedi, A. M., Upadhyay, S., Johanson, G., Ernstgård, L., and Palmberg, L. (2018). Inflammatory effects of acrolein, crotonaldehyde and hexanal vapors on human primary bronchial epithelial cells cultured at air-liquid interface. *Toxicol. Vitro* 46, 219–228. doi:10.1016/j.tiv.2017.09.016
- Faber, S. C., and McCullough, S. D. (2018). Through the looking glass: *in vitro* models for inhalation toxicology and interindividual variability in the airway. *Appl. Vitro Toxicol.* 4 (2), 115–128. doi:10.1089/aivt.2018.0002
- Faber, S. C., and McCullough, S. D. (2020). FITC-dextran trans-epithelial permeability assay. *Protoc. Exch., PROTOCOL* (Version 1). doi:10.21203/rs.2.20495/v1
- Fulcher, M. L., Gabriel, S., Burns, K. A., Yankaskas, J. R., and Randell, S. H. (2005). Well-differentiated human airway epithelial cell cultures. *Methods Mol. Med. U. S.* 107, 183–206. doi:10.1385/1-59259-861-7:183
- Georas, S. N., and Rezaee, F. (2014). Epithelial barrier function: at the front line of asthma immunology and allergic airway inflammation. *J. Allergy Clin. Immunol.* 134 (3), 509–520. doi:10.1016/j.jaci.2014.05.049
- Gerloff, J., Sundar, I. K., Freter, R., Sekera, E. R., Friedman, A. E., Robinson, R., et al. (2017). Inflammatory response and barrier dysfunction by different e-cigarette flavoring chemicals identified by gas chromatography-mass spectrometry in e-liquids and e-vapors on human lung epithelial cells and fibroblasts. *Appl. Vitro Toxicol.* 3 (1), 28–40. doi:10.1089/aivt.2016.0030
- Goodman, R. B., Pugin, J., Lee, J. S., and Matthay, M. A. (2003). Cytokine-mediated inflammation in acute lung injury. *Cytokine Growth Factor Rev.* 14 (6), 523–535. doi:10.1016/S1359-6101(03)00059-5
- Goralski, J. L., Wu, D., Thelin, W. R., Boucher, R. C., and Button, B. (2018). The *in vitro* effect of nebulized hypertonic saline on human bronchial epithelium. *Eur. Respir. J.* 51 (5), 1702652. doi:10.1183/13993003.02652-2017
- Graeber, A. Y., Zhou-Suckow, Z., Schatterny, J., Hirtz, S., Boucher, R. C., and Mall, M. A. (2013). Hypertonic saline is effective in the prevention and treatment of mucus obstruction, but not airway inflammation, in mice with chronic obstructive lung disease. *Am. J. Respir. Cell Mol. Biol.* 49 (3), 410–417. doi:10.1165/rcmb.2013-0050OC
- Grytting, V. S., Chand, P., Låg, M., Øvrevik, J., and Refsnes, M. (2022). The pro-inflammatory effects of combined exposure to diesel exhaust particles and mineral particles in human bronchial epithelial cells. *Part. Fibre Toxicol.* 19 (1), 14–22. doi:10.1186/s12989-022-00455-0
- Gui, T., Sun, Y., Shimokado, A., and Muragaki, Y. (2012). The roles of mitogen-activated protein kinase pathways in TGF- β -induced epithelial-mesenchymal transition. *J. Signal Transduct.* 2012, 289243. doi:10.1155/2012/289243
- Guo, Y., Pan, W. W., Liu, S. B., Shen, Z. F., Xu, Y., and Hu, L. L. (2020). ERK/MAPK signalling pathway and tumorigenesis. *Exp. Ther. Med.* 19, 1997–2007. doi:10.3892/etm.2020.8454
- Hashimoto, S., Gon, Y., Takeshita, I., Matsumoto, K., Jibiki, I., Takizawa, H., et al. (2000). Diesel exhaust particles activate p38 MAP kinase to produce interleukin 8 and RANTES by human bronchial epithelial cells and N-acetylcysteine attenuates p38 MAP kinase activation. *Am. J. Respir. Crit. Care Med.* 161 (1), 280–285. doi:10.1164/ajrccm.161.1.9904110
- Herfs, M., Hubert, P., Poirrier, A. L., Vandevenne, P., Renoux, V., Habraken, Y., et al. (2012). Proinflammatory cytokines induce bronchial hyperplasia and squamous metaplasia in smokers implications for chronic obstructive pulmonary disease therapy. *Am. J. Respir. Cell Mol. Biol.* 47 (1), 67–79. doi:10.1165/rcmb.2011-0353OC
- Hewitt, R. J., and Lloyd, C. M. (2021). Regulation of immune responses by the airway epithelial cell landscape. *Nat. Rev. Immunol.* 21 (6), 347–362. doi:10.1038/s41577-020-00477-9
- Hiemstra, P. S., Grootaers, G., van der Does, A. M., Krul, C. A. M., and Kooter, I. M. (2018). Human lung epithelial cell cultures for analysis of inhaled toxicants: lessons learned and future directions. *Toxicol. Vitro* 47, 137–146. doi:10.1016/j.tiv.2017.11.005
- Hiemstra, P. S., McCray, P. B., and Bals, R. (2015). The innate immune function of airway epithelial cells in inflammatory lung disease. *Eur. Respir. J.* 45 (4), 1150–1162. doi:10.1183/09031936.00141514
- Ioannidis, I., Ye, F., McNally, B., Willette, M., and Flaño, E. (2013). Toll-like receptor expression and induction of type I and type III interferons in primary airway epithelial cells. *J. Virology. U. S.* 87 (6), 3261–3270. doi:10.1128/JVI.01956-12
- Kelly, F. L., Weinberg, K. E., Nagler, A. E., Nixon, A. B., Star, M. D., Todd, J. L., et al. (2019). EGFR-dependent IL8 production by airway epithelial cells after exposure to the food flavoring chemical 2,3-butanedione. *Toxicol. Sci.* 169 (2), 534–542. doi:10.1093/toxsci/kfz066
- Kendall, R. T., and Feghali-Bostwick, C. A. (2014). Fibroblasts in fibrosis: novel roles and mediators. *Front. Pharmacol.* 5, 123. doi:10.3389/fphar.2014.00123
- Klasovogt, S., Zuschtratter, W., Schmidt, A., Kröber, A., Vorwerk, S., Wolter, R., et al. (2017). Air-liquid interface enhances oxidative phosphorylation in intestinal epithelial cell line IPEC-J2. *Cell Death Discov.* 3 (1), 17001. doi:10.1038/cddiscovery.2017.1
- Kouthouridis, S., Goepp, J., Martini, C., Matthes, E., Hanrahan, J. W., and Moraes, C. (2021). Oxygenation as a driving factor in epithelial differentiation at the air-liquid interface. *Integrative biology: quantitative biosciences from nano to macro. England* 13 (3), 61–72. doi:10.1093/intbio/zyab002
- Lamouille, S., Xu, J., and Derynck, R. (2014). Molecular mechanisms of epithelial-mesenchymal transition. *Nat. Rev. Mol. Cell Biol.* 15 (3), 178–196. Nature Publishing Group. doi:10.1038/nrm3758
- Lu, Z., and Xu, S. (2006). ERK1/2 MAP kinases in cell survival and apoptosis. *IUBMB Life* 58 (11), 621–631. doi:10.1080/15216540600957438
- Lucas, K., and Maes, M. (2013). Role of the Toll like receptor (TLR) radical cycle in chronic inflammation: possible treatments targeting the TLR4 pathway. *Mol. Neurobiol.* 48 (1), 190–204. doi:10.1007/s12035-013-8425-7
- Luettich, K., Talikka, M., Lowe, F. J., Haswell, L. E., Park, J., Gaca, M. D., et al. (2017). The adverse outcome pathway for oxidative stress-mediated EGFR activation leading to decreased lung function. *Appl. Vitro Toxicol.* 3 (1), 99–109. doi:10.1089/aivt.2016.0032
- Madala, S. K., Schmidt, S., Davidson, C., Ikegami, M., Wert, S., and Hardie, W. D. (2012). MEK-ERK pathway modulation ameliorates pulmonary fibrosis associated with epidermal growth factor receptor activation. *Am. J. Respir. Cell Mol. Biol.* 46 (3), 380–388. doi:10.1165/rcmb.2011-0237OC
- Mallek, N. M., and McCullough, S. D. (2021a). Culture of IMR90 cells in advanced MEM with reduced serum. *Protoc. Exch., PROTOCOL* (Version 1). doi:10.21203/rs.3.pex-1673/v1
- Mallek, N. M., and McCullough, S. D. (2021b). Measurement of trans-epithelial electrical resistance with EVOM2 and EndOhm cup. *Protoc. Exch., PROTOCOL* (Version 1). doi:10.21203/rs.3.pex-1672/v1
- Martínez-Limón, A., Joaquín, M., Caballero, M., Posas, F., and de Nadal, E. (2020). The p38 pathway: from biology to cancer therapy. *Int. J. Mol. Sci.* 21 (6), 1–18. doi:10.3390/ijms21061913
- Masoud, G. N., and Li, W. (2015). HIF-1 α pathway: role, regulation and intervention for cancer therapy. *Acta Pharm. Sin. B* 5 (5), 378–389. doi:10.1016/j.apsb.2015.05.007
- McCullough, S. D., Duncan, K. E., Swanton, S. M., Dailey, L. A., Diaz-Sanchez, D., and Devlin, R. B. (2014). Ozone induces a proinflammatory response in primary human

bronchial epithelial cells through mitogen-activated protein kinase activation without nuclear factor- κ B activation. *Am. J. Respir. Cell Mol. Biol.* 51 (3), 426–435. doi:10.1165/rcmb.2013-0515OC

McNabb, N., and McCullough, S. D. (2020). Isolation of total RNA with the Life Technologies PureLink kit. *Protoc. Exch., PROTOCOL* (Version 1) doi:10.21203/rs.2.21222/v1

Mitra, S., Schiller, D., Anderson, C., Gamboni, F., D'Alessandro, A., Kelher, M., et al. (2017). Hypertonic saline attenuates the cytokine-induced pro-inflammatory signature in primary human lung epithelia. *PLOS One* 12 (12), e0189536. doi:10.1371/journal.pone.0189536

Moretto, N., Bertolini, S., Iadicicco, C., Marchini, G., Kaur, M., Volpi, G., et al. (2012). Cigarette smoke and its component acrolein augment IL-8/CXCL8 mRNA stability via p38 MAPK/MK2 signaling in human pulmonary cells. *Am. J. Physiology - Lung Cell. Mol. Physiology* 303 (10), 929–938. doi:10.1152/ajplung.00046.2012

Murray, L. A., Dunmore, R., Camelo, A., Da Silva, C. A., Gustavsson, M. J., Habel, D. M., et al. (2017). Acute cigarette smoke exposure activates apoptotic and inflammatory programs but a second stimulus is required to induce epithelial to mesenchymal transition in COPD epithelium. *Respiratory Research. Respir. Res.* 18 (1), 1–12. doi:10.1186/s12931-017-0565-2

Nagle, D., and Zhou, Y.-D. (2006). Natural product-derived small molecule activators of hypoxia-inducible factor-1 (HIF-1). *Curr. Pharm. Des.* 12 (21), 2673–2688. doi:10.2174/13816120677698783

National Research Council (2007) Toxicity testing in the 21st century: a vision and strategy, risk analysis. doi:10.1111/j.1539-6924.2009.01222.x

Nichols, W., Murphy, D. G., Cristofalo, V. J., Toji, L. H., Greene, A. E., and Dwight, S. A. (1977). Characterization of a new human diploid cell strain, IMR-90. *Science* 196 (4285), 60–63. doi:10.1126/science.841339

Ning, Y., Tao, F., Qin, G., Imrich, A., Goldsmith, C. A., Yang, Z., et al. (2004). Particle-epithelial interaction: effect of priming and bystander neutrophils on interleukin-8 release. *Am. J. Respir. Cell Mol. Biol.* 30 (5), 744–750. doi:10.1165/rcmb.2003-0123OC

Olson, N., Hristova, M., Heintz, N. H., Lounsbury, K. M., and van der Vliet, A. (2011). Activation of hypoxia-inducible factor-1 protects airway epithelium against oxidant-induced barrier dysfunction. *Am. J. physiology. Lung Cell. Mol. physiology. U. S.* 301 (6), L993–L1002. doi:10.1152/ajplung.00250.2011

Pain, M., Bermudez, O., Lacoste, P., Royer, P. J., Botturi, K., Tissot, A., et al. (2014). Tissue remodelling in chronic bronchial diseases: from the epithelial to mesenchymal phenotype. *Eur. Respir. Rev.* 23 (131), 118–130. doi:10.1183/09059180.00004413

Paulo, H. (2020). *Chlorothalonil - in vitro measurement of the airway irritation potential of Bravo 720 SC formulation using different exposure scenarios in MucilAir pooled donor tissues*. Charles River Report No. 785136, Syngenta Task No. TK0510120.

Peterson, M. W., Walter, M. E., and Gross, T. J. (1993). Asbestos directly increases lung epithelial permeability. *Am. J. Physiology - Lung Cell. Mol. Physiology* 265 (3 9-3), L308–L317. doi:10.1152/ajplung.1993.265.3.308

Pezzulo, A. A., Starner, T. D., Scheetz, T. E., Traver, G. L., Tilley, A. E., Harvey, B. G., et al. (2011). The air-liquid interface and use of primary cell cultures are important to recapitulate the transcriptional profile of *in vivo* airway epithelia. *Am. J. Physiology - Lung Cell. Mol. Physiology* 300 (1), 25–31. doi:10.1152/ajplung.00256.2010

Pfaffl, M. W. (2001). A new mathematical model for relative quantification in real-time RT-PCR. *Nucleic Acids Res.* 29 (9), e45–e2007. doi:10.1093/nar/29.9.e45

Polito, A. J., and Proud, D. (1998). Epithelial cells as regulators of airway inflammation. *J. Allergy Clin. Immunol.* 102 (5), P714–P718. doi:10.1016/S0091-6749(98)70008-9

Randell, S. H., Fulcher, M. L., O'Neal, W., and Olsen, J. C. (2011). Primary epithelial cell models for cystic fibrosis research. *Methods Mol. Biol. Clift. N.J.). U. S.* 742, 285–310. doi:10.1007/978-1-61779-120-8_18

Rayner, R. E., Makena, P., Prasad, G. L., and Cormet-Boyaka, E. (2019). Optimization of normal human bronchial epithelial (NHBE) cell 3D cultures for *in vitro* lung model studies. *Sci. Rep.* 9 (1), 500–511. doi:10.1038/s41598-018-36735-z

Renda, T., Baraldo, S., Pelaia, G., Bazzan, E., Turato, G., Papi, A., et al. (2008). Increased activation of p38 MAPK in COPD. *Eur. Respir. J.* 31 (1), 62–69. doi:10.1183/09031936.00036707

Reynolds, C. J., Quigley, K., Cheng, X., Suresh, A., Tahir, S., Ahmed-Jushuf, F., et al. (2018). Lung defense through IL-8 carries a cost of chronic lung remodeling and impaired function. *Am. J. Respir. Cell Mol. Biol.* 59 (5), 557–571. doi:10.1165/rcmb.2018-0007OC

Rezaee, F., and Georas, S. N. (2014). Breaking barriers: new insights into airway epithelial barrier function in health and disease. *Am. J. Respir. Cell Mol. Biol.* 50 (5), 857–869. doi:10.1165/rcmb.2013-0541RT

Robinson, M., Hemming, A. L., Regnis, J. A., Wong, A. G., Bailey, D. L., Bautovich, G. J., et al. (1997). Effect of increasing doses of hypertonic saline on mucociliary clearance in patients with cystic fibrosis. *Thorax* 52 (10), 900–903. doi:10.1136/thx.52.10.900

Ross, A. J., Dailey, L. A., Brighton, L. E., and Devlin, R. B. (2007). Transcriptional profiling of mucociliary differentiation in human airway epithelial cells. *Am. J. Respir. Cell Mol. Biol.* 37 (2), 169–185. doi:10.1165/rcmb.2006-0466OC

Roux, P. P., and Blenis, J. (2004). ERK and p38 MAPK-activated protein kinases: a family of protein kinases with diverse biological functions. *Microbiol. Mol. Biol. Rev.* 68 (2), 320–344. doi:10.1128/mmbr.68.2.320-344.2004

Saitoh, M. (2018). Involvement of partial EMT in cancer progression. *J. Biochem.* 164 (4), 257–264. doi:10.1093/jb/mvy047

Shahzad, A., Knapp, M., Lang, I., and Köhler, G. (2010). Interleukin 8 (IL-8)-a universal biomarker? *Int. Archives Med.* 3 (1), 11–15. doi:10.1186/1755-7682-3-11

Shimoda, L. A., and Semenza, G. L. (2011). HIF and the lung: role of hypoxia-inducible factors in pulmonary development and disease. *Am. J. Respir. Crit. Care Med.* 183 (2), 152–156. doi:10.1164/rccm.201009-1393PP

Smyth, T., Veazey, J., Eliseeva, S., Chalupa, D., Elder, A., Georas, S. N., et al. (2020). Diesel exhaust particle exposure reduces expression of the epithelial tight junction protein Tricellulin. *Particle and Fibre Toxicology. Part. Fibre Toxicol.* 17 (1), 1–13. doi:10.1186/s12989-020-00383-x

Srinivasan, B., Kolli, A. R., Esch, M. B., Abaci, H. E., Shuler, M. L., and Hickman, J. J. (2015). TEER measurement techniques for *in vitro* barrier model systems. *J. Laboratory Automation* 20 (2), 107–126. doi:10.1177/2211068214561025

Stoehr, L. C., Endes, C., Radauer-Preiml, I., Boyles, M. S. P., Casals, E., Balog, S., et al. (2015). Assessment of a panel of interleukin-8 reporter lung epithelial cell lines to monitor the pro-inflammatory response following zinc oxide nanoparticle exposure under different cell culture conditions. *Part. Fibre Toxicol.* 12 (1), 29–12. doi:10.1186/s12989-015-0104-6

Stuart, J. A., Fonseca, J., Moradi, F., Cunningham, C., Seliman, B., Worsfold, C. R., et al. (2018). How supraphysiological oxygen levels in standard cell culture affect oxygen-consuming reactions. *Oxidative Med. Cell. Longev.* 8238459. doi:10.1155/2018/8238459

Takeyama, K., Fahy, J. V., and Nadel, J. A. (2001). Relationship of epidermal growth factor receptors to goblet cell production in human bronchi. *American journal of respiratory and critical care medicine. U. S.* 163 (2), 511–516. doi:10.1164/ajrccm.163.2.2001038

Tam, S. Y., Wu, V. W. C., and Law, H. K. W. (2020). Hypoxia-induced epithelial-mesenchymal transition in cancers: HIF-1 α and beyond. *Front. Oncol.* 10, 486. doi:10.3389/fonc.2020.00486

Tutkun, L., İritaş, S. B., Deniz, S., Öztan, Ö., Abuşoğlu, S., Ünlü, A., et al. (2019). TNF- α and IL-6 as biomarkers of impaired lung functions in dimethylacetamide exposure. *J. Med. Biochem.* 38 (3), 276–283. doi:10.2478/jomb-2018-0040

United States Environmental Protection Agency (2020). New approach methods work plan: reducing use of animals in chemical testing. (615B2001).

US Environmental Protection Agency (2021). New approach methods work plan (v2). EPA/600/X-. Available at: https://www.epa.gov/system/files/documents/2021-11/nams-work-plan_11_15_21_508-tagged.pdf.

van der Geer, P., Hunter, T., and Lindberg, R. A. (1994). Receptor protein-tyrosine kinases and their signal transduction pathways. *Annu. Rev. cell Biol.* 10, 251–337. doi:10.1146/annurev.cb.10.110194.001343

Vermee, P. D., Einwalter, L. A., Moninger, T. O., Rokhlina, T., Kern, J. A., Zabner, J., et al. (2003). Segregation of receptor and ligand regulates activation of epithelial growth factor receptor. *Nat. Engl.* 422 (6929), 322–326. doi:10.1038/nature01440

Vinall, J. (2017). *In vitro* measurement of the airway irritation potential of Bravo 720 SC formulation using MucilAir tissues from five different donors. Available at: <https://www.regulations.gov/document/EPA-HQ-OPP-2018-0517-0005>.

Vitos-Faleato, J., Real, S. M., Gutierrez-Prat, N., Villanueva, A., Llonch, E., Drosten, M., et al. (2020). Requirement for epithelial p38 α in KRAS-driven lung tumor progression. *Proc. Natl. Acad. Sci. U. S. A.* 117 (5), 2588–2596. doi:10.1073/pnas.1921404117

Voelkel, N. F., Vandivier, R. W., and Tudor, R. M. (2006). Vascular endothelial growth factor in the lung. *Am. J. Physiology - Lung Cell. Mol. Physiology* 290 (2), L209–L221. doi:10.1152/ajplung.00185.2005

Walker, R. A. (1998). The erbB/HER type 1 tyrosine kinase receptor family. *J. pathology* 185, 234–235. doi:10.1002/(SICI)1096-9896(199807)185:3<234::AID-PATH128>3.0.CO;2-8

Welch, J., Wallace, J., Lansley, A. B., and Roper, C. (2021). Evaluation of the toxicity of sodium dodecyl sulphate (SDS) in the MucilAir™ human airway model *in vitro*. *Regul. Toxicol. Pharmacol.* 125, 105022. doi:10.1016/j.yrtph.2021.105022

White, E. S. (2015). Lung extracellular matrix and fibroblast function. *Ann. Am. Thorac. Soc.* 12, S30–S33. doi:10.1513/AnnalsATS.201406-240MG

Wohlauer, M., Moore, E. E., Silliman, C. C., Fragos, M., Gamboni, F., Harr, J., et al. (2012). Nebulized hypertonic saline attenuates acute lung injury following trauma and hemorrhagic shock via inhibition of matrix metalloproteinase-13. *Crit. Care Med.* 40 (9), 2647–2653. doi:10.1097/CCM.0b013e3182592006

Woo, I. S., Park, M. J., Byun, J. H., Hong, Y. S., Lee, K. S., Park, Y. S., et al. (2004). Expression of placental growth factor gene in lung cancer. *Tumor Biol.* 25 (1–2), 1–6. doi:10.1159/000077716

Wu, D., Yuan, Y., Lin, Z., Lai, T., Chen, M., Li, W., et al. (2016). Cigarette smoke extract induces placental growth factor release from human bronchial epithelial cells via ROS/MAPK (ERK-1/2)/Egr-1 axis. *Int. J. COPD* 11 (1), 3031–3042. doi:10.2147/COPD.S120849

- Xian, M., Ma, S., Wang, K., Lou, H., Wang, Y., Zhang, L., Wang, C., et al. (2020). Particulate matter 2.5 causes deficiency in barrier integrity in human nasal epithelial cells. *Allergy, Asthma Immunol. Res.* 12 (1), 56–71. doi:10.4168/aaair.2020.12.1.56
- Xiong, R., Wu, Q., Muskhelishvili, L., Davis, K., Shemansky, J. M., Bryant, M., et al. (2018). Evaluating mode of action of acrolein toxicity in an *in vitro* human airway tissue model. *Toxicol. Sci.* 166 (2), 451–464. doi:10.1093/toxsci/kfy226
- Xu, X., Balsiger, R., Tyrrell, J., Boyaka, P. N., Tarran, R., and Cormet-Boyaka, E. (2015). Cigarette smoke exposure reveals a novel role for the MEK/ERK1/2 MAPK pathway in regulation of CFTR. *Biochimica et Biophysica Acta - general Subjects. Elsevier B.V.* 1850 (6), 1224–1232. doi:10.1016/j.bbagen.2015.02.004
- Yarden, Y., and Sliwkowski, M. X. (2001). Untangling the ErbB signalling network. *Nat. Rev. Mol. cell Biol. Engl.* 2 (2), 127–137. doi:10.1038/35052073
- Yoshida, K., Kuwano, K., Hagimoto, N., Watanabe, K., Matsuba, T., Fujita, M., et al. (2002). MAP kinase activation and apoptosis in lung tissues from patients with idiopathic pulmonary fibrosis. *J. Pathology* 198 (3), 388–396. doi:10.1002/path.1208
- Yu, X.-Y., Takahashi, N., Croxton, T. L., and Spannhake, E. W. (1994). Modulation of bronchial epithelial cell barrier function by *in vitro* ozone exposure. *Environ. Health Perspect.* 102 (12), 1068–1072. doi:10.1289/ehp.941021068
- Zarubin, T., and Han, J. (2005). Activation and signaling of the p38 MAP kinase pathway. *Cell Res.* 15 (1), 11–18. doi:10.1038/sj.cr.7290257
- Zeglinski, M. R., Turner, C. T., Zeng, R., Schwartz, C., Santacruz, S., Pawluk, M. A., et al. (2019). Soluble wood smoke extract promotes barrier dysfunction in alveolar epithelial cells through a MAPK signaling pathway. *Sci. Rep.* 9 (1), 10027. doi:10.1038/s41598-019-46400-8
- Zhou, Z., Liu, Y., Duan, F., Qin, M., Wu, F., Sheng, W., et al. (2015). Transcriptomic analyses of the biological effects of airborne PM2.5 exposure on human bronchial epithelial cells. *PLoS ONE* 10 (9), e0138267. doi:10.1371/journal.pone.0138267
- Ziello, J. E., Jovin, I. S., and Huang, Y. (2007). Hypoxia-Inducible Factor (HIF)-1 regulatory pathway and its potential for therapeutic intervention in malignancy and ischemia. *Yale J. Biol. Med.* 80 (2), 51–60.
- Ziment, I. (1978). *Respiratory pharmacology and therapeutics*. Philadelphia: WB Saunders, 60–104.



OPEN ACCESS

EDITED BY

Mary Catherine McElroy,
Charles River Laboratories, United Kingdom

REVIEWED BY

Madhuri Singal,
AeroTox Consulting Services, LLC, United States
Prathyusha Bagam,
National Center for Toxicological Research
(FDA), United States

*CORRESPONDENCE

Marjory Moreau,
✉ mmoreau@scitovation.com

RECEIVED 19 January 2024

ACCEPTED 28 March 2024

PUBLISHED 11 April 2024

CITATION

Moreau M, Simms L, Andersen ME,
Trelles Sticken E, Wiecezorek R, Pour SJ,
Chapman F, Roewer K, Otte S, Fisher J and
Stevenson M (2024), Use of quantitative *in vitro*
to *in vivo* extrapolation (QIVIVE) for the
assessment of non-combustible next-
generation product aerosols.
Front. Toxicol. 6:1373325.
doi: 10.3389/ftox.2024.1373325

COPYRIGHT

© 2024 Moreau, Simms, Andersen, Trelles
Sticken, Wiecezorek, Pour, Chapman, Roewer,
Otte, Fisher and Stevenson. This is an open-
access article distributed under the terms of the
[Creative Commons Attribution License \(CC BY\)](https://creativecommons.org/licenses/by/4.0/).
The use, distribution or reproduction in other
forums is permitted, provided the original
author(s) and the copyright owner(s) are
credited and that the original publication in this
journal is cited, in accordance with accepted
academic practice. No use, distribution or
reproduction is permitted which does not
comply with these terms.

Use of quantitative *in vitro* to *in vivo* extrapolation (QIVIVE) for the assessment of non-combustible next-generation product aerosols

Marjory Moreau^{1*}, Liam Simms², Melvin E. Andersen¹,
Edgar Trelles Sticken³, Roman Wiecezorek³, Sarah Jean Pour³,
Fiona Chapman², Karin Roewer³, Sandra Otte³, Jeffrey Fisher¹
and Matthew Stevenson²

¹Scitovation LLC, Durham, NC, United States, ²Imperial Brands PLC, Bristol, United Kingdom, ³Reemtsma
Cigarettenfabriken GmbH, An Imperial Brands PLC Company, Hamburg, Germany

With the use of *in vitro* new approach methodologies (NAMs) for the assessment of non-combustible next-generation nicotine delivery products, new extrapolation methods will also be required to interpret and contextualize the physiological relevance of these results. Quantitative *in vitro* to *in vivo* extrapolation (QIVIVE) can translate *in vitro* concentrations into in-life exposures with physiologically-based pharmacokinetic (PBPK) modelling and provide estimates of the likelihood of harmful effects from expected exposures. A major challenge for evaluating inhalation toxicology is an accurate assessment of the delivered dose to the surface of the cells and the internalized dose. To estimate this, we ran the multiple-path particle dosimetry (MPPD) model to characterize particle deposition in the respiratory tract and developed a PBPK model for nicotine that was validated with human clinical trial data for cigarettes. Finally, we estimated a Human Equivalent Concentration (HEC) and predicted plasma concentrations based on the minimum effective concentration (MEC) derived after acute exposure of BEAS-2B cells to cigarette smoke (1R6F), or heated tobacco product (HTP) aerosol at the air liquid interface (ALI). The MPPD-PBPK model predicted the *in vivo* data from clinical studies within a factor of two, indicating good agreement as noted by WHO International Programme on Chemical Safety (2010) guidance. We then used QIVIVE to derive the exposure concentration (HEC) that matched the estimated *in vitro* deposition point of departure (POD) (MEC cigarette = 0.38 puffs or 11.6 µg nicotine, HTP = 22.9 puffs or 125.6 µg nicotine) and subsequently derived the equivalent human plasma concentrations. Results indicate that for the 1R6F cigarette, inhaling 1/6th of a stick would be required to induce the same effects observed *in vitro*, *in vivo*. Whereas, for HTP it would be necessary to consume 3 sticks simultaneously to induce *in vivo* the effects observed *in vitro*. This data further demonstrates the reduced physiological potency potential of HTP aerosol compared to cigarette smoke. The QIVIVE approach demonstrates great promise in assisting human

health risk assessments, however, further optimization and standardization are required for the substantiation of a meaningful contribution to tobacco harm reduction by alternative nicotine delivery products.

KEYWORDS

physiologically based pharmacokinetic (PBPK) modelling, respiratory toxicity, *in vitro*, aerosol, heated tobacco product (HTP), cigarette, multiple-path particle dosimetry

1 Introduction

Heated tobacco products (HTPs) offer an alternative to consuming nicotine without the need to burn tobacco or produce smoke. A portion of refined tobacco is heated in a controlled manner, never burnt, producing an inhalable aerosol which contains nicotine and flavor aromas from the tobacco. As HTPs eliminate the need to burn tobacco, and do not produce smoke, the aerosols they produce contain fewer and lower levels of harmful chemicals compared to cigarette smoke (Chapman et al., 2023). As such, heated tobacco products have the potential to provide a meaningful contribution to tobacco harm reduction (COT, 2017).

Traditionally, inhalation toxicity testing has been performed using animal models to identify various physiological outcomes, including the lethal concentration of airborne materials or maximum tolerable concentration. *In vitro* studies in which a solution of the aerosol ingredients is directly applied to cells in culture are not representative of an *in vivo* inhalation exposure due to a lack of gas phase exposure (Mulhopt et al., 2020). Additionally, these submerged *in vitro* conditions neither reflect realistic cell-cell communication within organ systems, cell-particle interactions and particle deposition characteristics as occurs with *in vivo* inhalation exposures. Another limitation would be reduced delivery of short-lived reactive compounds to the cells. In the case of aerosols, all constituents might not be delivered to the cell if compounds have poor solubility in the aqueous media. More recently, novel *in vitro* methods have been developed that allow the direct exposure of airborne material to cultured human target cells on permeable porous membranes at the air liquid interface (ALI), with apical surface of the cell exposed directly to smoke/aerosol and the dorsal surface of the cells bathed with cell media (Wieczorek et al., 2023). The effects of HTP and cigarette aerosols on respiratory cells cultured at the ALI can be used to study potential cell injury or activation and the release of bioactive mediators.

With these new testing approaches, new extrapolation methods will be required to interpret and contextualize the *in vitro* assay results. *In silico* simulation is a promising approach to linking *in vitro* inhalation exposure back to *in vivo* exposure (Moreau et al., 2022). Key considerations to enable interpretation and extrapolation of the data to in-life exposure include aerosol particle size distribution, fluid mechanics impacting local deposition rates, and *in vivo* lung morphometries (Tsuda et al., 2013).

The chemical concentration applied *in vitro* that elicits biological activity may be different from the blood or tissue concentration required to elicit a comparable *in vivo* response due to chemical bioavailability, clearance, and other pharmacokinetic (PK) considerations. Quantitative *in vitro* to *in vivo* extrapolation (QIVIVE) can provide an estimate of the

likelihood of harmful effects from expected environmental exposures by effectively combining *in silico* and *in vitro* approaches including physiologically based pharmacokinetic (PBPK) modelling, and information on metabolism, transport, binding, and other model parameters from cell- and/or cell derived material-based assays.

PBPK models permit estimation of concentration-time profiles of a compound in various tissues or organs. A whole-body PBPK model contains an explicit representation of the organs that are most relevant to the absorption, distribution, excretion, and metabolism of the test articles due to their physiological/pharmacological function or their volume. The tissues are linked by the arterial and venous blood compartments, and each one of them is characterized by an associated blood-flow rate, volume, tissue-partition coefficient, and permeability. A major advantage of PBPK modeling is the creation of a comprehensive structural representation of the physiology of an organism. The various parameters in the model are either obtained from prior knowledge or calculated from specific and carefully validated formulas (Kuepfer et al., 2016). Inhalation PBPK models coupled to computational dosimetry approaches like the Multiple-Path Particle Dosimetry [MPPD, Applied Research Associates 4300 San Mateo Blvd Albuquerque; (Anjilvel and Asgharian, 1995; Asgharian et al., 1995)] are recommended for development of inhalation exposures and are probably the most effective, practical, and accurate approach (Kolli et al., 2020). The MPPD model predicts the deposition of particles in the entire respiratory tract or in a region of the respiratory tract, in adult and other age groups. These estimates of local dosimetry are usually used to characterize dose-response relationship, extrapolate between species or from *in vitro* assays or predict the distribution of a compound in the body when coupled to PBPK modeling.

In the present study we combined a PBPK model for nicotine with a lung deposition model (MPPD) to better understand the *in vitro* assay results in terms of *in vivo* exposure in humans of nicotine which is used as the biomarker of exposure to cigarette smoke and HTP aerosol.

2 Materials and methods

2.1 *In vitro* assays

2.1.1 Cell culture

BEAS-2B cells were maintained at 37°C in an atmosphere of 5% CO₂ in Airway Epithelial Cell Growth Medium (AEGM), that consisted of AEGM (Promocell, C-21060) complemented with SupplementMix (Promocell, C-39165) containing Bovine

TABLE 1 Smoke/aerosolization and sample conditions used with the SAEIVS for the high content screening experiments for the ALI exposure of BEAS-2B cell to derive a MEC.

Test article	Puff interval/volume/profile	Dilution factor 1/x	Number of sticks/devices per run	Runs	Puffs per run	Final puff number applied ^(a)
1R6F	30 s/55 mL/bell shape/vent block	5	3	1	7 (1.4 ^a)	7 (1.4 ^a)
HTP	30 s/55 mL/bell shape/no vent block	1	3	5	8	40

^aThe Smoke machine was used according to ISO, 20768.

Pituitary Extract 0.004 mL/mL, epidermal growth factor (10 ng/mL), insulin (5 µg/mL), Hydrocortisone (0.5 µg/mL), Epinephrine (0.5 µg/mL), Triiodo-L-thyronine (6.7 ng/mL); holo-Transferrin (10 µg/mL), Retinoic acid (0.1 ng/mL). Sub-cultivation was performed twice a week in T175 cell culture flasks with a cell seeding density of 8.7E5 and 5E5 cells per flask when cultivated over 3 and 4 days respectively.

2.1.2 Cell seeding and treatment

Cells were seeded on cell culture inserts designed to be used with microscopic analysis technologies (Millicell Cell culture inserts: Millipore PICM01250). In brief: Cells were seeded using 400 µL of a cell suspension with 3.5E5 cells/mL per cell culture insert. The loaded cell culture inserts were placed into 24-well plates filled with 250 µL AEGM medium. Cells were incubated overnight (appr. 18 h) at 37°C and 5% CO₂ to allow adherence and growth on the cell culture insert membrane. On the next day just before exposure, the medium from the apical compartment of the inserts was removed and the inserts were transferred into new 24-well plates with 250 µL HEPES buffered Dulbecco's minimal essential medium per well. A 24-well plate with the inserts was placed into one of the exposure chambers of the Smoke Aerosol Exposure *In Vitro* System [SAEIVS, (Wieczorek et al., 2023)]. Smoke/aerosol exposure was executed as described in Table 1. Following exposure, the plate with the inserts was removed from the SAEIVS.

Cell culture inserts with the treated cells were transferred into new 24-well plates filled with 250 µL AEGM medium. Pre-warmed AEGM medium (400 µL) was added to the cells in the apical compartment of the inserts. Cells were allowed to recover and kept in the incubator for 24 h at 37°C and 5% CO₂. Medium was removed from both compartments and 200 µL 4% formaldehyde in PBS was added to the apical part of the insert for a 15-min fixation step at room temperature.

To compare the effective concentrations of each product type, a study was designed to assess both the number of puffs delivered to the cells (BEAS-2B) and the amount of nicotine delivered at the cell surface. Separate experiments were adopted using glass plates of the same surface areas as the Millipore inserts (and therefore the cell layer surface) and the same puffing parameters and diluted/undiluted smoke/aerosol from the same product variants. For cell exposure, cigarette smoke (1R6F) was diluted 1:5 (smoke: fresh humidified filtered air) and 1:1 (aerosol: fresh humidified filtered air) for the HTP. The aim of this experiment was to determine the number of puffs required for each product to cause a minimum effective concentration (MEC) for the c-jun cellular marker, measured using high-content screening (HCS)

and to determine the number of puffs required to deliver nicotine to the cell surface (using glass plates to collect the deposited material). The marker c-jun was chosen as this was the most sensitive of a panel of selected cellular stress markers used with the HCS technique in-house. The aim was to be as conservative as possible, by using the most sensitive cellular marker using our experience with HCS. The MEC is defined as the lowest effective concentration outside of the background negative control range. The MEC had to exceed the calculated background [=3x median absolute deviation (mad)], that was determined by linear or non-linear regression (decided by the best curve fit). For comparative MEC calculation, the average 3x mad of all treatments for c-jun was used as target value. The Phosphorylation of c-jun (p-c-jun) defines a cellular stress marker which is involved in several signal pathways including proliferation, apoptosis, survival, tumorigenesis, and tissue morphogenesis (Schmeck et al., 2006; Dreij et al., 2010).

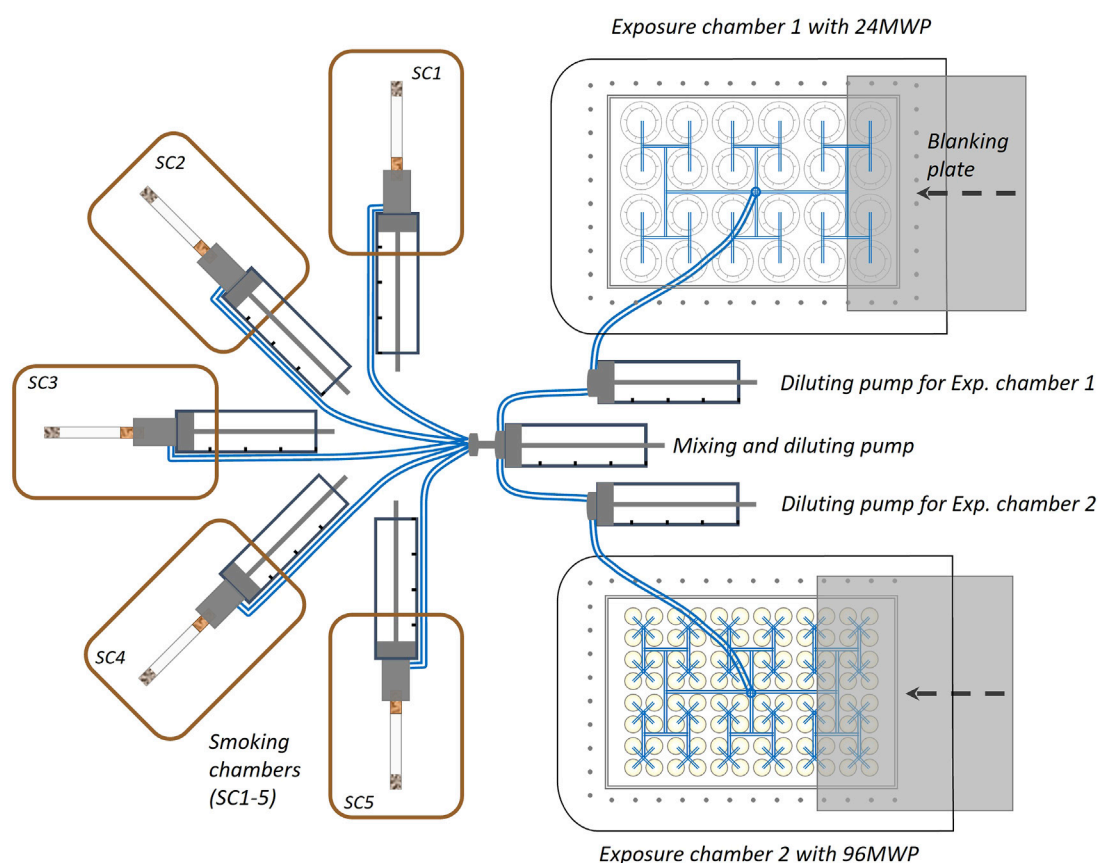
2.1.3 Cell surface for nicotine deposition

Previous work has assessed the effect of adding cells (V79 Chinese Hamster lung fibroblast cells and BEAS-2B) to the surface of the glass and compared to the cell-free glass surface. The deposition of nicotine on both surfaces was comparable and so clean glass slides were subsequently used (Wieczorek et al., 2023).

2.1.4 Nicotine evaluation from glass plates and cell medium

Nicotine was quantified using LC-MS/MS method (Internal Standard: Nicotine-d4). Nicotine trapped in cell media and PBS was measured directly without any further sample preparation. Whereas the nicotine trapped on the surface of the glass disc was eluted with isopropanol prior to final measurement.

Nicotine quantification of isopropanol extracts from exposed glass discs and basal medium was conducted using LC-MS/MS (AB Sciex API 6500 QTRAP (SCIEX, Darmstadt, Germany)). For analysis, medium samples were diluted 1:100 with MilliQ water/MeOH (1:1) and 1:1 in the autosampler with the internal standard solution in methanol. A Gemini NX-C18 column (110 Å, 100 × 2.0 mm, 3 µm) (Phenomenex, Aschaffenburg, Germany) was used for the liquid chromatography (oven temperature, 55°C), sample injection volume was 5 µL and the autosampler temperature was 5°C. The eluent gradient was applied according to the following: 0min: 2% B (methanol)/98% A (0.05% acetic acid in water) (flow rate: 400 µL/min); 1.2 min: 65% B/35% A (400 µL/min); 1.5 min: 95% B/5% A (400 µL/min); 2.5 min: 98% B/2% A (400 µL/min); 3.0 min: 98% B/2% A (400 µL/min). The following conditions were used for the mass spectrometry: Ion spray voltage: 4500V,



Both blanking plates are in the start positions for 24 and 96 multiwell plate
Each pump is equipped with an additional valve for fresh air and excess aerosol

FIGURE 1

Diagram of the Aerial view of the smoke/aerosol exposure *in vitro* system (SAEIVS). The system consists of five smoking chambers (SCs), which can accommodate cigarettes, electronic nicotine delivery systems and heated tobacco products (in respective runs). The smoke/aerosol generated is then drawn through tubing to a mixing and diluting pump (with charcoal filtered, humidified air). Each exposure chamber also has a further individual diluting pump to allow cells to be exposed different concentrations if required. The exposure chambers can accommodate either 24 or 96 well plates, and smoke/aerosol is delivered to individual wells via ports situated above each individual well. Between the exposure ports and the cell culture plate, a blanking plate can be moved (robotically) to prevent exposure to rows. As the blanking plate moves across the row of wells exposed, preventing subsequent exposure, an increasing dose can be delivered to uncovered rows.

Ion source temperature: 500°C, MRM: 163/132 quantification; 163/106 qualifier. The isopropanol samples were diluted 1:100 with MilliQ water/MeOH (1:1) and without autosampler dilution because internal standards were present in samples extraction and calibration solution. All other measurement parameters were the same as above.

To trigger the p-c-jun response in BEAS-2B cells, the cells were exposed to fresh smoke/aerosol from 1R6F/Pulze used with iD sticks (HTP). For details of the Pulze device and the iD sticks please see Chapman et al. (2023). The BEAS-2B cells were pre-grown on microporous membranes of dedicated cell culture inserts and supplied with medium apically and basally. For exposure to fresh smoke from the Reference Cigarette 1R6F and aerosol from Pulze and iD the cells were switched to ALI conditions (i.e., apical medium was aspirated) where nutrification of the cells is achieved from the lower compartment below the insert-containing well only. The use of the ALI exposure is key. *In vitro* exposure systems that deliver aerosols to the surface of human cells

cultured at ALI are of particular importance being the most physiologically relevant exposure route, and highly preferable to using submerged cell lines (Upadhyay and Palmberg, 2018). Upadhyay and Palmberg (2018) identified several factors influencing the successful development of ALI-models including the choice of cell line (preferably human), the source of any primary cells, and the use of co-culture systems consisting of multiple cell types (Clippinger et al., 2016). The use of an ALI system is also considered to be a feasible alternative approach and can be used to implement the “3 Rs principle” replacement, reduction, and refinement of animal usage—in conducting pulmonary toxicity studies (Upadhyay and Palmberg, 2018). The apical surface of the inserts with the cells were exposed directly to fresh aerosol and smoke in the in-house Smoke and Aerosol Exposure *In vitro* System (SAEIVS). This is an in-house built system to enable the delivery of whole aerosols directly to cells at the ALI, being able to deliver different dilutions of aerosol/smoke to two separate cell exposure chambers in under 10 s of

generation [for more details and characterization of the system see Figure 1; Wiczeorek et al. (2023)]. Following exposure to the aerosol/smoke the cells were covered with recovery medium and were incubated for 24 h before fixation and subsequent antibody staining for p-c-jun.

The study was composed of two parts.

- 1 - The quantification of phosphorylated c-jun protein in nuclei of BEAS-2B cells after direct exposure to diluted fresh smoke of 1R6F Reference cigarette and to undiluted fresh aerosol of Pulze and iD sticks at the ALI using the SAEIVS. The aim of this part of the study was to determine the p-c-jun MEC for both test articles on a puff basis by means of HCS technology.
- 2 - A dosimetry approach to determine the amount of nicotine delivered in the SAEIVS per well equipped with inserts corresponding to those used in part 1 of the study. Glass plates were loaded on top of the membranes to mimic the cell surface for smoke/aerosol deposition, with nicotine as the key dosimetry marker. Following exposure of those glass plates, they were extracted with isopropanol and the amount of nicotine trapped per glass plate was measured.

2.1.5 Combination of HCS and nicotine data

Following the determination of MEC and finalization of nicotine dosimetry, the data were combined to determine the MEC on a nicotine basis. To this end the MEC_{puff} from the HCS approach was used to determine the MEC_{nic} by using the MEC_{puff} in the equation of the nicotine dosimetry.

2.2 MPPD modeling

Respiratory tract deposition models consider the anatomic structure of the respiratory tract, the air flow patterns and the aerodynamic characteristics of the particles to predict the deposited dose in each region. Lung deposition was calculated using the MPPD model (MPPD version 3.04) available from the Applied Research Associates webpage (<https://www.ara.com/mppd/>).

The MPPD model includes both human and rat respiratory tract models of the deposition and clearance of spherical particles. It predicts the deposition and clearance of monodisperse and polydisperse aerosols in the respiratory tracts for particles ranging in size from ultrafine (1 nm) to coarse (100 μ m). Several factors can influence deposition including the concentration of the chemical/particles in the air, the aerodynamic characteristics of particles, the frequency and duration of exposure, the physiological inhalation parameters such as the anatomical structure of the respiratory tract, breathing patterns, and interaction with other airborne particles (Rozman and Klaassen, 2001).

In the simulations presented here, the stochastic model was parameterized to have upright body positioning and oral breathing at constant exposure conditions. Different scenarios of exposure were tested and deep breathing at resting, with a short breath hold chosen for the simulations. This corresponds to a breathing rate of 12 breaths per min, a tidal volume of 1.3 L, an

inspiration fraction of 0.5, a pause fraction of 0.1 and finally inhalation and exhalation times of 2.5 and 2 s, respectively. This scenario was chosen as the best one based on smoking habits (McEwan et al., 2019). In his review, Bernstein (2004) describes a specific pattern of smoking with 2 phases: The initial puff is first taken into the mouth and after a pause of 1–4 s, the smoke is then inhaled into the lungs.

We used the stochastic lung model as it represents asymmetric structures of the tracheobronchial region of a human lung. This model describes the randomness and asymmetry of the airway branching system. This lung model is based on distributions of morphometric parameters such as length, diameter, branching angle, cross-sectional area of the daughter tubes, gravity angle, and correlations between these parameters as a function of airway generation (Asgharian et al., 2001). This provides more realistic lung geometry than the symmetric lung models in MPPD (Yeh-Schum Single path, Yeh-Schum 5-Lobes, PNNL symmetric model or Weibel symmetric model). There are 10 models within the stochastic lung model ordered in size (total number of airways) from the smallest to the largest and the approximate size percentile of each lung. The 60th percentile human stochastic lung model was used for our simulation.

Concerning the particle size diameter for IVIVE, the mass median aerodynamic diameter (MMAD) was set to 0.8 μ m with a geometric standard deviation (GSD) of 1.3 for 1R6F and 0.7 μ m with a GSD of 1.5 for HTP based on Schaller et al. (2016). GSD represents the geometric standard deviation, and the larger the GSD value, the greater the spread of the aerosol diameter of the particles.

We also chose to incorporate an inhalability adjustment to the simulations. This is an adjustment for particle size larger than 8 μ m. The probability that these are inhaled is less than 1 and decreases with increasing particle size. This correction is used to account for expected inertial deposition of the larger particles (Asgharian et al., 1995).

2.3 PBPK modeling

2.3.1 Model development and structure

The absorption, distribution, metabolism, and excretion (ADME) properties of nicotine have been previously studied in different species (Benowitz et al., 2009a; Benowitz et al., 2009b). Nicotine is metabolized quickly in the liver, primarily by cytochrome P450s (CYP2B6 and CYP2E1) and has relatively low plasma protein binding (Benowitz et al., 2009a; Benowitz et al., 2009b). Large venous blood nicotine concentrations are produced within minutes after nicotine inhalation as the lungs offer a large surface area for absorption and a favorable dissolution pH of 7.4. Several PBPK models have been developed for nicotine (Plowchalk et al., 1992; Robinson et al., 1992; Teeguarden et al., 2013; Haghnegahdar et al., 2018).

The PBPK model developed here has perfusion-limited compartments for liver and lung and lumped compartment for the remaining tissues (rest of the body). Inhalation of aerosols is a complex process, and PBPK models with regional lung compartments are more descriptive. Here, we use a multicompartment respiratory tract model. Based on anatomical

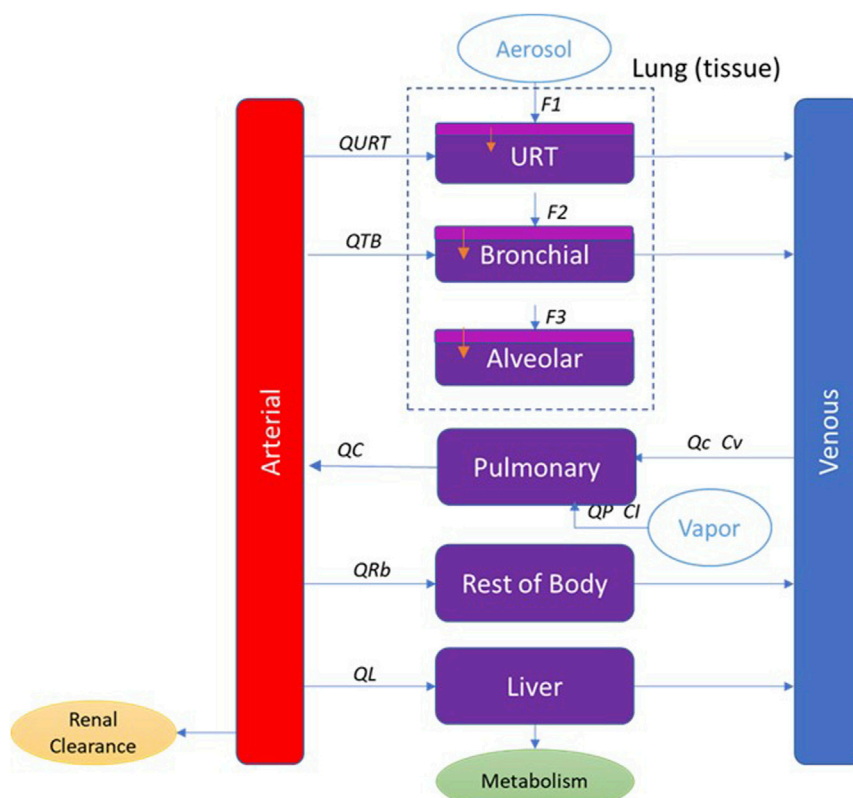


FIGURE 2

PBPK model schematic for nicotine showing the representation of the main organs considered with various sub-compartments in the lung for inhalation exposure. QL, QRB, QC, QTB, and QURT refer to blood flow to each tissue compartment. QP refers to the alveolar ventilation rate. Cv refers to the venous concentration and Ci to the inhaled vapor concentration. F1, F2, and F3 refer to the fraction deposited in each region of the respiratory tract. In the respiratory tract (URT, bronchial and alveolar), the light purple represents the mucus and epithelium, and the dark purple represents the submucosa region where blood perfusion occurs.

location and function, the respiratory tract is divided into three regions: upper respiratory tract (URT), trachea-bronchial region (TB) and alveolar region. There is also a pulmonary compartment which represents the gas exchange region of the lung. To include processes that transport the absorbed nicotine across the anterior respiratory tract compartments, these regions are further divided into a two-layered substructure: an epithelial cell layer with mucus, and a submucosal tissue layer. The submucosal tissue layer has blood perfusion and clears the absorbed nicotine from the airway compartments. Consistent with common practice, the tissue compartments are well-mixed reservoirs. Exposure is characterized in each lung (inhalation) compartment based on calculated deposition rates. Elimination occurred from both the liver and the blood compartment and was represented by hepatic and renal clearance, respectively. The model structure is shown schematically in Figure 2.

The physiologically-based biokinetic (PBBK) model was developed in Berkeley Madonna software (version 10.1.3; University of California, Berkeley, CA; www.berkeleymadonna.com). Model equations are in Supplemental 1.

2.3.2 Model parameters

Parameters used in the current model are summarized in Table 2. Tissue blood flows are from our ScitoVation database

for an adult male (internal database not shown), except for the blood flow to the upper respiratory tract (URT) that was set according to Campbell et al. (2015) and the blood flow to the alveolar region that was set according to Butler (1992). The ScitoVation database includes age-specific physiological parameters for body weight (BW), cardiac output, tissue weights (volumes), and tissue blood flows, and are adapted from published life-stage models (Wu et al., 2015; Song et al., 2016; Ruark et al., 2017).

Volumes were set to values from the ScitoVation database except for the lung volume. Tissue volumes for the three respiratory-tract compartments were estimated by multiplying the appropriate surface area with the tissue thickness. The surface area of the three lung regions was estimated using a standard lung model (MPPD) that quantifies airway length and diameter on a generation-by-generation basis. Epithelial thickness was obtained from Sarangapani et al. (2002b). The submucosal thickness was assumed to be approximately twice the epithelium thickness, based on histological sectioning (Matthew Bogdanffy, personal communication).

Chemical-specific parameters such as hepatic intrinsic clearance and renal clearance were obtained from previously published PBPK model from Robinson et al. (1992) and Yamazaki et al. (2010). Robinson et al. (1992) estimated a hepatic clearance of 1.09 L/min, using a PBPK model calibrated with *in vivo* human data.

TABLE 2 Physiological and biochemical parameters used for the nicotine PBPK model.

Parameters	Parameters description	Values		References
		Original	Fitted	
BW	Body weight—kg	81.2	—	Scitovation database
QC	Cardiac output—L/h	423.37	—	Scitovation database
QLc	Blood flow to the liver—Fraction of QC	0.235	—	Scitovation database
QURTc	Blood flow to the URT—Fraction of QC	0.00247	—	Campbell et al. (2015)
QTBc	Blood flow to the TB region—Fraction of QC	0.0075	—	Campbell et al. (2015)
QALVc	Blood flow to the pulmonary region—Fraction of QC	0.0067	—	Butler (1992)
VLc	Liver volume—Fraction of BW	0.0197	—	Scitovation database
VArc	Arterial blood volume—Fraction of BW	0.0142	—	Scitovation database
VVc	Venous blood volume—Fraction of BW	0.0427	—	Scitovation database
SAurt	URT surface area—cm ²	154.8	—	MPPD
SAtb	TB surface area—cm ²	4440	—	MPPD
SAta	Transitional airway surface area—cm ²	6220	—	Sarangapani et al. (2002a)
SAPulm	Pulmonary region surface area—cm ²	700146.6	—	MPPD
TmucepthURT	Mucus and epithelium thickness in the upper respiratory tract—cm	0.006	—	Sarangapani et al. (2002a)
TmucepthTB	Mucus and epithelium thickness in the tracheo-bronchial region—cm	0.0066	—	Sarangapani et al. (2002a)
TmucepthTA	Mucus and epithelium thickness in the transitional airway—cm	0.001	—	Sarangapani et al. (2002a)
TmucepthPULM	Mucus and epithelium thickness in the pulmonary region—cm	0.0005	—	Sarangapani et al. (2002a)
TURT	Submucosa thickness—cm	0.012	—	Bogdanffy, personal communication
TTB	Submucosa thickness—cm	0.0132	—	Bogdanffy, personal communication
TTA	Submucosa thickness—cm	0.002	—	Bogdanffy, personal communication
TV	Tidal volume—L	1.3	—	Brown et al. (1997)
DS	Dead space in the lung—L	0.15	—	Brown et al. (1997)
BR	Breathing rate—/h	720	—	Brown et al. (1997)
DLc	Nicotine diffusion—cm ² /h	4.87E-9	—	QSAR
PL	Liver: blood partition coefficient	7.8	7	Teeguarden et al. (2013)
PURT	URT: blood partition coefficient	2	1.23	Robinson et al. (1992)
PTB	TB: blood partition coefficient	2	0.1	Robinson et al. (1992)
PALV	ALV: blood partition coefficient	2	0.1	Robinson et al. (1992)
PRB	Rest of the body: blood PC	7.8	1.48	Teeguarden et al. (2013)
Fu	Plasma unbound fraction	0.95	—	Robinson et al. (1992)
CLr	Renal clearance—L/h	4.25	—	Yamazaki et al. (2010)
CL _{int}	Intrinsic clearance—L/h	63	128.5	Robinson et al. (1992)
FURT	Particle fraction deposited in the URT	0.014	—	MPPD
FTB	Particle fraction deposited in the TB	0.07	—	MPPD
FPULM	Particle fraction deposited in PULM	0.1629	—	MPPD
Fvapor	Vapor fraction for Cigarette	0.0247	0.20	Haghnegahdar et al. (2018)
BPR	Blood plasma ratio	1	—	Values range from 0.82 to 1.2 so estimation at 1

Tissue: blood partition coefficients (PC) are defined as the ratio of the concentration of a test chemical in two media (i.e., tissue and plasma), once equilibrium is reached. PCs are important determinants of the disposition of chemicals in different tissues. Liver PC was from [Teeguarden et al. \(2013\)](#). The other PCs (the rest of the body and lung compartments) were fitted to the *in vivo* human data. Plasma protein binding of approximately 5% has been reported by [Robinson et al. \(1992\)](#).

Nicotine permeability was taken from literature. There was some variability in reported values: 1.0E-4 cm/s from [Gowadia and Dunn-Rankin \(2010\)](#), 1.28E-4 cm/s from [Waddell and Marlowe \(1976\)](#), 2.5E-5 cm/s and 1.14E-5 cm/s from a QSAR model used by Symcyp. We opted to use the QSAR value as it was giving a better fit with the *in vivo* PK data. The nicotine permeability was multiplied by the tissue thickness in the experiment to derive a diffusion coefficient in cm²/s.

The fraction of particles deposited in each of the lung compartments was estimated using the MPPD model. To validate the model, we simulated individuals with deep breathing at rest with a short breath hold. Most of the studies used to validate the model did not provide direct information about the scenario of exposure. In most of the studies, volunteers were at rest, i.e., reading quietly, working, or engaging with social media. Based on smoking behavior found in different publications ([Pichelstorfer et al., 2016](#); [McEwan et al., 2019](#)), a deep breath at resting and a short breath hold seemed to be the more appropriate scenario to reflect the human *in vivo* data used to validate the model.

The fraction of vapor inhaled for cigarettes was fitted to the data. Here the particle size diameter, the count median diameter (CMD) was set to 163 nm with a geometric standard deviation (GSD) of 1.44 for cigarettes based on [Fuoco et al. \(2014\)](#) and [Sosnowski and Kramek-Romanowska \(2016\)](#). These values were used for the calibration and validation of the model.

2.3.3 Model calibration and validation

The performance of the model was first evaluated using the *in vivo* pharmacokinetic (PK) data (plasma concentrations between 0–4 h post exposure) from [McEwan et al. \(2019\)](#) where 48 healthy subjects smoked a single assigned test cigarette and had blood drawn on the morning of each visit. In the afternoon, the smoking behavior assessment was carried out with a single use of the same test product.

The model was also validated using 2 other *in vivo* PK datasets from [Picavet et al. \(2016\)](#), and [Digard et al. \(2013\)](#).

[Picavet et al. \(2016\)](#) assessed the PK of nicotine after a single use of cigarette in 28 healthy smokers. The cigarettes assessed in this study were non-menthol, manufactured, commercially available cigarettes, with a maximum ISO yield of 1 mg nicotine per cigarette. The pharmacokinetics of nicotine were measured on the days of single use. The first blood sample was collected within 15 min before a single use of the allocated product in the morning, and then at 2, 4, 6, 8, 10, 15, 30, 45, and 60 min, and at 3, 4, 6, 9, 12 and 24 h.

[Digard et al. \(2013\)](#) conducted a study with 20 healthy cigarette users. A cigarette was smoked, and blood samples taken at intervals over 120 min. The subjects were instructed to smoke the cigarette naturally according to their usual smoking behavior for 5 min or until the cigarette had been smoked to 30 mm from the mouth end (if this occurred in less than 5 min), at which point the cigarette was extinguished.

All the puffing scenario and dose (1 mg nicotine) used in each of these studies were the same with a puff duration of 2.3 s, puff interval of 30 s, puff volume of 69.5 mL and number of puffs per cigarettes of 14. Puff duration, number of puffs and puff volume for cigarette were based on [McEwan et al. \(2019\)](#). The puff interval was assumed to be 30 s ([Bernstein, 2004](#)).

The dose of nicotine in one cigarette was assumed to be 1 mg (the amount varies between brands but is usually between 0.7 and 1 mg) ([EU, 2014](#)).

2.3.4 Normalized sensitivity analysis

To evaluate the relative impact of each of the model parameters on nicotine plasma maximal concentration (C_{max}) and area under the curve (AUC), a sensitivity analysis was performed. The sensitivity coefficient (SC) was calculated according to the equation below ([Teeguarden et al., 2005](#)).

SC = Fractional change in model output / Fractional change in parameter

Each parameter was individually increased by 1% of its original value, with the other parameters held constant. The larger the absolute value of the sensitivity coefficient, the more important the parameter. A normalized sensitivity coefficient of 1 represents a 1:1 relationship between the change in the parameter and the internal dose metric of choice. A negative SC indicates the given parameter influences the dose metric in an inverse direction. The SCs are grouped into one of three categories: namely, high (absolute SC values greater than or equal to 0.5), medium (absolute SC values greater than or equal to 0.2 but less than 0.5), or low (absolute SC values greater than or equal to 0.1 but less than 0.2), according to the IPCS guideline ([WHO, 2010](#)).

2.4 *In vitro* to *in vivo* extrapolation

The goal was to estimate the Human Equivalent Concentration (HEC) from *in vitro* assays and nicotine plasma concentration. Three steps were followed to derive a tracheobronchial epithelium concentration equivalent to an MEC from an *in vitro* assay ([Figure 3](#)).

- Estimate the fraction deposited for a scenario type with MPPD.
- Use the fraction deposited from MPPD in the PBPK model and by reverse dosimetry derive the exposure concentration that matches the estimated *in vitro* deposition POD. BEAS2B cells were used so we used the amount deposited in the tracheobronchial region to perform reverse dosimetry (AT2 in the model code).
- Simulate plasma concentration using the PBPK model.

3 Results

3.1 *In vitro* assays

1R6F exposure of BEAS2B to air-diluted smoke (1:5) with a subsequent recovery of 24 h was performed. [Figure 4](#) shows the calculation of the minimum effective concentration (MEC), and [Figure 5](#) is the calculation of nicotine mass corresponding to the MEC threshold captured on glass plates.

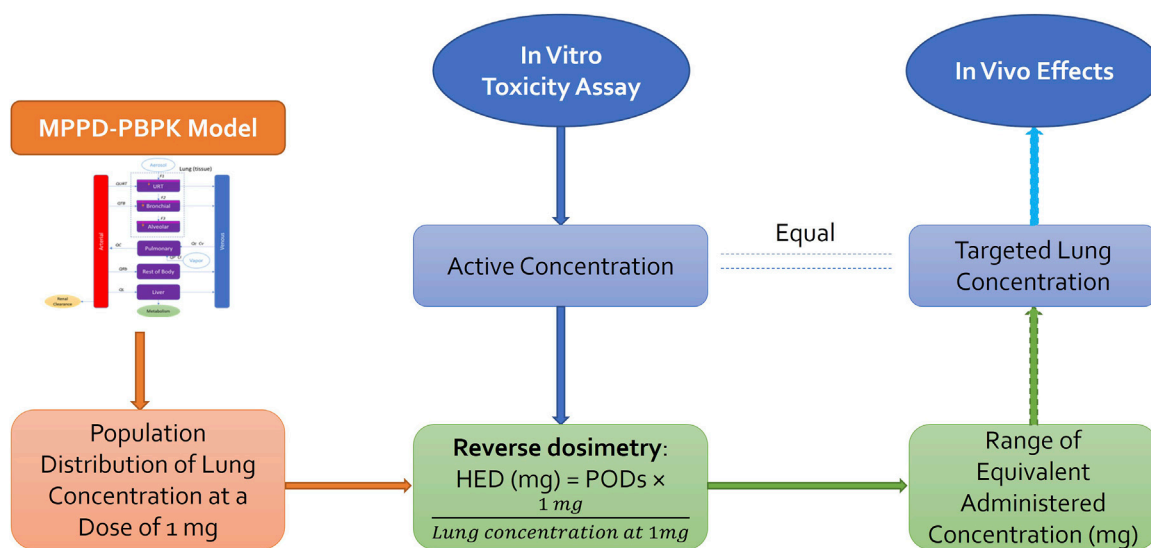


FIGURE 3

In vitro to *in vivo* extrapolation. Physiological parameters as well as parameters describing ADME processes of the chemical through the system were used to develop a PBPK model that can be used to predict the population distribution of lung concentration from any given daily dose. Reverse dosimetry predicts administered doses equivalent to *in vitro* active concentration, which can be compared to the *in vivo* measurements [Adapted from Bell et al. (2018)].

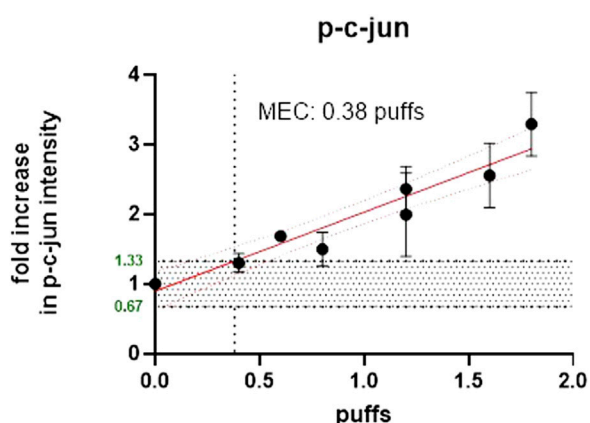


FIGURE 4

Number of puffs of 1R6F to reach the MEC for p-c-jun using high content screening.

The same experiments were also conducted for HTP and Figures 6, 7 below shows the p-c-jun HTP results, with the MEC and number of puffs required to reach the MEC.

3.2 MPPD modeling

Cigarette deposition fractions in the respiratory tract used to calibrate and validate the PBPK model can be found in Table 2. With a CMD of 0.163 μm and GSD of 1.44 and according to the scenario of exposure described in the method section, the deposition fractions in the head, the trachea-bronchial region and the pulmonary region

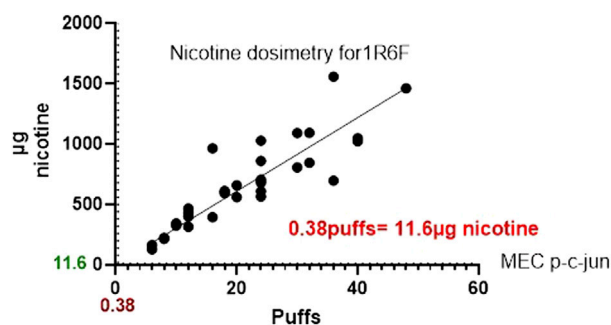


FIGURE 5

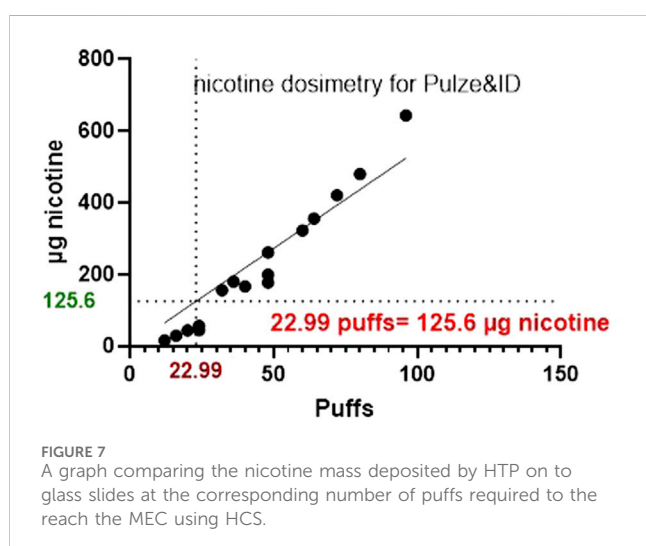
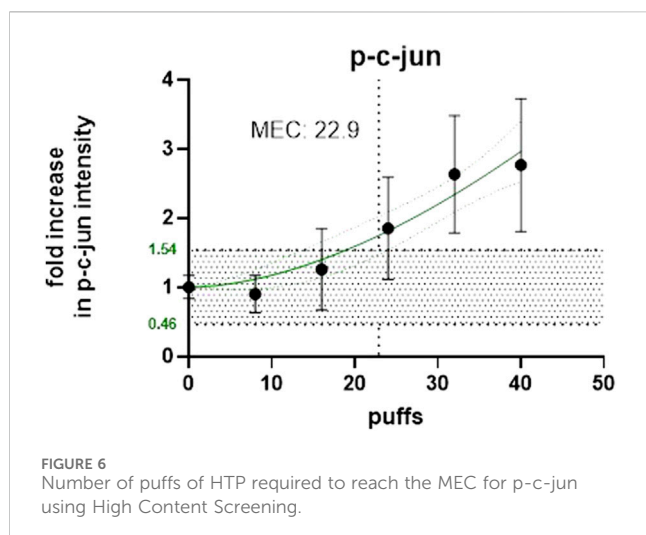
Graph comparing the nicotine mass deposited by 1R6F on to glass slides at the corresponding number of puffs required to reach the MEC using High Content Screening.

were 0.0147, 0.0673 and 0.1629, respectively. The total deposition fraction equaled 0.2449.

3.3 PBPK modeling

3.3.1 Model calibration and evaluation

Figure 8 shows the results of the performance of the model when evaluated using the *in vivo* PK data for nicotine from McEwan et al. (2019). A qualitative evaluation of the agreement between experimental plasma concentration and simulations was conducted through visual inspection of the time-course, where good agreement is generally defined as simulations falling within a factor of two of the data (EPA, 2006). In addition, IPCS (2010)



guidance on “Principles of Characterizing and Applying PBPK Models in Risk Assessment” states that “In PBPK modeling, predictions that are, on average, within a factor of 2 of the experimental data have frequently been considered adequate”.

Monte Carlo (MC) analysis was also conducted to investigate the population variability. Only the sensitive parameters from the sensitivity analysis were varied. Partition coefficients, body weight, breathing rates, and metabolic constants were simulated as log normally distributed; and cardiac output, blood flows, tissue volumes and parameters related to puffing scenario (puff volume, puff duration, puff interval) were simulated as normally distributed. The coefficients of variation (CV) for partition coefficients were 30%, a CV of 22% and 16% were used for the body weight and for the blood flow to the liver, respectively (Price et al., 2003), while a CV of 30% was assumed for the remaining model parameters. The distributions were truncated at 2 Standard deviations (Clewell and Clewell, 2008) to ensure physiological plausibility. Parameters distribution can be found in Supplementary Table S1. Monte-Carlo simulations were performed with 100 iterations to perform population-level simulations. Mean or median plasma

concentration as well as the 5th and 95th percentiles are graphically represented in Figures 8–10. For IVIVE, Monte-Carlo simulations were performed with 1,000 iterations to perform population-level simulations.

The performance of the model was also evaluated using *in vivo* nicotine PK studies with cigarettes (Digard et al., 2013; Picavet et al., 2016). Simulations results can be found in Figures 9, 10. The PBPK model predictions were consistent with the nicotine concentrations in plasma in adult humans.

3.3.2 Sensitivity analysis

The sensitivity of model parameters was calculated with the human PBPK model for the plasma maximum concentration (C_{max}) and area under the curve (AUC) after low and high inhalation doses of nicotine (1.2 and 12 mg). Results from the normalized sensitivity analysis are in Supplementary Figure S1. The most sensitive parameters are the ones related to inhaled dose: puff duration, puff interval, breathing rate, tidal volume, puff volume and fraction of vapor. The analysis showed that physiological parameters, including body weight, cardiac output and blood flow to the liver are medium to highly sensitive. The parameter for particle deposition in the pulmonary region is also a medium-sensitivity parameter. Note that hepatic metabolism parameters showed no sensitivity for plasma C_{max} but medium sensitivity for the plasma AUC. This does not mean that metabolism is not influential in plasma C_{max} , but indicates that metabolism is so efficient, i.e., $CL_{int_in\ vivo}$ very much exceeds liver plasma flow and a 1% increase in the parameter value would not make a difference, as it is largely limited by liver plasma flow, which is one of the most sensitive parameters.

The uncertainty of a model reflects the level of confidence in model predictions. The structure of the model is based on previously published models (Plowchalk et al., 1992; Robinson et al., 1992) where we included a more complex description of the lung to be able to link a dosimetry model (MPPD). The vapor fraction for cigarette was fitted to the data. For vapor absorption, we assumed that vapor would be completely absorbed in the deep lung. A more complex description of vapor absorption along the respiratory tract may provide simulations more similar to the observed data.

3.4 *In vitro* to *in vivo* extrapolation

The mass median aerodynamic diameter (MMAD) was set to 0.8 µm with a geometric standard deviation (GSD) of 1.3 for 1R6F and 0.7 µm with a GSD of 1.5 for HTP based on Schaller et al. (2016). For the PBPK model, we used values from McEwan et al. (2019) and O’Connell et al. (2019) with a puff duration of 2.3 s, a puff interval of 30 s, a puff volume of 69.5 mL and a number of puffs per cigarettes of 10. Results from MPPD modeling are presented in table 3.

We used the PBPK model and predicted the dose of nicotine per cigarette necessary to reach the MEC for both 1R6F and HTP. Monte Carlo simulations were used to estimate median, 5th and 95th percentiles for the amount of nicotine in the epithelium of the tracheobronchial region (AT2) for individuals exposed to the same, fixed dose (1 mg). Since the upper 95th percentile individuals have higher amounts for the same exposure, they are an example of a sensitive population. Then, reverse dosimetry predicted

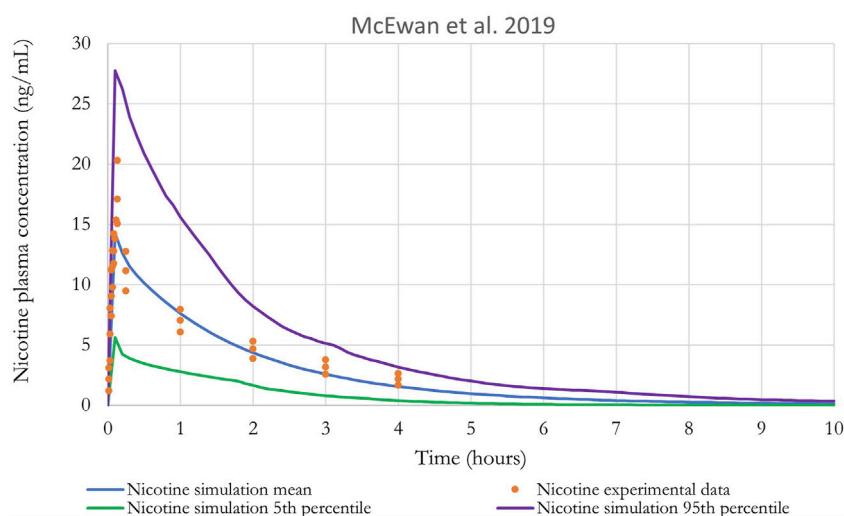


FIGURE 8

Nicotine plasma concentration in adult humans following inhalation exposure (1 mg). The solid line is the simulated venous concentration in ng/mL and the red circles are the PK data from [McEwan et al. \(2019\)](#) in ng/mL (mean \pm SEM).

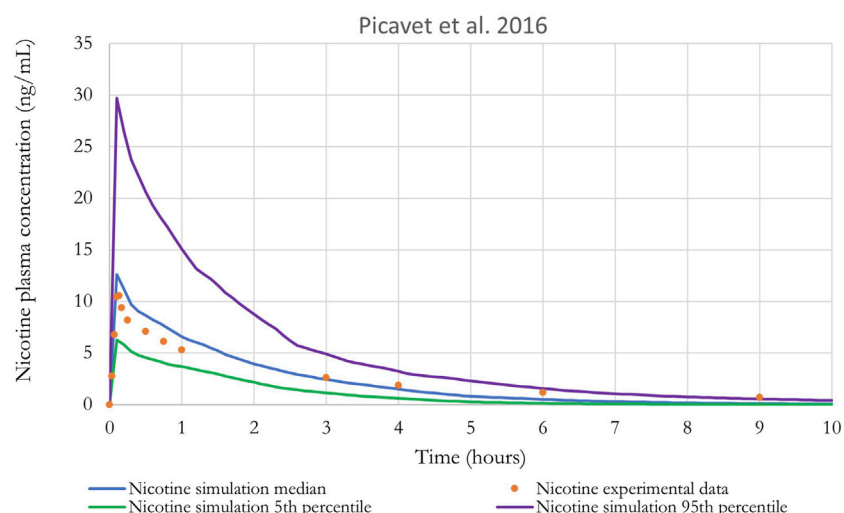


FIGURE 9

Nicotine plasma concentration in adult humans following inhalation exposure (1 mg). The solid line is the simulated venous concentration in ng/mL and the red circles are the PK data from [Picavet et al. \(2016\)](#) in ng/mL.

administered doses equivalent to the active concentrations from the *in vitro* assays (MEC of 0.072 and 0.77 μ mol for 1R6F and HTP, respectively). The exposure concentration necessary to reach the MEC are in [Table 4](#), and equivalent plasma concentrations are shown in [Table 5](#).

To derive the plasma concentration, we used two scenarios, one where only one cigarette is consumed (at the HEC for both cigarettes and HTP stick and at 1.03 mg nicotine for comparison with nicotine content in cigarettes or 1.85 mg nicotine for HTP stick) and a second scenario where 10 cigarettes are consumed over time (at the HEC \times 10 for the total dose of nicotine over the 10 sessions and at 10.3 mg or 18.5 mg nicotine which means 1.03 mg nicotine per cigarette or

1.85 mg nicotine per HTP stick \times 10 sessions). For each session, the parameters used were that a cigarette was smoked entirely after 10 puffs, a single puff every 30 s (5 min) and a single cigarette was smoked every hour.

[Table 4](#) shows the margin of exposure (MOE), which is the ratio between the nicotine content necessary to reach the MEC and the classic nicotine content of each cigarette. Results mean that after smoking the equivalent of 1/6th of a 1R6F cigarette, the MEC is already reached. However, for HTP, puffing almost 3 HTP sticks at the same time would be required to reach the MEC.

Plasma concentrations predicted after exposure to the classic nicotine content (1.85 and 1.03 for 1R6F and HTP, respectively) and

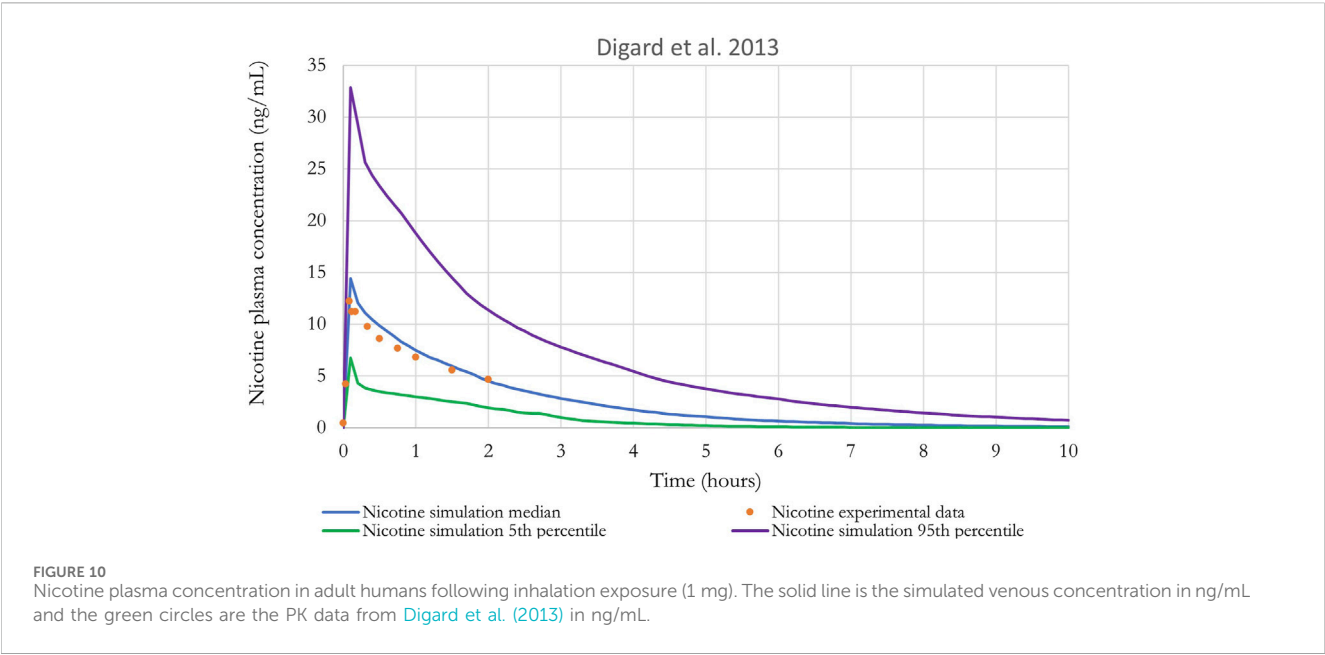


TABLE 3 Nicotine fraction deposited for 1R6F and HTP in MPPD.

Deposition	Head	Tracheobronchial region	Pulmonary region
1R6F	0.0082	0.0608	0.1454
HTP	0.0089	0.0615	0.1456

TABLE 4 Human equivalent exposure concentrations predictions using MPPD-PBPK modeling and the MEC values reported in Figures 4–6 and typical cigarettes and HTP nicotine content for comparison.

	MEC (μmol)	HEC (mg nicotine/stick) median (5th–95th percentiles)	Nicotine concentration (mg nicotine/stick)	Margin of exposure (MOE)
1R6F	0.072	0.288 (0.25–0.337) ^a	1.85	0.16
HTP	0.77	3.05 (2.64–3.58) ^a	1.03	2.96

^aMonte-Carlo simulations were performed with 1,000 iterations as described in model evaluation.

TABLE 5 Plasma concentrations of nicotine are predicted using MPPD-PBPK modeling, and the HEC values reported in Table 4 and blood concentrations predicted after exposure to the classic nicotine content.

	HEC (mg nicotine/cig)	Plasma concentration after 1 stick (ng/mL) ^a	HEC at steady state (mg nicotine/10 sticks)	Plasma concentration at steady state (ng/mL) ^a
1R6F	0.288	4.16 (1.84–10.02)	2.88	9.38 (4.34–21.42)
1R6F	1.85 ^b	28.18 (11.85–65.74)	18.5	60.83 (27.17–139.80)
HTP	3.05	46.48 (20.09–110.98)	30.5	101.43 (46.01–228.11)
HTP	1.03 ^b	15.50 (6.47–38.79)	10.3	34.30 (15.32–77.45)

^aMedian (fifth–95th percentile).

^bNicotine concentration in the Smoke/Aerosol from cigarettes or HTP sticks.

after exposure to the nicotine content at the MEC are in Table 5. Concentrations in plasma are reported after exposure to a single cigarette/stick and after 10 cigarettes/sticks to approximate a plasma steady state for nicotine. Table 5 shows that nicotine plasma concentrations range from 4 to 28 ng/mL after exposure to 1 stick of 1R6F at the MEC and at a nicotine concentration of a

classic cigarette, respectively. For HTP, nicotine plasma concentrations range from 15.5 to 46.5 ng/mL after exposure to 1 stick at a nicotine concentration of a classic HTP and at the MEC, respectively.

When a steady state is reached after 10 cigarettes or 10 HTP sticks (1R6F and HTP), simulations suggest that plasma concentrations have doubled. The plasma concentration of nicotine is not higher because between each stick, nicotine is rapidly eliminated.

4 Discussion

To better understand the applicability of *in vitro* assay results in terms of *in vivo* exposure in humans, it is necessary to develop computational tools to describe the PK of nicotine, a key biomarker of exposure to cigarettes and HTPs. In this study, we have combined a PBPK model for nicotine with a lung deposition model (MPPD) to better predict nicotine deposition and to model the pharmacokinetics of nicotine with use of either a HTP or cigarette. We have parameterized and exercised the MPPD model to characterize particle deposition in the respiratory tract and developed a PBPK model for nicotine that was validated by comparisons with human data from *in vivo* clinical studies. Finally, we estimated Human Equivalent Concentration (HEC) and plasma concentrations based on minimum effective concentration (MEC). This was derived by exposing BEAS-2B cells to 1R6F or HTP diluted smoke/aerosol and detecting c-jun activation using high content screening to then calculate the MEC as the point of departure.

Regarding the health consequences associated with tobacco use, several biomarkers of exposure for smoking have been reported (Benowitz et al., 2009b; Chang et al., 2017). In this study, we chose to measure nicotine as it has been studied extensively and is routinely measured in human clinical studies investigating exposure to nicotine-containing products and because of its relative stability for measurement (Crooks et al., 2013). Overall, the MPPD-PBPK model adequately recapitulated the *in vivo* kinetic data of nicotine from human studies with cigarettes. Good agreement with model predictions, generally within a factor of two of the data, was obtained. IPCS (2010) guidance on “Principles of Characterizing and Applying PBPK Models in Risk Assessment” states that “In PBPK modelling, predictions that are, on average, within a factor of 2 of the experimental data have frequently been considered adequate”.

One advantage of PBPK models is their potential to account for population variability. Interindividual variations in metabolism is usually well-documented in humans (Tyndale and Sellers, 2002; Hukkanen et al., 2005). Other causes of variability include the absorption of nicotine (different scenario of exposure depending on product uses) or differences in products used for nicotine delivery (e.g., cigarettes vs. HTP) and the physico-chemical characteristics of particles. The impact of changes in particle size through MPPD modelling or in scenarios of exposure (smoking habits) can be studied with a PBPK model. Supplementary Figure S2 in supplemental, for example, shows the regional deposition fractions of inhaled aerosol particles as a function of different breathing scenarios (Supplementary Material S1, Supplementary

Table S2). MPPD calculations of deposition in the head and tracheobronchial regions were very similar for many breathing patterns. However, deposition in the pulmonary region is highly dependent on breathing pattern and increases with longer breath hold and deeper, slower breath. In all cases, the total deposition is less than 40%. Concerning smoking habits, Jones et al. (2020) reported that the puffing data also provides evidence suggesting that consumers are, on average, more likely to take larger puff volumes when using a HTP compared to a classic cigarette. This observation is consistent with studies showing that HTPs lead to lower nicotine exposure (Bekki et al., 2017; Uchiyama et al., 2018; Vukas et al., 2023). Lower nicotine delivery could lead to compensatory puffing when product use does not sufficiently satisfy cravings (Vukas et al., 2023). Consumer use-behaviour and consumption data help ensure that modelling is reflective of real-world consumers. In this study, we assumed the same use-behaviour for cigarettes and HTPs users as the difference in nicotine levels between cigarettes and HTPs were not clear in all studies (Mallock et al., 2018; Salman et al., 2019; Rabenstein et al., 2023). Nicotine delivery and consumer satisfaction has also been shown to remain comparable between cigarette smoking and HTP use (Ogden et al., 2015; Picavet et al., 2016; Brossard et al., 2017; Roulet et al., 2019).

Public health experts worldwide have concluded that it is the toxicants in cigarette smoke generated by burning tobacco, and not the nicotine, which is the cause of smoking-related diseases. Therefore, whilst nicotine is a reliable biomarker for exposure to tobacco products, it does not provide any indication of health risks associated with smoking or the use of nicotine-containing products (Royal College of Physicians, 2016; FDA, 2022). Other biomarkers and health assessments are often used in conjunction to provide a more comprehensive understanding of the health impact of tobacco use. Both traditional cigarettes and HTP contain tobacco, but methods of consumption and associated health risk for these products differ. Cigarettes burn tobacco, producing smoke which contains numerous harmful chemicals with the number of smoke constituents being around 7,000 chemicals (Rodgman et al., 2000). Around 100 of these chemicals are classified by public health experts as causes or potential causes of smoking related disease (FDA, 2012). HTPs do not operate at temperatures high enough to burn tobacco. Since HTPs do not burn tobacco, they produce significantly fewer and lower levels of harmful chemicals compared to smoke from cigarettes (Schaller et al., 2016; Mallock et al., 2018; Salman et al., 2019; Vukas et al., 2023). Salman et al. (2019) for example, showed that reactive oxygen species (ROS) and carbonyl compound emissions were lower in HTP aerosol compared to cigarettes. Oxidative stress has been suggested as important part of several smoking-related diseases (Luettich et al., 2021).

In vitro experiments are essential to better understand differences in the potential effects of tobacco products. Several studies have demonstrated that measured reductions in toxicants in HTP aerosols compared to cigarette smoke can translate into reductions in *in vitro* toxicological effects (Schaller et al., 2016; Jaunky et al., 2018; Hattori et al., 2020; Dusautoir et al., 2021; Wang et al., 2021). Here, we investigated the effects of HTPs and the 1R6F Reference Cigarette, on the Phosphorylation of AP-1 transcription factor component, c-jun, which is a process involved in regulation of cellular stress responses such as cell cycling control and apoptosis

(Dreij et al., 2010). Studies suggest that exposure to both HTP aerosol and cigarette smoke can lead to the activation of c-jun (Kogel et al., 2015; Chapman et al., 2023). However, the specific effects and the extent of c-jun activation may vary between these two forms of tobacco use. The elevated levels of c-jun observed in response to tobacco products' exposure, make it a potentially useful biomarker for assessing tobacco-related effects on cellular processes.

In this work, to compare the effective concentrations of each product type, a study was designed to look at both the number of puffs delivered to cells (BEAS-2B) and the amount of nicotine delivered at the cell surface. The aim of this experiment was to determine the number of puffs required for the products to cause a minimum effective concentration for the c-jun cellular marker, measured using high content screening (HCS) and to relate the number of puffs with the delivery of nicotine to the cell surface. IVIVE was used to derive the exposure concentration (HEC) that matches the estimated *in vitro* effect (MEC) and then derive the equivalent plasma concentrations. Results show that it would be necessary to consume 3 HTP sticks at the same time to produce *in vivo* the effects seen *in vitro* under the conditions of this test. However, for the 1R6F cigarette, smoking only 1/6th of a stick would lead to the *in vivo* effect seen *in vitro* under the conditions of the test. Nicotine plasma concentrations ranged from 4 to 28 ng/mL after exposure to 1 stick of 1R6F at the MEC and at a nicotine concentration of a classic cigarette, respectively. For HTP, nicotine plasma concentrations range from 15.5 to 46.5 ng/mL after exposure to 1 stick of HTP at a nicotine concentration of a classic HTP stick and to 1 stick of HTP at the MEC, respectively. In comparison, plasma concentrations in clinical PK studies were between 14 and 20 ng/mL (Digard et al., 2013; Picavet et al., 2016; McEwan et al., 2019). At steady state, concentrations are higher, which is explained by the half-life of nicotine (1–3 h in blood). In the simulations with repeated use, sticks (1R6F and HTP) are consumed every hour for 10 h and therefore we can see an accumulation of nicotine in plasma over time until a steady state is achieved.

One of the modeling challenges in this study was that the *in vitro* testing was conducted with cigarettes and HTP smoke/aerosol which are complex mixtures including nicotine, organic acids, and carrier chemicals (propylene glycol and vegetable glycerol). The *in vitro* assays assessed the toxicity of the whole mixture, whereas the PBPK model and its parameterization was carried out for a specific compound, nicotine. Because of the various PK and pharmacodynamic properties of individual compounds in a mixture as well as the potential interactions between those chemicals, mixtures present a special challenge for conducting IVIVE (Hernandez and Tsatsakis, 2017). While important, these factors were not taken into consideration as the goal was to compare the potency of HTPs *versus* cigarettes. However, as a range of nicotine delivery products such as e-vapor products are gaining popularity among adult smokers, IVIVE modeling for mixtures must be considered (Zhang et al., 2021). Qualitatively, differences in irritant properties of the inhaled mixtures may be the primary cause of the c-jun responses being greater with cigarettes compared to the HTP. C-jun is an important marker as it plays a key role in cell cycle progression, that is achieved via the transcriptional repression of cell cycle inhibitors and the transcriptional activation of cell cycle progression machinery (Lukey et al., 2016).

Rodrigo et al. (2021) have suggested that the use of HTP may be associated with potentially reduced cancer and non-cancer endpoints based on their reduced harmful and potentially harmful constituent yields measured in aerosol when compared to cigarette smoke. Kusonic et al. (2023) stated that whilst HTP products have shown a reduced risk to human health when compared to the cigarettes, they still, however, contain compounds in the aerosol that can be detrimental to human health. The authors went on to state that there was not enough data obtained from independent studies indicating that the reduced amounts of toxic chemicals in the aerosol of HTP do not induce any harmful effects.

In conclusion, the results of this study demonstrate that for the 1R6F cigarette, consuming 1/6th of a stick would be required to induce the c-jun activation effects observed *in vitro*. Whereas, for HTP it would be necessary to consume 3 sticks simultaneously to produce *in vivo* the effects observed *in vitro*. This data further demonstrates the reduced potency of the HTP aerosol compared to cigarette smoke thereby adding to the weight of evidence that non-combustible next-generation products have the potential for reduced harm when compared to cigarettes. The QIVIVE approach demonstrates great promise in assisting human health risk assessments; however, further optimization and standardization is required to gain regulatory acceptance. Furthermore, biomarkers and health assessments other than nicotine and the measure of cellular stress also need to be studied to provide a more comprehensive understanding of the impact of tobacco use on an individual's health.

Data availability statement

The raw data supporting the conclusion of this article will be made available by the authors, without undue reservation.

Ethics statement

Ethical approval was not required for the studies on animals in accordance with the local legislation and institutional requirements because only commercially available established cell lines were used.

Author contributions

MM: Formal Analysis, Investigation, Methodology, Software, Visualization, Writing—original draft, Writing—review and editing. LS: Conceptualization, Methodology, Project administration, Writing—review and editing. MA: Writing—review and editing, Methodology. ES: Data curation, Formal Analysis, Writing—review and editing. RW: Methodology, Validation, Writing—review and editing, Formal Analysis. SP: Methodology, Validation, Writing—review and editing, Formal Analysis. FC: Conceptualization, Writing—review and editing. KR: Writing—review and editing, Formal Analysis. SO: Writing—review and editing, Formal Analysis. JF: Writing—review and editing, Methodology. MS: Conceptualization, Funding acquisition, Supervision, Writing—review and editing.

Funding

The author(s) declare that financial support was received for the research, authorship, and/or publication of this article. Funding was provided by Imperial Brands PLC.

Conflict of interest

Authors LS, FC, and MS are employed by Imperial Brands PLC. Authors ES, RW, SP, KR, and SO are employed by Reemtsma Cigarettenfabriken GmbH, An Imperial Brands PLC company. Authors MM, MA, and JF are employed by ScitoVation LLC.

References

- Anjilvel, S., and Asgharian, B. (1995). A multiple-path model of particle deposition in the rat lung. *Fundam. Appl. Toxicol.* 28, 41–50. doi:10.1006/faat.1995.1144
- Asgharian, B., Hofmann, W., and Bergmann, R. (2001). Particle deposition in a multiple-path model of the human lung. *Aerosol Sci. Technol.* 34, 332–339. doi:10.1080/02786820119122
- Asgharian, B., Wood, R., and Schlesinger, R. B. (1995). 'Empirical modeling of particle deposition in the alveolar region of the lungs: a basis for interspecies extrapolation. *Fundam. Appl. Toxicol.* 27, 232–238. doi:10.1006/faat.1995.1128
- Bekki, K., Inaba, Y., Uchiyama, S., and Kunugita, N. (2017). 'Comparison of chemicals in mainstream smoke in heat-not-burn tobacco and combustion cigarettes. *J. UOEH* 39, 201–207. doi:10.7888/juoeh.39.201
- Bell, S. M., Chang, X., Wambaugh, J. F., Allen, D. G., Bartels, M., Brouwer, K. L. R., et al. (2018). 'in vitro to in vivo extrapolation for high throughput prioritization and decision making. *Toxicol. Vitro* 47, 213–227. doi:10.1016/j.tiv.2017.11.016
- Benowitz, N. L., Dains, K. M., Dempsey, D., Herrera, B., Yu, L., and Jacob, P., 3rd. (2009a). Urine nicotine metabolite concentrations in relation to plasma cotinine during low-level nicotine exposure. *Nicotine Tob. Res.* 11, 954–960. doi:10.1093/ntr/ntp092
- Benowitz, N. L., Hukkanen, J., and Jacob, P., 3rd (2009b). 'Nicotine chemistry, metabolism, kinetics and biomarkers. *Handb. Exp. Pharmacol.*, 29–60. doi:10.1007/978-3-540-69248-5_2
- Bernstein, D. (2004). A review of the influence of particle size, puff volume, and inhalation pattern on the deposition of cigarette smoke particles in the respiratory tract. *Inhal. Toxicol.* 16, 675–689. doi:10.1080/08958370490476587
- Brossard, P., Weitkunat, R., Poux, V., Lama, N., Haziza, C., Picavet, P., et al. (2017). Nicotine pharmacokinetic profiles of the Tobacco Heating System 2.2, cigarettes and nicotine gum in Japanese smokers. *Regul. Toxicol. Pharmacol.* 89, 193–199. doi:10.1016/j.yrtph.2017.07.032
- Brown, R. P., Delp, M. D., Lindstedt, S. L., Rhomberg, L. R., and Beliles, R. P. (1997). Physiological parameter values for physiologically based pharmacokinetic models. *Toxicol. Ind. Health* 13, 407–484. doi:10.1177/074823379701300401
- Butler, J. (1992). "The bronchial circulation," in *Lung biology in health and disease*. Editor C. Lenfant (New York: Marcel Dekker Inc.).
- Campbell, J., Van Landingham, C., Crowell, S., Gentry, R., Kaden, D., Fiebelkorn, S., et al. (2015). A preliminary regional PBPK model of lung metabolism for improving species dependent descriptions of 1,3-butadiene and its metabolites. *Chem. Biol. Interact.* 238, 102–110. doi:10.1016/j.cbi.2015.05.025
- Chang, C. M., Edwards, S. H., Arab, A., Del Valle-Pinero, A. Y., Yang, L., and Hatsukami, D. K. (2017). 'Biomarkers of tobacco exposure: summary of an FDA-sponsored public workshop. *Cancer Epidemiol. Biomarkers Prev.* 26, 291–302. doi:10.1158/1055-9965.EPI-16-0675
- Chapman, F., Sticken, E. T., Wiczorek, R., Pour, S. J., Dethloff, O., Budde, J., et al. (2023). 'Multiple endpoint in vitro toxicity assessment of a prototype heated tobacco product indicates substantially reduced effects compared to those of combustible cigarette. *Toxicol. Vitro* 86, 105510. doi:10.1016/j.tiv.2022.105510
- Clewell, R. A., and Clewell, H. J., 3rd. (2008). Development and specification of physiologically based pharmacokinetic models for use in risk assessment. *Regul. Toxicol. Pharmacol.* 50, 129–143. doi:10.1016/j.yrtph.2007.10.012
- Clippinger, A. J., Ahluwalia, A., Allen, D., Bonner, J. C., Casey, W., Castranova, V., et al. (2016). Expert consensus on an in vitro approach to assess pulmonary fibrogenic potential of aerosolized nanomaterials. *Arch. Toxicol.* 90, 1769–1783. doi:10.1007/s00204-016-1717-8
- COT (2017). "Annual report," in *Committee on toxicity of chemicals in food, consumer products and the environment*.
- Crooks, I., Dillon, D. M., Scott, J. K., Ballantyne, M., and Meredith, C. (2013). The effect of long term storage on tobacco smoke particulate matter in in vitro genotoxicity

Publisher's note

All claims expressed in this article are solely those of the authors and do not necessarily represent those of their affiliated organizations, or those of the publisher, the editors and the reviewers. Any product that may be evaluated in this article, or claim that may be made by its manufacturer, is not guaranteed or endorsed by the publisher.

Supplementary material

The Supplementary Material for this article can be found online at: <https://www.frontiersin.org/articles/10.3389/ftox.2024.1373325/full#supplementary-material>

and cytotoxicity assays. *Regul. Toxicol. Pharmacol.* 65, 196–200. doi:10.1016/j.yrtph.2012.11.012

Digard, H., Proctor, C., Kulasekaran, A., Malmqvist, U., and Richter, A. (2013). Determination of nicotine absorption from multiple tobacco products and nicotine gum. *Nicotine Tob. Res.* 15, 255–261. doi:10.1093/ntr/nts123

Dreij, K., Rhrissorakrai, K., Gunsalus, K. C., Geacintov, N. E., and Scicchitano, D. A. (2010). 'Benzo[a]pyrene diol epoxide stimulates an inflammatory response in normal human lung fibroblasts through a p53 and JNK mediated pathway. *Carcinogenesis* 31, 1149–1157. doi:10.1093/carcin/bgq073

Dusautoir, R., Zarcone, G., Verrielle, M., Garcon, G., Fronval, I., Beauval, N., et al. (2021). Comparison of the chemical composition of aerosols from heated tobacco products, electronic cigarettes and tobacco cigarettes and their toxic impacts on the human bronchial epithelial BEAS-2B cells. *J. Hazard Mater.* 401, 123417. doi:10.1016/j.jhazmat.2020.123417

EPA (2006). "Approaches for the application of physiologically based pharmacokinetic (pbpk) models and supporting data in risk assessment," in edited by Office of Research and Development National Center for Environmental Assessment. (Washington, D.C: U.S. Environmental Protection Agency).

EU (2014). *Tighter rules on tobacco*. European Union. Available at: <https://eur-lex.europa.eu/EN/legal-content/summary/tighter-eu-rules-on-tobacco.html>.

FDA (2012). *Harmful and potentially harmful constituents in tobacco products and tobacco smoke*. Established List, 20034–20037.

FDA (2022). Nicotine is why tobacco products are addictive. Available at: <https://www.fda.gov/tobacco-products/health-effects-tobacco-use/nicotine-why-tobacco-products-are-addictive>.

Fuoco, F. C., Buonanno, G., Stabile, L., and Vigo, P. (2014). Influential parameters on particle concentration and size distribution in the mainstream of e-cigarettes. *Environ. Pollut.* 184, 523–529. doi:10.1016/j.envpol.2013.10.010

Gowadia, N., and Dunn-Rankin, D. (2010). A transport model for nicotine in the tracheobronchial and pulmonary region of the lung. *Inhal. Toxicol.* 22, 42–48. doi:10.3109/08958370902862442

Haghegahdar, A., Feng, Y., Chen, X., and Lin, J. (2018). Computational analysis of deposition and translocation of inhaled nicotine and acrolein in the human body with E-cigarette puffing topographies. *Aerosol Sci. Technol.* 52, 483–493. doi:10.1080/02786826.2018.1447644

Hattori, N., Nakagawa, T., Yoneda, M., Nakagawa, K., Hayashida, H., and Ito, T. (2020). Cigarette smoke, but not novel tobacco vapor products, causes epigenetic disruption and cell apoptosis. *Biochem. Biophys. Rep.* 24, 100865. doi:10.1016/j.bbrep.2020.100865

Hernandez, A. F., and Tsatsakis, A. M. (2017). Human exposure to chemical mixtures: challenges for the integration of toxicology with epidemiology data in risk assessment. *Food Chem. Toxicol.* 103, 188–193. doi:10.1016/j.fct.2017.03.012

Hukkanen, J., Jacob, P., 3rd, and Benowitz, N. L. (2005). 'Metabolism and disposition kinetics of nicotine. *Pharmacol. Rev.* 57, 79–115. doi:10.1124/pr.57.1.3

International Programme on Chemical Safety (IPCS) (2010). *Characterization and application of physiologically based pharmacokinetic models in risk assessment*. World Health Organization. Geneva, Switzerland: International Programme on Chemical Safety.

Jaunky, T., Adamson, J., Santopietro, S., Terry, A., Thorne, D., Breheny, D., et al. (2018). 'Assessment of tobacco heating product THP1.0. Part 5: in vitro dosimetric and cytotoxic assessment. *Regul. Toxicol. Pharmacol.* 93, 52–61. doi:10.1016/j.yrtph.2017.09.016

Jones, J., Slayford, S., Gray, A., Brick, K., Prasad, K., and Proctor, C. (2020). A cross-category puffing topography, mouth level exposure and consumption study among Italian users of tobacco and nicotine products. *Sci. Rep.* 10, 12. doi:10.1038/s41598-019-55410-5

- Kogel, U., Gonzalez Suarez, I., Xiang, Y., Dossin, E., Guy, P. A., Mathis, C., et al. (2015). 'Biological impact of cigarette smoke compared to an aerosol produced from a prototypic modified risk tobacco product on normal human bronchial epithelial cells. *Toxicol. Vitro* 29, 2102–2115. doi:10.1016/j.tiv.2015.08.004
- Kolli, A. R., Kuczaj, A. K., Martin, F., Hayes, A. W., Peitsch, M. C., and Hoeng, J. (2020). Bridging inhaled aerosol dosimetry to physiologically based pharmacokinetic modeling for toxicological assessment: nicotine delivery systems and beyond. *Crit. Rev. Toxicol.* 1–17. doi:10.1080/10408444.2019.1692780
- Kuepfer, L., Niederalt, C., Wendt, T., Schlender, J. F., Willmann, S., Lippert, J., et al. (2016). Applied concepts in PBPK modeling: how to build a PBPK/PD model. *CPT Pharmacometrics Syst. Pharmacol.* 5, 516–531. doi:10.1002/psp4.12134
- Kusonic, D., Bijelic, K., Kladar, N., Bozin, B., Torovic, L., and Srdencovic Conic, B. (2023). Comparative health risk assessment of heated tobacco products versus conventional cigarettes. *Subst. Use Misuse* 58, 346–353. doi:10.1080/10826084.2022.2161315
- Luetlich, K., Sharma, M., Yepiskoposyan, H., Breheny, D., and Lowe, F. J. (2021). An adverse outcome pathway for decreased lung function focusing on mechanisms of impaired mucociliary clearance following inhalation exposure. *Front. Toxicol.* 3, 750254. doi:10.3389/ftox.2021.750254
- Lukey, M. J., Greene, K. S., Erickson, J. W., Wilson, K. F., and Cerione, R. A. (2016). The oncogenic transcription factor c-Jun regulates glutaminase expression and sensitizes cells to glutaminase-targeted therapy. *Nat. Commun.* 7, 11321. doi:10.1038/ncomms11321
- Mallock, N., Boss, L., Burk, R., Danziger, M., Welsch, T., Hahn, H., et al. (2018). Levels of selected analytes in the emissions of "heat not burn" tobacco products that are relevant to assess human health risks. *Arch. Toxicol.* 92, 2145–2149. doi:10.1007/s00204-018-2215-y
- McEwan, M., Coburn, S., Ghosh, D., Simms, L., Giles, L., Yuki, D., et al. (2019). 'Assessment of priority tobacco additives per the requirements of the EU Tobacco Products Directive (2014/40/EU): Part 3, Smoking behavior and plasma nicotine pharmacokinetics. *Regul. Toxicol. Pharmacol.* 104, 29–38. doi:10.1016/j.yrtph.2019.02.012
- Moreau, M., Fisher, J., Andersen, M. E., Barnwell, A., Corzine, S., Ranade, A., et al. (2022). 'NAM-based prediction of point-of-contact toxicity in the lung: a case example with 1,3-dichloropropene. *Toxicology* 481, 153340. doi:10.1016/j.tox.2022.153340
- Mulhopt, S., Schlager, C., Berger, M., Murugadoss, S., Hoet, P. H., Krebs, T., et al. (2020). A novel TEM grid sampler for airborne particles to measure the cell culture surface dose. *Sci. Rep.* 10, 8401. doi:10.1038/s41598-020-65427-w
- O'Connell, G., Pritchard, J. D., Prue, C., Thompson, J., Verron, T., Graff, D., et al. (2019). A randomised, open-label, cross-over clinical study to evaluate the pharmacokinetic profiles of cigarettes and e-cigarettes with nicotine salt formulations in US adult smokers. *Intern. Emerg. Med.* 14, 853–861. doi:10.1007/s11739-019-02025-3
- Ogden, M. W., Marano, K. M., Jones, B. A., and Stiles, M. F. (2015). Switching from usual brand cigarettes to a tobacco-heating cigarette or snus: Part 1. Study design and methodology. *Biomarkers* 20, 382–390. doi:10.3109/1354750X.2015.1094133
- Picavet, P., Haziza, C., Lama, N., Weitkunat, R., and Ludicé, F. (2016). Comparison of the pharmacokinetics of nicotine following single and *ad libitum* use of a tobacco heating system or combustible cigarettes. *Nicotine Tob. Res.* 18, 557–563. doi:10.1093/ntr/ntv220
- Pichelstorfer, L., Hoffman, W., Winkler-Heil, R., Yurteri, C. U., and McAughey, J. (2016). Simulation of aerosol dynamics and deposition of combustible and electronic cigarette aerosols in the human respiratory tract. *J. Aerosol Sci.* 99, 125–132. doi:10.1016/j.jaerosci.2016.01.017
- Plowchalk, D. R., Andersen, M. E., and deBethizy, J. D. (1992). A physiologically based pharmacokinetic model for nicotine disposition in the Sprague-Dawley rat. *Toxicol. Appl. Pharmacol.* 116, 177–188. doi:10.1016/0041-008x(92)90297-6
- Price, P. S., Conolly, R. B., Chaisson, C. F., Gross, E. A., Young, J. S., Mathis, E. T., et al. (2003). 'Modeling interindividual variation in physiological factors used in PBPK models of humans. *Crit. Rev. Toxicol.* 33, 469–503. doi:10.1080/713608360
- Rabenstein, A., Rahofer, A., Vukas, J., Rieder, B., Storzehofecker, K., Stoll, Y., et al. (2023). Usage pattern and nicotine delivery during *ad libitum* consumption of pod E-cigarettes and heated tobacco products. *Toxics* 11, 434. doi:10.3390/toxics11050434
- Robinson, D. E., Balter, N. J., and Schwartz, S. L. (1992). A physiologically based pharmacokinetic model for nicotine and cotinine in man. *J. Pharmacokinet. Biopharm.* 20, 591–609. doi:10.1007/BF01064421
- Rodgman, A., Smith, C. J., and Perfetti, T. A. (2000). The composition of cigarette smoke: a retrospective, with emphasis on polycyclic components. *Hum. Exp. Toxicol.* 19, 573–595. doi:10.1191/096032700701546514
- Rodrigo, G., Jaccard, G., Tabin Djoko, D., Korneliou, A., Esposito, M., and Belushkin, M. (2021). 'Cancer potencies and margin of exposure used for comparative risk assessment of heated tobacco products and electronic cigarettes aerosols with cigarette smoke. *Arch. Toxicol.* 95, 283–298. doi:10.1007/s00204-020-02924-x
- Roulet, S., Chrea, C., Kanitscheider, C., Kallischnigg, G., Magnani, P., and Weitkunat, R. (2023). Potential predictors of adoption of the Tobacco Heating System by U.S. adult smokers: an actual use study. *F1000Res* 8, 214. doi:10.12688/f1000research.17606.1
- Royal College of Physicians (2016). Nicotine without smoke. Available at: <https://www.rcplondon.ac.uk/projects/outputs/nicotine-without-smoke-tobacco-harm-reduction>.
- Rozman, K. K., and Klaassen, C. D. (2001). "Absorption, distribution and excretion of toxicants," in *Casarett and Doull's toxicology: the basic science of poisons*. Editor C. D. Klaassen (New York: McGraw-Hill).
- Ruark, C. D., Song, G., Yoon, M., Verner, M. A., Andersen, M. E., Clewell, H. J., 3rd, et al. (2017). Quantitative bias analysis for epidemiological associations of perfluoroalkyl substance serum concentrations and early onset of menopause. *Environ. Int.* 99, 245–254. doi:10.1016/j.envint.2016.11.030
- Salman, R., Talih, S., El-Hage, R., Haddad, C., Karaoghlanian, N., El-Hellani, A., et al. (2019). Free-base and total nicotine, reactive oxygen species, and carbonyl emissions from IQOS, a heated tobacco product. *Nicotine Tob. Res.* 21, 1285–1288. doi:10.1093/ntr/nty235
- Sarangapani, R., Clewell, H. J., Cruzan, G., and Andersen, M. E. (2002a). Comparing respiratory-tract and hepatic exposure-dose relationships for metabolized inhaled vapors: a pharmacokinetic analysis. *Inhal. Toxicol.* 14, 835–854. doi:10.1080/08958370290084656
- Sarangapani, R., Teeguarden, J. G., Cruzan, G., Clewell, H. J., and Andersen, M. E. (2002b). Physiologically based pharmacokinetic modeling of styrene and styrene oxide respiratory-tract dosimetry in rodents and humans. *Inhal. Toxicol.* 14, 789–834. doi:10.1080/08958370290084647
- Schaller, J. P., Keller, D., Poget, L., Pratte, P., Kaelin, E., McHugh, D., et al. (2016). 'Evaluation of the Tobacco Heating System 2.2. Part 2: chemical composition, genotoxicity, cytotoxicity, and physical properties of the aerosol. *Regul. Toxicol. Pharmacol.* 81 (Suppl. 2), S27–S47. doi:10.1016/j.yrtph.2016.10.001
- Schmeck, B., Moog, K., Zahlten, J., van Laak, V., N'Guessan, P. D., Opitz, B., et al. (2006). Streptococcus pneumoniae induced c-Jun-N-terminal kinase- and AP-1-dependent IL-8 release by lung epithelial BEAS-2B cells. *Respir. Res.* 7, 98. doi:10.1186/1465-9921-7-98
- Song, G., Peeples, C. R., Yoon, M., Wu, H., Verner, M. A., Andersen, M. E., et al. (2016). Pharmacokinetic bias analysis of the epidemiological associations between serum polybrominated diphenyl ether (BDE-47) and timing of menarche. *Environ. Res.* 150, 541–548. doi:10.1016/j.envres.2016.07.004
- Sosnowski, T. R., and Kramek-Romanowska, K. (2016). Predicted deposition of E-cigarette aerosol in the human lungs. *J. Aerosol Med. Pulm. Drug Deliv.* 29, 299–309. doi:10.1089/jamp.2015.1268
- Teeguarden, J. G., Deisinger, P. J., Poet, T. S., English, J. C., Faber, W. D., Barton, H. A., et al. (2005). Derivation of a human equivalent concentration for n-butanol using a physiologically based pharmacokinetic model for n-butyl acetate and metabolites n-butanol and n-butyric acid. *Toxicol. Sci.* 85, 429–446. doi:10.1093/toxsci/kfi103
- Teeguarden, J. G., Housand, C. J., Smith, J. N., Hinderliter, P. M., Gunawan, R., and Timchalk, C. A. (2013). A multi-route model of nicotine-cotinine pharmacokinetics, pharmacodynamics and brain nicotinic acetylcholine receptor binding in humans. *Regul. Toxicol. Pharmacol.* 65, 12–28. doi:10.1016/j.yrtph.2012.10.007
- Tsuda, A., Henry, F. S., and Butler, J. P. (2013). Particle transport and deposition: basic physics of particle kinetics. *Compr. Physiol.* 3, 1437–1471. doi:10.1002/cphy.c100085
- Tyndale, R. F., and Sellers, E. M. (2002). 'Genetic variation in CYP2A6-mediated nicotine metabolism alters smoking behavior. *Ther. Drug Monit.* 24, 163–171. doi:10.1097/00007691-200202000-00026
- Uchiyama, S., Noguchi, M., Takagi, N., Hayashida, H., Inaba, Y., Ogura, H., et al. (2018). Simple determination of gaseous and particulate compounds generated from heated tobacco products. *Chem. Res. Toxicol.* 31, 585–593. doi:10.1021/acs.chemrestox.8b00024
- Upadhyay, S., and Palmberg, L. (2018). Air-liquid interface: relevant *in vitro* models for investigating air pollutant-induced pulmonary toxicity. *Toxicol. Sci.* 164, 21–30. doi:10.1093/toxsci/kfy053
- Vukas, J., Mallock-Ohnesorg, N., Ruther, T., Pieper, E., Romano-Brandt, L., Stoll, Y., et al. (2023). Two different heated tobacco products vs. Cigarettes: comparison of nicotine delivery and subjective effects in experienced users *Toxics* 11, 525. doi:10.3390/toxics11060525
- Waddell, W. J., and Marlowe, C. (1976). 'Localization of nicotine-14C, cotinine-14C, and nicotine-1'-N-oxide-14C in tissues of the mouse. *Drug Metab. Dispos.* 4, 530–539.
- Wang, H., Chen, H., Huang, L., Li, X., Wang, L., Li, S., et al. (2021). *In vitro* toxicological evaluation of a tobacco heating product THP COO and 3R4F research reference cigarette on human lung cancer cells. *Toxicol. Vitro* 74, 105173. doi:10.1016/j.tiv.2021.105173
- WHO (2010). *Characterization and application of physiologically based pharmacokinetic models in risk assessment*. Geneva, Switzerland: World Health Organization.
- Wieczorek, R., Trelles Sticklen, E., Pour, S. J., Chapman, F., Rower, K., Otte, S., et al. (2023). Characterisation of a smoke/aerosol exposure *in vitro* system (SAEIVS) for delivery of complex mixtures directly to cells at the air-liquid interface. *J. Appl. Toxicol.* 43, 1050–1063. doi:10.1002/jat.4442
- Wu, H., Yoon, M., Verner, M. A., Xue, J., Luo, M., Andersen, M. E., et al. (2015). Can the observed association between serum perfluoroalkyl substances and delayed menarche be explained on the basis of puberty-related changes in physiology and pharmacokinetics? *Environ. Int.* 82, 61–68. doi:10.1016/j.envint.2015.05.006
- Yamazaki, H., Horiuchi, K., Takano, R., Nagano, T., Shimizu, M., Kitajima, M., et al. (2010). Human blood concentrations of cotinine, a biomonitoring marker for tobacco smoke, extrapolated from nicotine metabolism in rats and humans and physiologically based pharmacokinetic modeling. *Int. J. Environ. Res. Public Health* 7, 3406–3421. doi:10.3390/ijerph7093406
- Zhang, J., Chang, X., Holland, T. L., Hines, D. E., Karmaus, A. L., Bell, S., et al. (2021). 'Evaluation of inhalation exposures and potential health impacts of ingredient mixtures using *in vitro* to *in vivo* extrapolation. *Front. Toxicol.* 3, 787756. doi:10.3389/ftox.2021.787756



OPEN ACCESS

EDITED BY

Victoria Hutter,
University of Hertfordshire, United Kingdom

REVIEWED BY

Michael Oldham,
University of California, Irvine, United States
Lindsay Marshall,
Humane Society of the United States,
United States

*CORRESPONDENCE

Marianna Gaca,
✉ marianna_gaca@bat.com

RECEIVED 25 January 2024

ACCEPTED 30 April 2024

PUBLISHED 13 June 2024

CITATION

Thorne D, McHugh D, Simms L, Lee KM,
Fujimoto H, Moses S and Gaca M (2024),
Applying new approach methodologies to
assess next-generation tobacco and
nicotine products.
Front. Toxicol. 6:1376118.
doi: 10.3389/ftox.2024.1376118

COPYRIGHT

© 2024 Thorne, McHugh, Simms, Lee,
Fujimoto, Moses and Gaca. This is an open-
access article distributed under the terms of the
[Creative Commons Attribution License \(CC BY\)](https://creativecommons.org/licenses/by/4.0/).
The use, distribution or reproduction in other
forums is permitted, provided the original
author(s) and the copyright owner(s) are
credited and that the original publication in this
journal is cited, in accordance with accepted
academic practice. No use, distribution or
reproduction is permitted which does not
comply with these terms.

Applying new approach methodologies to assess next-generation tobacco and nicotine products

David Thorne¹, Damian McHugh², Liam Simms³, K. Monica Lee⁴,
Hitoshi Fujimoto⁵, Sara Moses⁶ and Marianna Gaca^{1*}

¹BAT (Investments) Ltd., Southampton, Hampshire, United Kingdom, ²PMI R&D Philip Morris Products S. A., Neuchâtel, Switzerland, ³Imperial Brands, Bristol, United Kingdom, ⁴Altria Client Services LLC, Richmond, VA, United States, ⁵Japan Tobacco Inc., R&D Group, Yokohama, Kanagawa, Japan, ⁶Swedish Match, Stockholm, Sweden

In vitro toxicology research has accelerated with the use of *in silico*, computational approaches and human *in vitro* tissue systems, facilitating major improvements evaluating the safety and health risks of novel consumer products. Innovation in molecular and cellular biology has shifted testing paradigms, with less reliance on low-throughput animal data and greater use of medium- and high-throughput *in vitro* cellular screening approaches. These new approach methodologies (NAMs) are being implemented in other industry sectors for chemical testing, screening candidate drugs and prototype consumer products, driven by the need for reliable, human-relevant approaches. Routine toxicological methods are largely unchanged since development over 50 years ago, using high-doses and often employing *in vivo* testing. Several disadvantages are encountered conducting or extrapolating data from animal studies due to differences in metabolism or exposure. The last decade saw considerable advancement in the development of *in vitro* tools and capabilities, and the challenges of the next decade will be integrating these platforms into applied product testing and acceptance by regulatory bodies. Governmental and validation agencies have launched and applied frameworks and “roadmaps” to support agile validation and acceptance of NAMs. Next-generation tobacco and nicotine products (NGPs) have the potential to offer reduced risks to smokers compared to cigarettes. These include heated tobacco products (HTPs) that heat but do not burn tobacco; vapor products also termed electronic nicotine delivery systems (ENDS), that heat an e-liquid to produce an inhalable aerosol; oral smokeless tobacco products (e.g., Swedish-style snus) and tobacco-free oral nicotine pouches. With the increased availability of NGPs and the requirement of scientific studies to support regulatory approval, NAMs approaches can supplement the assessment of NGPs. This review explores how NAMs can be applied to assess NGPs, highlighting key considerations, including the use of appropriate *in vitro* model systems, deploying screening approaches for hazard identification, and the importance of test article characterization. The importance and opportunity for fit-for-purpose testing and method standardization are

discussed, highlighting the value of industry and cross-industry collaborations. Supporting the development of methods that are accepted by regulatory bodies could lead to the implementation of NAMs for tobacco and nicotine NGP testing.

KEYWORDS

new approach methodologies (NAM), organs on a chip (OoC), human 3D tissues, next-generation products (NGP), airway models, high-content analysis, adverse outcome pathway (AOP), dosimetry

1 Introduction

Toxicological risk assessment methods have remained largely unchanged for half a century, with the traditional default approach using high doses administered in animal studies, human exposure estimates, and the use of conservative assessment (uncertainty) factors or linear extrapolations to establish whether a given chemical exposure is deemed “safe” or “unsafe” based on human exposure as well as estimating levels of potential risk. Despite the implementation of some changes to animal testing protocols over the years, the results from new *in vitro* approaches are still judged against this process of extrapolating the adverse effects of high doses in animals to low-dose exposures in humans. Refinements to animal studies have come in the form of reducing numbers of animals or ultimately waiving certain *in vivo* tests completely (e.g., acute *in vivo* toxicity “6-pack” testing for oral, dermal, and inhalation acute lethality; eye and skin irritation; and skin sensitization) (Mansouri et al., 2021; Lee et al., 2022). This is consistent to the guiding principles (3Rs) for ethical use of animals in product testing and scientific research that has been introduced by Russel and Burch (Russell and Burch, 1959).

The 3Rs are:

- *Replacement* that seeks to use methods to avoid or replace the use of animals;
- *Reduction* using methods that allow researchers to obtain information using fewer numbers of animals in scientific studies; and
- *Refinement* using methods to reduce potential pain, suffering or distress, and enhance animal welfare.

These broadly accepted ethical principles are now embedded in the conduct of animal-based science in many countries. In 2004, the UK government funded the creation of the National Centre for Reduction Refinement and Replacement of Animals in Research (NC3Rs) with the goal that research trends do not lead to increased animal usage or suffering (Burden et al., 2015). In the U.S., the Toxic Substances Control Act (TSCA), as amended by the Chemical Safety for the 21st Century Act, directs the U.S. Environmental Protection Agency (EPA) to “reduce and replace, to the extent practicable and scientifically justified, the use of vertebrate animals in the testing of chemical substances or mixtures; and promote the development and timely incorporation of alternative test methods or strategies that do not require new vertebrate animal testing” (U.S. Environmental Protection Agency, 2023).

The challenges to use of animal models have arisen from several different applications of toxicology. Issues with animal models have been reported, including questioning the usefulness of current mouse models due to irreproducibility and poor recapitulation of

human conditions and highlighting the fact that almost no animal models are validated (Justice and Dhillon, 2016; Perlman, 2016). There is also difficulty in extrapolating high doses in animal studies to low doses in humans, with 22% of all the chemicals tested in high-dose *in vivo* carcinogenicity studies being positive for cancer (Ennever and Lave, 2003). During development, 30% of drugs in Phase 1 (first use in humans) fail due to unexpected side effects or lack of efficacy, but the overall failure rate is ~90% for drugs in Phase 1 clinical trials due to other causes such as low efficacy (Sun et al., 2022). In light of this issue, the U.S. National Academies of Science, Engineering, and Medicine (NASEM) were asked to radically rethink traditional toxicological testing methodology, based on the large numbers of chemicals already released into the environment (>10,000) that had no associated toxicological data and the potential time and cost required to implement animal tests. The primary goals for the report were: to provide as wide a coverage of chemicals, outcomes and life stages as possible; reduce the costs and time for testing; use fewer animals with less suffering; and develop more robust methods for environmental chemical assessment. It was further recommended that assays chosen should also reflect the large gains in science that have been made in the last decades such as the use of the omics technologies. The U.S. National Research Council (NRC) released a 2007 report entitled “Toxicity Testing in the 21st Century: A Vision and a Strategy” (TT21C) (National Research Council, 2007) that proposed an alternative assessment testing paradigm where virtually all routine toxicity testing would be conducted *in vitro* (in human cells or cell lines). The underlying concept was that high-throughput toxicity pathway assays could evaluate disruption in key cellular processes. Toxicological risk assessment based on results from such assays would help avoid significant perturbations of known key cellular pathways in exposed human populations. Instead, dose-response modeling of altered pathway functions could be organized based on computational systems biology models of the networks underlying each toxicity pathway (Andersen and Krewski, 2009). This concept of pathway-based approaches to risk assessment was expanded by the description of “Adverse Outcome Pathways” (AOPs). Now the challenges are translating the AOP/TT21C vision into practical tools that will be useful to those making safety decisions and determining how to provide new mechanistic data not normally reviewed by risk assessors.

Following the release of the 2007 NRC report, consortia, collaborations, and initiatives were adopted to apply TTC21 *in vitro* toxicological approaches. In the US, Toxicology in the 21st Century (Tox21) was formed as part of a federal agency consortium, bringing together the EPA, the National Toxicology Program at the National Institute of Environmental Health Science, National Institutes of Health’s National Center for Advancing Translational Sciences, and the Food and Drug Administration

(Thomas et al., 2019). The goal of this program set out to develop assays to measure the pathways that lead to adverse effects in humans and develop models that can predict toxicity by using robotic technology to screen tens of thousands of environmental chemicals. Phase 1 of Tox21 involved testing 2,800 chemicals in 50 *in vitro* assays, with Phase 2 covering a further 10,000 chemicals (Attene-Ramos et al., 2013). European initiatives were developed following the ban on testing of cosmetic ingredients that came in to force in Europe 2013 (76/768EEC) (Silva and Tamburic, 2022) and continued as part of the European Union's Horizon 2020 project (Vinken, 2020). Similar to U.S. approaches, they have goals of looking for alternative testing methods via the Safety Evaluation Ultimately Replacing Animal Testing (SEURAT) (Daston et al., 2015). More recently in 2018, the Interagency Coordinating Committee on the Validation of Alternative Methods (ICCVAM, 2018) released its roadmap for the evaluation and implementation of new approach methodologies (NAMs) to support agile validation of scientific data from TT21C-based methods to be accepted by regulatory agencies without going through full Organisation for Economic Cooperation and Development (OECD)-like validation that could take 20 years or more. At the same time, utilization of NAM approaches including extrapolating *in vitro* data to *in vivo* exposures in humans would require computational and pharmacokinetic models to predict human blood and tissue concentrations under specific exposure conditions. Unfortunately, the scientific tools needed to make these changes in toxicological risk assessment practices are still in various stages of development and qualification (ICCVAM, 2023).

Realizing this vision for the future of toxicity testing will require wide-ranging scientific discussion among stakeholders and regulators, with a potential education program to motivate a shift from animal-based toxicological tests toward an appropriate approach more firmly based on human biology. This review focuses on how such a paradigm could be applied for the evaluation of alternative next-generation tobacco and nicotine products (NGPs). The review explores how NAMs approaches can be used to assess NGPs, and will highlight key considerations, such as the use of appropriate *in vitro* model systems, the use of screening approaches for hazard identification, and test article characterization. Furthermore other considerations such as AOPs, acute versus repeated-exposures, and *in vitro* to *in vivo* extrapolation will be explored. The value of industry and cross-industry collaborations are discussed outlining the importance and opportunity for fit-for-purpose testing and method standardization. With the increased requirement of scientific studies to support regulatory approval of NGPs, use of NAMs approaches should be considered for the assessment of NGPs as part of a testing strategy.

2 Next-generation inhaled tobacco and nicotine products (NGPs)

Next-generation tobacco and nicotine products (NGPs) have evolved significantly over the last decade as adults who smoke seek less-harmful alternatives to conventional cigarettes. Increased global consumer uptake has driven innovation and development, which has led to greater product complexity. Toxicological risk assessment and the development of technical ingredient and product standards have enabled the development and maintenance of product quality

standards and product material and ingredient quality for responsible manufacturers (Simms et al., 2019). Inclusion and adaptation of *in vitro* testing strategies can play a critical role in supporting NGP assessment, especially of inhalable products in filling the data gap in potential inhalation toxicity. NGPs not only offer the consumer an alternative choice to smoking, but these products have been reported to typically contain fewer toxicants and in lower levels compared to cigarette smoke (Margham et al., 2016; Schaller et al., 2016; Forster et al., 2018; Lu et al., 2021), offering a significant opportunity to potentially reduce the health impact of cigarette smoking on a global scale (McNeill et al., 2018; McNeil et al., 2022). This paper primarily discusses the *in vitro* testing of inhalable NGPs such as heated tobacco products (HTPs) and vapor products (also known as electronic nicotine delivery system (ENDS) or e-cigarettes (e-cigs)). While other oral products (e.g., Swedish-style smokeless tobacco products (snus) and oral nicotine pouches (ONPs) (Back et al., 2023) are increasingly available, the focus of this review is on inhalable products, so ONPs are out of scope.

HTPs utilize a specifically designed tobacco rod for use in a corresponding device that consists of a heating element, a battery, and a microprocessor controller. For HTPs to yield emissions with drastically reduced levels of harmful and potentially harmful constituents (HPHCs) as compared to cigarette smoke, the heating element should only reach temperatures below those leading to combustion of the tobacco rod (Baker, 1981; Malt et al., 2021; Lang et al., 2023; Sussman et al., 2023). The chemical composition of the resulting aerosol is typically significantly simpler than traditional cigarette smoke, with on average 90%–95% reductions in HPHC levels (Schaller et al., 2016; Forster et al., 2018). ENDS consist of a battery that powers an atomizer (microprocessor and a heating system/coil) to aerosolize an e-liquid (typically containing vegetable glycerin, propylene glycol, to United States Pharmacopoeia (USP) or European Pharmacopoeia (EP) specifications, and food-grade flavors, with or without pharmaceutical-grade nicotine). Compared to cigarette smoke, ENDS aerosols are simpler, with studied ENDS manufactured to a high-quality standard reported to yield emissions with on average 95%–99% reductions in selected HPHCs depending on the analyte assessed (Margham et al., 2016; Lu et al., 2021).

With the increased availability of NGPs and the requirement for scientific studies to support regulatory approval, NAMs may be more suitable for the assessment of such products with less complex emissions than combustible cigarettes. Recently, a number of *in vitro* toxicological approaches evaluating NGPs compared to cigarette smoke have been applied and reported (see Table 1). The use of a wide variety of different NAMs assays indicating the reduced bioactivity of both HTP and ENDS aerosols indicates the reduced harm potential of these NGPs when compared to cigarettes. However, in order to be able to compare these products against cigarettes, the test materials must be consistently generated and characterized, allowing the resulting *in vitro* exposures to be translated to human-relevant exposures.

3 Test articles

The laboratory assessment of NGPs involves multiple test matrices evolved from classical cigarette smoke testing using

TABLE 1 Summary of alternative nicotine and tobacco product characteristics and *in vitro* approaches—Examples from the literature.

Product category	HTP	ENDS
Format	• Tobacco component, battery, and heating element	• E-liquid (propylene glycol, vegetable glycerin, ± nicotine, flavorings), battery, and heating element
Consumption method	• Aerosol	• Aerosol
Chemical profile Average % reductions compared to a References cigarette	• 90%–95% (Schaller et al., 2016; Forster et al., 2018)	• 95%–99% (Margham et al., 2016)
Examples of <i>in vitro</i> data	• Significant reductions in cytotoxicity, genotoxicity, and mutagenicity (Schaller et al., 2016; Jaunky et al., 2018; Takahashi et al., 2018; Thorne et al., 2018; Ito et al., 2019; Hashizume et al., 2023) • No observed increases in tumor promotion (Crooks et al., 2018) • No impairment of endothelial cell migration and reduced effect on monocyte-endothelial cell adhesion (Poussin et al., 2016; Bishop et al., 2020) • High-content screening showed favorable differences in responses compared to cigarettes (Gonzalez-Suarez et al., 2016; Taylor et al., 2018)	• Significant reductions in cytotoxicity, genotoxicity, and mutagenicity (Thorne et al., 2016; Czekala et al., 2021; Bishop et al., 2023; Caruso et al., 2023) • No impairment of endothelial cell migration (Taylor et al., 2017) • High-content screening showed favorable differences in responses compared to cigarettes (Czekala et al., 2019)

TABLE 2 Summary of NGP test matrices.

Test matrix	Test matrix description	Predominant fraction assessed	HTP	ENDS
ACM	Aerosol collected on a filter pad and eluted with a solvent. This approach is comparable to the generation of TPM. Traditionally used in genotoxicity testing	Particulate	X	X
Aqueous extracts* (inc. GVP partitioning)	Aerosol bubbled through an impinger to extract soluble fractions. Has been referred to as conditioned media or bubbled extracts. Traditionally used in cytotoxicity/mechanistic-based research. The particulate can be filtered, leaving just the vapor fraction	Soluble constituents (focused on vapor phase solubility using GVP)	X	X
ACM* (TPM) + GVP	Particulate matter captured and prepared and eluted using a solvent. The GVP is also captured in a bubbled aqueous solution and both fractions are recombined to create an aerosol proxy. Has been extensively used for cigarette smoke assessment, with information on NGPs recently coming online	Particulate and vapor combined in a 1:1 ratio	X	X
Whole aerosol (incl. GVP partitioning)	Freshly generated whole aerosol (or GVP based on particulate exclusion) using an <i>in vitro</i> aerosol-generating and exposure system	Complete aerosol (focused on vapor phase solubility using GVP)	X	X

ACM, aerosol collected mass; GVP, gas vapor phase; TPM, total particulate matter.

X, denotes test article has been used for *in vitro* assessments.

*Can also trap non-aqueous gas phase depending on the choice of solvent.

Health Canada methods to capture the various smoke fractions (Health Canada, 2024). While the test articles should most appropriately mimic the mechanism by which humans are exposed, this is not always technically feasible. The following test articles have been utilized for the assessment of NGPs: 1) aerosol captured mass (ACM), which is equivalent to classical total particulate matter (TPM) capture approaches; 2) gas vapor phase (GVP), which involves filtering the particulate material from the test article, leaving predominately the vapor phase constituents; 3) aqueous trapping approaches, where the aqueous soluble components of the aerosol are captured in an aqueous trap; 4) ACM + GVP, a combination designed to be a proxy for whole aerosol approaches by individually capturing the various phases and recombining into a single test article; and 5) whole aerosol exposure, which often requires specialized equipment to expose cells to freshly

generated aerosol and maintain them at an exposure interface (Moore et al., 2023).

Whole aerosol approaches are designed to more appropriately capture the chemical-to-chemical interactions in the various phases of the aerosol and human exposures. When combined with complex co-culture or 3D human constructs, it represents the most physiologically advanced system achievable *in vitro* (Lacroix et al., 2018). However, not all assays are compatible with aerosol-generating systems (Thorne et al., 2020), and not all laboratories have the capacity to conduct aerosol-based studies. Comprehensive reviews have been published detailing the use of *in vitro* aerosolization systems and their applications (Thorne and Adamson, 2013; Klus et al., 2016; Li, 2016; Rudd et al., 2020; Cao et al., 2021; Thorne et al., 2021).

Capturing the particulate phase is a traditional, well-documented approach for cigarette smoke *in vitro* assessment

(Baker et al., 2004) and has been used to assess the ACM of HTPs and ENDS (see Table 2), (Misra et al., 2014; Schaller et al., 2016; Takahashi et al., 2018; Thorne et al., 2018; Thorne et al., 2019a; Thorne et al., 2019b; Iskandar et al., 2019; Miller-Holt et al., 2023). Aqueous extracts were previously used, but typically for mechanistic studies. These are also well characterized and utilized, but they are limited to the soluble fraction of the aerosol and may preferentially filter for the vapor phase constituents rather than particulates based on solubility (Bozhilova et al., 2020; Taylor et al., 2020). More recently, TPM + GVP has been used as a whole aerosol “proxy” for those occasions where the assay is not compatible with whole-aerosol methodologies or where aerosols are not standardized or available. Such approaches can capture both fractions in a 1:1 ratio and deliver more than just the particulate fraction to the cell cultures (Crooks et al., 2022). More information is available in more detail in a recent aerosol collection methods review (Smart and Phillips, 2021).

3.1 Dosimetry

A major challenge in evaluating inhalation toxicity is accurate determination of the delivered dose. In humans, breathing is a complex physical process (inhalation-pause-exhalation), and the complex anatomy of the respiratory tract makes it challenging to estimate the delivered doses to the cell surface (Alexander et al., 2008). After a substance is inhaled and deposited in the lung, particles can dissolve and absorb into the systemic/pulmonary circulation. Others are cleared from the lung by pulmonary metabolism or alveolar macrophages, and those deposited higher up in the respiratory tract are removed by mucociliary clearance (Clara et al., 2023).

The exact application of dosimetry measurements also largely depends on the exposure system being used, which should be selected based on the deposition and interaction of particles and vapors at the cell surface. Characterization of the exposure system is key to understanding the delivery of smoke/aerosol to the cell surface (Miller-Holt et al., 2023; Wiczkorek et al., 2023). Ideally, dosimetry is the measure of the internal dose, or even the concentration at the molecular target (biologically effective dose) within the target cells for the chemicals of interest (Paustenbach, 2000; Escher and Hermens, 2004; Proença et al., 2021). However, directly measuring cellular dose in submerged cultures poses a significant obstacle to the application of target tissue dosimetry. For example, for nanoparticles and microparticle toxicity assessment, particularly for *in vitro* systems, due to nanoparticle agglomeration in liquids, which can alter the density of the nano particles has the ability to alter the particle transport and deposition, ultimately altering the dose response relationship (Hinderliter et al., 2010; Watson et al., 2016; Deloid et al., 2017; Thomas et al., 2018). As a consequence, the target tissue paradigm for dosimetry and hazard assessment for nanoparticles has largely been ignored in favor of using alternative indirect methods of potential or surrogate exposure such as μg particle/mL culture medium, particle surface area/mL, or particle number/mL for submerged cultures (Hinderliter et al., 2010).

Air-liquid interface (ALI) exposure is the most physiologically relevant approach to accurately determine both the dose deposited on the cell surface and the dose ultimately available to be absorbed

by the cells. The most common methods are deposition of mass onto quartz crystal microbalance and the use of particle counters, photometers, or specialized gas analyzers. For a recent review of recommendations for conducting dosimetry studies in inhalable tobacco products please see the review by Miller-Holt and colleagues (Miller-Holt et al., 2023).

4 *In Vitro* model systems and high-content analysis

Animal experiments are being strongly scrutinized or entirely replaced (e.g., in the case of the cosmetics industry in certain countries) to respect the guiding principles of the 3Rs to “Replace, Reduce, Refine” in animal testing (Russell and Burch, 1959; van Meer et al., 2015). It is important that 21st Century Toxicity testing provide sufficient data that can be used for read-across purposes and ultimately to reduce animal experiments (Settivari et al., 2015). Traditional *in vitro* toxicity testing is often based on simple, single endpoints that quantify the global impact of toxicants on cells by determining increased cell permeability or reduced cell viability. However, these endpoints do not provide information on the underlying toxicological mechanism. Technological advances have facilitated the development of a series of high-content screening (HCS) *in vitro* technologies that offer a wide range of toxicological endpoints, thus increasing predictive value and complementary readouts to current regulatory toxicity testing. The goal of HCS is to provide more mechanistic information faster than traditional approaches, giving more flexibility to assess the growing diverse product landscape in a time and cost-effective manner. In general, the approaches listed below are in line with Tox21 goals (National Research Council, 2007), offering key advantages over traditional toxicity testing. Some of these NAMs have tradeoffs, but all have increased throughput, added mechanistic value, greater human and/or biological relevance, and multiplexing opportunities to maximize tissue and increase information gained. Furthermore, they provide mechanistic insights could also be used to inform AOPs (Wheeldon et al., 2020). Additionally, prior to selecting the appropriate *in vitro* models, there are a series of question(s) to be first addressed—for example, Figure 1 lists key questions in designing inhalation *in vitro* testing (Lee et al., 2022; Sharma et al., 2023).

The following summary highlights the strengths and weaknesses of *in vitro* alternatives to animal testing for inhaled toxicants relevant to tobacco and nicotine products. In particular the focus will be on screening approaches such as HCS, ToxTracker™ and MultiFlow® and respiratory *in vitro* models including 2D and 3D approaches, use of *ex vivo* models and organs-on-a-chip (OoC).

4.1 High-content screening (HCS)

HCS enables investigative toxicity testing *in vitro* to provide knowledge about the affected biologic processes and functions. It generally refers to automated (high-throughput) microscopy, multi-parameter image processing, and visualization to extract quantitative data from cells growing in multi-well cell culture plates. HCS typically uses fluorescent imaging to trace the effect



FIGURE 1

Main considerations when selecting an *in vitro* model. Reproduced with permission from Lee et al. (2022), Sharma et al. (2023). Note: 1) Test chemical and its physicochemical properties, 2) *In vitro* exposure system and aerosol characterization, 3) *In vitro* 2D/3D systems including 2D/3D, 4) cellular types and relevant tissues, and 5) assay endpoints and clinical relevance.

of chemicals on different toxicity pathways including oxidative stress, apoptotic cell death, DNA damage, and mitochondrial health and can be performed in a multiplexed fashion (Gonzalez-Suarez et al., 2016; Taylor et al., 2018; Czekala et al., 2019). In addition, HCS allows morphometric analysis for evaluating toxicant-induced effects on the morphology or size of cells and organelles. All these analyses can be performed with fixed cells or in a time-resolved mode by using live-cell imaging. HCS is also commonly used to monitor spatial (re)distribution of target molecules inside cells, which is pertinent to transcriptional activation following cell stress and inflammatory challenges (Czekala et al., 2019). Similar to flow cytometry, HCS enables information to be collected for multiple endpoints at an individual cell level or from an entire cell population, allowing analysis of dynamic ranges across treated cells in culture.

HCS methodologies are continuously expanding; they are now being applied to two-dimensional (2D) culture systems and three-dimensional (3D) organotypic tissue culture models (Booij et al., 2019). Artificial intelligence adds another level to HCS by allowing predictive *in vitro* toxicology analysis of new chemicals (Su et al., 2016; Lee et al., 2018).

HCS is generally perceived as a powerful *in vitro* screening technology for assessing the toxicity and efficacy of chemicals. There are also several associated limitations, especially as the technology is routinely used for screening cells growing in a 2D format:

- Lack of standardization
- Unavailability of specific tracer molecules or antibodies to stain and quantify targets of interest
- Increased data storage requirements
- Lower sensitivity than other quantitative methods (e.g., quantitative polymerase chain reaction)
- Limited applications for 3D image analysis
- Autofluorescence of test items (e.g., TPM) from cigarette smoke
- HCS of 3D organotypic ALI cultures is technically more demanding than for standard 2D culture systems
- Limited markers (e.g., cytotoxicity and H2AX for genotoxicity) have been demonstrated with whole aerosol approaches, but focusing and imaging the ALI can be problematic

Several groups have employed HCS to assess the biological impact of NGP aerosol fractions (Gonzalez-Suarez et al., 2016;

Taylor et al., 2018; Czekala et al., 2019). All of these studies demonstrated the utility of HCS as a tool for NGP product assessment. They also provided *in vitro* evidence for reduced biological impacts of fractions generated from HTPs and other nicotine-containing products compared to those of cigarette smoke fractions. Moreover, complementary test methods, such as those sensitive for oxidative stress toxicity pathways (gene-expression analysis or reporter-gene assays), confirmed the trends observed by HCS. Once qualified, HCS may be applied as a standard platform for modern toxicologic analysis of NGPs.

4.2 ToxTracker™

ToxTracker™ (Toxys, Oegstgeest, the Netherlands) is a high-content assay that employs a series of mouse embryonic stem cell reporter gene cell-lines (Czekala et al., 2021). It consists of six green fluorescent protein (GFP) reporter gene lines plus a control wild-type line, providing readouts on biomarkers for oxidative stress (Srxn1 Nrf2 dependent and Blvr2 Nrf2 independent), DNA damage (Bsc1 and Rtnk), cell stress (Btg2), and protein damage/misfolding (Ddit3). ToxTracker has been qualified against >450 known compounds and possesses ≥95% sensitivity and selectivity for both the Ames and *in vivo* micronucleus assays for mutagenicity and genotoxicity, respectively (Hendriks et al., 2016). ToxTracker could prove particularly valuable as it exhibits good/excellent concordance with classical genotoxicity testing and also offers mechanistic data on mode of action. Accordingly, ToxTracker can be a potential screening tool and/or a follow-up assay to identify mode of action in a positive *in vitro* response.

Several caveats exist for the application of ToxTracker:

- Although excellent concordance has been shown with classical toxicological approaches, the assay utilizes a mouse (not human) embryonic cell line
- As the assay is based on GFP expression, there are autofluorescence issues when using TPM from cigarette smoke (Johnson et al., 2009)
- It has not yet been combined or demonstrated to be applicable to whole aerosol approaches
- The assay is currently undergoing OECD validation, and there are few data on its use with NGPs

- Limited information exists on the assays ability to deal with complex mixtures where multiple direct and indirect acting chemicals are at play

4.3 MultiFlow®

The *in vitro* MultiFlow® (Litron Laboratories, Rochester, NY, USA) genotoxicity flow cytometric assay multiplexes several biomarkers that are responsive to diverse forms of DNA damage. The multiplexed biomarkers include: 1) phosphorylation of H2AX at serine 139 to detect double-strand DNA breaks, 2) phosphorylation of histone H3 at serine 10 to identify mitotic cells, 3) nuclear p53 content as an indicator of p53 activation, 4) frequency of 8n + cells to monitor polyploidization, and 5) relative nuclei counts to provide information about treatment-related cytotoxicity (Bryce et al., 2016; Bryce et al., 2017; Dertinger et al., 2019). Some multiplexing adaptations to the methodology have been described for a more integrated genotoxicological approach, such as the combination of the MultiFlow® with a flow-based *in vitro* micronucleus assays (Smart et al., 2020). The MultiFlow assay has also undergone significant inter-laboratory comparisons (Bryce et al., 2017). Eighty-four chemicals split between aneugen, clastogen, and nongenotoxin groups were collectively compared and cross-analyzed to determine inter-laboratory assay variability. Compared to historical mode of actions for the three class of chemicals, the MultiFlow assay demonstrated ≥92% sensitivity, specificity, and concordance. As a result, an excellent “training” list and established data are available to cross-reference results (Bryce et al., 2017).

Some limitations of MultiFlow include:

- The variability observed in the biomarker endpoints could confound result interpretation in less experienced laboratories. Analyzing multiplexed data requires careful interpretation and consideration.
- It has not been combined or demonstrated to be applicable to whole aerosol approaches
- Limited information exists on the assays ability to deal with mixtures where multiple direct and indirect acting chemicals are at play.

4.4 In Vitro airway models

Common *in vitro* models for studying the biological impact of inhaled toxicants on human airway epithelial cells are based on 2D cell culture systems. Tumor cell lines and immortalized primary epithelial cells (Calu-3, BEAS-2B, 16HBE14o-, NCI-H292, NCI-H441, RERF-LC-AI, and A549) grown in submerged (2D) culture conditions have been frequently used; however, they do not accurately recapitulate the native airway epithelia (Gordon et al., 2015). Although most of them can also be grown at the ALI (Haswell et al., 2010), drawbacks of using these epithelial cell lines for *in vitro* toxicity studies include their limited metabolic competency that might affect their responsiveness to toxic stimuli (Garcia-Canton et al., 2013), the absence or reduced formation of tight junctions, and their refractoriness to differentiation (Stewart et al., 2012). Non-differentiated primary epithelial cells grown in submerged conditions do not fully reflect native airway epithelia because

they either lack the polarized morphology and expression of markers (ion channels) normally found in airway epithelia (Kunzelmann et al., 1996) or show altered responsiveness to solid-particle exposure relative to differentiated primary epithelial cells (Ghio et al., 2013). Due to technical convenience (propagation and possibility for higher throughput), 2D culture systems based on cell lines are most suited for screening purposes to investigate the toxicity of a greater number of test items. Transformation techniques based on hTERT/Cdk4 allowed the generation of immortalized cell lines from primary lung epithelial cells that can differentiate into mucin-producing and ciliated airway models that more closely resemble the lung epithelium (Vaughan et al., 2006).

Reconstituted 3D organotypic culture systems from primary epithelial cells grown at the ALI (Nichols et al., 2013) also replicate the cellular complexity of pseudostratified epithelium found in human airways, containing ciliated/non-ciliated epithelial cells as well as basal (progenitor) cells (Gray et al., 1996; Prytherch et al., 2011). Furthermore, they closely mimic epithelial functionality by means of cilia beating, apical mucus secretion, ion channel expression, and the presence of tight junctions (Berube et al., 2009). These models also match the metabolic competency of the native tissue (Iskandar et al., 2013) and are amenable to whole aerosol exposure. The last characteristic can make an important difference regarding the potential underestimation of the biological impact of complex mixtures such as cigarette smoke, because frequently used smoke extracts such as TPM or GVP do not contain the totality of cigarette smoke constituents.

Three-dimensional epithelial cells from different zones of the human aerodigestive tract are commercially available as ready-to-use ALI cultures under brand names such as EpiAirway™ (MatTek Corporation, Ashland, MA, USA) MucilAir™, and SmallAir™ (both from Epithelix Sàrl, Geneva, Switzerland). They can be cultured for weeks to months and may be used for repeated (chronic) exposure (Czekala et al., 2021). The primary alveolar test model systems is increasing in use and commercial availability, with models currently available from suppliers such as Epithelix, ImmuONE (Hatfield, UK), and Invitorize (Belvaux, Luxembourg). The use of these models is relatively new and beyond the scope of this paper.

Even though 3D organotypic cell cultures closely resemble the native tissue, they usually lack the cellular components of the immune system. More complex model systems have been evaluated as potential candidates for routine aerosol testing (Lehmann et al., 2011; Klein et al., 2013; Marescotti et al., 2019). They use ALI conditions and combine immune cells from the innate immune system or fibroblasts with epithelial cell layers. Attempts to produce functional airway epithelial model systems originating from pluripotent stem cells are also promising and might provide additional mechanistic understanding of aerosol-induced toxicity while also allowing the generation of *in vitro* models from specific patient populations (Wong et al., 2015). No single *in vitro* model can answer every study question, so a pragmatic approach should be tailored depending upon the exact hypotheses.

4.5 Ex Vivo models and organ(s)-on-a-chip

The use of precision-cut lung slices (Behrsing et al., 2013; Sewald and Braun, 2013) and lung-on-chip model systems (Huh et al., 2010;

TABLE 3 Summary of major advantages/challenges of OoC and MOC models.

Advantages of OoC- and MOC-based <i>in vitro</i> models
More physiologically relevant, as the phenotype and functionality of used 3D organotypic model systems more closely resemble the human tissue counterparts
<ul style="list-style-type: none">• Organ-to-organ cross-talk (MOC)
<ul style="list-style-type: none">• Mechanical forces mimicking blood flow or breathing create more physiological conditions. For instance, endothelial barrier formation is promoted upon shear stress [Buchanan et al. (2014); Ohashi et al. (2023)]
<ul style="list-style-type: none">• Allow <i>in vitro</i> investigation of ADME
<ul style="list-style-type: none">• Compound metabolism by a liver surrogate in the chip can be analyzed, as can its systemic toxicity/efficacy on different organs (MOC)
<ul style="list-style-type: none">• Support PBPK modeling
Challenges of OoC- and MOC-based <i>in vitro</i> models
Stability of organ models in the chip
<ul style="list-style-type: none">• Co-culture medium and material compatibility
<ul style="list-style-type: none">• Technical challenges such as contamination and air-bubble trapping
<ul style="list-style-type: none">• OoC and MOC properties depend mainly on the source of the cells used to create the model (e.g., primary cells versus iPSCs or multiple cell types in one model)
<ul style="list-style-type: none">• No model standardization (standard protocols to produce, load, and culture the chips, as well as qualification of OoC and MOC functionality)
<ul style="list-style-type: none">• Scaling of components (e.g., medium volume or number of cells) might not fully reflect the <i>in vivo</i> counterpart, which could lead to inaccurate PBPK
<ul style="list-style-type: none">• Adsorption of test compounds to chip surfaces (common issue with PDMS-based chips)
<ul style="list-style-type: none">• Most OoC and MOC platforms provide only low-throughput capacity
<ul style="list-style-type: none">• Only a few systems designed for whole aerosol exposure of lung models on the chip
<ul style="list-style-type: none">• High cost

ADME, absorption, distribution, metabolism, and excretion; iPSC, induced pluripotent stem cell; MOC, multi organ on a chip; OoC, organ on a chip; PBPK, physiologically based pharmacokinetic; PDMS, polydimethylsiloxane.

Stucki et al., 2015) resembling additional aspects of the human respiratory tract provide opportunities for characterizing aerosol-induced toxicity *in vitro*, with an even greater relevance to native tissue and the possibility to emulate pharmacokinetics. Other approaches include using co-cultures of various organ cell types as a cell-based disease screening model (BioMap®) to screen drugs and NGPs for potential adverse effects (Simms et al., 2021).

In vitro organ models have received considerable attention in the attempt to reduce animal experiments and decrease the rate of preclinical failure associated with drug development. Two major advances in the *in vitro* research field are helping address the weaknesses of the simple models used in the past, rendering them more physiologically relevant and predictive for the effects of compounds in humans: 1) simple 2D cell culture systems are increasingly replaced by organotypic culture systems with 3D architecture, and 2) static culture systems have been switched to dynamic exposure models. The merging of these two developments has culminated in OoC technology, which combines 3D organotypic culture systems (organs) with microfluidic devices (Alepee et al., 2014; Bovard et al., 2017).

Microfluidics enable interconnection of different organ models on the same chip platform by circulating culture medium from a common reservoir. These multi-organ-on-a-chip (MOC) devices permit organ-to-organ crosstalk, which allows compounds to be tested in a more *in vivo*-like environment (Rogal et al., 2017). To date, long-term, MOC-based co-cultures of different organ

combinations have been established for liver spheroids with human 3D lungs (Bovard et al., 2018) or intestine (Maschmeyer et al., 2015a), neuronal (Materne et al., 2015) and pancreatic islet (Bauer et al., 2017) tissue models, as well as a skin–intestine–liver kidney chip (Maschmeyer et al., 2015b). At least two reported OoC systems have been designed for whole aerosol exposure of 3D lung models (Benam et al., 2016; Stucki et al., 2018). However, these platforms are not compatible with smoking machines or the *in vitro* exposure instruments commonly used in the tobacco industry.

Current OoC or MOC models have potentially improved the human relevance of *in vitro* assessment of chemicals (see Table 3 for systems strengths and challenges). While there are demonstrated examples in drug candidate profiling and investigative toxicology, their application for NGPs is currently in its infancy.

In summary, there are a number of established alternative *in vitro* models to animal testing that are more sophisticated than simple cell lines and suitable for investigating the biological impact of inhaled toxicants in an environment more relevant to human exposure. However, model validation remains important for ensuring acceptance by regulatory bodies. Additionally, inter-donor differences are difficult to capture in *in vitro* aerosol exposure studies, particularly with 3D organotypic ALI exposure, which is usually not sufficiently scalable to test a variety of donors (Mori et al., 2022). The development of a relevant human lung tissue model is of ultimate importance for

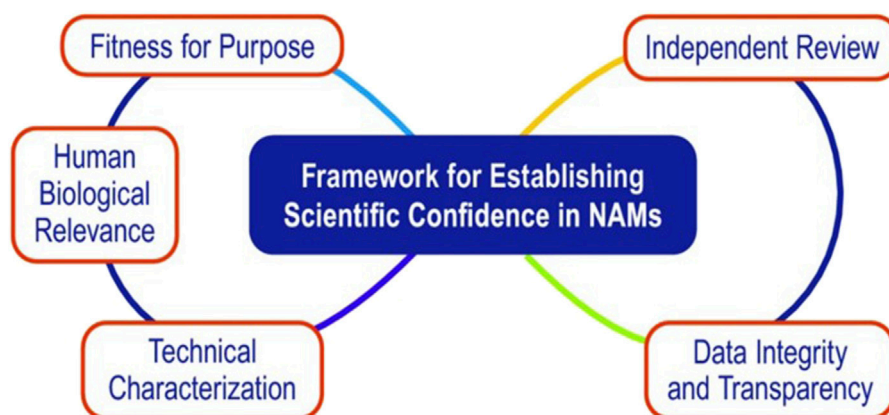


FIGURE 2

Key considerations in developing and qualifying NAM tools. Reproduced with permission from [van der Zalm et al. \(2022\)](#). Note: the figures illustrates the five inter-connected elements that are essential in establishing scientific confidence in NAM applications.

method standardization; the *in vitro* model must have high reproducibility and clinical relevance for inhalation toxicity assessment. However, constructing an *in vitro* lung tissue model derived from human cells currently remains challenging due to the inherent complexity of the human lung and the number of different cell types involved ([Petpiroon et al., 2023](#)).

5 Other considerations

5.1 Use of adverse outcome pathways (AOPs)

An AOP is defined as “an analytical construct that describes a sequential chain of causally linked events at different levels of biological organization that leads to an adverse health or ecotoxicological effect” as defined by the OECD ([OECD, 2023](#)). AOPs are used to help to organize the available mechanistic information relating to an adverse outcome into the key events (KEs) that are required for the adverse outcome, spanning all organizational levels of a biological system(s) ([Lowe et al., 2017](#); [Luettich et al., 2017](#)). Key event relationships (KERs) define the relationship between a pair of KEs by showing which is up-/downstream and are supported by both biological plausibility and empirical evidence ([Villeneuve et al., 2014](#)). The use of AOPs to organize information into AOP networks has the potential to improve the use of mechanistic data and lead to improved regulatory decision making ([Villeneuve et al., 2014](#)). In this way, the use of AOPs can greatly improve the biological understanding of a particular disease process through a simplified series of events. The critical element is causality as the AOP moves from 1 KE to another (i.e., KE 1 always occurs before KE 2, etc.). AOPs can also help link biological exposures to the eventual toxic effects at the population level.

In terms of regulatory context, knowledge of disease mechanisms can guide the design of testing strategies using *in vitro* methods that can measure or predict KEs relevant to the biological effect of interest. AOPs are not chemical specific, but they link the molecular initiating event (MIE) for a chemical to the apical end point, which is the observable outcome in the whole organism and typically a clinical sign or pathological state

([Burden et al., 2015](#)). The well-considered use of AOPs could drive positive changes in toxicology testing, moving toward less reliance on making predictions based on animal models and focusing on the measurement of apical toxicity endpoints ([Burden et al., 2015](#)).

5.2 Acute vs repeated exposure

The vast majority of *in vitro* toxicity testing is restricted to one-time (acute) treatment of cells with a test item for a relatively short exposure duration (hours to a few days) before endpoint measurement. Such tests include escalation of the dose to a point where toxic (adverse) effects are either visible at the morphological level or quantifiable by standard cytotoxicity (viability) tests. While dose–response analyses in cell-based assays to determine acute effects on cell cultures are commonly used to rank the toxicity of different chemicals, they have several limitations: 1) the doses for inducing adverse effects are often selected based on potential toxicity hazard that are not relevant for human exposure levels (environmental or use levels); 2) therefore, the toxicity mechanisms observed *in vitro*, especially after high dosing for eliciting acute toxicity in cell-based assays also may not reflect relevant mechanisms in humans; and 3) they cannot fully predict the effects of subtoxic concentrations of a chemical when administered repeatedly ([Ito et al., 2020](#); [Czekala et al., 2021](#); [Chapman et al., 2023](#)). The latter is pertinent, as smoking-related diseases such as chronic obstructive pulmonary disease or cardiovascular diseases only manifest after chronic exposure to cigarette smoke ([Yoshida and Tuder, 2007](#); [Luettich et al., 2021](#); [Farcher et al., 2023](#)). Chronic exposure may also result in distinct adverse effects not seen after acute exposure or cause adaptive responses that are not detectable following a single treatment. Adaptations often invoke compensatory repair mechanisms elicited upon chronic stress. These considerations are also relevant for testing inhalable toxicants *in vitro* and are reflected in a number of published studies on assessing NGPs through repeated exposure of cells, as discussed below.

5.2.1 Repeated exposure of lung epithelial cells to aerosol or smoke fractions

Long-term (repeated) exposure to subtoxic concentrations of cigarette smoke condensate (CSC) or total particulate matter (TPM) from 3R4F reference cigarettes for up to 12 weeks has been reported to induce an epithelial to mesenchymal transition-like phenotype in BEAS-2B cells, along with anchorage-independent growth of the cells and transient effects on both oxidative stress and DNA damage (Veljkovic et al., 2011; van der Toorn et al., 2018). These effects are only visible when cells are exposed to a much higher concentration of ACM from an NGP. Another study evaluating the short- and long-term effects of TPM on mitochondrial function in BEAS-2B cells (Malinska et al., 2018) revealed a short-term decrease in mitochondrial respiration rate after 1 week of repeated exposure, accompanied by an increase in oxidative stress markers upon 3R4F TPM treatment and cellular adaptation to stress after repeated exposure for 12 weeks. In case of ACM from a NGP, the concentrations required to elicit these effects were again much higher than those derived from reference cigarettes. A similar study on the effects of prolonged exposure to 3R4F cigarette smoke extract (CSE) on BEAS-2B cells reported increased mitochondrial capacity (Hoffmann et al., 2013). These contradictory results may be explained by the different smoke extract used, as well as the applied dose and overall duration of exposure. In a different study, the long-term effects of 1–16 weeks of exposure to nicotine or CSE from 3R4F has been analyzed in BEAS-2B cells (Stabile et al., 2018). In this repeated exposure study, distinct effects of CSE *versus* pure nicotine were observed when analyzing cell viability and other cellular parameters, including nerve growth factor/receptor gene expression.

Repeated exposure experiments were also extended to differentiated primary human bronchial epithelial organotypic cell cultures, which showed cumulative effects on inflammatory responses and tissue morphology after 1-month repeated exposure to 3R4F TPM (Ito et al., 2018). Interestingly, repeated exposure of bronchial epithelial organotypic cells to 3R4F CSE or TPM during the differentiating phase of the culture had profound effects on cell composition when measured after 28 days; although the number of ciliated cells decreased, those of Clara and goblet cells increased (Haswell et al., 2010; Schamberger et al., 2015).

5.2.2 Repeated exposure of lung epithelial cells to whole aerosols

Several studies evaluated the short-to-long-term effects of subtoxic concentrations of whole cigarette smoke on 3D organotypic ALI tissue cultures reconstituted from human primary epithelial cells, which were tested as either mono- or co-cultures with fibroblasts. The authors reported transition of normal bronchial epithelia towards a metaplastic phenotype and fewer cilia-bearing cells after repeated exposure (4–13 times) to mainstream 3R4F smoke (Aufderheide et al., 2015; Aufderheide et al., 2017). This suggests that the effect on cilia is caused by volatile organic constituents present in mainstream smoke. Similarly, reductions of ciliated, mucus-producing, and club cells were observed when differentiated immortalized primary normal human bronchial epithelial cells were repeatedly exposed to cigarette smoke or e-cigarette vapor (Aufderheide and Emura, 2017). In that study, metaplastic areas positively stained for the basal cell marker cytokeratin-13 were also identified after exposure to both

cigarette smoke and e-cigarette vapor. In a co-culture model with ‘omics’ analysis using human 3D bronchial tissue cultures combined with human fibroblasts, the central carbon metabolism in relation to oxidative stress response was perturbed after 21 days of repeated exposure to 3R4F whole smoke; additionally, the epidermal growth factor receptor was identified as a key regulator of perturbed processes (Ishikawa et al., 2019). Repeated exposure (21 days) of differentiating bronchial epithelial 3D organotypic cultures to 3R4F whole smoke, in contrast to repeated exposure to CSE, did not result in an increase in goblet cells (Ishikawa and Ito, 2017).

5.3 *In vitro*-to-*in vivo* extrapolation (IVIVE)

While *in vitro* experiments have many advantages over *in vivo* testing in terms of increased human relevance as presented above, using *in vitro* data for the purpose of risk assessment (e.g., quantifying the margin of safety) has many challenges, including uncertainty around how to interpret and link exposure or dose. Quantitative *in vitro*-to-*in vivo* extrapolation (IVIVE) is an emerging NAM-based computational tool to facilitate this process, generally referred as an extrapolation of (human tissue-derived) cellular (*in vitro*) data to predict the exposures or outcomes in humans (*in vivo*). IVIVE implies certain quantitative extrapolations of “dose (or exposure)” and “response” to enable *in vitro*-based toxicological risk assessment (Zhang et al., 2021; Hines et al., 2022; Zhang and Wright, 2022). Dose extrapolation is necessary to estimate the human exposure or intake level (e.g., daily human equivalent dose) of individual toxicants, commonly by computational (e.g., physiologically-based pharmacokinetic [PBPK]) models and *in silico* and/or human-based *in vitro* data. The human equivalent dose can be extrapolated back to the corresponding exposure levels (commonly called “reverse” dosimetry) and compared to measured (environmental) exposures to evaluate the safety margin or guide regulatory safety decision-making. Therefore, one may first define and characterize the *in silico* or *in vitro*-based dose–response relationship, and the relevance of the MIEs or KEs can be selected based on the AOPs of interest. Then, using the *in vitro* dosimetry and disease-relevant response data and with the help of computational modeling, IVIVE enables “human-relevant” safety assessment, moving away from a need for conventional animal toxicity data.

While the concept of IVIVE is gaining interest in scientific communities (Bell et al., 2018; Chang et al., 2021; Hines et al., 2022), it is still an emerging field with limited application to regulatory risk assessment, especially for tobacco and nicotine products. The early successes—mostly from pharmaceutical and environmental safety assessment—typically involve single chemicals, although concerted effort is being made to apply IVIVE to mixtures (Chang et al., 2021; Zhang et al., 2021; Zhang and Wright, 2022). Many of the challenges in using IVIVE for tobacco or nicotine products are similar, including uncertainty in dose selection and quantification (which individual toxicants should be modeled as is or as mixtures in the complex and dynamically unstable aerosol mixtures) and the target test systems (which cellular/tissue systems should be used to reflect what clinically relevant outcomes at cellular levels). Additionally, there is a lack of chemical or mixture-related *in vitro* data that can be used for IVIVE model development and the independent verification of modeling outcomes.

6 Summary

NAMs are gaining traction as chemical toxicity and biologically relevant assessment tools based on *in vitro* and *in silico* (computational) methodologies that support 3R *in vivo* animal testing traditionally necessary for risk assessment. Significant progress has been made toward the adoption of NAMs for human health and environmental toxicity assessment, although they are not yet fully embraced for routine use in regulatory decision making. This review summarized the current NAMs in use by major tobacco and nicotine product manufacturers. The NAMs were chosen in line with the concepts/criteria displayed in Figure 2, with a focus on the human relevance of NAMs and their potential ability to model and predict key elements of human disease processes.

As part of the effort to promote NAM applications for use in tobacco and nicotine products, two symposiums were held during the annual Cooperation Centre for Scientific Research Relative to Tobacco (CORESTA) Smoke Science and Product Technology conferences in 2021 and 2023 to introduce the concepts and potential application of NAMs for evaluating NGPs (Lee et al., 2022; Lee et al., 2023). Many of the promises are tangible based on successful case examples demonstrating that NAMs can be a pragmatic and effective approach in terms of cost, time, and resources, in addition to offering enhanced sensitivity for predicting human-relevant health impacts. At the same time, there are ample opportunities to increase confidence in NAM context of use and standardization. Finally, clarity on the degree of validation/qualification by regulatory bodies is required. This last point is essential before NAM-based risk assessments achieve full legitimacy for regulatory risk assessment.

Author contributions

DT: Conceptualization, Writing–original draft, Writing–review and editing. DM: Conceptualization, Writing–review and editing. LS: Conceptualization, Writing–review and editing. KL: Conceptualization, Writing–review and editing. HF: Writing–review and editing. SM: Conceptualization,

Writing–review and editing. MG: Conceptualization, Writing–original draft, Writing–review and editing.

Funding

The author(s) declare that financial support was received for the research, authorship, and/or publication of this article. All authors were employees of the respective companies in the affiliations and received a salary while working on this manuscript.

Acknowledgments

The authors would like to thank Stefan Frentzel and Gaddamnugu L Prasad for their inputs to an earlier draft version of the manuscript, Lindsay Reese who supported an editorial review, and the CORESTA Scientific Committee for their support and review.

Conflict of interest

Authors DT and MG were employed by BAT (Investments) Ltd. Author LS was employed by Imperial Brands. Author KL was employed by Altria Client Services LLC. Author HF was employed by Japan Tobacco Inc., R&D Group. Author DM was employed by Philip Morris International. Author SM was employed by Swedish Match.

Publisher's note

All claims expressed in this article are solely those of the authors and do not necessarily represent those of their affiliated organizations, or those of the publisher, the editors and the reviewers. Any product that may be evaluated in this article, or claim that may be made by its manufacturer, is not guaranteed or endorsed by the publisher.

References

- Alepee, N., Bahinski, A., Daneshian, M., De Wever, B., Fritsche, E., Goldberg, A., et al. (2014). State-of-the-art of 3D cultures (organs-on-a-chip) in safety testing and pathophysiology. *ALTEX* 31, 441–477. doi:10.14573/altex.1406111
- Alexander, D. J., Collins, C. J., Coombs, D. W., Gilkison, I. S., Hardy, C. J., Healey, G., et al. (2008). Association of Inhalation Toxicologists (AIT) working party recommendation for standard delivered dose calculation and expression in non-clinical aerosol inhalation toxicology studies with pharmaceuticals. *Inhal. Toxicol.* 20, 1179–1189. doi:10.1080/08958370802207318
- Andersen, M. E., and Krewski, D. (2009). Toxicity testing in the 21st century: bringing the vision to life. *Toxicol. Sci.* 107, 324–330. doi:10.1093/toxsci/kfn255
- Attene-Ramos, M. S., Miller, N., Huang, R., Michael, S., Itkin, M., Kavlock, R. J., et al. (2013). The Tox21 robotic platform for the assessment of environmental chemicals—from vision to reality. *Drug Discov. Today* 18, 716–723. doi:10.1016/j.drudis.2013.05.015
- Aufderheide, M., and Emura, M. (2017). Phenotypical changes in a differentiating immortalized bronchial epithelial cell line after exposure to mainstream cigarette smoke and e-cigarette vapor. *Exp. Toxicol. Pathol.* 69, 393–401. doi:10.1016/j.etp.2017.03.004
- Aufderheide, M., Ito, S., Ishikawa, S., and Emura, M. (2017). Metaplastic phenotype in human primary bronchiolar epithelial cells after repeated exposure to native mainstream smoke at the air-liquid interface. *Exp. Toxicol. Pathol.* 69, 307–315. doi:10.1016/j.etp.2017.01.015
- Aufderheide, M., Scheffler, S., Ito, S., Ishikawa, S., and Emura, M. (2015). Ciliotoxicity in human primary bronchiolar epithelial cells after repeated exposure at the air-liquid interface with native mainstream smoke of K3R4F cigarettes with and without charcoal filter. *Exp. Toxicol. Pathol.* 67, 407–411. doi:10.1016/j.etp.2015.04.006
- Back, S., Masser, A. E., Rutqvist, L. E., and Lindholm, J. (2023). Harmful and potentially harmful constituents (HPHCs) in two novel nicotine pouch products in comparison with regular smokeless tobacco products and pharmaceutical nicotine replacement therapy products (NRTs). *BMC Chem.* 17, 9. doi:10.1186/s13065-023-00918-1
- Baker, R. R. (1981). Product formation mechanisms inside a burning cigarette. *Prog. Energy Combust. Sci.* 7, 135–153. doi:10.1016/0360-1285(81)90008-3
- Baker, R. R., Massey, E. D., and Smith, G. (2004). An overview of the effects of tobacco ingredients on smoke chemistry and toxicity. *Food Chem. Toxicol.* 42, 53–83. doi:10.1016/j.fct.2004.01.001
- Bauer, S., Wennberg Hult, C., Kanebratt, K. P., Durieux, I., Gunne, D., Andersson, S., et al. (2017). Functional coupling of human pancreatic islets and liver spheroids on-a-chip: towards a novel human *ex vivo* type 2 diabetes model. *Sci. Rep.* 7, 14620. doi:10.1038/s41598-017-14815-w
- Behrsing, H. P., Furniss, M. J., Davis, M., Tomaszewski, J. E., and Parchment, R. E. (2013). *In vitro* exposure of precision-cut lung slices to 2-(4-amino-3-methylphenyl)-5-fluorobenzothiazole lysylamide dihydrochloride (NSC 710305, Phortress) increases

- inflammatory cytokine content and tissue damage. *Toxicol. Sci.* 131, 470–479. doi:10.1093/toxsci/kfs319
- Bell, S. M., Chang, X., Wambaugh, J. F., Allen, D. G., Bartels, M., Brouwer, K. L. R., et al. (2018). *In vitro* to *in vivo* extrapolation for high throughput prioritization and decision making. *Toxicol. Vitro* 47, 213–227. doi:10.1016/j.tiv.2017.11.016
- Benam, K. H., Villenave, R., Lucchesi, C., Varone, A., Hubeau, C., Lee, H. H., et al. (2016). Small airway-on-a-chip enables analysis of human lung inflammation and drug responses *in vitro*. *Nat. Methods* 13, 151–157. doi:10.1038/nmeth.3697
- Berube, K., Aufderheide, M., Breheny, D., Clothier, R., Combes, R., Duffin, R., et al. (2009). *In vitro* models of inhalation toxicity and disease. The report of a FRAME workshop. *Altern. Lab. Anim.* 37, 89–141.
- Bishop, E., Breheny, D., Hewitt, K., Taylor, M., Jaunky, T., Camacho, O. M., et al. (2020). Evaluation of a high-throughput *in vitro* endothelial cell migration assay for the assessment of nicotine and tobacco delivery products. *Toxicol. Lett.* 334, 110–116. doi:10.1016/j.toxlet.2020.07.011
- Bishop, E., East, N., Miazzi, F., Fiebelkorn, S., Breheny, D., Gaca, M., et al. (2023). A contextualised e-cigarette testing strategy shows flavourings do not impact lung toxicity *in vitro*. *Toxicol. Lett.* 380, 1–11. doi:10.1016/j.toxlet.2023.03.006
- Booij, T. H., Price, L. S., and Danen, E. H. J. (2019). 3D cell-based assays for drug screens: challenges in imaging, image analysis, and high-content analysis. *SLAS Discov.* 24, 615–627. doi:10.1177/2472555219830087
- Bovard, D., Iskandar, A., Luettich, K., Hoeng, J., and Peitsch, M. (2017). Organs-on-a-chip: new *in vitro* tools multi-organ-on-a-chip challenges, limitations, and future prospects for fluidic devices. *Toxicol. Res. Appl.* 1, 1–16. doi:10.1177/2397847317726351
- Bovard, D., Sandoz, A., Luettich, K., Frentzel, S., Iskandar, A., Marescotti, D., et al. (2018). A lung/liver-on-a-chip platform for acute and chronic toxicity studies. *Lab. Chip* 18, 3814–3829. doi:10.1039/c8lc01029c
- Bozhilova, S., Baxter, A., Bishop, E., Breheny, D., Thorne, D., Hodges, P., et al. (2020). Optimization of aqueous aerosol extract (AqE) generation from e-cigarettes and tobacco heating products for *in vitro* cytotoxicity testing. *Toxicol. Lett.* 335, 51–63. doi:10.1016/j.toxlet.2020.10.005
- Bryce, S. M., Bernacki, D. T., Bemis, J. C., and Dertinger, S. D. (2016). Genotoxic mode of action predictions from a multiplexed flow cytometric assay and a machine learning approach. *Environ. Mol. Mutagen.* 57, 171–189. doi:10.1002/em.21996
- Bryce, S. M., Bernacki, D. T., Bemis, J. C., Spellman, R. A., Engel, M. E., Schuler, M., et al. (2017). Interlaboratory evaluation of a multiplexed high information content *in vitro* genotoxicity assay. *Environ. Mol. Mutagen.* 58, 146–161. doi:10.1002/em.22083
- Buchanan, C. F., Verbridge, S. S., Vlachos, P. P., and Rylander, M. N. (2014). Flow shear stress regulates endothelial barrier function and expression of angiogenic factors in a 3D microfluidic tumor vascular model. *Cell. Adh. Migr.* 8, 517–524. doi:10.4161/19336918.2014.970001
- Burden, N., Sewell, F., Andersen, M. E., Boobis, A., Chipman, J. K., Cronin, M. T., et al. (2015). Adverse Outcome Pathways can drive non-animal approaches for safety assessment. *J. Appl. Toxicol.* 35, 971–975. doi:10.1002/jat.3165
- Cao, X., Coyle, J. P., Xiong, R., Wang, Y., Heflich, R. H., Ren, B., et al. (2021). Invited review: human air-liquid-interface organotypic airway tissue models derived from primary tracheobronchial epithelial cells—overview and perspectives. *Vitro Cell. Dev. Biol. Anim.* 57, 104–132. doi:10.1007/s11626-020-00517-7
- Caruso, M., Distefano, A., Emma, R., Zuccarello, P., Copat, C., Ferrante, M., et al. (2023). *In vitro* cytotoxicity profile of e-cigarette liquid samples on primary human bronchial epithelial cells. *Drug Test. Anal.* 15, 1145–1155. doi:10.1002/dta.3275
- Chang, X., Abedini, J., Bell, S., and Lee, K. M. (2021). Exploring *in vitro* to *in vivo* extrapolation for exposure and health impacts of e-cigarette flavor mixtures. *Toxicol. Vitro* 72, 105090. doi:10.1016/j.tiv.2021.105090
- Chapman, F., Pour, S. J., Wiecek, R., Trelles Sticken, E., Budde, J., Rower, K., et al. (2023). Twenty-eight day repeated exposure of human 3D bronchial epithelial model to heated tobacco aerosols indicates decreased toxicological responses compared to cigarette smoke. *Front. Toxicol.* 5, 1076752. doi:10.3389/ftox.2023.1076752
- Clara, P. C., Jerez, F. R., Ramirez, J. B., and Gonzalez, C. M. (2023). Deposition and clinical impact of inhaled particles in the lung. *Arch. Bronconeumol.* 59, 377–382. doi:10.1016/j.arbres.2023.01.016
- Crooks, I., Hollings, M., Leverette, R., Jordan, K., Breheny, D., Moore, M. M., et al. (2022). A comparison of cigarette smoke test matrices and their responsiveness in the mouse lymphoma assay: a case study. *Mutat. Res. Genet. Toxicol. Environ. Mutagen.* 879–880, 503502. doi:10.1016/j.mrgentox.2022.503502
- Crooks, I., Neilson, L., Scott, K., Reynolds, L., Oke, T., Forster, M., et al. (2018). Evaluation of flavourings potentially used in a heated tobacco product: chemical analysis, *in vitro* mutagenicity, genotoxicity, cytotoxicity and *in vitro* tumour promoting activity. *Food Chem. Toxicol.* 118, 940–952. doi:10.1016/j.fct.2018.05.058
- Czekala, L., Simms, L., Stevenson, M., Trelles-Sticken, E., Walker, P., and Walele, T. (2019). High Content Screening in NHBE cells shows significantly reduced biological activity of flavoured e-liquids, when compared to cigarette smoke condensate. *Toxicol. Vitro* 58, 86–96. doi:10.1016/j.tiv.2019.03.018
- Czekala, L., Wiecek, R., Simms, L., Yu, F., Budde, J., Trelles Sticken, E., et al. (2021). Multi-endpoint analysis of human 3D airway epithelium following repeated exposure to whole electronic vapor product aerosol or cigarette smoke. *Curr. Res. Toxicol.* 2, 99–115. doi:10.1016/j.crtox.2021.02.004
- Daston, G., Knight, D. J., Schwarz, M., Gocht, T., Thomas, R. S., Mahony, C., et al. (2015). SEURAT: safety evaluation ultimately replacing animal testing—recommendations for future research in the field of predictive toxicology. *Arch. Toxicol.* 89, 15–23. doi:10.1007/s00204-014-1421-5
- DeLoid, G., Cohen, J., Pyrgiotakis, G., and Demokritou, P. (2017). Preparation, characterization, and *in vitro* dosimetry of dispersed, engineered nanomaterials. *Nat. Protoc.* 12, 355–371. doi:10.1038/nprot.2016.172
- Dertinger, S. D., Kraynak, A. R., Wheeldon, R. P., Bernacki, D. T., Bryce, S. M., Hall, N., et al. (2019). Predictions of genotoxic potential, mode of action, molecular targets, and potency via a tiered multistage assay data analysis strategy. *Environ. Mol. Mutagen.* 60, 513–533. doi:10.1002/em.22274
- Ennever, F. K., and Lave, L. B. (2003). Implications of the lack of accuracy of the lifetime rodent bioassay for predicting human carcinogenicity. *Regul. Toxicol. Pharmacol.* 38, 52–57. doi:10.1016/s0273-2300(03)00068-0
- Escher, B. I., and Hermens, J. L. (2004). Internal exposure: linking bioavailability to effects. *Environ. Sci. Technol.* 38, 455A–462A. doi:10.1021/es0406740
- Farcher, R., Syleouni, M. E., Vinci, L., and Mattli, R. (2023). Burden of smoking on disease-specific mortality, DALYs, costs: the case of a high-income European country. *BMC Public Health* 23, 698. doi:10.1186/s12889-023-15535-9
- Forster, M., Fiebelkorn, S., Yurteri, C., Mariner, D., Liu, C., Wright, C., et al. (2018). Assessment of novel tobacco heating product THP1.0. Part 3: comprehensive chemical characterisation of harmful and potentially harmful aerosol emissions. *Regul. Toxicol. Pharmacol.* 93, 14–33. doi:10.1016/j.yrtph.2017.10.006
- Garcia-Canton, C., Minet, E., Anadon, A., and Meredith, C. (2013). Metabolic characterization of cell systems used in *in vitro* toxicology testing: lung cell system BEAS-2B as a working example. *Toxicol. Vitro* 27, 1719–1727. doi:10.1016/j.tiv.2013.05.001
- Ghio, A. J., Dailey, L. A., Soukup, J. M., Stonehurner, J., Richards, J. H., and Devlin, R. B. (2013). Growth of human bronchial epithelial cells at an air-liquid interface alters the response to particle exposure. *Part. Fibre Toxicol.* 10, 25. doi:10.1186/1743-8977-10-25
- Gonzalez-Suarez, I., Martin, F., Marescotti, D., Guedj, E., Acali, S., John, S., et al. (2016). *In vitro* systems toxicology assessment of a candidate modified risk tobacco product shows reduced toxicity compared to that of a conventional cigarette. *Chem. Res. Toxicol.* 29, 3–18. doi:10.1021/acs.chemrestox.5b00321
- Gordon, S., Daneshian, M., Bouwstra, J., Caloni, F., Constant, S., Davies, D. E., et al. (2015). Non-animal models of epithelial barriers (skin, intestine and lung) in research, industrial applications and regulatory toxicology. *ALTEX* 32, 327–378. doi:10.14573/altex.1510051
- Gray, T. E., Guzman, K., Davis, C. W., Abdullah, L. H., and Nettesheim, P. (1996). Mucociliary differentiation of serially passaged normal human tracheobronchial epithelial cells. *Am. J. Respir. Cell Mol. Biol.* 14, 104–112. doi:10.1165/ajrcmb.14.1.8534481
- Hashizume, T., Ishikawa, S., Matsumura, K., Ito, S., and Fukushima, T. (2023). Chemical and *in vitro* toxicological comparison of emissions from a heated tobacco product and the 1R6F reference cigarette. *Toxicol. Rep.* 10, 281–292. doi:10.1016/j.toxrep.2023.02.005
- Haswell, L. E., Hewitt, K., Thorne, D., Richter, A., and Gaca, M. D. (2010). Cigarette smoke total particulate matter increases mucous secreting cell numbers *in vitro*: a potential model of goblet cell hyperplasia. *Toxicol. Vitro* 24, 981–987. doi:10.1016/j.tiv.2009.12.019
- Health Canada (2024). Health Canada. Health Canada official methods for the testing of tobacco products (mainstream smoke). Available at: <https://open.canada.ca/data/en/dataset/71394df3-ae88-4117-92cb-a035360972a2> (Accessed January 2, 2024).
- Hendriks, G., Derr, R. S., Misovic, B., Morolli, B., Calleja, F. M., and Vrieling, H. (2016). The extended ToxTracker assay discriminates between induction of DNA damage, oxidative stress, and protein misfolding. *Toxicol. Sci.* 150, 190–203. doi:10.1093/toxsci/kfv323
- Hinderliter, P. M., Minard, K. R., Orr, G., Chrisler, W. B., Thrall, B. D., Pounds, J. G., et al. (2010). ISDD: a computational model of particle sedimentation, diffusion and target cell dosimetry for *in vitro* toxicity studies. *Part. Fibre Toxicol.* 7, 36–20. doi:10.1186/1743-8977-7-36
- Hines, D. E., Bell, S., Chang, X., Mansouri, K., Allen, D., and Kleinstreuer, N. (2022). Application of an accessible interface for pharmacokinetic modeling and *in vitro* to *in vivo* extrapolation. *Front. Pharmacol.* 13, 864742. doi:10.3389/fphar.2022.864742
- Hoffmann, R. F., Zarrintan, S., Brandenburg, S. M., Kol, A., De Bruin, H. G., Jafari, S., et al. (2013). Prolonged cigarette smoke exposure alters mitochondrial structure and function in airway epithelial cells. *Respir. Res.* 14, 97. doi:10.1186/1465-9921-14-97
- Huh, D., Matthews, B. D., Mammoto, A., Montoya-Zavala, M., Hsin, H. Y., and Ingber, D. E. (2010). Reconstituting organ-level lung functions on a chip. *Science* 328, 1662–1668. doi:10.1126/science.1188302

- Interagency Coordinating Committee on the Validation of Alternative Methods (ICCVAM) (2023). Validation, qualification, and regulatory acceptance of new approach methodologies. Available at: https://ntp.niehs.nih.gov/sites/default/files/2023-08/VWG%20Report%20Draft_for%20public%20comment_08Aug2023.pdf (Accessed December 12, 2023).
- Interagency Coordinating Committee on the Validation of Alternative Methods (ICVAM) (2018). A strategic roadmap for establishing new approaches to evaluate the safety of chemicals and medical products in the United States. Available at: https://ntp.niehs.nih.gov/iccvm/docs/roadmap/iccvm_strategicroadmap_january2018_document_508.pdf [Accessed December 12, 2023].
- Ishikawa, S., and Ito, S. (2017). Repeated whole cigarette smoke exposure alters cell differentiation and augments secretion of inflammatory mediators in air-liquid interface three-dimensional co-culture model of human bronchial tissue. *Toxicol. Vitro* 38, 170–178. doi:10.1016/j.tiv.2016.09.004
- Ishikawa, S., Matsumura, K., Kitamura, N., Takanami, Y., and Ito, S. (2019). Multi-omics analysis: repeated exposure of a 3D bronchial tissue culture to whole-cigarette smoke. *Toxicol. Vitro* 54, 251–262. doi:10.1016/j.tiv.2018.10.001
- Iskandar, A. R., Martin, F., Talikka, M., Schlage, W. K., Kostadinova, R., Mathis, C., et al. (2013). Systems approaches evaluating the perturbation of xenobiotic metabolism in response to cigarette smoke exposure in nasal and bronchial tissues. *Biomed. Res. Int.* 2013, 512086. doi:10.1155/2013/512086
- Iskandar, A. R., Zanetti, F., Marescotti, D., Titz, B., Sewer, A., Kondylis, A., et al. (2019). Application of a multi-layer systems toxicology framework for *in vitro* assessment of the biological effects of Classic Tobacco e-liquid and its corresponding aerosol using an e-cigarette device with MESH technology. *Arch. Toxicol.* 93, 3229–3247. doi:10.1007/s00204-019-02565-9
- Ito, S., Ishimori, K., and Ishikawa, S. (2018). Effects of repeated cigarette smoke extract exposure over one month on human bronchial epithelial organotypic culture. *Toxicol. Rep.* 5, 864–870. doi:10.1016/j.toxrep.2018.08.015
- Ito, S., Matsumura, K., Ishimori, K., and Ishikawa, S. (2020). *In vitro* long-term repeated exposure and exposure switching of a novel tobacco vapor product in a human organotypic culture of bronchial epithelial cells. *J. Appl. Toxicol.* 40, 1248–1258. doi:10.1002/jat.3982
- Ito, S., Taylor, M., Mori, S., Thorne, D., Nishino, T., Breheny, D., et al. (2019). An inter-laboratory *in vitro* assessment of cigarettes and next generation nicotine delivery products. *Toxicol. Lett.* 315, 14–22. doi:10.1016/j.toxlet.2019.08.004
- Jaunky, T., Adamson, J., Santopietro, S., Terry, A., Thorne, D., Breheny, D., et al. (2018). Assessment of tobacco heating product THP1.0. Part 5: *in vitro* dosimetric and cytotoxic assessment. *Regul. Toxicol. Pharmacol.* 93, 52–61. doi:10.1016/j.yrtph.2017.09.016
- Johnson, M. D., Schilz, J., Djordjevic, M. V., Rice, J. R., and Shields, P. G. (2009). Evaluation of *in vitro* assays for assessing the toxicity of cigarette smoke and smokeless tobacco. *Cancer Epidemiol. Biomarkers Prev.* 18, 3263–3304. doi:10.1158/1055-9965.EPI-09-0965
- Justice, M. J., and Dhillon, P. (2016). Using the mouse to model human disease: increasing validity and reproducibility. *Dis. Model Mech.* 9, 101–103. doi:10.1242/dmm.024547
- Klein, S. G., Serchi, T., Hoffmann, L., Blomeke, B., and Gutleb, A. C. (2013). An improved 3D tetra-culture system mimicking the cellular organisation at the alveolar barrier to study the potential toxic effects of particles on the lung. *Part. Fibre Toxicol.* 10, 31. doi:10.1186/1743-8977-10-31
- Klus, H., Boenke-Nimphius, B., and Müller, L. (2016). Cigarette mainstream smoke: the evolution of methods and devices for generation, exposure and collection. *Contrib. Tob. Nicotine Res.* 27, 137–274. doi:10.1515/cttr-2016-0015
- Kunzelmann, K., Kathofer, S., Hipper, A., Gruenert, D. C., and Gregner, R. (1996). Culture-dependent expression of Na⁺ conductances in airway epithelial cells. *Pflügers Arch.* 431, 578–586. doi:10.1007/BF02191906
- Lacroix, G., Koch, W., Ritter, D., Gutleb, A., Larsen, S. T., Loret, T., et al. (2018). Air-liquid interface *in vitro* models for respiratory toxicology research: consensus workshop and recommendations. *Appl. Vitro Toxicol.* 4, 91–106. doi:10.1089/aivt.2017.0034
- Lang, G., Henao, C., Almstetter, M., Arndt, D., Goujon, C., and Maeder, S. (2023). Non-targeted analytical comparison of a heated tobacco product aerosol against mainstream cigarette smoke: does heating tobacco produce an inherently different set of aerosol constituents? *Anal. Bioanal. Chem.* 416, 1349–1361. doi:10.1007/s00216-024-05126-x
- Lee, J. J., Miller, J. A., Basu, S., Kee, T. V., and Loo, L. H. (2018). Building predictive *in vitro* pulmonary toxicity assays using high-throughput imaging and artificial intelligence. *Arch. Toxicol.* 92, 2055–2075. doi:10.1007/s00204-018-2213-0
- Lee, K. M., Corley, R., Jarabek, A. M., Kleinstreuer, N., Paini, A., Stucki, A. O., et al. (2022). Advancing new approach methodologies (NAMs) for tobacco harm reduction: synopsis from the 2021 CORESTA SSPT-NAMs symposium. *Toxics* 10, 760. doi:10.3390/toxics10120760
- Lee, K. M., Pour, S. J., Zhang, J., Keyser, B., Iskandar, A., Ito, S., et al. (2023). New approach methods (NAMs) symposium-II: applications in tobacco regulatory sciences, the 2023 CORESTA SSPT symposium. Available at: https://www.coresta.org/sites/default/files/events/CORESTA_SSPT2023-NAM-Symposium_20231013_final.pdf (Accessed January 22, 2024).
- Lehmann, A. D., Daum, N., Bur, M., Lehr, C. M., Gehr, P., and Rothen-Rutishauser, B. M. (2011). An *in vitro* triple cell co-culture model with primary cells mimicking the human alveolar epithelial barrier. *Eur. J. Pharm. Biopharm.* 77, 398–406. doi:10.1016/j.ejpb.2010.10.014
- Li, X. (2016). *In vitro* toxicity testing of cigarette smoke based on the air-liquid interface exposure: a review. *Toxicol. Vitro* 36, 105–113. doi:10.1016/j.tiv.2016.07.019
- Lowe, F. J., Luettich, K., Talikka, M., Hoang, V., Haswell, L. E., Hoeng, J., et al. (2017). Development of an adverse outcome pathway for the onset of hypertension by oxidative stress-mediated perturbation of endothelial nitric oxide bioavailability. *Appl. Vitro Toxicol.* 3, 131–148. doi:10.1089/aivt.2016.0031
- Lu, F., Yu, M., Chen, C., Liu, L., Zhao, P., Shen, B., et al. (2021). The emission of VOCs and CO from heated tobacco products, electronic cigarettes, and conventional cigarettes, and their health risk. *Toxics* 10, 8. doi:10.3390/toxics10010008
- Luettich, K., Sharma, M., Yepiskoposyan, H., Breheny, D., and Lowe, F. J. (2021). An adverse outcome pathway for decreased lung function focusing on mechanisms of impaired mucociliary clearance following inhalation exposure. *Front. Toxicol.* 3, 750254. doi:10.3389/ftox.2021.750254
- Luettich, K., Talikka, M., Lowe, F. J., Haswell, L. E., Park, J., Gaca, M. D., et al. (2017). The adverse outcome pathway for oxidative stress-mediated EGFR activation leading to decreased lung function. *Appl. Vitro Toxicol.* 3, 99–109. doi:10.1089/aivt.2016.0032
- Malinska, D., Szymanski, J., Patalas-Krawczyk, P., Michalska, B., Wojtala, A., Prill, M., et al. (2018). Assessment of mitochondrial function following short- and long-term exposure of human bronchial epithelial cells to total particulate matter from a candidate modified-risk tobacco product and reference cigarettes. *Food Chem. Toxicol.* 115, 1–12. doi:10.1016/j.fct.2018.02.013
- Malt, L., Thompson, K., Mason, E., Wale, T., Nahde, T., and O'Connell, G. (2022). The product science of electrically heated tobacco products: a narrative review of the scientific literature. *F1000Research* 11, 121. doi:10.12688/f1000research.74718.1
- Mansouri, K., Karmaus, A. L., Fitzpatrick, J., Patlewicz, G., Pradeep, P., Alberga, D., et al. (2021). CATMoS: collaborative acute toxicity modeling suite. *Environ. Health Perspect.* 129 (4), 47013. doi:10.1289/EHP8495
- Marescotti, D., Serchi, T., Luettich, K., Xiang, Y., Moschini, E., Talikka, M., et al. (2019). How complex should an *in vitro* model be? Evaluation of complex 3D alveolar model with transcriptomic data and computational biological network models. *ALTEX* 36, 388–402. doi:10.14573/altex.1811221
- Margham, J., Mcadam, K., Forster, M., Liu, C., Wright, C., Mariner, D., et al. (2016). Chemical composition of aerosol from an E-cigarette: a quantitative comparison with cigarette smoke. *Chem. Res. Toxicol.* 29, 1662–1678. doi:10.1021/acs.chemrestox.6b00188
- Maschmeyer, I., Hasenberg, T., Jaenicke, A., Lindner, M., Lorenz, A. K., Zech, J., et al. (2015a). Chip-based human liver-intestine and liver-skin co-cultures--A first step toward systemic repeated dose substance testing *in vitro*. *Eur. J. Pharm. Biopharm.* 95, 77–87. doi:10.1016/j.ejpb.2015.03.002
- Maschmeyer, I., Lorenz, A. K., Schimek, K., Hasenberg, T., Ramme, A. P., Hubner, J., et al. (2015b). A four-organ-chip for interconnected long-term co-culture of human intestine, liver, skin and kidney equivalents. *Lab. Chip* 15, 2688–2699. doi:10.1039/c5lc00392j
- Materne, E. M., Ramme, A. P., Terraso, A. P., Serra, M., Alves, P. M., Brito, C., et al. (2015). A multi-organ chip co-culture of neurospheres and liver equivalents for long-term substance testing. *J. Biotechnol.* 205, 36–46. doi:10.1016/j.jbiotec.2015.02.002
- McNeil, A., Simonavičius, E., Brose, L. S., Taylor, E., East, K., Zuikova, E., et al. (2022). *Nicotine vaping in England: an evidence update including health risks and perceptions, September 2022. A report commissioned by the Office for Health Improvement and Disparities*. London: Office for Health Improvement and Disparities.
- McNeill, A., Brose, L. S., Calder, R., and Bauld, L. (2018). *Evidence review of e-cigarettes and heated tobacco products 2018. A report commissioned by Public Health England*. London: Public Health England.
- Miller-Holt, J., Behrsing, H., Crooks, I., Curren, R., Demir, K., Gafner, J., et al. (2023). Key challenges for *in vitro* testing of tobacco products for regulatory applications: recommendations for dosimetry. *Drug Test. Anal.* 15, 1175–1188. doi:10.1002/dta.3344
- Misra, M., Leverette, R. D., Cooper, B. T., Bennett, M. B., and Brown, S. E. (2014). Comparative *in vitro* toxicity profile of electronic and tobacco cigarettes, smokeless tobacco and nicotine replacement therapy products: E-liquids, extracts and collected aerosols. *Int. J. Environ. Res. Public Health* 11, 11325–11347. doi:10.3390/ijerph111111325
- Moore, M. M., Abraham, I., Ballantyne, M., Behrsing, H., Cao, X., Clements, J., et al. (2023). Key challenges and recommendations for *in vitro* testing of tobacco products for regulatory applications: consideration of test materials and exposure parameters. *Altern. Lab. Anim.* 51, 55–79. doi:10.1177/02611929221146536
- Mori, S., Ishimori, K., Matsumura, K., Ishikawa, S., and Ito, S. (2022). Donor-to-donor variability of a human three-dimensional bronchial epithelial model: a case study of cigarette smoke exposure. *Toxicol. Vitro* 82, 105391. doi:10.1016/j.tiv.2022.105391
- National Research Council (NRC) (2007). *Toxicity testing in the 21st century: a vision and a strategy*. Available at: <https://nap.nationalacademies.org/catalog/11970/toxicity-testing-in-the-21st-century-a-vision-and-a> (Accessed December 12, 2023).

- Nichols, J. E., Niles, J. A., Vega, S. P., and Cortiella, J. (2013). Novel *in vitro* respiratory models to study lung development, physiology, pathology and toxicology. *Stem Cell Res. Ther.* 4 (1), S7. doi:10.1186/s13287
- Ohashi, K., Hayashida, A., Nozawa, A., Matsumura, K., and Ito, S. (2023). Human vasculature on-a-chip with macrophage-mediated endothelial activation: the biological effect of aerosol from heated tobacco products on monocyte adhesion. *Toxicol. Vitro* 89, 105582. doi:10.1016/j.tiv.2023.105582
- Organisation for Economic Co-operation and Development (OECD) (2023). Welcome to the collaborative adverse outcome pathway wiki (AOP-Wiki). Available at: <https://aopwiki.org/> (Accessed December 12, 2023).
- Paustenbach, D. J. (2000). The practice of exposure assessment: a state-of-the-art review. *J. Toxicol. Environ. Health B Crit. Rev.* 3, 179–291. doi:10.1080/10937400050045264
- Perlman, R. L. (2016). Mouse models of human disease: an evolutionary perspective. *Evol. Med. Public Health* 2016, 170–176. doi:10.1093/emph/eow014
- Petpiroon, N., Netkueakul, W., Sukrak, K., Wang, C., Liang, Y., Wang, M., et al. (2023). Development of lung tissue models and their applications. *Life Sci.* 334, 122208. doi:10.1016/j.lfs.2023.122208
- Poussin, C., Laurent, A., Peitsch, M. C., Hoeng, J., and De Leon, H. (2016). Systems toxicology-based assessment of the candidate modified risk tobacco product THS2.2 for the adhesion of monocytic cells to human coronary arterial endothelial cells. *Toxicology* 339, 73–86. doi:10.1016/j.tox.2015.11.007
- Proença, S., Escher, B. I., Fischer, F. C., Fisher, C., Grégoire, S., Hewitt, N. J., et al. (2021). Effective exposure of chemicals in *in vitro* cell systems: a review of chemical distribution models. *Toxicol. Vitro* 73, 105133. doi:10.1016/j.tiv.2021.105133
- Prytherch, Z., Job, C., Marshall, H., Oreffo, V., Foster, M., and Berube, K. (2011). Tissue-Specific stem cell differentiation in an *in vitro* airway model. *Macromol. Biosci.* 11, 1467–1477. doi:10.1002/mabi.201100181
- Rogal, J., Probst, C., and Loskill, P. (2017). Integration concepts for multi-organ chips: how to maintain flexibility? *Future Sci. OA* 3, FSO180. doi:10.4155/fsoa-2016-0092
- Rudd, K., Stevenson, M., Wiczorek, R., Pani, J., Trelles-Sticken, E., Dethloff, O., et al. (2020). Chemical composition and *in vitro* toxicity profile of a pod-based E-cigarette aerosol compared to cigarette smoke. *Appl. Vitro Toxicol.* 6, 11–41. doi:10.1089/avt.2019.0015
- Russell, W. M. S., and Burch, R. L. (1959) *The principles of humane experimental technique*. Massachusetts: Methuen.
- Schaller, J. P., Keller, D., Poget, L., Pratte, P., Kaelin, E., Mchugh, D., et al. (2016). Evaluation of the Tobacco Heating System 2.2. Part 2: chemical composition, genotoxicity, cytotoxicity, and physical properties of the aerosol. *Regul. Toxicol. Pharmacol.* 81 (2), S27–S47. doi:10.1016/j.yrtph.2016.10.001
- Schamberger, A. C., Staab-Weijnitz, C. A., Mise-Racek, N., and Eickelberg, O. (2015). Cigarette smoke alters primary human bronchial epithelial cell differentiation at the air-liquid interface. *Sci. Rep.* 5, 8163. doi:10.1038/srep08163
- Settivari, R. S., Ball, N., Murphy, L., Rasoulpour, R., Boverhof, D. R., and Carney, E. W. (2015). Predicting the future: opportunities and challenges for the chemical industry to apply 21st-century toxicity testing. *J. Am. Assoc. Lab. Anim. Sci.* 54, 214–223.
- Sewald, K., and Braun, A. (2013). Assessment of immunotoxicity using precision-cut tissue slices. *Xenobiotica* 43, 84–97. doi:10.3109/00498254.2012.731543
- Sharma, M., Stucki, A. O., Verstraalen, S., Stedeford, T. J., Jacobs, A., Maes, F., et al. (2023). Human cell-based *in vitro* systems to assess respiratory toxicity: a case study using silanes. *Toxicol. Sci.* 195 (2), 213–230. doi:10.1093/toxsci/kfad074
- Silva, R. J., and Tamburic, S. (2022). A state-of-the-art review on the alternatives to animal testing for the safety assessment of cosmetics. *Cosmetics* 9, 90. doi:10.3390/cosmetics9050090
- Simms, L., Clarke, A., Paschke, T., Manson, A., Murphy, J., Stabbert, R., et al. (2019). Assessment of priority tobacco additives per the requirements of the EU Tobacco Products Directive (2014/40/EU): Part 1: background, approach, and summary of findings. *Regul. Toxicol. Pharmacol.* 104, 84–97. doi:10.1016/j.yrtph.2019.02.011
- Simms, L., Mason, E., Berg, E. L., Yu, F., Rudd, K., Czekala, L., et al. (2021). Use of a rapid human primary cell-based disease screening model, to compare next generation products to combustible cigarettes. *Curr. Res. Toxicol.* 2, 309–321. doi:10.1016/j.crt.2021.08.003
- Smart, D. J., Helbling, F. R., Verardo, M., Huber, A., Mchugh, D., and Vanscheuwijk, P. (2020). Development of an integrated assay in human TK6 cells to permit comprehensive genotoxicity analysis *in vitro*. *Mutat. Res. Genet. Toxicol. Environ. Mutagen.* 849, 503129. doi:10.1016/j.mrgentox.2019.503129
- Smart, D. J., and Phillips, G. (2021). Collecting e-cigarette aerosols for *in vitro* applications: a survey of the biomedical literature and opportunities to increase the value of submerged cell culture-based assessments. *J. Appl. Toxicol.* 41, 161–174. doi:10.1002/jat.4064
- Stabile, A. M., Marinucci, L., Balloni, S., Giuliani, A., Pistilli, A., Bodo, M., et al. (2018). Long term effects of cigarette smoke extract or nicotine on nerve growth factor and its receptors in a bronchial epithelial cell line. *Toxicol. Vitro* 53, 29–36. doi:10.1016/j.tiv.2018.07.020
- Stewart, C. E., Torr, E. E., Mohd Jamili, N. H., Bosquillon, C., and Sayers, I. (2012). Evaluation of differentiated human bronchial epithelial cell culture systems for asthma research. *J. Allergy (Cairo)* 2012, 943982. doi:10.1155/2012/943982
- Stucki, A. O., Stucki, J. D., Hall, S. R., Felder, M., Mermoud, Y., Schmid, R. A., et al. (2015). A lung-on-a-chip array with an integrated bio-inspired respiration mechanism. *Lab. Chip* 15, 1302–1310. doi:10.1039/c4lc01252f
- Stucki, J. D., Hobi, N., Galimov, A., Stucki, A. O., Schneider-Daum, N., Lehr, C. M., et al. (2018). Medium throughput breathing human primary cell alveolus-on-chip model. *Sci. Rep.* 8, 14359. doi:10.1038/s41598-018-32523-x
- Su, R., Xiong, S., Zink, D., and Loo, L. H. (2016). High-throughput imaging-based nephrotoxicity prediction for xenobiotics with diverse chemical structures. *Arch. Toxicol.* 90, 2793–2808. doi:10.1007/s00204-015-1638-y
- Sun, D., Gao, W., Hu, H., and Zhou, S. (2022). Why 90% of clinical drug development fails and how to improve it? *Acta. Pharm. Sin. B* 12, 3049–3062. doi:10.1016/j.apsb.2022.02.002
- Sussman, R. A., Sipala, F., Emma, R., and Ronsisvalle, S. (2023). Aerosol emissions from heated tobacco products: a review focusing on carbonyls, analytical methods, and experimental quality. *Toxics* 11 (12), 947. doi:10.3390/toxics11120947
- Takahashi, Y., Kanemaru, Y., Fukushima, T., Eguchi, K., Yoshida, S., Miller-Holt, J., et al. (2018). Chemical analysis and *in vitro* toxicological evaluation of aerosol from a novel tobacco vapor product: a comparison with cigarette smoke. *Regul. Toxicol. Pharmacol.* 92, 94–103. doi:10.1016/j.yrtph.2017.11.009
- Taylor, M., Jaunky, T., Hewitt, K., Breheny, D., Lowe, F., Fearon, I. M., et al. (2017). A comparative assessment of e-cigarette aerosols and cigarette smoke on *in vitro* endothelial cell migration. *Toxicol. Lett.* 277, 123–128. doi:10.1016/j.toxlet.2017.06.001
- Taylor, M., Santopietro, S., Baxter, A., East, N., Breheny, D., Thorne, D., et al. (2020). *In vitro* biological assessment of the stability of cigarette smoke aqueous aerosol extracts. *BMC Res. Notes* 13, 492. doi:10.1186/s13104-020-05337-2
- Taylor, M., Thorne, D., Carr, T., Breheny, D., Walker, P., Proctor, C., et al. (2018). Assessment of novel tobacco heating product THP1.0. Part 6: a comparative *in vitro* study using contemporary screening approaches. *Regul. Toxicol. Pharmacol.* 93, 62–70. doi:10.1016/j.yrtph.2017.08.016
- Thomas, D. G., Smith, J. N., Thrall, B. D., Baer, D. R., Jolley, H., Munusamy, P., et al. (2018). ISD3: a pharmacokinetic model for predicting the combined effects of particle sedimentation, diffusion and dissolution on cellular dosimetry for *in vitro* systems. *Part Fibre Toxicol.* 15, 6. doi:10.1186/s12989-018-0243-7
- Thomas, R. S., Bahadori, T., Buckley, T. J., Cowden, J., Deisenroth, C., Dionisio, K. L., et al. (2019). The next generation blueprint of computational toxicology at the US Environmental Protection Agency. *Toxicol. Sci.* 169, 317–332. doi:10.1093/toxsci/kfz058
- Thorne, D., and Adamson, J. (2013). A review of *in vitro* cigarette smoke exposure systems. *Exp. Toxicol. Pathol.* 65, 1183–1193. doi:10.1016/j.etp.2013.06.001
- Thorne, D., Breheny, D., Proctor, C., and Gaca, M. (2018). Assessment of novel tobacco heating product THP1.0. Part 7: comparative *in vitro* toxicological evaluation. *Regul. Toxicol. Pharmacol.* 93, 71–83. doi:10.1016/j.yrtph.2017.08.017
- Thorne, D., Crooks, I., Hollings, M., Seymour, A., Meredith, C., and Gaca, M. (2016). The mutagenic assessment of an electronic-cigarette and reference cigarette smoke using the Ames assay in strains TA98 and TA100. *Mutat. Res. Genet. Toxicol. Environ. Mutagen.* 812, 29–38. doi:10.1016/j.mrgentox.2016.10.005
- Thorne, D., Hollings, M., Kilford, J., Clements, J., Payne, R., Ballantyne, M., et al. (2020). An experimental aerosol air–agar interface mouse lymphoma assay methodology. *Mutat. Res. Genet. Toxicol. Environ. Mutagen.* 856–857, 503230. doi:10.1016/j.mrgentox.2020.503230
- Thorne, D., Leverette, R., Breheny, D., Lloyd, M., Mcenaney, S., Whitwell, J., et al. (2019a). Genotoxicity evaluation of tobacco and nicotine delivery products: Part One. Mouse lymphoma assay. *Food Chem. Toxicol.* 132, 110584. doi:10.1016/j.fct.2019.110584
- Thorne, D., Leverette, R., Breheny, D., Lloyd, M., Mcenaney, S., Whitwell, J., et al. (2019b). Genotoxicity evaluation of tobacco and nicotine delivery products: Part Two. *in vitro* micronucleus assay. *Food Chem. Toxicol.* 132, 110546. doi:10.1016/j.fct.2019.05.054
- Thorne, D., Wiczorek, R., Fukushima, T., Shin, H.-J., Leverette, R., Ballantyne, M., et al. (2021). A survey of aerosol exposure systems relative to the analysis of cytotoxicity: a Cooperation Centre for Scientific Research Relative to Tobacco (CORESTA) perspective. *Toxicol. Res. Appl.* 5, 239784732110222. doi:10.1177/23978473211022267
- U.S. Environmental Protection Agency (2023). Alternative test methods and strategies to reduce vertebrate animal testing. Available at: <https://www.epa.gov/assessing-and-managing-chemicals-under-tsca/alternative-test-methods-and-strategies-reduce> (Accessed December 6, 2023).
- Van Der Toorn, M., Sewer, A., Marescotti, D., John, S., Baumer, K., Bornand, D., et al. (2018). The biological effects of long-term exposure of human bronchial epithelial cells to total particulate matter from a candidate modified-risk tobacco product. *Toxicol. Vitro* 50, 95–108. doi:10.1016/j.tiv.2018.02.019
- Van Der Zalm, A. J., Barroso, J., Browne, P., Casey, W., Gordon, J., Henry, T. R., et al. (2022). A framework for establishing scientific confidence in new approach methodologies. *Arch. Toxicol.* 96, 2865–2879. doi:10.1007/s00204-022-03365-4
- Van Meer, P. J., Graham, M. L., and Schuurman, H. J. (2015). The safety, efficacy and regulatory triangle in drug development: impact for animal models and the use of animals. *Eur. J. Pharmacol.* 759, 3–13. doi:10.1016/j.ejphar.2015.02.055

- Vaughan, M. B., Ramirez, R. D., Wright, W. E., Minna, J. D., and Shay, J. W. (2006). A three-dimensional model of differentiation of immortalized human bronchial epithelial cells. *Differentiation* 74, 141–148. doi:10.1111/j.1432-0436.2006.00069.x
- Veljkovic, E., Jiricny, J., Menigatti, M., Rehrauer, H., and Han, W. (2011). Chronic exposure to cigarette smoke condensate *in vitro* induces epithelial to mesenchymal transition-like changes in human bronchial epithelial cells, BEAS-2B. *Toxicol. Vitro* 25, 446–453. doi:10.1016/j.tiv.2010.11.011
- Villeneuve, D. L., Crump, D., Garcia-Reyero, N., Hecker, M., Hutchinson, T. H., Lalone, C. A., et al. (2014). Adverse outcome pathway (AOP) development I: strategies and principles. *Toxicol. Sci.* 142, 312–320. doi:10.1093/toxsci/kfu199
- Vinken, M. (2020). 3Rs toxicity testing and disease modeling projects in the European Horizon 2020 research and innovation program. *EXCLI J.* 19, 775–784. doi:10.17179/excli2020-1463
- Watson, C. Y., DeLoid, G. M., Pal, A., and Demokritou, P. (2016). Buoyant nanoparticles: implications for nano-biointeractions in cellular studies. *Small* 12 (23), 3172–3180. doi:10.1002/sml.201600314
- Wheeldon, R. P., Bernacki, D. T., Dertinger, S. D., Bryce, S. M., Bemis, J. C., and Johnson, G. E. (2020). Benchmark dose analysis of DNA damage biomarker responses provides compound potency and adverse outcome pathway information for the topoisomerase II inhibitor class of compounds. *Environ. Mol. Mutagen.* 61, 396–407. doi:10.1002/em.22360
- Wieczorek, R., Trelles Sticklen, E., Pour, S. J., Chapman, F., Röwer, K., Otte, S., et al. (2023). Characterisation of a smoke/aerosol exposure *in vitro* system (SAEIVS) for delivery of complex mixtures directly to cells at the air-liquid interface. *J. Appl. Toxicol.* 43, 1050–1063. doi:10.1002/jat.4442
- Wong, A. P., Chin, S., Xia, S., Garner, J., Bear, C. E., and Rossant, J. (2015). Efficient generation of functional CFTR-expressing airway epithelial cells from human pluripotent stem cells. *Nat. Protoc.* 10, 363–381. doi:10.1038/nprot.2015.021
- Yoshida, T., and Tuder, R. M. (2007). Pathobiology of cigarette smoke-induced chronic obstructive pulmonary disease. *Physiol. Rev.* 87, 1047–1082. doi:10.1152/physrev.00048.2006
- Zhang, J., Chang, X., Holland, T. L., Hines, D. E., Karmaus, A. L., Bell, S., et al. (2021). Evaluation of inhalation exposures and potential health impacts of ingredient mixtures using *in vitro* to *in vivo* extrapolation. *Front. Toxicol.* 3, 787756. doi:10.3389/ftox.2021.787756
- Zhang, X., and Wright, S. H. (2022). Transport turnover rates for human OCT2 and MATE1 expressed in Chinese hamster ovary cells. *Int. J. Mol. Sci.* 23, 1472. doi:10.3390/ijms23031472



OPEN ACCESS

APPROVED BY
Frontiers Editorial Office,
Frontiers Media SA, Switzerland

*CORRESPONDENCE
Marianna Gaca,
✉ marianna_gaca@bat.com

RECEIVED 05 July 2024
ACCEPTED 09 July 2024
PUBLISHED 19 July 2024

CITATION
Thorne D, McHugh D, Simms L, Lee KM,
Fujimoto H, Moses S and Gaca M (2024),
Corrigendum: Applying new approach
methodologies to assess next-generation
tobacco and nicotine products.
Front. Toxicol. 6:1460271.
doi: 10.3389/ftox.2024.1460271

COPYRIGHT
© 2024 Thorne, McHugh, Simms, Lee,
Fujimoto, Moses and Gaca. This is an open-
access article distributed under the terms of the
[Creative Commons Attribution License \(CC BY\)](#).
The use, distribution or reproduction in other
forums is permitted, provided the original
author(s) and the copyright owner(s) are
credited and that the original publication in this
journal is cited, in accordance with accepted
academic practice. No use, distribution or
reproduction is permitted which does not
comply with these terms.

Corrigendum: Applying new approach methodologies to assess next-generation tobacco and nicotine products

David Thorne¹, Damian McHugh², Liam Simms³, K. Monica Lee⁴,
Hitoshi Fujimoto⁵, Sara Moses⁶ and Marianna Gaca^{1*}

¹BAT (Investments) Ltd., Southampton, Hampshire, United Kingdom, ²PMI R&D Philip Morris Products S. A., Neuchâtel, Switzerland, ³Imperial Brands, Bristol, United Kingdom, ⁴Altria Client Services LLC, Richmond, VA, United States, ⁵Japan Tobacco Inc., R&D Group, Yokohama, Kanagawa, Japan, ⁶Swedish Match, Stockholm, Sweden

KEYWORDS

new approach methodologies (NAM), organs on a chip (OoC), human 3D tissues, next-generation products (NGP), airway models, high-content analysis, adverse outcome pathway (AOP), dosimetry

A Corrigendum on Applying new approach methodologies to assess next-generation tobacco and nicotine products

by Thorne D, McHugh D, Simms L, Lee KM, Fujimoto H, Moses S and Gaca M (2024). *Front. Toxicol.* 6:1376118. doi: [10.3389/ftox.2024.1376118](https://doi.org/10.3389/ftox.2024.1376118)

In the published article, there was an error in the **Conflict of interest** statement. The **Conflict of interest** statement was displayed as “Authors DT and MG were employed by BAT (Investments) Ltd. Author LS was employed by Imperial Brands. Author KML was employed by Altria Client Services LLC. Author HF was employed by Japan Tobacco Inc., R&D Group. The remaining authors declare that the research was conducted in the absence of any commercial or financial relationships that could be construed as a potential conflict of interest.”

The correct **Conflict of interest** statement appears below.

Conflict of interest

Authors DT and MG were employed by BAT (Investments) Ltd. Author LS was employed by Imperial Brands. Author KL was employed by Altria Client Services LLC. Author HF was employed by Japan Tobacco Inc., R&D Group. Author DM was employed by Philip Morris International. Author SM was employed by Swedish Match.

The authors apologize for this error and state that this does not change the scientific conclusions of the article in any way. The original article has been updated.

Publisher's note

All claims expressed in this article are solely those of the authors and do not necessarily represent those of their affiliated

organizations, or those of the publisher, the editors and the reviewers. Any product that may be evaluated in this article, or claim that may be made by its manufacturer, is not guaranteed or endorsed by the publisher.



OPEN ACCESS

EDITED BY

Victoria Hutter,
University of Hertfordshire, United Kingdom

REVIEWED BY

Madhuri Singal,
AeroTox Consulting Services, LLC, United States
Mary Catherine McElroy,
Charles River Laboratories, United Kingdom

*CORRESPONDENCE

Lynne T. Haber,
✉ lynne.haber@uc.edu

†PRESENT ADDRESSES

Amanda N. Buerger,
ToxStrategies, Inc., Cincinnati, OH, United States
Phillip W. Clapp,
Independent, Winston-Salem, NC, United States
Phillip W. Clapp,
Department of Cell Biology and Physiology,
UNC/NCSSU Joint Department of Biomedical
Engineering, University of North Carolina at
Chapel Hill, Chapel Hill, NC, United States
Shaun D. McCullough,
Exposure and Protection, RTI International,
Durham, NC, United States
Nathan Pechacek,
3M, St. Paul, MN, United States

RECEIVED 12 May 2024

ACCEPTED 19 September 2024

PUBLISHED 08 October 2024

CITATION

Haber LT, Bradley MA, Buerger AN, Behrsing H,
Burla S, Clapp PW, Dotson S, Fisher C,
Genco KR, Kruszewski FH, McCullough SD,
Page KE, Patel V, Pechacek N, Roper C,
Sharma M and Jarabek AM (2024) New
approach methodologies (NAMs) for the *in vitro*
assessment of cleaning products for respiratory
irritation: workshop report.
Front. Toxicol. 6:1431790.
doi: 10.3389/ftox.2024.1431790

COPYRIGHT

© 2024 Haber, Bradley, Buerger, Behrsing,
Burla, Clapp, Dotson, Fisher, Genco,
Kruszewski, McCullough, Page, Patel,
Pechacek, Roper, Sharma and Jarabek. This is
an open-access article distributed under the
terms of the [Creative Commons Attribution
License \(CC BY\)](https://creativecommons.org/licenses/by/4.0/). The use, distribution or
reproduction in other forums is permitted,
provided the original author(s) and the
copyright owner(s) are credited and that the
original publication in this journal is cited, in
accordance with accepted academic practice.
No use, distribution or reproduction is
permitted which does not comply with these
terms.

New approach methodologies (NAMs) for the *in vitro* assessment of cleaning products for respiratory irritation: workshop report

Lynne T. Haber^{1*}, Mark A. Bradley¹, Amanda N. Buerger^{2†},
Holger Behrsing³, Sabina Burla⁴, Phillip W. Clapp^{5†},
Scott Dotson⁶, Casey Fisher⁷, Keith R. Genco⁸,
Francis H. Kruszewski⁹, Shaun D. McCullough^{10†},
Kathryn E. Page¹¹, Vivek Patel³, Nathan Pechacek^{7†}, Clive Roper¹²,
Monita Sharma¹³ and Annie M. Jarabek¹⁴

¹Risk Science Center, Department of Environmental and Public Health Sciences, University of Cincinnati, Cincinnati, OH, United States, ²Stantec ChemRisk, Cincinnati, OH, United States, ³Institute for In Vitro Sciences, Inc., Gaithersburg, MD, United States, ⁴Invitrolize sarl, Belvaux, Luxembourg, ⁵Wake Forest Institute for Regenerative Medicine, Winston-Salem, NC, United States, ⁶Insight Exposure and Risk Sciences Group, Cincinnati, OH, United States, ⁷Ecolab, St. Paul, MN, United States, ⁸Arkema Inc., King of Prussia, PA, United States, ⁹American Cleaning Institute®, Washington, DC, United States, ¹⁰Public Health and Integrated Toxicology Division, Center for Public Health and Environmental Assessment, Office of Research and Development, U.S. EPA, Chapel Hill, NC, United States, ¹¹The Clorox Company, Pleasanton, CA, United States, ¹²Roper Toxicology Consulting Limited, Edinburgh, United Kingdom, ¹³PETA Science Consortium International e.V., Stuttgart, Germany, ¹⁴Health and Environmental Effects Assessment Division, Center for Public Health and Environmental Assessment, Office of Research and Development, U.S. EPA, Chapel Hill, NC, United States

The use of *in vitro* new approach methodologies (NAMs) to assess respiratory irritation depends on several factors, including the specifics of exposure methods and cell/tissue-based test systems. This topic was examined in the context of human health risk assessment for cleaning products at a 1-day public workshop held on 2 March 2023, organized by the American Cleaning Institute® (ACI). The goals of this workshop were to (1) review *in vitro* NAMs for evaluation of respiratory irritation, (2) examine different perspectives on current challenges and suggested solutions, and (3) publish a manuscript of the proceedings. Targeted sessions focused on exposure methods, *in vitro* cell/tissue test systems, and application to human health risk assessment. The importance of characterization of assays and development of reporting standards was noted throughout the workshop. The exposure methods session emphasized that the appropriate exposure system design depends on the purpose of the assessment. This is particularly important given the many dosimetry and technical considerations affecting relevance and translation of results to human exposure scenarios. Discussion in the *in vitro* cell/tissue test systems session focused on the wide variety of cell systems with varying suitability for evaluating key mechanistic steps, such as molecular initiating events (MIEs) and key events (KEs) likely present in any putative respiratory irritation adverse outcome pathway (AOP). This suggests the opportunity to further develop guidance around *in vitro* cell/tissue test system endpoint selection, assay design, characterization and validation, and analytics that provide information about a given assay's utility. The

session on applications for human health protection emphasized using mechanistic understanding to inform the choice of test systems and integration of NAMs-derived data with other data sources (e.g., physicochemical properties, exposure information, and existing *in vivo* data) as the basis for *in vitro* to *in vivo* extrapolation. In addition, this group noted a need to develop procedures to align NAMs-based points of departure (PODs) and uncertainty factor selection with current human health risk assessment methods, together with consideration of elements unique to *in vitro* data. Current approaches are described and priorities for future characterization of *in vitro* NAMs to assess respiratory irritation are noted.

KEYWORDS

new approach methodologies, cleaning products, respiratory irritation, adverse outcome pathway, air-liquid interface, inhalation dosimetry, *in vitro*, best practices

1 Introduction

The American Cleaning Institute® (ACI)¹ sponsored a workshop in Arlington, Virginia on 2 March 2023, regarding the use of *in vitro* new approach methodologies (NAMs) for the assessment of cleaning products and ingredients for respiratory irritation. To avoid limiting the discussion, NAMs were not defined in the context of the workshop, and definitions may vary across different organizations. A recent definition from the US EPA is “any technologies, methodologies, approaches, or combinations thereof that can be used to provide information on chemical hazard and potential human exposure that can avoid or significantly reduce the use of testing on animals” (U.S. EPA, 2023). Respiratory irritation is one of the leading health concerns associated with the inhalation of chemicals in consumer and workplace scenarios. In a review of the health risks of chemicals in consumer products, Li and Suh (2019) found that 50% of the identified chemicals caused irritation. Similarly, almost 1/3 of the occupational exposure limits (OELs) reviewed by Paustenbach (2000) were based on odor or irritation. Irritation was not defined in the studies by Li and Suh (2019) or Paustenbach (2000), but for the purposes of this workshop, respiratory irritation was defined as disruption of the epithelial lining fluid (ELF) or epithelial perturbation (e.g., disruption of the cell membrane, inflammation, or cytotoxicity). Thus, respiratory irritation can occur throughout the respiratory tract, including in the pulmonary region. Conversely, respiratory sensitization, sensory irritation (i.e., irritation resulting from stimulation of specific nerve receptors), and neurogenic inflammation were not included within the workshop scope.

Animal studies conducted to characterize respiratory responses to potential chemical irritants pose unique technical and scientific challenges and are often high cost and low throughput. To address these concerns, toxicity testing in Organisation for Economic Co-operation and Development (OECD) member countries is being

increasingly directed towards systems that can provide data relevant to human biology and mechanisms of toxicity while moving away from animal testing. Key milestones include the European Union (EU) directive limiting cosmetic product testing on animals (European Union, 2003), the associated regulation (European Union, 2009), and the 2007 National Research Council (NRC) report on toxicity testing in the 21st Century (National Research Council, 2007). More recently, a key objective of the Registration, Evaluation, Authorisation and Restriction of Chemicals (REACH) legislation in the EU was to promote non-animal test methods, as exemplified by European Chemicals Agency (ECHA) guidance (European Chemicals Agency, 2011; European Chemicals Agency, 2016). Similarly, the United States (U.S.) Environmental Protection Agency (EPA) released a strategic plan to promote the development and implementation of alternative test methods within the Toxic Substances Control Act (TSCA) program (U.S. EPA, 2018), as well as a workplan for reducing vertebrate animal testing and increasing scientific confidence in and application of alternative methods (U.S. EPA, 2021). These alternative methods, including *in vitro* testing, testing of non-vertebrate organisms, *in silico* modeling, read-across, among others, are collectively termed NAMs and are increasingly being used for both regulatory and non-regulatory internal decision making (Stucki et al., 2022; Lee et al., 2022; Westmoreland et al., 2022; Miller-Holt et al., 2022; Schmeisser et al., 2023).

An important advantage of *in vitro* testing is that it uses cells from the species of interest (i.e., humans), with the potential to allow for the evaluation of inter-individual variability, and for the study of population variability (e.g., children and susceptible populations) where *in vivo* exposure studies may not be ethical. There are, however, additional parameters that need to be considered for the incorporation of *in vitro* NAMs to predict respiratory irritation and for decision making. Limitations of *in vitro* testing for respiratory irritation may include the use of single cell lines or limited cell types to represent a spatially diverse and complex system of at least 41 cell types, limited capacity for long-term exposures, lack of metabolic capacity, inadequate replicates, limited understanding or measurement of internal dose, no consideration of systemic sequelae; as well as the use of systems, assays, and methods that have not been thoroughly optimized and/or characterized. Several of these challenges may be resolved with additional research and modification of test methods and test systems, but some are likely to be inherent to *in vitro* testing. Creating a single *in vitro*

¹ ACI is a non-profit trade association made up of more than 150 member companies, representing manufacturers of household, industrial, and institutional cleaning products, their ingredients and finished packaging, as well as oleochemical producers, and chemical distributors to the cleaning products industry. <https://www.cleaninginstitute.org/>

TABLE 1 Cleaning product and ingredient assessment types and uses for industry and regulatory purposes.

	Assessment type and use		
	Screening (qualitative or semi-quantitative)	Intermediate (qualitative or semi-quantitative)	Full (quantitative)
Industry – Internal Activities and Decision Making	Include/exclude ingredient or product candidates	Internal risk assessment for ingredients or product formulations	Submission of full risk assessment for regulatory approval of ingredients and product formulations (if applicable)
Regulatory	Screening/prioritization for full risk assessment (hazard and/or exposure)	N/A	Review of full regulatory risk assessments for ingredients Derivation of TRVs Not applicable to cleaning product mixtures

Key: N/A: not applicable; TRV: toxicity reference value, a term equivalent to health benchmark value.

test system that contains all cell types found in the respiratory tract is not technically feasible, but the effects on specific regions of the respiratory tract might be predicted with experimental systems containing the cells critical to a given pathogenesis (Clippinger et al., 2018a).

The workshop focused on issues related to cleaning products and their components and was specifically targeted to issues faced by manufacturers and formulators of cleaning products and of their ingredients and intermediates when designing toxicity testing for the intended use of these materials. The organizers defined a cleaning product as any product whose purpose is to remove a “soil”². “Soils” can be complex and variable. Examples of “soils” include grass stains on clothing, scale on shower walls, and biological material on a scalpel. The chemical heterogeneity of soils, together with the diversity of surfaces to be cleaned, necessitates the use of a variety of different types of chemical agents. Addressing cleaning products is a challenge, since cleaning products are typically complex formulations, with each component serving a specific function. Thus, a single cleaning product may be a mixture of surfactants, builders with an array of functions (e.g., anti-corrosion, deflocculation, chelation), solvents, antimicrobials, enzymes, dyes, fragrances, preservatives, and water (ACI, 2024).

Broadly, participants recognized three potential applications of *in vitro* respiratory irritation assays for cleaning product formulations and/or ingredients, with the idea that the test should fit the objective and context of use: (1) qualitative or semi-quantitative screening-level hazard identification, (2)

industry qualitative or semi-quantitative risk assessment, and (3) deriving a toxicity reference value (TRV, a generic term for health benchmark values such as a Reference Concentration, RfC) or a quantitative risk assessment conducted for the purposes of regulatory acceptance (Table 1). Industry may utilize qualitative screening-level hazard identification to inform inclusion or exclusion of ingredients in formulations, or to identify product formulation candidates for further development; regulatory bodies may use screening-level hazard and/or exposure assessments to prioritize chemicals for TRV derivation or a full risk assessment. For example, a negative respiratory irritation result in a simpler *in vitro* test may be sufficient to pass hazard screening of an ingredient or cleaning product internally, so that the ingredient/product can undergo further testing in a more complex *in vitro* system. Alternatively, a positive result may result in a decision not to proceed with development or use of that formulation or ingredient.

In industry, internal risk assessments (qualitative or semi-quantitative) can be conducted for product formulations or ingredients. This may be the final risk assessment step for cleaning product formulations, or this step may act as a precursor to the quantitative risk assessment for regulatory purposes for single chemical ingredients used in the cleaning product. For example, under Federal Insecticide, Fungicide and Rodenticide Act (FIFRA)³, which regulates cleaning products with antimicrobial claims, there are different regulatory testing requirements for product formulations (which are typically complex mixtures) versus individual ingredients. Specifically, evaluation of antimicrobials under FIFRA requires acute inhalation toxicity studies of the active ingredient and end-use product; a repeated dose (90-day) animal study may be required for the active ingredient(s) but repeat-dose testing is not required for the mixture in the final product (CFR, 2013). Risk is evaluated for new and existing chemicals under the TSCA, and for worker exposure under the Occupational Safety and Health Act (OSHA), but there are no associated minimum data requirements. The FIFRA testing requirements and lack of specific testing requirements under TSCA and OSHA mean that respiratory irritation may not have been evaluated *in vivo* for the cleaning product. Therefore,

2 The State of California (Breast Cancer Prevention Partners, 2017) defines a general cleaning product as “a soap, detergent, or other chemically formulated consumer product labeled to indicate that the purpose of the product is to clean, disinfect, or otherwise care for fabric, dishes, or other wares; surfaces including, but not limited to, floors, furniture, countertops, showers, and baths; or other hard surfaces, such as stovetops, microwaves, and other appliances.” The U.S. EPA Safer Choice Program for cleaning products addresses products that clean in the following categories: all-purpose, hard surface, glass, degreasers, kitchen and bath, hand dish, drain cleaning and maintenance, floor care, carpet care, car care, laundry, dish detergents, marine cleaning, graffiti removal, and odor removal (U.S. EPA, 2015).

3 Antimicrobials were not the intended focus for this workshop.

manufacturers and formulators may use NAMs internally to inform respiratory irritancy and potency of cleaning product formulations that are not captured in *in vivo* tests and not required in regulatory submissions. This internal use of NAMs by manufacturers and formulators was the primary, but not exclusive, focus of the workshop.

The quantitative or final assessment in industry for cleaning product formulations and ingredients may be submitted for regulatory approval, which requires different types of acute and repeated dose toxicity tests, as described above. The regulatory authorities review these quantitative risk assessments or may develop their own risk assessments and derive TRVs. This level of regulatory review and acceptance is not covered in detail in this manuscript, as the intent is to cover evaluation of cleaning products prior to when this type of quantitative assessment is applicable.

Due to the wide variety of cleaning products, chemical classes were not specified as part of defining the scope of the workshop. However, it is acknowledged that certain approaches (exposure systems, calculation methods, *in vitro* cellular or tissue test systems, etc.) are not appropriate, not relevant, or are less desirable for certain chemical classes and/or physicochemical characteristics, and this was noted when appropriate. It was noted that typical liquid aerosol particle sizes generated during cleaning product use would be expected to be $>10\ \mu\text{m}$, and that pulmonary deposition is often considered to be restricted to particles smaller than $10\ \mu\text{m}$. Thus, it is generally assumed that cleaning products are unlikely to generate particles small enough to reach the pulmonary region of the lung. However, some products/ingredients may increase or reduce particle size prior to reaching the breathing zone. Additionally, all particulate exposures occur with a size distribution, rather than as a single uniform size, and may even be multi-modal, such that an aerosol with a particle median diameter $>10\ \mu\text{m}$ could still have a substantial fraction of smaller particles depending on its size distribution. Further, particles of $10\text{--}30\ \mu\text{m}$ can deposit in the tracheobronchial region and upper airways. Therefore, consideration of the entire particle size distribution and characterization of the particle size distribution under relevant exposure scenarios is important, especially as it determines the location of deposition in the respiratory tract. As further addressed in [Sections 3.1.2, 6.2](#), the Multi-path Particle Dosimetry (MPPD) model uses particle size distribution in calculating deposited dose.

[Delmaar and Bremmer \(2009\)](#) conducted an extensive investigation of the mass generation rate and particle size distribution of spray cans and trigger sprays, as part of the development of the ConsExpo spray model, which is commonly used for modeling exposures to consumer products. They found that trigger sprays, which use mechanical force, produce larger aerosols than spray cans, which use a pressurized propellant gas. For almost all of the cleaning products tested, 1.3% or less of the total mass sprayed had a particle size $\leq 10\ \mu\text{m}$; the sole exception was a spray can product with 9% of the mass having a particle size $\leq 10\ \mu\text{m}$. These data support the assumptions described in the previous paragraph, but it is important to ensure that particle size distribution is assessed during product development.

For the purposes of the workshop, exposure scenarios of interest were defined as acute episodic exposures and repeated exposures, relevant to consumer and occupational exposure environments (e.g.,

workers at commercial cleaning companies). The workshop specifically excluded from its scope issues related to assessment of effects after subchronic or chronic repeat dose inhalation testing, including evaluating systemic effects. Rather, the assays addressed by the workshop would often be used for ranking and screening or creating context regarding effects as part of a weight of evidence (WOE) evaluation for product safety.

The public was invited to the workshop, and specific expert panelists from industry, government organizations, and non-governmental organizations were invited to attend. It is acknowledged that this method of invitation likely did not result in attendance fully representative of worldwide experts. The goals of this workshop were to (1) review *in vitro* cellular and tissue-based NAMs for evaluation of respiratory irritation, (2) examine different perspectives on current challenges and suggested solutions, and (3) publish a manuscript of the proceedings. The aim of these proceedings is to assist the cleaning products industry in best practices and principles (including identification of potential issues and concerns) when selecting testing methods to assess the respiratory irritation potential of their products.

The plenary session included an introduction to adverse outcome pathways (AOPs), as well as an overview of available exposure systems and *in vitro* cell/tissue culture test systems. [Section 2](#) of this manuscript introduces the use of AOPs to inform application of NAMs data. The panel discussions were focused primarily on three-dimensional (3D) transwell insert test systems derived from either primary cells (also known as reconstituted human airways [RHuA]) or cell lines cultured at the air-liquid interface (ALI). Other test systems are available but were not considered in detail by the panelists. These additional test systems include submerged cultures, cell lines (e.g., H292 [muco-epidermoid carcinoma], A549 [alveolar basal epithelial cells], and BEAS-2B [normal human bronchial epithelium, immortalized]), organoids and spheroids, lung on chip systems (often with 3D test systems, cell lines, and organoids incorporated into them), and human precision cut lung slices (hPCLS). Further information on different test systems and their advantages and disadvantages are discussed in other literature ([Zavala et al., 2020](#); [Polk et al., 2016](#); [Clippinger et al., 2018b](#)). Specific issues identified include choice of cell/tissue test system and exposure system, and the importance of considering inter-individual variability in the test systems and time course of potential responses.

The initial plenary introduction was followed by three concurrent breakout sessions, on exposure methods, *in vitro* cell/tissue test systems, and application considerations for human health protection. Charge questions for the breakouts are presented in the [Supplementary Material](#). These breakout sessions are summarized in [Sections 3, 4, 6](#), respectively. [Section 5](#) summarizes an illustrative (and not specifically recommended) option for a tiered testing approach that was discussed by the breakout group on *in vitro* cell/tissue test systems. The breakouts were followed by plenary summaries of the breakout sessions and associated discussion.

A key feature of the workshop was to provide the opportunity for sharing diverse perspectives, especially as NAMs represent an emergent technology. Therefore, no attempt was made to reach consensus, although areas of agreement are noted. Where participants disagreed, alternative perspectives are presented in these proceedings. Finally, the focus of these proceedings is to

summarize the discussions that occurred *at the workshop*. Some additional explanations have been added for clarity, but these proceedings are not intended to be a comprehensive review of the literature. Where specific examples are listed, this is intended to provide context, rather than being exhaustive.

2 Use of adverse outcome pathways to inform application of NAMs data

AOPs play a key role in the use of NAMs in human health risk assessment. An AOP is defined as “a sequence of events commencing with initial interactions of a stressor with a biomolecule in a target cell or tissue (i.e., molecular initiating event [MIE]), progressing through a dependent series of intermediate events, and culminating in an adverse outcome” (OECD, 2017; OECD, 2018b). These intermediate events are termed Key Events (KEs), and the response-response relationship between KEs are termed Key Event Relationships (KERs). An AOP is similar to mode of action (MOA), but the AOP begins with the molecular interaction of the chemical and a target, and does not consider physicochemical properties or absorption, distribution, metabolism and elimination (ADME), which are key determinants of a MOA. By excluding the chemical-specific parts of the MOA, an AOP is “chemically agnostic,” facilitating application of an AOP in a modular fashion to various chemicals and additional stressors (Villeneuve et al., 2014a; Villeneuve et al., 2014b).

An advantage of the AOP conceptual construct is that it provides the structure for designing a testing strategy based on MIE, KEs, and KERs within an AOP, which can then be assessed using *in vitro* methods (Clippinger et al., 2018a; Carusi et al., 2018; Leutlich et al., 2021). A fully defined AOP is not always needed to comprehensively understand likely and important key events of pathogenesis induced by an exposure; instead, testing may be focused on mechanistically characterizing one or a few KEs. It is important to evaluate NAMs data based on mechanistic understanding and based on data from other, well-studied chemicals. An Integrated Approach to Testing and Assessment (IATA) provides a framework for integrating all of the available data and data types in support of the application of NAMs (Worth and Patlewicz, 2016; Kang et al., 2021). An IATA is designed to obtain and combine salient information to allow a decision to be made in the most efficient way, accounting for the context of use. As defined by the U.S. National Toxicology Program⁴, an IATA “provides a means by which all relevant and reliable information about a chemical is used to answer a defined hazard characterization question. Information considered can include toxicity data, computational model predictions, exposure routes, use cases, and production volumes” and may include various AOPs. A defined approach (DA) consists of a selection of information sources (e.g., *in silico* predictions, *in chemico*, *in vitro* data) used in a specific combination, and resulting data are interpreted using a fixed data interpretation procedure (DIP) (e.g., a mathematical, rule-based

model). A DA can be used in an IATA or on its own to satisfy the need for hazard information. A DA “can be applied to data ... generated with a defined set of information sources to derive a prediction without the need for expert judgment ...” and is intended to overcome some limitations of the individual, stand-alone methods (OECD, 2020; OECD, 2022; OECD, 2023). For example, several DAs were developed to characterize various key events based on an established AOP for skin sensitization (Kleinstreuer et al., 2018).

Although no respiratory irritation AOP has been developed⁵, some efforts have used existing AOPs to inform human health risk assessment for respiratory toxicity, including respiratory irritation. Clippinger et al. (2018a), Clippinger et al. (2018b) described considerations and tools that are useful to develop an IATA for assessing acute inhalation toxicity, informed by KEs in various possible AOPs. Ramanarayanan et al. (2022) described an AOP-based approach to assess respiratory toxicity of a contact irritant using a NAM, which was subsequently developed into an OECD case study (OECD, 2022). Pauluhn (2022) noted the importance of considering respiratory tract region and physicochemical properties in the context of AOP development. Sharma et al. (2023) have developed a case study on *in vitro* systems to assess respiratory toxicity. As discussed further in the rest of these proceedings, establishing confidence in a testing approach is critical for its use in health risk assessment (van der Zalm et al., 2022).

3 Exposure methods

Rather than identifying a set of prescriptive standards for the exposure methods to be used in *in vitro* assessments of respiratory irritation, the workshop participants defined key considerations in the selection of appropriate *in vitro* exposure methods based upon the intended application of the data obtained. Such considerations are linked to the purpose and question(s) of interest in the respiratory irritation assessment, as outlined in Table 1. Therefore, it was suggested that exposure methods be selected on a fit-for-purpose basis or for the intended application or context of use (van der Zalm et al., 2022). For example, screening level or prioritization assessments may utilize submerged exposures, whereas assessments for regulatory submissions or contributions to TRV derivation may utilize *in vitro* exposures more relevant to human inhalation exposures. Given the fit-for-purpose nature of selecting *in vitro* exposure methods, documentation of the rationale for the choice of *in vitro* exposure method is needed. Use of inadequate exposure methods or lack of proper documentation of *in vitro* exposure methods can limit the applicability and reliability of the results in the hazard or risk assessment (Whalan et al., 2019; Petersen et al., 2023). Thus, participants emphasized the necessity of establishing reporting standards that adequately document the methods and provide scientific justification for the selection of those methods (van der Zalm et al., 2022). At the time the

⁴ Integrated Approaches to Testing and Assessment (nih.gov)

⁵ The respiratory irritation case study (OECD, 2022) discussed later in this report references an AOP, but that AOP is not specific to the respiratory tract.

workshop was held, no *in vitro* reporting guidelines were available; however, the United Kingdom-based National Centre for Replacement, Refinement, & Reduction of Animals in Research has since submitted the Reporting *In Vitro* Experiments Responsibly (RIVER) Recommendations (2023).

3.1 Connecting *in vitro* exposure scenario to anticipated or known human exposure

The participants highlighted the importance of the relevant *in vivo* occupational or consumer exposure scenario in selection of *in vitro* delivery method, dose selection, exposure regimen (both duration of exposure and use of recovery periods), and exposure method. However, it was acknowledged that cleaning product or ingredient characteristics must be considered in, and sometimes drive, the *in vitro* exposure design. These considerations include the testing of a single ingredient or the cleaning product mixture, the physicochemical properties of the cleaning product and/or ingredient (including aerosol size distribution), and the product packaging (e.g., spray bottle versus aerosol canister). Such aspects of the cleaning product or ingredient may inform aspects of the exposure scenario (e.g., mode of delivery based on product form) as they affect the intended use of the product and could impact performance of the assay. This section (Section 3.1) outlines considerations in selection of a relevant *in vitro* exposure based on the pertinent human exposure.

3.1.1 *In Vivo* user exposure scenario

Proper problem formulation of the *in vivo* exposure(s) of interest is foundational in the design of relevant *in vitro* exposure methods. The *in vivo* exposure scenario was discussed in terms of tailoring the *in vitro* system to the exposed populations and their range of expected and potential use scenarios. Broadly, the intended exposure scenarios of cleaning products and/or ingredients were expected to fall into three categories: (1) manufacturers/formulators (i.e., those manufacturing raw ingredients or those combining the raw ingredients into a cleaning product), (2) industrial cleaners (i.e., those using cleaning products under an occupational exposure scenario), and (3) retail consumers (i.e., those using cleaning products residentially). Each of these intended users has a different usage pattern and exposure profile, as well as varying use and types of personal protective equipment (PPE). For example, a worker in a manufacturing scenario may be exposed to a particular ingredient for intermittent periods during 8-hour or 12-hour production days or an industrial cleaner may be exposed to a cleaning product daily for the entire duration of their employment (e.g., 8 h per day for years, leading to a subchronic or chronic exposure), with or without PPE; while a retail consumer may be exposed for a short duration (e.g., 15 min) once per week over months or years with little or no use of PPE. Another categorization of user types that the participants considered was the use of three broad categories of users for the cleaning product or chemical ingredient of interest: average users, high end users, and bystanders. For example, the average retail consumer may use a product once per week, while a retail high end user may use the cleaning product once per day or more; a bystander may be a spouse or child in the home where the cleaning product is used by either an

average or superuser. Category definitions of average users, high end users, and bystanders can be established on a case-by-case basis.

In addition to consideration of the *in vivo* exposure scenario through the lens of the anticipated cleaning product or ingredient user, there are additional attributes that need to be considered in the selection of exposure methods for risk assessment of respiratory irritation. Risk assessment has historically assumed (implicitly or explicitly) a 70 kg adult male to be the receptor for hazard identification and risk calculation purposes, whereas current practice is moving toward expanding the life stages, genders, sizes, and other susceptibility factors (e.g., people with asthma; evaluation of different activity levels, which can affect minute volume) to be considered during the assessment process. Concern about potential exposure of susceptible populations to cleaning products or ingredients may affect the frequency and duration of their use in certain settings (e.g., hospitals). Further, assessments should consider not only exposure from the intended use of a product, but also the potential for exposures resulting from unintended or unexpected use of the cleaning product or ingredient, such as an acute high dose exposure from a spill. The pertinent dosing regimen may need to consider both potential for aggregate exposure to the cleaning product and/or ingredient via multiple routes, and cumulative exposure to multiple cleaning products and/or ingredients. The exposure scenario incorporates aspects of not only the duration and the intensity of exposure but may also need to consider recovery times to account for the intermittent use of cleaning products by some users (e.g., retail users). Additionally, the product form and packaging (e.g., spray bottle, pump, aerosol) will impact the use and exposure profile. These challenges related to the user populations and their use scenarios are not unique to *in vitro* models, as the same considerations are made in determining *in vivo* experimental exposure methods.

3.1.2 Determining *in vitro* exposure scenario

The variety of use scenarios described in Section 3.1.1 illustrate the importance of both the intensity and duration of the *in vivo* exposure, which in turn impacts the choice of *in vitro* exposure concentration and duration. Participants highlighted the importance of selecting a biologically relevant dose, tying the *in vitro* dose to the dose *in vivo* under the exposure scenario of interest. For example, the relevant dose metric for cytotoxicity is typically the inhaled dose per unit area. Potential dose metrics might include the external air concentration, the total inhaled deposited dose, or the inhaled dose deposited in a particular respiratory region, or amount absorbed (uptake) into cells (Phalen et al., 2021). Deposited dose is generally preferred over the external air concentration, as a better description of the amount of the chemical interacting with the target tissue. The particle size distribution (e.g., mass median aerodynamic diameter [MMAD] and geometric standard deviation [GSD]) are key determinants of particle deposition, and these in turn depend on the form of the product (e.g., spray bottle, pump, aerosol). The same cleaning product formulation in different types of packaging can produce different particle size distribution profiles. Dosimetry models, which consider the respiratory tract physiology, different breathing conditions, and particle size distribution, are useful to translate exposure to delivered dose metrics and thereby help connect the *in vitro* exposure method to the *in vivo* exposure of interest as

addressed further in [Section 6.2](#). Application of dosimetry models allows for determination of the dose delivered to various respiratory regions under the physiological breathing condition(s) of interest such as breathing mode (nasal, oronasal, or mouth breathing only) and breathing rate ([Jarabek et al., 2005](#); [Kuempel et al., 2015](#); [Asgari et al., 2021](#)). The user or bystander respiratory tract physiology and breathing rate should be considered in the *in vitro* cell/tissue test system ([Section 4](#)).

Participants noted that dosimetry models can calculate a wide variety of dose metrics, reflecting the tissue dose under the human *in vivo* exposure conditions, and informing the target delivered dose level for the *in vitro* respiratory irritation model. Deposition can be calculated on a regional basis, or models may make more localized predictions, helping to inform potential target cell types. Deposition can be calculated for a cleaning product formulation or for an individual ingredient. Depending on the physicochemical properties of the inhaled aerosol or gas, other potential dose metrics include flux to the tissue (a measure of mass per area per unit time) (e.g., [Kimbell et al. \(2001\)](#)) or measures of the amount of reactivity within the tissue, such as DNA-protein crosslinks (e.g., [Conolly et al. \(2023\)](#)). Some models also account for systemic absorption and distribution (e.g., [Sweeney et al. \(2013\)](#)). In the case of a mixture, such as a cleaning product, the flux could potentially vary for each chemical although flux of the mixture is what would be needed as input to such models and could potentially be adjusted by molecular diffusivity for individual components. One participant noted that the flux of that chemical could be influenced by the mixture itself. Some participants opined that incorporation of flux into dosimetry models for respiratory irritation could add unnecessary complexity to the model, but others noted that it is a fundamental input parameter to compute internal dose of most models (e.g., PBPK, CFD, single pass mass transfer) and is easily characterized.

Some participants discussed the additional utility of dosimetry models (e.g., the MPPD model, the International Commission on Radiological Protection Human Respiratory Tract Model [ICRP HRTM], and computational fluid dynamics [CFD] or computational fluid particle dynamics [CFPD] models) in informing selection of the relevant *in vitro* cell/tissue test system by aiding in identification of the respiratory tract region or cell types with the greatest deposition or flux ([ICRP, 2015](#); [Corley et al., 2021](#); [OECD, 2022](#); [Ramanarayanan et al., 2022](#); [ARA \(Applied Research Associates\), 2024](#)). Alternatively, participants discussed that the most sensitive respiratory tract region or cell type, rather than the region with the greatest deposition, could be used as the basis for the *in vitro* cell/tissue test system. Based on the description of particle sizes generated from cleaning product use as $>10\ \mu\text{m}$, it is assumed that it is unlikely for a significant portion of the aerosol distribution to reach the pulmonary region, but this depends on the geometric size distribution. Importantly, post-generation characteristics of aerosols should also be evaluated. For example, evaporation of volatile components can result in a reduction of aerodynamic diameter between generation, inhalation, and deposition. Consideration of the entire particle size distribution is also important, and if the distribution includes particles small enough to reach the pulmonary region, the implication of their exposure needs to be considered.

In selecting or designing an *in vitro* cell/tissue test system, one must consider the biological relevance of the cells or tissues exposed

in vitro to those that are exposed *in vivo*, since different cell types may have qualitatively or quantitatively different responses to the same exposure ([Faber et al., 2020](#)). Considerations related to cell and tissue test system selection based on deposition distribution and anchoring to AOPs are discussed in further detail in the *In Vitro* Cell/Tissue Test Systems section ([Section 4](#)) of this report.

Participants noted that exhalation and clearance *in vivo* have an impact on the tissue dose, but these processes are not well characterized or represented in *in vitro* assays. For particles, *in vivo* clearance mechanisms such as mucociliary clearance or removal via alveolar macrophages can reduce the tissue dose; particle transport and deposition during *in vivo* exhalation can also affect local cell/tissue dose. Some participants considered the lack of clearance mechanisms *in vitro* to be a challenge in utilizing dosimetry models to inform dose selection and duration of exposure. Other participants noted the utility of dosimetry models to predict the net deposition (*i.e.*, deposition occurring on both inhalation and exhalation) and that computational fluid-particle dynamics (CFPD) models can predict doses localized to specific cell types, to aid in comparing *in vivo* and *in vitro* doses. Some participants emphasized the use of washing and recovery periods *in vitro* to simulate *in vivo* clearance but acknowledged that this does not capture the intricacies of the biological process of clearance *in vivo*; further, it was noted that washing may remove important components, such as ELF. The ELF plays several complex roles that were acknowledged, but not fully explored at the workshop, including metabolic activation of chemicals ([Pulfer et al., 2005](#); [Squadrito et al., 2010](#); [Pauluhn, 2021](#)). *In vitro* cell/tissue test systems may be unable to capture the complex *in vivo* dynamics of ELF production and transport, or of tissue remodeling after chemical insult that may impact exposure *in vivo* ([Mudway and Kelly, 2000](#); [Ng et al., 2004](#); [Henderson, 2005](#); [Ciencewicki et al., 2008](#); [Chanez and Bourdin, 2008](#); [Darquenne, 2012](#); [U.S. EPA, 2019b](#); [US EPA, 2020](#)). The major implication of the inability to adequately represent respiratory tract clearance *in vitro* is uncertainty regarding how accurately *in vitro* dose reflects *in vivo* exposure and effects. Some participants wondered whether the lack of such clearance mechanisms *in vitro* allows for use of shorter duration exposures to simulate the human *in vivo* exposures. Other participants noted that consideration of ADME and MOA is important. For example, the relevant dose metric may be the parent or the metabolite, and peak versus area under the curve (AUC) for either might be the most relevant. Generally, some participants recommended that better characterization of the *in vitro* dose is needed to build confidence in the use of *in vitro* models.

3.2 Technical considerations in *in vitro* exposure

In addition to tailoring the *in vitro* exposure design based on the pertinent *in vivo* exposure scenario(s), there are technical considerations regarding basics of study design and quality that are important in all scientific endeavors, *in vitro* and *in vivo* alike. Just as detailed and accurate documentation of exposure protocols are necessary for *in vivo* studies, similarly detailed documentation is needed for *in vitro* studies ([Percie du Sert et al., 2020a](#); [Percie du Sert](#)

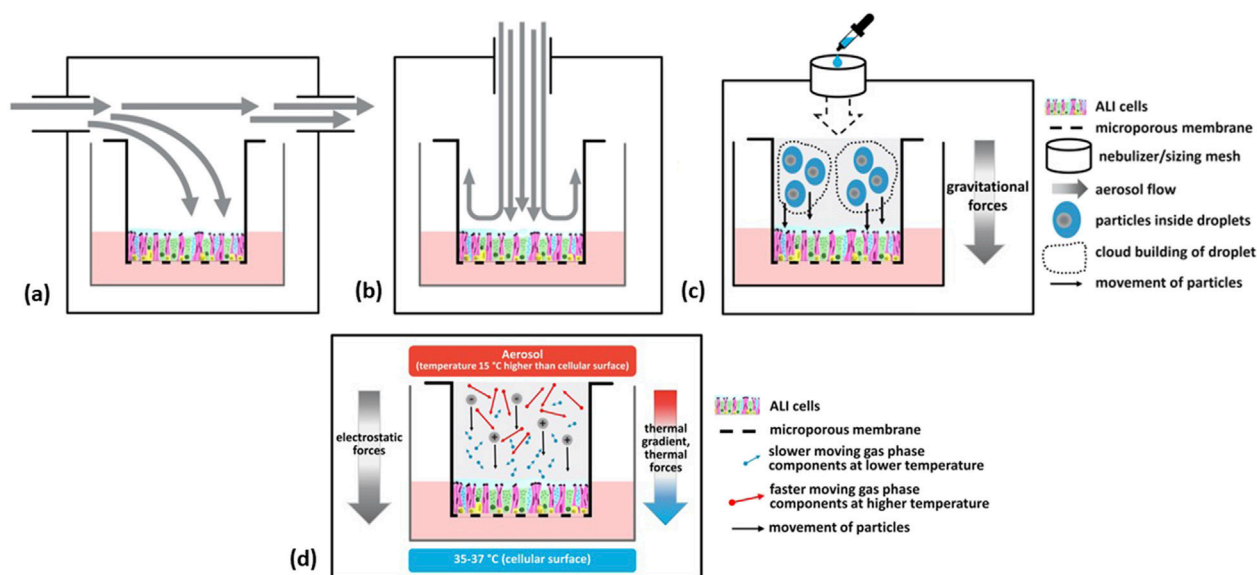


FIGURE 1
Schematics of various air-liquid interface (ALI) exposure systems. Continuous flow exposure systems include parallel horizontal (A) and perpendicular (B) that can provide for alignment of fluid dynamics; or cloud (droplet sedimentation) in an incubator/box type or stagnation point flow type that relies on gravitational forces (C). Electrostatic forces or thermal gradients may be used to enhance deposition (D). (Figure courtesy of A.M. Jarabek).

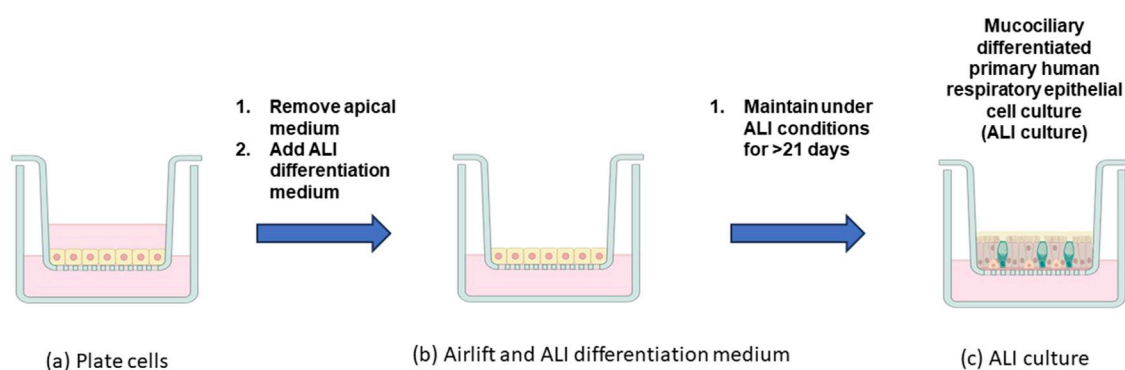


FIGURE 2
Differentiation of primary human respiratory epithelial cell models. Cells are plated on cell culture inserts containing porous membranes (A). After the cells reach confluence, the apical medium is removed ("airlifted"), and the basolateral medium is replaced with ALI differentiation medium (B). The airlifted cultures are maintained under ALI conditions for >21 days, resulting in the (differentiated) ALI culture (C). Created with BioRender. (Figure courtesy of S. McCullough).

et al., 2020b; Whalan et al., 2019; Wong, 2007). For example, documentation of the exposure system should include the accurate identification and characterization of the cleaning product and/or ingredient, exposures utilized and details regarding preparation of dilutions, exposure method, analytical methods, exposure duration, and washing protocols if used, among others. In addition, the rationale for the exposure protocol should be included. The participants addressed three categories of important technical considerations for the use of *in vitro* NAMs in evaluation of the respiratory irritation of cleaning products and ingredients: exposure delivery method, dose quantification, and utilization of controls.

3.2.1 Exposure delivery method

The three main types of exposure delivery systems that the participants discussed were: (1) submerged culture exposures (i.e., cultures that have never been cultures under ALI conditions), (2) direct liquid application to cells that have been grown at the ALI, and (3) ALI exposures. ALI exposure systems include continuous flow (parallel or incubator/box type and perpendicular or stagnation point flow type) that can provide for alignment of fluid dynamics, and cloud or droplet sedimentation types (e.g., ALICE-Cloud; Vitrocell® Cloud) that rely on gravitational settling (Lewinski et al., 2017; Lacroix et al., 2018; Braakhuis et al., 2023). Various ALI exposure systems are illustrated

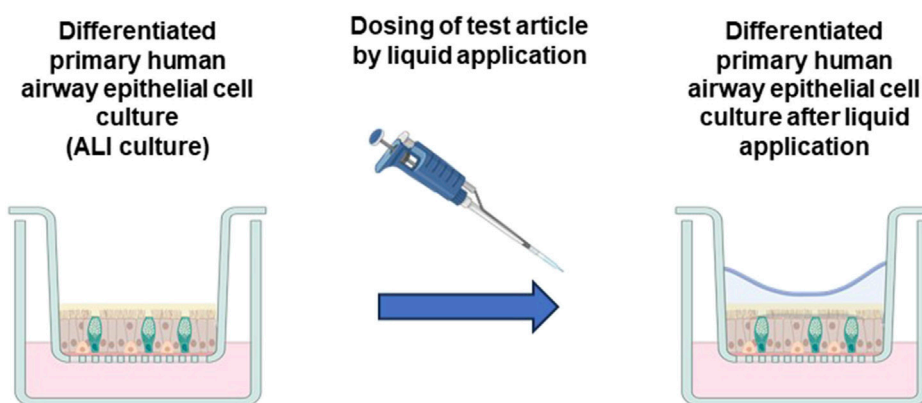


FIGURE 3

Transition of ALI cultures to liquid-liquid interface by liquid application dosing. ALI respiratory tract models are differentiated under ALI conditions, which involve exposure of the apical culture surface to ambient air and mimic the environment of the respiratory epithelium *in vivo*. Test article dosing by liquid application involves the addition of liquid to the apical culture surface, thus abolishing ALI conditions and resulting in a liquid-liquid interface. Created with BioRender. (Figure courtesy of S. McCullough).

schematically in Figure 1. Continuous flow systems are used for gases, complex mixtures, or particles of chemicals or materials which are available in larger quantities (several g) under a constant delivery for longer exposure durations. Cloud systems are used for single chemical droplet sedimentation or dry powders of materials that are scarce or expensive and for shorter exposure durations. The three main types of exposure delivery systems introduced at the beginning of this paragraph are discussed in greater detail in the following paragraphs.

It was acknowledged that these exposure methods coupled with cell/tissue systems represent different degrees of biological fidelity pertaining to the endpoints and nature of the responses. The level of biological fidelity required for the exposure depends on the exposure scenario being modeled. Numerous viewpoints regarding the appropriate use of these three exposure systems, as well as the degree of biological fidelity, were expressed by participants. Notably, discussions largely excluded detailed aspects of exposure relating to electrostatic or thermophoresis particle deposition, lung-on-a-chip technologies, and hPCLS.

Some participants felt that submerged culture exposures have limited or no value in respiratory irritation hazard and risk assessment due to a high degree of uncertainty and lack of biological fidelity (Lenz et al., 2009); others asserted that the ease of conducting submerged exposures make them useful for certain applications, such as high-throughput screening.

In contrast to submerged culture, ALI culture systems allow for the basal surface of the cells to be maintained on a membrane in contact with cell medium while the apical surface of the cells are exposed to air with the toxicant. Establishing and maintaining ALI conditions is critical for the *in vitro* differentiation of primary human respiratory epithelial cell cultures (Figure 2) (Fulcher et al., 2005; Ross et al., 2007; Rayner et al., 2019; Randell et al., 2011; Pezzulo et al., 2011; Kouthouridis et al., 2021). The generation of ALI respiratory tract models involves plating primary respiratory epithelial cells on cell culture inserts containing porous membranes (Figure 2A). Once they reach confluence, the apical medium is removed (“airlifted”) and the basolateral medium is replaced with

ALI differentiation medium (Figure 2B). Airlifted cultures are then maintained under ALI conditions, with regular basolateral medium changes, for >21 days (actual duration differs based on the medium formulation used and how the completion of differentiation is defined). Following the ALI differentiation period, nasal and tracheobronchial cultures exhibit columnar ciliated epithelial cells with beating cilia, goblet cells that secrete mucus (shown in yellow), and basal epithelial cells (Figure 2C). A549 adenocarcinoma cells maintained under ALI conditions for extended periods of time (i.e., weeks) can differentiate to express type I and type II pneumocyte markers (Wu et al., 2017). As noted in Figure 1, ALI exposures utilize different delivery systems to expose cells at the ALI to gases, vapors, or aerosols. ALI exposure systems using various cell/tissue models represent promising exposure systems for nanoparticles, and they have been shown to provide transferability and reproducibility (Braakhuis et al., 2023). Recommendations for refinement of ALI exposure systems include developing a stepwise standard operating procedure (SOP) for operation and training personnel (Braakhuis et al., 2023).

Direct liquid application involves applying small volumes of test chemicals to the apical surface of ALI cultures; the delivery liquid may or may not be washed off at various durations, depending on the design of the experiment. Importantly, however, the addition of the liquid abolishes ALI conditions and results in a liquid-liquid interface (Figure 3). Reported usage of liquid application dosing includes a wide range of volumes; however, the ability of those volumes to completely cover the cell layer at the beginning and end of experimental exposures is typically not demonstrated. Further, the effect of applying the vehicle liquid on ALI cultures is similarly not demonstrated. A recently published study empirically determined the smallest liquid volume that would maintain complete coverage of ALI cultures for a 24-hour exposure and evaluated the effects of those conditions on ALI culture physiology (Mallek et al., 2024). This study demonstrated that application of liquid alone (i.e., in the absence of a test article) caused substantial changes to the physiology of ALI-differentiated primary human bronchial epithelial cells, including reduction in

epithelial barrier integrity, activation of several cellular signaling pathways, and induction of pro-inflammatory cytokines and growth factors (Mallek et al., 2024). These changes were consistent with a range of respiratory diseases, as well as the effects of inhaled irritants, and the authors indicated that the effects of liquid application alone were likely to confound the interpretation of test article exposures. The observations reported in the Mallek et al. (2024) study were made with a single liquid vehicle at two liquid exposure durations. Thus, additional studies are required to determine whether similar effects occur under other liquid dosing conditions. The Mallek et al. (2024) study also demonstrated that commonly used applied liquid volumes, when applied to larger membrane diameters, do not maintain complete coverage of the cell layer after 24 h of exposure. While small volumes are typically used to minimize applied liquid depth, Mallek et al. asserted that the ability to maintain consistent coverage of the cell layer and thus avoid inconsistencies in culture conditions and test article exposures should be demonstrated for each set of exposure conditions used.

Some participants asserted that ALI exposures may be more biologically relevant than submerged exposures or direct liquid application to cells that were grown at the ALI for inhaled exposure to cleaning products and ingredients with intended applications as aerosols or sprays. Participants recognized that limitations of sedimentation cloud systems may include an inability to characterize how airflow affects particle transport and deposition *in vitro*, so that translation to *in vivo* particle sizes or airway concentrations is limited. Others felt that the value of data from an ALI exposure system outweighs the associated costs and challenges. Introduction of salts to the cleaning product for the nebulizer to create the exposure clouds is another limitation of sedimentation type ALI systems. In contrast to continuous flow systems, which allow for a slower deposition and accumulation of test article on exposed cultures, cloud systems deliver one or more bolus dose(s) of the test article. While cloud exposures can be highly relevant for the modeling of brief exposures (e.g., exposure of a consumer during the use of a cleaning product), they may not represent the kinetics of exposure that occur in longer occupational exposures (e.g., continuous exposure during an eight-hour workday). Importantly, the generation of large diameter liquid droplets for cloud exposures may result in the sedimentation of total liquid volumes over a short period of time that could be similar conditions to liquid application (Loret et al., 2016). When using cloud-based exposures, actual liquid volume deposition should be evaluated and comparisons between vehicle and incubator control cultures should be conducted to evaluate effects of the exposure method.

Some participants said that, in their experience, direct liquid application to cells that were grown at the ALI allows greater ease of conducting experiments and for more control of dosing than cloud exposure; but the range of ALI exposure systems is noted in the literature as providing a wide range of optimized fluid dynamics and effective cell contact (Lacroix et al., 2018). Finally, some participants mentioned some of the challenges of the ALI exposures, such as creating a setup that delivers a physiologically appropriate flow of material to the cell surface (Lacroix et al., 2018), but these considerations can be addressed with proper characterization

(Lacroix et al., 2018; Braakhuis et al., 2023) or may be addressed by other emerging *in vitro* systems, such as lung-on-a-chip technologies (Bajaj et al., 2016).

The physicochemical properties of the cleaning product or ingredient may necessitate use of either liquid application or ALI exposures. For example, participants noted that ALI exposures are more appropriate for the delivery of volatile compounds that are insoluble in liquids (Zavala et al., 2018; Mistry et al., 2020). In another example of the importance of physicochemical properties, the INSPIRE project (*IN vitro* System to Predict Respiratory toxicity) required a modification to methods related to the mode of exposure, as vapor exposures had to be reduced in duration (from 1 h to 30 min) because the silanes being tested hydrolyzed rapidly in humid conditions (Sharma et al., 2023). This is likely a widespread issue for both volatile organic compounds (VOCs) and reactive gases given that ALI exposures require high relative humidity (RH) to mimic physiological conditions. Both RH and exposure concentration should be measured to address this concern, as nominal concentrations will likely be inaccurate and do not reflect actual exposure concentrations. Other participants noted that other, less-characterized, exposure methods may provide approaches for testing materials with low solubility in aqueous solutions, or that degrade in water-based solvents. An example of such methods includes the microvolume deposition of dimethyl sulfoxide (DMSO)-based liquids in the form of very small volume droplets (Behrsing et al., 2017). Participants recognized that some physicochemical properties, such as viscosity, may limit the feasibility for ALI exposures, necessitating liquid exposure. However, viscosity would decrease substantially when the ingredient is incorporated into the cleaning product formulation, which could then be tested via ALI exposure.

Participants also acknowledged that the exposure delivery method can impact the biological properties of the *in vitro* cell/tissue model and the toxicity of some xenobiotics. For example, direct liquid applications to an *in vitro* differentiated primary respiratory cell model altered the transcriptome, biological pathways, activation of several cellular signaling pathways, induced the secretion of pro-inflammatory cytokines and growth factors, and compromised epithelial barrier function relative to cultures maintained at the ALI and exposed to the same delivered dose (Mallek et al., 2024). Similarly, some participants postulated that powders of low or minimal toxicity may become toxic once mixed with the mucus (irrespective of dosing method), due to facilitated delivery into cells by the liquid components of mucus and/or formulation. Another example was that exposure to zinc oxide nanoparticles resulted in different toxic responses following submerged liquid and ALI exposures (Lenz et al., 2009). These studies demonstrate that (1) adherence to recommendations of the exposure system manufacturer for operating parameters is important; (2) biological responses may differ based on the exposure method used rather than the chemical, (3) biological changes should be interpreted in the context of the exposure application to identify chemically induced toxicological effects, and (4) biologically relevant systems (e.g., delivery method, particle size, chemistry, etc.) should be utilized to predict *in vivo* responses.

3.2.2 Measurement and quantification

The administered concentration, the dose delivered to the *in vitro* system, and the intracellular dose represent three different important aspects of exposure. It was noted that the internal dose is the driver of the toxicological response and is the most appropriate dose metric, although it is difficult to measure and is a product of ADME. Therefore, the delivered dose, rather than the administered concentration, should be measured (Schmid and Cassee, 2017; Phalen et al., 2021). Methods for measuring the dose delivered, but not taken up by the cells, were discussed by the participants. The choice of method for measuring the concentration delivered to the cells depends on the physicochemical properties of the cleaning product.

The participants noted that one measuring approach used filter disks to collect particles to estimate deposition efficiency and determine deposition uniformity across cell culture inserts (Oldham et al., 2020b). Different deposition efficiencies based on particle size were demonstrated (Oldham et al., 2020b). Others noted that limitations of the filter paper approach include low deposition efficiency and that deposition on a dry filter disk does not mimic deposition on a moist cell surface.

In contrast, an integrated quartz crystal microbalance (QCM) was used in an inter-laboratory effort to harmonize delivered dose from the Vitrocell® Cloud system (Bannuscher et al., 2022). Use of the QCM addressed variability observed by measurement of deposition fraction on transwell inserts alone (Ding et al., 2020; Bannuscher et al., 2022). Measurements from the QCM can be used to verify homogeneity of the exposure in the chamber and across transwell inserts, which may not always occur; however, quantifying exposure homogeneity may be limited by the ability to use the QCM in wells in the middle rows/columns of devices intended for use with 12- or 24-well inserts. Regardless of the measurement method, adherence to recommended or standardized procedures or SOPs helps to promote homogeneity and reproducibility in the net deposition (Ding et al., 2020; Bannuscher et al., 2022).

Participants also acknowledged the influence of flow in the chamber on exposure delivery, especially when comparing between parallel and perpendicular flow delivery systems. Uniform mixing of aerosols was obtained with use of a dilution unit (Kuczaj et al., 2016), but others reported heterogeneous mixing of aerosols in flow chambers in a perpendicular flow system (Oldham et al., 2020a; Oldham et al., 2020b).

Participants also noted that, similar to challenges with *in vivo* chamber exposures, the measurement of a concentration in the chamber does not represent the dose delivered to the cells. Accurately characterizing the dose to the cells in ALI systems is challenging because of the variability in particle deposition in ALI systems, which is influenced by the physicochemical properties of the aerosols and the type of exposure system utilized by the study (Oldham et al., 2020a; Oldham et al., 2020b; Steiner et al., 2017). For example, in continuous flow aerosol exposure systems, losses of aerosol constituents at the inner surfaces of the exposure system components (e.g., tubing, trumpets, etc.) are commonly observed due to adsorption and other particle transport mechanisms such as impaction, and sedimentation (Steiner et al., 2018; Wong, 2007; Yi et al., 2013). In sedimentation aerosol exposure systems (e.g., Vitrocell® Cloud), the aerosol droplets tend to adhere to the inner surfaces of the chamber (polycarbonate) and the nebulizer

(Bannuscher et al., 2022). The aerosolization and deposition efficiency vary for different materials based on their physicochemical properties, such as hydrophilicity. While some of the materials may react with the polycarbonate parts of the chamber and nebulizer (with high concentrations and sufficient contact time), participants noted that this reaction may not have a significant effect on particle deposition due to comparatively shorter exposure duration (i.e., 5–10 min). Characterizing the settling velocity and time for particles generated by nebulizers using varying mesh sizes for the cloud delivery system will be important for quantifying dose delivered to the cells. Hydrophobic constituents may also adhere to the materials of cell culture insert (e.g., polyester terephthalate [PET]) at the ALI (Steiner et al., 2018). Additional parameters that affect deposition of the aerosol at the ALI include solubility in mucus, culture medium, volume, and transwell surface area, and volume (Steiner et al., 2018).

For volatile chemicals, a known volume of trapping liquid can be placed within the exposure chamber to collect deposited material. The total amount of material deposited can be determined based on the concentration of the material in the known volume of trapping liquid. Steiner et al. (2018) demonstrated that the trapping liquid influences the delivery efficiencies of constituents in smoke exposures.

For liquid application exposures, representative samples for analysis can be taken at dosing to confirm the concentration, homogeneity, and the actual (rather than nominal) exposure applied in the test system. The homogeneity has been demonstrated to be dependent on both the volume applied as well as the duration of the application (Mallek et al., 2024). Participants noted that this application concentration does not capture the dose that the cells are exposed to or take up, but rather the applied exposure dose. Further, participants recognized that, as for aerosol exposures, hydrophobic constituents in submerged cultures may also adhere to the materials of the cell culture insert (e.g., PET), and that the solubility in mucus, surface area, and volume may also affect deposition (Steiner et al., 2018).

In addition to the measurement of the exposure of the cleaning product or ingredient, participants noted that other experimental conditions should be recorded due to their potential to influence both the amount of test article delivered and the results of the *in vitro* assays. Such factors include the temperature, humidity, particle size distribution (e.g., MMAD, GSD), and density. Temperature, humidity, and ventilation can affect the experimental conditions and may or may not be controlled; they should be reported to aid in interpretation of results. Some participants felt that these challenges are not unique to *in vitro* methods and present a challenge in *in vivo* exposures as well, while others noted the use of controlled temperature and humidity *in vivo*. For liquid exposures, some participants noted that a unique challenge remains the influence of the volume of test chemical on the assay. For example, when determining the threshold for irritation for a cleaning product mixture, different volumes may be required to achieve different exposure doses, as dilution changes the composition of the mixture. This may impact the dose that directly interacts with the apical surface of the cells. Other participants noted that many assays require the use of a specific volume, and therefore this issue is not always pertinent.

3.2.3 Utilization of exposure controls

Use of appropriate controls for the *in vitro* test method selected is essential to have confidence in the data and allow for proper interpretation in the context of the control responses. Six broad types of controls were identified for use *in vitro* respiratory irritation assays: (1) vehicle controls, (2) cleaning formulation solvent controls, (3) single blank (processing) controls, (4) double blank (no processing and no dose) controls, (5) negative controls, and (6) positive controls. However, it was acknowledged that additional controls may be needed for certain assays and endpoints. Vehicle controls are essential to evaluate whether the vehicle used in the assay, rather than the cleaning product or ingredient being tested, is causing the observed outcome in the assay. If the product is intended to be diluted prior to use, the diluent is also tested as a vehicle control. Selection of the vehicle control is impacted by the assay endpoint of interest. In cases where more than one vehicle control is used, all vehicles should be characterized in the assay to evaluate the variability elicited by choice of vehicle. Solvent controls may be necessary to evaluate the effect of the cleaning product formulation solvent on the outcome of the assay. For example, if the cleaning product solvent is ethanol, the toxicity of ethanol should be evaluated separately, in addition to the toxicity of the entire cleaning product formulation. In some cases, the cleaning product solvent may inform the choice of the assay vehicle such that both are the same. Therefore, the solvent control may be the same as the assay vehicle control (e.g., both a water solvent and a water vehicle) or different (e.g., ethanol solvent control and a water vehicle control). Single blank or processing controls, which are not dosed but undergo processing, may also be necessary to evaluate the system itself. For example, in an ALI exposure chamber, while a vehicle control may be aerosolized water droplets, the blank controls may consist of pumped air or no air current (i.e., an incubator control). Double blank controls are those that receive no dosing and do not undergo the processing. For example, when using a wash, the double blank control will not be washed, to evaluate the effect of that process on the outcome of the assay. The use of positive and negative controls demonstrates that the *in vitro* test system is producing the expected response (i.e., known respiratory non-irritants are eliciting negative results and known respiratory irritants are eliciting positive results). Identification of reference chemicals to serve as positive controls that elicit positive responses in the selected *in vitro* cell/tissue system is critical to avoid false negative results (Bisig et al., 2019). Further, the use of controls contributes to characterizing the nature of the response (e.g., benchmark level) as well as intra- and interlaboratory variability in the assays (OECD, 2018a).

3.3 Conclusion

Substantial advancements have been made in recent years in the exposure methods used for assessment of respiratory toxicity. The choice of the appropriate exposure design for an *in vitro* respiratory irritation assay depends on consideration of the likely effect and the intended use of the data based on the purpose and assessment type. Thus, there is not a single correct way to design the exposure across *in vitro* respiratory irritation assessments, but there are considerations that should be kept in mind when choosing a particular exposure system. One such major consideration is the

physicochemical properties of the cleaning products and ingredients; a comprehensive review of these properties and their impact on selection of exposure methods would be useful guidance for developers and users of NAM technologies targeting these chemicals. The exposure scenario has implications in the *in vitro* cell/tissue test system selection (e.g., relevant cells or tissues based on dosimetry) and for the risk assessment (e.g., reducing uncertainties). The exposure methods utilized in an *in vitro* cell/tissue test system of respiratory irritation, and the appropriate justification and documentation of these methods, guide and can limit the scope of interpretation of the resulting data. This will help to make the resulting data useful for the desired application in screening or risk assessment.

4 In Vitro cell/tissue test systems

4.1 Considerations in characterization and standardization of *in vitro* cell/tissue test systems, assays, and reporting

To maximize the use of *in vitro* NAMs to predict respiratory irritation in response to cleaning products, the participants identified a need to use well-characterized systems and standardized procedures and develop reporting standards. These tools will facilitate reproducibility across laboratories and interpretation of data generated using *in vitro* methods. This section (Section 4) outlines some considerations relevant to these systems, procedures, and reporting standards, but is not meant to cover all possible items.

Variability in *in vitro* methods and assays can be due to several factors such as the type and “lifespan” of cell/tissue test system, culturing conditions (medium components, cell seeding density, etc.), and how the assay is performed and reported. These variations can affect the outcomes of assays, and thus pose a challenge to the use, integration, and interpretation of the results. Some participants noted that *in vivo* studies face similar challenges, with variation by species, strain, food and water, housing, and other factors. Consistent information from standardized reporting of assays can assist with the characterization of assays within defined study plans used to conduct those studies. This will, in turn, provide a clearer understanding of how differences in methods may contribute to variation in results.

Participants particularly noted an urgent need to be proactive in characterizing and potentially standardizing *in vitro* respiratory irritation assays and reporting, instead of merely summarizing comparisons or conducting retrospective analyses after data are gathered. Such characterization and standardization will facilitate the use of data from assays for a broader range of applications, including filling data gaps. As mentioned in Section 3, to further characterize assays and establish confidence in NAMs, *in vitro* test systems and assays also need to be considered in the context of Good Laboratory Practices (GLP). The principles outlined in the Guidance Document on Good *In Vitro* Method Practices (GIVIMP) (OECD, 2018a) and RIVER working group (2023) should also be considered, though GIVIMP does not have the same regulatory status as GLP and does not guarantee discussion of the rationale for choice of assay or test system. Critically, assays used in conjunction with *in vitro*

respiratory tract models would benefit from improved reporting to aid in characterization.

The longer that any research proceeds without well-characterized and/or standardized assays, the more data that may need to be regenerated to fit into standardized assays and any necessary framework. In a broader context, [Jarabek and Hines \(2019\)](#) discussed a workflow for coherent integration of *in vitro* and other evidence across a range of risk assessment and regulatory applications, including sufficiency of metadata, transparency of assumptions, and explanation of applicability domain for assays. A recent paper on liver-chip methods provides one possible model approach for standardization of *in vitro* methods, including considerations of both technical and cost aspects ([Ewart et al., 2022](#)). One example of an effort towards standardization of inhalation toxicity testing (though not specific to respiratory irritation) is the Respiratory Toxicity (RespTox) Collaborative—an international, cross-sector consortium of experts conducting *in vitro* inhalation toxicity testing (publications in preparation). The collaborative was established for developing and gaining consensus on the minimum information reporting needs for different assays. Participants were unaware of any such efforts specific to *in vitro* respiratory irritation.

Conducting a literature survey or review would identify existing data and knowledge gaps to guide generation of additional information. For example, participants noted that identifying the data available regarding the appropriateness of different assays and models for different physicochemical properties of cleaning product ingredients or formulations is a key step towards assay standardization. There will be significant challenges for conducting this survey/review in the context of respiratory irritation and cleaning products or ingredients, and for any characterization and standardization effort more broadly. Publication bias will pose a challenge as negative results from assays are critical for overall understanding of the assays. Further, small differences in methodology can also produce different results, and so incomplete documentation of methods will also be a barrier to fully understanding assays and test systems. Therefore, engagement of stakeholders and those with hands-on knowledge is critical to ensure that this additional information is captured in the analysis, as these groups will likely have the best insight into unpublished results or missing methodological details. Workshops such as the one that is the basis for the current publication can play an important role in gathering perspectives from a diversity of scientists and can inform or supplement a literature survey/review. The following paragraphs outline some considerations that may be addressed in more detail by such a literature survey/review and/or future workshop, but this list is not exhaustive.

There is a wide range of available cell/tissue models that have been utilized to evaluate respiratory irritation potential *in vitro*. Most discussion at the workshop focused on primary monocultures versus cocultures, but the considerations apply more broadly to cell/tissue test system selection. First, resemblance between *in vivo* and *in vitro* responses needs to be considered when characterizing *in vitro* cell/tissue culture methods and developing standardized approaches. For example, primary cells and immortalized cell lines will respond differently under the same exposure conditions for

some, but not all, assays and exposures. Therefore, understanding the differences in response and identifying which more closely resembles the *in vivo* response is critical in selection of the cell/tissue test system. Second, accessory cell types (e.g., fibroblasts, macrophages) may act as mediators or moderators or exert more direct effects on the responses to exposure, even if these cells are not directly in contact with the chemical. A mechanistic understanding of respiratory irritation can provide information on when accessory cell types need to be included and which cell types should be considered. Third, the appropriateness of cell/tissue test systems is dependent on the KEs under investigation, which are affected by the physicochemical properties of the test article. For example, there are at least 41 cell types in the lung, including bronchiolar and alveolar epithelial cells, and different cell types are known to respond differently to the same compounds, due to their different biology ([Parent, 2015](#); [Harkema et al., 2018](#)). Finally, it will be necessary to characterize the background response variability of the available *in vitro* cell/tissue test systems to differentiate test system variability from exposure-related effects ([van der Zalm et al., 2022](#)). Generally, the factors listed here inform test system selection, but both the feasibility of use and the access to relevant cell/tissue test system must be considered. For example, primary cells can be expected to be more representative of *in vivo* responses but there may be logistical or cost barriers to using them.

There is a tradeoff between phenotypic complexity of the *in vitro* cell/tissue test system and throughput. More complex systems (e.g., ones including multiple cell types and/or 3D structure) tend to be more expensive and time-intensive to run, while the higher throughput systems tend to be less sophisticated but may not produce fully tissue-relevant data. These opposing forces will need to be balanced, and this balance may be prioritized differently depending on the purpose and stage of the assessment ([Table 1](#)).

Participants noted that some *in vitro* cell/tissue test systems or assays relevant to respiratory irritation will be easier to standardize than others. For example, ciliary beat frequency (CBF) can indicate impaired ciliary motility and mucociliary transport via mucin hypersecretion triggered by respiratory irritants, as seen in diseases such as asthma and cystic fibrosis ([Bustamante-Marin and Ostrowski, 2017](#)). CBF may be relatively easy to standardize and technical considerations and recommendations have been made ([Behrsing et al., 2022](#)). For technical proficiency in this endpoint, it will be key to record video with maximum contrast between light and dark, making it easier to identify the effect with appropriate analysis software. Additional examples were not discussed as part of this workshop, but similar suggestions and considerations for characterizing and standardizing assays would apply to other endpoints.

The medium used in a particular cell/tissue test system may affect what endpoints can be tested. Different medium choices can have an impact on physicochemical properties of the test article and have different effects on cell morphology/physiology/function and response in the same cell system ([Saint-Criq et al., 2020](#); [Leung et al., 2020](#); [Lee et al., 2020](#)). Each *in vitro* cell/tissue test system has particular medium requirements, especially for co-cultures with different media and media mixtures being used at various stages of culturing ([Klein et al., 2013](#)), and laboratories may use in-house formulations rather than commercial media. These in-house media

are likely to differ across laboratories and therefore should be reported. Some commercially available test systems (e.g., from Mattek and Epithelix) can be purchased with medium specifically developed for the test system. When new endpoint assays are implemented, they should be optimized to the manufacturer's media whenever possible. Where the medium has to be changed, careful evaluation of the medium change should be conducted with suitable control groups.

Another consideration is that the choice of *in vitro* cell/tissue test systems, respiratory irritation assays, and modes of exposure depends on the physicochemical properties of test chemicals. An understanding of the relationship between different sets of physicochemical properties and the appropriate choice among emerging cell/tissue test systems will be useful. For example, the choice of hPCLS culture method has implications for hPCLS assays used for cleaning products with aerosol exposure. Aerosol exposures are possible using the hPCLS ALI (tissue culture insert) method, but not possible using hPCLS roller culture method or submerged cultures (Patel et al., 2021). More generally, in exposure at the ALI (e.g., complex coculture or hPCLS), the test article (including solid, liquid, or aerosol) can be applied indirectly (by aerosolization) or directly (hand pipetted, automatically dispensed in a pattern distributed across the ALI surface (Behrsing et al., 2017)) onto the *in vitro* test system and thus is not required to be soluble in the chosen cell culture medium. In contrast, in submerged exposure of an *in vitro* monoculture (i.e., single layer, 2D cell culture), the test article needs to dissolve in the chosen cell culture medium, limiting the applicability of submerged culture systems. Mode of exposure can also have implications for interpretation of assay results. In one study, submerged exposures led to higher production of reactive oxygen species and secretion of IL-8 relative to cloud ALI exposures (Klein et al., 2013). Considerations of volatility of the test article also has implications for *in vitro* test systems and exposure. For example, volatile compounds may evaporate rapidly if dissolved in warm media. Different particle size distributions impact cellular uptake. Thus, the choice of *in vitro* assays, test systems, and modes of exposure is critical for any assessment of respiratory irritation.

In addition, the physicochemical properties of cleaning product formulations may differ from those of their individual chemical components, with associated implications for the assays that can be conducted. Testing a single chemical or component of a cleaning product alone, even at a dilution similar to that used in the final formulation, may not accurately reflect physicochemical properties and behavior of the ingredient in the final formulation.

4.2 Capturing population variability *in vitro*

It is important to characterize population variability in the context of a risk assessment model. This might be done using default approaches or using information on variability derived from *in vitro* assays. Susceptible populations are currently accounted for *post-hoc* by using uncertainty factors (UF) to address human variability, but *in vitro* cell/culture test systems may be able to provide or inform a quantitative understanding of variability, which can result in more scientifically informed UFs. However, for some risk assessment purposes (e.g., screening), default UFs may be sufficient. UFs are discussed further in Section 6.4.

Possible sources of population variability include sex, age, race, geographical source, disease status, and susceptibility windows. Ambient air quality differs across geographical areas (Brody et al., 2002; Vrijheid, 2014), potentially resulting in different baseline characteristics in primary samples collected from donors in different areas. Susceptibility windows of interest noted were early development (Goldizen et al., 2016) and menopause (Ziller et al., 2023). Younger populations are often considered to be more at risk due to differences in dosimetry and respiratory tract development (Ginsberg et al., 2008; Ginsberg et al., 2017; Dietert et al., 2000). Participants also noted that some subpopulations may be *more* resilient (less susceptible) to respiratory irritation, though specific examples were not given.

Population variability might be dependent on the endpoint of interest, the chemical/formulation of interest, or both; these dependencies may influence the choice of *in vitro* cell/tissue culture model. As an example of the former, males and females are likely to have similar CBF of around 12–15 Hz in healthy adults (Roth et al., 1991; Tilley et al., 2015), but may have differences in airway inflammation and remodeling (Ekpru and Silveyra, 2022).

One aspect of population variability and susceptible populations that is particularly relevant for the testing of cleaning products is consideration of the anticipated biological features (e.g., ventilation rate and airway anatomy) of both the intended end-user and of those who may be unintentionally exposed in the presence of the end-user. *In vitro* cell/tissue test systems representative of the biology of some susceptible populations are available (Faber and McCullough, 2018). ALI-differentiated primary human bronchial epithelial cell models have been shown to exhibit inter-individual variability across donors (McCullough et al., 2016; Bowers et al., 2018; Bowers et al., 2021). The use of cryopreserved lung slices allows for consideration of population variability to some degree, at the cost of a greater level of complexity and study scope (Patel et al., 2023). Depending on the assessment purpose, it may be possible to address such considerations through selection of particular *in vitro* test systems.

5 Tiered testing framework/approach

The *in vitro* cell/tissue test systems breakout group proposed an option (described in Section 5.1) for development of an approach for *in vitro* test systems and assays to evaluate respiratory irritation for cleaning products, with room for customization to specific needs of each assessment. Some additional background and context relevant to the development and use of an approach are discussed in Section 5.2. This approach includes an initial tier of screening chemicals based on physicochemical characterization and computational approaches (Tier 1), followed by up to two tiers (Tiers 2 and 3) of testing in appropriate *in vitro* cell/tissue test systems informed by mechanistic understanding. This is explicitly not a recommended approach but is meant as an illustrative example of how such an approach might look. The participants acknowledge that this is a starting point and may need to be modified based on the outstanding questions (below), findings from a literature survey/review (above), and/or the specific problem formulation or goal of testing (Section 1). Depending on the purpose to which the approach is applied, some tiers may not be needed. Lower tiers (Tier 1 and possibly Tier 2) may be adequate for screening, while more sophisticated

applications, including regulatory applications, may require elucidation of mechanisms or filling data gaps in higher tiers (Tier 2 and Tier 3) potentially coupled with data from *in vivo* cell/tissue test systems.

5.1 An illustrative option for a tiered approach to screen thousands of ingredients/mixtures

One option for a proposed tiered approach is presented herein. As noted above, this is explicitly not a recommendation but is meant as an illustrative example of how such an approach might be designed. Similar approaches have been proposed for evaluating natural complex substances for a range of endpoints, including local respiratory toxicity (Api et al., 2022; Clippinger et al., 2018a). Though not specific to respiratory irritation, this tiered approach for complex mixtures may also inform considerations relevant to cleaning product formulations.

5.1.1 Tier 1: Physicochemical characterization and computational screening

The main goal of this tier would be to inform later testing. The goal at this level is explicitly not to identify test products or ingredients as non-irritants, but to identify appropriate assays and *in vitro* cell/tissue models that can be used to assess them. In addition, this tier could be used to “screen out” test articles that are not good candidates for use in cleaning products because they are highly likely to be irritants, though specific examples of physicochemical properties that would indicate that a test article is likely to be an irritant were not discussed in detail. Since cleaning product ingredient manufacturers and cleaning product formulators aim to use non-irritant ingredients/formulations, it does not make sense for ingredients/formulations that are identified in this tier as highly likely to be irritants to proceed to further testing. Screening out very likely irritants at this early stage could optimize the use of resources in the *in vitro* testing in Tiers 2 and 3. Ingredients/formulations that are identified in this tier as likely to be non-irritants, or those which may or may not be irritants, should proceed to further tiers, so that predictions can be confirmed or refuted with experimental data. The exact threshold to determine when an ingredient/formulation is “highly likely to be an irritant” was beyond the scope of this workshop, but may vary depending on the purpose of the assessment. Care may need to be taken to not be overly restrictive at this early stage, given the “screening level” nature of this tier.

Before performing any laboratory testing, computational approaches based on physicochemical properties and/or structural flags can identify appropriate test systems and exposure systems, and flag ingredients/formulations of obvious concern for respiratory irritation. Physicochemical properties should be known before beginning laboratory testing and need to be considered throughout the process. Consideration of physicochemical properties can guide users to choose *in vitro* cell/tissue test systems appropriate for such properties and can have a big impact on readout of tests. Similar to considerations for exposure systems (Section 3.3.1), some test systems or assays will be better for, or more sensitive to, certain chemistries.

5.1.2 Tier 2: Simpler *in vitro* models

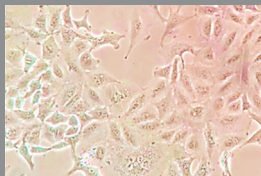
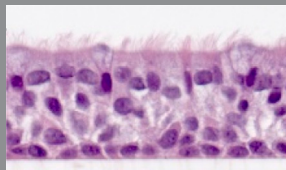
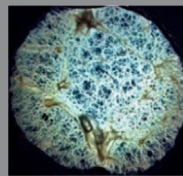
Due to considerations of cost, time, and throughput, *in vitro* testing of ingredients/formulations may begin with using a simpler cell/tissue test system (e.g., a simple 2D mono-culture using submerged exposure), with the aim of collecting data on multiple relevant endpoints from a single cell/tissue system (i.e., multiplex). The specific choice of cell/tissue test system in this tier may depend on the purpose of the assessment, and some purposes may demand a higher level of complexity than others. For example, if specific effector cells are expected to be involved in the irritation response, a co-culture test system including those cells would be preferred. The mode of exposure should also be considered at this stage. Submerged and liquid application exposures are faster, easier, and less expensive than ALI exposure, and so may be favored at this early step when possible. However, there are efforts to improve liquid application exposures (e.g., Behrsing et al. (2017), Mistry et al. (2020)), and this may enable the use of these systems for rapid screening.

To determine an ideal *in vitro* cell/tissue test system around which to base a “multiplex-centered” testing strategy, it is necessary to first identify the *in vitro* cell/tissue test system that addresses the greatest number of relevant KEs, then fill in gaps with other models. KEs can be selected from any established AOP or informed by a broader IATA that contributes additional evidence. This is especially relevant to respiratory irritation, given the lack of a well-developed and accepted AOP for this endpoint (Section 2). For example, inflammation may contribute to both irritation and sensitization (though it is not required for irritation). If there are relevant mechanistic steps that are not included in an AOP or IATA (or if an AOP or IATA do not yet exist), these steps should also be considered.

Multiplexing may be achieved by conducting non-destructive assays (i.e., monitoring various functional readouts that do not damage the structure or integrity of the cells) in an *in vitro* cell/tissue test system first, and then letting those findings guide the next steps in the process (which may include destructive testing). Cortesi and Giordano (2022) recently reviewed such assays for 3D cultures. For example, one could evaluate changes in CBF initially (a relatively non-destructive test) and then immediately assay mitochondrial toxicity (a destructive test such as the MTT [3-[4,5-dimethylthiazol-2-yl]-2,5 diphenyl tetrazolium bromide] assay). In this example, the value of assessing multiple endpoints in a single test system is prioritized over the challenge of conducting the more complex/expensive endpoint first; depending on the purpose, the relative priorities of these aspects may be different. Multiplexing may also be achieved by choosing a non-destructive test (such as WST-8 [2-(2-methoxy-4-nitrophenyl)-3-(4-nitrophenyl)-5-(2,4-disulfophenyl)-2H-tetrazolium, monosodium salt]) instead of a destructive test (such as MTT). This substitution would allow samples already used for WST-8 to be multiplexed for omics (Phillips et al., 2021) or other biochemical evaluation, or to be fixed for histological examination following assays for cell viability.

Results from submerged exposures in simple 2D monoculture (or co-cultures with accessory cells, if required) in this tier can determine whether progression to the next tier, with more complex cell/tissue test systems and/or modes of exposure, is warranted and can inform the selection of cell/tissue test systems and modes of exposure. Results from this tier can also increase the efficiency of

TABLE 2 Example of Endpoints that can be Tested in Different Cell/Tissue Test Systems.

	<div>Exposure</div> <div>Aqueous - Solvent - Aerosol</div> <div>Test system</div>			
	Biomarkers/Events	2D cells	3D RHuA	3D hPCLS
<div>Molecular Initiating Events</div> <div>Cellular Key Events</div> <div>Tissue/Organ Key Events</div>	Oxidative Stress	✓	✓	✓
	DNA Binding/Strand Breaks	✓	✓	✓
	Mitotoxicity	✓	✓	✓
	Cytotoxicity	✓	✓	✓
	Viability	✓	✓	✓
	Macrophage Activation ^a		✓	✓
	Cytokine/Chemokine Response	✓	✓	✓
	Tight Junction Integrity		☑	
	ECM Deposition		✓	✓
	ECM stiffness	✓	✓	☑
	Spatial context (histology) ^b		✓	✓
	Mucociliary Clearance ^c		✓	✓
	Airway Contractility			☑
	Vessel contractility			☑
	Goblet Cell Increase		☑	
	Mucin/surfactant Expression		✓	✓
	<i>In vivo</i> -comparable tissue dosimetry ⁴		☑	

These examples reflect capabilities at the time of the workshop discussion/publication and may change over time or differ across institutions. 3D RHuA = 3D reconstructed human airway. 3D hPCLS, = 3D human precision cut lung slices. (ECM, extracellular matrix). A checkmark (✓) indicates that a given test system can address a biomarker/event. A checked box (☑) indicates that the biomarker/event is uniquely addressed by the test system.

^aBoth RHuA and hPCLS, offer activated macrophage detection, however, hPCLS, immune cells are already present in the tissue at the time of culture (same donor) and in a spatial context (e.g., intra-alveolar vs interstitial location). RHuA tissue can be supplemented with immune cells (typically from a different donor) after tissue maturation and prior to experimental use. It is unclear how effects of immune cells from a different donor impact the RHuA tissue response/performance during experimentation.

^bhPCLS, offer a native tissue architecture, including respiratory parenchyma and pulmonary vasculature. This environment allows the observation of histological changes in a spatial context (e.g., alveolar vs small airway response) where the presence of specific cell types may indicate changes reflective of disease progression and/or hallmark KE (e.g., interstitial collagen deposition). When generated as co-cultures, RHuA can inform on some aspects of tissue architecture, but in a more limited scope than hPCLS.

^chPCLS, can contain airways with beating cilia and whose beat frequency can be quantified. However, due to the infrequent presence of cilia-bearing airways, efforts for this endpoint assay in hPCLS, would likely be low-throughput.

^dExposures conducted using RHuA under ALI, conditions most closely reflect the dosimetry of *in vivo* exposures in represented cell types. Since hPCLS, are generated by slicing lung tissue, the luminal-albuminal compartmentalization is disrupted. This means that there is no longer an epithelial barrier between the test article and underlying non-epithelial cell types (e.g., fibroblasts, endothelial cells, *et cetera*). However, the impact of a disrupted epithelial barrier and whether assay endpoint results are adversely impacted through the loss of this barrier has not been investigated.

testing in the following tier. For example, cleaning product manufacturers may be able to screen out ingredients/formulations that are clearly irritants in this earlier tier, thus reserving further testing for those that are unlikely to be irritants, or those that may or may not be irritants. For some assessment purposes (e.g., a simple hazard characterization), the results at this tier may not require progression to the next tier. For other purposes (e.g., a full regulatory risk assessment), the next tier (and more) would likely be required.

5.1.3 Tier 3: More complex *in vitro* models

Based on outcomes from Tier 2, the aim in Tier 3 is to address as many relevant KEs or other mechanistic supporting endpoints as possible in a single test cell/tissue system (i.e., maximize data output from a single experimental model), and use additional test systems to address additional KEs and/or other mechanistic endpoints not addressed by the primary test system. An example from respiratory sensitization may provide a model for multiplexing endpoints in a single test system (Gibb and Sayes, 2022). Such multiplexing may be a challenge for some endpoints, considering that other, well-characterized endpoints (e.g., skin sensitization) require multiple assays that are not amenable to multiplexing to address separate KEs. However, this challenge may not be relevant for respiratory irritation. Table 2 presents an illustrative example of how two different 3D culture systems (RHuA and hPCLS) can each cover a range of endpoints relevant to respiratory irritation (as currently conducted at one organization at the time of publication; some specific model-endpoint capabilities may change as additional assay capabilities are developed or may be different between organizations). For example, 3D RHuA can be used for tight junction integrity, mucociliary clearance, goblet cell increase, macrophage activation, and mucin expression, while 3D hPCLS can be used for macrophage activation, extracellular matrix (ECM) deposition, and airway contractility. Depending on the particular purpose and the results from the simpler Tier 2 testing, one or both 3D culture systems could be chosen. Choice of test systems will also depend on the capabilities of the performing laboratory. Participants also mentioned that specific pairing of assays and irritation KEs would be beneficial, but specifics were not discussed at the workshop. Future work could build on Table 2 to include more specifics on which assays can address specific KEs to contribute data to a framework. Progress toward an AOP would be complementary to this future work.

5.2 Outstanding questions and considerations for a tiered framework

Workshop participants discussed the amount and type of data needed to establish confidence in the utility of a NAM. There was broad agreement on the need to ground any tiered framework in mechanistic considerations. As understanding of the mechanisms of respiratory irritation improves, mechanistic considerations may be grounded in AOPs, developed into an IATA, or ultimately incorporated into a DA, or some other option. Although there was general agreement on the utility of AOPs for setting biological context for NAMs, there were different perspectives regarding the details. Some participants suggested that a more complete AOP is

better but left open the possibility that a “complete enough” AOP would still be useful (and left open the definition of “complete enough”). Others focused on the integration of NAM data with other data (i.e., *in silico* or existing *in vivo* data) in a systematic approach leading to a coherent conceptual model in the form of an IATA (Clippinger et al., 2018a; van der Zalm et al., 2022), regardless of the completeness (or even existence) of an AOP. A conceptual model would aid in understanding how particular NAM-based data may or may not be able to inform the understanding of a chemical’s potential hazard. An AOP (or multiple AOPs) provides one way to inform such a conceptual model, but the lack of a well-defined AOP should not prevent the development of this coherent conceptual model. Indeed, a key purpose of AOPs is to provide a structure for organizing the data (Villeneuve et al., 2014a; Villeneuve et al., 2014b). Some participants also noted that AOPs are living documents and are thus never considered fully complete (Villeneuve et al., 2014a).

There was general agreement among participants that any tiered approach should rely on a customizable battery of tests, rather than a single *in vitro* cell/tissue test system that is tuned perfectly for just one test/mechanism/endpoint or one set of physicochemical properties. Any test or set of tests that is too narrow in focus on mechanism or endpoint could miss key markers of irritation. A battery of tests can account for the strengths and weaknesses of different tests and capture a more complete biological picture. From an industry perspective, a requirement for multiple tests could make a testing program more challenging, though this could be mitigated somewhat by development of an IATA and specific DA aimed at KEs. For example, to assess respiratory irritation, one of the biological effects to consider is secretion of inflammatory markers. Models such as ImmuLungTM, ImmuPHAGETM, ALIsens[®], and others (Chary et al., 2019; Marescotti et al., 2019) include macrophages (albeit from different donors than the other cell lines in the model), and allow measurement of inflammatory biomarkers (Cook et al., 2019). A participant noted that secretion of inflammatory markers by epithelial cells would also be of interest. Depending on the purpose of the study, one way to build a relevant battery would be to identify the most comprehensive ALI test system that can evaluate as many endpoints as possible, including inflammation markers. After identifying the ALI test system that fits the purpose of the study, an approach could then be built around it.

Participants discussed that a tiered approach could be structured in several different ways. One possibility is as a flow diagram or a decision tree, where one key event from an AOP is tested, and if the test result is positive, the testing proceeds to the next key event. Another option would be a structure similar to the “2 out of 3” KEs approach used for the skin sensitization DA, wherein a certain number of KEs with positive hits results in a “flag” for sensitization (OECD, 2023). These may not be the only ways of structuring a tiered approach. It is also possible that rules for proceeding between different tiers of a tiered approach could be structured in different ways.

Another decision point is whether to focus on inexpensive test systems with limited capabilities but higher throughput or more complex test systems addressing multiple endpoints with greater biological fidelity but lower throughput. These alternatives are not necessarily mutually exclusive but may reflect the need to answer

specific questions and have different priorities across stages of the process or for different assessment purposes. Essential to answering this question is identifying which KEs can be assessed relatively inexpensively and quickly, and then using the data generated from these initial tests to inform the next steps. For example, in an initial screening test it may make sense to use tests that are relatively easy to perform and produce reproducible results to obtain a go/no-go decision for ingredients/formulations, while later tiers might use more complex *in vitro* cell/tissue test systems.

There are hundreds of thousands of possible ingredients in cleaning products, and many potential ways of formulating cleaning products. While some contexts (e.g., a regulatory context for a specific formulation) may require testing of only a small number of combinations of possible cleaning product formulations, others (e.g., an early screening effort by a chemical manufacturer for determining ingredients for use in a product) may require testing of a larger number of combinations of ingredients. As such, high (er)-throughput methods would be of benefit in screening, for example by harnessing high throughput transcriptomic methods to identify concentrations that alter relevant biological pathways (Harrill et al., 2019; Harrill et al., 2021a). Use of a transcriptomic approach would add the need for standardization of transcriptomic signatures considered indicative of respiratory irritation. For transcriptomic signatures, a time course is a key variable to consider. The potential for evaluating multiple alternative formulations in a higher throughput format is one potential strength of *in vitro* testing (Price et al., 2020). There is ongoing progress toward an OECD reporting framework for transcriptomics data use in regulatory toxicology (Harrill et al., 2021b) that should also be considered in any framework for identifying respiratory irritation by cleaning products; similar reporting requirements may also be relevant for other high (er)-throughput methods. Some participants noted that increasing throughput can also limit the number of endpoints that can be investigated, so the applicability may vary by purpose.

There are also considerations related to cell culture plate dimensions that pose a challenge to utilization of higher throughput methods. Increasing the number of wells also means decreasing the size of the wells (and thus the mass of the cells/tissues each well can hold, or “biological material”). Thus, one of the disadvantages of using a format with more wells is that the degree of possible multiplexing *can be* reduced (i.e., reducing the variety or number of assay endpoints that can be evaluated with material from a single well). This may be mitigated in some cases by increases in the total biological material per plate (instead of per well) when more wells are added, but this increase is not universal. The relationship between well size and number of wells per plate, and its implications for assay scale, multiplexing, and throughput, should be considered on a case-by-case basis. Further, there are edge effects related to mucociliary phenotype when culturing reconstituted tissues in wells, where mucociliary phenotype is not maintained close to the edge of culture wells. The participants’ opinion was that at this time, culturing in 96-well plates while retaining mucociliary phenotype is possible, but such cultures in 384-well plates primarily consist of phenotypes altered by these edge effects. More research is needed to fully understand the extent of edge effects. As such, different purposes may have a different

optimal choice of well size, driven by a balance between throughput and assay scale/multiplexing.

6 Applications to human health risk assessment

6.1 Importance of NAMs evidence integration with other data in systematic approaches

As noted in the Introduction (Section 1), respiratory irritation was defined for this workshop as disruption of the ELF or epithelial perturbation, but even this limited definition includes challenging biological complexities. Therefore, broader biological understanding of respiratory irritation will be critical in validating and creating context for *in vitro* data, though the specifics of exposure in clinical data may be unknown. These data should be integrated in a systematic manner, leading to a coherent conceptual model in the form of an IATA. Clear documentation of the methods followed to obtain the *in vitro* data is essential to developing confidence in the results and their reproducibility.

The translation between clinical and *in vivo* data to *in vitro* data should be based on mechanistic understanding (informed where possible by KEs and KERs in an AOP) relevant to both physicochemical properties and respiratory irritation. A key challenge will be quantifying the KERs, such as defining how much cytotoxicity results in compensatory cell proliferation. Another key concern of participants in this session was defining criteria for a positive signal in *in vitro* assays. Some suggested approaches were to compare results with those obtained with a reference chemical or spike a product with a known respiratory irritant.

There was a consensus in the human health risk assessment (HHRA) breakout group that participants would not be comfortable using *in vitro*⁶ results alone for respiratory irritation risk assessment, but many would use such data for screening or prioritization or as part of the WOE, if the context of use is clear. For example, using *in vitro* assays in an early tier for screening, and followed up by more traditional tests in a tiered approach might be more acceptable for certain purposes (e.g., regulatory submissions, exposure limit derivation), while such follow up testing might not be needed for internal assessment purposes. Some participants felt that benchmarking the *in vitro* assay results relative to more traditional tests may boost acceptance among users and stakeholders. This could be accomplished by conducting an *in vitro* assay for a chemical with existing animal data as has been done historically. Others stated that the current state of the

6 It is recognized that other portions of this report note the importance of considering *in vitro* data together with *in silico* data and AOPs, but the consensus question was framed specifically in terms of use of *in vitro* data. The framing of the question was intended to distinguish between the use of *in vitro* data in the absence of broader biological understanding and the growing opportunities for moving to *in vitro* testing when the underlying biology is well-understood based on prior testing.

science is that direct concordance of data from human cell-based *in vitro* assays and animal data should not be expected, and any such analysis should be conducted with caution (Van der Zalm et al., 2022). Biological understanding of the processes leading to respiratory irritation represented by direct cytotoxicity was important in the development of a case study on an IATA for using NAMs to refine an inhalation risk assessment for respiratory irritation (OECD, 2022). Importantly, a FIFRA scientific advisory panel (SAP) reviewing a case study of an *in vitro* approach for refining a pesticide inhalation risk assessment indicated several limitations with the use of cytotoxicity to represent respiratory irritation (U.S. EPA, 2019a). The report also highlighted the need for more data linking effects observed in *in vitro* systems with *in vivo* exposure outcomes.

6.2 Dosimetry

Consideration of dosimetry will be critical for applying *in vitro* methods to HHRA, including benchmarking the *in vitro* test conditions to exposure in the *in vivo* use scenario. As described in this section (Section 6.2), choice of the appropriate dose metric is determined based on the chemical's physicochemical characteristics and the mechanistic step (e.g., MIE or KE) that is the basis for the assay. This dose metric is then used to calculate the human equivalent concentration (HEC), the concentration in air that would result in the same dose to the target as was delivered in the *in vitro* cell/tissue test system of interest, using *in vitro* to *in vivo* extrapolation (IVIVE).

As noted in prior sections (Sections 3, 4), it is important to distinguish the exposure concentration in air or liquid from the internal dose achieved in the assay. The “target site exposure” in the assay can refer to deposited or retained dose at the tissue, cellular, or molecular level. The best dose measures (“metrics”) show a correlation with toxicity, or at least with the response in the KE/endpoint being measured. The definition of dose will be key for appropriate dosimetry. When choosing a dose metric for use in the *in vitro* assay, the scale of the metric should be the same as the observation or the KE used (NASEM, 2017). Internal dose is strongly preferred over external exposure whenever possible. Typically, the internal inhaled dose will be what is delivered to the epithelium, or preferably, the intracellular dose, similar to that used in the *in vivo* assays. This can be normalized to surface area, or, if the MOA or other evidence points to a specific effector cell, dose could be normalized to the number of effector cells (e.g., the number of alveolar macrophages). More generally, for effects in tissues, dose could be based on how many cells are in that tissue; for cellular effects, the dose metric should be intracellular dose.

The goal of the dosimetric adjustment is to integrate *in vivo* and *in vitro* data to systematically account for how physicochemical properties (e.g., particle size, solubility) and product form (e.g., spray, mist, or fog) interact with differences in exposure systems or exposure regimen, respiratory tract anatomy, and physiology (e.g., breathing mode and ventilation activity pattern) to determine the “target site exposure.” Depending on the cell/tissue test system, a variety of different parameters and processes determine the relevant target site exposure. These include protein binding, degradation, metabolism, partitioning, particle size and density, and solubility for

cell cultures, and aerosol properties, deposition, uptake, solubility, and agglomeration for ALI systems that utilize cloud rather than liquid exposures (see Figure 4). These various processes mean that the amount of chemical added to a cell or tissue culture does not necessarily directly translate to a dose delivered to the cell/tissue. Thus, while the target site exposure typically is not measured, it is important for coherent evidence integration across experimental platforms in the calculation of the HEC to account for differences between the amount of chemical added to the culture and the actual target site exposure. The same deposition mechanisms occur in air and in liquid media and can be addressed quantitatively. It is also necessary to account for the viscosity of fluid, and whether the fluid is flowing or static. All these elements affect the *in vitro* toxicokinetics (TK) and can factor into the uncertainty factors selected (see Section 6.4).

Characterizing and reporting the determinants of dose will also be important. The choice of dose metric is informed by the level of biological organization of KE (e.g., molecular, cellular). It is possible to select any dose-response relationship along an AOP, based on where there is the most confidence in the causal relationship of KE to adverse outcome (AO). Alternatively, the specific KEs may not be known, but risk assessors will still want to know the internal/intracellular dose. This dose then needs to be scaled appropriately to the HEC based on the dose metric of choice, such as the delivered or intracellular dose per unit area for cytotoxicity related to the internal inhaled dose of the relevant region of the respiratory tract and its surface area. CFD or CFPD models can refine these relationships to localized cell types if relevant.

The choice of specific dosimetry model will be determined by the *in vitro* cell/tissue test system and the physicochemical properties of the test article. The *in vitro* sedimentation, diffusion, and dosimetry model (ISDD; Hinderliter et al., 2010) and *in vitro* sedimentation, diffusion, dissolution, and dosimetry model (ISD3; Thomas et al., 2018) are for submerged test systems; the latter includes dissolution (e.g., for when the ion is the toxic form). CFD or CFPD models can predict localized flux or localized particle deposition from *in vivo* gas or aerosol exposures (Corley et al., 2015; Corley et al., 2021; Lee et al., 2022). Physiologically based pharmacokinetic (PBPK) models are useful for considering systemic dose, and can address metabolism (e.g., Tan et al. (2020), OECD (2023)). Hybrid CFD-PBPK models can address respiratory tract tissue metabolism (Schroeter et al., 2006) and predict localized internal doses such as the area under the curve for parent compound or various metabolites in specific regions. The MPPD model can be used to predict inhaled particle deposition and clearance to estimate retained mass in humans, rats, and mice (ARA (Applied Research Associates), 2024). The U.S. EPA has developed its own version of the MPPD model (U.S. EPA MPPD v2.0 2024) that underwent external expert peer review; it is scheduled for release in 2024. In addition to the capabilities of the version of MPPD released by Applied Research Associates (ARA), the U.S. EPA version will be able to address clearance in the head, has revised clearance rates using more data for rodents (rats and mice), and includes adjustment capabilities for hygroscopicity and solubility. Participants noted that at this time, there are not yet any adequate dosimetry models for ALI exposure systems.

Participants identified several uncertainties around dosimetry and *in vitro* cell/tissue test systems for respiratory irritation. One uncertainty was the impact of a lack of clearance *in vitro*. There was discussion, but no resolution, regarding whether *in vitro* test systems can be considered a worst-case scenario in the absence of clearance. For example, retained dose represents an accumulation over time that does not occur *in vitro*. Participants also questioned whether cumulative dose considerations would apply in the absence of clearance in *in vitro* test systems. Another uncertainty was the impact of washing and recovery in the *in vitro* test systems. Conversely, the *in vitro* test system may not have the appropriate enzymes for metabolism, depending on the cell types used (e.g., carboxylesterase is highest in nasal tissue and lower in the lower respiratory tract), though metabolism might be less important for direct contact irritation, which is often related to reactivity of the parent chemical. Another consideration is that, while *in vitro* respiratory irritation models are frequently applicable only to the upper or conducting airway (e.g., use bronchial epithelial cells), *in vitro* respiratory irritation models should also consider the lower airway. Some participants in the broader workshop suggested some of this can be handled with the application of uncertainty factors (UFs); other participants suggested that UFs are an acceptable default in the absence of additional information, but that further characterizing uncertainty or variability might be preferred for some purposes. Using *in vitro* cell/tissue test systems to characterize variability was discussed in Section 4.2. Finally, uncertainties remain regarding other aspects affecting the dose, such as how to account qualitatively and quantitatively for the test article binding with the plate equipment.

6.3 Identifying the point of departure for dose-response analysis

Benchmark dose (BMD) modeling is preferred over the No Observed Adverse Effect Level/Lowest Observed Adverse Effect Level (NOAEL/LOAEL) approach to dose-response analysis, because the latter is dependent on study design and doses chosen (U.S. EPA, 2012; EFSA Scientific Committee et al., 2022). In standard BMD modeling, each relevant endpoint is modeled separately, with the effect level based on the benchmark response (BMR), a predetermined change in the level of response. The TRV⁷ or exposure limit is then based on determining the most sensitive relevant BMD (or, typically, the 95% lower confidence limit on the BMD, the BMDL) and dividing this point of departure (POD) by appropriate UFs. Thus, there are three key decision points in deriving TRVs: (1) identifying the appropriate degree of change for the BMR, (2) choosing the appropriate mathematical model(s), and (3) applying appropriate UFs. The first two decision points are discussed in this section (Section 6.3), while UFs are discussed in Section 6.4. As described in the previous section (Section 6.2), dosimetric adjustments or other adjustments to the POD may also be needed to match the experimental exposure conditions

and physiology/biology to the exposure scenario of interest (United States Environmental Protection Agency, 1994; NASEM, 2017).

There was a general agreement among participants in the HHRA breakout session that there is a need to evaluate the visual fit to the data from multiple mathematical models and statistically demonstrate goodness of fit, though the specifics of how this should be done were not discussed. One possibility is based on the U.S. EPA BMD guidance: run three different statistical models on each endpoint, demonstrate goodness of fit, and provide the rationale for choice of model, including consideration of the Akaike Information Criterion (AIC) (U.S. EPA, 2012). Alternatively, one could run all relevant models available in the software being used.

The choice of the appropriate BMR (which ultimately determines the POD) is challenging (Haber et al., 2018). There is a lot of uncertainty in defining adverse responses *in vitro*, as well as uncertainty related to technical issues in the assays. It is necessary to understand what causes variability in responses *in vitro* to determine the appropriate BMR. This necessity was discussed in more detail in Section 4. In making this choice, there are a few options and issues to consider. The BMR could be based on a change of one standard deviation from the mean of the reference group or it could be related to the degree of change considered adverse (related to severity). The BMR is likely to be different for different endpoints. Many questions remain for how to systematize an approach to choosing a POD for *in vitro* assays. Some participants noted the use of a BMR of a one standard deviation change in the control mean in the OECD (2022) case study, while others questioned whether this choice was adequately supported. Several recent publications discuss methods of integrating and using transcriptomic data for regulatory purposes (Harrill et al., 2021a; Harrill et al., 2021b; Harrill et al., 2019). Other recent publications that discuss ways of conducting BMD modeling across various assays, often in the context of transcriptomic data (e.g., Speen et al. (2022), Drake et al. (2023)), may also provide insights into how to conduct BMD modeling across multiple assays in a framework like the one above, including evaluation of their relationship to the *in vivo* POD. The need for quantitative AOP (qAOP) has been emphasized to help improve IVIVE and integrate exposure and key events in support of computational modeling and risk assessment (Perkins et al., 2019).

Participants highlighted the importance of standards for reporting data and analysis methods, echoing the importance of GLP and GIVIMP highlighted earlier.

6.4 Uncertainty factors

Workshop participants considered the “classical” UFs used with *in vivo* studies to provide an appropriate background on the use of *in vitro* data in HHRA. Although different organizations vary in the details of their approach to UFs, UFs related to human variability (UF_H) and interspecies extrapolation (UF_A) are considered by most organizations in standard risk assessments using *in vivo* data. Both the interspecies and intraspecies variability includes uncertainty due to data deficiencies and variability with respect to TK and toxicodynamics (TD). Considerations include the nature of the dosimetry adjustment (e.g., default or optimal model) and the

⁷ Note that the BMD is a point of departure that is divided by UFs to result in a TRV, or health “benchmark.”

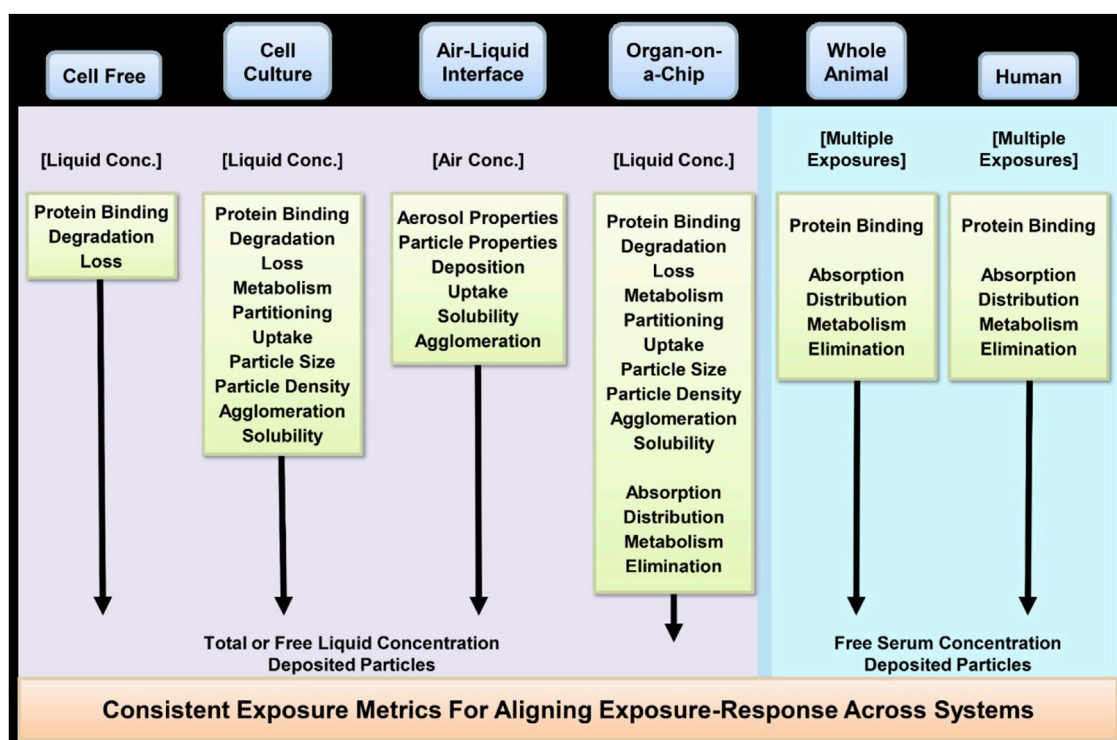


FIGURE 4

Chemical characteristics, experimental parameters, and mechanistic processes that affect delivered dose. (NASEM, 2017). Note that in 2017, at the time of the NASEM report, lung on a chip used liquid exposure, but advances since then mean that lung on a chip is now more frequently done at ALI, so air concentration would be the exposure metric. In addition, note that “particle properties” includes particle size distribution, and this characteristic is among those determining deposition, and therefore absorption, in the whole animal and human systems.

need to account for variability of susceptible populations due to differences in life stage, disease state, and other features. The U.S. EPA also considers UFs related to (1) severity or nature of the endpoint, or LOAEL to NOAEL extrapolation (UF_L), (2) duration extrapolation (UF_S), and (3) database uncertainties (UF_D), typically related to comprehensiveness of the foundational data and questions of whether the appropriate critical effect has been identified (United States Environmental Protection Agency, 1994; U.S. EPA, 2002). Other organizations may use different UFs but consider the same general areas of uncertainty (Haber et al., 2012). Where a specific regulatory organization has jurisdiction, it is important to follow the approach of that organization. Regardless of the approach used, documenting the rationale for the choice of each UF provides needed transparency.

The U.S. EPA and other organizations partition the interspecies and intraspecies UFs into TK and TD components, where chemical-specific data can replace the default values for any of the subfactors (e.g., intraspecies variability in TK) (IPCS, 2005; U.S. EPA, 2014). Such partitioning for intraspecies variability can provide an incentive to address the key questions needed to apply *in vitro* data in HHRA. The discussion below presents perspectives on both use of default approaches and on how available data can replace defaults. Van der Zalm et al. (2022) addressed uncertainties and issues needed to establish scientific confidence in NAMs more broadly, which largely apply to NAMs for respiratory irritation here. They highlight the importance of fitness-for-purpose, reliability, relevance to human biology, independent review, and

transparent communication. The text below expands on this approach.

6.4.1 UF_A – interspecies extrapolation

Interspecies extrapolation typically addresses TK and TD considerations to account for the differences between animals and humans. The use of human cells or cell lines for *in vitro* assays negates the need for interspecies extrapolation. However, some workshop participants considered a new *in vitro* UF (discussed below in Section 6.4.5) as analogous to the extrapolations involved with applying interspecies UF (e.g., the degree of dosimetry adjustment to characterize the TK determinants of the exposure system, and the reliability and utility of the cell/tissue model as relevant to the *in vivo* target tissue).

6.4.2 UF_H – intraspecies variability

Participants agreed that it is useful to continue to divide this UF into default subfactors of 3 each for TK and TD. These subfactors reflect the need to address population variability in ADME and in response (TD) with cell/tissue models from a small number of individuals. Other related uncertainties include consideration of whether the human cells are from immortalized cell lines or primary cells, as well as the adequacy of the number of replicates, and the resulting impact on estimates of central tendency and variability. It was noted that chemical-specific data can replace the default subfactors, and determining the primary causes of variability can help to refine the subfactors.

Understanding population variability in the dose metric of interest for a given exposure level can address intraspecies TK, and donor variability in the response for a given dose (using the appropriate dose metric) addresses intraspecies TD (e.g., McCullough et al. (2016), Bowers et al. (2018), Bowers et al. (2021)). In using donor samples to characterize population variability (Section 4.2) and replace the default factor for intraspecies TD, it would be important to test an adequate sample size, and to ensure that potential sensitive populations are included. It should also be noted that total variability reflects a combination of sampling variability, technical variability, and population variability (Rusyn et al., 2022). It will also be critical to demonstrate that inter-individual variability in exposure outcomes in primary cell-based respiratory tract models is a biological characteristic that is reproducible over time and not just the cumulative impact of technical variation across different exposure experiments. Note that the individual subfactors are not intended to capture the entire range of population variability. Rather, they reflect the range from a measure of central tendency (e.g., the mean) to a high percentile (e.g., 95th) on the sensitive end of the distribution (IPCS, 2005; U.S. EPA, 2014). Another perspective, based on a case study on use of an IATA for a respiratory irritant, was that variability in ADME was likely to have minimal impact for a direct-acting irritant, and so the UF for intraspecies TK could be reduced to 1 (OECD, 2022). These two perspectives are not necessarily mutually exclusive, though there may be disagreements about precisely when it is appropriate to reduce UF_H.

6.4.3 UF_L – severity

UF_L is usually set to 1 with the use of a BMDL (Haber et al., 2018). Participants discussed uncertainty in how this should be handled in relation to the challenge of selecting appropriate BMR levels for *in vitro* assays. As noted in Section 6.3, it is not clear what an *in vitro* BMR should be, and the appropriate BMR may vary by assay. Some of the early literature on choice of BMR for dichotomous and continuous *in vivo* endpoints may inform such decisions for *in vitro* endpoints (Faustman et al., 1994; Allen et al., 1994a; Allen et al., 1994b; Kavlock et al., 1995).

6.4.4 UF_S – duration (classically, subchronic to chronic)

Participants generally agreed that the UF_S should be 1 if the duration of assay is comparable to the duration indicated in the problem formation. Depending on the MOA and whether response increases with exposure duration, UF_S may need to be larger than 1 for repeated and/or episodic exposures. For example, mild irritation may be driven by concentration, not cumulative exposure, while irritation that results in tissue damage and remodeling increases with exposure duration. The exact magnitude of UF_S for various endpoints remains to be decided.

6.4.5 UF_{IV} – *in Vitro* UF

Some participants in the HHRA breakout proposed a new *in vitro* UF to address the uncertainty of using *in vitro* testing as surrogate for *in vivo* testing. In part, this new UF is analogous to the interspecies UF and would need to reflect both TK and TD uncertainties related to IVIVE. Additionally, this UF would address other uncertainties, such as the connections between KE

and AO, and how well an *in vitro* cell/tissue test system can represent *in vivo* human response. There was some disagreement among the broader workshop participants about the necessity of the *in vitro* UF.

Those in favor of this new UF suggested it could be modeled after the interspecies UF, with default subfactors of 3 each for TK and TD uncertainties. The TK subfactor would address uncertainties in differences between *in vitro* and *in vivo* dosimetry, as well as the quality of the dosimetry adjustment applied, while the TD factor would address differences in response. Areas of uncertainty and variability specific to *in vitro* systems include issues related to the choice of target system surrogate, target tissue specificity and variability, spatial representation and variability, and metabolic competence and variability. Specific TK considerations include issues related to (1) the *in vitro* delivery mechanisms, (2) well and insert sizes, (3) reactivity of the generation/exposure system with physicochemical properties of the test substance, (4) relevance to target exposure scenario, and (5) cell/tissue system specifications. TD considerations include issues related to consideration of (1) the intended application of the assay relative to the effect or KE it represents, (2) the degree of verification of the assay; (3) target response level (BMR); and (4) existence of performance standards.

Appropriate data could be used to modify default subfactors when available. For example, a submerged cell culture with ISDD addresses dosimetry, and thus the *in vitro* TK is addressed. Similarly, if CFD is used to perform IVIVE for an ALI exposure with appropriate scale up to an HEC, it may not be necessary to apply additional dosimetry adjustments. However, it would be necessary in these cases to characterize the determinants of dose or to recognize that as an uncertainty. In addition, the TD component would need to be addressed by how well the *in vitro* test system captures issues of susceptible populations.

Those opposed to an *in vitro* UF noted that the OECD (2022) case study did not include an *in vitro* UF. They argued that other aspects of *in vitro* testing, such as the absence of clearance, compensate for the IVIVE, and thus they believe that an *in vitro* uncertainty factor would not be required. Others felt that the absence of biologically-relevant ADME including clearance processes (M and E) increases uncertainty compared to an *in vivo* experiment. This premise raised the issue of whether *in vitro* cell/tissue test systems are always conservative from the dose perspective. Exposure is dynamic *in vivo*. This dynamic aspect is not reflected *in vitro*, but other aspects of dosimetry are often not well-characterized. For example, *in vitro*, the chemical is often sticking to the plate, meaning that the delivered dose is less than expected based on the applied dose.

The question was also raised about how well a single assay, or even a battery of assays, can address the respiratory tract as a system. In addition to uncertainties about the respiratory tract, uncertainties about systemic effects were also noted. Such uncertainties could be part of this UF or UF_D, but such issues were beyond the scope of the workshop.

6.4.6 UF_D – database

The database uncertainty factor addresses whether the correct endpoint is being considered (i.e., whether the NAM provided comprehensive coverage of potential toxicity). In other words, UF_D addresses whether all of the assays conducted provide adequate confidence that all relevant potential effects have been

considered and the appropriate endpoint is being used for the POD. A single assay will be unable to do this, although it may be possible with a specified battery of assays. Further, it is not clear how the possibility of systemic effects should be considered.

It is uncertain at this point whether the proposed *in vitro* UF would address coverage, or whether a separate UF_D is needed. There is a possibility of overlap between the two if a battery of assays is deployed, so it is not clear whether the two factors should be conceptualized separately. Others felt that the *in vitro* and database factors represent separate areas of extrapolation.

7 Conclusion

Although the purpose of this workshop was not necessarily to reach consensus among workshop participants, several key themes emerged from multiple breakout groups. These key themes often led to recommendations for next steps. Common themes included.

- Some of the challenges related to characterizing respiratory irritation are not unique to *in vitro* cell/tissue test systems and are shared with *in vivo* models. These challenges include ensuring intra- and inter-laboratory reproducibility and ensuring that both assays and controls perform as expected. Variability in exposure (both real-world and in experimental systems), *in vitro* test systems, and human populations need to be characterized and understood.
- The nature of the assessment informs the choice of experimental exposure system, the *in vitro* cell/tissue test system and method, and the use of the data to inform human health assessments. Assessments can be categorized as (1) qualitative screening-level hazard identification, (2) industry semi-quantitative or qualitative risk assessment, and (3) deriving a TRV or a quantitative risk assessment conducted for the purposes of regulatory acceptance. The burden of proof increases sequentially across these assessment types.
- The physicochemical properties of the cleaning product ingredient or formulation can guide the choice of both the exposure system and *in vitro* cell/tissue test system. A literature survey/review to identify how the physicochemical properties influence the selection of exposure method and cell/tissue test system is recommended as a key step towards characterization and standardization of exposure and cell/tissue test system methods.
- Building confidence in the use of NAMs requires use of all available data—*in vivo* data from clinical studies and animal data, *in vitro* data, and *in silico* analyses/data—to create context and a better basis for understanding and inference.
- Systematic integration of NAM data with other data (existing *in vivo* data from humans and animals, mechanistic data, *in silico* data, etc.) into a coherent conceptual model or an IATA is critical. The NAMs being evaluated will usually be linked to specific KEs, although a fully described AOP is not necessary.
- Consideration of dosimetry and identification of an appropriate dose metric(s) are essential. It is important to coordinate the choice and measurement of dose metric across the experimental exposure system, *in vitro* cell/tissue system, and quantification approach.
- Characterization of assay methods and standardization of reporting is needed and will facilitate the use of data from assays for a range of applications. Until reporting standards are developed, it is important to document all elements of experimental systems to aid in reproducibility and in determining which design elements have important impacts on the results. It is important to note that exposure concentration for an exposure at ALI is not an appropriate dose metric given that deposition efficiencies vary across ALI exposure systems and are influenced by the physicochemical properties of the test article. Similarly, nominal solution concentration in liquid dosing does not reflect the impact of various factors (e.g., molecular diffusivity, volatility) that influence the exposure of the cells in the *in vitro* system to the test article.
- A tiered approach (such as one like the illustrative example outlined in Section 5.1) is recommended to help make the complex problem of *in vitro* testing for respiratory irritation by cleaning products tractable. Consideration of physicochemical properties, together with *in silico* analyses, is important in early tiers. Further work is needed to develop the tiering, including the specifics of the decision logic.
- Many of the elements of developing risk values from *in vivo* data can be applied to NAMs. For example, BMD modeling is preferred over the NOAEL/LOAEL approach for dose-response analysis, although more research is needed regarding the choice of the BMR.
- The UFs used for *in vivo* assessments can also be adapted for use with NAMs. There was general agreement that the use of human cells removes the need for an interspecies factor, although other aspects of IVIVE need to be considered. Dividing the human variability UF into TK and TD subfactors can provide an incentive for obtaining data to address key questions and replace subfactor defaults with chemical-specific data. Additional research is needed regarding a database UF for adequacy of assay or test battery coverage, and whether a separate UF is needed to address uncertainties related to using *in vitro* testing as a surrogate for *in vivo* testing.
- There is a need for cross-sector collaboration on characterization/standardization and framework development. Engagement from industry, non-governmental organizations (NGOs) and non-profits, consultants, and government agencies will be needed, including those with laboratory expertise and those experienced in the application of such data. This collaboration should consider the different requirements for different types of assessments (e.g., screening versus regulatory-related).
- There will need to be sponsorship and funding for a characterization/standardization effort, from multiple organizations.
- It is important to recognize that buy-in and characterization/standardization requires an ongoing, collaborative effort; a high-quality paper or presentation at a meeting does not automatically lead to standardization without further support.

Author contributions

LH: Conceptualization, Writing–original draft, Writing–review and editing, Methodology. MB: Conceptualization, Writing–original draft, Writing–review and editing, Methodology. AB: Conceptualization, Writing–original draft, Writing–review and editing, Project administration, Methodology. HB: Writing–original draft, Writing–review and editing. PC: Writing–original draft, Writing–review and editing. SD: Writing–original draft, Writing–review and editing. CF: Conceptualization, Methodology, Writing–original draft, Writing–review and editing. KG: Conceptualization, Methodology, Writing–original draft, Writing–review and editing. FK: Conceptualization, Funding acquisition, Methodology, Writing–original draft, Writing–review and editing. SM: Conceptualization, Writing–original draft, Writing–review and editing. KP: Conceptualization, Methodology, Writing–original draft, Writing–review and editing. VP: Writing–original draft, Writing–review and editing. NP: Conceptualization, Methodology, Writing–original draft, Writing–review and editing. CR: Conceptualization, Methodology, Writing–original draft, Writing–review and editing. MS: Conceptualization, Writing–original draft, Writing–review and editing, Methodology. AJ: Conceptualization, Methodology, Writing–original draft, Writing–review and editing.

Funding

The author(s) declare that financial support was received for the research, authorship, and/or publication of this article. Funding for the workshop and the preparation of the workshop proceedings manuscript was provided by the American Cleaning Institute® (ACI) (Washington, DC), including funding to Stantec ChemRisk for the workshop support and authorship roles of LH, MB, and AB.

Acknowledgments

The technical assistance of Sydney Hess (University of Cincinnati) is gratefully acknowledged, as is Andy Maier (Stantec ChemRisk) for his ideas and support. The contributions of the workshop participants to the scientific discussion are also recognized. Drs. Jessica R. Murray (US EPA ORD CPHEA) and Martin B. Phillips (US EPA OSCPP OPPT) are thanked for their critical and constructive review of the draft manuscript. Keith Tarpley of AttainX is acknowledged for excellent graphical design and support.

Conflict of interest

The authors declare that this workshop and the preparation of the workshop proceedings manuscript were funded by the

American Cleaning Institute® (ACI). The funder was involved in conceptualization and organization of the workshop, and in a high-level review of the written proceedings. FK was an employee of ACI. KP was an employee of Clorox, a member company of ACI, which manufactures cleaning products and may use the methods/approaches outlined in this manuscript. KG was an employee of Arkema, a member company of ACI, which manufactures chemicals, some of which are used in cleaning products and may use the methods/approaches outlined in this manuscript. CF was an employee of Ecolab, a member company of ACI, which manufactures cleaning products and may use the methods/approaches outlined in this manuscript. NP was an employee of Ecolab at the time of the workshop, and moved to 3M during the preparation of this manuscript. LH, MB, and AB were consultants paid by ACI. LH and MB were employees of the University of Cincinnati. AB was an employee of Stantec ChemRisk at the time of the workshop and moved to ToxStrategies, Inc. during the preparation of this manuscript. HB and VP were employees of the Institute for *in vitro* Sciences, which uses some of the *in vitro* experimental models described in this manuscript for commercial purposes. SB was an employee of Invitrolize, which markets *in vitro* models for the respiratory tract. PC was an employee of the Wake Forest Institute for Regenerative Medicine at the time of the workshop, became an independent consultant during the writing of this manuscript and is now at UNC Chapel Hill. SD was an employee of the Insight Exposure and Risk Sciences Group. AMJ was an employee of the U.S. EPA Office of Research and Development. SDM was an employee of the U.S. EPA Office of Research and Development at the time of the workshop and was an employee of RTI during the writing of the proceedings. CR was the owner of Roper Toxicology Consulting Limited. MS was an advisor to PETA Science Consortium International e.V.

The remaining author declares that the research was conducted in the absence of any commercial or financial relationships that could be construed as a potential conflict of interest.

Publisher's note

All claims expressed in this article are solely those of the authors and do not necessarily represent those of their affiliated organizations, or those of the publisher, the editors and the reviewers. Any product that may be evaluated in this article, or claim that may be made by its manufacturer, is not guaranteed or endorsed by the publisher.

Supplementary Material

The Supplementary Material for this article can be found online at: <https://www.frontiersin.org/articles/10.3389/ftox.2024.1431790/full#supplementary-material>

References

- ACI (2024). *Ingredient functions*. The American Cleaning Institute. Downloaded 1/30/2024.
- Allen, B. C., Kavlock, R. J., Kimmel, C. A., and Faustman, E. M. (1994a). Dose-response assessment for developmental toxicity II. Comparison of generic benchmark dose estimates with no observed adverse effect levels. *Fundam. Appl. Toxicol.* 23 (4), 487–495. doi:10.1006/faat.1994.1133
- Allen, B. C., Kavlock, R. J., Kimmel, C. A., and Faustman, E. M. (1994b). Dose-response assessment for developmental toxicity III. Statistical models. *Fundam. Appl. Toxicol.* 23 (4), 496–509. doi:10.1006/faat.1994.1134
- Api, A. M., Belsito, D., Botelho, D., Bruze, M., Burton, G. A., Jr, Buschmann, J., et al. (2022). The RIFM approach to evaluating natural complex substances (NCS). *Food Chem. Toxicol.* 159 (Suppl. 1), 112715. Epub 2021 Nov 27. doi:10.1016/j.fct.2021.112715
- ARA (Applied Research Associates) (2024). *Multiple path particle dosimetry (MPPD) model (MPPD v3.04)*. Raleigh, NC: ARA. Available at: <https://www.ara.com/mppd/>.
- Asgari, M., Lucci, F., and Kuczaj, A. (2021). Multispecies aerosol evolution and deposition in a human respiratory tract cast model. *J. Aerosol Sci.* 153, 105720. doi:10.1016/j.jaerosci.2020.105720
- Bajaj, P., Harris, J. F., Huang, J. H., Nath, P., and Iyer, R. (2016). Advances and challenges in recapitulating human pulmonary systems: at the cusp of biology and materials. *ACS Biomater. Sci. Eng.* 2 (4), 473–488. Epub 2016 Mar 14. doi:10.1021/acsbomaterials.5b00480
- Bannuscher, A., Schmid, O., Drasler, B., Rohrbasser, A., Braakhuis, H. M., Meldrum, K., et al. (2022). An inter-laboratory effort to harmonize the cell-delivered *in vitro* dose of aerosolized materials. *NanoImpact* 28, 100439. Epub 2022 Nov 17. doi:10.1016/j.impact.2022.100439
- Behrsing, H. P., Huang, S., and Constant, S. (2017). The use of human 3D reconstructed airway cultures for tobacco product evaluation: precision low-volume exposures at the apical site. *Appl. Vitro Toxicol.* 3 (1), 56–67. doi:10.1089/aivt.2016.0028
- Behrsing, H. P., Wahab, A., Ukishima, L., Grodi, C., Frentzel, S., John, S., et al. (2022). Ciliary beat frequency: proceedings and recommendations from a multi-laboratory ring trial using 3-D reconstituted human airway epithelium to model mucociliary clearance. *Altern. Lab. Anim.* 50 (4), 293–309. Epub 2022 Aug 7. doi:10.1177/02611929221114383
- Bisig, C., Voss, C., Petri-Fink, A., and Rothen-Rutishauser, B. (2019). The crux of positive controls - pro-inflammatory responses in lung cell models. *Toxicol. Vitro* 54, 189–193. doi:10.1016/j.tiv.2018.09.021
- Bowers, E. C., Martin, E. M., Jarabek, A. M., Morgan, D. S., Smith, H. J., Dailey, L. A., et al. (2021). Ozone responsive gene expression as a model for describing repeat exposure response trajectories and interindividual toxicodynamic variability *in vitro*. *Toxicol. Sci.* 185 (1), 38–49. doi:10.1093/toxsci/kfab128
- Bowers, E. C., McCullough, S. D., Morgan, D. S., Dailey, L. A., and Diaz-Sanchez, D. (2018). ERK1/2 and p38 regulate inter-individual variability of exposed air-liquid gene expression in primary human bronchial epithelial cells. *Sci. Rep.* 8 (1), 9398. doi:10.1038/s41598-018-27662-0
- Braakhuis, H. M., Gremmer, E. R., Bannuscher, A., Drasler, B., Keshavan, S., Rothen-Rutishauser, B., et al. (2023). Transferability and reproducibility of exposed air-liquid interface co-culture lung models. *NanoImpact* 31, 100466. doi:10.1016/j.impact.2023.100466
- Breast Cancer Prevention Partners (2017). *SB-258. Cleaning product right to know act of 2017. Section (j). Bill text - SB-258 cleaning product right to know act of 2017. (ca.gov)*.
- Brody, J. G., Vorhees, D. J., Melly, J., Swedis, S. R., Drivas, P. J., and Rudel, R. A. (2002). Using GIS and historical records to reconstruct residential exposure to large-scale pesticide application. *J. Expo. analysis Environ. Epidemiol.* 12 (1), 64–80. doi:10.1038/sj.jea.7500205
- Bustamante-Marin, X. M., and Ostrowski, L. E. (2017). Cilia and mucociliary clearance. *Cold Spring Harb. Perspect. Biol.* 9 (4), a028241. doi:10.1101/cshperspect.a028241
- Carusi, A., Davies, M. R., De Grandis, G., Escher, B. I., Hodges, G., Leung, K. M. Y., et al. (2018). Harvesting the promise of AOPs: an assessment and recommendations. *Sci. Total Environ.* 628–629, 1542–1556. Epub 2018 Feb 22. doi:10.1016/j.scitotenv.2018.02.015
- CFR (Code of Federal Regulations) (2013). Antimicrobial pesticide data requirements. Toxicology. Available at: <https://www.ecfr.gov/current/title-40/chapter-I/subchapter-E/part-158/subpart-W>.
- Chanez, P., and Bourdin, A. (2008). “Chapter 3. Pathophysiology of asthma,” in *Histopathology and natural history of asthma* (Elsevier). doi:10.1016/B978-0-323-04289-5.X1000-4
- Chary, A., Serchi, T., Moschini, E., Hennen, J., Cambier, S., Ezendam, J., et al. (2019). An *in vitro* coculture system for the detection of sensitization following aerosol exposure. *ALTEX* 36 (3), 403–418. Epub 2019 Feb 20. doi:10.14573/altex.1901241
- Ciencewicz, J., Trivedi, S., and Kleeberger, S. R. (2008). Oxidants and the pathogenesis of lung diseases. *J. Allergy Clin. Immunol.: Pract.* 122 (3), 456–470. doi:10.1016/j.jaci.2008.08.004
- Clippinger, A. J., Allen, D., Behrsing, H., Bérubé, K. A., Bolger, M. B., Casey, W., et al. (2018a). Pathway-based predictive approaches for non-animal assessment of acute inhalation toxicity. *Toxicol. Vitro* 52, 131–145. Epub 2018 Jun 20. doi:10.1016/j.tiv.2018.06.009
- Clippinger, A. J., Allen, D., Jarabek, A. M., Corvaro, M., Gaça, M., Gehen, S., et al. (2018b). Alternative approaches for acute inhalation toxicity testing to address global regulatory and non-regulatory data requirements: an international workshop report. *Toxicol. Vitro* 48, 53–70. doi:10.1016/j.tiv.2017.12.011
- Conolly, R. B., Campbell, J. L., Clewell, H. J., Schroeter, J., Kimbell, J. S., and Gentry, P. R. (2023). Relative contributions of endogenous and exogenous formaldehyde to formation of deoxyguanosine monoadducts and DNA-protein crosslink adducts of DNA in rat nasal mucosa. *Toxicol. Sci.* 191 (1), 15–24. doi:10.1093/toxsci/kfac119
- Cook, D. B., McLucas, B. C., Montoya, L. A., Brotski, C. M., Das, S., Miholits, M., et al. (2019). Multiplexing protein and gene level measurements on a single Luminex platform. *Methods* 158, 27–32. Epub 2019 Feb 8. doi:10.1016/j.ymeth.2019.01.018
- Corley, R. A., Kabilan, S., Kuprat, A. P., Carson, J. P., Jacob, R. E., Minard, K. R., et al. (2015). Comparative risks of aldehyde constituents in cigarette smoke using transient computational fluid dynamics/physiologically based pharmacokinetic models of the rat and human respiratory tracts. *Toxicol. Sci.* 146 (1), 65–88. Epub 2015. doi:10.1093/toxsci/kfv071
- Corley, R. A., Kuprat, A. P., Suffield, S. R., Kabilan, S., Hinderliter, P. M., Yugulis, K., et al. (2021). New approach methodology for assessing inhalation risks of a contact respiratory cytotoxicant: computational fluid dynamics-based aerosol dosimetry modeling for cross-species and *in vitro* comparisons. *Toxicol. Sci.* 182 (2), 243–259. doi:10.1093/toxsci/kfab062
- Cortesi, M., and Giordano, E. (2022). Non-destructive monitoring of 3D cell cultures: new technologies and applications. *PeerJ* 10, e13338. doi:10.7717/peerj.13338
- Darquenne, C. (2012). Aerosol deposition in health and disease. *J. Aerosol Med. Pulm. Drug Deliv.* 25, 140–147. doi:10.1089/jamp.2011.0916
- Delmaar, J. E., and Bremmer, H. J. (2009). *The ConsExpo spray model - modelling and experimental validation of the inhalation exposure of consumers to aerosols from spray cans and trigger sprays*. RIVM Report 320104005.
- Dietert, R. R., Etzel, R. A., Chen, D., Halonen, M., Holladay, S. D., Jarabek, A. M., et al. (2000). Workshop to identify critical windows of exposure for children's health: immune and respiratory systems work group summary. *Environ. Health Perspect.* 108 (Suppl. 3), 483–490. doi:10.1289/ehp.00108s3483
- Ding, Y., Weindl, P., Lenz, A. G., Mayer, P., Krebs, T., and Schmid, O. (2020). Quartz crystal microbalances (QCM) are suitable for real-time dosimetry in nanotoxicological studies using VITROCELL®Cloud cell exposure systems. *Part Fibre Toxicol.* 17 (1), 44. doi:10.1186/s12989-020-00376-w
- Drake, C., Wehr, M. M., Zobl, W., Koschmann, J., De Lucca, D., Kühne, B. A., et al. (2023). Substantiate a read-across hypothesis by using transcriptome data-A case study on volatile diketones. *Front. Toxicol.* 5, 1155645. doi:10.3389/ftox.2023.1155645
- EFSA Scientific Committee (2022). More, S. J., Bampidis, V., Benford, D., Bragard, C., Halldorsson, T. I., Hernández-Jerez, A. F., et al. (2022). Guidance on the use of the benchmark dose approach in risk assessment. *EFSA J.* 20 (10), e07584. doi:10.2903/j.efsa.2022.7584
- Ekpruke, C. D., and Silveyra, P. (2022). Sex differences in airway remodeling and inflammation: clinical and biological factors. *Front. Allergy* 3, 875295. doi:10.3389/falgy.2022.875295
- European Chemicals Agency (ECHA) (2011). *The use of alternatives to testing animals for the REACH regulation*. ISBN -13: 978-92-95035-96-6.
- European Chemicals Agency (ECHA) (2016). *Practical Guide: how to use alternatives to animal testing to fulfil your information requirements for REACH registration*, V2. doi:10.2823/194297
- European Union (EU) (2003). *Directive 2003/15/EC of the European parliament and of the Council of 27 february 2003 amending Council directive 76/768/EEC on the approximation of the laws of the member states relating to cosmetic products*. OJEU, 10. Available at: <https://eur-lex.europa.eu/LexUriServ/LexUriServ.do?uri=OJ:L:2003:066:0026:0035:en:PDF>.
- European Union (EU) (2009). *Regulation (EC) No 1223/2009 of the European parliament and the Council of 30 november 2009 on cosmetic products*. OJEU. Available at: https://health.ec.europa.eu/system/files/2016-11/cosmetic_1223_2009_regulation_en_0.pdf.
- Ewart, L., Apostolou, A., Briggs, S. A., Carmin, C. V., Chaff, J. T., Heng, A. R., et al. (2022). Performance assessment and economic analysis of a human Liver-Chip for predictive toxicology. *Commun. Med.* 2, 154. doi:10.1038/s43856-022-00209-1
- Faber, S. C., and McCullough, S. D. (2018). Through the looking glass: *in vitro* models for inhalation toxicology and interindividual variability in the airway. *Appl. Vitro Toxicol.* 4 (2), 115–128. doi:10.1089/aivt.2018.0002
- Faber, S. C., McNabb, N. A., Ariel, P., Aungst, E. R., and McCullough, S. D. (2020). Exposure effects beyond the epithelial barrier: transepithelial induction of oxidative stress by diesel exhaust particulates in lung fibroblasts in an organotypic human airway model. *Toxicol. Sci.* 177 (1), 140–155. doi:10.1093/toxsci/kfaa085

- Faustman, E. M., Allen, B. C., Kavlock, R. J., and Kimmel, C. A. (1994). Dose-response assessment for developmental toxicity I. Characterization of database and determination of no observed adverse effect levels. *Fundam. Appl. Toxicol.* 23 (4), 478–486. doi:10.1006/faat.1994.1132
- Fulcher, M. L., Gabriel, S., Burns, K. A., Yankaskas, J. R., and Randell, S. H. (2005). Well-differentiated human airway epithelial cell cultures. *Methods Mol. Med.* 107, 183–206. PMID: 15492373. doi:10.1385/1-59259-861-7:183
- Gibb, M., and Sayes, C. (2022). An *in vitro* alveolar model allows for the rapid assessment of chemical respiratory sensitization with modifiable biomarker endpoints. *Chem. Biol. Interact.* 368, 110232. Epub 2022 Oct 26. doi:10.1016/j.cbi.2022.110232
- Ginsberg, G., Vulimiri, S. V., Lin, Y. S., Kancherla, J., Foos, B., and Sonawane, B. (2017). A framework and case studies for evaluation of enzyme ontogeny in children's health risk evaluation. *J. Toxicol. Environ. Health A* 80 (10–12), 569–593. doi:10.1080/15287394.2017.1369915
- Ginsberg, G. L., Asgharian, B., Kimbell, J. S., Ultman, J. S., and Jarabek, A. M. (2008). Modeling approaches for estimating the dosimetry of inhaled toxicants in children. *J. Toxicol. Environ. Health A* 71 (3), 166–195. doi:10.1080/15287390701597889
- Goldizen, F. C., Sly, P. D., and Knibbs, L. D. (2016). Respiratory effects of air pollution on children. *Pediatr. Pulmonol.* 51 (1), 94–108. Epub 2015 Jul 24. doi:10.1002/ppul.23262
- Haber, L. T., Dourson, M. L., Allen, B. C., Hertzberg, R. C., Parker, A., Vincent, M. J., et al. (2018). Benchmark dose (BMD) modeling: current practice, issues, and challenges. *Crit. Rev. Toxicol.* 48 (5), 387–415. doi:10.1080/10408444.2018.1430121
- Haber, L. T., Strawson, J. E., Maier, A., Baskerville-Abraham, I. M., Parker, A., and Dourson, M. L. (2012). “Noncancer risk assessment: principles and practice in environmental and occupational settings,” in *Patty's toxicology*. Editors E. Bingham, and B. Cohnsen Sixth edition (Wiley and Sons, Inc).
- Harkema, J. R., Nikula, K. J., and Haschek, W. M. (2018). “Chapter 14 - respiratory system,” in *Fundamentals of toxicologic pathology*. Editors M. A. Wallig, W. M. Haschek, C. G. Rousseaux, and B. Bolon Third Edition (Academic Press), 351–393. doi:10.1016/B978-0-12-809841-7.00014-9
- Harrill, J., Shah, I., Setzer, R. W., Haggard, D., Auerbach, S., Judson, R., et al. (2019). Considerations for strategic use of high-throughput transcriptomics chemical screening data in regulatory decisions. *Curr. Opin. Toxicol.* 15, 64–75. doi:10.1016/j.cotox.2019.05.004
- Harrill, J. A., Everett, L. J., Haggard, D. E., Sheffield, T., Bundy, J. L., Willis, C. M., et al. (2021a). High-throughput transcriptomics platform for screening environmental chemicals. *Toxicol. Sci.* 181 (1), 68–89. doi:10.1093/toxsci/kfab009
- Harrill, J. A., Viant, M. R., Yauk, C. L., Sachana, M., Gant, T. W., Auerbach, S. S., et al. (2021b). Progress towards an OECD reporting framework for transcriptomics and metabolomics in regulatory toxicology. *Regul. Toxicol. Pharmacol.* 125, 105020. Epub 2021b Jul 29. doi:10.1016/j.yrtph.2021.105020
- Henderson, R. F. (2005). Use of bronchoalveolar lavage to detect respiratory tract toxicity of inhaled material. *Exp. Toxicol. Pathol.* 57 (Suppl. 1), 155–159. doi:10.1016/j.etp.2005.05.004
- Hinderliter, P. M., Minard, K. R., Orr, G., Chisler, W. B., Thrail, B. D., Poiunds, J. G., et al. (2010). ISDD: a computational model of particle sedimentation, diffusion and target cell dosimetry for *in vitro* toxicity studies. *Part Fibre Toxicol.* 7, 36. doi:10.1186/1743-8977-7-36
- ICRP (International Commission on Radiological Protection) (2015). Occupational intakes of radionuclides: Part 1. ICRP publication 130. Chapter 3: biokinetic and dosimetric models. *Ann. ICRP* 44, 57–94.
- International Programme on Chemical Safety (IPCS) and IPCS Workshop on Incorporating Uncertainty and Variability into Risk Assessment (2005). *Chemical-specific adjustment factors for interspecies differences and human variability: guidance document for use of data in dose/concentration-response assessment*. Geneva, Switzerland: World Health Organization. Available at: <https://apps.who.int/iris/handle/10665/43294>.
- Jarabek, A. M., Asgharian, B., and Miller, F. J. (2005). Dosimetric adjustments for interspecies extrapolation of inhaled poorly soluble particles (PSP). *Inhal. Toxicol.* 17 (7–8), 317–334. doi:10.1080/08958370590929394
- Jarabek, A. M., and Hines, D. E. (2019). Mechanistic integration of exposure and effects: advances to apply systems toxicology in support of regulatory decision-making. *Syst. Toxicol.* 16, 83–92. doi:10.1016/j.cotox.2019.09.001
- Kang, Y., Jeong, B., Lim, D. H., Lee, D., and Lim, K. M. (2021). *In silico* prediction of the full United Nations Globally Harmonized System eye irritation categories of liquid chemicals by IATA-like bottom-up approach of random forest method. *J. Toxicol. Environ. Health A* 84 (23), 960–972. Epub 2021 Jul 30. doi:10.1080/15287394.2021.1956661
- Kavlock, R. J., Allen, B. C., Faustman, E. M., and Kimmel, C. A. (1995). Dose-response assessments for developmental toxicity. IV. Benchmark doses for fetal weight changes. *Fundam. Appl. Toxicol.* 26 (2), 211–222. doi:10.1006/faat.1995.1092
- Kimbell, J. S., Subramaniam, R. P., Gross, E. A., Schlosser, P. M., and Morgan, K. T. (2001). Dosimetry modeling of inhaled formaldehyde: comparisons of local flux predictions in the rat, monkey, and human nasal passages. *Toxicol. Sci.* 64 (1), 100–110. doi:10.1093/toxsci/64.1.100
- Klein, S. G., Serchi, T., Hoffmann, L., Blömeke, B., and Gutleb, A. C. (2013). An improved 3D tetraculture system mimicking the cellular organisation at the alveolar barrier to study the potential toxic effects of particles on the lung. *Part Fibre Toxicol.* 10, 31. doi:10.1186/1743-8977-10-31
- Kleinstreuer, N. C., Hoffmann, S., Alépée, N., Allen, D., Ashikaga, T., Casey, W., et al. (2018). Non-animal methods to predict skin sensitization (II): an assessment of defined approaches. *Crit. Rev. Toxicol.* 48 (5), 359–374. Epub 2018 Feb 23. doi:10.1080/10408444.2018.1429386
- Kouthouridis, S., Goepp, J., Martini, C., Matthes, E., Hanrahan, J. W., and Moraes, C. (2021). Oxygenation as a driving factor in epithelial differentiation at the air-liquid interface. *Integr. Biol. (Camb)* 13 (3), 61–72. PMID: 33677549; PMCID: PMC7965866. doi:10.1093/intbio/zyab002
- Kuczaj, A. K., Nordlund, M., Jayaraju, A., Komen, E., Krebs, T., Peitsch, M. C., et al. (2016). Aerosol flow in the vitroculture 24/48 exposure system: flow mixing and aerosol coalescence. *Appl. Vitro Toxicol.* 2, 165–174. doi:10.1089/avt.2016.0009
- Kuempel, E. D., Sweeney, L. M., Morris, J. B., and Jarabek, A. M. (2015). Advances in inhalation dosimetry models and methods for occupational risk assessment and exposure limit derivation. *J. Occup. Environ. Hyg.* 12 (Suppl. 1), S18–S40. doi:10.1080/15459624.2015.1060328
- Lacroix, G., Koch, W., Ritter, D., Gutleb, A. C., Larsen, S. T., Loret, T., et al. (2018). Air-liquid interface *in vitro* models for respiratory toxicology research: consensus workshop and recommendations. *Appl. vitro Toxicol.* 4 (2), 91–106. doi:10.1089/avt.2017.0034
- Lee, D. D. H., Petris, A., Hynds, R. E., and O'Callaghan, C. (2020). Ciliated epithelial cell differentiation at air-liquid interface using commercially available culture media. *Methods Mol. Biol.* 2109, 275–291. doi:10.1007/978-1-299-26929-9_269
- Lee, K. M., Corley, R., Jarabek, A. M., Kleinstreuer, N., Paini, A., Stucki, A. O., et al. (2022). Advancing new approach methodologies (NAMs) for tobacco harm reduction: synopsis from the 2021 CORESTA SSPT-NAMs Symposium. *Toxics* 10 (12), 760. doi:10.3390/toxics10120760
- Lenz, A. G., Karg, E., Lentner, B., Dittrich, V., Brandenberger, C., Rothen-Rutishauser, B., et al. (2009). A dose-controlled system for air-liquid interface cell exposure and application to zinc oxide nanoparticles. *Part Fibre Toxicol.* 6, 32. doi:10.1186/1743-8977-6-32
- Leung, C., Wadsworth, S. J., Yang, S. J., and Dorscheid, D. R. (2020). Structural and functional variations in human bronchial epithelial cells cultured in air-liquid interface using different growth media. *Am. J. Physiol. Lung Cell Mol. Physiol.* 318 (5), L1063–L1073. Epub 2020 Mar 25. doi:10.1152/ajplung.00190.2019
- Lewinski, N. A., Liu, N. J., Asimakopoulou, A., Papaioannou, E., Konstandopoulos, A., and Riediker, M. (2017). “Air-liquid interface cell exposures to nanoparticle aerosols,” in *Biomedical nanotechnology. Methods in molecular biology*, vol 1570. Editors S. Petrosko, and E. Day (New York, NY: Humana Press). doi:10.1007/978-1-4939-6840-4_21
- Li, D., and Suh, S. (2019). Health risks of chemicals in consumer products: a review. *Environ. Int.* 123, 580–587. Epub 2019 Jan 7. doi:10.1016/j.envint.2018.12.033
- Loret, T., Peyret, E., Dubreuil, M., Aguerre-Chariol, O., Bressot, C., le Bihan, O., et al. (2016). Air-liquid interface exposure to aerosols of poorly soluble nanomaterials induces different biological activation levels compared to exposure to suspensions. *Part Fibre Toxicol.* 13 (1), 58. doi:10.1186/s12989-016-0171-3
- Luetlich, K., Sharma, M., Yepiskoposyan, H., Breheny, D., and Lowe, F. J. (2021). An adverse outcome pathway for decreased lung function focusing on mechanisms of impaired mucociliary clearance following inhalation exposure. *Front. Toxicol.* 3, 750254. doi:10.3389/ftox.2021.750254
- Mallek, N. M., Martin, E. M., Dailey, L. A., and McCullough, S. D. (2024). Liquid application dosing alters the physiology of air-liquid interface (ALI) primary human bronchial epithelial cell/lung fibroblast co-cultures and *in vitro* testing relevant endpoints. *Front. Toxicol.* 5, 1264331. doi:10.3389/ftox.2023.1264331
- Marescotti, D., Serchi, T., Luetlich, K., Xiang, Y., Moschini, E., Talikka, M., et al. (2019). How complex should an *in vitro* model be? Evaluation of complex 3D alveolar model with transcriptomic data and computational biological network models. *ALTEX* 36 (3), 388–402. Epub 2019 Feb 12. doi:10.14573/alte.1811221
- McCullough, S. D., Bowers, E. C., On, D. M., Morgan, D. S., Dailey, L. A., Hines, R. N., et al. (2016). Baseline chromatin modification levels may predict interindividual variability in ozone-induced gene expression. *Toxicol. Sci.* 150, 216–224. doi:10.1093/toxsci/kfv324
- Miller-Holt, J., Behrsing, H. P., Clippinger, A. J., Hirn, C., Stedeford, T. J., and Stucki, A. O. (2022). Use of new approach methodologies (NAMs) to meet regulatory requirements for the assessment of tobacco and other nicotine-containing products. *Front. Toxicol.* 4, 943358. doi:10.3389/ftox.2022.943358
- Mistry, A., Bowen, L. E., Dzierlenga, M. W., Hartman, J. K., and Slattery, S. D. (2020). Development of an *in vitro* approach to point-of-contact inhalation toxicity testing of volatile compounds, using organotypic culture and air-liquid interface exposure. *Toxicol. Vitro* 69, 104968. Epub 2020 Aug 15. doi:10.1016/j.tiv.2020.104968
- Mudway, I. S., and Kelly, F. J. (2000). Ozone and the lung: a sensitive issue. *Mol. Asp. Med.* 21 (1–2), 1–48. doi:10.1016/S0098-2997(00)00003-0

- NASEM (National Academies of Sciences, Engineering, and Medicine) (2017). *Using 21st Century science to improve risk-related evaluations*. Washington, DC: The National Academies Press. doi:10.17226/24635
- National Research Council (2007). *Toxicity testing in the 21st Century: a vision and a strategy*. Washington, DC: The National Academies Press. doi:10.17226/11970
- Ng, A. W., Bidani, A., and Heming, T. A. (2004). Innate host defense of the lung: effects of lung-lining fluid pH. *Lung* 182, 297–317. doi:10.1007/s00408-004-2511-6
- OECD (2017). Guidance document for the use of adverse outcome pathways in developing integrated approaches to testing and assessment (IATA). ENV/JM/MONO. 2016; 67. OECD Series on Testing and Assessment. Available at: <https://www.oecd-ilibrary.org/content/publication/44bb06c1-en>.
- OECD (2018a). *Guidance document on good in vitro method practices (GIVIMP)*, OECD Series on Testing and Assessment, 286. doi:10.1787/9789264304796-en
- OECD (2018b). *Users' handbook supplement to the guidance document for developing and assessing adverse outcome pathways*. OECD Series on Adverse Outcome Pathways, 1. doi:10.1787/5jlvm9d1g32-en
- OECD (2020). Overview of concepts and available guidance related to integrated approaches to testing and assessment (IATA), OECD Series on Testing and Assessment. Available at: <https://www.oecd.org/chemicalsafety/risk-assessment/concepts-and-available-guidance-related-to-integrated-approaches-to-testing-and-assessment.pdf>.
- OECD (2022). Case Study on the use of an integrated approach for testing and assessment (IATA) for new approach methodology (NAM) for refining inhalation risk assessment from point of contact toxicity of the pesticide, Chlorothalonil, OECD Series on Testing and Assessment, No. 367, ENV/CBC/MONO. Available at: <https://www.oecd.org/officialdocuments/publicdisplaydocumentpdf/>.
- OECD (2023). Guideline on defined approaches for skin sensitisation. Available at: https://www.oecd-ilibrary.org/fr/environment/guideline-no-497-defined-approaches-on-skin-sensitisation_b92879a4-en.
- Oldham, M. J., Castro, N., Zhang, J., Lucci, F., Kosachevsky, P., Rostami, A. A., et al. (2020a). Comparison of experimentally measured and computational fluid dynamic predicted deposition and deposition uniformity of monodisperse solid particles in the Vitrocell® AMES 48 air-liquid-interface *in-vitro* exposure system. *Toxicol Vitro* 67, 104870. Epub 2020 Apr 21. doi:10.1016/j.tiv.2020.104870
- Oldham, M. J., Castro, N., Zhang, J., Rostami, A., Lucci, F., Pithawalla, Y., et al. (2020b). Deposition efficiency and uniformity of monodisperse solid particle deposition in the Vitrocell® 24/48 Air-Liquid-Interface *in vitro* exposure system. *Aerosol Sci. Technol.* 54 (1), 52–65. doi:10.1080/02786826.2019.1676877
- Parent, R. A. (2015). *Comparative biology of the normal lung*. Second ed. London UK: Academic Press.
- Patel, V., Amin, K., Allen, D., Ukishima, L., Wahab, A., Grodi, C., et al. (2021). Comparison of long-term human precision-cut lung slice culture methodology and response to challenge: an argument for standardisation. *Altern. Lab. Anim.* 49, 209–222. doi:10.1177/02611929211061884
- Patel, V. S., Amin, K., Wahab, A., Marimoutou, M., Ukishima, L., Alvarez, J., et al. (2023). Cryopreserved human precision-cut lung slices provide an immune competent pulmonary test system for “on-demand” use and long-term cultures. *Toxicol. Sci.* 191, 253–265. doi:10.1093/toxsci/kfac136
- Pauluhn, J. (2021). Phosgene inhalation toxicity: update on mechanisms and mechanism-based treatment strategies. *Toxicology* 450, 152682. doi:10.1016/j.tox.2021.152682
- Pauluhn, J. (2022). Derivation of thresholds for inhaled chemically reactive irritants: searching for substance-specific common denominators for read-across prediction. *Regul. Toxicol. Pharmacol.* 130, 105131. doi:10.1016/j.yrtph.2022.105131
- Paustenbach, D. J. (2000). “The history of biological basis of occupational exposure limits for chemical agents,” in *Patty's industrial hygiene*. Editor R. Harris (New York: Wiley), 1903–2000. as cited in Paustenbach and Gaffney 2006.
- Percie du Sert, N., Ahluwalia, A., Alam, S., Avey, M. T., Baker, M., Browne, W. J., et al. (2020b). Reporting animal research: explanation and elaboration for the ARRIVE guidelines 2.0. *PLoS Biol.* 18 (7), e3000411. doi:10.1371/journal.pbio.3000411
- Percie du Sert, N., Hurst, V., Ahluwalia, A., Alam, S., Avey, M. T., Baker, M., et al. (2020a). The ARRIVE guidelines 2.0: updated guidelines for reporting animal research. *BMC Vet. Res.* 16 (1), 242. doi:10.1186/s12917-020-02451-y
- Perkins, E. J., Ashauer, R., Burgoon, L., Conolly, R., Landesmann, B., Mackay, C., et al. (2019). Building and applying quantitative adverse outcome pathway models for chemical hazard and risk assessment. *Environ. Toxicol. Chem.* 38 (9), 1850–1865. doi:10.1002/etc.4505
- Petersen, E. J., Elliott, J. T., Gordon, J., Kleinstreuer, N. C., Reinke, E., Roesslein, M., et al. (2023). Technical framework for enabling high quality measurements in new approach methodologies (NAMs). *ALTEX* 40 (1), 174–186. Epub 2022 Jul 15. doi:10.14573/alte.2205081
- Pezzulo, A. A., Starnier, T. D., Scheetz, T. E., Traver, G. L., Tilley, A. E., Harvey, B. G., et al. (2011). The air-liquid interface and use of primary cell cultures are important to recapitulate the transcriptional profile of *in vivo* airway epithelia. *Am. J. Physiol. Lung Cell Mol. Physiol.* 300 (1), L25–L31. Epub 2010 Oct 22. PMID: 20971803; PMCID: PMC3023285. doi:10.1152/ajplung.00256.2010
- Phalen, R. F., Hoover, M. D., Oldham, M. J., and Jarabek, A. M. (2021). Inhaled aerosol dosimetry: research-related needs and recommendations. *J. Aerosol Sci.* 155, 105755. doi:10.1016/j.jaerosci.2021.105755
- Phillips, G., Czekala, L., Behrsing, H. P., Amin, K., Budde, J., Stevenson, M., et al. (2021). Acute electronic vapour product whole aerosol exposure of 3D human bronchial tissue results in minimal cellular and transcriptomic responses when compared to cigarette smoke. *Toxicol. Res. Appl.* 5, 239784732098849. doi:10.1177/2397847320988496
- Polk, W. W., Sharma, M., Sayes, C. M., Hotchkiss, J. A., and Clippinger, A. J. (2016). Aerosol generation and characterization of multi-walled carbon nanotubes exposed to cells cultured at the air-liquid interface. *Part Fibre Toxicol.* 13, 20. doi:10.1186/s12989-016-0131-y
- Price, P. S., Jarabek, A. M., and Burgoon, L. D. (2020). Organizing mechanism-related information on chemical interactions using a framework based on the aggregate exposure and adverse outcome pathways. *Environ. Int.* 138, 105673. Epub 2020 Mar 24. doi:10.1016/j.envint.2020.105673
- Pulfer, M. K., Taube, C., Gelfand, E., and Murphy, R. C. (2005). Ozone exposure *in vivo* and formation of biologically active oxysterols in the lung. *J. Pharmacol. Exp. Ther.* 312 (1), 256–264. doi:10.1124/jpet.104.073437
- Ramanarayanan, T., Szarka, A., Flack, S., Hinderliter, P., Corley, R., Charlton, A., et al. (2022). Application of a new approach method (NAM) for inhalation risk assessment. *Regul. Toxicol. Pharmacol.* 133, 105216. Epub 2022 Jul 8. doi:10.1016/j.yrtph.2022.105216
- Randell, S. H., Fulcher, M. L., O'Neal, W., and Olsen, J. C. (2011). Primary epithelial cell models for cystic fibrosis research. *Methods Mol. Biol.* 742, 285–310. PMID: 21547740. doi:10.1007/978-1-61779-120-8_18
- Rayner, R. E., Makena, P., Prasad, G. L., and Cormet-Boyaka, E. (2019). Optimization of normal human bronchial epithelial (NHBE) cell 3D cultures for *in vitro* lung model studies. *Sci. Rep.* 9 (1), 500. PMID: 30679531; PMCID: PMC6346027. doi:10.1038/s41598-018-36735-z
- RIVER working group (2023). *Reporting in vitro experiments responsibly – the RIVER recommendations*. MetaArXiv. doi:10.31222/osf.io/x6aut
- Ross, A. J., Dailey, L. A., Brighton, L. E., and Devlin, R. B. (2007). Transcriptional profiling of mucociliary differentiation in human airway epithelial cells. *Am. J. Respir. Cell Mol. Biol.* 37 (2), 169–185. Epub 2007 Apr 5. PMID: 17413031. doi:10.1165/rcmb.2006-0466OC
- Roth, Y., Aharonson, E. F., Teichtahl, H., Baum, G. L., Priel, Z., and Modan, M. (1991). Human *in vitro* nasal and tracheal ciliary beat frequencies: comparison of sampling sites, combined effect of medication, and demographic relationships. *Ann. Otol. Rhinol. Laryngol.* 100 (5 Pt 1), 378–384. PMID: 2024898. doi:10.1177/000348949110000506
- Rusyn, I., Chiu, W. A., and Wright, F. A. (2022). Model systems and organisms for addressing inter- and intra-species variability in risk assessment. *Regul. Toxicol. Pharmacol.* 132, 105197. doi:10.1016/j.yrtph.2022.105197
- Saint-Criq, V., Delpiano, L., Casement, J., Onuora, J. C., Lin, J., and Gray, M. A. (2020). Choice of differentiation media significantly impacts cell lineage and response to CFTR modulators in fully differentiated primary cultures of cystic fibrosis human airway epithelial cells. *Cells* 9 (9), 2137. doi:10.3390/cells9092137
- Schmeisser, S., Miccoli, A., von Bergen, M., Berggren, E., Braeuning, A., Busch, W., et al. (2023). New approach methodologies in human regulatory toxicology - not if, but how and when. *Environ. Int.* 178, 108082. doi:10.1016/j.envint.2023.108082
- Schmid, O., and Cassee, F. R. (2017). On the pivotal role of dose for particle toxicology and risk assessment: exposure is a poor surrogate for delivered dose. *Part Fibre Toxicol.* 14 (1), 52. doi:10.1186/s12989-017-0233-1
- Schroeter, J. D., Kimbell, J. S., Andersen, M. E., and Dorman, D. C. (2006). Use of a pharmacokinetic-driven computational fluid dynamics model to predict nasal extraction of hydrogen sulfide in rats and humans. *Toxicol. Sci.* 94 (2), 359–367. Epub 2006 Sep 19. doi:10.1093/toxsci/kfl112
- Sharma, M., Stucki, A. O., Verstraeten, S., Stedeford, T. J., Jacobs, A., Maes, F., et al. (2023). Human cell-based *in vitro* systems to assess respiratory toxicity: a case study using silanes. *Toxicol. Sci.* 195, 213–230. doi:10.1093/toxsci/kfad074
- Speen, A. M., Murray, J. R., Krantz, Q. T., Davies, D., Evansky, P., Harrill, J. A., et al. (2022). Benchmark dose modeling approaches for volatile organic chemicals using a novel air-liquid interface *in vitro* exposure system. *Toxicol. Sci.* 188 (1), 88–107. doi:10.1093/toxsci/kfac040
- Squadrito, G. L., Postlethwait, E. M., and Matalon, S. (2010). Elucidating mechanisms of chlorine toxicity: reaction kinetics, thermodynamics, and physiological implications. *Am. J. Physiol. Lung Cell Mol. Physiol.* 299 (3), L289–L300. doi:10.1152/ajplung.00077.2010
- Steiner, S., Diana, P., Dossin, E., Guy, P., Vuillaume, G., Kondylis, A., et al. (2018). Delivery efficiencies of constituents of combustion-derived aerosols across the air-liquid interface during *in vitro* exposures. *Toxicol. Vitro* 52, 384–398. Epub 2018 Jul 9. doi:10.1016/j.tiv.2018.06.024
- Steiner, S., Majeed, S., Kratzer, G., Vuillaume, G., Hoeng, J., and Frentzel, S. (2017). Characterization of the Vitrocell® 24/48 aerosol exposure system for its use in exposures to liquid aerosols. *Toxicol. Vitro* 42, 263–272. doi:10.1016/j.tiv.2017.04.021

- Stucki, A. O., Barton-Maclaren, T. S., Bhuller, Y., Henriquez, J. E., Henry, T. R., Hirn, C., et al. (2022). Use of new approach methodologies (NAMs) to meet regulatory requirements for the assessment of industrial chemicals and pesticides for effects on human health. *Front. Toxicol.* 4, 964553. doi:10.3389/ftox.2022.964553
- Sweeney, L. M., Parker, A., Haber, L. T., Tran, C. L., and Kuempel, E. D. (2013). Application of Markov chain Monte Carlo analysis to biomathematical modeling of respirable dust in US and UK coal miners. *Regul. Toxicol. Pharmacol.* 66 (1), 47–58. Epub 2013 Feb 27. doi:10.1016/j.yrtph.2013.02.003
- Tan, Y. M., Chan, M., Chukwudebe, A., Domoradzki, J., Fisher, J., Hack, C. E., et al. (2020). PBPK model reporting template for chemical risk assessment applications. *Regul. Toxicol. Pharmacol.* 115, 104691. Epub 2020 Jun 2. doi:10.1016/j.yrtph.2020.104691
- Thomas, D. G., Smith, J. N., Thrall, B. D., Baer, D. R., Jolley, H., Munusamy, P., et al. (2018). ISD3: a particokinetic model for predicting the combined effects of particle sedimentation, diffusion and dissolution on cellular dosimetry for *in vitro* systems. *Part Fibre Toxicol.* 15, 6. doi:10.1186/s12989-018-0243-7
- Tilley, A. E., Walters, M. S., Shaykhiev, R., and Crystal, R. G. (2015). Cilia dysfunction in lung disease. *Annu. Rev. Physiol.* 77, 379–406. Epub 2014 Oct 29. doi:10.1146/annurev-physiol-021014-071931
- United States Environmental Protection Agency (EPA) (1994). Methods for derivation of inhalation reference concentrations and application of inhalation dosimetry. Available at: https://www.epa.gov/sites/default/files/2014-11/documents/rfc_methodology.pdf.
- U.S. EPA (2002). A review of the reference dose and reference concentration processes. U.S. Environmental Protection Agency, Risk Assessment Forum. Available at: <https://www.epa.gov/osa/review-reference-dose-and-reference-concentration-processes>.
- U.S. EPA (2012). *Benchmark dose technical guidance*. EPA/100/R-12/001. Washington, DC: Risk Assessment Forum US Environmental Protection Agency.
- U.S. EPA (2014). Guidance for applying quantitative data to develop data-derived extrapolation factors for interspecies and intraspecies extrapolation. Available at: <https://www.epa.gov/risk/guidance-applying-quantitative-data-develop-data-derived-extrapolation-factors-interspecies>.
- U.S. EPA (2015). *EPA's safer choice standard; EPA's safer choice standard*.
- U.S. EPA (2018). *Strategic plan to promote the development and implementation of alternative test methods within the TSCA program*. U.S. EPA. Available at: https://www.epa.gov/sites/default/files/2018-06/documents/epa_alt_strat_plan_6-20-18_clean_final.pdf (Accessed June 22, 2018).
- U.S. EPA (2019a). *FIFRA scientific advisory panel meeting minutes and final report No. 2019-01 peer review on evaluation of a proposed approach to refine the inhalation risk assessment for point of contact toxicity: a case study using a new approach methodology (NAM) december 4 and 6, 2018 FIFRA scientific advisory panel meeting*. Washington, DC: U.S. EPA. EPA-HQ-OPP-2018-0517-0030.
- U.S. EPA (2019b). *Integrated science assessment (ISA) for particulate matter (final report, dec 2019)*. Washington, DC: U.S. Environmental Protection Agency. EPA/600/R-19/188, 2019.
- U.S. EPA (2020). *Integrated science assessment (ISA) for ozone and related photochemical oxidants (final report, apr 2020)*. Washington, DC: U.S. Environmental Protection Agency. EPA/600/R-20/012, 2020.
- U.S. EPA (2021). *New approach methods work plan (v2)*. Washington, DC: U.S. Environmental Protection Agency. Available at: <https://www.epa.gov/chemical-research/new-approach-methods-work-plan>.
- U.S. EPA (2023). *EPA releases updated new approach methodologies (NAMs) work plan*. Last updated January 12, 2023.
- van der Zalm, A. J., Barroso, J., Browne, P., Casey, W., Gordon, J., Henry, T. R., et al. (2022). A framework for establishing scientific confidence in new approach methodologies. *Arch. Toxicol.* 96 (11), 2865–2879. Epub 2022 Aug 20. doi:10.1007/s00204-022-03365-4
- Villeneuve, D. L., Crump, D., Garcia-Reyero, N., Hecker, M., Hutchinson, T. H., LaLone, C. A., et al. (2014a). Adverse outcome pathway (AOP) development I: strategies and principles. *Toxicol. Sci.* 142 (2), 312–320. doi:10.1093/toxsci/kfu199
- Villeneuve, D. L., Crump, D., Garcia-Reyero, N., Hecker, M., Hutchinson, T. H., LaLone, C. A., et al. (2014b). Adverse outcome pathway development II: best practices. *Toxicol. Sci.* 142 (2), 321–330. doi:10.1093/toxsci/kfu200
- Vrijheid, M. (2014). The exposome: a new paradigm to study the impact of environment on health. *Thorax* 69 (9), 876–878. doi:10.1136/thoraxjnl-2013-204949
- Westmoreland, C., Bender, H. J., Doe, J. E., Jacobs, M. N., Kass, G. E. N., Madia, F., et al. (2022). Use of new approach methodologies (NAMs) in regulatory decisions for chemical safety: report from an EPAA deep dive workshop. *Regul. Toxicol. Pharmacol.* 135, 105261. Epub 2022 Sep 11. doi:10.1016/j.yrtph.2022.105261
- Whalan, J. E., Stanek, J., Woodall, G., Reinhart, P., Galizia, A., Glenn, B., et al. (2019). The evaluation of inhalation studies for exposure quality: a case study with formaldehyde. *Toxicol. Lett.* 312, 167–172. Epub 2019 May 14. doi:10.1016/j.toxlet.2019.05.011
- Wong, B. A. (2007). Inhalation exposure systems: design, methods and operation. *Toxicol. Pathol.* 35 (1), 3–14. doi:10.1080/01926230601060017
- Worth, A. P., and Patlewicz, G. (2016). Integrated approaches to testing and assessment. *Adv. Exp. Med. Biol.* 856, 317–342. doi:10.1007/978-3-319-33826-2_13
- Wu, J., Wang, Y., Liu, G., Jia, Y., Yang, J., Shi, J., et al. (2017). Characterization of air-liquid interface culture of A549 alveolar epithelial cells. *Braz J. Med. Biol. Res.* 51 (2), e6950. doi:10.1590/1414-431X20176950
- Yi, J., Chen, B. T., Schwegler-Berry, D., Frazer, D., Castranova, V., McBride, C., et al. (2013). Whole-body nanoparticle aerosol inhalation exposures. *J. Vis. Exp.* 7 (75), e50263. doi:10.3791/50263
- Zavala, J., Freedman, A. N., Szilagyi, J. T., Jaspers, I., Wambaugh, J. F., Higuchi, M., et al. (2020). New approach methods to evaluate health risks of air pollutants: critical design considerations for *in vitro* exposure testing. *Int. J. Environ. Res. Public Health* 17 (6), 2124. doi:10.3390/ijerph17062124
- Zavala, J., Ledbetter, A. D., Morgan, D. S., Dailey, L. A., Puckett, E., McCullough, S. D., et al. (2018). A new cell culture exposure system for studying the toxicity of volatile chemicals at the air-liquid interface. *Inhal. Toxicol.* 30 (4–5), 169–177. Epub 2018 Aug 8. doi:10.1080/08958378.2018.1483983
- Ziller, V., Oppermann, T. S., Cassel, W., Hildebrandt, O., Kroidl, R. F., and Koehler, U. (2023). Chronic cough in postmenopausal women and its associations to climacteric symptoms. *BMC Women's Health.* 23 (1), 93. doi:10.1186/s12905-023-02225-2

Glossary

ACI	American Cleaning Institute	OSHA	Occupational Safety and Health Act
ADME	absorption, distribution, metabolism and elimination	PBPK	physiologically based pharmacokinetic
ALI	air-liquid interface	PET	polyester terephthalate
AOP	adverse outcome pathway	POD	point of departure
BMD	benchmark dose	PPE	personal protective equipment
BMDL	95% lower confidence limit on the BMD	QCM	quartz crystal microbalance
BMR	benchmark response	REACH	Registration, Evaluation, Authorisation, and Restriction of Chemicals
CBF	ciliary beat frequency	RfC	Reference Concentration
CFD	computational fluid dynamics	RH	relative humidity
CFPD	computational fluid particle dynamics	RHuA	reconstituted human airways
2D	two dimensional	SOP	standard operating procedure
3D	three dimensional	TD	toxicodynamic(s)
DA	defined approach	TK	toxicokinetic(s)
ECHA	European Chemicals Agency	TRV	toxicity reference value
ECM	extracellular matrix	TSCA	Toxic Substances Control Act
ELF	epithelial lining fluid	UF	uncertainty factor
EU	European Union	WOE	weight of evidence
DA	defined approach		
FIFRA	Federal Insecticide, Fungicide and Rodenticide Act		
GIVIMP	Guidance Document on Good <i>In Vitro</i> Method Practices		
GLP	Good Laboratory Practices		
GSD	geometric standard deviation		
HEC	human equivalent concentration		
HHRA	human health risk assessment		
hPCLS	human precision cut lung slices		
IATA	integrated approach to testing and assessment		
ICRP	International Commission on Radiological Protection		
ISDD	<i>in vitro</i> sedimentation, diffusion, and dosimetry model		
IVIVE	<i>in vitro</i> to <i>in vivo</i> extrapolation		
KE	key event		
KER	key event relationship		
LOAEL	lowest observed adverse effect level		
MMAD	mass median aerodynamic diameter		
MPPD	multiple-path particle dosimetry		
MIE	molecular initiating event		
MOA	mode of action		
MTT	3-[4,5-dimethylthiazol-2-yl]-2,5 diphenyl tetrazolium bromide		
NAM(s)	new approach methodologies		
n.d.	no date		
NOAEL	no-observed-adverse effect level		
NRC	National Research Council		
OECD	Organisation for Economic Co-operation and Development		



OPEN ACCESS

EDITED BY

Stina Oredsson,
Lund University, Sweden

REVIEWED BY

Robert Landsiedel,
BASF, Germany
Lan Ma-Hock,
BASF, Germany
Cynthia Bosquillon,
University of Nottingham, United Kingdom
Louis Scott,
ImmuONE, United Kingdom

*CORRESPONDENCE

Maria Teresa Baltazar,
✉ maria.baltazar@unilever.com

†PRESENT ADDRESS

Daniilo Basili,
Société des Produits Nestlé S.A., Nestlé
Research, Lausanne, Switzerland

RECEIVED 30 April 2024

ACCEPTED 13 January 2025

PUBLISHED 21 February 2025

CITATION

de Ávila RI, Müller I, Barlow H, Middleton AM,
Theiventhran M, Basili D, Bowden AM, Saib O,
Engi P, Pietrenko T, Wallace J, Boda B,
Constant S, Behrsing HP, Patel V and
Baltazar MT (2025) Evaluation of a non-animal
toolbox informed by adverse outcome
pathways for human inhalation safety.
Front. Toxicol. 7:1426132.
doi: 10.3389/ftox.2025.1426132

COPYRIGHT

© 2025 de Ávila, Müller, Barlow, Middleton,
Theiventhran, Basili, Bowden, Saib, Engi,
Pietrenko, Wallace, Boda, Constant, Behrsing,
Patel and Baltazar. This is an open-access article
distributed under the terms of the [Creative
Commons Attribution License \(CC BY\)](#). The use,
distribution or reproduction in other forums is
permitted, provided the original author(s) and
the copyright owner(s) are credited and that the
original publication in this journal is cited, in
accordance with accepted academic practice.
No use, distribution or reproduction is
permitted which does not comply with these
terms.

Evaluation of a non-animal toolbox informed by adverse outcome pathways for human inhalation safety

Renato Ivan de Ávila¹, Iris Müller¹, Hugh Barlow¹,
Alistair Mark Middleton¹, Mathura Theiventhran¹, Daniilo Basili^{1†},
Anthony M. Bowden¹, Ouarda Saib¹, Patrik Engi¹,
Tymoteusz Pietrenko¹, Joanne Wallace², Bernadett Boda³,
Samuel Constant³, Holger Peter Behrsing⁴, Vivek Patel⁴ and
Maria Teresa Baltazar^{1*}

¹Safety, Environmental and Regulatory Science (SERS), Unilever, Colworth Science Park, Sharnbrook, Bedfordshire, United Kingdom, ²Charles River Laboratories, Edinburgh, United Kingdom, ³Epithelix Sarl, Plan-les-Outes, Switzerland, ⁴Respiratory Toxicology Program, Institute for In Vitro Sciences, Inc., Gaithersburg, MD, United States

Introduction: This work evaluated a non-animal toolbox to be used within a next-generation risk assessment (NGRA) framework to assess chemical-induced lung effects using human upper and lower respiratory tract models, namely MucilAir™-HF and EpiAlveolar™ systems, respectively.

Methods: A 12-day substance repeated exposure scheme was established to explore potential lung effects through analysis of bioactivity readouts from the tissue integrity and functionality, cytokine/chemokine secretion, and transcriptomics.

Results: Eleven benchmark chemicals were tested, including inhaled materials and drugs that may cause lung toxicity following systemic exposure, covering 14 human exposure scenarios classified as low- or high-risk based on historical safety decisions. For calculation of bioactivity exposure ratios (BERs), obtained chemical-induced bioactivity data were used to derive *in vitro* points of departures (PoDs) using a nonlinear state space model. PoDs were then combined with human exposure estimates, i.e., predicted lung deposition for benchmark inhaled materials using multiple path particle dosimetry (MPPD) exposure computational modeling or literature maximum plasma concentration (C_{max}) for systemically available benchmark drugs.

Discussion: In general, PoDs occurred at higher concentrations than the corresponding human exposure values for the majority of the low-risk chemical-exposure scenarios. For all the high-risk chemical-exposure scenarios, there was a clear overlap between the PoDs and lung deposited mass and C_{max} for the benchmark inhaled materials and therapeutic drugs, respectively. Our findings suggest that combining computational and *in vitro*

new approach methodologies (NAMs) informed by adverse outcome pathways (AOPs) associated with pulmonary toxicity can provide relevant biological coverage for chemical lung safety assessment.

KEYWORDS

inhalation risk assessment, lung exposure modelling, lung toxicity, new approach methodologies, nonanimal testing, point of departure, bioactivity exposure ratio

1 Introduction

Unlike nebulized pharmaceuticals which are inhaled for therapeutic reasons, consumer spray products (e.g., antiperspirants, hairsprays, cleaning sprays) do not need to be inhaled to perform their function but may lead to unintentional inhalation exposure during normal daily use. It is therefore important for the safety assessment of such consumer products to consider the potential for ingredients to cause adverse effects in the lung under the conditions of product use. Lung hazard data have historically been obtained by performing testing in animals. In the case of inhaled materials, animal data have been taken from studies that consist of exposing rodents to chemicals in whole-body or nose-only systems, such as rodent acute (OECD, 2009a; OECD, 2009b; OECD, 2018c), 28-day subacute (OECD, 2018a), and 90-day subchronic (OECD, 2018b; US EPA, 1998) inhalation toxicity studies from which no observed effect concentration (NOEC) or no observed adverse effect concentration (NOAEC) are derived to inform human health inhalation risk assessments (Ramanarayanan et al., 2022).

In vivo studies have been used in risk assessment for many decades. However, it is clear that significant uncertainties arise from using animal data in the prediction of human toxicity responses due to anatomical, physiological, and biochemical differences between rodent and human respiratory systems and differences in breathing patterns (Cao et al., 2021; Clippinger et al., 2018b). Additionally, ethics related to animal welfare, and changes in the legislation in several geographies have motivated the development of more human-relevant tools and approaches that do not rely on the generation of new animal data to test chemicals (Brescia et al., 2023; Fentem, 2023). For example, animal testing of cosmetic ingredients has been banned in the European Union (EU) since 2009 (European Union, 2009). Other legislation, including the REACH (Registration, Evaluation and Authorization of Chemicals) regulation in the EU, also clearly states that registrants should only use animal testing as a last resort to obtain chemical hazard and safety information (European Commission, 2006).

In this context, recent research anchored in human-relevant science has focused on developing human-relevant *in silico* and *in vitro* tools and approaches (New Approach Methodologies, NAMs) that can be employed, together with existing information, within the next-generation risk assessment (NGRA) of materials to assess the risk of lung toxicity (Bedford et al., 2022; Clippinger et al., 2018b; Corley et al., 2021; OECD, 2022; Ramanarayanan et al., 2022; Stucki et al., 2022). NGRA aims to conduct safety assessments that are “human-relevant, exposure-led, hypothesis-driven and designed to prevent harm” (Dent et al., 2018). Therefore, NGRA focus on determining whether a substance triggers *in vitro* bioactivity at

human-relevant concentrations and, consequently, adverse health effects, *in lieu* of replicating apical endpoints that would traditionally be obtained using high-dose animal studies (Baltazar et al., 2020; Dent et al., 2021; Middleton et al., 2022; OECD, 2017; Thomas et al., 2019). NGRA uses information from NAMs and conservative decision-making to protect human health, aligning with the way regulatory decision-making has been conducted using traditional approaches (Browne et al., 2024).

Inspired by the NGRA concepts applied to other safety areas, such as systemic toxicity (Middleton et al., 2022), skin sensitisation (Gilmour et al., 2020; Gilmour et al., 2022), and development and reproductive toxicity (DART) (Rajagopal et al., 2022), we developed a strategy for inhalation safety assessment of consumer goods which considered the context of use (i.e. product formats and duration of application), the exposure of the ingredients to the respiratory tract (regional lung deposition/dosimetry), the types of ingredients of interest (e.g., polymers, preservatives) and the associated potential human adverse effects (e.g., lung inflammation and fibrosis) (Figure 1). The two main product formats are pressurised propellant-driven aerosols (e.g., antiperspirants and hairsprays) and pump/trigger sprays (e.g., hair and household cleaning products) which may be used daily through multiple applications. These two product formats produce different particle/droplet size distribution patterns. For example, pressurised propellant-driven aerosol hairsprays generally produce droplets with mass median aerodynamic diameters (MMAD) in the range of 2–7 μm , whereas hair pump sprays generate MMADs in the region of 5–15 μm . Given this difference, it is important to understand the realistic human exposure scenarios and then estimate the respiratory tissue dosimetry of materials potentially inhaled from these products. The predicted regional lung deposition using computational models, such as the multiple path particle dosimetry (MPPD) (<https://www.ara.com/mppd/>), can differ between these two formats, with pressurised propellant-driven aerosols leading to alveolar (particles < 7 μm), tracheobronchial and head (nasal and pharynx) exposures, whereas pump/trigger sprays mostly lead to distribution in tracheobronchial and head regions.

The current mechanistic understanding behind chemically-induced respiratory adverse effects through adverse outcome pathways (AOPs) can facilitate the establishment of appropriate NAM-based toolboxes with broad coverage of bioactivity readouts/biomarkers relevant to inhalation hazards which can provide *in vitro* point of departures (PoDs). In turn, *in vitro* PoDs and exposure estimates can be combined into a single metric to understand safe levels in humans, i.e., the bioactivity exposure ratio (BER), also known as margin of safety or margin of exposure (Health Canada, 2021; Middleton et al., 2022; Paul Friedman et al., 2019; Reardon et al., 2023; Wetmore et al., 2015).

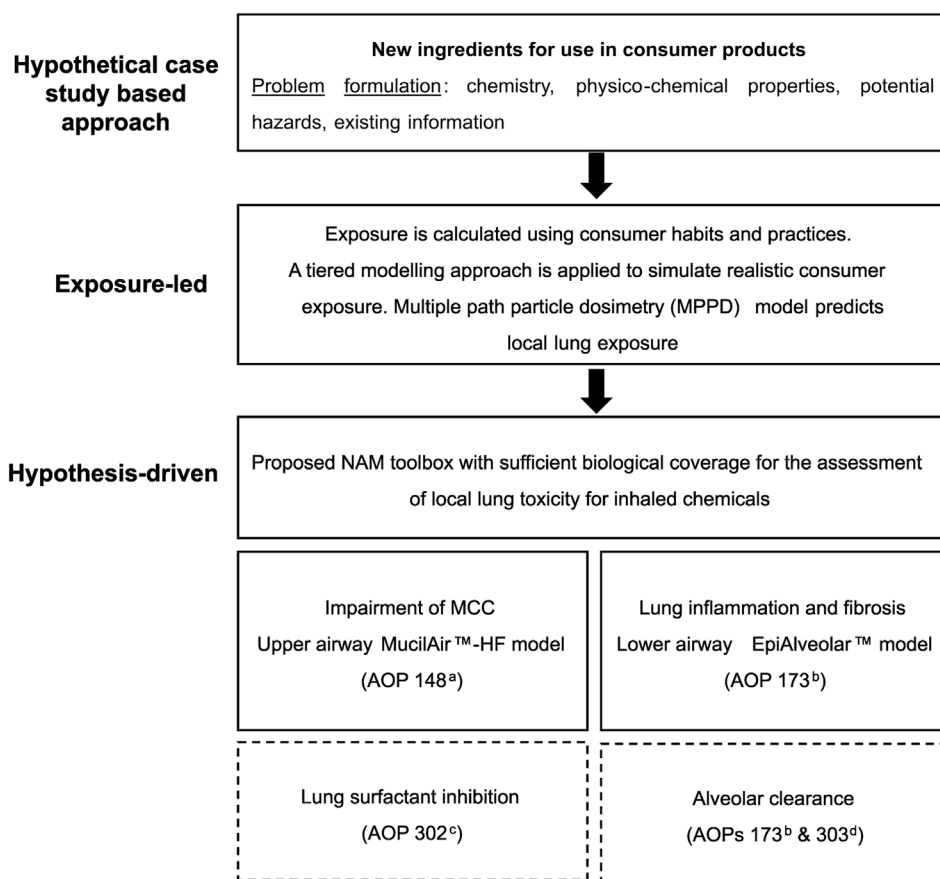


FIGURE 1

Human-relevant strategy for inhalation safety assessment recommended within next-generation risk assessment (NGRA). The strategy is structured around the context of use (i.e. product formats and duration of application), exposure to the respiratory tract (regional lung deposition), the types of chemicals of interest (e.g., polymers, preservatives) and the associated potential adverse effects. The two main product formats are pressurised propellant-driven aerosols (e.g., antiperspirants and hairsprays) and pump/trigger sprays (e.g., hair and cleaning products). These two product formats produce different particle/droplet size distribution patterns. The predicted regional lung deposition using the multiple path particle dosimetry (MPPD) will differ between these two formats, with pressurised propellant-driven aerosols leading to alveolar (particles < 7 µm), tracheobronchial and head (nasal and pharynx) exposures, whereas pump/trigger sprays mostly lead to distribution in tracheobronchial and head regions. The selection of new approach methodologies (NAMs) to assess inhalation toxicity was informed by this extensive knowledge of product use and human exposure. The establishment of a comprehensive NAM toolbox relied on adverse outcome pathways (AOPs) associated with inhalation toxicity. Several adverse outcomes stem from a common molecular initiating event (MIE), which is the interaction of chemicals with lung cells, and involve similar intermediate key events (KEs). Based on this, pulmonary inflammation/fibrosis, impairment of mucociliary clearance (MCC), lung surfactant inhibition, and alveolar clearance were prioritized as the key endpoints of concern. This study focuses on evaluating the NAM toolbox for only two of these endpoints - impairment of MCC and pulmonary inflammation/fibrosis using upper (MucilAir™-HF) and lower (EpiAlveolar™) respiratory tract models. ^a<https://aopwiki.org/aops/148> ^b<https://aopwiki.org/aops/173>/OECD Series on AOP No. 33 (Halappanavar et al., 2023) ^c<https://aopwiki.org/aops/302> ^d<https://aopwiki.org/aops/303>.

In this pilot work, we aimed to investigate the feasibility of defining an NAM toolbox for lung toxicity assessment using two commercial 3D reconstructed human lung models to represent the upper and lower respiratory tract, namely MucilAir™-HF and EpiAlveolar™ systems, respectively. The different bioactivity readouts (from which PoDs are derived) are mixture of readouts directly mapped into the AOPs relevant for lung toxicity (specific) and non-specific bioactivity. For example, specific lung biomarkers such as cilia beating frequency or mucin secretion were selected, in comparison to general markers of cell integrity and transcriptomics. Both are intended to be used in a protective manner, i.e. they represent a measure of bioactivity that can be used in an exposure-led safety assessment (Cable et al., 2024). To investigate the feasibility of these assays to provide protective PoDs and BER estimates, a panel of benchmark chemicals, selected based on

historical safety decisions and covering several human exposure scenarios (e.g., consumer goods products and occupational use scenarios), was tested.

2 Materials and methods

2.1 Human-relevant strategy for selecting NAMs for lung toxicity NGRA

The selection of NAMs for use in risk assessments for both acute and chronic lung toxicity was informed by an extensive knowledge of product use and human exposure, as previously mentioned (Figure 1). The aim was to identify assays that provide broad biological coverage of the key adverse outcomes across the upper

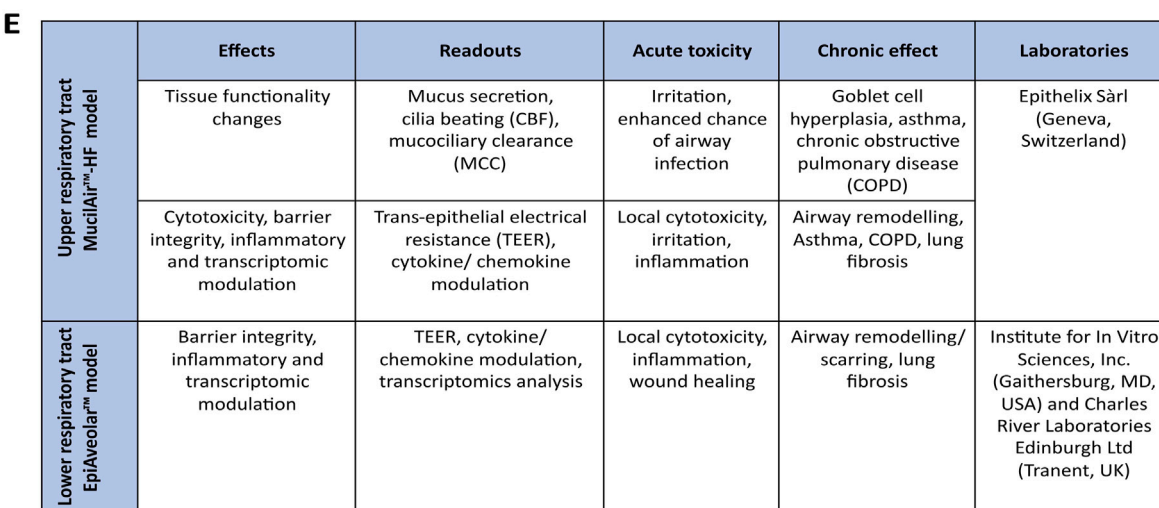


FIGURE 2 Schematic illustration of the upper MucilAir™-HF and lower EpiAveolar™ respiratory tract models, test material exposure, study design and selection of bioactivity readouts aligned to adverse outcome of pathways (AOPs)/endpoints of interest. **(A)** MucilAir™ model (Epithelix, Geneva, Switzerland) is a commercial air-liquid interface system composed of primary human cells that are differentiated into a ciliated pseudostratified respiratory epithelium with barrier function, including ciliated, basal, and goblet cells that produce mucus. **(B)** EpiAlveolar™ model (MatTek Corporation, Ashland, MA, United States) is a commercial air-liquid interface system composed of human primary alveolar epithelial cells, fibroblasts, endothelial cells, and macrophages and have shown to replicate biological responses to known pro-fibrotic compounds after sub-chronic exposures **(C)** Both models are stable for extended periods and allows for single or repeated exposure, either via liquid application or a nebulization system. The nebulization process occurs during 3–5 min through test material-containing cloud emission, homogeneous mixing, and droplets gravitational settling phases. **(D)** For toxicity

(Continued)

FIGURE 2 (Continued)

testing, tissues were exposed to the test materials once a day repeatedly for 30 min/6 h (for MucilAir™) or 24 h (for EpiAlveolar™) over 12 consecutive days. (E) Several bioactivity readouts, that translate to substance-induced acute and chronic effects examinations, were investigated at different time points over a 12-day experimental period by three laboratories.

(nose to larynx) and lower (trachea to alveoli) respiratory tract to support risk assessments that will protect the exposed human population. The establishment of a comprehensive NAM toolbox was anchored in several AOPs associated with lung toxicity (Clippinger et al., 2018a; Clippinger et al., 2018b; Halappanavar et al., 2020; Luettich et al., 2021; Luettich et al., 2017), details of which can be found on the virtual platform for the development and storage of AOPs (<https://aopwiki.org/>). Literature shows that several adverse outcomes can stem from a common molecular initiating event (MIE), defined as the initial interaction between a molecule and a biomolecule or biosystem that can be causally linked to an outcome via a pathway (Allen et al., 2014). This common MIE occurs at the level of the epithelial lung cells, and the AOPs also involve similar intermediate key events (KEs) (Halappanavar et al., 2020). Based on this, pulmonary inflammation/fibrosis, impairment of mucociliary clearance (MCC), lung surfactant inhibition, and alveolar clearance can be highlighted as the key endpoints of concern for inhaled materials (Figure 1). This paper focuses on our preliminary evaluation of the NAM toolbox for KEs linked to only two of these adverse effects - impairment of MCC and pulmonary fibrosis in upper and lower respiratory tract, respectively, considering that these regions are generally the most sensitive targets to chemicals in which humans may be repeatedly exposed via inhalation (Escher et al., 2010).

MCC plays a vital role in the innate immune defence against airborne pathogens and inhaled xenobiotics. The protective mucous layer, the airway surface liquid layer, and the cilia on the surface of ciliated cells are the key functional components responsible for this process. Any disturbance in the processes regulating these components can lead to MCC dysfunction. This dysfunction has been associated with the development of lung diseases such as chronic obstructive pulmonary disease (COPD) and asthma, which pose a significant risk of increased morbidity and mortality. AOP 148 (<https://aopwiki.org/aops/148>) outlines the mechanism by which exposure to inhaled toxicants can lead to mucus hypersecretion and subsequently affect pulmonary function (Luettich et al., 2017). Later, Luettich et al. (2021) expanded AOP 148 further to include oxidative stress as an MIE, decrease cilia beating frequency (CBF) and decrease MCC as KE6 and KE7, respectively. To obtain bioactivity associated with the MIEs or KEs outlined in both AOPs, the MucilAir™-HF model (Epithelix, Geneva, Switzerland) was selected. This system is composed of primary human cells that are differentiated into a ciliated pseudostratified respiratory epithelium with barrier function, including ciliated, basal, and goblet cells that produce mucus (Huang et al., 2011) (Figure 2A). The model has been shown to be stable for extended periods and allows for both single and repeated substance exposure, either via liquid application or nebulization system, and provides a realistic representation of the route of administration of inhaled materials, using, for instance, the Vitrocell® Cloud 12 system chamber (Vitrocell Systems GmbH,

Waldkirch, Germany). Measurements of mucin secretion, CBF, MCC, and a panel of cytokines/chemokines were taken at three timepoints over a 12-day experimental period (Figures 2C–E).

Lung fibrosis is characterised by the progressive and irreversible destruction of lung architecture caused by a dysregulated tissue repair process (Wynn, 2011). AOP 173 (<https://aopwiki.org/aops/173>), also summarized in the OECD Series on AOP No. 33 (Halappanavar et al., 2023), describes the relationship between the initial interaction of a test material with components of the resident lung cellular membrane (considered the MIE), and the subsequent KEs triggered by the release of pro-inflammatory and pro-fibrotic mediators that signal the recruitment of immune cells into the lungs. If the chemical/stressor is not cleared effectively and/or, in particular, if there is repeated exposure, the persistent inflammation triggers to fibroblast proliferation and myofibroblast differentiation, leading to synthesis and deposition of extracellular matrix, such as collagen. In turn, excessive collagen deposition results in alveolar septa thickening, decrease in total lung volume and lung fibrosis (the adverse outcome). Pulmonary fibrosis is a complex condition that is difficult to model *in vitro* because it involves multiple cell types and typically develops over a prolonged period after repeated exposures. Nevertheless, the objective here was to evaluate a human tissue model that is intended to represent the alveolar region and that can deliver a range of readouts critical in the AOPs (Figures 2B–E). These readouts include the secretion of pro-inflammatory and pro-fibrotic mediators, loss of alveolar membrane integrity, and fibroblast/myofibroblast proliferation. When the experiments were being planned, the EpiAlveolar™ model (MatTek Corporation, Ashland, MA, United States) was deemed the most favourable commercial option. This model includes human primary alveolar epithelial cells, fibroblasts, endothelial cells, and macrophages (Figure 2B) and had shown to replicate biological responses to known pro-fibrotic compounds after sub-chronic exposures (Barosova et al., 2020). Experiments with EpiAlveolar™ model were conducted in two laboratories to compare how the results vary across different testing facilities.

Finally, a series of well-known benchmark chemicals and documented exposures that are known to be associated with or without adverse effects in humans were selected for the evaluation of the performance of each tissue model (Tables 1–3).

2.2 Test materials and exposure scenario selection

For the evaluation of the upper and lower respiratory models, two groups of test materials were selected: reference materials and benchmark chemicals (Tables 1, 2). Reference materials were selected to test whether the model was sensitive to chemicals known to cause a specific effect *in vitro* as described in the literature. Supplementary Table S1 describes in detail the

TABLE 1 Benchmark chemicals and reference materials used for the upper respiratory toxicity testing using MucilAir™-HF systems.

Test materials	CAS no.	Abbreviation	Solvent	Exposure method ^a	Exposure time/day	Tested concentrations
Benchmark chemicals						
AKEMI® anti-fleck super	-	Akemi	Saline	Aerosol	30 min ^b	1, 6, 12 µg/cm²
					6 h ^c	6 µg/cm²
ACUDYNE™ DHR copolymer	-	Acrylate copolymer	Saline	Aerosol	30 min ^b	0.1, 10, 100 µg/cm²
					6 h ^c	100 µg/cm²
Butyl ester of poly (methyl vinyl ether-alt-maleic acid monoethyl ester) copolymer	-	BE PVM/MA	Saline	Apical liquid	30 min ^d	0.1, 10, 100 µg/cm²
					6 h ^c	100 µg/cm²
Carboxymethylcellulose sodium salt	9004-32-4	CMC	Saline	Aerosol	30 min ^b	2.5, 5, 10, 100 µg/cm²
Coumarin	91-64-5	Coumarin	Saline	Aerosol	30 min ^b	0.5, 4.7, 9.4 µg/cm²
					6 h ^c	4.7 µg/cm²
Polyhexamethyleneguanidine phosphate	89697-78-9	PHMG	Saline	Aerosol	30 min ^d	0.8, 2.4, 4.8 µg/cm²
					6 h ^c	2.4 µg/cm²
Reference materials						
Nicotine	54-11-5	Nicotine	Saline	Aerosol	30 min ^d	0.04, 0.4, 4 µg/cm²
Lipopolysaccharide from <i>Pseudomonas aeruginosa</i> 10	-	LPS	Saline	Apical liquid	30 min ^d	0.2, 1.6, 16 µg/cm²
				Aerosol	6 h ^c	1.6 µg/cm²
Benzalkonium chloride	63449-41-2	BAC	Saline	Apical liquid	30 min ^b	0.1, 0.5, 5, 10 µg/cm²
Acrolein	107-02-8	Acrolein	Saline	Apical liquid	30 min ^d	500, 750, 1,000 µM
4-Chloro-3-methylphenol	59-50-7	Chlorocresol	Saline	Apical liquid	30 min ^d	1.3, 2.6, 26 µg/cm²
Isoproterenol hydrochloride	5984-95-2	Isoproterenol	Medium	Basal liquid	30 min ^d	1, 50, 100 µM
CFTR _{inh} -172	307510-92-5	CFTR _{inh} -172	DMSO	Basal liquid	30 min ^d	1, 10, 100 µM
Recombinant human TNF-α (carrier-free)	-	TNF-α	PBS + FCS	Basal liquid	30 min ^d	10, 50, 100 ng/mL
R,S-Sulforaphane	4478-93-7	Sulforaphane	Saline	Aerosol	30 min ^d	0.1, 1.4, 2.9 µg/cm²
					6 h ^d	1.4 µg/cm²

^aVolumes used for aerosol, apical liquid or basal liquid exposures were 0.47, 10 or 700 µL, respectively.

^bMale healthy donor, 41 years (batch number MD072001); age of tissue culture: 53 days.

^cMale healthy donor, 41 years (batch number MD072001); age of tissue culture: 81 days.

^dFemale healthy donor, 56 years (batch number HF-MD078701); age of tissue culture: 42 days.

^eMale healthy donor, 41 years (batch number MD072001); age of tissue culture: 67 days.

supporting evidence for the 7 reference materials which can trigger lung toxicity via different mechanisms, including inflammation (e.g., LPS), oxidative stress (e.g., Acrolein), CBF (e.g., Chlorocresol), and mucus production/viscosity changes (e.g., CFTR_{inh}-172). However, for the purposes of evaluating NAMs for use in safety assessment, it is also necessary to define exposure scenarios, that are associated either with no effects in humans or have been reported to cause adverse respiratory effects. This approach allows the evaluation of a set of tools not only in the context of hazard but incorporating exposure in the context of risk assessment (Middleton et al., 2022). The underpinning hypothesis of this benchmarking approach as an evaluation strategy is that the

magnitude of the BER (i.e., the ratio between bioactivity expressed through *in vitro* PoD derivation and predicted human exposure) is correlated with level of risk in humans. In simple terms, for each benchmark chemical-exposure, a BER is calculated by dividing the lowest *in vitro* PoD across all bioactivity readouts by the predicted exposure (Middleton et al., 2022; Paul Friedman et al., 2019). In principle, a NAM toolbox is deemed successful if it is capable of distinguishing between low- and high-risk exposure scenarios as a function of the BER size.

The criteria used for the selection of benchmark chemicals included the following: 1) a human exposure can be defined (e.g., inclusion level of a chemical in a given product type, and how it is

TABLE 2 Benchmark chemicals and reference materials used for the lower respiratory toxicity testing using EpiAlveolar™ systems.

Test materials	CAS no.	Abbreviation	Solvent	Exposure method ^a	Exposure time	Tested concentrations
Benchmark chemicals						
AKEMI® Anti-Fleck Super	-	Akemi	Saline	Aerosol, daily for 12 days	24 h	0.3, 0.8, 1.6, 8 µg/cm²
Crystalline silica	7631-86-9	Crystalline silica	Saline	Aerosol, daily for 12 days	24 h	0.01, 1, 5, 50 µg/cm²
Amorphous silica	112945-52-5	Amorphous silica	Saline	Aerosol, daily for 12 days	24 h	0.01, 1, 5, 50 µg/cm²
Polyhexamethyleneguanidine phosphate	89697-78-9	PHMG	Saline	Aerosol, daily for 12 days	24 h	Lab 1: 0.005, 0.01, 0.05, 0.2 µg/cm² Lab 2: 0.1, 0.5, 0.9, 9.4 µg/cm²
Amiodarone hydrochloride	19774-82-4	Amiodarone	DMSO	Basal liquid, daily for 12 days	24 h	0.01, 0.1, 1 and 10 µM
Doxorubicin hydrochloride	25316-40-9	Doxorubicin	Medium (Lab 1) or ultrapure water (Lab 2)	Basal liquid, daily for 6 days +6 days without exposure	24 h	0.18, 0.36, 0.72 µM
Reference materials						
LPS from <i>Pseudomonas aeruginosa</i> 10 (Lab 1) or <i>Escherichia coli</i> 055:B5 (Lab 2)	-	LPS	DMSO (Lab 1) or saline (Lab 2)	Apical liquid, daily for 12 days	24 h	0.01, 0.1, 1, 10 µg/mL
R,S-Sulforaphane	4478-93-7	Sulforaphane	Saline	Aerosol, daily for 12 days	24 h	0.03, 0.1, 0.6, 3 µg/cm²

^aVolumes used for aerosol, apical liquid or basal liquid exposures were 200–250 µL, 75 µL or 5 mL, respectively.

used); 2) existing toxicological information (animal, human, *in vitro*); and 3) evidence to support the high- or low-risk classification for each chemical-exposure scenario pair based on existing safety assessment and/or regulatory limits. For example, the Research Institute for Fragrance Material (RIFM) reviewed the safety of Coumarin and concluded it was safe to be used in antiperspirant aerosols up to 0.08% (Api et al., 2019; Api et al., 2020). Similarly, acrylate copolymers are frequently used as hair fixatives and supported by inhalation risk assessment at the inclusion level of 5% in hairspray aerosol (CIR, 2018). For high-risk exposure scenarios, we selected Crystalline silica, a well-known particle responsible for several cases of pulmonary fibrosis developed over many years at exposure levels higher than the permissible exposure limit (PEL) of 0.05 mg/m³ calculated as an 8-h time-weighted average (TWA) (Steenland and Brown, 1995). Another example of a high-risk scenario is the use of the antimicrobial polyhexamethylene guanidine phosphate (PHMG) which caused serious adverse effects in humans in Korea at the inclusion level of 1.3% in humidifiers, which were also observed in animal and *in vitro* experiments (Jung et al., 2014; Kim et al., 2016; Song et al., 2022). This paper focuses primarily on exposure to inhaled materials, however, two compounds (Amiodarone and Doxorubicin) with robust human data from oral or intravenous (i.v.) administration were tested to assess the EpiAlveolar™ model's response to known pro-fibrotic drugs. The exposure scenarios, risk classification and associated rationale are presented in detail in Table 3. For some chemicals it was possible to find more than one scenario. In the case of Crystalline silica, different risk classifications were identified, one low risk and one high risk (see Table 3).

2.3 Local lung exposure estimation

2.3.1 Exposure modelling

For most of the exposure scenarios related to inhaled materials (see Table 3), the objective was to obtain a worst-case human estimate of deposited aerosol concentrations in each region of the upper and lower respiratory tract (µg/cm²). This single value of exposure was then compared to the *in vitro* PoDs obtained from each readout of the correspondent experiment using MucilAir™-HF and EpiAlveolar™ for upper and lower respiratory tract, respectively.

Several steps were needed to predict these exposure values. The first step was to collate information about the use scenario (consumer, patient, or worker), product type, benchmark chemical inclusion level, duration of exposure, route of exposure, and particle size distribution (Table 3; Supplementary Material S1). For Amiodarone and Doxorubicin, which are administered via the oral and i.v. routes, respectively, plasma levels corresponding to a typical therapeutic dose scheme were obtained from the literature (Andreasen et al., 1981; Barpe et al., 2010). For these compounds, PoDs were expressed in µM given that this would be the most relevant metric for the risk assessment.

For the inhalation exposures, the second step was to calculate an airborne concentration which was either derived from the literature (e.g. PHMG and Akemi) or experimentally derived (Acrylate copolymer, Amorphous silica, Coumarin, BE PVM/MA, and BAC) using simulated use evaluation testing (SUET; see details below in item 2.3.3).

TABLE 3 Exposure scenarios, risk classification and associated rationale for the investigated benchmark chemicals.

Benchmark chemical	Risk classification	Risk classification reasoning	Product	Exposure scenario		Concentration or dose	Particle size (µm)	References
BE PVM/MA ^a	Low	Used safely in cosmetic products. Exposure level supported by existent toxicological data	Hair spray ^a	10% inclusion pump spray	10 min Once a day	0.017383 mg/m ³	8.53	Carthew et al. (2006) , Burnett et al. (2011)
Coumarin ^a	Low	Used safely in cosmetic products. Exposure level supported by existent toxicological data	Anti-perspirant ^a	0.08% Inclusion Spray rate 1 g/s Breathing zone volume 1 m ³ 2s/axillae	10 min Twice a day	0.00183 mg/m ³	5.22	Api et al. (2020)
Acrylate copolymer	Low	Used safely in cosmetic products. Exposure level supported by existing toxicological data	Hair Spray ^a	5% Inclusion Spray rate 0.59 g/s Breathing zone volume 1 m ³ 10s application	10 min Once a day	0.022518 mg/m ³	3.632	CIR (2019)
Amorphous silica	Low	Used safely in cosmetic products. Exposure level supported by existent toxicological data	Anti-perspirant ^a	Inclusion 0.06% Spray rate 1 g/s Breathing zone volume 1 m ³ 8s spray time	10 min Twice a day	0.001461 mg/m ³	6.317	CIR (2019)
	Low	The National Institute for Occupational Safety and Health recommended exposure limit (REL)	Occupational Scenario	Worker shift	8 h Shift	6 mg/m ³	3	Barsan (2007)
CMC	Low	Used safely in nasal sprays products	Nasal spray	Single dose 0.1% inclusion level (1.25 µg/cm ²)	N/A	N/A	N/A	Gizurarson (2012) , Ugwoke et al. (2000)
BAC	Low	Used safely in nasal sprays and ophthalmic products	Nasal spray	0.01% inclusion level (0.5 µg/cm ²)	N/A	N/A	N/A	Johnson (2017)
	Low	Used safely in homecare products. Exposure level supported by existent toxicological data	Cleaning spray	Inclusion level 0.75%	10 min Once a day	0.0081 mg/m ³	7	Johnson (2017)
Crystalline silica	Low	OSHA: <i>Permissible exposure limit (PEL)</i> . The employer shall ensure that no employee is exposed to an airborne concentration of respirable Crystalline silica in excess of 0.05 mg/m ³ , calculated as an 8 h time-weighted average (TWA)	Occupational scenario (Low Risk)	Worker shift	8 h shift 5 days a week	0.05 mg/m ³	3	US Occupational Safety and Health Administration (2013)
	High	Exposure likely to result in silicosis after cumulative exposure	Occupational scenario (High Risk)			5 mg/m ³	3	Mannetje et al. (2002)

(Continued on following page)

TABLE 3 (Continued) Exposure scenarios, risk classification and associated rationale for the investigated benchmark chemicals.

Benchmark chemical	Risk classification	Risk classification reasoning	Product	Exposure scenario		Concentration or dose	Particle size (μm)	References
PHMG	High	Evidence of serious adverse lung effects such as diffuse pulmonary fibrosis	Humidifier	From measurements taken of humidifier in low humidity environment	11 h Once a day	0.95 mg/m ³	5.5	Park et al. (2014), Lee and Yu (2017)
Akemi	High	Acute lung toxicity characterised by coughing, tachypnoea, chest pain, fever, and shortness of breath	Tile coating product	Worker scenario	150 min Once per day	563 mg/m ³	3	Duch et al. (2014)
Doxorubicin	High	Evidence of occurrence of interstitial lung disease in cancer patients	Therapeutic dose	Plasma conc 1.3 μM		Infusion of 60 mg/m ² for 40 min		Schwaiblmair et al. (2012), Nevadunsky et al. (2013), Hoshina and Takei (2021), Li et al. (2021), Barpe et al. (2010)
Amiodarone	High	Alveolar/interstitial pneumonitis with a subacute onset	Therapeutic dose	Plasma conc: 2 μM		Single dose of 400 mg via oral route		Wolkove and Baltzan (2009), Andreasen et al. (1981)

*Scenarios for which SUET data was used to determine airborne concentration and particle size.

The third step was to use the MPPD model to calculate the deposition of each benchmark chemical in the lung based on the airborne concentration and particle size. For most exposures, particle size information was either experimentally derived (SUET data) or based on the literature (Table 3); however, for the two occupational exposure scenarios (Crystalline and Amorphous silica), a corresponding measured particle diameter was not found. In lieu, a worst-case assumption that the particle diameter in both cases was 3 μm was made, corresponding to the highest deposition fraction in the lower respiratory tract according to MPPD (version 3.04).

In the case of nasal spray based scenarios, MPPD was not used, and all exposure was assumed to be confined to the nasal cavity. Therefore, only the airborne concentration and nasal cavity areas were required to calculate a mass per unit area (Gizurason, 2012; Johnson, 2017).

In this study, we compared a calculated local concentration in the lung for each exposure scenario to the PoD obtained in the *in vitro* lung models. For this purpose, MPPD was used to calculate the deposited mass in each lung generation. Using the mass deposited and the corresponding area of each generation, a local average concentration is determined as the ratio between the mass deposited in generation and the area of generation. This quantity is a function of the particle diameter as measured or estimated for each exposure scenario.

Once deposited, clearance mechanisms in the upper and lower respiratory tract regions begin to remove the material. These mechanisms for the clearance of material from the upper and lower respiratory tracts were modelled as described in item 2.3.2.

2.3.2 *In silico* lung dosimetry modelling

MPPD (<https://www.ara.com/mppd/>) is a widely used tool which models human lungs as a series of interconnected pipes, i.e., it models the lungs as connected bifurcating paths, which each new bifurcation corresponding to a “lung generation”, with the trachea corresponding to generation 1 and terminating at generation 23 (terminal bronchioles) (Asgharian and Price, 2006; Asgharian and Price, 2007; Asgharian et al., 2006; Rostami, 2009; Patwa and Shah, 2015). Within each of these pipes, which vary in length and diameter according to lung generations, the deposition of a given particle/droplet is estimated based on gravitational effects, diffusion and impaction. For the purposes of this study, the lung geometry used was the symmetric Weh-Shum model with a fixed breathing rate of 12 breaths per minute, with a functional residual capacity of 3,300 mL. The upper respiratory tract volume was set at 50 mL. The tidal volume of the lung was assumed to be 625 mL with no pause between inhalation and exhalation and an inspiratory fraction of 0.5.

With these assumptions and the parameters determined for each of the exposure scenarios above (see Supplementary Material S1), the dose rate within the lung (mg/min) for each exposure scenario in each generation of the lung was calculated. In absence of any clearance, the local concentration would simply be the local dose-rate multiplied by the total exposure duration as specified in each scenario.

To make the exposure scenarios realistic, we modelled the clearance for both the upper and lower respiratory tract using the human respiratory clearance model as developed by the International Congress on Radiological Protection (ICRP, 1994), as described in

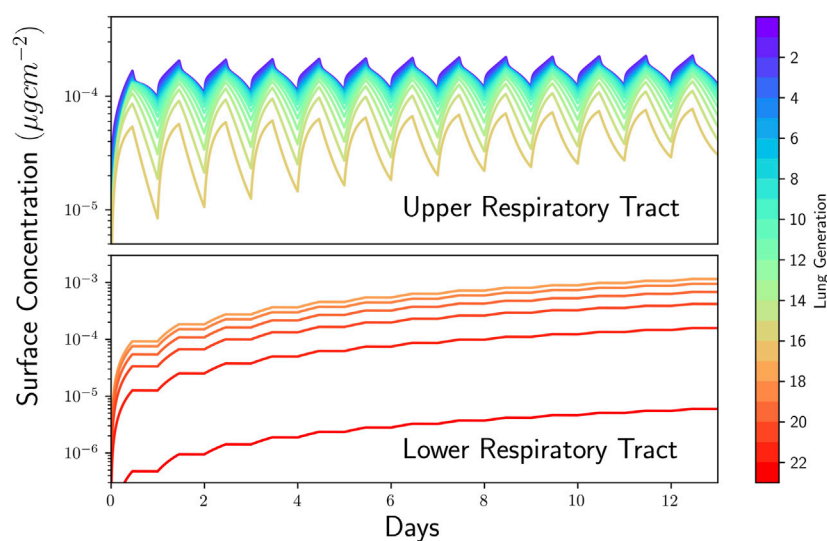


FIGURE 3

Lung dosimetry modelling using multiple path particle dosimetry (MPPD). Concentration in each generation of the lung as a function of time for Polyhexamethyleneguanidine phosphate (PHMG) humidifier exposure. Upper airway concentration (top) and lower airway concentrations (bottom) shown separately. Lung generations (i.e., tracheobronchial tree, a system partitioned into 23 generations of dichotomous branching, from trachea to the last order of terminal bronchioles, respectively, generations 0 and 23) are indicated by numbers as shown in the colour bar.

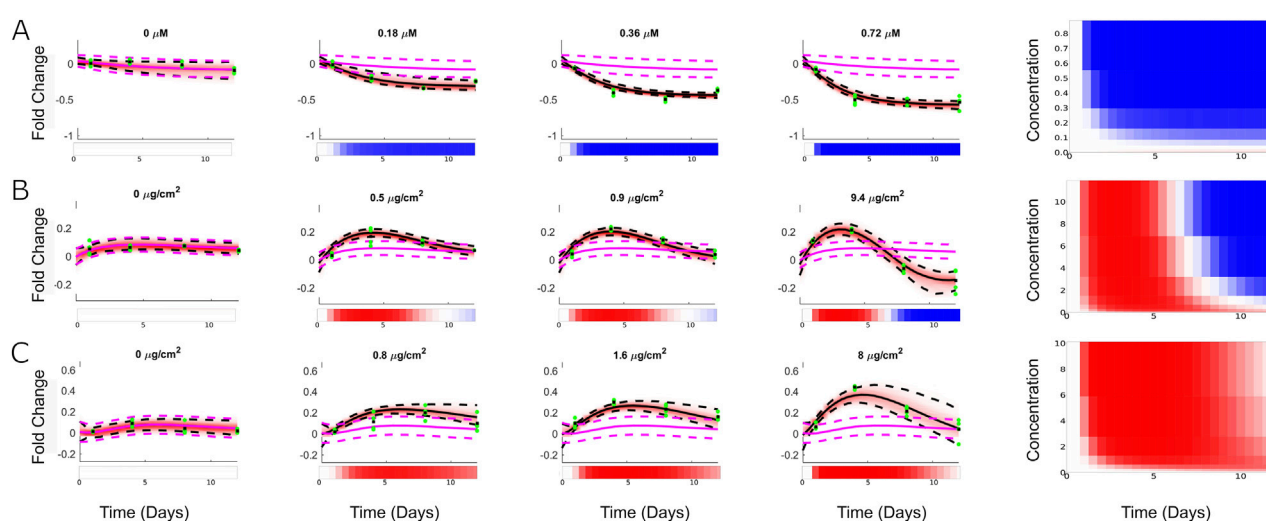


FIGURE 4

Representative concentration response data and model fits using the state space model. Left) Posterior predictive plots comparing the inferred trajectories of the different readouts in response to chemical treatment to the normalised data for (A) Doxorubicin for MMP -3, (B) PHMG for IL-1ra, (C) Akemi for IL-1a. Pink and black dashed lines represent 95% credible range of vehicle control and cred range of mean response, respectively. Green dots are the data points, whereas the depth of red shading reflects the probability distribution of the mean response. Blank, blue, and red colours represent no changes, down- or upregulation in relation to control (at same timepoint), respectively, whereas the colour variation shows the intensity of such effects. Right) Corresponding heat map representations of the biomarker response as described by the state space model blank, blue, and red colours represent no changes, down- or upregulation in relation to control (at same timepoint), respectively, whereas the colour variation shows the intensity of such effects.

Supplementary Material S2. The methodology here therefore combines the mechanistic MPPD model for predicting exposure, with the semi-empirical ICRP model for clearance. Hereafter, the ICRP model, when mentioned here, only refers to clearance modelling, as ICRP model for deposition was not used in this study. Such a hybridised approach is

already taken in the commercially available MPPD software but does not return a local concentration as we desired here. The value obtained using the commercially available form of MPPD only produces a total retained mass in the upper and lower lung and so does not give the additional granularity we seek to compare *in vitro* to *in vivo* dose.

However, we have used the default clearance parameters implemented in MPPD and so when compared for total mass retained our results correspond to the value obtained using the commercial software.

In this study, to determine the local dose within each generation of the lung, the ICRP clearance model was implemented to predict a retained mass in each lung generation over time. The average local concentration is determined by dividing the mass retained in the lung generation by the area of the corresponding generation of the lung for each given day. An example of the local concentration as a function of time is shown in Figure 3. The exposure used to compare to the *in vitro* dose response is taken to be the highest predicted exposure for each region of the lung on a measured day. By combining *in silico* deposition and clearance, this method offers a better approximation of the *in vivo* concentration for each scenario, while remaining conservative.

2.3.3 Simulated use evaluation testing (SUET)

SUET is a measurement method for sprayed particles/droplets released during simulated consumer use scenarios of products, allowing the generation of realistic consumer exposure data for use in safety assessments (Carthew et al., 2002; Steiling et al., 2014). In brief, a mannequin, placed in a room of a standardised size, was positioned (e.g., arms up for axilla spraying) and equipped accordingly (e.g., wearing a full length, real hair wig for hair products), and was exposed in a realistic manner (i.e., equivalent to the expected use scenario based on the product type and user under investigation) to the sprayed product (e.g., a short burst spray at each axilla for antiperspirants). The number/mass of any airborne particles/droplets in the mannequin's "breathing zone" during product use was determined by sampling the room air for a short duration (i.e., similar to the expected time the user remains in the vicinity of the spray cloud), via a short tube (representing the upper respiratory tract) attached to the "mouth" of the mannequin, using a TSI Model 3,321 Aerodynamic Particle Sizer time-of-flight spectrometer (TSI Incorporated, Shoreview, MN, United States) (FEA, 2009). These data were used to calculate the particle size (μm) and estimate the inhalable dose (mg/m^3 ; fraction potentially depositing anywhere within the respiratory tract) during the sampling period, and then used as input for the MPPD modelling.

2.4 Materials

All reagents used are listed in Supplementary Material S2.

2.5 Upper respiratory toxicity assessment using MucilAir™-HF model

2.5.1 MucilAir™-HF culture

The MucilAir™-HF system (EP11MD) and ready-to-use chemically-defined, serum-free culture medium (EP04AM) were obtained from Epithelix Sàrl (Geneva, Switzerland). Tissues were handled as recommended by manufacturer's instruction. Epithelia (MucilAir™-HF) were used containing bronchial cells isolated from 2 healthy donors (male, 41 years, batch number MD072001; and female, 56 years, batch number HF-MD078701). After differentiation for 42 up to 81 days at the air-liquid interface

(ALI) under standard culture conditions ($37^\circ\text{C} \pm 1^\circ\text{C}$ in a humidified atmosphere of $5\% \pm 1\%$ CO_2 in air), tissues were washed 3 days before first exposure and each insert was inspected for beating cilia and mucus production. This washing step (one or twice with PBS) were performed to remove accumulated mucus and cell debris to minimize the risk of interference with the toxicity tests. Over 12-day experimental period, washing steps as well as media changes was performed every 2-3 days. Trans-epithelial electrical resistance (TEER) was measured and only inserts which passed morphological inspection and showed $\text{TEER} > 200 \Omega \cdot \text{cm}^2$ were used.

2.5.2 Test material exposure

To prepare the stock solutions to perform the test material exposures, buffered saline solution (0.9% NaCl, 10 mM HEPES, 1.25 mM CaCl_2), DMSO or culture medium (Table 1). See Supplementary Material S2 for additional details.

For toxicity testing performed over a 12-day experimental period, tissues were daily exposed to 3 different concentrations of each test material for 30 min or 6 h (for detailed information on each material see Table 1). The test material exposure time was chosen based on the average time (30 min) for which the upper airway mucociliary beating transport mechanism propels inhaled particles out of the human airways (Koparal et al., 2021), and previous experimental design in which MucilAir systems were daily exposed to inhaled drugs for 6 h over 12-day period (Balogh Sivars et al., 2017). Tissues were exposed by test materials via nebulization, liquid apical application, or liquid basal application. These differences in the exposure type were due to solubility of the test material, route of exposure (inhaled or systemic), or comparison with previous publications. A nebulized exposure was performed using a Vitrocell® Cloud 12 system chamber equipped with a quartz crystal microbalance (QCM) (VitroCell, Germany). A 10- μm size nebulizer was used for the exposures. Untreated/vehicles (i.e. tissues exposed with medium only or vehicles used to solubilize/nebulize each material) and positive control groups were used to check the performance of the systems by evaluating TEER, CBF, mucin secretion and Mucin 5AC detection. The following agents were used as positive controls: cytomix (known inflammatory-inducing agent, prepared using 500 ng/mL TNF- α , 0.2 mg/mL lipopolysaccharide, 1% FCS, tissue exposure via liquid basal), Triton X-100 (cytotoxic at 10%, via liquid basal exposure) or IL-13 (a goblet cell hyper-, metaplasia agent at 10 ng/mL, via liquid basal exposure). For CBF analysis, tissues kept at 4°C for 1 h were also used as positive control groups since low temperatures inhibit CBF activity (data not shown).

2.5.3 TEER analysis

TEER measurements were performed daily after test item exposure to evaluate tissue barrier function. Tissues were washed, 200 μL of buffered saline solution was added to the apical compartment of MucilAir™-HF cultures, and resistance was measured using an EVOMX volt-ohmmeter with chopstick style probes (World Precision Instruments, Stevenage, UK). Resistance values (Ω) were converted to TEER ($\Omega \cdot \text{cm}^2$) using the following formula, where 100 Ω is the resistance of the membrane and 0.33 cm^2 is the total surface of the epithelium: $\text{TEER} = (\text{resistance value}(\Omega) - 100(\Omega)) \times 0.33$.

2.5.4 CBF analysis

CBF was analysed using a system consisting of a high-speed acquisition camera (Sony XCD V60, Tokyo, Japan) connected to an Olympus BX51 microscope with a $\times 5$ objective (Tokyo, Japan) and a specific software package (Sony ZCL Viewer, Tokyo, Japan), as previously described (Huang et al., 2017). CBF was calculated using an Epithelix software (Cilia-X) through analysis of 256 images/tissue (recording of an area corresponding to 1/10 of the total surface), captured at high frequency rate (125 frames/s) at room temperature, and expressed in Hertz (Hz).

2.5.5 MCC analysis

MCC was monitored using a high-speed acquisition camera (Sony XCD-U100CR, Tokyo, Japan) connected to a microscope with a $\times 5$ objective (Olympus BX51), as previously described (Huang et al., 2017).

2.5.6 Mucin secretion measurement

Mucin production was quantified using an enzyme-linked lectin assay, following a protocol previously published (Rossner et al., 2019).

2.5.7 Mucin-5AC detection analysis

The presence of goblet cells was assessed through immunohistochemistry analysis for mucin-5AC protein (Muc5AC) detection. IL-13 and cytomix were used as positive controls (see item 2.5.2 for additional details). On last day of experiment (day 12), cultures ($n = 3$ tissues/group) were rinsed in PBS and fixed by immersion in 4% formaldehyde for 20 min. Fixed tissues were embedded into paraffin, sectioned, and processed for staining on paraffin sections. The immunostaining of the sections was performed with the Benchmark automated platform (Ventana-Roche, Hoffmann-La Roche Ltd, Basel, Switzerland) and the Autostainer Link 48 (Agilent, Santa Clara, CA, United States) with the detection kit Ultraview DAB (DAB chromogeny, Hoffmann-La Roche Ltd). Sections were pre-treated using heat mediated antigen retrieval with sodium citrate buffer, pH 6, for 20 min. The section was then incubated with recombinant anti-mucin 5AC antibody (ab3649, Abcam) for 1 h at room temperature, followed by biotinylated secondary antibody (Dako) and HRP detection (HRP conjugated ABC system, Vector Laboratories), according to manufacturer's instruction. The section was then counterstained with hematoxylin (Sigma-Aldrich) and mounted with DPX, a synthetic non-aqueous mounting medium for microscopy. Digital images of the slides were then acquired, and quantitative image analysis performed using Image Pro Plus 6.2 (Media Cybernetics) to quantify the goblet cells on a section. The whole images of stained sections were scanned, and an average 15 images/section were analysed. The results are the ratio between the mucin 5AC stained area and the total surface area of the epithelium on the section.

2.5.8 Cytokine and chemokine measurements

Basolateral medium samples of the tissue cultures were collected and stored at -80°C until analysis. The following cytokines/chemokines were quantified using customized Human Luminex® Discovery Assay kits (R&D Systems):

chemokine (C-C motif) ligand (CCL) 2, CCL7, CCL26, C-X-C motif chemokine ligand (CXCL) 10, CXCL11, intercellular adhesion molecule-1 (ICAM-1), IL-1 α , IL-6, IL-8, matrix metalloproteinase (MMP)-1, MMP-2, MMP-3, MMP-7, MMP-9, osteopontin, interferon (IFN)- γ , IL-1 receptor antagonist (IL-1Ra), urokinase-type plasminogen activator receptor (uPAR), tumour necrosis factor (TNF)- α , urokinase (uPA), serpin E1, tissue inhibitor of metalloproteinase 1 (TIMP-1), and TGF- β 1. Samples were measured in technical triplicates according to the manufacturer's recommendation using a Luminex Bio-Plex® 200 RUO System (R&D Systems).

2.6 Lower respiratory tract toxicity assessment using EpiAlveolar™ model

The histology/immunohistochemistry, TEER, cytokine/chemokine measurements involving EpiAlveolar™ model were performed by testing facilities located in different geographies: the Institute for *In Vitro* Sciences, Inc. (Gaithersburg, MD, United States) (Laboratory 1) and Charles River Laboratories Edinburgh Ltd (Tranent, UK) (Laboratory 2). In cytokine/chemokine measurements, apical culture media samples of the tissues collected by Laboratory 2 were sent to our laboratory facility (Unilever SERS, Sharnbrook, UK), where the analyses were performed. Oxidative stress and Mitotracker staining assays were performed by Laboratory 1 only, whereas tissues material exposure for high-throughput transcriptomics analysis was performed by Laboratory 2. In this case, Laboratory 2 sent RNA samples to another laboratory facility (Cambridge Genomics Services, Cambridge, UK) to proceed with additional steps of RNA sequencing; the differential expression and pathway analyses were then performed by Unilever SERS. The laboratory work was performed independently by the laboratories, i.e., each facility used its own *in house* implemented protocols to perform test material exposure and investigate material-induced bioactivity. Additional details of all procedures are described in the next sections.

2.6.1 EpiAlveolar™ culture

EpiAlveolar™ system was obtained from MatTek Corporation (Ashland, MA, United States, cat. no. ALV-100-FT-MAC, ALV-100-FT-MAC-PE12). According to the supplier, the tissue systems were derived from primary human alveolar epithelial cells and primary pulmonary fibroblasts, both from a same healthy donor (male, 50 years), and pulmonary endothelial cells from another healthy donor (male, 6 years), and THP-1 cell line derived macrophages. These tissues were differentiated by the manufacturer prior to shipping to the testing facilities. Upon receipt, systems were maintained, for 2–7 days prior to use, at the ALI in modified 6-well hanging top plates with 5 mL of EpiAlveolar™ culture medium (MatTek) in the basolateral compartment and 75 μL of media on the apical surface and incubated at standard culture conditions ($37^{\circ}\text{C} \pm 1^{\circ}\text{C}$ in a humidified atmosphere of 5% CO_2 in air). TEER was measured and only systems with confirmed quality of the tight junction barrier ($>300 \Omega \cdot \text{cm}^2$) and with approved morphological inspection were used in the experiments.

2.6.2 Test material exposure

To prepare the stock solutions/suspensions to perform the test material exposures, saline, medium, ultrapure water or DMSO were used to dilute the test materials (Table 2). See [Supplementary Material S2](#) for additional details.

Tissues were exposed to eight test items, including known fibrotic, inflammation inducing agents (e.g., PHMG and Doxorubicin). Vehicle control groups were also tested in parallel. Except for Doxorubicin (which underwent a 6-day chemical exposure + 6-day without exposure), exposures were conducted daily, on 12 consecutive days with different concentrations, through aerosol, apical or basolateral liquid exposure methods (Table 2). In the aerosol exposure method, the procedure was performed using a Vitrocell® Cloud 12 system chamber equipped with a QCM. A 10-μm size nebulizer was used for the exposures. Each of the insert holders of the instrument base module was filled with Hanks' Balanced Salt solution (HBSS) or PBS prior to placing the tissue inserts. Then, each test item solution/suspension was placed into the nebulizer reservoir for aerosol material exposure. The nebulizer was activated until the material solution/suspension was consumed and discharged into the main exposure chamber and allowed to fully gravity deposit out of the Cloud 12 (determined using a QCM). After exposure, the tissues were placed back into their multi-well culture plates containing the same medium, a further aliquot of media was added apically (20 μL for Akemi, 75 μL for all others except LPS) and returned to incubator until next exposure. Media used during the 6- or 12-day experimental period was prepared without Supplement X by MatTek. In medium exposure, the apical or basolateral liquid of each tissue was removed and replaced with each test item medium solution/suspension and returned to the incubator until the next exposure. After the beginning of the exposure cycles, tissues were only re-fed with new culture medium every 3–4 days.

2.6.3 Histology and immunohistochemistry analyses

To evaluate the quality of EpiAlveolar™ tissues over the 12-day experimental period, histological and immunohistochemistry assessments for detection of pan-cytokeratin, vimentin, aquaporin 5, pro-surfactant C, CD68, caspase-3, and/or αSMA were performed by Laboratories 1 and 2. Details can be found in [Supplementary Material S2](#).

2.6.4 TEER analysis

2.6.4.1 Laboratory 1

Tissue inserts were removed and placed into a 12-well plate containing 0.75 mL of HBSS well and 0.25 mL of HBSS were added into each apical compartment of the culture inserts. Resistance was then measured using an EVOM volt-ohm-meter with chopstick style probes (World Precision Instruments, Stevenage, UK). Resistance values (Ohm, Ω) were converted to TEER (Ω.cm²) using the following formula, where 1.12 cm² is the total surface area of the tissue inserts: $TEER = (resistance\ value - tissue\ free\ membranes\ resistance\ value) \times 1.12$. The change in barrier function (ΔTEER) was then calculated using the time point specific reading (day 1, 4, 8 or 12) subtracted from the initial reference reading (day 0).

2.6.4.2 Laboratory 2

TEER was measured using the Millicell Electrical Resistance System-2 meter with an Endohm™ 12 Tissue Resistance

Measurement Chamber electrode (Merck, Darmstadt, Germany). Tissue inserts were removed and placed into a 12-well plate containing TEER buffer (1 mL/well, MatTek) and the top surface of each tissue was gently rinsed with 0.5 mL of the same buffer. The units were then emptied and added sequentially to the measurement chamber containing 4 mL of TEER buffer. After adding 0.75 mL of TEER buffer in each tissue apical compartment, electrodes were submerged to measure the resistance. TEER values (Ω.cm²) were calculated as described above by Laboratory 1.

2.6.5 Cytokine and chemokine measurements

In Laboratory 1, basal media samples collected from the tissues were collected and stored at ≤ −60°C until analysis. For cytokine/chemokine measurements, 17-Plex, duplex and single-plex analyte detection panels were run on the samples using Human Luminex™ Multiplex Immunoassay kits (R&D Systems). The analytes quantified were TNF-α, IL-6, MMP-9, MMP-3, MMP-1, MMP-2, CXCL10, CCL2, IFN-γ, IL-1ra, CCL7, IL-1a, CCL26, CXCL9, VCAM-1, ICAM-1, and CXCL11 in a 17-plex assay; whereas IL-8 and Serpin E1 in a duplex assay and TGF-β1 in a single-plex assay.

In Laboratory 2, apical culture media samples of the tissues were collected, stored at −80°C until shipment, in dry ice with temperature monitor control, to Unilever SERS, where the analyses were performed. Upon receipt, samples were again stored in the −80°C until the analysis using Human Luminex® Discovery Assay kits (R&D Systems). The same readouts investigated for MucilAir™-HF tissue samples were quantified in these samples.

2.6.6 Oxidative stress assay

Reduced glutathione (GSH) and oxidized glutathione (GSSG) levels in tissue lysate samples were determined using a GSH/GSSG-Glo™ assay kit (Promega) by Laboratory 1, as previously described ([Vivek et al., 2023](#)).

2.6.7 Mitotracker staining assay

Mitochondrial toxicity assessment was performed by the Laboratory 1 using MitoTracker® Red FM reagent, a cell-permeant dye able to stain active mitochondria in live cells. Tissues were loaded on the apical surface with MitoTracker® Red FM dye solution (500 Nm in HBSS) for 30 min in empty 12-well plates. Afterwards, the dye solution was removed from each tissue followed by rinsing the tissue apical surfaces with 200 μL HBSS. Fluorescence reads at an excitation and emission wavelength of 581/644 nm, respectively, were performed using FlexStation® 3 microplate reader. Empty inserts were utilized as a negative control to subtract the background noise or fluorescence of the dye.

2.6.8 High-throughput transcriptomics analysis

2.6.8.1 RNA extraction, assessment of quality, library construction and sequencing

Following material exposure for 12 days, tissues were cut from the plastic unit, transferred into 2 mL Precellys tubes (Bertin Technologies, Montigny-le Bretonneux, France) containing 700 μL of QIAzol lysis reagent and stored at −80°C until RNA extraction. For this, samples were homogenized followed by

centrifugation at 12000 g at 4°C for 5 min. The supernatants were used to extract RNA through a combined semi-automated method using a Qiagen RNeasy 96 QIAcube HT kit. All samples were DNase treated using a Thermo Fisher DNA-free kit, following manufacturer's instructions. All these steps were performed by Laboratory 2 which, then, stored RNA samples ($n = 5/\text{group}$) in 96-well plates until shipment on dry ice with a temperature monitor to the RNA sequencing laboratory facility (Cambridge Genomics Services). Samples then underwent quality control (QC) using Agilent RNA ScreenTape assay, following manufacturer's instructions, to generate RNA integrity number (RIN) score and traces for the samples. RNA library construction was performed using Illumina TruSeq™ Stranded mRNA kit, following manufacturer's protocol. RNA-seq data mapping was processed using Spliced Transcripts Alignment to a Reference (STAR) method, as previously described (Dobin et al., 2013).

2.6.8.2 Differential expression and pathway-level data extraction

The raw data for the EpiAlveolar™ experiments underwent QC. Probes whose median counts across treatment and timepoint was less than 5 were removed. All the samples had more than 5 M reads, thus no sample was removed from the analysis. No outlier samples were detected as all the replicates had a high degree of correlation (>0.9). A total of 64 samples were removed due to low quality, this was a particular issue for PHMG when the following concentrations were removed: 2nd highest concentration ($0.5 \mu\text{g}/\text{cm}^2$) on day 12, and the two highest concentrations (0.9 and $9.4 \mu\text{g}/\text{cm}^2$) across all timepoints (Supplementary Material S3). Datasets were then normalized and transformed using the $rlog()$ function in DESeq2 (Love et al., 2014), to minimize differences between samples for rows with small counts and to normalize with respect to library size.

With the aim of identifying patterns of co-regulated genes in a way that is neither fully data-driven nor fully constrained by biological knowledge, Pathway-level information extractor (PLIER) (Mao et al., 2019) was used. PLIER approximates the expression pattern of every gene as a linear combination of eigengene-like latent variables (LVs) and aims to optimize alignment of LVs to relevant biological knowledge. The compendium of prior knowledge chosen for the analysis includes the full Reactome database (v. 7.5.1) (Gillespie et al., 2021) and the Hallmark gene sets (v. 7.5.1) (Liberzon et al., 2015), as provided by The Molecular Signatures Database (MsigDB). Genes sets included in the MsigDB are annotated with official gene symbols hence, the Ensembl ID used to annotate the probes needed to be converted. This step was performed using the `bitr()` function from the clusterProfile R package (Guangchuang Yu et al., 2012) and led to the loss of 7.8% genes from the EpiAlveolar™ dataset. Since different Ensembl IDs could match the same official gene symbol ID, this redundancy had to be removed for PLIER to work optimally. This was achieved by keeping the gene with the highest median expression. Reliable associations between LVs and gene sets as identified by PLIER were filtered for $\text{AUC} > 0.7$ and $\text{fdr} < 0.05$. As the EpiAlveolar™ model underwent material exposure at different concentrations, the LVs expression dataset was then used as to analyse time concentration-dependent effects and to estimate PoDs for each LV for each test material at different timepoints. Data

has been submitted to the European Bioinformatics Institute (EBI) data repository, Array Express (<https://www.ebi.ac.uk/biostudies/arrayexpress>) under the accession number E-MTAB-14272.

2.7 Data analysis

2.7.1 Concentration and time-dependent response analysis and *in vitro* PoD determination

Concentration and time-dependent changes in the bioactivity readout data were analyzed using a nonlinear state space model, based on the work of Svensson and Schön (2017). The method was adapted to allow for experimental measurements where the same readout was observed for multiple different test material treatments and concentrations, observed at different timepoints (Middleton et al., in preparation). All bioactivity readouts were included in the analysis (where available), i.e., measurements for tissue integrity loss (TEER) and functionality (MCC, CBF, and mucin secretion), cytokine/chemokine secretion, and the transcriptional LV values obtained using PLIER. The datasets were grouped so that a single state space model was used to capture all the responses (across time, concentration, and test material) for a single readout obtained within a particular study (laboratory/tissue model). Data were transformed to the log base 10 scale and normalized using z-scores, so that for a given readout Y_t^{ij} from a laboratory/tissue model, the corresponding normalized value was given by $\hat{y}_t^{ij} = (\log_{10}(Y_t^{ij}) - \mu)/\sigma$. Here, the indexes i, j, t correspond to the different test materials, concentrations and timepoints, μ and σ are the sample mean and standard deviation of the control readout values obtained for the first timepoint. All measurement were then scaled so that the maximum median value across different replicates was one for all timepoints, readouts and test materials within a given laboratory/tissue model.

The model consists of state variables $x_t^{i,j}$, response variables $y_t^{i,j}$ and the concentrations of material $c_t^{i,j}$. The response variables $y_t^{i,j}$ represent the normalized (see below) readout values at timepoint t for material exposure i, j . The mean of the response variable is given by $x_t^{i,j}$, so that $y_t^{i,j} \sim x_t^{i,j} + e_t$, where e_t represents random fluctuations in the readout values, due to observational noise, which are taken to be normally distributed. Dynamical changes in state values are given by $x_t^{i,j} = f(x_{t-1}^{i,j}, c_t^{i,j}) + v_t$. Here, $f(x_{t-1}^{i,j}, c_t^{i,j})$ is a non-linear function that represents interactions between different state variables and the perturbation caused by the test material at a given exposure at concentration $c_t^{i,j}$, and v_t represents random fluctuations in state dynamics (which are also normally distributed). Following Svensson and Schön (2017), the nonlinear terms are based on an approximation to Gaussian processes, which are obtained using a basis function expansion-based approach. Inference of the model parameters was performed in the framework of Bayesian inference, wherein random draws of the posterior distribution were obtained using Sequential Monte Carlo (SMC), see Svensson and Schön (2017) and Chopin and Papaspiliopoulos (2020). For each state space model representing a particular laboratory/readout dataset, SMC simulation was run for three chains at 5,000 iterations each, and first 1,000 iterations were discarded from the final posterior samples. The Rhat convergence diagnostic ($\text{Rhat} < 1.1$) was used to ensure the simulations had converged.

The state space model and posterior model parameter samples were then used to construct posterior predictive distributions of the response of each readout to a given test material for a given concentration and timepoint (see [Figure 4](#)). The posterior predictive distributions were used to estimate various statistics on the readout responses (median, 95% credible range etc.), PoDs, Concentration Dependency Scores (CDS) and two Effect Scores (increase and decrease). PoDs were defined as the concentration at which the mean response to a test material exceeded the 95% credible range of control for each timepoint (otherwise the mean response remains within the range of control). PoDs distribution for each timepoint, test material and readout, from which different statistical measures (e.g., the median, 95% credible range etc.) were calculated. The CDS was designed to provide confidence metric in whether an effect in the data was truly concentration dependent. Following [Hatherell et al. \(2020\)](#), the CDS (for a given timepoint, test material and readout) was calculated as the proportion of posterior samples there was a PoD. CDS values could vary between 0 and 1 (0 indicating high confidence that there was no effect, 1 indicating high confidence there is an effect). A CDS > 0.5 was required for an effect to be considered concentration dependent. The Effect Score was subdivided into a metric of increasing responses and decreasing responses (ES_increase and ES_decrease). These were calculated as the proportion of posterior samples where the mean response increases above (for ES_increase) or below (ES_decrease) the control range. ES_increase and ES_decrease values vary between 0 and 1 (so that the maximum value of ES_increase plus ES_decrease is 1). The ES_increase and decrease values were plotted as heatmaps to visualize the effect of the test material over time and concentration (see [Figure 4](#)).

2.7.2 BER calculation

A BER is defined as the ratio between the *in vitro* PoD and predicted human exposure ([Health Canada, 2021](#); [Middleton et al., 2022](#)). If a PoD was determined, a BER was calculated for each benchmark chemical-exposure scenario, using the lowest PoD among the different readouts (i.e. lowest across readouts from TEER, tissue functionality, cytokine/chemokine secretion and/or transcriptional LVs) investigated across the two respiratory tract models and laboratories. As such, the following BERs could be calculated per benchmark chemical-exposure scenario (see [Table 3](#)) and upper and lower respiratory tract tissue model (i.e. MucilAir™-HF and EpiAlveolar™ models, respectively):

- Ratio between the lowest PoD from all MucilAir™-HF model readouts and the highest exposure estimate in the upper respiratory tract;
- Ratio between the lowest PoD from all EpiAlveolar™ model readouts in Laboratory 1 and the highest exposure estimate in the lower respiratory tract;
- Ratio between the lowest PoD from all EpiAlveolar™ model readouts (except transcriptomics) in Laboratory 2 and the highest exposure estimate in the lower respiratory tract;
- Ratio between the lowest transcriptional PoD in the EpiAlveolar™ model in Laboratory 2 and the highest exposure estimate in the lower respiratory tract.

3 Results

This section describes in detail the main results obtained when MucilAir™-HF and EpiAlveolar™ models were exposed daily to benchmark chemicals and reference materials ([Tables 1, 2](#)), in three different exposure methods (aerosol, apical and/or basal liquid), over a 12-day experimental period. Several bioactivity readouts were investigated, including TEER, tissue functionality, cytokine/chemokine secretion and/or gene expression. The effects induced by the reference materials as well as relevant literature data are also summarized in [Supplementary Table S1](#). A comparison between the concentration- and time-dependent response analysis and corresponding readout data can be found in the [Supplementary Material S4](#), whereas the main analyses are shown in [Figures 5–8](#).

3.1 Effects of materials in the upper respiratory tract MucilAir™-HF model

3.1.1 Tissue barrier integrity loss

[Table 4](#) summarizes the effects in the tissue barrier integrity through TEER measurement analysis when the MucilAir™-HF tissues were exposed to test items for 30 min/day and/or 6 h/day. Among the benchmark chemicals, only BAC were able to trigger changes in tissue barrier integrity at 30 min/day exposure; however, this finding was observed mainly at high tested concentrations ([Table 4](#); [Figure 5](#)). Interestingly, no effects were observed following exposure to BE PVM/MA at 30 min/day, unlike following the 6 h exposure/day regimen ([Table 4](#); [Supplementary Figure S1](#)). Except TNF- α , the reference materials were not able to trigger changes in the TEER measurements ([Table 4](#); [Supplementary Figure S2](#)).

3.1.2 Tissue functionality

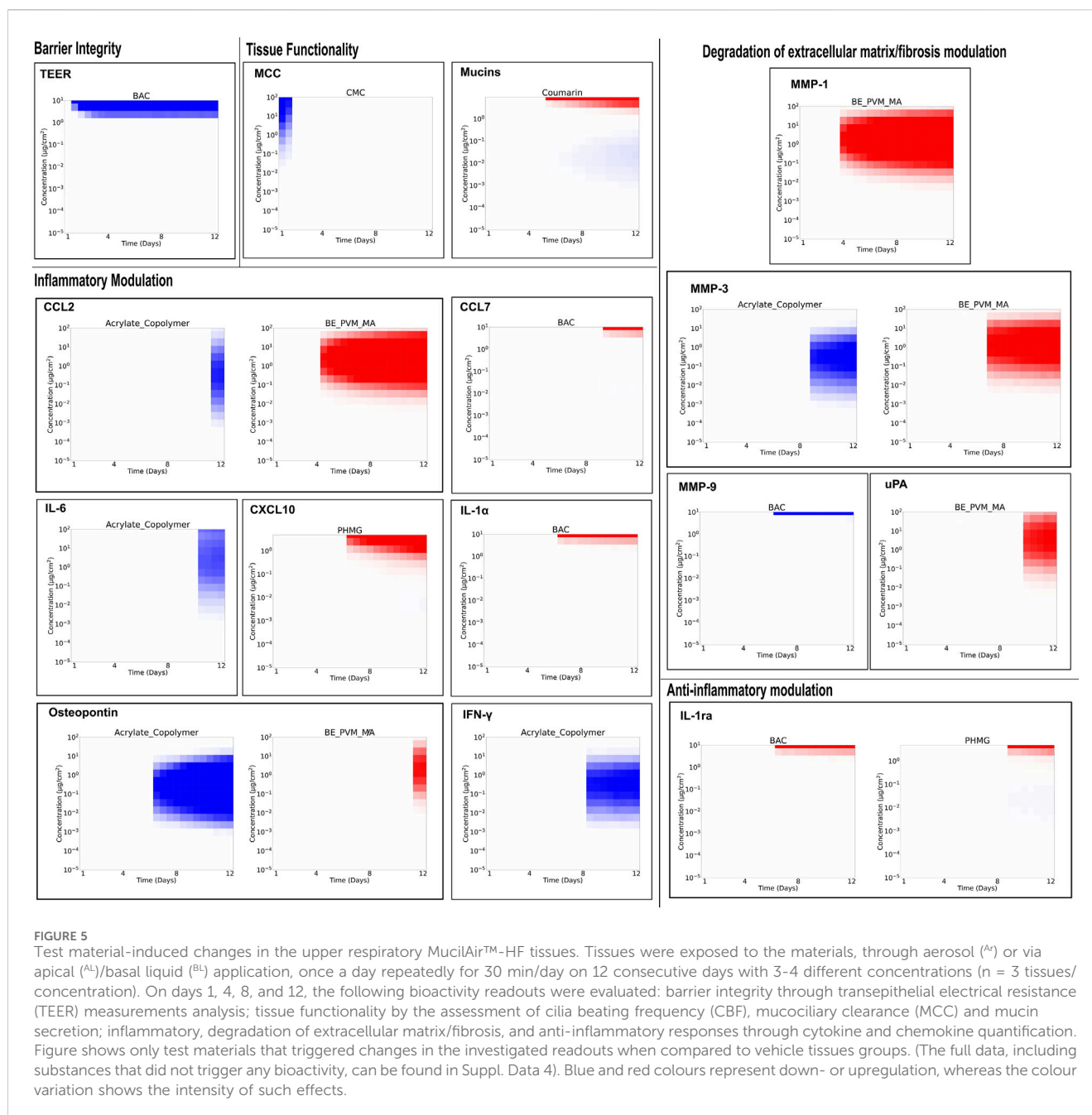
Tissue functionality was investigated through the assessment of CBF, MCC and mucin secretion. Even though there is evidence that some of the reference materials (see [Supplementary Table S1](#)) have the potential to induce changes in those parameters, no bioactivity was observed in the MucilAir™-HF tissues ([Table 4](#)). Regarding the benchmark chemicals, only BE PVM/MA reduced CBF at 6 h exposure/day ([Table 4](#); [Supplementary Figure S1](#)), whereas CMC at 30 min exposure/day promoted a concentration-dependent reduction in the MCC only on day 1 ([Table 4](#); [Figure 5](#)), suggesting that this finding may be of no concern due to the fast reversibility ([Ugwoke et al., 2000](#)). Regarding mucin production, PHMG triggered increased mucin secretion at 6 h exposure/day, mainly from day 8 onward; a similar effect was observed for Coumarin at 30 min exposure/day, but not at 6 h exposure/day ([Table 4](#); [Figure 5](#); [Supplementary Figure S1](#)).

The presence of mucin-producing goblet cells was investigated using Muc5AC immunohistochemical staining ([Table 4](#); [Supplementary Figure S3](#); [Supplementary Table S2](#)). It was observed that the goblet cell hyper-, metaplasia agent IL-13 triggered an expected 4-fold increase in cells expressing Muc5AC protein, when compared to unexposed tissues. Similarly, Isoproterenol also induced a 2.5- and 3-fold increase in this parameter at 50 and 100 μ M, respectively. However, other test materials were not able to promote any changes in Muc5AC

TABLE 4 Observed effects in the test material-exposed MucilAir™-HF tissues over 12-day period.

Test materials ^a	Exposure time/day	Tissue barrier integrity loss	Tissue functionality				Modulation of cytokines and chemokines		
			Increased mucin secretion	Reduced CBF	Reduced MCC	Increased Muc5AC protein	Inflammatory modulation	Extracellular matrix/fibrosis modulation	Anti-inflammatory modulation
Benchmark chemicals									
Akemi ^{Ar}	30 min	×	×	×	×	×	×	×	×
	6 h	×	×	×	×	×	✓	✓	×
Acrylate copolymer ^{Ar}	30 min	×	×	×	×	×	✓	✓	×
	6 h	×	×	×	×	×	✓	✓	×
BAC ^{AL}	30 min	✓	×	×	×	×	✓	✓	✓
BE PVM/MA ^{AL}	30 min	×	×	×	×	×	✓	✓	×
	6 h	✓	×	✓	×	×	✓	✓	✓
CMC ^{Ar}	30 min	×	×	×	✓	×	×	×	×
Coumarin ^{Ar}	30 min	×	✓	×	×	×	×	×	×
	6 h	×	×	×	×	×	×	×	×
PHMG ^{Ar}	30 min	×	×	×	×	×	✓	×	✓
	6 h	×	✓	×	×	×	✓	×	✓
Reference materials									
Nicotine ^{Ar}	30 min	×	×	×	×	×	×	×	×
LPS ^{AL/Ar}	30 min	×	×	×	×	×	×	×	×
	6 h	×	×	×	×	×	✓	✓	×
Sulforaphane ^{Ar}	30 min	×	×	×	×	×	×	×	×
	6 h	×	×	×	×	×	×	×	×
Acrolein ^{AL}	30 min	×	×	×	×	×	×	×	×
Chlorocresol ^{AL}	30 min	×	×	×	×	×	×	×	×
Isoproterenol ^{BL}	30 min	×	×	×	×	✓	×	✓	×
CFTR _{inh} -172 ^{BL}	30 min	×	×	×	×	×	×	×	×
TNF-α ^{BL}	30 min	✓	×	×	×	×	✓	×	×

The symbols × and ✓ absence or presence of bioactivity induced by the related chemical, respectively.
^aTissues were exposed to test materials via aerosol (^{Ar}), apical liquid (^{AL}) and/or basal liquid (^{BL}) application.



protein expression, including CFTR_{inh}-172, experimentally used to mimic the inflammatory profile found in cystic fibrosis, a disease marked by mucus hyperproduction.

3.1.3 Modulation of cytokines and chemokines

Quantification of different cytokines and chemokines was performed with focus on those proteins involved in the inflammation (CCL2, CCL7, CCL26, CXCL10, CXCL11, ICAM-1, IL-1 α , osteopontin, IFN- γ , TNF- α , IL-6, and IL-8), degradation of extracellular matrix/fibrosis (MMP-1, MMP-2, MMP-3, MMP-7, MMP-9, TIMP-1, uPAR, uPA, serpin E1, and TGF- β 1) and anti-inflammatory (IL-1ra) responses, as summarized in Table 4.

In general, benchmark chemicals (Akemi, Acrylate copolymer, BE PVM/MA, PHMG, and BAC) and reference materials (LPS,

Isoproterenol, and TNF- α) produced differentially modulated cytokines and chemokines release over the 12-day experimental period (Table 4; Figure 5; Supplementary Figures S1, S2). Those materials exposed at 6h/day showed a tendency to induce stronger changes in the investigated biomarkers release, demonstrating that the exposure time was related to the extent of the induced biological effects. For instance, LPS, a material well-known for its ability to induce inflammatory responses, did not promote modulation of the different cytokines/chemokines at 30min/day exposure (Table 4); however, the 6h/day exposure triggered increased levels of proteins involved in the inflammatory response (e.g., IL-6, IL-8, and TNF- α) and degradation of extracellular matrix/fibrosis (e.g., MMP-3 and uPAR) (Table 4; Supplementary Figures S1, S2).

Regarding inflammatory modulation, BE PVM/MA (Figure 5) and the reference material TNF- α (Supplementary Figure S2), both at 30 min/day exposure, were able to trigger the upregulation of CCL2 and osteopontin. Also, the former induced production of TNF- α itself and of IL-8 (Supplementary Figure S2), concordant with literature data using other lung cell models (see Supplementary Table S1). At 6h/day exposure, BE PVM/MA triggered upregulation of a higher number of biomarkers, such as IL-6 and IL-8 (Supplementary Figure S1). Similarly, PHMG triggered increased levels of CXCL10 only at 30 min/day exposure (Figure 5), while the 6h/day exposure induced the upregulation of CXCL10, IL-6, and IL-8 (Supplementary Figure S1). Also, BAC promoted an increase in CCL7, IL-1 α and IL-6, mainly at high concentration (Figure 5). Interestingly, Acrylate copolymer promoted a dual effect related to its time of exposure in MucilAir™-HF model: a downregulation of some released inflammatory biomarkers at 30 min/day exposure (Figure 5), whereas it triggered an upregulation profile at 6h/day exposure (Supplementary Figure S1).

Concerning the degradation of extracellular matrix/fibrosis, PHMG and TNF- α did not induce any modulation of related biomarkers, even though they have triggered the modulation of inflammatory cytokines (Table 4; Figure 5). BAC and Isoproterenol promoted downregulation of MMP-7 only (Figure 5), while Akemi (Supplementary Figure S1) and LPS (Supplementary Figure S2) induced upregulation of MMP-3 and both MMP-3/uPAR, respectively, at 6 h/day exposure. On the other hand, Acrylate copolymer and BE PVM/MA showed changes in a high number of biomarkers, such as MMP-3 and MMP-7 (Figure 5; Supplementary Figure S1).

In general, test materials promoted mainly upregulation of IL-6, IL-8 and MMP-3 and downregulation of MMP-7 levels. Regarding the anti-inflammatory modulation, IL-1ra showed upregulated levels induced by BE PVM/MA, PHMG, and BAC (Figure 5; Supplementary Figures S1, S2). As IL-1ra has been linked to modulation of inflammation in cystic fibrosis (Fritzsche et al., 2015), this finding suggests its role in preserving cell function against the inflammatory process induced by those chemicals.

3.2 Effects of materials in the lower respiratory tract EpiAlveolar™ model

3.2.1 Histology and immunohistochemistry analyses

To evaluate the quality of EpiAlveolar™ tissues over the 12-day experimental period, histological and immunohistochemistry assessments were performed by Laboratories 1 and 2. In addition, changes induced by the test materials were also performed by Laboratory 2. Detailed findings can be found in Supplementary Material S2.

In general, the cell morphology and viability of the tissues were not significantly impacted. However, Laboratory 1 observed that overall cellularity appeared to be decreased with flattening/thinning of cell layers from day 8 onward, while Laboratory 2 found early signs degeneration with a minor increase in thinning of the epithelial layers and a minor increase in numbers of degenerate cells from day 4 onward. Both laboratories also observed expected expression patterns for pan-cytokeratin, vimentin and/or aquaporin 5;

nevertheless, no strong pro-surfactant C staining was evident over 12-day period, suggesting that type II pneumocytes were not present, contrasting with previous findings (Barosova et al., 2020). Moreover, rare CD68 positive macrophages, seen on days 1 and 4, were not found later by Laboratory 2, suggesting that those cells likely vanished out of the system due to tissue washing off steps procedures.

Moreover, Laboratory 2 observed that, in general, the concentration related changes induced by the benchmark chemicals ranged from increased cell degeneration, separation/detachment, multifocal thinning (e.g., Crystalline silica, Amorphous silica, and Doxorubicin) and with more severe injury locally extensive cell death/necrosis (e.g., PHMG and Akemi).

3.2.2 Tissue barrier integrity loss

Over the 12-day experimental period, Crystalline silica, Amiodarone, and the reference materials LPS and Sulforaphane showed no effects on barrier integrity in either laboratory. The same results were observed for Akemi, Amorphous silica, and Doxorubicin in Laboratory 1, in contrast to Laboratory 2 which observed changes induced by those chemicals at high concentrations (Table 5; Figure 6).

Regarding PHMG (Figure 6), different concentrations were tested by both laboratories. In Laboratory 2, PHMG (0.1–9.4 $\mu\text{g}/\text{cm}^2$) triggered a marked concentration-dependent tissue barrier integrity loss at all concentrations on the first day of the experiment. From day 4 on, TEER values were at the background level, indicating that the tissue barrier was irreversibly perturbed. In view of this, lower concentrations (0.005–0.2 $\mu\text{g}/\text{cm}^2$) were tested by Laboratory 1. Results showed that only the highest concentration triggered a slight barrier integrity loss on day 4. This loss was markedly increased until the end of the experiment, therefore, this concentration triggered barrier integrity loss in a time-dependent manner.

3.2.3 Modulation of cytokines and chemokines

As with upper respiratory tract toxicity assessments using the MucilAir™-HF model, quantification of cytokines/chemokines was performed in test material-exposed EpiAlveolar™ tissues. Data are shown in Table 5; Figure 6.

In Laboratories 1 and 2, the reference positive material LPS, a well-known inflammatory agent, failed to induce changes in the levels of the investigated cytokines and chemokines. Also, as expected, the reference negative material Sulforaphane did not trigger any marked changes in such proteins. Moreover, in both laboratories, PHMG showed concordant outcomes regarding the modulation of the inflammatory, degradation of extracellular matrix/fibrosis, and anti-inflammatory responses, as expected. However, different patterns in the up- or downregulation of biomarkers were observed due to different concentrations tested by both laboratories (i.e., tested concentrations range from 0.005–0.2 $\mu\text{g}/\text{cm}^2$ or 0.1–9.4 $\mu\text{g}/\text{cm}^2$ in Laboratories 1 and 2, respectively). In Laboratory 1, it was observed a tendency to increase the release of the investigated proteins at high tested concentration. On the other hand, in Laboratory 2, where a marked tissue barrier integrity loss was observed for all tested concentrations, a downregulation profile was observed. Also, IL-1ra showed upregulation profile initially for all concentrations until day 8 followed by biphasic response from day 8 onward.

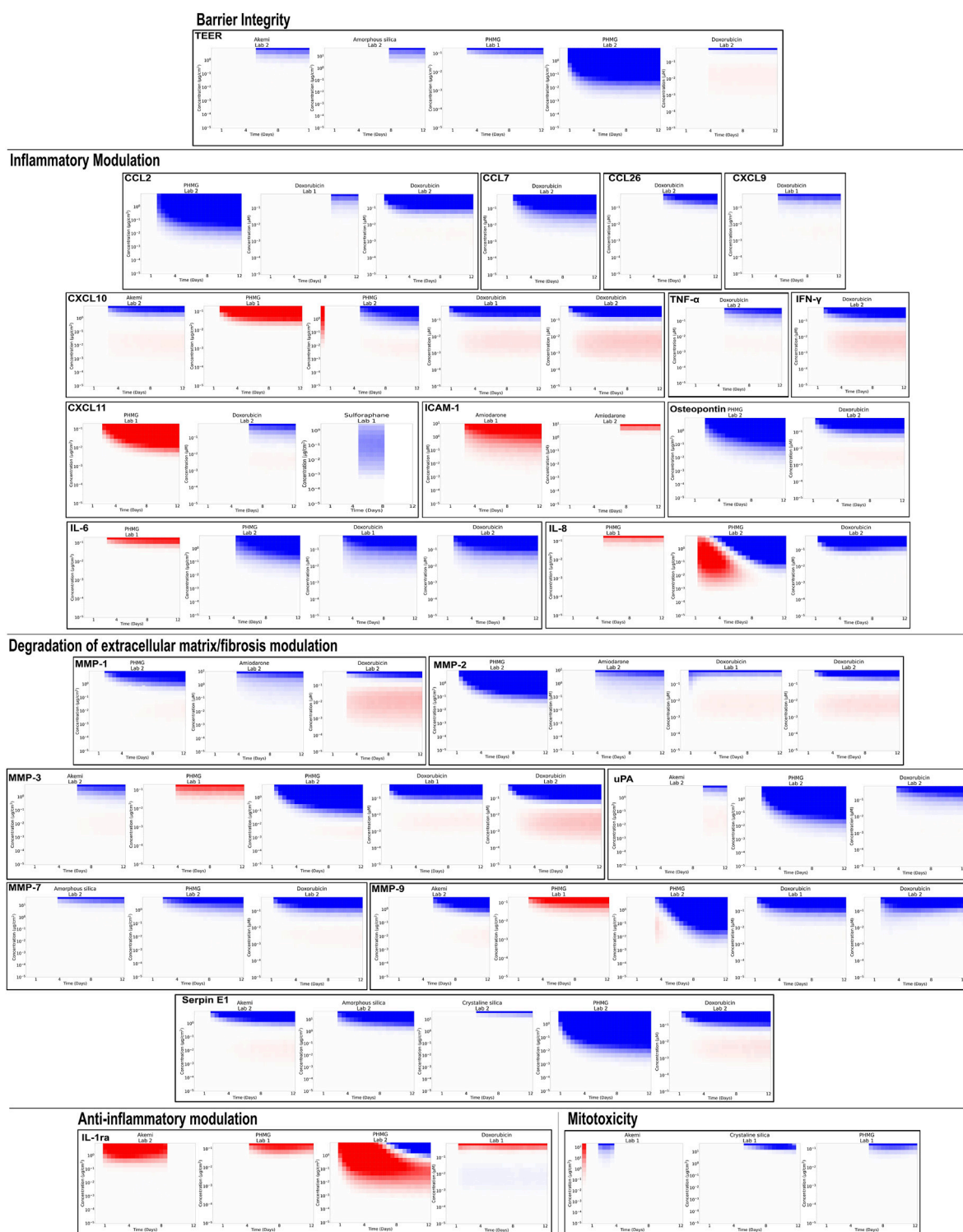


FIGURE 6

Test material-induced changes in the lower respiratory EpiAveolar™ tissues. Except for Doxorubicin (which underwent a 6-day exposure + 6-day without exposure), tissues were exposed to the materials, with 3–4 different concentrations ($n = 3$ tissues/concentration), were conducted on 12 consecutive days through aerosol (^A), apical (^A) or basolateral (^B) liquid exposure methods. On days 1, 4, 8, and 12, basolateral culture medium samples of each tissue were collected for assessment of the following readouts: barrier integrity through transepithelial electrical resistance (TEER) measurements analysis; inflammatory, degradation of extracellular matrix/fibrosis, and anti-inflammatory responses through cytokine and chemokine quantification. Figure shows only test materials that triggered changes in the investigated readouts when compared to vehicle tissues groups. (The full data, including substances that did not trigger any bioactivity, can be found in Suppl. Data 4). Blue and red colours represent down- or upregulation, whereas the colour variation shows the intensity of such effects.

TABLE 5 Observed effects in test materials exposed EpiAlveolar™ tissues over 12-day period and qualitative concordance between laboratories 1 and 2.

Test materials ^a	Tissue barrier integrity loss		Modulation of cytokines and chemokines						Changes in GSH and GSSS levels ^b	Mitotoxicity ^b
			Inflammatory modulation		Extracellular matrix/fibrosis modulation		Anti-inflammatory modulation			
	Lab 1	Lab 2	Lab 1	Lab 2	Lab 1	Lab 2	Lab 1	Lab 2	Lab 1	Lab 1
Benchmark chemicals										
Akemi ^{Ar}	×	✓	×	✓	×	✓	×	✓	×	✓
Crystalline silica ^{Ar}	×	×	×	×	×	✓	×	×	×	✓
Amorphous silica ^{Ar}	×	✓	×	✓	×	✓	×	×	×	×
PHMG ^{Ar}	✓	✓	✓	✓	✓	✓	✓	✓	×	✓
Amiodarone ^{BL}	×	×	✓	✓	×	✓	×	×	×	×
Doxorubicin ^{BL}	×	✓	✓	✓	✓	✓	✓	×	×	×
Reference materials										
LPS ^{AL}	×	×	×	×	×	×	×	×	×	×
Sulforaphane ^{Ar}	×	×	×	×	×	×	×	×	×	×

The symbols × and ✓ absence or presence of bioactivity induced by the related chemical, respectively.
^aTissues were exposed to test materials via aerosol (^{Ar}), apical liquid (^{AL}) and/or basal liquid (^{BL}) application.
^bThis readout was investigated by Laboratory 1 only.

Despite having shown changes in different biomarkers induced by Doxorubicin, both laboratories also observed a tendency towards downregulation of the inflammatory and degradation of extracellular matrix/fibrosis responses; also, a dual effect with the anti-inflammatory IL-1ra response was observed by the Laboratory 1 only. Moreover, a tendency for downregulation of biomarkers related to inflammation and/or degradation of extracellular matrix/fibrosis was observed for Amorphous silica, Crystalline silica, and Akemi only by Laboratory 2. Regarding Amiodarone, both laboratories observed upregulated levels of ICAM-1, but only Laboratory 2 showed downregulated levels of MMP-1 and MMP-2.

Taking the results found in both laboratories together, levels of CXCL10, IL-8, IL-1 α , matrix metalloproteinases (MMP-1, -2, -3, -7, and -9), uPA, and serpin E1 had greater magnitude of response compared to other investigated readouts. Given the range of proteins evaluated, this finding suggests the fundamental role of these readouts in the bioactivity induced by the benchmark chemicals.

3.2.4 Changes in GSH and GSSG levels and mitotoxicity

No benchmark chemical induced alterations in GSH and GSSG levels (Table 5; Supplementary Material S4), suggesting that the GSH pathway was not linked to oxidative stress induced by some chemicals, e.g., PHMG. Nonetheless, effects in mitochondria were observed for Akemi, Crystalline silica and PHMG at higher concentrations mainly (Table 5; Figure 6).

3.2.5 Elucidation of mechanism of action using transcriptomics

Here, we explored the potential utility of transcriptomics as a technology, not only for establishing a PoD but also for gaining mechanistic insights to generate hypotheses within the context of a risk assessment framework. Therefore, we set out to investigate if, by using this type of analysis, the mechanisms of lung toxicity (especially pulmonary fibrosis) associated with the benchmark chemicals could be identified.

Figure 7 displays the LVs that showed significant concentration- and time-dependent responses after benchmark chemical exposure relative to the vehicle control. The number of LVs altered increased over time, with maximum effects observed at day 12 for all chemicals. The most active chemicals were PHMG ($n = 22$), Amorphous silica ($n = 15$) and Doxorubicin ($n = 12$), followed by Crystalline silica ($n = 6$), Akemi ($n = 5$), Amiodarone ($n = 5$), and the reference materials LPS ($n = 4$) and Sulforaphane ($n = 1$). Importantly, most of the LVs modulated by PHMG, Amorphous silica, and Doxorubicin captured biological activity corresponding to the key factors leading to pulmonary fibrosis (Sieber et al., 2023; Todd et al., 2012): inflammation, oxidative stress, epithelial-mesenchymal transition which ultimately leads to excessive deposition of extracellular matrix. For example, LV62, LV80, and LV76, have strong associations with pathways such as “extracellular matrix organization,” “epithelial mesenchymal transition,” and “collagen formation.” In addition, LV7 and LV11 contain bioactivity related to inflammation, keratinization and oxidative stress (see Supplementary Material S5). It is worth mentioning that several LVs share the same pathways, e.g., keratinization can be found for LVs 2, 7, 62, and 80, corroborating the involvement of this

pathway in the bioactivity induced by the materials (Supplementary Figure S4). In a risk assessment context this information would suggest that PHMG, Amorphous silica, and Doxorubicin could cause pulmonary fibrosis *in vivo* and would warrant further investigation. This is consistent with the evidence of pulmonary fibrosis observed in humans and animal models after exposure to PHMG (Kim et al., 2021; Park et al., 2014) and Doxorubicin (Minchin et al., 1988; Nevadunsky et al., 2013). In contrast, research on the health effects of Amorphous silica has shown that the initial inflammatory and fibrogenesis response is reversible in animal studies (Sun et al., 2016; Weber et al., 2018), supported by the long-term safe use in products and based on epidemiological studies from occupational exposures (ECETOC, 2006; Merget et al., 2002; Yong et al., 2022). Surprisingly, only 3 out of the 24 pathways perturbed by Crystalline silica, a well-known pro-fibrotic compound, were related to fibrosis.

For the water repellent polymer (Akemi), LVs 7, 11, 30, and 33 contain pathways related to fibrosis. Whether this compound leads to this adverse outcome *in vivo* is unknown, as all existing human (Duch et al., 2014) and animal data is limited to short-term exposures and concentrates on its effects on the lung surfactant (Sørli et al., 2018).

Amiodarone-induced pulmonary fibrosis develops in 5%–7% of patients following typical Amiodarone pneumonitis (Budin et al., 2022). There are several mechanisms potentially involved, however, it has been suggested that mitochondrial dysfunction could play a critical role (Bolt et al., 2001). Amiodarone has been shown to cause uncoupling of oxidative phosphorylation, and inhibition of the electron transport chain and fatty acid β -oxidation (Fromenty et al., 1990a; Fromenty et al., 1990b). Most of the pathways perturbed by Amiodarone in this dataset are associated with these mechanisms (LVs 28 and 81), for example the pathways: “oxidative_phosphorylation,” “reactome_complex_i_biogenesis,” “reactome_fatty_acyl_coa_biosynthesis.”

For the reference negative chemical, Sulforaphane, only one LV was weakly modulated (LV 31). While it was not possible to derive a mechanism of lung toxicity for LPS from this dataset, for most of the other benchmark chemicals, this analysis was able to provide further insights into their putative mechanism of toxicity.

3.3 Comparison between PoD and exposure estimates for the use scenarios

Figure 8 shows the PoD medians for all readouts in which benchmark chemical-induced bioactivity (either up or downregulation) were observed. The corresponding exposures predicted for day 12 for upper and lower respiratory tract regions are shown as vertical lines. A comparison was performed between the predicted exposure using *in silico* methods (described in item 2.3) and the measured bioactivity responses (i.e., PoDs as determined using the state-space model approach). The exposure was taken from the maximum predicted value across all relevant generations on that day (1, 4, 8, and 12), which was recorded for both the upper and lower lung (Table 3; Supplementary Material S1). Corresponding BERs for all benchmark chemical scenarios are shown in Supplementary Figure S5. Plots of *in vitro* PoDs and calculated exposures for each day are shown in Supplementary Figures S6, S7.

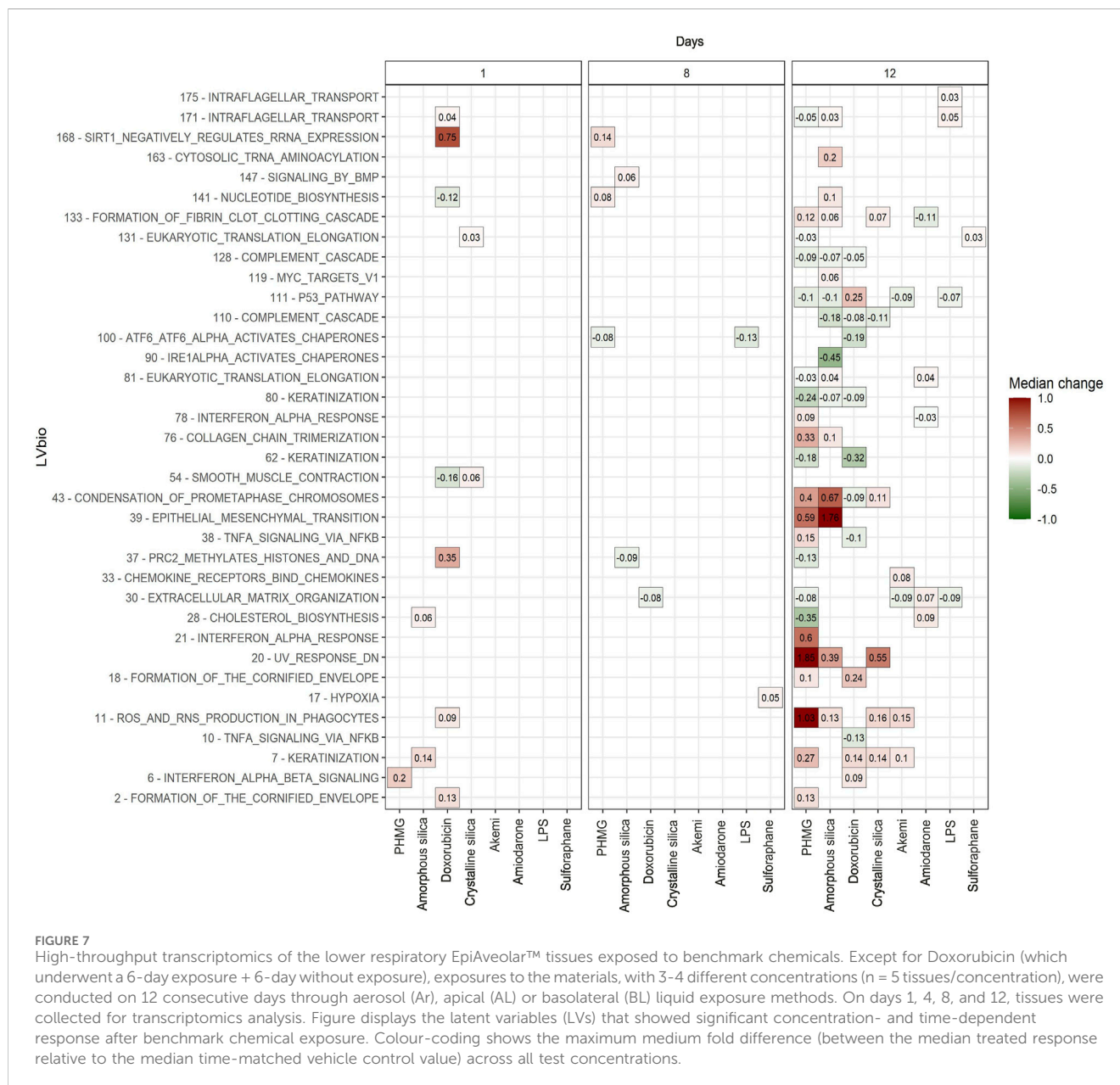


FIGURE 7

High-throughput transcriptomics of the lower respiratory EpiAveolar™ tissues exposed to benchmark chemicals. Except for Doxorubicin (which underwent a 6-day exposure + 6-day without exposure), exposures to the materials, with 3–4 different concentrations ($n = 5$ tissues/concentration), were conducted on 12 consecutive days through aerosol (Ar), apical (AL) or basolateral (BL) liquid exposure methods. On days 1, 4, 8, and 12, tissues were collected for transcriptomics analysis. Figure displays the latent variables (LVs) that showed significant concentration- and time-dependent response after benchmark chemical exposure. Colour-coding shows the maximum medium fold difference (between the median treated response relative to the median time-matched vehicle control value) across all test concentrations.

For the low-risk consumer product use scenarios, namely Amorphous silica (antiperspirant), BAC (nasal and cleaning sprays), Acrylate copolymer (hair spray) and Coumarin (antiperspirant), the exposure levels were lower than minimum observed PoDs, as expected. The BERs obtained for day 12 in these scenarios were between $\sim 25,000$ for Coumarin and ~ 5 for Acrylate copolymer. In these five cases, the airborne concentration and particle size obtained from the SUET data were used as inputs into the calculation performed with MPPD (Supplementary Material S1), which likely helped to make the parameters used to model said scenarios more realistic.

For the occupational exposure low-risk scenarios for Amorphous and Crystalline silicas, the exposure values were much higher relative to the PoDs, leading to BERs less than 1. This may be attributed to the very low clearance rate in the ICRP

model for lower respiratory tract clearance or to the sensitive transcriptomics PoDs. In general, it is found that the bioactivity observed with the transcriptomics analysis was more sensitive to changes than for other readouts investigated using the EpiAlveolar™ model (Figure 8; Supplementary Figures S6, S7). For Crystalline silica, for both the occupational low- and high-risk scenarios, the predicted lower respiratory exposure was higher than the minimum PoD from transcriptomics, but neither scenario led to exposures which exceed the minimum PoDs for other readouts.

Since both BAC and one of the investigated CMC scenarios were for nasal sprays, only the upper respiratory tract was considered in this situation. In the case of CMC, only one readout (MCC) had an observed PoD in the MucilAir™-HF model, which was only observed on day 1 and was greater than

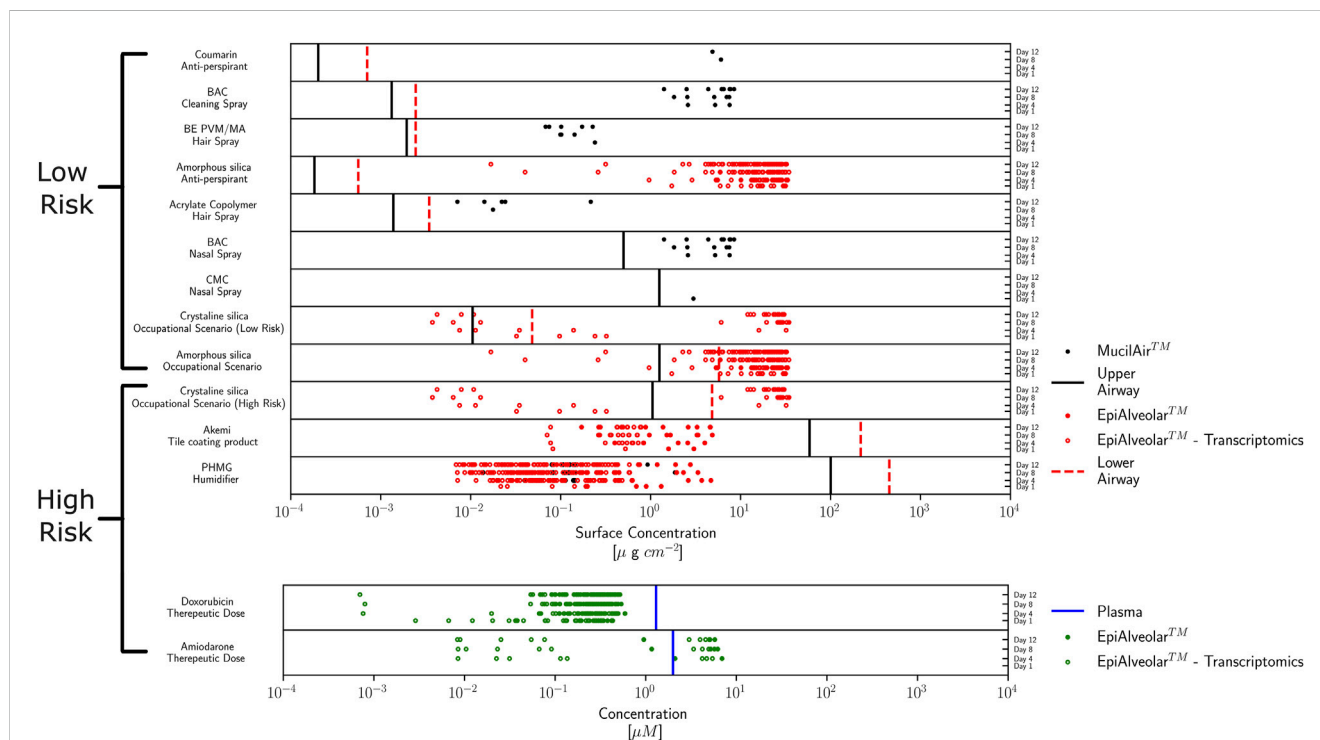


FIGURE 8

Comparison of human internal exposure (upper/lower respiratory tract or plasma) and *in vitro* point of departures (PoDs) per benchmark chemical using MucilAirTM-HF or EpiAveolarTM models. All obtained PoDs, bioactivity readouts and timepoints (days 1, 4, 8 or 12) are plotted together with the associated lung regional concentration estimates (top) or maximum plasma concentration, C_{max} (bottom). The points correspond to the median PoD values from different concentration-response datasets for which the concentration dependency scores (CDS) > 0.5 (where the legend indicates the corresponding tissue model). PoDs determined from transcriptomics are indicated by unfilled symbols and other readouts (e.g., barrier integrity, tissue functionality, or cytokines/chemokines levels) by filled symbols.

the predicted exposure ($BER \approx 2.4$) (Figure 8; Supplementary Figures S5–7).

For the remaining two chemicals studied in this work, PHMG and Akemi (humidifier and tile coating product scenarios, respectively), our findings agreed with the high-risk classification for all scenarios investigated. For both chemicals, the predicted exposures exceeded even the largest PoD on all days measured, corresponding to a Day 12 BER of approximately 10^{-5} for PHMG and 10^{-4} for Akemi.

For both non-aerosolised drugs, Doxorubicin and Amiodarone, covering therapeutic dose high-risk scenarios, the exposure (i.e. maximum plasma concentration C_{max}) was taken from literature values (see Table 3). For Doxorubicin, this led to a very high exposure which exceeded the PoD for all readouts for all days, corresponding to BERs between 0.0005–0.2. Amiodarone by contrast, gave more variable results, with the C_{max} exceeding the transcriptomics PoDs at all timepoints (minimum BER of 0.004) but higher PoDs from the other readouts with BERs between 0.5 and 3.5 depending on timepoint and laboratory.

4 Discussion

Following the trends and perspectives of the toxicity testing in the 21st Century vision (National Research Council, 2007), there is an ongoing need to develop robust and relevant tools and

approaches that can be used to characterize the kinetics, bioactivity and risk of chemicals using NGRA without generation of new animal data. For assessing respiratory toxicity, ALI human lung models have shown promise, as they represent a complex tissue structure that physiologically recapitulates many aspects of the human respiratory epithelium as well as allowing *in vivo*-like exposure to pulmonary toxicants (Bedford et al., 2022; Cao et al., 2021; Xiong et al., 2021). In this context, the present work evaluated the applicability of the commercially available upper MucilAirTM-HF and lower EpiAlveolarTM human lung models to be used as *in vitro* systems within a NAM toolbox to identify the bioactivity (i.e., *in vitro* PoD derivation) and risk of materials that may reach the respiratory tract and induce lung toxicity. A 12-day substance exposure protocol was established to explore potential adverse effects in the lung following repeated exposure. The obtained PoDs were combined with exposure estimates using MPPD and ICRP modeling to calculate BER values. The performance of this approach is determined by its ability to differentiate between chemical/exposure scenarios of low and high risk to humans based on the size of the BER. In this pilot work, we have not conducted a formal evaluation as previously reported for NGRA approaches for systemic toxicity (Cable et al., 2024; Middleton et al., 2022), but rather we have investigated a proof-of-concept to establish the feasibility of defining a NAM toolbox to be included within an NGRA approach for lung toxicity. For the 11 benchmark chemicals (Table 3; Figure 8) investigated in 14 human exposure scenarios, it was possible to

correctly separate their risk classification by using the lowest BER per readout and lung model. Generally, for the low-risk chemical-exposure scenarios (except Crystalline and Amorphous silica occupational scenarios), the PoDs occurred at higher concentrations than the corresponding human exposure values, whereas for all the high-risk chemical-exposure scenarios, there was a clear overlap between the PoDs and lung deposited mass (benchmark inhaled materials) or maximum plasma concentration (systemically available benchmark drugs). This is only true if the transcriptomic PoDs are included in the analysis. If the transcriptomics analysis were not included, results for the high risk Crystalline silica scenario would have clustered with the low-risk chemical-exposure scenarios. One of the limitations of this work was that transcriptomics was not performed in a concentration-response manner for the upper MucilAir™-HF respiratory model, and therefore not all benchmark chemicals have transcriptomics PoDs.

Risk assessments for human inhalation toxicity based on traditional animal studies generally include a safety factor of 25 to account for uncertainties related to interspecies (animal-to-human: 2.5-safety factor) and inter-individual (human-to-human: 10-safety factor) variabilities (ECHA, 2012). Therefore, a margin of safety over 25 compared to no observed adverse effects levels in animals has been judged to be protective for human health for several decades regarding local lung effects. Defining a safe BER threshold or the appropriate use of uncertainty factors remains a challenge in NGRA. A recent regulatory example, accepted by the US EPA, of a non-animal risk assessment for the fungicide chlorothalonil in an occupational scenario combined *in vitro* PoDs from MucilAir™ readouts (i.e., TEER, lactate dehydrogenase leakage and resazurin metabolism analyses) with dosimetry information obtained from a computational fluid-particle dynamics (CFPD) model (Corley et al., 2021; Li et al., 2018; McGee Hargrove et al., 2021; Ramanarayanan et al., 2022). In this specific case, the total uncertainty safety factor, to account the response among human population, was 3 considering inter-individual toxicodynamic variability only. The inter-individual toxicokinetic and interspecies uncertainty factors were waived on the premise that the *in vitro* model was derived from human lung biopsies, the readouts measure MIEs for the mode of action (direct acting contact irritation) and the exposure modelling is sufficiently realistic and accurate. Applying a BER threshold of 3 to our dataset would be protective for all benchmark chemicals, only when including the transcriptomics PoDs for the high-risk exposure scenarios for Amiodarone and Crystalline silica. To be able to identify low-risk BER thresholds that would be protective for a range of chemicals and human exposure scenarios would require additional work to characterize further the uncertainties in both the exposure and toxicodynamic parts of our NAM toolbox, as discussed below.

Our work addressed the challenge of bridging the gap between realistic human exposures and toxicological responses, employing the widely used MPPD model. Although upper respiratory tract CFD models offer detailed dose resolution as demonstrated in the chlorothalonil case study, conducting full simulations in the lower respiratory tract proved computationally burdensome due to the vast scale of the human pulmonary system (Corley et al., 2021;

Kuempel et al., 2015). Therefore, such models would be a potential next step in a tiered approach to exposure assessment if refinement is needed. Recent studies attempted to overcome this by combining upper respiratory CFD models with lower respiratory multi-path models, albeit at a considerable computational expense (Kuprat et al., 2021; Kuprat et al., 2023). Limitations of the MPPD model include its inability to predict hotspots forming at airway junctions and points of extreme curvature, potentially leading to underestimated local doses. A significant source of inaccuracy in *in silico* modeling arises from the ICRP model used to predict chemical clearance within the lung. The lower respiratory clearance model, calibrated from clinical data on the clearance of radioactive dust particles from worker exposures (ICRP, 1994), may be excessively conservative when applied to small molecules. In the exposure scenarios explored in this paper, a combination of literature values and experimentally measured data formed the basis for estimates. Where data was lacking, a conservative approach was taken, as exemplified by assuming a MMAD of 3 μm for Crystalline silica and Akemi, predicting the highest lower respiratory exposure upon inhalation. Despite employing conservative assumptions in this work, the primary source of uncertainty stems from the absence of any formal guidance on the parameterization of these models and validation data, unlike the well-established validation of physiologically based kinetic models against human clinical data (Li et al., 2021; Punt et al., 2022).

The *in vitro* lung models used in this work demonstrated some limitations which impacted on their sensitivity to some toxicants and their ability to replicate expected physiological responses. Despite selecting reference materials known for specific *in vitro* lung effects (Supplementary Table S1), some well-documented biological responses to these materials were mild or absent in both *in vitro* human lung systems. For instance, tissue apical exposure to Chlorocresol failed to induce a CBF decrease in MucilAir™-HF tissues, and LPS via apical exposure did not trigger intense inflammatory cytokine secretion in EpiAlveolar model, whereas a mild response was observed in MucilAir™-HF tissues exposed to TNF- α and LPS (at 6h/day aerosol exposure only); on the other hand, no effects were triggered by Nicotine and Sulforaphane, both via aerosol exposure, similar to other *in vitro* systems (see details in Supplementary Table S1). The absence of dendritic cells in MucilAir™-HF tissues might have led to the lack of marked inflammatory response to LPS and TNF- α , while the lack of macrophages in EpiAlveolar™ tissues might have impacted the response to Crystalline silica, Amorphous silica, Amiodarone, and LPS given the lack of response in the cytokine/chemokine panel. However, the transcriptomics data provided insights about both the potency and mechanism of toxicity of these substances. Similarly, the absence of epithelial alveolar type II cells, the site of toxicity for the polymer contained in the Akemi formulation, did not impact classification of this chemical, with all PoDs generated in the EpiAlveolar™ tissues being lower than the predicted human exposure. Similar results were observed in the recently evaluated systemic NAM toolbox (Cable et al., 2024). While the toolbox was not always able to identify the critical mode of action for some chemicals, it was almost always able to correctly assess the risk of the chemical-exposure scenario based on a general measure of bioactivity, such as transcriptomics.

It was clear from our experience with two laboratories, that there is a need to develop and evaluate standardized protocols for dosing methodologies (e.g., Bannuscher et al., 2022), measurement of readouts [e.g., CBF and TEER analyses as proposed by Behrsing et al. (2022); Sharma et al. (2024), respectively], number of donor requirements, timepoints and duration of exposure. In this regard, recent research showed that apical liquid dosing in the primary human bronchial epithelial cell/lung fibroblast ALI co-culture model can reprogram gene expression and alter cell physiology, potentially introducing confounding factors that compromise the accuracy of inhaled substance evaluations (Mallek et al., 2024). Corroborating this, our data showed that LPS from *P. aeruginosa* 10, via aerosol exposure, induced upregulation of MMP-3 and uPAR levels in MucilAir™-HF tissues; however, no effects were observed when tissues were exposed to LPS via apical liquid dosing. Similarly, no effects were observed in EpiAlveolar™ tissues exposed, via apical, to LPS from *P. aeruginosa* 10 or *E. coli* 055:B5. Therefore, this may also explain the lack of marked inflammatory response induced by LPS, besides the use of different bacterial strain sources that can to significantly impact the results of *in vitro* and *in vivo* experiments (Ernst et al., 2021; Lin et al., 2020; Pulendran et al., 2001). Moreover, the *in vitro* systems used here were composed of primary cells derived from limited number of human samples. In fact, sample size estimates have indicated the need for a reasonable number of donors ($n = 13$ –299) to detect 2-fold changes in a panel of inflammatory readouts (e.g., IL-6 and IL-8 transcripts) to account for interindividual variability in studies using an *in vitro* primary cell-based model exposed to ozone (Bowers et al., 2022). Therefore, an approach using multiple donors, donor-matched tissue and pooled-donor samples in ALI exposures may support the understanding of inter-individual variability within *in vitro* assays (Moreau et al., 2022) by ideally using a broad set of different inhaled materials covering a diversity regarding chemical structures.

Despite some of the limitations discussed above, the NAM toolbox for respiratory safety used in this work appeared to separate the low- and high-risk benchmark exposure scenarios for 12 out of the 14 scenarios evaluated when using the BER, suggesting that our strategy of selecting NAMs informed by AOPs associated with pulmonary toxicity, can provide relevant biological coverage. In addition, the benchmarking approach provides an alternative to the traditional validation of NAMS against apical effects in rodent studies but rather tries to evaluate the NAMs in the context of making protective safety decisions (Browne et al., 2024). Our findings pave the way for further evaluation of the performance of NAM toolboxes for a wider substance dataset with varied mechanisms of action, uses, and balanced low and high-risk benchmarks to build confidence in the protectiveness of the approach. In addition, there is a need to establish scientific confidence by improving the reproducibility, standardization of protocols, and *in vitro* culture methodologies (ICCVAM, 2024; van der Zalm et al., 2022). This pioneering work together with future research will ensure confidence in the use of *in vitro* testing to generate human-relevant and mechanistically driven PoDs that, together with estimates of human exposure, can be used in safety assessments of ingredients in consumer goods products without the need for the generation of new animal data.

Data availability statement

The data related to transcriptomics analysis presented in the study are deposited in the European Bioinformatics Institute (EBI) data repository, Array Express (<https://www.ebi.ac.uk/biostudies/arrayexpress>), accession number E-MTAB-14272. The other original contributions presented in the study are included in the article/Supplementary Material, further inquiries can be directed to the corresponding author.

Ethics statement

The studies involving humans were approved by Epithelix Sarl review board and MatTek Life Sciences Biotechnology Company. The MucilAir™-HF and EpiAlveolar™ primary human tissue models were acquired from Epithelix Sarl (Geneva, Switzerland) and MatTek Corporation (Ashland, MA, USA), respectively. In all cases, consent was obtained by these institutions from the donor or the donor's legal next of kin, for use of the cells or derivatives of the tissue for research purpose. All procedures were conducted in accordance with the local legislation and institutional requirements.

Author contributions

RdA: Data curation, Formal Analysis, Supervision, Writing—original draft, Writing—review and editing. IM: Conceptualization, Data curation, Formal Analysis, Methodology, Project administration, Writing—review and editing. HuB: Data curation, Formal Analysis, Methodology, Visualization, Writing—original draft, Writing—review and editing. AM: Data curation, Formal Analysis, Visualization, Writing—original draft, Writing—review and editing. MT: Data curation, Formal Analysis, Writing—original draft, Writing—review and editing. DB: Data curation, Formal Analysis, Methodology, Visualization, Writing—original draft, Writing—review and editing. AB: Data curation, Methodology, Resources, Writing—original draft, Writing—review and editing. OS: Data curation, Formal Analysis, Writing—review and editing. PE: Data curation, Formal Analysis, Writing—review and editing. TP: Data curation, Formal Analysis, Writing—review and editing. JW: Investigation, Methodology, Writing—review and editing. BB: Investigation, Methodology, Writing—original draft, Writing—review and editing. SC: Investigation, Methodology, Writing—original draft, Writing—review and editing. HoB: Investigation, Methodology, Writing—original draft, Writing—review and editing. VP: Investigation, Methodology, Writing—original draft, Writing—review and editing. MB: Conceptualization, Funding acquisition, Methodology, Project administration, Supervision, Writing—original draft, Writing—review and editing.

Funding

The author(s) declare that financial support was received for the research, authorship, and/or publication of this article. This work

was funded by Unilever as part of Unilever's ongoing effort to develop new ways of assuring human safety.

Acknowledgments

We thank Dr Maja Aleksic, Dr Matthew Dent, and Dr Carl Westmoreland for providing comments that improved the manuscript; Zoë Deag for her technical support for the SUET data; Dr Claire Peart and Mark Liddell for their support for the high-throughput transcriptomics work; and Dr Beate Nicol for providing invaluable leadership for the data management part of the project.

Conflict of interest

Author JW was employed by Charles River Laboratory Edinburgh Ltd. Authors BB and SC were employed by Epithelix Sarl. Authors HB and VP were employed by Institute for In Vitro Sciences, Inc.

References

- Allen, T. E. H., Goodman, J. M., Gutsell, S., and Russell, P. J. (2014). Defining molecular initiating events in the adverse outcome pathway framework for risk assessment. *Chem. Res. Toxicol.* 27, 2100–2112. doi:10.1021/tx500345j
- Andreasen, F., Agerbaek, H., Bjerregaard, P., and Gøtzsche, H. (1981). Pharmacokinetics of amiodarone after intravenous and oral administration. *Eur. J. Clin. Pharmacol.* 19, 293–299. doi:10.1007/BF00562807
- Api, A. M., Belmonte, F., Belsito, D., Biserta, S., Botelho, D., Bruze, M., et al. (2019). RIFM fragrance ingredient safety assessment, coumarin, CAS Registry Number 91-64-5. *Food Chem. Toxicol.* 130, 110522. doi:10.1016/j.fct.2019.05.030
- Api, A. M., Belsito, D., Biserta, S., Botelho, D., Bruze, M., Burton, G. A., Jr, et al. (2020). Corrigendum to "RIFM fragrance ingredient safety assessment, coumarin, CAS registry number 91-64-5" [Food Chem. Toxicol. 130 (Suppl. 1) (2019) 110522]. *Food Chem. Toxicol.* 141, 111406. doi:10.1016/j.fct.2020.111406
- Asgharian, B., and Price, O. T. (2006). Airflow distribution in the human lung and its influence on particle deposition. *Inhal. Toxicol.* 18, 795–801.
- Asgharian, B., and Price, O. T. (2007). Deposition of ultrafine (NANO) particles in the human lung. *Inhal. Toxicol.* 19, 1045–1054.
- Asgharian, B., Price, O. T., and Hofmann, W. (2006). Prediction of particle deposition in the human lung using realistic models of lung ventilation. *J. Aero. Sci.* 37, 1209–1221.
- Balogh Sivars, K., Sivars, U., Hornberg, E., Zhang, H., Brändén, L., Bonfante, R., et al. (2017). A 3D human airway model enables prediction of respiratory toxicity of inhaled drugs *in vitro*. *Toxicol. Sci.* 162, 301–308. doi:10.1093/toxsci/kfx255
- Baltazar, M. T., Cable, S., Carmichael, P. L., Cubberley, R., Cull, T., Delagrangé, M., et al. (2020). A next-generation risk assessment case study for coumarin in cosmetic products. *Toxicol. Sci.* 176, 236–252. doi:10.1093/toxsci/kfaa048
- Bannuscher, A., Schmid, O., Drasler, B., Rohrbasser, A., Braakhuis, H. M., Meldrum, K., et al. (2022). An inter-laboratory effort to harmonize the cell-delivered *in vitro* dose of aerosolized materials. *NanoImpact* 28, 100439. doi:10.1016/j.nimpact.2022.100439
- Barosova, H., Maione, A. G., Septiadi, D., Sharma, M., Haeni, L., Balog, S., et al. (2020). Use of EpiAlveolar lung model to predict fibrotic potential of multiwalled carbon nanotubes. *ACS Nano* 14, 3941–3956. doi:10.1021/acsnano.9b06860
- Barpe, D. R., Rosa, D. D., and Froehlich, P. E. (2010). Pharmacokinetic evaluation of doxorubicin plasma levels in normal and overweight patients with breast cancer and simulation of dose adjustment by different indexes of body mass. *Eur. J. Pharm. Sci.* 41, 458–463. doi:10.1016/j.ejps.2010.07.015
- Bedford, R., Perkins, E., Clements, J., and Hollings, M. (2022). Recent advancements and application of *in vitro* models for predicting inhalation toxicity in humans. *Toxicol. Vitro* 79, 105299. doi:10.1016/j.tiv.2021.105299
- Behrsing, H. P., Wahab, A., Ukishima, L., Grodi, C., Frentzel, S., John, S., et al. (2022). Ciliary beat frequency: proceedings and recommendations from a multi-laboratory ring trial using 3-D reconstituted human airway epithelium to model mucociliary clearance. *Altern. Lab. Anim.* 50, 293–309. doi:10.1177/0261192922114383
- Bolt, M. W., Card, J. W., Racz, W. J., Brien, J. F., and Massey, T. E. (2001). Disruption of mitochondrial function and cellular ATP levels by amiodarone and N-desethylamiodarone in initiation of amiodarone-induced pulmonary cytotoxicity. *J. Pharmacol. Exp. Ther.* 298, 1280–1289. doi:10.1016/s0022-3565(24)29503-3
- Bowers, E. C., Martin, E. M., Jarabek, A. M., Morgan, D. S., Smith, H. J., Dailey, L. A., et al. (2022). Ozone responsive gene expression as a model for describing repeat exposure response trajectories and interindividual toxicodynamic variability *in vitro*. *Toxicol. Sci.* 185, 38–49. doi:10.1093/toxsci/kfab128
- Brescia, S., Alexander-White, C., Li, H., and Cayley, A. (2023). Risk assessment in the 21st century: where are we heading? *Toxicol. Res.* 12, 1–11. doi:10.1093/toxres/tfac087
- Browne, P., Paul Friedman, K., Boekelheide, K., and Thomas, R. S. (2024). Adverse effects in traditional and alternative toxicity tests. *Regul. Toxicol. Pharmacol.* 148, 105579. doi:10.1016/j.yrtph.2024.105579
- Burnett, C. L., Bergfeld, W. F., and Andersen, F. A. (2011). Final Report of the Amended Safety Assessment of PVM/MA Copolymer and Its Related Salts and Esters as Used in Cosmetics. *Inter. J. Toxicol.* 30, 1285–1445.
- Barsan, M. E. (2007). NIOSH pocket guide to chemical hazards. Available at: <https://stacks.cdc.gov/view/cdc/21265>.
- Budin, C. E., Cocuz, I. G., Sabău, A. H., Niculescu, R., Ianos, I. R., Ioan, V., et al. (2022). Pulmonary fibrosis related to amiodarone—is it a standard pathophysiological pattern? A case-based literature review. *Diagn. (Basel)* 12, 3217. doi:10.3390/diagnostics12123217
- Cable, S., Baltazar, M. T., Bunglawala, F., Carmichael, P. L., Contreas, L., Dent, M. P., et al. (2024). Advancing systemic toxicity risk assessment: evaluation of a NAM-based toolbox approach. *Toxicol. Sci.* kfae159. doi:10.1093/toxsci/kfae159
- Cao, X., Coyle, J. P., Xiong, R., Wang, Y., Heflich, R. H., Ren, B., et al. (2021). Invited review: human air-liquid-interface organotypic airway tissue models derived from primary tracheobronchial epithelial cells—overview and perspectives. *Vitro Cell. and Dev. Biol. - Animal* 57, 104–132. doi:10.1007/s11626-020-00517-7
- Carthew, P., Griffiths, H., Keech, S., and Hartop, P. (2002). Safety assessment for hair-spray resins: risk assessment based on rodent inhalation studies. *Inhal. Toxicol.* 14, 401–416. doi:10.1080/08958370252871023
- Chopin, N., and Papaspiliopoulos, O. (2020). *An introduction to sequential Monte Carlo*. Cham: Springer, 378.
- CIR (2018). Amended safety assessment of acrylates copolymers as used in cosmetics. Available at: <https://www.cir-safety.org/sites/default/files/Acrylates%20Copolymers.pdf>.
- CIR (2019). Amended safety assessment of amorphous silica and synthetically-manufactured amorphous silicates as used in cosmetics. Available at: <https://cir-safety.org/sites/default/files/silica092019FR.pdf>.
- Clippinger, A. J., Allen, D., Behrsing, H., Bérubé, K. A., Bolger, M. B., Casey, W., et al. (2018a). Pathway-based predictive approaches for non-animal

Publisher's note

All claims expressed in this article are solely those of the authors and do not necessarily represent those of their affiliated organizations, or those of the publisher, the editors and the reviewers. Any product that may be evaluated in this article, or claim that may be made by its manufacturer, is not guaranteed or endorsed by the publisher.

Supplementary material

The Supplementary Material for this article can be found online at: <https://www.frontiersin.org/articles/10.3389/ftox.2025.1426132/full#supplementary-material>

assessment of acute inhalation toxicity. *Toxicol Vitro* 52, 131–145. doi:10.1016/j.tiv.2018.06.009

Clippinger, A. J., Allen, D., Jarabek, A. M., Corvaro, M., Gaça, M., Gehen, S., et al. (2018b). Alternative approaches for acute inhalation toxicity testing to address global regulatory and non-regulatory data requirements: an international workshop report. *Toxicol Vitro* 48, 53–70. doi:10.1016/j.tiv.2017.12.011

Corley, R. A., Kuprat, A. P., Suffield, S. R., Kabilan, S., Hinderliter, P. M., Yugulis, K., et al. (2021). New approach methodology for assessing inhalation risks of a contact respiratory cytotoxicant: computational fluid dynamics-based aerosol dosimetry modeling for cross-species and *in vitro* comparisons. *Toxicol. Sci.* 182, 243–259. doi:10.1093/toxsci/kfab062

Dent, M., Amaral, R. T., Da Silva, P. A., Ansell, J., Boislevé, F., Hatao, M., et al. (2018). Principles underpinning the use of new methodologies in the risk assessment of cosmetic ingredients. *Comput. Toxicol.* 7, 20–26. doi:10.1016/j.comtox.2018.06.001

Dent, M. P., Vaillancourt, E., Thomas, R. S., Carmichael, P. L., Ouedraogo, G., Kojima, H., et al. (2021). Paving the way for application of next generation risk assessment to safety decision-making for cosmetic ingredients. *Regul. Toxicol. Pharmacol.* 125, 105026. doi:10.1016/j.yrtph.2021.105026

Dobin, A., Davis, C. A., Schlesinger, F., Drenkow, J., Zaleski, C., Jha, S., et al. (2013). STAR: ultrafast universal RNA-seq aligner. *Bioinformatics* 29, 15–21. doi:10.1093/bioinformatics/bts635

Duch, P., Nørgaard, A. W., Hansen, J. S., Sørli, J. B., Jacobsen, P., Lynggaard, F., et al. (2014). Pulmonary toxicity following exposure to a tile coating product containing alkylsiloxanes. A clinical and toxicological evaluation. *Clin. Toxicol. (Phila.)* 52, 498–505. doi:10.3109/15563650.2014.915412

ECETOC (2006). JACC REPORT No. 51, synthetic amorphous silica. Available at: <https://www.ecetoc.org/publication/jacc-report-51-synthetic-amorphous-silica/>.

ECHA (2012). Guidance on information requirements and chemical safety assessment: chapter R8: characterisation of dose [Concentration]-Response for human health. Available at: https://echa.europa.eu/documents/10162/17224/information_requirements_r8_en.pdf/e153243a-03f0-44c5-8808-88af66223258.

Ernst, O., Khan, M. M., Oyler, B. L., Yoon, S. H., Sun, J., Lin, F. Y., et al. (2021). Species-specific endotoxin stimulus determines toll-like receptor 4- and caspase 11-mediated pathway activation characteristics. *mSystems* 6, e0030621. doi:10.1128/mSystems.00306-21

Escher, S. E., Tluczkiewicz, I., Batke, M., Bitsch, A., Melber, C., Kroese, E. D., et al. (2010). Evaluation of inhalation TTC values with the database RepDose. *Regul. Toxicol. Pharmacol.* 58, 259–274. doi:10.1016/j.yrtph.2010.06.009

European Commission (2006). Regulation (EC) No 1907/2006 of the European parliament and of the Council of 18 december 2006 concerning the registration, evaluation, authorisation and restriction of chemicals (REACH), establishing a European chemicals agency, amending directive 1999/45/EC and repealing Council regulation (EEC) No 793/93 and commission regulation (EC) No 1488/94 as well as Council directive 76/769/EEC and commission directives 91/155/EEC, 93/67/EEC, 93/105/EC and 2000/21/EC. *Off. J. Euro. Union* L396, 1–849.

European Union (2009). Regulation (EC) No 1223/2009 of the European parliament and of the Council of 30 november 2009 on cosmetic products. *Off. J. Euro. Union* L342, 1–59.

FEA (2009). Guide on particle size measurement from aerosol products. Available at: <http://www.aerosol.org>.

Fentem, J. H. (2023). The 19th FRAME annual lecture, november 2022: safer chemicals and sustainable innovation will be achieved by regulatory use of modern safety science, not by more animal testing. *Altern. Lab. Anim.* 51 (2), 90–101. doi:10.1177/02611929231158236

Fritzsching, B., Zhou-Suckow, Z., Trojanek, J. B., Schubert, S. C., Schatterny, J., Hirtz, S., et al. (2015). Hypoxic epithelial necrosis triggers neutrophilic inflammation via IL-1 receptor signaling in cystic fibrosis lung disease. *Am. J. Respir. Crit. Care Med.* 191, 902–913. doi:10.1164/rccm.201409-1610OC

Fromenty, B., Fisch, C., Berson, A., Letteron, P., Larrey, D., and Pessayre, D. (1990a). Dual effect of amiodarone on mitochondrial respiration. Initial protonophoric uncoupling effect followed by inhibition of the respiratory chain at the levels of complex I and complex II. *J. Pharmacol. Exp. Ther.* 255, 1377–1384.

Fromenty, B., Fisch, C., Labbe, G., Degott, C., Deschamps, D., Berson, A., et al. (1990b). Amiodarone inhibits the mitochondrial beta-oxidation of fatty acids and produces microvesicular steatosis of the liver in mice. *J. Pharmacol. Exp. Ther.* 255, 1371–1376.

Gillespie, M., Jassal, B., Stephan, R., Milacic, M., Rothfels, K., Senff-Ribeiro, A., et al. (2021). The reactome pathway knowledgebase 2022. *Nucleic Acids Res.* 50, D687–D692. doi:10.1093/nar/gkab1028

Gilmour, N., Kern, P. S., Alépée, N., Boislevé, F., Bury, D., Clouet, E., et al. (2020). Development of a next generation risk assessment framework for the evaluation of skin sensitization of cosmetic ingredients. *Regul. Toxicol. Pharmacol.* 116, 104721. doi:10.1016/j.yrtph.2020.104721

Gilmour, N., Reynolds, J., Przybylak, K., Aleksic, M., Aptula, N., Baltazar, M. T., et al. (2022). Next generation risk assessment for skin allergy: decision making using new

approach methodologies. *Regul. Toxicol. Pharmacol.* 131, 105159. doi:10.1016/j.yrtph.2022.105159

Gizurason, S. (2012). Anatomical and histological factors affecting intranasal drug and vaccine delivery. *Curr. Drug Deliv.* 9, 566–582. doi:10.2174/156720112803529828

Yu, G., Wang, L. G., Han, Y., and He, Q. Y. (2012). clusterProfiler: an R Package for comparing biological themes among gene clusters. *OMICS A J. Integr. Biol.* 16, 284–287. doi:10.1089/omi.2011.0118

Halappanavar, S., Sharma, M., Solorio-Rodriguez, S., Richard Wallin, E. H., Vogel, U., Sullivan, K., et al. (2023). *Substance interaction with the pulmonary resident cell membrane components leading to pulmonary fibrosis*. OECD.

Halappanavar, S., van den Brule, S., Nymark, P., Gaté, L., Seidel, C., Valentino, S., et al. (2020). Adverse outcome pathways as a tool for the design of testing strategies to support the safety assessment of emerging advanced materials at the nanoscale. *Part Fibre Toxicol.* 17, 16. doi:10.1186/s12989-020-00344-4

Hatherell, S., Baltazar, M. T., Reynolds, J., Carmichael, P. L., Dent, M., Li, H., et al. (2020). Identifying and characterizing stress pathways of concern for consumer safety in next-generation risk assessment. *Toxicol. Sci.* 176, 11–33. doi:10.1093/toxsci/kfaa054

Health Canada (2021). *Bioactivity exposure ratio: application in priority setting and risk assessment*. Ottawa: Health Canada Publishing. Available at: <https://www.canada.ca/en/environment-climate-change/services/evaluating-existing-substances/science-approach-document-bioactivity-exposure-ratio-application-priority-setting-risk-assessment.html>.

Hoshina, H., and Takei, H. (2021). Drug-induced interstitial lung disease after anthracycline-combined chemotherapy for breast cancer: A case report and literature review. *Case. Rep. Oncol.* 14, 1671–1676.

Huang, S., Boda, B., Vernaz, J., Ferreira, E., Wiszniewski, L., and Constant, S. (2017). Establishment and characterization of an *in vitro* human small airway model (SmallAir™). *Eur. J. Pharm. Biopharm.* 118, 68–72. doi:10.1016/j.ejpb.2016.12.006

Huang, S., Wiszniewski, S., and Constant, S. (2011). “The use of *in vitro* 3D cell models in drug development for respiratory diseases.” in *Drug Discovery and development*. Editor M. K. Izet (Rijeka: IntechOpen). Ch. 8.

Iccvam, V. (2024). Qualification, and regulatory acceptance of new approach methodologies. A Rep. Interag. Coord. Comm. Validation Altern. Methods (ICCVAM) Validation Workgr. Available at: <https://ntp.niehs.nih.gov/whatwestudy/niceatm/resources-for-test-method-developers/submissions>. doi:10.22427/NICEATM-2

ICRP (1994). Human respiratory tract model for radiological protection ICRP publication 66. *Ann. ICRP* 24. doi:10.1016/0146-6453(94)90029-9

Johnson, N. F. (2017). Pulmonary toxicity of benzalkonium chloride. *J. Aerosol Med. Pulm. Drug Deliv.* 31, 1–17. doi:10.1089/jamp.2017.1390

Jung, H. N., Zerin, T., Podder, B., Song, H. Y., and Kim, Y. S. (2014). Cytotoxicity and gene expression profiling of polyhexamethylene guanidine hydrochloride in human alveolar A549 cells. *Toxicol Vitro* 28, 684–692. doi:10.1016/j.tiv.2014.02.004

Kim, C., Jeong, S. H., Kim, J., Lee, K. Y., Cha, J., Lee, C. H., et al. (2021). Evaluation of polyhexamethylene guanidine-induced lung injuries by chest CT, pathologic examination, and RNA sequencing in a rat model. *Sci. Rep.* 11, 6318. doi:10.1038/s41598-021-85662-z

Kim, H. R., Lee, K., Park, C. W., Song, J. A., Shin, D. Y., Park, Y. J., et al. (2016). Polyhexamethylene guanidine phosphate aerosol particles induce pulmonary inflammatory and fibrotic responses. *Arch. Toxicol.* 90, 617–632. doi:10.1007/s00204-015-1486-9

Koparal, M., Kurt, E., Altuntas, E. E., and Dogan, F. (2021). Assessment of mucociliary clearance as an indicator of nasal function in patients with COVID-19: a cross-sectional study. *Eur. Arch. Otorhinolaryngol.* 278, 1863–1868. doi:10.1007/s00405-020-06457-y

Kuempel, E. D., Sweeney, L. M., Morris, J. B., and Jarabek, A. M. (2015). Advances in inhalation dosimetry models and methods for occupational risk assessment and exposure limit derivation. *J. Occup. Environ. Hyg.* 12 (Suppl. 1), S18–S40. doi:10.1080/15459624.2015.1060328

Kuprat, A. P., Jalali, M., Jan, T., Corley, R. A., Asgharian, B., Price, O., et al. (2021). Efficient bi-directional coupling of 3D computational fluid-particle dynamics and 1D Multiple Path Particle Dosimetry lung models for multiscale modeling of aerosol dosimetry. *J. Aerosol Sci.* 151, 105647. doi:10.1016/j.jaerosci.2020.105647

Kuprat, A. P., Price, O., Asgharian, B., Singh, R. K., Colby, S., Yugulis, K., et al. (2023). Automated bidirectional coupling of multiscale models of aerosol dosimetry: validation with subject-specific deposition data. *J. Aerosol Sci.* 174, 106233. doi:10.1016/j.jaerosci.2023.106233

Lee, J., and Yu, I. J. (2017). Human exposure to polyhexamethylene guanidine phosphate from humidifiers in residential settings: Cause of serious lung disease. *Toxicol. Ind. Health.* 33, 835–842.

Li, H., Yuan, H., Middleton, A., Li, J., Nicol, B., Carmichael, P., et al. (2021). Next generation risk assessment (NGRA): bridging *in vitro* points-of-departure to human safety assessment using physiologically-based kinetic (PBK) modelling - a case study of

- doxorubicin with dose metrics considerations. *Toxicol Vitro* 74, 105171. doi:10.1016/j.tiv.2021.105171
- Li, L., Mosquin, P., and Brambilla, D. (2018). MRID 50610401 chlorothalonil - benchmark dose (BMD) analysis of MucilAir data to establish a toxicological point of departure (POD) for use in human risk assessment final report. Available at: <https://www.regulations.gov/document/EPA-HQ-OPP-2018-0517-0006>.2018.
- Liberzon, A., Birger, C., Thorvaldsdóttir, H., Ghandi, M., Mesirov, J. P., and Tamayo, P. (2015). The Molecular Signatures Database (MSigDB) hallmark gene set collection. *Cell Syst.* 1, 417–425. doi:10.1016/j.cels.2015.12.004
- Lin, T. L., Shu, C. C., Chen, Y. M., Lu, J. J., Wu, T. S., Lai, W. F., et al. (2020). Like cures like: pharmacological activity of anti-inflammatory lipopolysaccharides from gut microbiome. *Front. Pharmacol.* 11, 554. doi:10.3389/fphar.2020.00554
- Love, M. I., Huber, W., and Anders, S. (2014). Moderated estimation of fold change and dispersion for RNA-seq data with DESeq2. *Genome Biol.* 15, 550. doi:10.1186/s13059-014-0550-8
- Luetlich, K., Sharma, M., Yepiskoposyan, H., Breheny, D., and Lowe, F. J. (2021). An adverse outcome pathway for decreased lung function focusing on mechanisms of impaired mucociliary clearance following inhalation exposure. *Front. Toxicol.* 3, 750254. doi:10.3389/ftox.2021.750254
- Luetlich, K., Talikka, M., Lowe, F. J., Haswell, L. E., Park, J., Gaca, M. D., et al. (2017). The adverse outcome pathway for oxidative stress-mediated EGFR activation leading to decreased lung function. *Appl. Vitro Toxicol.* 3, 99–109. doi:10.1089/avt.2016.0032
- Mallek, N. M., Martin, E. M., Dailey, L. A., and McCullough, S. D. (2024). Liquid application dosing alters the physiology of air-liquid interface (ALI) primary human bronchial epithelial cell/lung fibroblast co-cultures and *in vitro* testing relevant endpoints. *Front. Toxicol.* 5, 1264331. doi:10.3389/ftox.2023.1264331
- Mannetje, A., Steenland, K., Attfield, M., Boffetta, P., Checkoway, H., DeKlerk, N., et al. (2002). Exposure-response analysis and risk assessment for silica and silicosis mortality in a pooled analysis of six cohorts. *Occup. Environ. Med.* 59, 723–728.
- Mao, W., Zaslavsky, E., Hartmann, B. M., Sealfon, S. C., and Chikina, M. (2019). Pathway-level information extractor (PLIER) for gene expression data. *Nat. Methods* 16, 607–610. doi:10.1038/s41592-019-0456-1
- McGee Hargrove, M., Parr-Dobrzanski, B., Li, L., Constant, S., Wallace, J., Hinderliter, P., et al. (2021). Use of the MucilAir airway assay, a new approach methodology, for evaluating the safety and inhalation risk of agrochemicals. *Appl. Vitro Toxicol.* 7, 50–60. doi:10.1089/avt.2021.0005
- Merget, R., Bauer, T., Küpper, H. U., Philippou, S., Bauer, H. D., Breitstadt, R., et al. (2002). Health hazards due to the inhalation of amorphous silica. *Archives Toxicol.* 75, 625–634. doi:10.1007/s002040100266
- Middleton, A. M., Reynolds, J., Cable, S., Baltazar, M. T., Li, H., Bevan, S., et al. (2022). Are non-animal systemic safety assessments protective? A toolbox and workflow. *Toxicol. Sci.* 189, 124–147. doi:10.1093/toxsci/kfac068
- Minchin, R. F., Johnston, M. R., Schuller, H. M., Aiken, M. A., and Boyd, M. R. (1988). Pulmonary toxicity of doxorubicin administered by *in situ* isolated lung perfusion in dogs. *Cancer* 61, 1320–1325. doi:10.1002/1097-0142(19880401)61:7<1320::aid-cncr2820610708>3.0.co;2-j
- Moreau, M., Fisher, J., Andersen, M. E., Barnwell, A., Corzine, S., Ranade, A., et al. (2022). NAM-based prediction of point-of-contact toxicity in the lung: a case example with 1,3-dichloropropene. *Toxicology* 481, 153340. doi:10.1016/j.tox.2022.153340
- National Research Council (2007). *Toxicity testing in the 21st Century: a vision and a strategy*. Washington, DC: The National Academies Press.
- Nevadunsky, N. S., Mbagwu, C., Mizrahi, N., Burton, E., and Goldberg, G. L. (2013). Pulmonary fibrosis after pegylated liposomal Doxorubicin in a patient with uterine papillary serous carcinoma. *J. Clin. Oncol.* 31, e167–e169. doi:10.1200/JCO.2012.44.5767
- OECD (2009a). *Test No. 403: acute inhalation toxicity*.
- OECD (2009b). *Test No. 436: acute inhalation toxicity – acute toxic class method*.
- OECD (2017). *Guidance document for the use of adverse outcome pathways in developing integrated approaches to testing and assessment (IATA)*.
- OECD (2018a). *Test No. 412: subacute inhalation toxicity: 28-day study*.
- OECD (2018b). *Test No. 413: subchronic inhalation toxicity: 90-day study*.
- OECD (2018c). *Test No. 433: acute inhalation toxicity: fixed concentration procedure*.
- OECD (2022). Case study on the use of an integrated approach for testing and assessment (IATA) for new approach methodology (NAM) for refining inhalation risk assessment from point of contact toxicity of the pesticide, chlorothalonil. *Ser. Test. Assess. No.* 367.
- Park, S., Lee, K., Lee, E. J., Lee, S. Y., In, K. H., Kim, H. K., et al. (2014). Humidifier disinfectant-associated interstitial lung disease in an animal model induced by polyhexamethylene guanidine aerosol. *Am. J. Respir. Crit. Care Med.* 190, 706–708. doi:10.1164/rccm.201404-0710LE
- Paul Friedman, K., Gagne, M., Loo, L. H., Karamertzanis, P., Netzeva, T., Sobanski, T., et al. (2019). Utility of *in vitro* bioactivity as a lower bound estimate of *in vivo* adverse effect levels and in risk-based prioritization. *Toxicol. Sci.* 173, 202–225. doi:10.1093/toxsci/kfz01
- Patwa, A., and Shah, A. (2015). Anatomy and physiology of respiratory system relevant to anaesthesia. *Indian. J. Anaesth.* 59, 533–541.
- Pulendran, B., Kumar, P., Cutler, C. W., Mohamadzadeh, M., Van Dyke, T., and Banchereau, J. (2001). Lipopolysaccharides from distinct pathogens induce different classes of immune responses *in vivo*. *J. Immunol.* 167, 5067–5076. doi:10.4049/jimmunol.167.9.5067
- Punt, A., Louise, J., Beekmann, K., Pinckaers, N., Fabian, E., Van Ravenzwaay, B., et al. (2022). Predictive performance of next generation human physiologically based kinetic (PBK) models based on *in vitro* and *in silico* input data. *Altex* 39, 221–234–234. doi:10.14573/altex.2108301
- Rajagopal, R., Baltazar, M. T., Carmichael, P. L., Dent, M. P., Head, J., Li, H., et al. (2022). Beyond AOPs: a mechanistic evaluation of NAMs in DART testing. *Front. Toxicol.* 4, 838466. doi:10.3389/ftox.2022.838466
- Ramanarayanan, T., Szarka, A., Flack, S., Hinderliter, P., Corley, R., Charlton, A., et al. (2022). Application of a new approach method (NAM) for inhalation risk assessment. *Regul. Toxicol. Pharmacol.* 133, 105216. doi:10.1016/j.yrtph.2022.105216
- Reardon, A. J. F., Farmahin, R., Williams, A., Meier, M. J., Addicks, G. C., Yauk, C. L., et al. (2022). From vision toward best practices: evaluating *in vitro* transcriptomic points of departure for application in risk assessment using a uniform workflow. *Front. Toxicol.* 5, 1194895. doi:10.3389/ftox.2023.1194895
- Rostami, A. A. (2009). Computational modeling of aerosol deposition in respiratory tract: A review. *Inhala. Toxicol.* 21, 262–290.
- Rossner, P., Cervena, T., Vojtisek-Lom, M., Vrbova, K., Ambroz, A., Novakova, Z., et al. (2019). The biological effects of complete gasoline engine emissions exposure in a 3D human airway model (MucilAir™) and in human bronchial epithelial cells (BEAS-2B). *Int. J. Mol. Sci.* 20, 5710. doi:10.3390/ijms20225710
- Sharma, M., Huber, E., Arnesdottir, E., Behrsing, H. P., Bettmann, A., Brandwein, D., et al. (2024). Minimum information for reporting on the TEER (trans-epithelial/endothelial electrical resistance) assay (MIRTA). *Archives Toxicol.* 99, 57–66. doi:10.1007/s00204-024-03879-z
- Sieber, P., Schäfer, A., Lieberherr, R., Caimi, S. L., Lüthi, U., Ryge, J., et al. (2023). NF-κB drives epithelial-mesenchymal mechanisms of lung fibrosis in a translational lung cell model. *JCI Insight* 8, e154719. doi:10.1172/jci.insight.154719
- Song, J. H., Ahn, J., Park, M. Y., Park, J., Lee, Y. M., Myong, J. P., et al. (2022). Health effects associated with humidifier disinfectant use: a systematic review for exploration. *J. Korean Med. Sci.* 37, e257. doi:10.3346/jkms.2022.37.e257
- Schwaiblmair, M., Behr, W., Haeckel, T., Märkl, B., Foerg, W., Berghaus, T., et al. (2012). Drug induced interstitial lung disease. *Open. Respir. Med. J.* 6, 63–74.
- Sorli, J. B., Huang, Y., Da Silva, E., Hansen, J. S., Zuo, Y. Y., Frederiksen, M., et al. (2018). Prediction of acute inhalation toxicity using *in vitro* lung surfactant inhibition. *Altex* 35, 26–36. doi:10.14573/altex.1705181
- Steenland, K., and Brown, D. (1995). Silicosis among gold miners: exposure-response analyses and risk assessment. *Am. J. Public Health* 85, 1372–1377. doi:10.2105/ajph.85.10.1372
- Steiling, W., Bascompta, M., Carthew, P., Catalano, G., Corea, N., D'Haese, A., et al. (2014). Principle considerations for the risk assessment of sprayed consumer products. *Toxicol. Lett.* 227, 41–49. doi:10.1016/j.toxlet.2014.03.005
- Stucki, A. O., Barton-Maclaren, T. S., Bhuller, Y., Henriquez, J. E., Henry, T. R., Hirn, C., et al. (2022). Use of new approach methodologies (NAMs) to meet regulatory requirements for the assessment of industrial chemicals and pesticides for effects on human health. *Front. Toxicol.* 4, 964553. doi:10.3389/ftox.2022.964553
- Sun, B., Wang, X., Liao, Y. P., Ji, Z., Chang, C. H., Pokhrel, S., et al. (2016). Repetitive dosing of fumed silica leads to profibrogenic effects through unique structure-activity relationships and biopersistence in the lung. *ACS Nano* 10, 8054–8066. doi:10.1021/acsnano.6b04143
- Svensson, A., and Schön, T. B. (2017). A flexible state-space model for learning nonlinear dynamical systems. *Automatica* 80, 189–199. doi:10.1016/j.automatica.2017.02.030
- Thomas, R. S., Bahadori, T., Buckley, T. J., Cowden, J., Deisenroth, C., Dionisio, K. L., et al. (2019). The next generation blueprint of computational toxicology at the U.S. Environmental protection agency. *Toxicol. Sci.* 169, 317–332. doi:10.1093/toxsci/kfz058
- Todd, N. W., Luzina, I. G., and Atamas, S. P. (2012). Molecular and cellular mechanisms of pulmonary fibrosis. *Fibrogenes. Tissue Repair* 5, 11. doi:10.1186/1755-1536-5-11
- Ugwoke, M. I., Agu, R. U., Jorissen, M., Augustijns, P., Sciort, R., Verbeke, N., et al. (2000). Toxicological investigations of the effects carboxymethylcellulose on ciliary beat frequency of human nasal epithelial cells in primary suspension culture and *in vivo* on rabbit nasal mucosa. *Int. J. Pharm.* 205, 43–51. doi:10.1016/s0378-5173(00)00484-1

- US EPA (1998). Health effects test guidelines: OPPTS 870.3465 90-day inhalation toxicity. Available at: <https://www.regulations.gov/document/EPA-HQ-OPPT-2009-0156-0014>. 1998.
- US Occupational Safety and Health Administration (2013). Proposed rule: occupational exposure to respirable crystalline silica. Federal Register 78, 56273–56504. Available at: <https://www.osha.gov/laws-regs/federalregister/2013-09-12>.
- van der Zalm, A. J., Barroso, J., Browne, P., Casey, W., Gordon, J., Henry, T. R., et al. (2022). A framework for establishing scientific confidence in new approach methodologies. *Archives Toxicol.* 96, 2865–2879. doi:10.1007/s00204-022-03365-4
- Vivek, S. P., Wahab, A., and Behring, H. P. (2023). Determination of oxidative stress in 3-dimensional reconstructed human tissues grown at the air-liquid interface using Promega's GSH/GSSG-Glo™ Assay kit, using single lysate preparations. *Protoc. Exch.* doi:10.21203/rs.3.pex-2288/v1
- Weber, K., Bosch, A., Bühler, M., Gopinath, C., Hardisty, J. F., Krueger, N., et al. (2018). Aerosols of synthetic amorphous silica do not induce fibrosis in lungs after inhalation: pathology working group review of histopathological specimens from a subchronic 13-week inhalation toxicity study in rats. *Toxicol. Res. Appl.* 2, 2397847318805273. doi:10.1177/2397847318805273
- Wetmore, B. A., Wambaugh, J. F., Allen, B., Ferguson, S. S., Sochaski, M. A., Setzer, R. W., et al. (2015). Incorporating high-throughput exposure predictions with dosimetry-adjusted *in vitro* bioactivity to inform chemical toxicity testing. *Toxicol. Sci.* 148, 121–136. doi:10.1093/toxsci/kfv171
- Wolkove, N., and Baltzan, M. (2009). Amiodarone pulmonary toxicity. *Canad. Res. J.* 16, 282540.
- Wynn, T. A. (2011). Integrating mechanisms of pulmonary fibrosis. *J. Exp. Med.* 208, 1339–1350. doi:10.1084/jem.20110551
- Xiong, R., Wu, Y., Wu, Q., Muskhelishvili, L., Davis, K., Tripathi, P., et al. (2021). Integration of transcriptome analysis with pathophysiological endpoints to evaluate cigarette smoke toxicity in an *in vitro* human airway tissue model. *Archives Toxicol.* 95, 1739–1761. doi:10.1007/s00204-021-03008-0
- Yong, M., Morfeld, P., and McCunney, R. (2022). Extended investigation of exposure to respirable synthetic amorphous silica dust and its potential impact on non-malignant respiratory morbidity. *Front. Public Health* 10, 801619. doi:10.3389/fpubh.2022.801619

Glossary

Acrylate copolymer	ACUDYNE™ DHR copolymer	PoD	point of departure
Akemi	AKEMI® anti-fleck super	QC	quality control
ALI	air-liquid interface	QCM	quartz crystal microbalance
AOP	adverse outcome pathway	REACH	Registration, Evaluation and Authorization of Chemicals
BAC	Benzalkonium chloride	SMC	Sequential Monte Carlo
BE PVM/MA	Butyl ester of poly (methyl vinyl ether-alt-maleic acid monoethyl ester) copolymer	SUET	simulated use evaluation testing
BER	bioactivity exposure ratio	TEER	trans-epithelial electrical resistance
C_{max}	maximum plasma concentration	TIMP-1	tissue inhibitor of metalloproteinase 1
CBF	cilia beating frequency	TNF	tumour necrosis factor
CCL	chemokine (C-C motif) ligand	TWA	time-weighted average
CDS	Concentration Dependency Scores	uPA	urokinase
CFPD	computational fluid-particle dynamics	uPAR	urokinase-type plasminogen activator receptor
Chlorocresol	4-Chloro-3-methylphenol		
CMC	Carboxymethylcellulose sodium salt		
COPD	chronic obstructive pulmonary disease		
CXCL	C-X-C motif chemokine ligand		
DART	development and reproductive toxicity		
FCS	fetal calf serum		
GSH	Reduced glutathione		
GSSH	oxidized glutathione		
HBSS	Hanks' Balanced Salt solution		
ICAM-1	intercellular adhesion molecule-1		
ICRP	International Commission on Radiological Protection		
IFN	interferon		
IL-1Ra	IL-1 receptor antagonist		
KE	key event		
LPS	lipopolysaccharide		
LV	latent variable		
MCC	mucociliary clearance		
MIE	molecular initiating event		
MMAD	mass median aerodynamic diameters		
MMP	matrix metalloproteinase		
MPPD	multiple path particle dosimetry		
Muc5AC	mucin-5AC protein		
NAMs	New Approach Methodologies		
NGRA	next-generation risk assessment		
NOAEC	no observed adverse effect concentration		
NOEC	no observed effect concentration		
PBS	phosphate-buffered saline		
PHMG	polyhexamethylene guanidine phosphate		
PLIER	Pathway-level information extractor		



OPEN ACCESS

EDITED BY

Emanuela Corsini,
University of Milan, Italy

REVIEWED BY

Lang Tran,
Institute of Occupational Medicine,
United Kingdom
Jana Tulinska,
Slovak Medical University, Slovakia

*CORRESPONDENCE

Dori R. Germolec,
✉ germolec@nih.gov
Victor J. Johnson,
✉ vjohnson@brt-labs.com

RECEIVED 04 December 2024

ACCEPTED 02 May 2025

PUBLISHED 26 May 2025

CITATION

Johnson VJ, Walker NJ, Luster MI, Burleson GR, Cora M, Baker GL, Sparrow B and Germolec DR (2025) Immunotoxicity assessment of multiwalled carbon nanotubes following whole-body inhalation exposure for 30 and 90 days in B6C3F1/N mice and 30 days in HSD:Harlan Sprague Dawley SD[®] rats. *Front. Toxicol.* 7:1539810. doi: 10.3389/ftox.2025.1539810

COPYRIGHT

© 2025 Johnson, Walker, Luster, Burleson, Cora, Baker, Sparrow and Germolec. This is an open-access article distributed under the terms of the [Creative Commons Attribution License \(CC BY\)](https://creativecommons.org/licenses/by/4.0/). The use, distribution or reproduction in other forums is permitted, provided the original author(s) and the copyright owner(s) are credited and that the original publication in this journal is cited, in accordance with accepted academic practice. No use, distribution or reproduction is permitted which does not comply with these terms.

Immunotoxicity assessment of multiwalled carbon nanotubes following whole-body inhalation exposure for 30 and 90 days in B6C3F1/N mice and 30 days in HSD:Harlan Sprague Dawley SD[®] rats

Victor J. Johnson^{1*}, Nigel J. Walker², Michael I. Luster¹, Gary R. Burleson¹, Michelle Cora², Gregory L. Baker³, Barney Sparrow⁴ and Dori R. Germolec^{2*}

¹Burleson Research Technologies, Inc., Morrisville, NC, United States, ²Division of Translational Toxicology, National Institute of Environmental Health Sciences, National Institutes of Health, Research Triangle Park, NC, United States, ³Sarepta Therapeutics, Columbus, OH, United States, ⁴Battelle Memorial Institute, Columbus, OH, United States

Background: Several lines of evidence suggest the possibility that inhalation exposure to multi-walled carbon nanotubes (MWCNT) at occupationally relevant doses can lead to systemic immunotoxicity. To test this hypothesis, we undertook in-depth examination of immune function in mice and rats exposed by inhalation to relatively low levels of 1020 Long Multiwalled Carbon Nanotubes (L-MWNT-1020).

Methods: Studies were conducted to determine the systemic and pulmonary immunotoxic effects in mice and rats exposed to L-MWNT-1020 following whole-body inhalation for 6 h/day for 5 days/week for 30 (mice and rats) and 90 (mice) days at dose levels of 0, 0.06, 0.2, and 0.6 mg/m³. Additional groups were administered cyclophosphamide (CPS) as a positive control for each cohort. Following exposure, pulmonary macrophage phagocytosis, immunophenotypic analysis of immune cells populations in the spleen, and systemic immune function, including tests for humoral (T-dependent antibody response, TDAR), cell-mediated (cytotoxic T-lymphocyte [CTL] activity), and innate (Natural Killer [NK] cell activity) immunity were conducted.

Results: While exposure increased pulmonary macrophage activity, no major changes were observed in any of the systemic immune parameters measured in mice exposed for 30 or 90 days. In rats, there was a slight decrease in humoral immunity coinciding with an increase in the number of splenic T cell and NK cell populations.

Conclusion: Although pulmonary macrophage activity increased in mice following exposure to L-MWNT-1020, systemic immune function for the most part remained unaffected. In contrast, rats demonstrated a slight decrease in humoral immune function as well as an increase in spleen cell numbers, T cell,

and NK cell populations suggesting species-specific effects on systemic immunity, however, these effects were small and their biological significance with respect to altering disease susceptibility is unclear.

KEYWORDS

multiwalled carbon nanotubes, MWCNT, immunotoxicity testing, innate immunity, humoral immunity, 1020 long multiwalled carbon nanotubes, L-MWNT-1020

Introduction

Multi-walled carbon nanotubes (MWCNTs) are concentric tubes of rolled graphene up to 100 μm long and appear as needle-like structures. When functionalized, they have widespread industrial, mechanical engineering, and biomedical applications (NIOSH, 2013). However, in their pristine form where they tend to form agglomerates, their structure, durability, and potential for widespread exposure, particularly during manufacture, raises concerns that exposure may have significant adverse health effects. A systematic review of occupational exposure studies indicated that exposure concentrations in 85% of the studies were above the current NIOSH recommended exposure limit (REL) of 1 $\mu\text{g}/\text{m}^3$ as an 8-h time-weighted average (TWA) (Guseva Canu et al., 2020). *In vitro* studies have shown that these pristine nanotubes induce cell necrosis/apoptosis and oxidative stress when ingested by macrophages (Orecchioni et al., 2014), while pulmonary exposure (i.e., inhalation or intratracheal instillation) in experimental animals has repeatedly caused substantial lung inflammation, fibrosis and granuloma formation (Lam et al., 2004; Warheit et al., 2004; Shvedova et al., 2005; NIOSH, 2013). Mitchell et al. (2007), conducted immunotoxicology studies in mice following whole body inhalation of MWCNTs for 7 or 14 days at dose levels of 0.3, 1 or 5 mg/m^3 . Although pulmonary inflammation was not observed, a monotonic immunosuppression was induced after 14 days of exposure as evidenced by a reduced T-dependent antibody responses (TDAR) and lymphocyte proliferation to Con A mitogen. Natural killer (NK) cell activity was also reduced but only in animals exposed at 1 mg/m^3 . Follow-up studies suggested that immunosuppression was possibly due to activation of the COX-2 pathway in the lung and subsequent release of prostaglandins (Mitchell et al., 2009). More recently, whole body inhalation to L-MWNT-1020 was shown to inhibit serum IgE levels, IL-13 production in the lung, and airway mucus production in a house dust mite model of allergic airways disease (Ihrie et al., 2019). Interestingly, in the absence of pulmonary allergy, inhalation of L-MWNT-1020 resulted in minimal changes in the lung with no indications of pulmonary inflammation (Migliaccio et al., 2021). The exacerbating effect of MWCNT on respiratory allergy was later demonstrated to be due to the house dust mite (HDM) allergen corona after adsorbing to MWCNT when combined in aqueous solution for oropharyngeal aspiration exposure (Bartone et al., 2024).

Taken together previous studies suggests that immunomodulation could represent a sensitive physiological indicator adversely affected by MWCNT exposure. To help confirm and extend previous findings we undertook in-depth studies in mice and rats to determine the immunotoxicity of L-MWNT-1020 following whole body inhalation exposure for short term to subchronic durations. Exposure levels selected for these studies were previously demonstrated not to produce significant acute toxicity in lungs of experimental animals

(NTP, 2019). While these exposure levels were above the NIOSH REL of 1 $\mu\text{g}/\text{m}^3$ for elemental carbon as a respirable mass 8-h TWA concentration, they overlapped with airborne concentrations in occupational setting where levels have been measured up to 417.91 $\mu\text{g}/\text{m}^3$ (Dahm et al., 2018).

Materials and methods

Test material

A representative “long” and “thin” MWCNT was selected for testing in the Division of Translational Toxicology (DTT), NIEHS Immunotoxicology studies. The 1020 Long Multiwalled Carbon Nanotube (L-MWNT-1020) from Sun Innovations (Fremont, CA) was selected based on commercial availability of large quantities, high purity (98%), and the low amount of residual metal (nickel) catalyst (0.52% by weight). Identity and purity analyses were conducted by various analytical chemistry techniques (NTP, 2019) and the L-MWNT-1020 was stored in the original shipping containers at room temperature (approximately 25°C). Reanalysis of the lot 10031301M used for these studies showed an average length and width of 2,400 nm and 16 nm, respectively, which was in accordance with the characterization by the manufacturer as 10–30 μm length and 10–20 nm diameter. The L-MWNT-1020 was composed almost entirely of carbon and was stable and chemically unreactive; therefore, the potential pulmonary toxicity and hazard of L-MWNT-1020 should be primarily a function of physical dimensions, exposure concentration, and biopersistence.

Study design, aerosol generation, and exposure system

All animal procedures were approved by the institutional animal care and use committee (IACUC) at the appropriate institution, Battelle Memorial Institute (Headquarters, Columbus, OH) for the inhalation exposure phase, and Burleson Research Technologies, Inc. for the immunotoxicity assessments. Exposures were conducted by Battelle Memorial Institute using whole body inhalation systems as previously described in detail (Ihrie et al., 2019; NTP, 2019). Briefly, the aerosol generation system consisted of a linear feed dust metering device to m L-MWNT-1020 from a reservoir into an air stream. A particle attrition chamber was positioned immediately downstream of the metering device exhaust tube to reduce the particle size of the test material. A single jet disperser assisted in further dispersion and particle size reduction and a cyclone separator removed the larger particles from the distribution

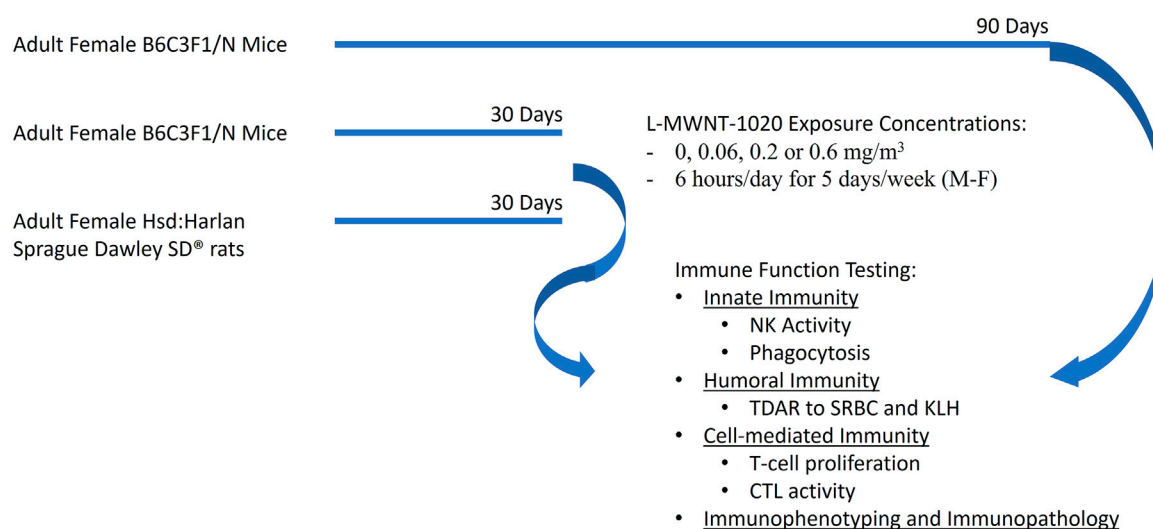


FIGURE 1
Study design for L-MWNT-1020 whole-body inhalation exposures in adult female B6C3F1/N mice and Hsd:Harlan Sprague Dawley SD® rats.

system. Generated aerosol was conveyed from an exposure control suite to the exposure room. The inhalation exposure chamber (Lab Products, Inc., Seaford, DE) was designed so uniform aerosol concentrations could be maintained throughout the chamber with a total active mixing volume for each chamber of 1.7 m³. The concentrations of L-MWNT-1020 in the exposure chambers and room air were monitored using three real-time aerosol monitors. Aerosol particle size distribution and uniformity of aerosol concentration in the inhalation exposure chambers without animals present were evaluated before the studies began (NTP, 2019). Female mice and rats were used for these studies as they tend to be more sensitive to immunotoxicity and show greater dynamic range in immune responses than males (Klein and Flanagan, 2016). Female B6C3F1/N mice (Taconic Biosciences, Hudson, NY) were exposed for 30 or 90 days to L-MWNT-1020 at concentrations of 0, 0.06, 0.2 or 0.6 mg/m³ while cohorts of female Hsd:Harlan Sprague Dawley SD® rats were exposed for 30 days at the same concentrations 6 h/day for 5 days/week, as shown in Figure 1. Following the prescribed exposure period, animals were transferred to Bureson Research Technologies, Inc. (BRT; Morrisville, NC) to provide immunizations or infections and subsequent immune function testing *ex vivo*. A positive control group was also included in which mice received 50 mg/kg bodyweight of cyclophosphamide (CPS) by intraperitoneal injection, once per day for 4–14 days (cohort dependent), prior to scheduled euthanasia and rats received 15 mg/kg bodyweight, once per day for 4–14 days (cohort dependent), prior to assessment of immune function. All animals were euthanized by CO₂ inhalation using 100% CO₂ introduced at 3.65 LPM into a 7.3 L chamber to displace 50% of the atmosphere per minute until breathing ceased and no pedal reflex was observed. Severing the diaphragm was used for confirmation of death.

Animals were single housed in individually ventilated cages and acclimated to the BRT vivarium for at least 7 days. Municipal tap water (Town of Cary, NC) and NTP-2000 pelleted diet were

provided *ad libitum*. All animals were kept in facilities with a 12-h light/dark cycle at 19.3°C–25.0°C and with a 30%–64% relative humidity. Following acclimation, animals were randomized by bodyweight ($\pm 20\%$ of mean bodyweight) to six independent cohorts (Table 1) for each study (30-day mouse, 90-day mouse, and 30-day rat studies). Each cohort for the mouse studies consisted of 8 animals/treatment group unless otherwise stated. Each cohort for the rat study consisted of 12 rats/treatment group with the exception of the CPS groups which consisted of 10 rats/group.

Hematology (cohort 1), pathology (cohort 1), and organ weights (all cohorts)

Blood was collected by the retro-orbital (RO) route in anesthetized animals into EDTA blood collection tubes for analysis (complete hematological profiles, white blood cell differentials and reticulocyte counts). Due to unsuccessful RO blood collection, several animals had blood collected via cardiac puncture. The blood was analyzed the day of collection on an Advia 120 hematology analyzer using associated V.6.3.2-MS software (Siemens Medical Solutions United States, Inc., Malvern, PA).

Following completion of blood collection, animals were euthanized with CO₂ and selected tissues for histopathology were collected. Gross observations were documented and the spleen, thymus, liver, right kidney with adrenals, and lungs were weighed. The spleen, thymus, mesenteric and popliteal lymph nodes, and liver (median, caudate, and right lobes) were preserved in 10% neutral buffered formalin (NBF). Other organs and tissues showing gross lesions were preserved in 10% NBF. Thymus, spleen, lymph nodes, bronchoalveolar lymphoid tissue (BALT), and bone marrow from the femur were examined using an enhanced histopathology method (Elmore, 2012), while the lung, liver, kidney (right), and adrenal gland (right) were evaluated using routine histopathology. Bone marrow cells from the right femur were removed and collected for total cell counts and cytospin preparations.

TABLE 1 Endpoints examined for each cohort.

Cohort	Study endpoints
1	<ul style="list-style-type: none"> • Clinical observations • Body and organ weights • Hematology • Pathology (enhanced immunopathology for immune tissues, traditional histology for non-immune tissues)
2	<ul style="list-style-type: none"> • Clinical observations • Body and organ weights • Antibody response to SRBC
3	<ul style="list-style-type: none"> • Clinical observations • Body and organ weights • Antibody response to KLH – In-life 5 days following immunization (IgM) and at terminal necropsy (IgG)
4	<ul style="list-style-type: none"> • Clinical observations • Body and organ weights • Pulmonary macrophage function • T-cell proliferation • Immunophenotyping of the spleen
5	<ul style="list-style-type: none"> • Clinical observations • Body and organ weights • CTL response to influenza infection
6	<ul style="list-style-type: none"> • Clinical observations • Body and organ weights • NK cell response to influenza infection

Pulmonary mononuclear cell phagocytosis (cohort 4)

BALF was collected, and mononuclear cells (50,000 cells) were mixed with opsonized *staphylococcus aureus* bioparticles (100 µg) labeled with pH sensitive pHrodo™ Red fluorochrome (Invitrogen; Eugene, OR) that fluoresces red within phagosomes due to the acidic pH. Cytochalasin D (15 µM; Sigma, St. Louis, MO), an *in vitro* inhibitor of phagocytosis, was added to selected samples for 45 min prior to the addition of bioparticles. Cells and bioparticles were incubated for 2 h (±5 min) and then cooled to 2°C–8°C to stop phagocytosis. Phagocytosis was quantified as the increase in cell-associated red fluorescence (peak emission at 587 nm) using an Accuri C6® flow cytometer using CFlow Plus® software v1.0.264.15. Data were expressed as the percentage of cells that engulfed bacteria and the mean fluorescent intensity of cells that engulfed bacteria (measure of number of bacteria engulfed per cell).

Humoral immunity (cohort 2 for SRBC and cohort 3 for KLH)

Humoral mediated immunity was assessed using two model T-dependent antigens, sheep red blood cells (SRBC, Colorado Serum Company, Denver, CO) and keyhole limpet hemocyanin (KLH; GMP-grade whole subunit, Stellar Biotechnologies, Inc., Los Angeles, CA). Four days following intravenous immunization with SRBC (7.5×10^7 /mouse and 1×10^8 /rat), the T-dependent antibody response (TDAR) was assessed by measuring the number of antibody forming cells (AFC) in the spleen using the hemolytic plaque assay, the number of IgM antibody producing B cells using ELISpot, and the serum titers of circulating IgM antibody to SRBC. A separate group received

intraperitoneal immunization with KLH 14 days prior to euthanasia and serum IgM and IgG antibody titers determined 5 (IgM) and 14 (IgG) days following immunization. We have described these methods in detail previously (Watson et al., 2021).

Splenic T-cell proliferation (cohort 4)

T-cell proliferation was examined in single cell suspensions from the spleen in response to *ex vivo* treatment with species specific monoclonal anti-CD3 antibodies (BD Bioscience, Franklin Lake, NJ), as previously described (Watson et al., 2021). Briefly, microtiter plates were coated overnight with anti-mouse CD3 antibody and then washed. Splenocytes in RPMI complete medium were added to the appropriate wells and incubated at 37°C and 5% CO₂ for up to 96 h. A non-radioactive assay system was used to determine T-cell proliferation (CyQuant Direct Cell Proliferation Assay®, Molecular Probes, Eugene, OR) according to the manufacturer's instructions. Fluorescence signal is directly proportional to DNA content and cell number. Data were collected using a SpectraMax M2e spectrofluorometer running Softmax Pro® (Molecular Devices, San Jose, CA) software v5.0.1.

Lung cytotoxic T lymphocyte (CTL) activity (cohort 5)

To stimulate an *in vivo* cell-mediated immune response, mice and rats from Cohort 5 were infected with influenza virus [$\sim 4 \times 10^4$ plaque forming units (pfu)/mouse or $\sim 2 \times 10^5$ pfu/rat] via intranasal instillation (Burleson et al., 2018; Watson et al., 2021) 8 days prior to scheduled termination. The *ex vivo* CTL assay was performed using lung effector cells isolated from the influenza-exposed animals

8 days following infection as previously described (Watson et al., 2021). Briefly, on the day of the assay either EL-4 (mice) or UMR-106 (rat) target cells (ATCC, Manassas, VA) were infected with influenza virus (multiplicity of 10) *in vitro* and then labeled with Chromium-51 (^{51}Cr at 100 μCi per 1×10^6 target cells for 90 min). Lung effector cells (isolated from bronchoalveolar lavage fluid from mice or lung tissue digests from rats) were separated from red blood cells and adherent cells and combined with labeled target cells in U-bottomed microtiter plates at the appropriate effector-to-target ratios (20:1, 10:1, and 5:1 for mice or 50:1, 25:1, and 12.5:1 for rat). Plates were briefly centrifuged to facilitate effector-to-target cell contact and incubated at 37°C/5%CO₂ for 6 h. Culture supernatants were harvested and release of ^{51}Cr was determined using a Cobra II Auto-Gamma counter (Packard Inc., Pamsey, MN). Specific target cell lysis is a direct measure of influenza-specific CTL killing activity.

Lung natural killer (NK) cell activity (cohort 6)

To stimulate *in vivo* recruitment and activation of NK cells in the lung, mice or rats from cohort 6 were infected with influenza virus [$\sim 4 \times 10^4$ plaque forming units (pfu)/mouse or $\sim 2 \times 10^5$ pfu/rat] via intranasal instillation (Watson et al., 2021) 2 days prior to scheduled termination for rats and 3–4 days prior to scheduled termination for mice. Pulmonary NK cell killing activity was evaluated using YAC-1 tumor target cells as previously described (Watson et al., 2021). Briefly, lung effector cells (100 μL) were added to wells of round-bottom microtiter plates containing 100 μL of YAC-1 target cells (1×10^5 cells/mL labeled with ^{51}Cr at 100 μCi per 1×10^6 target cells for 90 min) at effector to target ratios of 20:1, 10:1, and 5:1 for mice or 50:1, 25:1, and 12.5:1 for rats. The plates were centrifuged and then incubated at 37°C/5%CO₂ for 4 h. Culture supernatants were harvested and release of ^{51}Cr was determined using a Cobra II Auto-Gamma counter (Packard).

Immunophenotyping of the spleen (cohort 4)

Splenic immune cell populations were determined using flow cytometry and are presented as absolute cell numbers and relative percentages of CD45⁺ lymphocytes or total myeloid cells, as appropriate. Red blood cells (RBC) present in single cell suspensions from the spleen were removed by lysis prior to Fc receptor blocking and antibody staining. Detailed procedures including antibodies, staining, and gating strategies were previously published (Watson et al., 2021). Antibody cocktails for discrimination of immune cell populations were the following.

- Rat: (1) CD45, CD3, CD45RA, and CD161a; (2) CD45, CD3, CD4, CD8a; and (3) CD11b/c, CD103, RP-1, and CD161a.
- Mouse: (1) CD45, CD3, CD45R, and CD161a; (2) CD45, CD3, CD4, CD8a; and (3) CD11b, CD11c, Ly6G, and CD335 (NKP46).

Details of the antibodies used for these studies are provided in the CEBS Supplemental Antibody Table (10.22427/NTP-DATA-500-005-001-000-1). Cell populations examined in the spleen

included total lymphocytes, total T cells, CD4⁺ T cells, CD8⁺ T cells, B cells, NK cells, monocytes/macrophages, eosinophils, and neutrophils. In addition, T:B cell and CD4⁺:CD8⁺ T cell ratios were determined. Following staining, samples were stored at 2–8°C, protected from light, until analyzed on an Accuri C6 flow cytometer using CFlow Plus v 1.0.264.15 (BD Biosciences). In all cases, a minimum of 20,000 events/sample was acquired.

Lymphocyte gating was performed on CD45⁺ populations. The following lymphocyte subsets were identified; T-cells (CD3⁺CD45RA⁺), B-cells (CD3⁺CD45RA⁺), NK cells (CD3⁺CD161a⁺), T-helper cells (CD3⁺CD4⁺), and T-cytotoxic cells (CD3⁺CD8⁺). Myeloid cells were gated based on being positive for CD11b with low-to-mid intensity staining for CD11c (mouse) or CD103 (rats). Myeloid populations were differentiated from NK cells based on lack of CD335(NKP46) expression, (mouse) or lack of CD161a (rats). Further differentiation was based on expression of Ly6G (mouse) or RP-1 (rat) with positive cells being neutrophils and negative cells differentiated using SSC into monocytes/macrophages with low granularity and eosinophils with high granularity.

Data collection, data analysis, and statistical analysis

Data were collected into Provantis v9.3.2.1 (Instem, Philadelphia, PA) and calculation of endpoints was performed within this validated electronic data collection and management system. Results are presented as mean \pm SEM. Extreme values were identified by the outlier test of Dixon and Massey when sample size was <20 (Dixon and Massey, 1957) and by Tukey's outer fences method (Tukey, 1977) when sample size was ≥ 20 . All flagged outliers were examined by DTT, NIEHS personnel, and implausible values were eliminated from the final analyses. Jonckheere's test was used to test for dose-related trends (Jonckheere, 1954). The positive control group was excluded from the trend tests. Bodyweight and organ weight data, which exhibit a normal distribution, were analyzed using Jonckheere's trend test (Jonckheere, 1954) and Williams' or Dunnett's (pairwise) test depending on detection of a trend at a 0.01 significance level (Dunnett, 1955; Williams, 1971; Williams, 1972; Williams, 1986). Data for other endpoints were analyzed using a non-parametric multiple comparison procedure. Shirley's test was used if a significant trend was observed (Shirley, 1977) and Dunn's test was used if the trend was not significant (Dunn, 1964). Positive control group data were compared to the vehicle control group using the t-test for bodyweight and organ weight and Wilcoxon rank-sum test for all other endpoints. Data that were different from control at $p \leq 0.05$ were considered statistically significant.

Results

Summary findings pertinent for evaluating immunotoxicity of L-MWNT-1020 are presented below. All study findings including results that are discussed in this section but not presented in the manuscript can be found in the NTP Chemical Effects in Biological Systems (CEBS) database. (10.22427/NTP-DATA-500-005-001-000-1).

TABLE 2 Absolute counts of immune cell populations in the spleen of rodents following inhalation of L-MWNT-1020.

	L-MWNT-1020 (mg/m ³)				15 mg/kg CPS
	0	0.06	0.2	0.6	
30-day rat exposure study					
Total Leukocytes (x10 ³ /μL)	10.104 ± 0.691 [12]	10.619 ± 0.708 [11]	9.170 ± 0.677 [11]	11.353 ± 0.516 [12]	3.050 ± 0.164 [10]**
Absolute Counts					
Lymphocytes (x10 ³ /μL)	8.921 ± 0.615 [12]	9.181 ± 0.616 [11]	7.815 ± 0.543 [11]	9.633 ± 0.454 [12]	2.319 ± 0.100 [10]**
Neutrophils (x10 ³ /μL)	0.664 ± 0.061 [12] ^{††}	0.837 ± 0.104 [11]	0.758 ± 0.080 [11]**	1.054 ± 0.092 [12]**	0.479 ± 0.043 [10]*
Monocytes (x10 ³ /μL)	0.302 ± 0.027 [12]	0.358 ± 0.038 [11]	0.243 ± 0.033 [11]	0.317 ± 0.021 [12]	0.085 ± 0.008 [10]**
Eosinophils (x10 ³ /μL)	0.075 ± 0.004 [12] ^{††}	0.100 ± 0.021 [11]	0.175 ± 0.057 [11]*	0.173 ± 0.033 [12]**	0.100 ± 0.031 [10]
Basophils (x10 ³ /μL)	0.044 ± 0.006 [12]	0.041 ± 0.007 [11]	0.038 ± 0.006 [11]	0.049 ± 0.006 [12]	0.011 ± 0.002 [10]**
LUC (x10 ³ /μL)	0.098 ± 0.012 [12]	0.101 ± 0.009 [11]	0.144 ± 0.042 [11]	0.126 ± 0.017 [12]	0.056 ± 0.013 [10]*
Relative Counts					
Percent Lymphocytes (%)	88.23 ± 0.48 [12] ^{‡‡}	86.40 ± 0.89 [11]	85.61 ± 0.88 [11]*	84.82 ± 0.84 [12]**	76.45 ± 1.44 [10]**
Percent Neutrophils (%)	6.54 ± 0.30 [12] ^{††}	7.92 ± 0.72 [11]	8.17 ± 0.60 [11]*	9.27 ± 0.66 [12]**	15.63 ± 0.99 [10]**
Percent Monocytes (%)	3.09 ± 0.32 [12]	3.38 ± 0.29 [11]	2.58 ± 0.25 [11]	2.85 ± 0.21 [12]	2.77 ± 0.26 [10]
Percent Eosinophils (%)	0.78 ± 0.05 [12] ^{††}	0.99 ± 0.25 [11]	1.72 ± 0.46 [11]**	1.56 ± 0.29 [12]**	3.02 ± 0.76 [10]**
Percent Basophils (%)	0.41 ± 0.04 [12]	0.37 ± 0.05 [11]	0.39 ± 0.04 [11]	0.42 ± 0.04 [12]	0.36 ± 0.06 [10]
Percent LUC (%)	0.92 ± 0.06 [12]	0.95 ± 0.05 [11]	1.51 ± 0.43 [11]	1.08 ± 0.12 [12]	1.77 ± 0.37 [10]
30-day mouse exposure study					
Total Leukocytes (x10 ³ /μL)	11.088 ± 0.744 [6]	8.949 ± 0.806 [8]	9.933 ± 0.468 [7]	10.009 ± 0.559 [7]	2.636 ± 0.458 [7]**
Absolute Counts					
Lymphocytes (x10 ³ /μL)	9.377 ± 0.677 [6]	7.651 ± 0.716 [8]	8.403 ± 0.457 [7]	8.564 ± 0.522 [7]	2.299 ± 0.412 [7]**
Neutrophils (x10 ³ /μL)	1.143 ± 0.049 [6]	0.854 ± 0.057 [8]*	1.027 ± 0.079 [7]	0.903 ± 0.059 [7]	0.220 ± 0.035 [7]**
Monocytes (x10 ³ /μL)	0.162 ± 0.013 [6]	0.113 ± 0.005 [8]*	0.150 ± 0.010 [7]	0.161 ± 0.017 [7]	0.019 ± 0.005 [7]**
Eosinophils (x10 ³ /μL)	0.228 ± 0.051 [6]	0.121 ± 0.014 [8]	0.174 ± 0.025 [7]	0.193 ± 0.029 [7]	0.046 ± 0.015 [7]**
Basophils (x10 ³ /μL)	0.040 ± 0.010 [6]	0.045 ± 0.011 [8]	0.043 ± 0.006 [7]	0.037 ± 0.006 [7]	0.004 ± 0.002 [7]**
LUC (x10 ³ /μL)	0.140 ± 0.039 [6]	0.161 ± 0.045 [8]	0.141 ± 0.023 [7]	0.146 ± 0.027 [7]	0.049 ± 0.009 [7]**
Relative Counts					
Percent Lymphocytes (%)	84.42 ± 0.72 [6]	85.26 ± 0.65 [8]	84.43 ± 0.90 [7]	85.43 ± 0.75 [7]	86.86 ± 1.46 [7]
Percent Neutrophils (%)	10.43 ± 0.49 [6]	9.88 ± 0.75 [8]	10.56 ± 1.16 [7]	9.10 ± 0.54 [7]	8.67 ± 0.74 [7]
Percent Monocytes (%)	1.50 ± 0.18 [6]	1.31 ± 0.09 [8]	1.51 ± 0.07 [7]	1.60 ± 0.13 [7]	0.70 ± 0.14 [7]*
Percent Eosinophils (%)	2.10 ± 0.51 [6]	1.36 ± 0.07 [8]	1.71 ± 0.22	2.00 ± 0.33 [7]	1.73 ± 0.52 [7]
Percent Basophils (%)	0.37 ± 0.06 [6]	0.49 ± 0.10 [8]	0.40 ± 0.06	0.39 ± 0.06 [7]	0.19 ± 0.05 [7]
Percent LUC (%)	1.18 ± 0.23 [6]	1.70 ± 0.35 [8]	1.40 ± 0.20	1.49 ± 0.30 [7]	1.89 ± 0.44 [7]
90-day mouse exposure study					
Total Leukocytes (x10 ³ /μL)	9.186 ± 0.484 [8] [‡]	9.223 ± 0.356 [6]	8.253 ± 0.450 [8]	7.523 ± 0.852 [8]	2.870 ± 0.572 [7]**
Absolute Counts					
Lymphocytes (x10 ³ /μL)	7.378 ± 0.388 [8] [‡]	7.627 ± 0.254 [6]	6.694 ± 0.359 [8]	5.954 ± 0.713 [8]	2.775 ± 0.600 [6]**
Neutrophils (x10 ³ /μL)	0.969 ± 0.068 [8]	0.833 ± 0.109 [6]	0.899 ± 0.095 [8]	1.168 ± 0.176 [8]	0.202 ± 0.075 [6]**
Monocytes (x10 ³ /μL)	0.084 ± 0.007 [8]	0.075 ± 0.017 [6]	0.090 ± 0.018 [8]	0.066 ± 0.027 [8]	0.000 ± 0.000 [7]**
Eosinophils (x10 ³ /μL)	0.574 ± 0.055 [8]	0.503 ± 0.128 [6]	0.439 ± 0.106 [8]	0.276 ± 0.128 [8]	0.000 ± 0.000 [7]**
Basophils (x10 ³ /μL)	0.061 ± 0.010 [8] [‡]	0.062 ± 0.015 [6]	0.061 ± 0.018 [8]	0.023 ± 0.009 [8]	0.000 ± 0.000 [7]**
LUC (x10 ³ /μL)	0.120 ± 0.033 [8] ^{‡‡}	0.127 ± 0.036 [6]	0.068 ± 0.017 [8]	0.036 ± 0.014 [8]*	0.000 ± 0.000 [7]**
Relative Counts					
Percent Lymphocytes (%)	80.41 ± 1.08 [8]	82.95 ± 2.70 [6]	81.45 ± 2.44 [8]	78.83 ± 2.38 [8]	93.67 ± 1.09 [6]**
Percent Neutrophils (%)	10.51 ± 0.54 [8] ^{††}	8.97 ± 1.10 [6]	10.79 ± 0.91 [8]	16.01 ± 1.84 [8]*	6.33 ± 1.09 [6]*
Percent Monocytes (%)	0.93 ± 0.08 [8]	0.78 ± 0.17 [6]	1.06 ± 0.21 [8]	0.80 ± 0.30 [8]	0.00 ± 0.00 [7]**

(Continued on following page)

TABLE 2 (Continued) Absolute counts of immune cell populations in the spleen of rodents following inhalation of L-MWNT-1020.

	L-MWNT-1020 (mg/m ³)				15 mg/kg CPS
	0	0.06	0.2	0.6	
Percent Eosinophils (%)	6.19 ± 0.41 [8]	5.33 ± 1.33 [6]	5.16 ± 1.30 [8]	3.51 ± 1.59 [8]	0.00 ± 0.00 [7]**
Percent Basophils (%)	0.66 ± 0.08 [8]	0.65 ± 0.15 [6]	0.71 ± 0.21 [8]	0.29 ± 0.11 [8]	0.00 ± 0.00 [7]**
Percent LUC (%)	1.34 ± 0.37 [8]	1.35 ± 0.35 [6]	0.79 ± 0.19 [8]	0.51 ± 0.21 [8]	0.00 ± 0.00 [7]**

Data are presented as Mean ± SEM [n]. SEM, Standard error; CPS, cyclophosphamide; LUC, Large Unstained Cells. Significant increasing ([†]p < 0.05 or ^{††}p < 0.01) or decreasing ([‡]p < 0.05 or ^{‡‡}p < 0.01) trend with increasing dose of L-MWNT-1020. Significantly different from vehicle control at *p < 0.05 of **p < 0.01.

Clinical observations, pathology, bodyweights, and organ weights (all cohorts)

In all three experimental studies occasional minor clinical abnormalities were observed, such as alopecia in mice, but were not considered related to exposure as similar incidences were observed between control and treated groups (CEBS Summary Table I05). The exposures to L-MWNT-1020 were performed by the inhalation contractor followed by shipment of the animals to BRT for assessment of immune function. L-MWNT-1020 inhalation had minimal effects on in-life bodyweights in mice and rats (CEBS Summary Tables I04 and I04G). Exposures were not continued at BRT and there were no effects on terminal bodyweights in any of the cohorts. At necropsy, the thymus, spleen, liver, right kidney with adrenals, and lungs were removed, examined, and weighed. There were no significant gross pathology (CEBS Summary Table PA46) or organ weight changes (CEBS Summary Table PA06) in any of the organs collected when compared to the vehicle control group. Histological examination revealed low numbers of pulmonary macrophages that contained black pigment, consisting of agglomerated L-MWCT-1020, in the majority of rats treated for 30 days with ≥0.2 mg/m³ and in all mice from the 0.6 mg/m³ treatment group following 90 days of exposure, but not in mice treated for 30 days. There were no other histopathological changes that could be attributed to inhalation of L-MWNT-1020 in any lymphoid or non-lymphoid tissue examined in either mice or rats (CEBS Summary Table PA02, PA03, PA08, and PA10).

Hematology (cohort 1)

L-MWNT-1020 inhalation resulted in small, but statistically significant changes in hematological values and white blood cell (WBC) differentials. There was a significant decreasing trend with increasing exposure concentration in platelet counts in mice treated for 90 days and a significant decrease in mice treated with 0.6 mg/m³ L-MWNT-1020 compared to the vehicle control group. A similar negative trend in platelets was observed in rats treated for 30 days, however, no treatment groups were different from the vehicle group (CEBS Summary Table M04). Examination of WBC differentials (Table 2, CEBS Summary Table M03) indicated that there were significant increasing trends in absolute and relative neutrophils and eosinophils in rats exposed to L-MWNT-1020 for 30 days. There was also a decreasing trend in the relative lymphocyte counts in exposed rats. These trends were accompanied by significantly increased absolute neutrophil counts (0.6 mg/m³), relative

neutrophil counts (≥0.2 mg/m³), and absolute and relative eosinophil counts (≥0.2 mg/m³), as well as significantly decreased relative lymphocyte counts (≥0.2 mg/m³) in rats exposed to L-MWNT-1020 for 30 days. Mice exposed to L-MWNT-1020 for 30 days appeared less sensitive and only had significantly decreased numbers of monocytes and neutrophils in the 0.06 mg/m³ treatment group. Extending the exposure period in mice to 90 days resulted in a significantly increasing trend in relative neutrophil counts which was significantly increased in the 0.6 mg/m³ group relative to the vehicle group which is consistent with the findings in rats. Mice exposed to L-MWNT-1020 for 90 days also showed significantly decreasing trends in absolute lymphocytes, basophils, and large unstained cells but only large unstained cells in mice exposed to 0.6 mg/m³ were significantly decreased relative to the vehicle control group (CEBS Summary Table M03). No other changes were observed in hematology parameters in mice or rats treated with L-MWNT-1020. The positive control, CPS, produced a hemogram consistent with severe leukocytopenia as expected.

Phagocytosis (cohort 4)

The impact of L-MWNT-1020 exposure on the number and ability of bronchoalveolar lavage fluid (BALF) mononuclear cells to phagocytize opsonized *Staphylococcus aureus* bioparticles was determined (Figure 2; CEBS Summary Table M14). In mice exposed for 30 days, there was a significant increase in the number of pulmonary mononuclear cells present in the BALF in the 0.6 mg/m³ exposure group (Figure 2A) and in the percentage of mononuclear phagocytic cells actively engulfing opsonized *staphylococcus aureus* bioparticles in both the 0.2 and 0.6 mg/m³ exposure groups (Figure 2B). The relative number of opsonized *Staphylococcus aureus* bioparticles phagocytized per cell, as measured by mean fluorescent intensity (MFI), was not affected by exposure in mice (Figure 2C). Neither pulmonary mononuclear cell number nor phagocytosis were affected in rats exposed by inhalation for 30 days to L-MWNT-1020 (Figures 2D–F). There was insufficient uptake of the fluorescent bioparticles by the pulmonary phagocytic cells for all animals and assessment of phagocytic function was not possible in the 90-Day mouse study (data are not presented).

Humoral immune response to T-lymphocyte dependent antigens (cohort 2 for SRBC and cohort 3 for KLH)

L-MWNT-1020 exposure in rats significantly decreased the anti-SRBC AFC response (CEBS Summary Table M07) at the

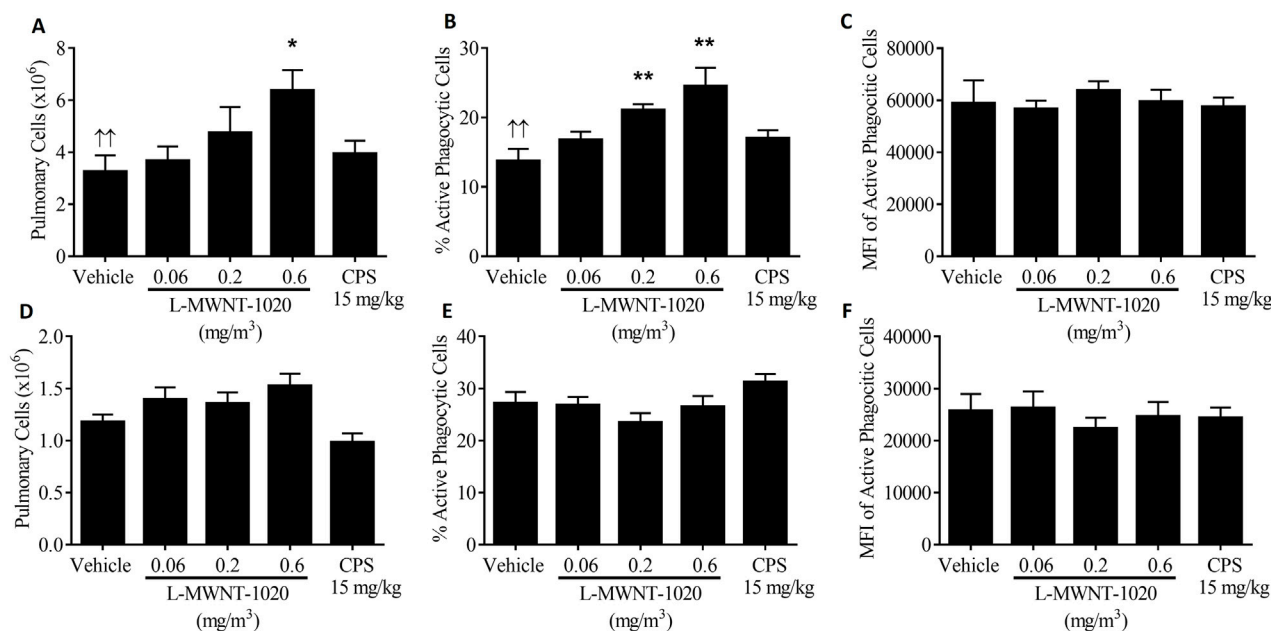


FIGURE 2 Pulmonary cell number, percent phagocytosis and mean fluorescent intensity (MFI) of phagocitized cells in mice exposed for 30 days (A–C), respectively or rats exposed for 30 days (D–F), respectively to 0, 0.06, 0.2 or 0.6 mg/m³ of L-MWNT-1020. CPS–cyclophosphamide was administered as a positive control to mice at 50 mg/kg and to rats at 15 mg/kg. SEM–standard error of the mean. Significantly different from the vehicle control group at *p < 0.05 or **p < 0.01. ††Significant increasing dose-response trend with increasing dose of L-MWNT-1020 (p < 0.01).

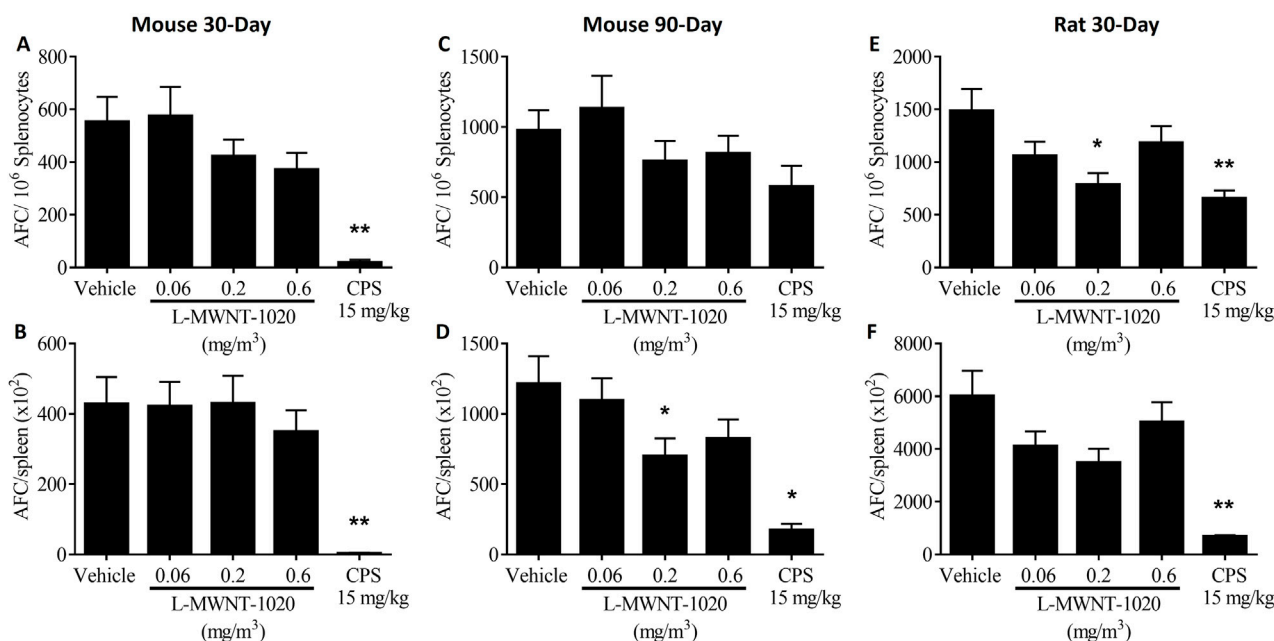


FIGURE 3 Antibody forming cell response to SRBC in rodents following inhalation of L-MWNT-1020 for 30 days in mice (A,B), 90 days in mice (C,D) and 30 days in rats (E,F). The AFC response is presented normalized per million splenocytes and as total numbers per spleen. AFC–Antibody forming cell, CPS–cyclophosphamide. Data are presented as Mean ± Standard Error (SEM). Group sizes for mice were 8 per treatment, except for vehicle group from the mouse 30 days study which was 7. Group sizes for rats were 12 per L-MWNT-1020 group and 10 per CPS group. Significantly different from the vehicle control at *p < 0.05 or **p < 0.01.

0.2 mg/m³ dose level when expressed as AFC/10⁶ spleen cells (Figure 3E). A decrease was also observed when expressed as AFC/spleen but did not reach statistical significance (Figure 3F). While the responses were also decreased at the 0.06 and 0.6 mg/m³ dose levels in rats, statistical significance was not achieved. Similar decreases were observed in the AFC responses in mice, but these changes did not reach statistical significance (Figures 3A–D). None of these groups showed significant dose response trends. Serum levels of anti-SRBC IgM antibodies (CEBS Summary Table M08) and anti-SRBC IgM producing B-cells (CEBS Summary Table M19) were negligibly impacted by inhalation of L-MWNT-1020 in mice and rats. In addition, antibody responses to KLH were not affected by L-MWNT-1020 inhalation in rats or mice (CEBS Summary Table M09). Humoral immune responses to SRBC and KLH were markedly decreased in all CPS treated animals as expected.

Cell mediated immunity (cohort 4 for T-cell proliferation and cohort 5 for CTL response)

Cell mediated immune function was assessed by quantitating splenic T cell proliferation in response to stimulation with anti-CD3 monoclonal antibodies and by determining the ability of pulmonary T cells from influenza-infected animals to lyse influenza-infected target cells in a cytotoxic T lymphocyte (CTL) assay. There was a statistically significant increase in anti-CD3 antibody stimulated T cell proliferation at the lowest (0.06 mg/m³) dose of L-MWNT-1020 in mice exposed for 30 days but no effect was observed after 90 days in mice. A significant decrease in proliferation occurred in rats exposed to L-MWNT-1020 for 30 days, but only in the 0.2 mg/m³ treatment group (CEBS Summary Table M11). These changes in T-cell proliferation were minor and not dose-related. CTL activity was unaffected following exposure to L-MWNT-1020 in either mice or rats (CEBS Summary Table M12). CPS treatment markedly decreased the CTL response as expected.

Natural Killer (NK) cell activity (cohort 6)

Natural killer (NK) cell activity was evaluated by examining the ability of pulmonary effector cells isolated 2 days following influenza infection to lyse YAC-1 tumor target cells. There was a significant decreasing trend in NK killing activity in mice exposed to L-MWNT-1020 for 90 days but only at the 5:1 E:T ratio. This trend was not observed in mice or rats exposed for 30 days. There were no other exposure-related effects on NK activity following inhalation of L-MWNT-1020 in either rats or mice (CEBS Summary Table M15).

Immunophenotypes in the spleen (cohort 4)

The absolute number and relative percentages of immune cell populations in the spleen are presented in Tables 3, 4, respectively. Mice exposed to L-MWNT-1020 for 90 days showed a significant decreasing trend in relative percentage and absolute number of neutrophils with both measures being significantly decreased in the 0.6 mg/m³ treatment group. Changes in other cell populations in the

spleen were mostly negligible in mice treated for 30 or 90 days. In rats exposed to 0.06 and 0.2 mg/m³ L-MWNT-1020 for 30 days there was a significant increase in the absolute number of spleen cells that corresponded with a significant increase in total lymphocytes in the same groups. The impact of L-MWNT-1020 on immune cell population numbers was on the T cell compartment as evidenced by significant increases in total T cells, CD4⁺ T cells, CD8⁺ T cells, and the total T cell:B cell ratios in rats treated with 0.06 and 0.2 mg/m³. In addition, there was a positive trend in NK cell numbers with all exposure levels being significantly elevated. CPS treatment was consistent with historical controls resulting in a marked reduction in the number of almost all cell phenotypes with B cells being the most affected and NK cells and monocytic cells the least.

Discussion

In depth immunotoxicity studies were conducted in mice exposed for 30 and 90 days and in rats for 30 days to whole body inhalation of L-MWNT-1020 at concentrations of 0.06, 0.2, and 0.6 mg/m³ 6 h/day for 5 days/week. The low and mid exposure levels used in the present studies were within the range of concentrations (<0.001–417.91 µg/m³) previously observed in US facilities manufacturing carbon nanotubes and nanofibers (Dahm et al., 2018). Critical effect levels have already been estimated for noncancerous lung effects from animal dose response data (e.g., BMD, benchmark dose and BMDL, the 95% lower confidence limit estimates of the BMD) and extrapolated to humans for MWCNTs by accounting for the factors influencing the lung dose in experimental animals. Based on BMD modeling of subchronic animal inhalation studies (Ma-Hock et al., 2009; Pauluhn, 2010), a working lifetime exposure of 0.2–2 µg/m³ (8-h TWA concentration) was estimated to be associated with a 10% excess risk of early-stage adverse lung effects (95% lower confidence limit estimates). In view of these health risks, and ongoing improvements in sampling and analytical methodologies, NIOSH has recommended a REL of 1 µg/m³ as an 8-h TWA respirable mass concentration using NIOSH Method 5040 (<https://www.cdc.gov/niosh/docs/2013-145/pdfs/2013-145.pdf>). The NIOSH REL is based on minimizing the risk of pulmonary inflammation, including neutrophil influx, and pulmonary fibrosis that were observed in animal studies following short-term and subchronic exposure to carbon nanotubes and nanofibers (Bergamaschi et al., 2021). Although there was systemic neutrophilia in the blood of rats exposed for 30 days to L-MWNT-1020, there was no histopathological evidence of inflammation and neutrophil influx into the lungs of rats or mice in these studies.

Experimental animal studies have established that the lung is the primary target following inhalation of single walled carbon nanotubes (SWCNTs) characterized by persistent pulmonary fibrosis, granulomas and other tissue injury (Lam et al., 2004; Shvedova et al., 2005). These studies were normally conducted at higher concentrations (e.g., 1–5 mg/kg bodyweight) than employed in the present studies and the materials were often administered as a bolus, i.e., instilled or aspirated. It is known that there can be significant differences in toxicity due to exposure method (e.g., inhalation vs aspiration or instillation) as well as between different lots of carbon nanotubes due to the length, presence of

TABLE 3 Absolute counts of immune cell populations in the spleen of rodents following inhalation of L-MWNT-1020.

	L-MWNT-1020 (mg/m ³)				15 mg/kg CPS
	0	0.06	0.2	0.6	
30-day rat exposure study					
Spleen Cells (x10 ⁶)	345.95 ± 16.00 (12)	456.95 ± 28.47 (12) **	434.15 ± 21.57 (12) *	409.80 ± 19.40 (12)	165.18 ± 19.49 (10) **
Total Lymphocytes	340.954 ± 15.738 (12)	451.685 ± 28.159 (12) **	429.145 ± 21.429 (12) *	404.909 ± 19.201 (12)	162.807 ± 19.745 (10) **
Total T Cells	102.024 ± 4.983 (12)	154.826 ± 11.171 (12) **	143.832 ± 8.819 (12) **	126.047 ± 7.065 (12)	80.965 ± 9.626 (10)
CD4 ⁺ T Cells	57.520 ± 4.024 (12)	88.327 ± 8.269 (12) **	83.264 ± 5.535 (12) **	68.792 ± 4.107 (12)	42.012 ± 6.242 (10)
CD8 ⁺ T Cells	39.540 ± 2.564 (12)	60.507 ± 4.075 (12) **	54.213 ± 4.162 (12) *	51.805 ± 3.128 (12)	36.691 ± 3.383 (10)
B Cells	172.003 ± 9.675 (12)	213.994 ± 14.403 (12)	201.592 ± 11.929 (12)	194.959 ± 10.078 (12)	46.339 ± 6.996 (10) **
NK Cells	8.754 ± 0.606 (12) ^{††}	11.014 ± 0.762 (12) *	10.873 ± 0.371 (12) *	12.391 ± 1.061 (12) **	7.973 ± 1.259 (10)
Mono/Mac Cells	6.560 ± 0.651 (12)	6.962 ± 0.613 (12)	6.738 ± 0.269 (12)	6.655 ± 0.568 (12)	2.137 ± 0.370 (10) **
Neutrophils	5.749 ± 0.379 (12)	5.820 ± 0.325 (12)	6.982 ± 0.467 (12)	5.855 ± 0.362 (12)	4.072 ± 0.485 (10) *
Eosinophils	0.521 ± 0.046 (12)	0.488 ± 0.055 (12)	0.558 ± 0.093 (12)	0.416 ± 0.065 (12)	0.252 ± 0.032 (10) **
Total T Cells: B Cells Ratio	0.604 ± 0.028 (12)	0.727 ± 0.025 (12) **	0.716 ± 0.025 (12) *	0.650 ± 0.027 (12)	1.853 ± 0.106 (10) **
CD4 ⁺ T Cells: CD8 ⁺ T Cells Ratio	1.513 ± 0.143 (12)	1.485 ± 0.138 (12)	1.583 ± 0.102 (12)	1.339 ± 0.059 (12)	1.117 ± 0.095 (10) *
30-day mouse exposure study					
Spleen Cells (x10 ⁶)	78.48 ± 8.07 (8)	70.90 ± 3.65 (8)	75.20 ± 4.70 (7)	74.38 ± 3.08 (8)	19.88 ± 1.59 (8) **
Total Lymphocytes	70.403 ± 7.494 (8)	65.746 ± 3.957 (8)	70.824 ± 5.143 (7)	67.541 ± 2.900 (8)	19.357 ± 1.527 (8) **
Total T Cells	21.088 ± 2.375 (8)	20.014 ± 1.474 (8)	20.643 ± 2.052 (7)	19.558 ± 0.760 (8)	9.534 ± 0.727 (8) **
CD4 ⁺ T Cells	11.935 ± 1.393 (8)	11.518 ± 0.916 (8)	12.019 ± 1.216 (7)	11.036 ± 0.488 (8)	5.288 ± 0.403 (8) **
CD8 ⁺ T Cells	7.574 ± 0.828 (8)	7.093 ± 0.495 (8)	7.058 ± 0.760 (7)	6.999 ± 0.241 (8)	3.690 ± 0.289 (8) **
B Cells	42.438 ± 4.404 (8)	39.452 ± 2.152 (8)	43.374 ± 2.811 (7)	41.201 ± 1.966 (8)	8.284 ± 0.716 (8) **
NK Cells	3.403 ± 0.447 (8)	2.873 ± 0.193 (8)	3.550 ± 0.233 (7)	3.321 ± 0.155 (8)	0.746 ± 0.083 (8) **
Mono/Mac Cells	1.502 ± 0.175 (8)	1.339 ± 0.088 (8)	1.395 ± 0.087 (7)	1.457 ± 0.091 (8)	0.263 ± 0.023 (8) **
Neutrophils	0.067 ± 0.007 (8)	0.064 ± 0.007 (8)	0.075 ± 0.010 (7)	0.081 ± 0.009 (8)	0.008 ± 0.001 (7) **
Eosinophils	0.069 ± 0.009 (8)	0.051 ± 0.004 (8)	0.050 ± 0.005 (7)	0.066 ± 0.004 (8)	0.015 ± 0.001 (8) **
Total T Cells: B Cells Ratio	0.496 ± 0.012 (8)	0.505 ± 0.017 (8)	0.473 ± 0.031 (7)	0.477 ± 0.011 (8)	1.167 ± 0.056 (8) **
CD4 ⁺ T Cells: CD8 ⁺ T Cells Ratio	1.569 ± 0.027 (8)	1.619 ± 0.032 (8)	1.716 ± 0.044 (7) *	1.574 ± 0.023 (8)	1.434 ± 0.019 (8) **
90-day mouse exposure study					
Spleen Cells (x10 ⁶)	61.25 ± 4.60 (8)	58.73 ± 3.51 (8)	67.70 ± 5.47 (8)	54.63 ± 6.02 (8)	13.39 ± 0.84 (8) **
Total Lymphocytes	59.106 ± 4.258 (8)	56.090 ± 3.460 (8)	65.677 ± 5.273 (8)	53.319 ± 5.932 (8)	13.170 ± 0.802 (8) **
Total T Cells	17.811 ± 1.654 (8)	16.875 ± 1.057 (8)	20.122 ± 1.447 (8)	16.921 ± 1.722 (8)	7.336 ± 0.426 (8) **
CD4 ⁺ T Cells	10.101 ± 0.971 (8)	9.778 ± 0.713 (8)	11.745 ± 0.887 (8)	9.853 ± 1.103 (8)	4.222 ± 0.238 (8) **
CD8 ⁺ T Cells	6.332 ± 0.576 (8)	5.797 ± 0.295 (8)	6.820 ± 0.486 (8)	5.754 ± 0.544 (8)	2.717 ± 0.169 (8) **
B Cells	37.166 ± 2.338 (8)	35.475 ± 2.427 (8)	41.381 ± 3.778 (8)	32.914 ± 3.945 (8)	4.970 ± 0.473 (8) **
NK Cells	0.721 ± 0.052 (8)	0.696 ± 0.056 (8)	0.780 ± 0.085 (8)	0.562 ± 0.048 (8)	0.133 ± 0.011 (8) **
Mono/Mac Cells	1.450 ± 0.118 (8)	1.444 ± 0.092 (8)	1.538 ± 0.157 (8)	1.199 ± 0.135 (8)	0.209 ± 0.017 (8) **
Neutrophils	0.115 ± 0.013 (8) ^{††}	0.114 ± 0.008 (8)	0.115 ± 0.016 (8)	0.061 ± 0.007 (8) **	0.013 ± 0.002 (8) **
Eosinophils	0.098 ± 0.010 (8)	0.100 ± 0.008 (8)	0.099 ± 0.014 (8)	0.105 ± 0.012 (8)	0.032 ± 0.003 (8) **

(Continued on following page)

TABLE 3 (Continued) Absolute counts of immune cell populations in the spleen of rodents following inhalation of L-MWNT-1020.

	L-MWNT-1020 (mg/m ³)				15 mg/kg CPS
	0	0.06	0.2	0.6	
Total T Cells: B Cells Ratio	0.475 ± 0.025 (8) [†]	0.480 ± 0.023 (8)	0.494 ± 0.022 (8)	0.522 ± 0.012 (8)	1.545 ± 0.141 (8) **
CD4 ⁺ T Cells: CD8 ⁺ T Cells Ratio	1.593 ± 0.041 (8)	1.678 ± 0.054 (8)	1.719 ± 0.020 (8)	1.703 ± 0.053 (8)	1.561 ± 0.036 (8)

Data are presented as Mean ± SEM (n). SEM, Standard error; CPS, cyclophosphamide; NK, Natural Killer; Mono/Mac–Monocyte/Macrophage. Significant increasing ([†]p < 0.05 or ^{††}p < 0.01) or decreasing ([‡]p < 0.05 or ^{‡‡}p < 0.01) trend with increasing dose of L-MWNT-1020. Significantly different from vehicle control at *p < 0.05 of **p < 0.01.

contaminants such as metal oxides, and the degree of agglomeration (Pauluhn, 2010; Vitkina et al., 2016; Fujita et al., 2020). Ninety-day studies in rats showed a moderate level of pathology at dose levels higher than 0.4–0.5 mg/m³ in the upper respiratory tract, including goblet cell hyper- and/or metaplasia, eosinophilic globules, and focal turbinate remodeling, but not at lower doses (Ma-Hock et al., 2009; Pauluhn, 2010). The exposures in the current studies were intentionally selected to not induce remarkable lung pathology. Previous studies conducted by the NTP using whole body inhalation exposure of L-MWNT-1020 in rats and mice indicated that chronic inflammation and alveolar (rats) or bronchiolar (mice) epithelial hyperplasia occurred only following exposure to ≥1 mg/m³. The chronic inflammation was characterized by diffusely scattered macrophages in alveoli as well as aggregates of cellular debris and neutrophils near alveolar ducts and terminal bronchioles indicating that the inflammation was associated mainly with the distal airways. The increased incidence of foreign body inclusions in the mediastinal and bronchial lymph nodes was mainly associated with macrophages in paracortex and medullary cords and showed increasing severity with increasing exposure concentration (NTP, 2019).

Despite the absence of lung tissue pathology, increased numbers of pulmonary macrophage and phagocytic capabilities were observed in mice exposed to L-MWNT-1020 for 30 days. This effect was not observed in rats. Shvedova et al. (Shvedova et al., 2008) has reported increased numbers of activated alveolar macrophages in the lungs of mice following a single oropharyngeal aspiration administration of single walled carbon nanotubes (SWCNTs) at doses as low as 10 µg/mouse. More importantly, they showed that pulmonary clearance of administered *Listeria monocytogenes* decreased despite the presence of these macrophages hypothesizing that the macrophages were already activated by the SWCNT exposure and were deficient in their antibacterial activities. This is consistent with *in vitro* studies investigating the impact of long MWCNTs on human primary macrophages. For up to 5 days following *in vitro* exposure, superoxide and inflammatory mediator release were increased. However, these cells had poor phagocytic capabilities, characterized by incomplete engulfment of the MWCNTs, which interfered with bacterial phagocytosis, a state known as frustrated phagocytosis (Sweeney et al., 2015). Since the phagocytosis assay performed in the present study utilized killed bioparticles, it was not possible to determine if the bactericidal activity of pulmonary macrophages was negatively impacted by inhalation of L-MWNT-1020.

Systemic effects on immune cell populations in the peripheral blood were observed in the present study. Interestingly, the effects on blood cells showed species and time differences in sensitivity.

Rats exposed to L-MWNT-1020 for 30 days showed evidence of systemic inflammation with increased neutrophils and eosinophils in the blood. In contrast, mice exposed for 30 days did not show any changes in peripheral blood leukocytes. Only after 90 days of exposure did mice show some changes, mainly a small increase in the percentage of neutrophils but not absolute counts. These data suggest that rats may be more sensitive to systemic inflammation following carbon nanotube inhalation. For the most part, systemic immune functions in mice were unaffected by exposure to L-MWNT-1020 including antibody-mediated immunity, NK cell function, T cell proliferation, CTL activity, and immunophenotypes in the spleen. Earlier studies conducted by Mitchell et al. (2007), demonstrated that a monotonic decrease in the AFC response occurred in mice exposed by inhalation to 0.3, 1 or 3 mg/m³ MWCNT for 14 days as well as decreases in NK cell activity. Although we did not confirm these findings in mice, we did observe a slight decrease in the AFC response in rats evidenced by a significant decrease only in the 0.2 mg/m³ treatment group, thus the effect was not dose responsive. The lack of an effect at the high dose may be due to different mechanisms of toxicity operating at higher doses due to a higher burden and reduced clearance of L-MWNT-1020. In fact, the 0.6 mg/m³ dose level may be approaching lung overload in the rat as previous studies have demonstrated moderate lung overload at doses as low as 0.4 mg/m³ of Baytubes® MWCNTs (Pauluhn, 2010) and clear evidence of lung overload in rats exposed to ≥3 mg/m³ L-MWNT-1020 (NTP, 2019). Consistent with the low dose effect on AFC, rats exposed to 0.06 and 0.2 mg/m³ showed significant changes in the constitution of immune cell populations in the spleen that were not apparent in the high dose group. These phenotypic changes included increases in total spleen cells accompanied by an increase in T-cell populations, both CD4 and CD8, and NK cells. These effects were more prominent at the lower exposure levels, further suggesting possible alterations in the exposure characteristics and/or delivery to and deposition in the airways, as the concentration MWCNTs increased. Systemic intravenous administration of PEGylated MWCNT was shown to suppress the TDAR following immunization with SRBC (Zhang et al., 2017). Although systemic distribution of the inhaled L-MWNT-1020 was not measured in the present study, it is possible that systemic absorption following inhalation exposure was responsible for the systemic effects on the immune system.

In conclusion, inhalation exposure to L-MWNT-1020 for 30 or 90 days in female B6C3F1/N mice and 30 days in female Harlan Sprague Dawley (HSD) rats at concentrations of 0, 0.06, 0.2 or 0.6 mg/m³ produced minimal evidence of systemic immunotoxicity.

TABLE 4 Relative percentages of immune cell populations in the spleen of rodents following inhalation of L-MWNT-1020.

	L-MWNT-1020 (mg/m ³)				
	0	0.06	0.2	0.6	15 mg/kg CPS
30-day rat exposure study					
Percent Total Lymphocytes	98.560 ± 0.126 (12)	98.854 ± 0.097 (12)	98.831 ± 0.080 (12)	98.801 ± 0.103 (12)	98.155 ± 0.834 (10)
Percent Total T Cells	30.126 ± 1.059 (12)	34.158 ± 0.818 (12) *	33.343 ± 0.788 (12)	31.096 ± 0.866 (12)	50.227 ± 1.259 (10) **
Percent CD4 ⁺ T Cells	56.102 ± 2.062 (12)	56.387 ± 1.748 (12)	57.882 ± 1.400 (12)	54.485 ± 0.943 (12)	50.467 ± 2.008 (10)
Percent CD8 ⁺ T Cells	38.963 ± 1.842 (12)	39.618 ± 1.623 (12)	37.588 ± 1.461 (12)	41.169 ± 0.990 (12)	46.730 ± 2.035 (10) *
Percent B Cells	50.256 ± 0.936 (12)	47.240 ± 0.657 (12)	46.847 ± 0.920 (12) *	48.114 ± 0.768 (12)	27.657 ± 1.191 (10) **
Percent NK Cells	2.558 ± 0.113 (12)	2.479 ± 0.151 (12)	2.591 ± 0.133 (12)	3.038 ± 0.200 (12)	4.806 ± 0.439 (10) **
Percent Mono/Mac Cells	1.917 ± 0.185 (12)	1.513 ± 0.087 (12)	1.589 ± 0.091 (12)	1.626 ± 0.112 (12)	1.277 ± 0.148 (10) **
Percent Neutrophils	1.666 ± 0.086 (12)	1.303 ± 0.075 (12) **	1.650 ± 0.147 (12)	1.429 ± 0.058 (12)	2.533 ± 0.259 (10) **
Percent Eosinophils	0.153 ± 0.014 (12) [↓]	0.108 ± 0.011 (12)	0.131 ± 0.021 (12)	0.101 ± 0.016 (12) *	0.155 ± 0.015 (10)
30-day mouse exposure study					
Percent Total Lymphocytes	89.389 ± 1.672 (8)	92.449 ± 1.291 (8)	93.834 ± 1.043 (7)	90.821 ± 1.060 (8)	97.420 ± 0.335 (8) **
Percent Total T Cells	29.871 ± 0.467 (8)	30.276 ± 0.671 (8)	28.851 ± 1.282 (7)	29.014 ± 0.391 (8)	49.399 ± 1.152 (8) **
Percent CD4 ⁺ T Cells	56.464 ± 0.428 (8)	57.396 ± 0.496 (8)	58.153 ± 0.475 (7)	56.350 ± 0.362 (8)	55.450 ± 0.398 (8)
Percent CD8 ⁺ T Cells	36.025 ± 0.375 (8)	35.511 ± 0.428 (8)	33.989 ± 0.659 (7) *	35.844 ± 0.363 (8)	38.701 ± 0.262 (8) **
Percent B Cells	60.374 ± 0.561 (8)	60.198 ± 0.780 (8)	61.533 ± 1.390 (7)	60.928 ± 0.598 (8)	42.679 ± 1.038 (8) **
Percent NK Cells	4.755 ± 0.187 (8)	4.364 ± 0.100 (8)	5.039 ± 0.140 (7)	4.928 ± 0.146 (8)	3.805 ± 0.136 (8) **
Percent Mono/Mac Cells	1.902 ± 0.060 (8)	1.885 ± 0.064 (8)	1.864 ± 0.073 (7)	1.962 ± 0.095 (8)	1.323 ± 0.031 (8) **
Percent Neutrophils	0.086 ± 0.005 (8)	0.091 ± 0.011 (8)	0.104 ± 0.018 (7)	0.108 ± 0.010 (8)	0.042 ± 0.005 (7) **
Percent Eosinophils	0.088 ± 0.007 (8)	0.073 ± 0.004 (8)	0.066 ± 0.006 (7)	0.089 ± 0.004 (8)	0.074 ± 0.003 (8)
90-day mouse exposure study					
Percent Total Lymphocytes	96.654 ± 0.557 (8)	95.464 ± 0.586 (8)	97.023 ± 0.400 (8)	97.578 ± 0.367 (8)	98.446 ± 0.208 (8) **
Percent Total Lymphocytes	96.654 ± 0.557 (8)	95.464 ± 0.586 (8)	97.023 ± 0.400 (8)	97.578 ± 0.367 (8)	98.446 ± 0.208 (8) **
Percent Total T Cells	29.830 ± 1.069 (8) [↑]	30.144 ± 0.968 (8)	30.854 ± 0.884 (8)	31.973 ± 0.468 (8)	55.973 ± 1.955 (8) **
Percent CD4 ⁺ T Cells	56.593 ± 0.643 (8)	57.716 ± 0.733 (8)	58.279 ± 0.458 (8)	57.925 ± 0.763 (8)	57.623 ± 0.543 (8)
Percent CD8 ⁺ T Cells	35.618 ± 0.542 (8)	34.554 ± 0.713 (8)	33.911 ± 0.256 (8)	34.164 ± 0.666 (8)	36.988 ± 0.531 (8)
Percent B Cells	63.281 ± 1.224 (8)	63.164 ± 0.971 (8)	62.723 ± 1.075 (8)	61.381 ± 0.556 (8)	37.490 ± 1.973 (8) **
Percent NK Cells	1.226 ± 0.046 (8)	1.235 ± 0.047 (8)	1.205 ± 0.102 (8)	1.083 ± 0.069 (8)	1.004 ± 0.036 (8) **
Percent Mono/Mac Cells	2.379 ± 0.111 (8)	2.467 ± 0.093 (8)	2.251 ± 0.096 (8)	2.198 ± 0.045 (8)	1.563 ± 0.076 (8) **
Percent Neutrophils	0.185 ± 0.013 (8) ^{↑↑}	0.193 ± 0.005 (8)	0.165 ± 0.013 (8)	0.118 ± 0.014 (8) **	0.095 ± 0.010 (8) **
Percent Eosinophils	0.161 ± 0.011 (8)	0.170 ± 0.008 (8)	0.143 ± 0.011 (8)	0.192 ± 0.011 (8)	0.244 ± 0.017 (8) **
Percent Mono/Mac Cells	2.379 ± 0.111 (8)	2.467 ± 0.093 (8)	2.251 ± 0.096 (8)	2.198 ± 0.045 (8)	1.563 ± 0.076 (8) **
Percent Neutrophils	0.185 ± 0.013 (8) ^{↑↑}	0.193 ± 0.005 (8)	0.165 ± 0.013 (8)	0.118 ± 0.014 (8) **	0.095 ± 0.010 (8) **
Percent Eosinophils	0.161 ± 0.011 (8)	0.170 ± 0.008 (8)	0.143 ± 0.011 (8)	0.192 ± 0.011 (8)	0.244 ± 0.017 (8) **

Data are presented as Mean ± SEM (n). SEM – Standard error, CPS – cyclophosphamide; NK – Natural Killer; Mono/Mac – Monocyte/Macrophage. Significant increasing ([↑]p < 0.05 or ^{↑↑}p < 0.01) or decreasing ([↓]p < 0.05 or ^{↓↓}p < 0.01) trend with increasing dose of L-MWNT-1020. Significantly different from vehicle control at *p < 0.05 of **p < 0.01.

While exposure increased pulmonary macrophage activity in mice, as well as systemic inflammation evidenced by increased neutrophils in rats and mice, no significant changes were observed in mice in any of the systemic functional immune parameters measured. However, in rats there was a slight decrease in humoral immunity coinciding with an increase in splenic T cell and NK cell populations. The biological significance of the minor systemic effects observed in rats at exposure levels similar to those observed in the workplace is unclear as there was a lack of pulmonary inflammation.

Data availability statement

The datasets presented in this study can be found in online repositories. The names of the repository/repository and accession number(s) can be found below: NIEHS CEBS ([10.22427/NTP-DATA-500-005-001-000-1](https://doi.org/10.22427/NTP-DATA-500-005-001-000-1)).

Ethics statement

The animal studies were approved by the IACUCs of Burleson Research Technologies, Inc. and Battelle. The studies were conducted in accordance with the local legislation and institutional requirements.

Author contributions

VJ: Conceptualization, Data curation, Formal Analysis, Funding acquisition, Investigation, Methodology, Project administration, Supervision, Writing – original draft, Writing – review and editing. NW: Conceptualization, Methodology, Writing – review and editing. ML: Writing – original draft, Writing – review and editing. GRB: Funding acquisition, Writing – review and editing. MC: Data curation, Writing – review and editing. GLB: Investigation, Methodology, Writing – review and editing. BS: Investigation, Methodology, Writing – review and editing. DG: Conceptualization, Funding acquisition, Methodology, Project administration, Supervision, Writing – original draft, Writing – review and editing.

Funding

The author(s) declare that financial support was received for the research and/or publication of this article. This work was supported

by the Intramural Research Program of the NIH, National Institute of Environmental Health Sciences, Intramural Research projects ES103374-01, and National Institute of Environmental Health Sciences, National Institutes of Health, U.S. Department of Health and Human Services, contracts HHSN273201000016C (Battelle Memorial Research Institute, Columbus, OH) and HHSN273201400017C (Burleson Research Technologies, Morrisville, NC).

Acknowledgments

The authors are grateful to William Gwinn for his critical review of this manuscript.

Conflict of interest

Authors VJ, ML, and GRB were employed by Burleson Research Technologies, Inc. Author GLB was employed by Sarepta Therapeutics.

The remaining authors declare that the research was conducted in the absence of any commercial or financial relationships that could be construed as a potential conflict of interest.

The author(s) declared that they were an editorial board member of Frontiers, at the time of submission. This had no impact on the peer review process and the final decision.

Generative AI statement

The author(s) declare that no Gen AI was used in the creation of this manuscript.

Publisher's note

All claims expressed in this article are solely those of the authors and do not necessarily represent those of their affiliated organizations, or those of the publisher, the editors and the reviewers. Any product that may be evaluated in this article, or claim that may be made by its manufacturer, is not guaranteed or endorsed by the publisher.

References

- Bartone, R. D., Tisch, L. J., Dominguez, J., Payne, C. K., and Bonner, J. C. (2024). House dust mite proteins adsorb on multiwalled carbon nanotubes forming an allergen corona that intensifies allergic lung disease in mice. *ACS Nano* 18, 26215–26232. doi:10.1021/acsnano.4c07893
- Bergamaschi, E., Garzaro, G., Jones, G. W., Buglisi, M., Caniglia, M., Godono, A., et al. (2021). Occupational exposure to carbon nanotubes and carbon nanofibres: more than a cobweb. *Nanomaterials* 11 (3), 1–15. doi:10.3390/nano11030745
- Burleson, G. R., Burleson, F. G., and Dietert, R. R. (2018). Evaluation of cell-mediated immune function using the cytotoxic T-lymphocyte assay. *Methods Mol. Biol.* 1803, 199–208. doi:10.1007/978-1-4939-8549-4_13
- Dahm, M. M., Schubauer-Berigan, M. K., Evans, D. E., Birch, M. E., Bertke, S., Beard, J. D., et al. (2018). Exposure assessments for a cross-sectional epidemiologic study of US carbon nanotube and nanofiber workers. *Int. J. Hyg. Environ. Health* 221 (3), 429–440. doi:10.1016/j.IJHEH.2018.01.006
- Dixon, W. J., and Massey, F. J. (1957). *Introduction to statistical analysis*. 2nd ed. New York, NY: McGraw-Hill Book Company, Inc. (International student edition).
- Dunn, O. J. (1964). Multiple comparisons using rank sums. *Technometrics* 6 (3), 241–252. doi:10.1080/00401706.1964.10490181
- Dunnnett, C. W. (1955). A multiple comparison procedure for comparing several treatments with a control. *J. Am. Stat. Assoc.* 50, 1096–1121. doi:10.2307/2281208
- Elmore, S. A. (2012). Enhanced histopathology of the immune system: a review and update. *Toxicol. Pathol.* 40 (2), 148–156. doi:10.1177/0192623311427571

- Fujita, K., Obara, S., Maru, J., and Endoh, S. (2020). Cytotoxicity profiles of multi-walled carbon nanotubes with different physico-chemical properties. *Toxicol. Mech. Methods* 30 (7), 477–489. doi:10.1080/15376516.2020.1761920
- Guseva Canu, I., Batsungnoen, K., Maynard, A., and Hopf, N. B. (2020). State of knowledge on the occupational exposure to carbon nanotubes. *Int. J. Hyg. Environ. Health* 225, 113472. doi:10.1016/j.ijheh.2020.113472
- Ihrle, M. D., Taylor-Just, A. J., Walker, N. J., Stout, M. D., Gupta, A., Richey, J. S., et al. (2019). Inhalation exposure to multi-walled carbon nanotubes alters the pulmonary allergic response of mice to house dust mite allergen. *Inhal. Toxicol.* 31 (5), 192–202. doi:10.1080/08958378.2019.1643955
- Jonckheere, A. R. (1954). A distribution free k-sample test against ordered alternatives. *Biometrika* 41 (1–2), 133–145. doi:10.1093/BIOMET/41.1-2.133
- Klein, S. L., and Flanagan, K. L. (2016). Sex differences in immune responses. *Nat. Rev. Immunol.* 16 (10), 626–638. doi:10.1038/nri.2016.90
- Lam, C. W., James, J. T., McCluskey, R., and Hunter, R. L. (2004). Pulmonary toxicity of single-wall carbon nanotubes in mice 7 and 90 days after intratracheal instillation. *Toxicol. Sci.* 77 (1), 126–134. doi:10.1093/TOXSCI/KFG243
- Ma-Hock, L., Treumann, S., Strauss, V., Brill, S., Luizi, F., Mertler, M., et al. (2009). Inhalation toxicity of multiwall carbon nanotubes in rats exposed for 3 months. *Toxicol. Sci.* 112 (2), 468–481. doi:10.1093/TOXSCI/KFP146
- Migliaccio, C. T., Hamilton, R. F., Shaw, P. K., Rhoderick, J. F., Deb, S., Bhargava, R., et al. (2021). Respiratory and systemic impacts following MWCNT inhalation in B6C3F1/N mice. *Part Fibre Toxicol.* 18 (1), 16. doi:10.1186/S12989-021-00408-Z
- Mitchell, L. A., Gao, J., Wal, R., Gigliotti, A., Burchiel, S. W., and McDonald, J. D. (2007). Pulmonary and systemic immune response to inhaled multiwalled carbon nanotubes. *Toxicol. Sci.* 100 (1), 203–214. doi:10.1093/toxsci/kfm196
- Mitchell, L. A., Lauer, F. T., Burchiel, S. W., and McDonald, J. D. (2009). Mechanisms for how inhaled multiwalled carbon nanotubes suppress systemic immune function in mice. *Nat. Nanotechnol.* 4 (7), 451–456. doi:10.1038/nnano.2009.151
- NIOSH (2013). *Current intelligence bulletin 65: occupational exposure to carbon nanotubes and nanofibers*. Cincinnati, OH: DHHS (NIOSH) Publication, 2013–2145.
- NTP (2019). Toxicity studies of 1020 long multiwalled carbon nanotubes (L-MWNT-1020) administered by inhalation to Sprague Dawley (Hsd:Sprague Dawley SD) rats and B6C3F1/N mice. *Toxic. Rep. Ser.* (94). doi:10.22427/NTP-TOX-94
- Orecchioni, M., Bedognetti, D., Sgarrella, F., Marincola, F. M., Bianco, A., and Delogu, L. G. (2014). Impact of carbon nanotubes and graphene on immune cells. *J. Transl. Med.* 12 (1), 138. doi:10.1186/1479-5876-12-138
- Pauluhn, J. (2010). Subchronic 13-week inhalation exposure of rats to multiwalled carbon nanotubes: toxic effects are determined by density of agglomerate structures, not fibrillar structures. *Toxicol. Sci.* 113 (1), 226–242. doi:10.1093/TOXSCI/KFP247
- Shirley, E. (1977). A non-parametric equivalent of Williams' test for contrasting increasing dose levels of a treatment. *Biometrics* 33 (2), 386–389. doi:10.2307/2529789
- Shvedova, A. A., Fabisiak, J. P., Kisin, E. R., Murray, A. R., Roberts, J. R., Tyurina, Y. Y., et al. (2008). Sequential exposure to carbon nanotubes and bacteria enhances pulmonary inflammation and infectivity. *Am. J. Respir. Cell. Mol. Biol.* 38 (5), 579–590. doi:10.1165/RCMB.2007-0255OC
- Shvedova, A. A., Kisin, E. R., Mercer, R., Murray, A. R., Johnson, V. J., Potapovich, A. I., et al. (2005). Unusual inflammatory and fibrogenic pulmonary responses to single-walled carbon nanotubes in mice. *Am. J. Physiol. Lung Cell. Mol. Physiol.* 289 (5 33-5), L698–L708. doi:10.1152/ajplung.00084.2005
- Sweeney, S., Grandolfo, D., Ruenaroengsak, P., and Tetley, T. D. (2015). Functional consequences for primary human alveolar macrophages following treatment with long, but not short, multiwalled carbon nanotubes. *Int. J. Nanomedicine* 10, 3115–3129. doi:10.2147/IJN.S77867
- Tukey, J. W. (1977). "Exploratory data analysis," in *The concise encyclopedia of statistics* (New York, NY: Springer), 61–100. doi:10.1007/978-0-387-32833-1_136
- Vitkina, T. I., Yankova, V. I., Gvozdenko, T. A., Kuznetsov, V. L., Krasnikov, D. V., Nazarenko, A. V., et al. (2016). The impact of multi-walled carbon nanotubes with different amount of metallic impurities on immunometabolic parameters in healthy volunteers. *Food Chem. Toxicol.* 87, 138–147. doi:10.1016/J.FCT.2015.11.023
- Warheit, D. B., Laurence, B. R., Reed, K. L., Roach, D. H., Reynolds, G. A. M., and Webb, T. R. (2004). Comparative pulmonary toxicity assessment of single-wall carbon nanotubes in rats. *Toxicol. Sci.* 77 (1), 117–125. doi:10.1093/TOXSCI/KFG228
- Watson, ALTD, Johnson, V. J., Luster, M. I., Burleson, G. R., Fallacara, D. M., Sparrow, B. R., et al. (2021). Immunotoxicity studies of sulfolane following developmental exposure in Hsd:Sprague Dawley SD rats and adult exposure in B6C3F1/N mice. *J. Immunotoxicol.* 18 (1), 1–12. doi:10.1080/1547691X.2020.1869355
- Williams, D. A. (1971). A test for differences between treatment means when several dose levels are compared with a zero dose control. *Biometrics* 27 (1), 103–117. doi:10.2307/2528930
- Williams, D. A. (1972). The comparison of several dose levels with a zero dose control. *Biometrics* 28 (2), 519–531. doi:10.2307/2556164
- Williams, D. A. (1986). A note on Shirley's nonparametric test for comparing several dose levels with a zero-dose control. *Biometrics* 42 (1), 183–186. doi:10.2307/2531254
- Zhang, T., Tang, M., Zhang, S., Hu, Y., Li, H., Zhang, T., et al. (2017). Systemic and immunotoxicity of pristine and PEGylated multi-walled carbon nanotubes in an intravenous 28 days repeated dose toxicity study. *Int. J. Nanomedicine* 12, 1539–1554. doi:10.2147/IJN.S123345

Frontiers in Toxicology

Explores the effects of toxins from molecular to population level

A multidisciplinary journal which presents the latest research on the adverse effects of substances, particles and mixtures on living organisms.

Discover the latest Research Topics

[See more →](#)

Frontiers

Avenue du Tribunal-Fédéral 34
1005 Lausanne, Switzerland
frontiersin.org

Contact us

+41 (0)21 510 17 00
frontiersin.org/about/contact

